DEPARTMENT OF COMMERCE PUBLICATION

NBS SPECIAL PUBLICATION 300

VOLUME 6

Precision Measurement and Calibration

Heat

U.S. DEPARTMENT OF COMMERCE
National Bureau of Standards

UNITED STATES DEPARTMENT OF COMMERCE • MAURICE H. STANS, Secretary
U.S., NATIONAL BUREAU OF STANDARDS • LEWIS M. BRANSCOMB, Director

Precision Measurement and Calibration

Selected NBS Papers on

Heat

Defoe C. Ginnings, Editor

A compilation of previously published papers by the staff of the National Bureau of Standards, including selected abstracts by NBS and non-NBS authors. Issued in several volumes, see page IV.

NBS Special Publication 300 — Volume 6

CODEN NAT. BUR. STAND. (U.S.), SPEC. PUBL. 300, V. 6, 387 pages, February 1970

Issued February 1970

For sale by the Superintendent of Documents, U.S. Government Printing Office, Washington, D.C. 20402
(Order by SD Catalog No. C 13.10: 300/v.6). Price $5.00

Abstract

This volume is one of an extended series which brings together the previously published papers, monographs, abstracts, and bibliographies by NBS authors dealing with the precision measurement of specific physical quantities and the calibration of the related metrology equipment. The contents have been selected as being useful to the standards laboratories of the United States in tracing to NBS standards the accuracies of measurement needed for research work, factory production, or field evaluation.

Volume 6 contains reprints through 1968 covering the following topics: General Calorimetry and Techniques, Low Temperature Calorimetry, High Temperature Calorimetry, Reaction Calorimetry, and Heat Transfer.

Key words: Heat measurements, calorimetric methods, calorimetric design principles, calorimetric theory, cryoscopic studies, differential thermal analysis, low temperature calorimetry, high temperature calorimetry, reaction calorimetry, bomb calorimetry, heat transfer.

Library of Congress Catalog Card Number: 68–60042

Foreword

In the 1950's the tremendous increase in industrial activity, particularly in the missile and satellite fields, led to an unprecedented demand for precision measurement, which, in turn, brought about the establishment of hundreds of new standards laboratories. To aid these laboratories in transmitting the accuracies of the national standards to the shops of industry, NBS in 1959 gathered together and reprinted a number of technical papers by members of its staff describing methods of precision measurement and the design and calibration of standards and instruments. These reprints, representing papers written over a period of several decades, were published as NBS Handbook 77, Precision Measurement and Calibration, in three volumes: Electricity and Electronics; Heat and Mechanics; Optics, Metrology, and Radiation.

Some of the papers in Handbook 77 are still useful, but new theoretical knowledge, improved materials, and increasingly complex experimental techniques have so advanced the art and science of measurement that a new compilation has become necessary. The present volume is part of a new reprint collection, designated NBS Special Publication 300, which has been planned to fill this need. Besides previously published papers by the NBS staff, the collection includes selected abstracts by both NBS and non-NBS authors. It is hoped that SP 300 will serve both as a textbook and as a reference source for the many scientists and engineers who fill responsible positions in standards laboratories.

Lewis M. Branscomb, *Director.*

Preface

The general plan for this compilation has been reviewed by the Information Committee of the National Conference of Standards Laboratories. The plan calls for Special Publication 300 to be published in 12 volumes having the following titles and editors:

Statistical Concepts and Procedures, H. H. Ku
Frequency and Time, A. H. Morgan
Electricity—Low Frequency, F. L. Hermach and R. F. Dziuba
Electricity—Radio Frequency, A. J. Estin
Heat, D. C. Ginnings
Temperature, J. F. Swindells
Mechanics, R. L. Bloss and Mary J. Orloski
Dimensional Metrology—Length and Angle, H. K. Hammond, III
Radiometry and Photometry, H. K. Hammond, III
Colorimetry and Image Optics, I. Nimeroff and C. S. McCamy
Spectrochemical Analysis, B. F. Scribner
Ionizing Radiation, E. H. Eisenhower

This division of subject matter has been chosen to assure knowledgeable selection of context rather than to attain uniform size. It is believed, however, that the larger volumes, of approximately 500 pages, will still be small enough for convenient handling in the laboratory.

The compilation consists primarily of original papers by NBS authors which have been reprinted by photoreproduction, with occasional updating of graphs or numerical data when this has appeared desirable. In addition, some important publications by non-NBS authors that are too long to be included, are represented by abstracts or references; the abstracts are signed by the individuals who wrote them, unless written by the author.

Each volume has a subject index and author index, and within each volume, contents are grouped by subtopics to facilitate browsing. Many entries follow the recent Bureau practice of assigning several key words or phrases to each document; these may be collated with titles in the index. Pagination is continuous within the volume, the page numbers in the original publications also being retained and combined with the volume page numbers, for example 100–10. The index notation 6–133 refers to volume 6, page 133 of this volume. A convenient list of SI (Système International) physical units and a conversion table are to be found inside the back cover.

The publications listed herein for which a price is indicated are available from the Superintendent of Documents, U.S. Government Printing Office, Washington, D.C. 20402 (foreign postage, one-fourth additional). Many documents in the various NBS nonperiodical series are also available from the NBS Clearinghouse for Federal Scientific and Technical Information, Springfield, Va. 22151. Reprints from the NBS Journal of Research or from non-NBS journals may sometimes be obtained directly from an author.

Suggestions as to the selection of papers which should be included in future editions will be welcome. Current developments in measurement technology at NBS are covered in annual seminars held at either the Gaithersburg (Maryland) or the Boulder (Colorado) laboratories. These developments are summarized, along with a running list of publications by NBS authors, in the monthly NBS Technical News Bulletin.

H. L. Mason,
Office of Measurement Services,
NBS Institute for Basic Standards.

Editor's Note

This volume supplements the papers on calorimetry and heat transfer given in NBS Handbook 77—Volume II, Heat and Mechanics, published in 1961. Because of its importance, an earlier paper on bomb calorimetry is repeated in this volume (5.1). Also, one abstract is given of a paper that is now in preparation (4.3). All the papers in this volume are entirely by NBS authors except two.

The emphasis in this volume is on methods and techniques of heat measurements, primarily in calorimetry but also in heat transfer measurements. In the field of calorimetry, there are discussed methods, design, and errors in calorimetry, and the application of calorimetry to the measurement of a variety of thermodynamic and other properties. A list of "SI" recommended units, and a table of conversion factors are given inside the back cover.

D. C. Ginnings, *Editor.*

Contents

Contents

2. Cryoscopic Measurements

3. Low Temperature Calorimetry

Contents

Contents

1. General Calorimetry and Techniques

1. General Calorimetry and Techniques—Continued

Reprinted from

Experimental Thermodynamics
Volume I

Calorimetry of Non-reacting Systems

Editors: John P. McCullough and Donald W. Scott

Chapter 1. Introduction

Defoe C. Ginnings

National Bureau of Standards

INTERNATIONAL UNION OF PURE AND APPLIED CHEMISTRY

1968

BUTTERWORTHS
LONDON

CHAPTER 1

Introduction

Defoe C. Ginnings

National Bureau of Standards, Washington, D.C., U.S.A.

Contents

I. General Principles and Terminology

The word *calorimeter* is derived from the Latin word for *heat* and the Greek word for *measure*. A calorimeter is accepted today to mean an instrument to measure the heat involved in a known change in state of a material. This can involve a change in phase, temperature, pressure, volume, chemical composition, or any other property of the material which is associated with the change in heat. Thus, it is possible that a calorimeter may really be used to measure several quantities besides heat. Ordinarily, however, in non-reacting systems, only one or two other quantities are significant. For example, in measuring the heat capacity of a solid at moderate temperatures and pressures, the temperature change in the solid is usually the only significant quantity, although the volume of the solid and the pressure on it have some slight effect.

A calorimeter can measure the heat involved either directly by comparison with a known electrical energy or indirectly by comparison with materials with known properties. Direct measurement usually involves the addition of a known amount of electrical energy in the form of heat, because with modern techniques, electrical energy can be measured more accurately and conveniently than other forms of energy. Frequently, one can avoid the use of electrical energy measurements by utilizing some thermal property which has already been measured electrically. An example of this is the "calibration" of a calorimeter, with a "standard" material such as aluminum oxide (sapphire), in heat capacity measurements. Whether direct or indirect measurements of heat are used, the heat involved in the change in state usually includes some heat (called *heat leak*) which is due to the non-ideality of the calorimeter and its application. This heat leak is usually significant for accurate heat measurements. The importance of heat leak

in accurate calorimetry was pointed out in 1928 by W. P. White in his book *The Modern Calorimeter*[20]. He says "There is a difference of opinion as to whether thermal leakage is necessarily the chief source of error in calorimetry, but it is undoubtedly responsible for most of the experimental features and devices in accurate work". With increased emphasis on accuracy this is more true today than it was in 1928!

The term *calorimeter* is commonly used with two different meanings. In the broad sense, it is used to describe an entire calorimetric apparatus. Although this meaning is very useful in a general description, it is more useful in much of this book to limit it to a particular part of the calorimetric apparatus. Specifically, when the word calorimeter is used in this limited sense, it is defined as that part of the apparatus in which the change in energy is accounted for. Sometimes, such terms as *calorimeter proper* and *calorimeter vessel* have been used to have the above meaning.

The calorimeter as defined above in the limited sense can consist of either few or many parts, depending on the type of calorimeter, accuracy desired, and many other factors. The exact geometric location of the boundary between the calorimeter (used in this limited sense) and its surroundings usually has little significance because of the method of using the calorimeter, as described later in this book.

Calorimeters may be classified in several ways. One method of classification is according to which physical variables are kept constant. Thus *isothermal calorimeters*, as the name implies, are those in which there is ideally no temperature change during the experiment. The general usage of the term isothermal here implies constancy of temperature with time of any part of the calorimeter, rather than the uniformity of temperature over the calorimeter at any one time. Many isothermal calorimeters utilize a phase change to maintain constancy of temperature. The solid–liquid phase change is used in the ice calorimeter[5], the resulting volume change being used as a measure of either the heat added or removed. The liquid–vapor phase change also has been used[7, 18]. Other methods that have been used to keep constancy of temperature during the experiment include use of electric heating to balance removal of heat and electric cooling (Peltier effect) to balance the addition of heat[9, 14]. Sometimes a heat flow is provided to balance out a heat source. Such a calorimeter may be called a *heat flow isothermal calorimeter* or simply a *heat flow calorimeter*. In a heat flow calorimeter, the heat may be removed either by fluid flow, such as in a *flow calorimeter*, or by using heat leak by radiation[21], convection or conduction. Twin "*conduction*" *calorimeters* have been used by Calvet in the microcalorimetric study of slow thermal processes.

A second class of calorimeters are referred to as *adiabatic*. An adiabatic calorimeter is one which ideally has no heat transfer across its boundary. Strictly speaking, the term adiabatic is used in a vague sense because no practical calorimeter is truly adiabatic. A calorimeter can be made more adiabatic by reducing the heat exchange between the calorimeter and its surroundings. This can be done by (*i*) minimizing the temperature difference between calorimeter and surroundings, (*ii*) minimizing the heat transfer coefficient (sometimes called leakage modulus), or (*iii*) minimizing the time for the heat exchange. It is true that common usage implies mainly the

minimizing of temperature difference when describing an adiabatic calorimeter, even though the other factors may be just as important. There is also a tendency in modern calorimetry to restrict the term adiabatic calorimeter to one which both changes in temperature and minimizes heat leak by control of the temperature of the surrounding surface of the shield to the same temperature as the calorimeter. The term *adiabatic shield* (or jacket) is used to describe the above shield. Such a restricted definition of adiabatic calorimeter would not include an ice calorimeter, even though its shield temperature is the same as that of the calorimeter. Possibly the greatest use of the term adiabatic calorimeter is to differentiate it from the calorimeter whose surrounding shield is kept at a constant temperature, rather than at the calorimeter temperature (*See* Chapter 6). The latter calorimeter could be named appropriately an *isothermal shield calorimeter* or *isothermal jacket calorimeter.* Since these names are somewhat cumbersome to use, this calorimeter has sometimes loosely and erroneously been called *isothermal* calorimeter. As an alternative name for this calorimeter, the term *isoperibol* has been suggested by Kubaschewski and Hultgren[15].

The use of the term adiabatic calorimeter has been questioned when electric energy passes through the calorimeter boundary. In this regard, it should be noted that the basic definition of adiabatic refers to heat, not any other form of energy. The accepted meaning of an adiabatic calorimeter permits measured electric energy to enter the calorimeter and be transformed to heat, as in a calorimeter heater. By carrying this principle even further, it would be possible in an adiabatic calorimeter to absorb γ-radiation from the surroundings, the resulting temperature change being a measure of the radiation energy[13]. Perhaps the dividing line in the case of radiation would depend on its frequency; that is, the radiation frequency must not be in the range produced by the temperatures involved in the calorimeter and shield.

Sometimes, a type of calorimeter is named after the scientist who first used it extensively. Examples are the *Bunsen ice calorimeter* (Chapter 8), which is an isothermal calorimeter using the ice–water phase change, the *Nernst calorimeter* (Chapter 6), which is the isothermal shield type (isoperibol) used frequently in combustion calorimetry and in low-temperature calorimetry, and the *Joule twin calorimeter* system, which uses two calorimeters differentially to minimize errors due to heat leak. Frequently, the latter calorimeters are called simply *twin* calorimeters or *differential* calorimeters. Of historical interest is the *Dewar low-temperature calorimeter* using evacuation and surfaces with low radiation emittance for insulation.

The *Calvet calorimeter*[3] is a twin microcalorimeter characterized by use of a metal block for isothermal surroundings, with evaluation of heat in one twin either by compensation (Peltier cooling or Joule heating) or by time integration of the temperature difference between the twins. The *Callendar radiation balance*[2], sometimes called *Callendar radio balance*, consists of twin microcalorimeters used to measure heats of radioactivity or solar radiation. Peltier cooling in a thermocouple is used to balance out the unknown heat.

The names of several calorimeters describe a characteristic property or function of the calorimeter. A *microcalorimeter* refers to a calorimeter used to measure small amounts of heat. It is not necessarily small in size[17] although

in modern microcalorimetry it usually is. A *flow calorimeter* is one used with fluid samples flowing through the calorimeter. Of historic value are the names *continuous* or *continuous electric calorimeters* used to describe early flow calorimeters[1]. Flow calorimeters have been used both to measure the thermal properties of a fluid in terms of electric energy (*See* Chapter 10) and to measure a steady heat source, by using the known thermal properties of the fluid. An *aneroid calorimeter* is usually interpreted as one which depends on solid conduction rather than liquids for distributing heat. Thus the usual combustion bomb calorimeter, with its reaction vessel immersed in a stirred liquid bath, is not an aneroid calorimeter. One aneroid calorimeter is the *copper block calorimeter* which has been used frequently in the drop method for measuring enthalpies at high temperatures. Sometimes, a calorimeter which is used in the drop method is called a *receiving calorimeter*. The term *radiation calorimeter* has sometimes been used to describe an isothermal calorimeter in which heat radiated to the surroundings is used to balance a heat evolution in the calorimeter plus a measured electric heat. In the field of chemical reactions such names as combustion, bomb, reaction, flame, and solution calorimeters are used to describe the various types of reactions studied[15].

The *method of mixtures* uses a mixing process to measure th thermal properties of one material in terms of the known thermal properties of another material. For example, when a known mass of sample at a known temperature is "mixed" with a known mass of water at another known temperature, the mixture will come to thermal equilibrium at a third known temperature. By using the known heat capacity of water, the average heat capacity of the sample over its change in temperature can be calculated. Sometimes the method of mixtures is considered perhaps loosely to include the case of the "standard" material changing in phase, rather than temperature, such as in the ice calorimeter. In this case, the amount of the phase change, and its corresponding heat change, must be known.

As pointed out earlier, a large part of the effort in accurate calorimetry is usually devoted to either minimizing and/or measuring the heat transfer between the calorimeter and its surroundings. The terminology for the immediate surroundings varies considerably among different laboratories. Among the various names for the surroundings are *shield*, *jacket*, *guard*, *envelope*, *thermostat*, etc. The reader must depend upon the author of a particular chapter to define his terms for the calorimeter surroundings. The term *shield* will be used in this introduction to describe the calorimeter surroundings.

II. Definitions and Symbols

In calorimetry there are a few thermodynamic properties which relate directly to the experimentally measured heat. The simplest property is the *internal energy*, E, of a system, which depends only on the state of the system. Thus, the difference in internal energy, ΔE, between two states is independent of the "path" the system follows in going from one state to the other.

An example of a direct calorimetric measurement of E as a function of temperature is that of a gas at a constant volume. In this case, because no

work is done by the gas on its surroundings, the heat input, q, corresponds directly to the change in internal energy, E, of the gas, so that $q = (E_2 - E_1)$.

Most calorimetry, however, is not carried out with the sample at constant volume. This is especially true with solids and liquids for which this procedure would be very difficult. Most calorimetry is carried out at approximately constant pressure so that the sample does work on the surroundings and the heat input does not correspond to the change in internal energy E. In this case, the heat measured, q, corresponds to the change in the thermodynamic quantity enthalpy, H, which is defined by $H = E + PV$, in which P and V represent the pressure and volume of the sample. In other words, at constant pressure P, $q = H_2 - H_1 = \Delta H = (E_2 - E_1) + P(V_2 - V_1)$. The quantity enthalpy was called *heat content* (or *total heat*) in earlier calorimetry. These older names are sometimes misleading because they describe a quantity whose change does not always correspond to the heat input. Such a case is the heat input, q, to a system in which the pressure changes so that $q \neq \Delta H$.

A system with changing pressure is frequently encountered in calorimetric measurements on liquids having significant vapor pressure (*see* Chapter 11). If the liquid sample is in equilibrium with its vapor in a calorimeter, the pressure in the calorimeter will vary with temperature.

The previous discussion covers measurements of heats corresponding to the three "paths", (*i*) constant volume, (*ii*) constant pressure, and (*iii*) "saturation" pressure (defined as equilibrium vapor pressure). In all these measurements if no transition or phase change is involved, a heat input q results in a temperature change ΔT. The ratio $q/\Delta T$ defines the term *average heat capacity* of the system over the temperature interval ΔT. The limit of this ratio as q is made indefinitely small is called the *heat capacity*, C, (sometimes *true heat capacity* or *thermal capacity*). Thus the dimensions of heat capacity are (energy) (temperature)$^{-1}$ and it is an extensive property. The three types of heat capacity defined by the three "paths" previously given are $C_V[= (\partial E/\partial T)_V]$, heat capacity at constant volume, $C_P[= (\partial/H\partial T)_P]$ heat capacity at constant pressure, and C_S, heat capacity at saturation pressure. The term *molal heat capacity* (or *molar heat capacity*) refers to the heat capacity of one gram-formula-weight of a material, and is an intensive property.

The term *specific* (*heat* or *specific heat capacity*) is frequently used interchangeably with heat capacity. Specific heat is generally interpreted as the *heat capacity per unit mass* of the sample, so that it is an intensive property. From these definitions, it is seen that the term heat capacity applies to *any* system, such as a calorimeter with many separate components. When the system is restricted to one mole of a compound, the term molal (or molar) heat capacity is used. In a strict sense, molal heat capacity is a specific heat, but the term specific heat is usually limited to other units of mass than one mole, such as one gram, etc. Although the distinction between the quantities heat capacity and specific heat is not always sharply defined, there should be no confusion if the authors give the units of the quantity. In most general discussions, they can be used interchangeably.

In the case of solutions involving two or more components, the terms *partial molal heat capacity* and *apparent molal heat capacity* are used to describe the behaviour of single components (*See* Chapter 12). In a similar way,

partial molal, *apparent molal*, and *relative molal* are applied to other thermodynamic properties of solutions.

The term *water equivalent* has been used as the heat capacity of the calorimeter (sometimes called *energy equivalent*). In modern calorimetry, use of the term water equivalent has little meaning because heat units are not defined in terms of the heat capacity of water.

The terms *heat of vaporization* and *latent heat of vaporization* are both used to describe the heat required to transform unit mass of liquid to vapor, so they have dimensions of (energy) $(\text{mass})^{-1}$. The older term latent heat is used very rarely in modern calorimetry. While in principle the term heat of vaporization can be applied to any process in which liquid is vaporized, it is generally interpreted to be limited to vaporization at a constant temperature and pressure. In this case, the term heat of vaporization, ΔH_v, is synonymous with *enthalpy of vaporization.* Since most heat of vaporization experiments correspond to enthalpies of vaporization, it is recommended that the term enthalpy of vaporization be used if it applies.

The terms *heat of fusion* and *latent heat of fusion* are analogous to the case of vaporization except they apply to the solid–liquid instead of the liquid–vapor phase change. Here again, the term latent heat is used rarely in modern calorimetry. The term *enthalpy of fusion* is synonymous with heat of fusion for a constant-pressure melting. Similarly, the term *enthalpy of sublimation* applies to a *heat of sublimation* at constant pressure.

The term *entropy*, S, applied to calorimetric experiments, is defined simply by the relation $dS = \delta q/T$, in which dS is the change in entropy in a *reversible* process and δq the heat involved at the temperature T. The term *free energy* has been used for many years to include the *Gibbs energy*, defined as $H - TS$ or *Helmholtz energy*, defined as $E - TS$. Of these two quantities, the Gibbs energy has been used more frequently. There has not been international agreement on symbols for these two quantities. European textbooks have used the symbol F and the name *free energy* or *Helmholtz energy* for the function, $E - TS$. These books also use the symbol G and names such as *Gibbs function*, *Gibbs energy*, or *free enthalpy* for the function, $H - TS$. On the other hand, in America, the quantity, $H - TS$, has been represented by the symbol F, and the quantity, $E - TS$, by the symbol A. As a result of the international confusion on these symbols, I.U.P.A.C. has recommended that the function, $H - TS$, be named the *Gibbs energy*, represented by the symbol G, and the function $E - TS$ be named the *Helmholtz energy*, represented by the symbol A. This notation will be used throughout in this book. A summary of notation used is given in the Appendix.

It seems appropriate to mention here the terms precision and accuracy for those who may not realize their difference in usage in modern science. The term *precision* is used to measure the *reproducibility* of experiments and may not be a measure of the accuracy of experiments. The precision may be so good that this source of error is negligible in comparison with the systematic error. On the other hand, the term *accuracy* is used to describe how close the experimental quantities are to the *true* quantities. In other words, systematic errors as well as random errors should be considered in estimating accuracy. In most calorimetric measurements it is believed that high precision is necessary in order to obtain high accuracy. In giving

either precision or accuracy, the number given is necessarily statistical, so that it is imperative that the statistical basis be given in order that the number be meaningful. In early calorimetry, the term *average deviation from the mean* was used frequently as a measure of precision of a set of experiments. This term, defined as the average of differences between each measurement and the average for the set, is not nearly so useful and meaningful as the term *standard deviation of the mean*, which is commonly used now[14] as an indication of the precision of a set of experiments. Standard deviation of the mean, s, is defined:

$$s = \sqrt{\frac{\Sigma(x_i - \bar{x})^2}{n\,(n-1)}}$$

in which $\bar{x}$ is the average of the observations, x_i, and n is the number of observations. The term *standard deviation of the mean* should not be confused with the term *standard deviation of an individual experiment*, which is defined as $\sqrt{n}$ times the standard deviation of the mean. Since there has been some question as to which of the above two meanings the term *standard deviation* applies to, the term *standard error* has been suggested to be synonymous with standard deviation of the mean. Most of the literature uses σ as the symbol for the standard deviation. However, statisticians use the symbol s when derived from a *finite* number of experiments, so that $s \rightarrow \sigma$ when $n \rightarrow \infty$. *Probable error* has also been used as a measure of precision. Representing an error which has a 50 per cent chance of being exceeded, the probable error, P, is related to the standard deviation of the mean by $P = 0{\cdot}6745\ s$, if there are a large number of observations. Another term is the *variance* which is the square of the standard deviation. This term is rarely used because it is not convenient to compare with the original measurements. The term *confidence limit* is used sometimes as a measure of the reproducibility of results. If an infinite number of observations have been made, the relation between confidence limits and standard deviation of the mean is fixed by the normal distribution curve. For 50 per cent confidence limit, error $= 0{\cdot}6745\ s$; for 90 per cent confidence limit, error $= 1{\cdot}64\ s$; for 95 per cent confidence limit, error $= 1{\cdot}96\ s$; for 99 per cent confidence limit, error $= 2{\cdot}58\ s$. A more complete discussion of assignment of calorimetric uncertainties has been given previously[14].

III. Heat Units and Constants

In early work in calorimetry in which most measurements were made near room temperature, it was convenient to both measure and express the heat in terms of a unit called the calorie which was defined as the heat required to raise the temperature of one gram of liquid water one degree C. As calorimetric measurements became more accurate, it was realized that the magnitude of the calorie so defined depends on the temperature of the water. Consequently, a variety of "calories" originated, such as the 4°-calorie, the 15°-calorie, the 20°-calorie, the mean (0–100°) calorie, etc.

Although the comparative heat measurements could be made with relative ease, it was recognized very early that it was necessary to determine the quantity of energy corresponding to a given calorie. The energy corresponding to a specific calorie was called J, the *mechanical equivalent of heat*[10].

Investigations of this quantity were carried out over most of a century with either mechanical or electrical sources of energy.

With the development of accurate electrical standards and instrumentation, it became possible to measure electrical energy more precisely than heat could be measured in terms of the heat capacity of water. After this time, the calorie and the mechanical equivalent of heat had little significance except as measurements of the heat capacity of water. Out of habit, however, the calorie continued to be used as a heat unit, so that it became desirable in accurate calorimetry to separate the definition of calorie from the heat capacity of water. As a result, there are two "dry" or defined calories used today[11]. In engineering steam tables, the *I.T. calorie* (International Table calorie) is used and defined as 4·1868 joules. In the field of calorimetry as applied by physicists and chemists, if the term calorie is used, it usually refers to the *thermochemical calorie*, which is defined as 4·1840 joules. The joule referred to here is by international agreement the absolute joule which was accepted in 1948 and is discussed in Chapter 3.

The name *mechanical equivalent of heat* is now obsolete, because it refers merely to a conversion factor to change from one to another unit of heat. Although the term calorie has lost its original utility, its use has persisted in many fields. No doubt it will be used for a long time, but logically it is destined ultimately for obsolescence along with many other superfluous units. It should be noted that in a Resolution which was adopted in 1948 by the 9th International General Conference on Weights and Measures[16], the recommendation on the unit of heat was the joule, and that it was requested that the results of calorimetric experiments be expressed in joules when possible. If the calorimetric results are expressed in units other than joules, the unit should be defined in terms of the joule.

IV. Standard Reference Substances

In evaluating the results of calorimetric research, uncertainties in the final results may arise from two sources, namely from errors in the calorimetry itself (energy, temperature, mass, etc.), or from uncertainties in the purity and state of the material whose properties are measured. In order to minimize the errors in the calorimetry, it may sometimes be a considerable advantage to check the reliability of the calorimetric measurements with a "reference" material whose state is reproducible and known. If the thermal properties of this reference material are known, this check yields evidence on the reliability of the calorimetric measurements. Of course, this requires that someone must have made accurate measurements on this reference material. When moderate calorimetric accuracy is adequate, it may not be difficult to find a reference material whose thermal properties have been measured with higher accuracy. When high calorimetric accuracy is required, this becomes more difficult because the accuracy of other calorimetric measurements may not be significantly better. However, even in this case, a reference material is useful. By having samples of any one material taken from one source of high purity, one has a means of *comparing* calorimetric measurements made in different laboratories under different experimental conditions. It was with this in mind that in 1949 the Fourth Calorimetry Conference[4] recommended three substances to be used as "standard" reference

materials for heat capacity measurements. These three substances were benzoic acid, n-heptane, and aluminum oxide (corundum). Benzoic acid and n-heptane were intended for the moderate to low temperature range, whereas aluminum oxide was intended primarily for the high temperature range, although it is also useful at lower temperatures.

For calorimetric measurements near room temperature, water has always been used as a reference material, partly because of its universal availability in a pure state, and partly because of the numerous measurements on its heat capacity. In the range 0–100°C, the specific heat of liquid water is believed to be known to within 0·01–0·02 per cent[12].

When using standard reference materials, some experimenters regard their use as a "calibration" of their calorimeters, with the conclusion that when using their calorimeters as a comparison device, the accuracy on the unknown sample is comparable to the accuracy of the standard reference materials. The experimenter should be warned against this conclusion. Although it is true that a comparison method does reduce certain errors, the degree of reduction depends upon the experimental conditions. The comparison method is no "cure-all" for experimental defects! The comparison method is most effective in reducing errors when the physical properties and amount of the material being investigated are identical with those of the standard reference material. Departure from this ideal results in errors whose magnitudes depend upon the particular calorimetric apparatus. Even when the material has identical physical properties, there is always the possibility of the variation of the performance of a calorimetric apparatus from day-to-day.

V. Choice of Calorimetric Method

The first question raised after embarking on a calorimetric project is the choice of method. There are numerous factors which should be considered in choosing a calorimetric method. Some of these factors will be discussed now.

One of the most important factors to be considered is the accuracy required. The effort required increases exponentially as higher accuracy is desired. Many calorimetric measurements near room temperature can be made with 1 per cent accuracy with an ordinary household Dewar flask and very simple instrumentation[15]. Measurements to 0·1 per cent accuracy, if possible, usually require at least one and possibly two or three orders of magnitude increased effort, depending upon circumstances. Measurements accurate to 0·01 per cent are usually impractical with most calorimeters, although there are special examples near room temperature in which this accuracy has been approached with great effort[12]. At extreme temperatures or other conditions, the difficulties in attaining 1 per cent may be as great as attaining 0·01 per cent near room temperature.

Another important factor related to the accuracy required is whether to make absolute or relative calorimetric measurements. If the accuracy required is not as high as the accuracy obtained in published calorimetric measurements on a certain material, then it may be advantageous to use this reference material to "calibrate" a less complicated calorimeter. In this regard, one must keep in mind that this "calibration" usually only

partially compensates for calorimeter errors, depending upon a number of factors. If possible, a reference material should be chosen which has thermal properties similar to those of the material being investigated.

The physical properties of the sample and its thermal property to be measured usually have considerable influence on the choice of method and calorimetric design. A flow method may be used with advantage to measure the heat capacity of a gas which requires large volumes to give the desired mass. The temperature and pressure range involved in the measurements are important, as well as the amount of sample available. If only a few milliliters of solid or liquid sample are available and if a large number of samples are to be measured, the use of the drop method offers simplicity in changing samples. The drop method is most useful for deriving heat capacity values if the heat capacity is not changing rapidly with temperature.

If the measurements involve very small heats, it may be advantageous to use twin calorimeters to minimize errors introduced by uncertainties in heat leak. In microcalorimetry, twin calorimeters are usually used for this reason. In measurements for which the time of experiment is necessarily very long, it may be necessary to choose a method having small heat leak (power) uncertainty.

As a practical matter, the choice of method is frequently determined by available apparatus and personnel. If a minimum of electrical measuring equipment is available, an isothermal calorimeter (such as the Bunsen ice calorimeter) might be considered because it does not require electrical instrumentation. Choice of a method using a platinum resistance thermometer for temperature measurement might not be possible if an expensive resistance bridge (or potentiometer) is not available. As a general rule, an adiabatic calorimeter would require more instrumentation (or personnel) than either an isothermal calorimeter or an isothermal shield calorimeter. The quality of personnel available may be a determining factor in choice of a method and apparatus. It is of little value to use a very elaborate and complicated apparatus if qualified personnel are not available for its operation.

It seems appropriate here to consider some of the advantages and disadvantages of various calorimetric methods. There is no "best" method for a general calorimetric problem. Even for a very specific problem, there may be no significant over-all advantage of one method over another. Consider first the *isothermal shield calorimeter* (*isoperibol calorimeter*) which has been used so extensively. Here, the calorimeter may change temperature (such as in heat capacity experiments) while the shield is kept at a constant temperature. One obvious advantage of this method is the simplicity of the operation of the shield, controlled either manually or automatically. Another advantage may be the relative independence from variable thermal contact in the shield, since it is at constant temperature. On the other side of the ledger, the corrections for "heat leak" from the calorimeter may be relatively large in some experiments, with the requirement that the heat leak coefficient (leakage modulus) be both constant and accurately known. In this regard, it should be pointed out that it is only the uncertainty in the heat leak correction which affects the results, not the magnitude of the correction. This is no doubt why in combustion bomb calorimetry, the isothermal shield

has been used almost universally. The rapid change in the calorimeter immediately following the combustion has made it very difficult to control the shield temperature to that of the calorimeter. Even though the actual heat leak corrections could no doubt be reduced by changing the temperature of the jacket, the uncertainties in the heat leak might be larger than if the jacket is kept at a constant temperature. With modern instrumentation and advanced jacket design this situation may not be the same! Isothermal shield calorimeters for measuring heat capacities are still used for accurate measurements in low temperature calorimetry for which heat leak becomes less important owing to the decrease in radiative heat transfer. The use of isothermal shield calorimeters at higher temperatures depends upon successfully keeping heat leaks down to a reasonable value. In a very special type of calorimetric experiment, it is possible to use an isothermal shield at room temperature and still measure heat capacities at high temperatures with little heat leak error[19]. However, this is accomplished by making the time of the experiment so short that the total energy transferred from the sample (wire) is still small compared to the energy used to heat the wire.

The *adiabatic calorimeter* has increased in use along with the availability of modern electronic instrumentation for temperature control and recording. However, the design of the calorimeter and its auxiliary parts is at least as important as the external instrumentation in obtaining good temperature control. For example, large thermal "lags" in parts of the apparatus can make it difficult if not impossible to control an adiabatic calorimeter properly. Also, the calorimeter becomes more difficult to use in going to higher temperatures, because of increased heat leak coefficients. At 500°C, it is very difficult to obtain 0·1 per cent accuracy and at higher temperatures difficulties are much greater. Consequently, most of the heat capacity measurements in the range above 500°C have been made by using the "drop" method which keeps the heat leak small by allowing unwanted heat transfer for only a very short time during the drop.

The *drop method* is an example of the method of mixtures in which the receiving calorimeter measures the change in heat in the sample between its initial and final temperatures. The principal application of the drop method has been in measuring enthalpies at high temperatures. With the drop method, the initial temperature of the sample (in a furnace) is varied, but the final temperature is kept essentially constant, usually near room temperature. This restriction of varying only one temperature places an important limitation on the application of the drop method. For this method to be valid requires that the sample be at a thermodynamically reproducible state at both temperatures. If the sample (or its container) has a solid–solid transition, it is possible that the transition will not be complete in the time of drop so that some energy of transition will be "frozen in"[6]. Consequently, whenever the drop method is used with materials having such transitions, the experimenter must be aware of this possibility of error. Another disadvantage of the drop method is that it obtains values of heat from differences in heats which may be quite large by comparison. For example, it may be necessary to measure over-all heats (relative enthalpies) to 0·01 per cent to obtain 0·1 per cent accuracy on the enthalpy derivative, heat capacity, if this heat capacity changes significantly with temperature. This disadvantage

is partly overcome in the drop method because the calorimeter is usually operated in a favorable temperature range (room temperature) so that measurements can be made very precisely. The drop method has an important advantage in its ease of changing from one sample to another. Sometimes, the drop method has been applied to enthalpy measurements at lower temperatures than the "receiving" calorimeter[8]. The principal value of this is its use when a receiving calorimeter already exists for measurements at higher temperatures. The drop method usually finds little application at low temperatures because (*i*) the heat capacity frequently changes more rapidly than at high temperatures, and (*ii*) the quantities of heat are smaller.

The *isothermal calorimeter* has an advantage that its heat capacity does not affect the results since its temperature does not change. Also the problem of minimizing uncertainty in heat leak is frequently made easier. In the ice calorimeter, for example, the heat in the inside ideally goes to melting ice and the outer part of the calorimeter is unaffected. In the history of calorimetry, this advantage has been considerable; however, with modern instrumentation, it is not so great. Even today, however, the isothermal calorimeter offers excellent heat leak control without elaborate instrumentation. With experiments of long duration, this control may be necessary. The isothermal calorimeter using vaporization (liquid–vapor equilibrium) may provide high sensitivity. If liquid hydrogen or helium is used, for example, a very small quantity of heat results in the evolution of a large volume of gas to be measured. This is partly because the heats of vaporization of hydrogen and helium are relatively low whereas the specific volumes of gas are large.

Recent developments in thermoelectricity have provided calorimetry with a useful tool with the availability of semi-conductor materials for refrigeration. With available thermocouples, it is now possible to make an isothermal calorimeter to measure heat quantities without using a change in phase of a material. The heat in a calorimeter can be balanced out with thermoelectric cooling to provide isothermal conditions, and the thermoelectric device can be calibrated in place with an electric heater. Even before semi-conductor thermocouples were available, metallic thermocouples were used in microcalorimetry for heat compensation[9, 14].

The use of *twin calorimeters* may be a real advantage if the necessary control of heat leak is difficult. In microcalorimetry, in which only very small heats are measured, the use of twin calorimeters minimizes the effect of changes in temperature of the environment. To be effective, the twin calorimeters should be as nearly alike as possible and located so that they are affected the same by their environment. One disadvantage of the twin calorimeters is the effort required to build an extra calorimeter and in many cases to prove that the two calorimeters have identical thermal characteristics. Another advantage of twin calorimeters is that differential thermo-elements can be used to best advantage for measuring the temperature difference between twin calorimeters. In most calorimetry involving large amounts of heat, twin calorimeters are not used.

Flow calorimeters have been used with both gases and liquids. When used to measure heat capacities, the flow calorimeter offers an advantage that the heat capacity of the calorimeter is not involved since ideally the

calorimeter does not change temperature during an experiment. Although the flow calorimeter was used in early calorimetry on liquids, its principal use in accurate calorimetry today is with gases. Here, the flow method provides a relatively large volume of sample per experiment, which would be impractical with non-flow calorimeters.

VI. Summary

The principal fundamental physical quantities measured in calorimetry are temperature, energy, and mass. Whereas the first two are covered in Chapters 2 and 3, the techniques for measuring mass are so generally known or available, that no treatment is given here. In calorimetry it is frequently necessary to measure other quantities such as pressure and volume. Since measurements of these two quantities are usually secondary in calorimetric measurements, a discussion of them will be deferred to Volume II, which will cover P–V–T and transport properties.

For the student in calorimetry, a brief bibliography is given. The field of reacting systems has recently been covered[14, 15] and some of the techniques are applicable to non-reacting systems. The specialized field of microcalorimetry is covered in two books in the following bibliography.

VII. Bibliography and References

Bibliography

White, W. P., *The Modern Calorimeter*, Chemical Catalog Co., New York (1928).
Swietoslawski, W., *Microcalorimetry*, Reinhold, New York (1964).
Calvet, E., and H. Prat, *Microcalorimétrie*, Masson et Cie, Paris (1956).
Roth, W. A., and F. Becker, *Kalorimetrische Methoden zur Bestimmung chemischer Reaktionswärmen*, F. Vieweg, Braunschweig (1956).
Rossini, F. D. (Ed.), *Experimental Thermochemistry*, Vol. I, Interscience, New York (1956).
Weissberger, A. (Ed.), "Calorimetry" in *Technique of Organic Chemistry—Vol. I. Physical Methods of Organic Chemistry*, Chap. X, Interscience, New York (1959).
Skinner, H. A. (Ed.), *Experimental Thermochemistry*, Vol. II, Interscience, London (1962).

References

[1] Callendar, H. L., *Phil. Trans. Roy. Soc. (London)*, **A199**, 55 (1902).
[2] Callendar, H. L., *Proc. Phys. Soc. (London)*, **23**, 1 (1911).
[3] Calvet, E., and H. Prat, *Microcalorimétrie*, Masson et Cie, Paris (1956).
[4] *Chem. Eng. News*, **27**, 2772 (1949).
[5] Ginnings, D. C., T. B. Douglas, and A. F. Ball, *J. Research Natl. Bur. Standards*, **45**, 23 (1950).
[6] Ginnings, D. C., *J. Phys. Chem.*, **67**, 1917 (1963).
[7] Kraus, C. A., and J. A. Ridderhof, *J. Am. Chem. Soc.*, **56**, 79 (1934).
[8] Lucks, C. F. and H. W. Deem, *Special Publication No. 227, Am. Soc. Testing Materials* (1958).
[9] Mann, W. B., *J. Research Natl. Bir. Standards*, **52**, 177 (1954).
[10] Mueller, E. F., *Mech. Eng.*, **52**, 139 (1930).
[11] Mueller, E. F., and F. D. Rossini, *Am. J. Phys.*, **12**, 1 (1944).
[12] Osborne, N. S., H. F. Stimson, and D. C. Ginnings, *J. Research Natl. Bur. Standards*, **23**, 197 (1939).
[13] Pruitt, J. S., and S. R. Domen, *J. Research Natl. Bur. Standards*, **60A**, 371 (1962).
[14] Rossini, F. D. (Ed.), *Experimental Thermochemistry*, Vol. I, pp. 239, 297, Interscience, New York, (1956).
[15] Skinner, H. A. (Ed.), *Experimental Thermochemistry*, Vol. II, pp. 343, 189, Interscience, London (1962).
[16] Stimson, H. F., *Am. J. Phys.*, **2**, 617 (1955).
[17] Swietoslawski, W., *Microcalorimetry*, Reinhold, New York (1946).
[18] Tong, L. K. J., and W. O. Kenyon, *J. Am. Chem. Soc.*, **67**, 1278 (1945).
[19] Wallace, D. C., P. H. Sidles, and G. C. Danielson, *J. Appl. Phys.*, **31**, 168 (1960).
[20] White, W. P., *The Modern Calorimeter*, p. 17, Chemical Catalog Co., New York (1928).
[21] Wittig, V. F. E., and W. Schilling, *Z. Elektrochem.*, **65**, 70 (1961).

Experimental Thermodynamics
Volume I

CHAPTER 4

Principles of Calorimetric Design

D. C. Ginnings and E. D. West
National Bureau of Standards, Washington, D.C., U.S.A.

Contents

I. Introduction

The design of calorimetric apparatus involves consideration of many factors. The first factor is obviously the choice of the calorimetric method, as discussed in Chapter 1. This choice depends upon temperature range, accuracy desired, properties of the sample, amount of heat involved, duration of experiment, available apparatus and personnel, cost of the apparatus, and many other factors. After the choice of method comes the detailed

*See complete ref. on page 1-I.

design of the calorimetric apparatus needed. If the scientific literature describes calorimeters suitable for the investigation, it sometimes is possible to obtain constructional details either from the published papers or directly from the authors. More often, however, either this is impractical or certain variations in design are needed for the particular investigation. In any case, the construction and operation of a calorimetric apparatus is probably facilitated if certain fundamentals of design are known. It is the purpose of this chapter to review some general principles which underlie the design and operation of accurate calorimeters. For details of design and construction, the reader is referred to the various chapters describing apparatus. To illustrate some of the principles, simple examples will be given together with corresponding calculations of significant quantities.

In the references at the end of this Chapter are listed some of the handbooks and other sources of values of properties of materials useful in calorimetric design. Such information may be found also in *Mechanical Engineers Handbook*, McGraw-Hill Book Co., Inc., New York, 1958 and *Handbook of Chemistry and Physics*, Chemical Rubber Publishing Co., Cleveland, Ohio, published annually.

The specific design of calorimetric apparatus involves mechanical, chemical, electrical, thermal, and perhaps other properties of construction materials. Usually, the actual design is a compromise with at least some of these properties. For example, it may be necessary to sacrifice mechanical rigidity to obtain low thermal conductance in certain parts, or in selecting the size of the calorimeter heater current leads, it is necessary to compromise between electrical heat developed in the leads and thermal conductance of the leads. Some discussion will be given of the mechanical, chemical, and electrical design factors, but the major part of this chapter will be devoted to consideration of heat flow because it is believed that lack of understanding of heat flow is the source of most errors in accurate calorimetry.

II. Chemical, Mechanical, and Electrical Considerations

1. *Chemical*

For most calorimetry at moderate and low temperatures, the problem of chemical properties of materials is not difficult to solve. In this temperature range, it is usually possible to select inexpensive metals or alloys which are sufficiently unreactive either to the sample material or to the environment. Sometimes the use of noble metals such as platinum and gold is warranted. Glass is usually considered to be unreactive to most materials in this temperature range, and in earlier calorimetry it was frequently used. However, its use in modern calorimetry is limited because of its other properties. If good thermal conductance is desired, glass is undesirable because of its low thermal conductivity. If poor thermal conductance is desired, it frequently turns out that for mechanical reasons it is necessary to use a greater cross sectional area than would be required with metal, so there may be no significant gain. For example, in a glass tube, it might be necessary to use a wall thickness many times that required for a metal tube. Although the use of metals for most calorimetry is most convenient, at higher temperatures

they become more reactive, both with the sample and with air when they are in contact with it. Although there has been some progress in the development of materials inert at high temperatures, the chemical problem here still may be the major one. Further discussion of the chemical problem will not be given here, partly because it is not difficult in most calorimetry, and partly because any problems involved are usually characteristic of the particular experiment.

2. *Mechanical*

In all calorimetric apparatus, it is necessary to contain the sample, and to position and support the various parts. The mechanical design is necessarily a compromise between mechanical and other considerations, such as thermal and chemical. First of all, in order to contain the sample, the calorimeter must be strong enough to withstand any pressure and temperature encountered. The term "strong" here means not only avoiding rupture, but also keeping down to a reasonable tolerance any change in dimension due to pressure In accurate calorimetry, for example, if there is any significant change in dimension due to either pressure or temperature, the dimensions should be a reproducible function of these variables. An example of irreproducibility is exceeding the mechanical elastic limit of the material. The *elastic limit* (which has values essentially the same as the *proportional limit*) of a material may be defined as the greatest stress to which a material may be subjected without developing a permanent set. The calculation of the pressure effect will be given for simple cases.

If the mechanical properties of the calorimeter are likely to be a serious limitation, the shape of the calorimeter should be designed to minimize strain. In this respect, a spherical shape might be ideal mechanically and also offers the smallest area for heat transfer to the outside. Since a sphere is not always convenient to fabricate, a cylindrical section having hemispherical ends frequently is used. In both cases the use of supporting internal struts gives added strength with relatively little additional material. The internal struts can serve also to distribute heat to reduce temperature gradients.

In considering the strengths of calorimeter sample containers, one must consider the effect of both external and internal pressure. Usually, the external pressure is limited to atmospheric pressure so that the sample container does not have to withstand more than one atmosphere differential pressure. Therefore, a small amount of metal can be used in order to minimize the heat capacity of the empty calorimeter. This is especially important at low temperatures where the heat capacity of the metal sample container may be a large fraction of the total. The reader is referred to Chapters 5, 6, 7, and 13 for details of low-temperature sample containers, including those designed for one atmosphere external pressure.

For sample containers with *internal* pressure, calculations are now given for the sphere and cylinder, which approximate most cases. Assume that the calorimeter is a spherical shell having a diameter D and thickness w, and containing an internal pressure P. The force operating to stretch the wall is $P(\pi D^2/4)$ and is exerted on a wall cross-sectional area (πDw), so

that the stress on the material (force/area) is $PD/4w$. If $P = 100$ lb/in^2, $D = 4$ in, and $w = 0{\cdot}02$ in, the stress is then 5000 lb/in^2. If the material is cold-worked copper, we find in tables of mechanical properties† that the "proportional limit" of this copper at room temperature is about 15 000 lb/in^2. This means that there is a safety factor on pressure of about three before the pressure will cause permanent set. In actual design, this safety factor seems too small, so that either the material or some other factor probably would be changed. Now calculate the change in the diameter D due to the pressure P. The material property which determines this change is called *modulus of elasticity*. The *fractional* increase in length of a specimen under tension is the ratio of stress to modulus of elasticity. For the copper, with a modulus of elasticity of about 16×10^6 lb/in^2, the pressure of 100 lb/in^2, which results in a stress of 5000 lb/in^2, increases the diameter D by $[(5 \times 10^3)/(16 \times 10^6)]\ D = 0{\cdot}00125$ in.

Using a length (l) of the same material in a cylinder of the same thickness (w) gives a force (PDl) operating on an area of $2wl$, so that the stress is $PDl/2wl = PD/2w = 10\,000$ lb/in^2. The increase in diameter is then $[10^4/(16 \times 10^6)]\ 4 = 0{\cdot}0025$ in.

There is another way in which modulus of elasticity enters into calorimetric design, namely in calculating stress in a material caused by increase in temperature in the material which is not allowed to expand significantly in one dimension. Assume in a simplified example that a specimen disk is held flat between two parallel fixed plates so that there is perfect contact at temperature T_1. Now heat the specimen to a temperature T_2. If the disk were free to expand, its thickness would increase by the factor $\alpha(T_2 - T_1)$ in which α is the coefficient of linear thermal expansion. Since we keep the disk from expanding axially, a stress is developed which can be calculated from the modulus of elasticity by using the relation, stress $= [\alpha(T_2 - T_1)]$ $\times$ [Modulus of Elas.]. Consider as an example a silver disk heated from 0° to 200°C. Taking an average value of $\alpha = 18 \times 10^{-6}$ and modulus of elasticity $= 10^7$ lb/in^2, one obtains stress $= 36\,000$ lb/in^2. However, this figure is considerably greater than the elastic limit of silver which is about 1000 lb/in^2, so that actually the silver would flow radially. When the specimen is cooled to room temperature, it will have a permanent set, its thickness being less than its original thickness. If the specimen is steel with an average coefficient of expansion of 10^{-5}/°C, a modulus of elasticity of 3×10^7 lb/in^2, and an elastic limit of 40 000 lb/in^2, then the calculated stress is 60 000 lb/in^2, which is also above the elastic limit, so that there would be some permanent set.

One application of the above principles to calorimetry is in the use of gasket materials for sealing two parts together, as in a "union". The above examples indicate that if a union is to be used over a wide temperature range, two precautions should be considered. First, the union body material might be made of a material having about the same coefficient of expansion, thereby minimizing the change in stress due to differential expansion. Second, the union might be designed to provide some flexure, so that large

† English units are used here because of their general use in engineering tables of properties of materials.

changes in stress in the gasket are avoided. This spring quality could be obtained either in a separate spring, or possibly in the configuration of the union body, if a material with high elastic limit is used.

The effect of thermal expansion in calorimetry over a wide temperature range is important also in choosing materials which are in contact, such as in soldered joints. As a general rule, the materials should be chosen so that the change in termperature results in a force tending to tighten the joint (compression) rather than loosen it (tension). For example, in a low temperature calorimeter, if there is a differential thermal expansion in a joint, the outer part preferably should have the higher coefficient of thermal expansion in the low temperature range.

A universal mechanical problem in calorimetry is the use of soldered joints, both in giving a "tight" joint and in providing strength. A variety of available solders[17] provides a melting temperature over a wide range of temperature. This is frequently useful in assembly of various calorimetric components. However, the lower melting solders are not generally as strong as the higher melting solders, especially at temperatures approaching melting. For example, in the design and preliminary testing of the 0–100° calorimeter described in Chapter 11, it was found that a lead-tin soldered joint holding the two hemispherical shells together failed at 100°C. When the lead-tin solder was replaced with a tin-antimony solder having both higher melting point and better mechanical properties at 100°C, the soldered joint was successful. Soldered joints should be subjected to the least possible stress and should depend as little as possible on the strength of the solder, which is usually considerably less than the strength of the metals being joined. In practice this means avoiding thick layers. The design of soldered joints is especially important in calorimeters used over large temperature ranges where differential expansion may cause large stresses in the joints.

In calorimeters operating over a large temperature range, account should be taken of the change in mechanical properties with temperature. Most materials are weaker at high temperatures so that their properties at the highest operational temperature must be used in the design. In the discussion earlier on modulus of elasticity, the modulus under tension or compression was used. Under special circumstances, the modulus in shear might be more appropriate.

A warning should be given on the use of certain "cast" metals or alloys if vacuum tightness is required. As an extreme example, when silver is cast in an air atmosphere, considerable oxygen in solution is expelled on solidification, thereby giving a porous structure. In this case a vacuum casting should be used to give a non-porous solid. The presence of oxygen in copper may lead to less desirable mechanical properties. For example, ordinary copper work hardens much faster than oxygen-free copper, which is now available commercially.

The design of the calorimeter supports, together with the choice of materials, is always a compromise among various requirements, which include mechanical, chemical, and heat flow. Discussion of the heat flow problems will be given later in this chapter. The shape of the mechanical support is a large factor in obtaining maximum support strength for a given

thermal conductance. The optimum shape is determined partly by the direction in which strength is needed. For example, with certain calorimeters which have no connecting tubes to the outside, vertical strength may be needed primarily for suspending the calorimeter, with little strength needed horizontally. In this circumstance it might be possible to use one or more small wires or "threads" under tension. If more horizontal strength is needed, the mechanical supports may consist of thin "struts" which may be tubes. For a given cross section of material (given thermal conductance) a tube gives greater mechanical rigidity than a rod. In one apparatus described in Chapter 11 the shield was suspended by three short thin mica strips spaced 120° apart so that they could be considered as narrow sections of a large "mica tube". This arrangement gave considerable strength horizontally, as well as vertically with the mica under tension. In general, if a minimum of material is desired, it is more stable under tension than compression. Also, because the deflection of "beams" is usually directly proportional to the cube of the length of the beam, it is better to use a short support piece, and keep to a minimum its dimension in a direction perpendicular to the force.

In choosing materials for mechanical supports, the thermal diffusivity of the material, together with dimensions, determines the time lag in the material as its ends are heated. Because ceramic materials usually have lower thermal diffusivities than metals, their time lags should be considered before using them in calorimeter design.

The above brief consideration of mechanical design is intended only to point out a few of the simple problems encountered in calorimetry. For detailed computations, the reader is referred to texts and handbooks covering the strength of materials[16] and to the various chapters in this book for specific calorimetric applications.

A question which arises repeatedly in calorimetric design is the thermal conduction between two surfaces in mechanical contact. The mechanism of heat transfer is by gas conduction, radiation, and by direct conduction at solid–solid contacts. Under pressure, the solid–solid contacts increase in number and in area and it is possible to gain considerably over gas conduction and radiation. The small amount of information available is for metallic surfaces.

For rather rough laminated steel surfaces at temperatures slightly above room temperature, aluminiun foil placed between surfaces increases the thermal contact conductance in air by a factor of about two with moderate contact pressures. An organic material in the space usually improves conduction considerably. For solid steel blocks, the largest contact conduction is for lapped surfaces. They show only slight dependence on contact pressure in air. Rougher surfaces show increased conduction by about a factor of two for pressures of 300 lb/in^2 (ref. 3).

Data for smooth aluminum alloys, steel, and bronze show considerable variation for different assemblies[20]. The conduction of aluminum joints is considerably better than steel at each pressure measured. Furthermore, copper plating one of the surfaces improves the conduction of the joints. Oil in the joint increases conduction, especially at low pressure, owing to the higher conductivity of oil compared to that of air.

For polished gold, silver and copper surfaces in vacuum at 25°C, the conduction of a metallic joint is negligible at zero contact pressure and increases linearly for copper to 0·3 W cm^{-2} deg^{-1} at 4 kg/cm^2. For gold and silver, the conductance is 0·22 W cm^{-2} deg^{-1} at a constant pressure of 1 kg/cm^2, increasing to 0·4 at 4 kg/cm^2 (ref. 11).

Qualitatively, conductance through metallic contact is increased by using softer metallic surfaces, smoother surfaces, and higher pressure. If such joints must be used, a large number of bolts or screws should be used to obtain a high pressure. If thermal conductance is needed in a contact in a vacuum, precaution should be taken either to apply sufficient force or to use a softer material at the contact. Some measurements of thermal contact resistance in vacuum at low temperatures have been made[2] on a few metals and non-metals.

3. *Electrical*

A. Thermocouples

Most of the factors involving the electrical system in the calorimetric apparatus also involve heat flow, so that both must be considered in the design. Consider first the sizes of electrical leads of thermocouples. Of course, the minimum size is that which can be handled safely during assembly and disassembly. In deciding how much larger to make the leads, one must compromise between electrical resistance and thermal conductance. If heat flow is important, one uses the smallest thermocouple wire compatible with the two requirements of strength for convenient handling and of tolerable resistance of the thermocouple circuit. This point depends upon the electrical resistance of the circuit external to the thermocouple, which frequently consists of a galvanometer and potentiometer. Consider the schematic circuit in *Figure 1*, in which E_1 and R_1 represent the e.m.f. and resistance of the

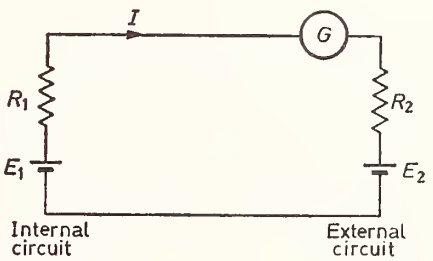

Figure 1. Thermocouple measuring circuit.

thermocouple and E_2 and R_2 represent the potentiometer bucking e.m.f. and the total resistance of the external circuit, considered to be a potentiometer and a galvanometer, G, for the simple case. At ideal balance, the current, I, is zero and $E_2 = E_1$. The actual balance occurs at some finite current, I_1, representing the smallest current which the galvanometer can detect. In this actual case, this error signal is $(E_2 - E_1) = I_1 (R_1 + R_2)$. If $R_2 \gg R_1$, then an increase in R_1, the thermocouple resistance, does not

change significantly the error signal I_1 $(R_1 + R_2)$. However, if $R_1 \gg R_2$, this error signal increases in proportion to the resistance R_1. With a given measuring circuit, the resistance of the thermocouples may determine the practical limit of the number of thermocouples which can be used in series (thermopile) to increase the sensitivity. If $R_1 \gg R_2$, then increasing the number of thermocouples increases the resistance $(R_1 + R_2)$ in proportion to the increase in E_1 so that the *relative* value of the error signal (precision of measurement) to the total e.m.f. (E_1) remains the same.

A typical resistance of a galvanometer–potentiometer circuit is perhaps 50 Ω, so that as a practical matter the resistance of any combination of thermocouples used should not be much larger than this resistance. Although higher resistance galvanometers can be used with thermocouple circuits having higher resistances, it is usually more practical to use electronic amplifiers because of their flexibility of input impedance. Even with low-resistance circuits, the use of electronic amplifiers has increased greatly in recent years. A comparison of the galvanometer with the electronic amplifier will be given later in this section (II–3–D).

In designing a temperature measuring system involving thermocouples, it is necessary to decide on thermocouple materials. Since this decision depends greatly upon the temperature range involved, only a brief discussion will be given here. In Chapter 2, the general subject of thermocouples has already been covered. In most accurate calorimetry, thermocouples have their main utility in measuring temperature differences in different parts of the apparatus. For this purpose, frequently it is convenient to use thermocouple materials having high thermoelectric powers, low thermal conductivities, and good mechanical properties. Reference should be made to the various chapters for the authors' choices of materials.

In the use of thermocouples in accurate calorimetry, it is necessary that the thermocouple e.m.f. be a true measure of difference in temperature between the components to which the principal and reference junctions of the thermocouple are attached. In order that this be true, several precautions should be taken. First, the thermocouple should be used under conditions which do not invalidate its calibration. The calibration of the thermocouple cannot be expected to apply to a thermocouple which has been contaminated after its calibration. For example, it is possible that a platinum–rhodium thermocouple becomes contaminated in use at high temperatures if it is in contact with certain materials in a chemically reducing atmosphere. Sometimes it is possible to calibrate thermocouples under the exact conditions of the experiment in which they are used. For example, in the calorimeters described in Chapter 11, thermocouples are used to measure the temperature difference between the calorimeter and a "reference block" containing platinum resistance thermometers. The thermoelectric coefficients of these thermocouples can be determined *in place* at any time during the experiments by comparing with the platinum resistance thermometer. This "in place" calibration also has the advantage that certain thermocouple errors are also accounted for. Another example of "in place" calibration of thermocouples is with differential thermocouples between the calorimeter and the surrounding shield. In this use, the calibration of the e.m.f. in terms of temperature difference is unnecessary. Instead, the e.m.f. is calibrated

directly in terms of heat flow by observing the resultant change in temperature of the calorimeter whose heat capacity is known with adequate accuracy.

A second precaution in the use of thermocouples concerns spurious e.m.f.s due, for example, to inhomogeneities in the thermocouple material. If an inhomogeneity is located in a region of temperature gradient in the thermocouple wire, there may be a spurious e.m.f. which will be measured along with the "true" e.m.f. of the thermocouple. Frequently, the thermocouple wires are tested for inhomogeneities before their use by moving a sharp temperature gradient along the wire and observing any resulting e.m.f. If the thermocouples are used only to measure small temperature differences, most of the effect of the inhomogeneities can be avoided by keeping the thermocouple material in relatively isothermal regions and using pure metal electrical leads which are relatively free from inhomogeneities. An example of this technique is described in Chapter 11 where many thermocouples measure temperatures relative to a "reference block" whose temperature is very close to that of the calorimeter.

A third precaution in using thermocouples is to make certain that their junctions are really at the temperatures of the components whose temperatures they measure. This problem usually is not serious if the thermojunction is soldered or welded to the component. However, it is not always possible or convenient to make this attachment. Frequently, it is necessary to insulate electrically the thermojunction from the component, so that thermocouples can be connected in series either for differential measurements, for increasing sensitivity, or for integration of temperature gradients. Electrical insulation of the thermojunction usually incurs some thermal insulation, so that if there is a heat flow from the thermojunction, its temperature necessarily will be different from the temperature of the component to which it is attached. Much of the heat flow from the thermojunction is along wires connected to it. It may be necessary, therefore, in accurate calorimetry to make sure that there is no significant heat flow along these wires. This can be accomplished by a technique sometimes called "*tempering*" of the thermocouple wires. Tempering of these wires may be defined as the process of bringing them to the temperature of the component *before* the wires reach the thermojunction. The tempering of wires will be discussed later in this chapter. A common method of tempering wires at moderate to low temperatures is to fasten the insulated wires in thermal contact with the component by using an organic cementing material to attach them, thereby providing both thermal contact and electrical insulation. At somewhat higher temperatures[5] in the presence of gas, bare wires may be placed in ceramic tubes or between strips of mica to be held in contact with the component.

Sometimes the choice of thermocouple material depends not only on temperature range but also on the environment. For example, at high temperatures, some materials should not be used in oxidizing atmospheres whereas other materials should not be used in reducing atmospheres. For an appropriate discussion of thermocouples, the readers are referred to books[4] covering the subject.

In addition to the requirement in accurate calorimetry that the thermocouple e.m.f. be a true measure of temperature difference, there is the prob-

lem of proper location of the junctions to evaluate properly the effective temperatures so that proper accounting can be made for both heat leak and temperature change, even if temperature gradients exist. Further discussion will be given later in this chapter on the problem of location of thermocouples.

B. Calorimeter Heater

The design of the calorimeter heater and its leads is important to accurate calorimetry in two different ways. The first way relates to the location of the potential leads in order to evaluate that part of the electrical heat in the leads which belongs to the calorimeter. Although this problem is discussed later in Section IV, it may be mentioned here that the calorimeter heater resistance should be large compared to its lead resistance, and that the thermal contacts between the ends of the heater current lead segment and the calorimeter and shield should be either good or equal and preferably both.

The second way design is important as it relates to changes in resistance in the heater and leads due to their temperature change. These changes in resistance make the accurate measurement of power more difficult. In the calorimeter heater, the change in temperature may be considered in two parts, the first due to the *initial* thermal transient as the heater wire attains its normal temperature excess, and the second due to the slower change in temperature as the calorimeter temperature increases†. When the current is first switched to the heater, its temperature is very near that of the calorimeter. Before it can deliver power to the calorimeter, its temperature must rise to provide a thermal head for heat flow. Since the heater itself has some heat capacity, usually an appreciable time is required for the initial rise to take place. In general, the resistance of the heater wire will increase during this time and the effect on the d.c. power measurements must be considered.

The thermal transient may be considered a simple exponential with time constant (time for 63 per cent of change) equal to the product of the heat capacity of the heater and the thermal resistance to the calorimeter. Since the total effect is small, only the order of magnitude is important and this "lumped constant" approximation is adequate. For small heater wires varnished to the calorimeter surface, the time constant is probably so small that the effect is negligible. More massive heaters and poor thermal contact depending on gas conduction or radiation across a mechanical space make the time constant larger and warrant considering it.

A typical case is a heater with heat capacity of 2 J/deg and thermal resistance to the calorimeter of 10 deg/W. This heater has a time constant of 20 sec, so that the effect would not be accounted for by "conventional" measurements of current and potential for which the first measurement is usually after 20 sec. A plot of resistance against time after turning on the heater is given in *Figure 2* for a linear resistance-temperature dependence

† The *electrical* transients in a calorimeter heater circuit are always over in such a short time that it is usually not necessary to consider them.

and constant heating rate. This heater resistance curve approaches exponentially the straight line which would be obtained by extrapolating from the current and potential measurements made later during the experiment. If a constant voltage is imposed on the heater, the electrical power is $P = E^2/R$, and there is a small error because the extrapolated resistance (dashed line)

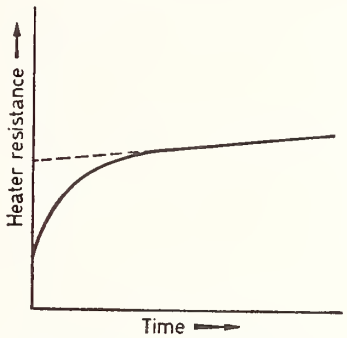

Figure 2. Change of heater resistance during experiment.

between start of the heating and the first measurement is different from the actual resistance. If the eventual excess temperature of the heater is ΔT, and R is a linear function of the temperature, the resistance at any time t can be written

$$R = R_0 \{1 + a [\Delta T(1 - e^{-t/\tau}) + \beta t]\}, \tag{1}$$

in which a is the temperature coefficient of resistance, β is the heating rate of the calorimeter, τ the heater time constant, and R_0 is the resistance at the beginning of the experiment. The difference between the extrapolated resistance and the true resistance is due to the exponential term in Equation (1). The difference ΔR between the true average value and observed average value is obtained by integrating over the heating period of length t_f. The fractional error when $t_f \gg \tau$ is then given approximately by the equation

$$\frac{\Delta R}{R_0} = a \Delta T \frac{\tau}{t_f}. \tag{2}$$

For our typical case $a = 4 \times 10^{-4}$ deg, $\Delta T = 30$ deg for 3 watts of heater power, so that $(\Delta R/R_0) = (0{\cdot}24/t_f)$. In a 600 sec experiment, the fractional error is four parts in 10 000. If the heating rate is doubled, ΔT is doubled and t_f is halved so that the fractional error is 4 times as great. If the calorimetric measurements have sufficient sensitivity, the error may be detected by changing the heating rate. In addition to the starting transient the slower change of resistance must be considered, but usually this is not bothersome except in very accurate calorimetry (see Chapter 5).

Several schemes have been developed to maintain constant power input when the calorimeter heater resistance changes owing either to the starting transient in the heater or to the gradual change of heater resistance with

the temperature of the calorimeter. In one scheme, approximately constant power with a moderate change in heater resistance can be obtained from a *constant current source* supplying the calorimeter heater shunted by an external resistance which is equal to the average calorimeter heater resistance[18]. In another scheme using a *constant voltage source*, the equal resistance is placed in series with the calorimeter heater[10]. Sometimes (see Chapter 5) the calorimeter heater leads are important in that they also change resistance during an experiment. This case is illustrated by *Figure 3* in which R_s is

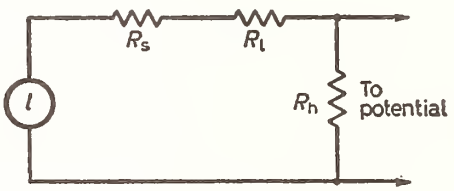

Figure 3. Calorimeter heater equivalent circuit.

constant whereas R_l and R_h are functions of the temperature of the calorimeter. For this circuit the power in the calorimeter is given by the equation

$$P = E^2 \frac{R_h}{(R_s + R_l + R_h)^2}. \tag{3}$$

To find the condition for no change in the power with a change in the heater and lead resistance we take the total differential of Equation (3) and set the result equal to zero. The condition for constant power is then given by the equation

$$\frac{R_s + R_l - R_h}{R_l} \frac{dR_h}{R_h} = \frac{2dR_l}{R_l}. \tag{4}$$

If the fractional changes in the heater and lead resistance are related by some proportionality constant m, $(m dR_h/R_h) = (dR_l/R_l)$, then the choice of R_s is determined from the following equation

$$R_s - R_h = (2m - 1)\, R_l. \tag{5}$$

A more convenient method is to make the change in the lead resistance dR_l negligible so that the condition for constant power is simply $R_s + R_l = R_h$.

The obvious solution to the problems resulting from change in resistance of the calorimeter heater and its leads is (*i*) to minimize the starting transient by keeping the heater in good thermal contact with the calorimeter, (*ii*) to construct the heater with a material having a small temperature coefficient of resistance, and (*iii*) to either make the heater leads of low electrical resistance or use a material with small temperature coefficient. Although the use of such a material is not always practical, it is available for calorimetry at low to moderate temperatures, as described in Chapter 5.

C. Heaters for Temperature Control

In the design of other heaters in calorimetric apparatus, it is usually also advantageous to have good thermal contact and low heat capacity in order to avoid lags. In addition, there are two other important factors. First, the resistance of a heater should be made to be compatible with an available power supply. With the extensive use of automatic controls in the past, the use of moderately high resistance heaters facilitated the use of electron tubes as power sources when the power required was not excessive. With the recent development of the transistor which has a lower impedance output than the electron tube, it may be more advantageous to use low-resistance heaters because of the high current available with the transistor. The availability of low-cost transistors controlling over 100 watts of power ensures their increasing use in calorimetric measurements.

In apparatus requiring larger power, it is frequently convenient to use magnetic amplifiers (saturable reactors) for control. The magnetic amplifier is usually used with a 60 c/s power supply and has a time constant longer than that of a transistor. In addition the output of the magnetic amplifier is either a.c. or d.c. with an a.c. component. As pointed out in the next section, this a.c. may cause trouble with pickup in other circuits if high sensitivity electronic amplifiers are used. Of course the rectified output of the magnetic amplifier can be filtered to eliminate the a.c. component at the expense of lengthening the time constant to perhaps a second. It should be pointed out that most magnetic amplifiers have the disadvantage in many control applications that their output powers cannot be reduced to zero.

Two other devices used for control of a.c. power are the thyratron and its modern solid-state equivalent, the SCR (silicon controlled rectifier) whose cost is decreasing steadily. The output of the SCR is pulsed so that it has a large a.c. component.

D. Galvanometers and Electronic Amplifiers

The use of d.c. electronic amplifiers in place of galvanometers has increased in recent years, so that it is believed appropriate here to compare their application to calorimetric measurements. The galvanometer has two fundamental disadvantages due to its mechanical nature. Most sensitive galvanometers are affected by mechanical vibration, so that considerable effort may be necessary to avoid motion of the moving coil due to this vibration. In addition, if a relatively large voltage is impressed on the galvanometer, the moving coil system may be damaged, possibly so that a new suspension wire is required. The electronic amplifier is essentially free from mechanical difficulties. The electronic amplifier also has the advantage of flexibility of power output and input impedance. The flexibility in the magnitude and impedance of the output of the electronic amplifier facilitates its use in recording and automatic control. In most calorimetric measurements the signal source is less than 100 ohms, so that a typical measuring circuit using a sensitive galvanometer is reasonably matched to the signal source; in other words, the power developed in the galvanometer approaches the maximum possible from the signal source. If the signal

source has a high resistance, a low-resistance galvanometer would be relatively insensitive to a voltage source. The electronic amplifier can easily be made with either high or low impedance input.

Most modern electronic d.c. amplifiers "chop" the d.c. signal before amplifying, so that an a.c. amplifier can be used. The purpose of this is two-fold. First, by chopping, any drift with time of the amplifier characteristics only changes its sensitivity so that its use as a null device is satisfactory†. Second, by use of a step-up transformer after the chopper, the signal voltage from a low-impedance source can be amplified before the first electron tube (or transistor). The practical limit of this transformer gain is determined by the ratio of impedances of the signal circuit to that of the grid circuit of the first amplifier tube. By using a phase detector (synchronized chopper on the amplifier signal), the amplifier gives a d.c. output.

Although the electronic amplifier can be designed for use with signal sources having high impedances, the reader should be aware of possible difficulties resulting from the high impedance. When using any detector, the theoretical minimum of the electrical noise in the input circuit is that due to "thermal" noise, which in a resistive circuit is directly proportional to the square root of the resistance. With circuits having resistance of about 100 Ω and with detectors having time constants about one second, the thermal noise equivalent (root mean square voltage) in the signal source at room temperature is about 0·001 μV. More often, the high impedance signal source gives trouble because of increased "pickup" of both transients and power line frequency (60 c/s). Consequently, when it is necessary to have very high sensitivity, high impedance signal sources should be avoided if possible.

When a typical galvanometer is used with a low-impedance signal source, not only is the "pickup" relatively small, but the inertia of the galvanometer serves as a high frequency filter which attenuates 60 c/s pickup. In most sensitive electronic amplifiers (d.c.), the effects of 60 c/s pickup are attenuated by an electrical filter in the early stages of the amplifier. To be completely free from first stage amplifier "saturation", the filter should precede the amplifier. However, this location of the filter requires it to have a low impedance when used with a low impedance signal source in order to avoid increased 60 c/s pickup in the signal circuit. Most commercial electronic amplifiers do not have this low-impedance input filter so that they are most susceptible to large 60 c/s pickup than galvanometers having the same time constant.

It follows from the previous discussion that electronic d.c. amplifiers have several advantages over galvanometers in many calorimetric measurements. For many applications, galvanometers are frequently less expensive. When very sensitive electronic amplifiers are used with signal sources susceptible to power line frequency pickup, a low-impedance signal source should be used and suitable steps should be taken to avoid using a.c. (60 c/s) close to any component leading to the input to the amplifier and to follow the usual precautions of shielding, twisted leads, etc.

† Negative feed-back is used sometimes to minimize change in sensitivity, to obtain a constant gain, and to make the amplifier have a high input impedance.

III. Heat Flow Considerations

1. *General*

For accurate calorimetry, the essential quantities to be measured are mass, temperature, and energy. Sometimes, additional quantities are measured, such as pressure and volume. Except in extreme ranges, it is possible to measure most of these quantities with all the accuracy that is needed. In most experiments, the major part of the energy is either derived from or compared with electric power which, with precautions, can be measured very accurately. However, the energy also includes heat from other sources, such as that resulting from heat leak. It is believed that the uncertainty in the evaluation of this heat leak is the principal source of error in a large fraction of measurements for accurate calorimetry. Of historical interest is the comment of W. P. White[23] on the first page of his book *The Modern Calorimeter* [1928]. He says "There is a difference of opinion as to whether thermal leakage is necessarily the chief source of error in calorimetry, but it is undoubtedly responsible for most of the experimental features and devices in accurate work." This is more true today than it was in 1928!

It should be pointed out that in calorimetric measurements, the absolute uncertainty in the evaluation of heat leak is not necessarily proportional to the value of the heat leak. For example, in Chapter 1, it has been pointed out that in calorimeters using an isothermal shield (surroundings), the absolute heat leak is usually considerably larger than with calorimeters with adiabatic shields. However, it must be emphasized that it is the absolute uncertainty in the heat leak that results in error, rather than the magnitude of the heat leak.

The problem of reducing heat leak is usually much more difficult than the problem of reducing electrical leakage. This is more obvious when one compares heat and electrical transport properties at room temperature. In electrical measurements, there are solid insulating materials available which have electrical resistivities about a factor of 10^{25} greater than the best electrical conductors. This means usually that it is not difficult, at least at moderate temperatures, to reduce electrical leakage to a very small amount. However, the best solid thermal insulators at room temperatures have thermal resistivities only a factor of about 10^4 greater than the best thermal conductor. Therefore, one cannot expect to minimize heat leakage to the extent that one can usually minimize electric current leakage. Furthermore, in thermal measurements, even when all material connections are removed, heat transfer by radiation may still persist. As shown later, at low temperatures, the radiative heat transfer may be relatively unimportant because radiation is proportional to T^4. On the other hand, at very high temperatures, radiation may be the predominant means of heat transfer.

In the ideal adiabatic calorimeter, for example, there is no heat transfer between the calorimeter and its surroundings. This ideal condition can be approximated if the heat transfer coefficient and the temperature difference between the calorimeter and surroundings are both very small. In the real adiabatic calorimeter, there are five principal steps which can be taken to reduce errors due to heat leak: (*i*) design the calorimeter to have a large

thermal resistance to its surrounding shield; (*ii*) design both calorimeter and shield to minimize temperature gradients in them; (*iii*) design the calorimeter and shield to have adequate temperature sensing devices at suitable locations to measure the *effective* temperature differences between the calorimeter and its surroundings, even with temperature gradients; (*iv*) design the calorimeter so that the experimental method or procedure can be made to compensate for at least some of the unknown heat leaks, such as by making two series of experiments; (*v*) make corrections for any measurable heat leak in an effort to account for it. Of the above five steps, all but the last involve calorimetric design requiring heat flow calculations. Many of these calculations can be made easily by assuming simple boundary conditions which are adequate for design purposes. It seems desirable to review briefly the fundamentals of heat flow before applying them to calorimeter design.

Heat flow is by radiation, convection, and conduction in most calorimetric operations. Although the separation of these three modes of heat flow is not always sharply defined, in most calorimetry at moderate temperatures, these modes can be treated independently for design purposes.

2. *Heat transfer by radiation*

In calorimetry we are concerned with heat radiated from one body at temperature T_1 to a cooler body at temperature T_2. The rate of heat (P_1) transferred to body (2) from unit area of body (1) is given by the relation

$$P_1 = \sigma A_2 F_{12} [T_1^4 - T_2^4] \tag{6}$$

in which P is in watts cm^{-2}, σ is the Stefan–Boltzman constant ($5{\cdot}67 \times 10^{-12}$ watts cm^{-2} deg K^{-4}), T_1 and T_2 are absolute temperatures (°K), A_2 is the area on body 2, and F_{12} is a dimensionless factor determined by the radiation emittances and geometric configuration of the surfaces. If T_1 and T_2 are nearly the same at about temperature T, the differential form of Equation (6) applies, i.e.,

$$\frac{\mathrm{d}P}{\mathrm{d}T} = 4\sigma A_2 F_{12} T^3. \tag{7}$$

The degree of approximation of Equation (7) can be shown by taking the case of $T = 300$°K and $\Delta T/2 = 5$ deg K. In this case the use of the value of $\mathrm{d}P/\mathrm{d}T$ at 300°K for the temperature difference between 295 to 305°K gives the same average heat transfer coefficient within less than 1 part in 5000 as that calculated from Equation (6). Nevertheless, the experimenter must be aware that the radiative heat transfer coefficient is greatly dependent upon absolute temperature, so that it cannot be considered constant over as large a temperature interval as heat transfer by conduction or convection. Between 295 and 305°K the increase in the radiative heat transfer coefficient due to temperature increase is about 7 per cent. Any experiment which depends on *constancy* of this coefficient should be examined to determine how great an error will result.

A discussion of the evaluation of the emissivity factor F_{12} is given in various books[13]. For the simplest case of a completely enclosed body, *small* compared to the enclosing body, the factor is given by $F_{12} = \epsilon_1$ in which ϵ_1 is the emittance of the enclosed body. For a completely enclosed body comparable in size and shape to the enclosure, the case becomes essentially the same as two infinite parallel planes for which

$$F_{12} = \frac{1}{\frac{1}{\epsilon_1} + \frac{1}{\epsilon_2} - 1} \tag{8}$$

in which ϵ_1 and ϵ_2 are the emittances of the two surfaces. In using these or other approximations, it is usually relatively easy to calculate radiative heat transfer to the accuracy needed in most design calculations, if values of ϵ are known. The difference in the usage of terms emissivity, effective emissivity, and emittance should be pointed out here. As used in this chapter, the above relation $F_{12} = \epsilon_1$ really defines ϵ_1 as either the *effective emissivity* or the *emittance* of the small enclosed body, such as a sphere. The outer surface A_1 of the sphere is considered in this case to be the ideal surface area $4\pi r^2$, even though the actual surface is rough and several times this area. If this surface is actually perfectly smooth such as with a highly polished metal, the value of its emittance is the same as what is called *emissivity*. In other words, the emissivity of a metal is for a smooth polished surface (no concave surfaces) but its emittance is for any surface. In most cases we do not have very smooth surfaces, so that the term emittance is more appropriate. As used in this chapter the term emittance is dimensionless, so that it should not be confused with a second meaning of emittance (radiant emittance) which has the dimensions of power.

In considering the effect of radiation on calorimetric design, simple calculations show how radiative heat transfer usually becomes relatively small at low temperatures. On the other hand, at room temperature with two infinite parallel planes each having an emittance of 0·6, and with a 1-cm still air space between them, the radiative heat transfer is about the same as the gaseous heat transfer (see *Figure 4*). At higher temperatures, the radiative heat transfer soon becomes the predominant heat transfer. In calorimetric design for accurate work, radiation shields can be quite useful even below room temperature, and at high temperatures extreme precautions may have to be taken.

Radiative heat transfer between two surfaces can be decreased by inserting one or more "floating" shields between them. One type of shield is a thin metallic surface completely surrounding the calorimeter. As soon as the steady state of heat flow has been established to a shield, the same amount of power, P_t, flows across each space. (The transient effect for a single shield is discussed in the next section.) This power can be written for the ith space as

$$P_t = \sigma A_{i+1} F_{i,\,i+1} (T_i^4 - T_{i+1}^4)$$

A series of equations can be written for n spaces and summed

$$P_t \frac{1}{\sigma A_1 F_{12}} = T_1^4 - T_2^4$$

$$P_t \frac{1}{\sigma A_2 F_{23}} = T_2^4 - T_3^4$$

$$\cdots\cdots = \cdots\cdots$$

$$\frac{P_t \dfrac{1}{\sigma A_n F_{n,\,n+1}} = T_n^4 - T_{n+1}^4}{P_t \left(\displaystyle\sum_{i=1}^{i=n} \frac{1}{\sigma A_i F_{i,\,i+1}} \right) = T_1^4 - T_{n+1}^4},$$

whence P_t can be found by

$$P_t = \frac{T_1^4 - T_{n+1}^4}{\displaystyle\sum_{i=1}^{i=n} \frac{1}{\sigma A_i F_{i,\,i+1}}}$$

The overall heat flow is still proportional to the difference in the fourth powers of the temperature, but is smaller than in the unshielded case. If the shields have equal areas and emittances, as is approximately true in many calorimeters the $A_i F_{ij}$ factors are equal and the heat flow is inversely proportional to $m + 1$, in which m is the number of "floating" shields. A simple case shows the advantage of the radiation shield. If a bright shield (such as one gold plated and polished to give an emittance of 0·02) is inserted between two black ($\epsilon = 1$) parallel planes, the radiative heat transfer is reduced by a factor of 100. Even a black shield would reduce the radiative heat transfer by a factor of 2. *Figure 4* given under Section III–3, illustrates the effectiveness of shields, both for radiation and convection.

In shielding a calorimeter or furnace, the area of the shield increases with the distance from the center and the effectiveness of successive shields decreases proportionately. It follows that the spacing of multiple shields should be the smallest compatible with mechanical and gas conduction considerations. At high temperatures the shields may be in the form of a fine powder which effectively inserts many shields in a narrow space. Because of surface roughness and higher intrinsic emissivities, a single powder surface is less effective than a metallic surface by perhaps a factor of 10, but ten particles of 1000 mesh powders at ~50 per cent bulk density occupy only 0·25 mm. Powder used for radiation shielding in vacuum should be placed in hot parts of the apparatus where it will outgas readily. Another consideration in selecting a powder is that a particle should not be transparent to the radiation at the highest temperature of operation.

A combination of this sort of radiation shielding with spaces shorter than the mean free path has resulted in an air-filled silica gel insulator being better than still air[14]. Although a powder is a useful insulating material, especially in furnaces, it is not generally used directly next to the calorimeter where energy must be accounted for. This is because of the heat capacity of the powder and the uncertainty of the calorimeter boundary, within which energy must be accounted for.

In making computations of heat transfer by radiation, it is sometimes difficult to select the proper value of the emittance for a particular problem. This is not so much because the data lack precision but because they may not apply to the particular surfaces under consideration. For example, the emittance of an aluminum surface changes by a factor of about 12 as the oxide layer increases from 0·25 μ to 7 μ. Another uncertainty in radiation computations is in the geometry of the calorimeter. The effective emittances of indentations and corners can be quite different from the emittances of the plane surface. The best approach is perhaps to choose the most unfavorable value of the emittance to make the calculation. More detailed treatment of radiant heat transfer is given by Jakob[13].

3. *Heat transfer by convection*

Heat transfer by convection is the result of mass transfer of a fluid (gas or liquid) from one region to another at another temperature. Convection is classified into two general types, (1) *forced convection* and (2) *free convection.* In forced convection the fluid is forced to move, such as by a stirrer in a liquid bath. In free convection the motion of the fluid is due to gravitational forces acting because of different densities of the fluid at different temperatures. The laws governing the behavior of convective heat transfer are the same for both liquids and gases, although values of their physical properties vary greatly. If these physical properties are known, calculations of both forced and free convection can be made by using engineering formulae[12]. Consideration will be given first to free convection.

Where the calorimeter is surrounded by a gas such as air, heat transfer by *free convection* (as well as by conduction) must be considered in designing and using the calorimeter. In precise calorimetry at room temperature and below, evacuation can be used advantageously to eliminate both gaseous convection and conduction between calorimeter and shield. At higher temperatures, at which radiation becomes more important, the use of evacuation depends on the particular design, which must weigh the advantages against the disadvantages of evacuation. Sometimes, partial evacuation is used to avoid convection while leaving gaseous conduction. In some apparatus, the gaseous conduction may be desirable to provide thermal contact between two components in poor mechanical contact. As a general rule, atmospheric gas pressure can be reduced by several orders of magnitude without much change in thermal conductivity while the effect of convection is made negligible.

In the case of convection with a gas between two parallel vertical surfaces at different temperatures, the denser gas near the cold surface moves down to displace the gas near the bottom of the warm surface which has been warmed by conduction. Warm gas at the top of the space is moved into contact with the top part of the cold surface, where it is cooled. Heat is thus transported by motion of the air as well as by direct gas conduction across the space. For horizontal surfaces with the hot surface above the cold surface, the low density gas is in stable equilibrium and ideally no convection occurs. When the hot surface is below, convection takes place as a local phenomenon, with upward and downward streams close to one another, sometimes resulting in considerable turbulence.

Early workers in calorimetry, recognizing the requirements for the linear relationship between heat transfer and temperature difference, performed experiments on the gaseous heat transfer in their apparatus. As long as heat transfer is *only* by gaseous conduction, this heat transfer is nearly proportional to the temperature difference (ΔT) because the thermal conductivity of a gas does not change very much with temperature. Of historical note, when this proportionality is valid, *Newton's Law of Cooling* is said to apply, i.e. the rate of cooling of a hot body is directly proportional to the temperature difference from its surroundings. As the temperature difference is made larger, convection begins to be significant. Since gas convection is not proportional to ΔT, the total heat transfer is no longer proportional to ΔT when the convection is significant.

In the calculation of the magnitude of free convection, the dimensionless quantity Grashof Number (N_{Gr}) is needed. This quantity is

$$N_{Gr} = \frac{\beta g \rho^2}{\eta^2} l^3 (T_1 - T_2) \tag{9}$$

in which β is the cubical expansion coefficient (deg K^{-1}), g is the acceleration due to gravity (cm sec^{-2}), ρ is the density (g/cm^3), l is the width of the gas space (cm), η is the dynamic viscosity (poise), and T is temperature (°K). Jakob[12] gives dimensionless plots of the equivalent conductivity (defined as conduction plus convection) against the Grashof Number, for cases of air layers bounded by horizontal planes, by vertical planes, and by coaxial cylinders. As a general rule, the convection is almost negligible for Grashof Numbers less than 1000. For horizontal planes and a Grashof Number of about two thousand, the ratio of equivalent to true conductivity is about 1·05; in other words, for this case the contribution of the convection is about 5 per cent of the thermal conductivity. The other cases yield similar results. For air near room temperature and one atmosphere pressure one can write that $l^3(T_1 - T_2)$ must be less than 11 cm^3 deg K to be reasonably sure that heat transfer is directly proportional to temperature difference. This is in reasonable agreement with the work of White[24] and Barry[1].

From the formula for the Grashof Number it is evident that the most useful experimental ways of decreasing this number are to work with small temperature differences, to reduce the spacing (at the expense of increasing the gas conduction) or to reduce the density. Of course, the ultimate step in reducing the effect of convection is to remove all of the gas, reducing the density to zero. In cases for which it is desirable to reduce convection but to retain gas conduction in order to maintain the thermal contact of heaters or temperature measuring devices with the calorimeter, it is possible to reduce the density of the gas substantially without impairing the thermal conduction of the gas. Until the pressure is reduced to the point at which the mean free path of the gas molecule is comparable to the dimensions of the gas space, the thermal conductivity of a gas is substantially independent of its pressure. At 0·1 atmosphere, the Grashof number is reduced by a factor of 100, but the mean free path in air is about 9×10^{-4} cm, so that gas conduction in spaces around thermometers and heaters is only slightly less than at 1 atm.

When calorimeters are used with gas at atmospheric pressure surrounding

the shield (and perhaps the calorimeter also), the problems of radiation and convection frequently can be solved simultaneously by the use of thin metal heaterless shields which act *both* to reduce radiative heat transfer (as noted in Section III–2) and to reduce convective heat transfer by reducing the thickness of the gas gap. *Figure 4* illustrates the effectiveness of

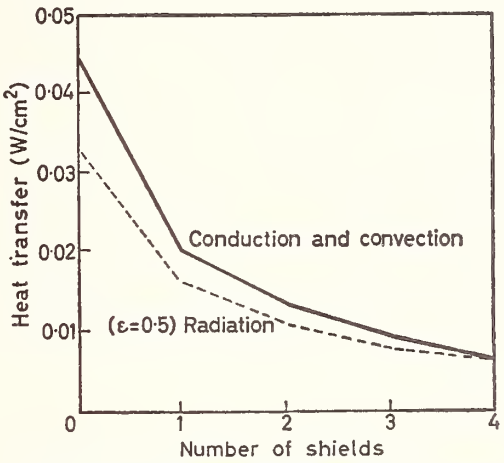

Figure 4. Effect of number of shields on heat transfer.

these radiation–convection shields in reducing the heat transfer coefficient between two parallel horizontal planes, spaced 5 cm apart with the lower plane at 400°K and the upper at 300°K with air between them. The emittance (ϵ) of both plane and shield surfaces is assumed to be 0·5. The figure shows that even with the large temperature difference of 100°, the use of shields 1 cm apart reduces the convection to a relatively small value. The figure also illustrates that the shields reduce the radiative heat transfer by the factor $1/(m + 1)$ in which m is the number of shields, if all surfaces are assumed to have the same emittance. In using convection shields, precautions should be taken to avoid "chimney" type convection which might occur if the shields allow gas to leak through.

One or more heaterless or "floating" shields can appreciably reduce both convection and radiation between the calorimeter and its surroundings, but only at the expense of introducing an additional time lag in the calorimeter temperature whenever either the calorimeter or surrounding temperature is changed. This lag may be calculated if the geometric and heat transfer data are known. The calculation will be illustrated for one floating shield between a calorimeter and its constant temperature surroundings, a water jacket, for example. Usually, the surfaces involved are of comparable areas, and it is an adequate approximation to treat them as parallel planes with heat flow perpendicular to the planes. Let p be the power (heat flow) per unit area, h the heat transfer coefficient, C the heat capacity per unit area of the floating shield, T the temperature, t the time, and the subscripts c, s and j refer to calorimeter, floating shield and jacket, respectively. For

small temperature differences, heat flow is proportional to the temperature difference

$$p_{cs} = h_{cs} (T_c - T_s) \tag{9a}$$

$$p_{sj} = h_{sj} (T_s - T_j). \tag{9b}$$

The change of temperature of the shield is equal to the heat absorbed divided by the heat capacity

$$dT_s = (p_{cs} - p_{sj})\, dt/C_s. \tag{9c}$$

These equations can be solved by substituting from Equations (9a) and (9b). The time constant τ is computed for the case in which the calorimeter, floating shield and jacket are at T_j initially and the calorimeter temperature is increased suddenly to a constant T_c. The time constant will be the same for any time–temperature relation for the calorimeter, and the amplitude factor will generally be less, so that we are considering a "worse" case. When $h_{cs} = h_{sj} \equiv h$, the heat flow from the calorimeter is given by the equation

$$p_{cs} = \frac{h}{2} (T_c - T_j)\, 1 + \exp\left(-\frac{2ht}{C_s}\right). \tag{9d}$$

To reduce the time constant, $C_s/2h$, the only practical step is to reduce the heat capacity of the shield, because increasing the heat transfer coefficient increases the uncertainty in heat loss from the calorimeter.

It is instructive to consider a particular case. For an aluminum shield spaced 1 cm from aluminum-surfaced calorimeter and shield in air at room temperature, the heat transfer coefficient is about $2{\cdot}5 \times 10^{-4}$ W cm^{-2} deg^{-1}. The heat capacity is 2·4 J cm^{-3} deg^{-1} and the time constant as a function of the thickness d of the shield is

$$\tau = 4{\cdot}8 \times 10^3\, d$$

in which τ is in sec if d is in cm. For ordinary aluminum foil, $d = 2{\cdot}5 \times 10^{-3}$ cm, and $\tau = 12$ sec. For p_{cs} to reach within 1/1000 of its ultimate value, 6·9 τ or 83 sec are required. If aluminum sheet having $d = 0{\cdot}025$ cm is used for its greater mechanical strength, 6·9 $\tau = 830$. If the aluminum floating shield is used in an evacuated space, the time constants for the 0·0025-cm and 0·025-cm thick shields are about 200 and 2000 sec, respectively, so that the total times for the power to reach within 1/1000 of its ultimate value are 1380 and 13 800 sec respectively. These figures show that in calorimetry using floating shields in evacuated spaces near room temperature, serious consideration should be given to errors resulting from the time lags.

In experiments using furnaces, frequently we need to know the power required to keep the inner core of the furnace at some given temperature and the corresponding temperature of the outside surface of the furnace. The calculation of the power required to maintain a given temperature difference in the furnace can be made simply by methods described later.

However, the temperature on the outside of the furnace depends upon the coefficient of heat transfer away from the outside surfaces. In this case, it is usually considered desirable to have a large enough heat transfer coefficient to hold the outside to a reasonable temperature. Radiative heat loss can be calculated as described earlier. The heat loss by free convection may be calculated with sufficient accuracy for furnace design, using methods described by Jakob[12]. If the heat flow is written proportional to the temperature difference ($P = h\Delta T$), the constant of proportionality, h, which we term the heat transfer coefficient, is a function of ΔT and may be calculated approximately for typical conditions by the following relations

horizontal surface — heat lost up

$$h = 2{\cdot}2 \times 10^{-4} (\Delta T)^{\frac{1}{4}} \tag{10}$$

horizontal surface — heat lost down

$$h = 1{\cdot}1 \times 10^{-4} (\Delta T)^{\frac{1}{4}} \tag{11}$$

vertical surface — (height $>$ 30 cm)

$$h = 1{\cdot}5 \times 10^{-4} (\Delta T)^{\frac{1}{4}} \tag{12}$$

in which ΔT is the difference between room temperature and the surface temperature in °K (or °C) and h is in W cm^{-2} deg^{-1}. For vertical surfaces less than 30 cm high, h may be somewhat larger, perhaps by as much as a factor of 2 or 3.

In addition to free convection which may or may not be desired in calorimetry, we sometimes use forced convection to obtain good thermal contact between a fluid and its surrounding tube. In forced convection, there are two distinct types of heat transfer, depending upon whether the fluid flow is *laminar* (streamline) or *turbulent*. For fluid flow in smooth tubes, the transition between laminar and turbulent flow occurs at a value of the dimensionless Reynolds Number ($vD\rho/\eta$) of approximately 2000. In this expression, v is the average velocity of the fluid (cm/sec), D is the diameter of the tube (cm), ρ is the density of the fluid (g/cm^3), and η is the dynamic viscosity of the fluid (poise). Turbulent flow is sometimes used to obtain a maximum heat transfer between the fluid and a solid surface. For laminar flow in a tube, the flow of gas at pressures for which the molecular mean free path is much less than the diameter of the tube may be calculated from Poiseuille's equation

$$\dot{v} = \frac{\pi D^4}{128\eta} \frac{(\Delta P)}{L} \tag{13}$$

in which $\dot{v}$ is the rate of volume flow (cm^3/sec), ΔP the pressure drop between the ends of the tube (in dynes/cm^2; note that 1 atm $\sim 10^6$ dynes/cm^2), L and D the length and diameter of the tube (cm), and η the dynamic viscosity of the fluid (poise). For laminar flow, for calculating the heat transfer coefficient between a tube and a fluid inside it, it is convenient for

design purposes to use a simple approximation to estimate a value of heat transfer coefficient which will be slightly less than the true value. This approximation is that the heat transfer coefficient (h) per unit length of tube per unit temperature difference is $5\pi\lambda$ in which λ is the thermal conductivity of the fluid in the tube. If λ is in W cm^{-1} deg^{-1}, then h will be in watts per cm length of tube per degree C difference in temperature between tube and the fluid. For turbulent flow in a tube, the relation

$$h = 0{\cdot}1\lambda \left(\frac{FC}{D\lambda}\right)^{0{\cdot}786} \tag{14}$$

will be adequate for most design purposes. In this relation, h is the heat transfer coefficient (W cm^{-1} deg^{-1}) for unit length of tube and unit temperature difference, λ is thermal conductivity (W cm^{-1} deg^{-1}), F the rate of mass flow of fluid (g/sec), C the heat capacity (J g^{-1} deg^{-1}), and D the inner diameter of the tube (cm).

4. *Heat transfer by thermal acoustical oscillation*

In apparatuses which have gas contained in a tube having a temperature gradient, there may be another mechanism of heat transfer which is unknown in most calorimetry. This mechanism, which may be called "thermal acoustical oscillation" may be important in low temperature calorimetry, especially in the liquid helium range. Under certain conditions depending on the tube dimensions, gas present, temperature gradient, etc., this gaseous oscillation may result in large pressure variations, together with a relatively large heat transfer which may make calorimetric measurements difficult or impossible. While a change in design of the apparatus may avoid this oscillation, a recent study[8] has developed a method to minimize the oscillation by using a "damping" device attached *externally* to the apparatus. With this device, consisting basically of a Helmholtz resonator, it is not necessary to redesign the apparatus.

5. *Heat transfer by mechanical vibration*

Another mechanism of energy transfer which may result in heat developed in a calorimeter is by mechanical vibration. This is a problem which sometimes arises where measurements are made of very small heats. In localities with large mechanical vibrations, detectable mechanical power has sometimes been transmitted to the calorimeter where it has been transformed into heat. This "anomalous" heat has been a problem in some calorimeters operating at liquid helium temperatures where a small amount of heat can be detected. One solution here is to mount the apparatus on a solid pier which is free from vibration. In case this is not practical, a mounting can be designed to attenuate the vibration before it reaches the calorimeter.

6. *Heat transfer by conduction*

In design calculation in most calorimetry except at high temperatures, heat transfer by solid conduction is probably more important than other modes of heat transfer. Frequently, conduction plays the predominant role in determining temperature gradients in the calorimeter and on its surface.

At low to moderate temperatures, solid conduction usually is the main source of heat transfer between calorimeter and shield. In many cases, dependence on thermal conduction is necessary in the evaluation of temperature, etc. As a consequence of the variety of calorimetric design problems in which conduction is important, this heat transfer mode will be considered in more detail, and some examples of calculations involving conduction will be given.

In most calorimetric work, thermal conductivity changes more slowly as a function of temperature than coefficients for heat transfer by radiation and convection. With most materials the changes with temperature of their thermal conductivities are sufficiently small over 10°C so that for design purposes, the heat conduction-heat transfer coefficient can be considered constant in an average experiment. One noteworthy exception is where a phase change takes place in the material. Consequently, materials of construction preferably should have no phase transitions in the temperature range of calorimeter operation. In all the following examples of heat flow calculations, it will be assumed that the thermal conductivity is constant and that there are no transitions in the material.

Heat flow calculations are usually classed into two types, *steady-state* and *unsteady-state*. In steady-state heat flow, the temperature at any point in the material does not change with time, whereas in unsteady-state heat flow, the temperature is a function of time.

The quantity thermal conductivity (λ) is the proportionality constant *defined* by the steady-state relation $P_x = -\lambda A\,(\partial T/\partial x)$ in which P_x is the power (rate of heat flow at x) in the x direction through an isotropic material having a cross sectional area A, and $\partial T/\partial x$ is the temperature gradient at x in the x direction. The minus sign in the defining equation is used to indicate that heat flow (power) is positive in the direction of increasing x if the temperature decreases with increasing x ($\partial T/\partial x$ is negative). Let us consider now a case in which $(\partial T/\partial x)$ is a function of x. If at x the power is $-\lambda A(\partial T/\partial x)$, then at $x + \mathrm{d}x$ the power is

$$-\lambda A \frac{\partial}{\partial x}\left(T + \frac{\partial T}{\partial x}\,\mathrm{d}x\right) = -\lambda A \frac{\partial T}{\partial x} - \lambda A \frac{\partial^2 T}{\partial x^2}\,\mathrm{d}x.$$

Thus, the *difference* in power at x and at $(x + \mathrm{d}x)$ is

$$P_x - P_{(x+\mathrm{d}x)} = \left[\lambda A \frac{\partial^2 T}{\partial x^2}\,\mathrm{d}x\right]. \tag{15}$$

The magnitude of this difference in power is determined by the boundary conditions for the particular heat flow problem. In solving any heat flow problem, the starting point is to set up the "heat balance" equation expressing the conditions of the particular problem. In principle, the solution of any such equation can be obtained if the boundary conditions are all known. The heat balance differential equation for a homogeneous isotropic solid has been derived for the general *three-dimensional* case in which temperature is changing with time and there is a power source (or sink) in the material. This general equation can be written as

$$\lambda\left[\frac{\partial^2 T}{\partial x^2} + \frac{\partial^2 T}{\partial y^2} + \frac{\partial^2 T}{\partial z^2}\right] - \rho c \frac{\partial T}{\partial t} = -F(x, y, z, t) \tag{16}$$

in which ρ and c are density and specific heat of the material, $\partial T/\partial t$ is the rate of change of temperature at a point (x, y, z) with time, t, and $F(x, y, z, t)$ is the power source per unit volume. The above equation is written conventionally as

$$\nabla^2 T - \left(\frac{\rho c}{\lambda}\right) \frac{\partial T}{\partial t} = \frac{-F(x, y, z, t)}{\lambda} \tag{17}$$

in which $(\lambda/\rho c)$ is a quantity known usually as thermal diffusivity, a. In the case of steady-state heat flow, $(\partial T/\partial t) = 0$, so that we have Poisson's equation

$$\nabla^2 T = \frac{-F(x, y, z, t)}{\lambda}. \tag{18}$$

If no heat is supplied to the body, this equation reduces to Laplace's equation $\nabla^2 T = 0$.

If instead of rectangular coordinates, cylindrical coordinates are used, the heat balance differential equation for the case of no heat generated in the cylinder is

$$\lambda \left[\frac{\partial^2 T}{\partial r^2} + \frac{1}{r}\frac{\partial T}{\partial r} + \frac{1}{r^2}\frac{\partial^2 T}{\partial \theta^2} + \frac{\partial^2 T}{\partial z^2}\right] = \rho c \frac{\partial T}{\partial t} \tag{19}$$

in which r is the radial distance from the cylindrical axis, θ the azimuth around the axis and z the distance along the axis. Many cylindrical heat flow problems of interest in calorimetry can be approximated by assuming T to be independent both of θ (symmetrical heat flow around axis) and of z (effectively infinitely long cylinders). In this case the cylindrical heat flow equation reduces to

$$\lambda \left[\frac{\partial^2 T}{\partial r^2} + \frac{1}{r}\frac{\partial T}{\partial r}\right] = \rho c \frac{\partial T}{\partial t}$$

or

$$\frac{\partial^2 T}{\partial r^2} + \frac{1}{r}\frac{\partial T}{\partial r} = \frac{1}{a}\frac{\partial T}{\partial t} \tag{20}$$

in which r is the radial distance from the axis of the cylinder.

There is a corresponding general heat flow differential equation for spherical polar coordinates[6]. Most applications in calorimetric design use the approximation that isothermal surfaces are concentric spheres. In this case the general equation reduces to

$$\frac{\partial^2 T}{\partial r^2} + \frac{2}{r}\frac{\partial T}{\partial r} = \frac{1}{a}\frac{\partial T}{\partial t} \tag{21}$$

in which r is the radial distance from the center of the sphere.

Steady-state heat flow will now be discussed because it is usually simpler and more frequently encountered in calorimetric design.

A. Steady-State Heat Flow

(1) *Rod.* The simplest steady-state heat flow case is for linear (unidirectional) heat flow in a rod having constant cross sectional area A in the direction of heat flow. We have linear heat flow if there is no lateral heat transfer. Here, the *defining* equation of thermal conductivity (λ) applies, so the power $P = -\lambda A \mathrm{d}T/\mathrm{d}x$ and $\mathrm{d}T/\mathrm{d}x = -P/(\lambda A)$. Integrating this equation between x_1 and x_2, corresponding to temperatures T_1 and T_2, gives

$$(T_2 - T_1) = \int_{x_1}^{x_2} -\frac{P}{\lambda A}\,\mathrm{d}x = \frac{P}{\lambda A}(x_1 - x_2). \tag{22}$$

In calorimetry, this simple equation may be used to calculate heat flow along a conductor (such as a wire or tube) corresponding to a known or estimated temperature difference across a known length.

The linear temperature–distance relation is common, but by no means general. For example, if the cross sectional area is not constant, as in a cone for which $A = Mx^2$, integration gives

$$(T_2 - T_1) = \int_{x_1}^{x_2} \frac{-P}{\lambda A}\,\mathrm{d}x = \frac{-P}{\lambda M}\int_{x_1}^{x_2} \frac{\mathrm{d}x}{x^2} = \frac{P}{\lambda M}\left[\frac{1}{x_2} - \frac{1}{x_1}\right]. \tag{23}$$

A more practical example is the heat flow along a tube of constant cross section for which the thermal conductivity changes drastically over the temperature variation on the tube. For example, take a stainless steel tube with constant cross section A, length l, and variable thermal conductivity λ. If this tube is used between a calorimeter at 4°K and a liquid nitrogen bath at 90°K, its thermal conductivity changes by about a factor of thirty over the temperature range. As a first approximation, adequate for most calorimetric design, $\lambda = 0{\cdot}0009\ T$ in this temperature range, with λ in watt cm^{-1} deg^{-1} and T in deg K. Integrating, we get $(0{\cdot}00045)\ T^2 = -(P/A)\ x + C$. From the boundary condition that $T = 4°$ when $x = 0$, the integration constant is 0·0072. Using the boundary condition that $T = 90°$ when $x = 10$ cm, and with $A = 0{\cdot}05\ \mathrm{cm}^2$, we get $P = 0{\cdot}018$ watt. The temperature distribution along this tube is $T = \sqrt{(808{\cdot}4\ x + 16)}$.

(2) *Wire Carrying Current.* An important example of a non-linear temperature–distance relationship arises when power is developed in the body, as in a heater lead. In calorimetry it is important that the heater lead wire not be excessively hot. A heater lead can be treated as a small rod of length l, cross sectional area A, and thermal conductivity λ, with power p developed per *unit length* of the wire. To simplify the problem, both ends of the wire are taken to be at temperature T_0 and losses from the surface of the wire by radiation and conduction are assumed negligible. The power developed in a differential length $\mathrm{d}x$ of the wire is simply $p\mathrm{d}x$. As shown earlier in Equation (15), this power can also be expressed in terms of the second differential

$\partial^2 T/\partial x^2$, so that the heat balance equation is

$$\lambda A \frac{\partial^2 T}{\partial x^2} \mathrm{d}x = -p \, \mathrm{d}x,$$

and by integrating,

$$T = \frac{-p}{2\lambda A} x^2 + C_1 x + C_2 \tag{24}$$

in which C_1 and C_2 are integration constants to be determined by the boundary conditions. Then

$$C_2 = T_0 \quad \text{and} \quad C_1 = \frac{pl}{2\lambda A},$$

so that

$$T = \frac{p}{2\lambda A} (lx - x^2) + T_0. \tag{25}$$

The above equation shows that the maximum temperature for this case is at $x = l/2$. As an example, take a 5 cm length of AWG#26 copper wire with a current of 0·5 amp. The excess temperature at the middle of the wire is calculated to be about 0·6°C.

(3) *Cylindrical Shell.* Consider the gradient in the axial (z) direction in a thin cylindrical shell (length l) due to constant power supplied per unit length of cylinder and removed at one end of the cylindrical shell ($z = l$). The heat balance equation is

$$-\lambda A \left(\frac{\partial T}{\partial z}\right)_{z=0} = pz$$

so that

$$(T_{z=0} - T_{z=l}) = \frac{p}{2\lambda A} l^2 \tag{26}$$

(4) *Radial Heat Flow in a Hollow Cylinder and Sphere.* A frequent problem in calorimetric design is steady-state radial heat flow in a cylinder for which the temperature is a function only of the radius r. Applying the defining equation for thermal conductivity (λ) to plane polar coordinates, and assuming a *constant* power P flowing radially for *unit length* of the cylinder, then one finds at any radius r, $P = -\lambda(2\pi r) \, \mathrm{d}T/\mathrm{d}r$. Integrating this between r_1 and r_2 gives the corresponding temperature difference

$$(T_2 - T_1) = \frac{-P}{2\pi\lambda} \ln \left(\frac{r_2}{r_1}\right) \tag{27}$$

A similar treatment for steady-state heat flow in a sphere gives a heat balance equation $P = -\lambda(4\pi r^2)\, dT/dr$ in which P is the total power flow. Integrating this between r_1 and r_2 gives

$$(T_2 - T_1) = \frac{-P}{4\pi\lambda}\left(\frac{1}{r_2} - \frac{1}{r_1}\right) \tag{28}$$

(5) *Thin Disk with Uniform Heating and Cooling.* A simple heat conduction case involving radial heat flow (such as in the top or bottom of a calorimeter sample container) is the calculation of the temperature in a thin disk in which there is introduced a constant power p per unit area which is dissipated at its circumference. The power crossing the cylindrical surface of radius r is $p(\pi r^2)$ so that $p(\pi r^2) = -\lambda(2\pi rw)\, dT/dr$ in which w and λ are the thickness and thermal conductivity respectively. The solution here for the temperature (T_r) at radius r is

$$T_r = -\left(\frac{p}{4\lambda w}\right) r^2 + C_1.$$

If we impose the boundary conditions that $T = T_0$ at the circumference ($r = a$, with a the radius of the disk), then

$$C_1 = T_0 + \frac{p}{4\lambda w} a^2$$

and

$$T_r = \frac{p}{4\lambda w}(a^2 - r^2) + T_0. \tag{29}$$

This solution also holds (except for sign) for the reverse case for which a constant power p per unit area is *removed* from the disk.

(6) *Tempering of Electrical Leads and Other Conductors.* Consider now a slightly more complicated case which is basic to most calorimetry. This is the problem of "tempering" of electrical leads, defined as bringing the temperature of leads to the temperature of the body by thermal contact. This problem is exceedingly important in accurate calorimetry if the true temperature of lead wires must be known in order to minimize and measure heat leak. Tempering of wires may be accomplished either *continuously* over a length of wire or in *steps*. These two methods will be considered separately.

(7) *Continuous Tempering.* For continuous tempering, consider a small wire having a thermal conductivity λ and cross sectional area A. Let the temperature of a wire be T_1 at $x = 0$, where the wire first comes in thermal contact with a body at a temperature T_0. Let h represent the *constant* heat transfer (power) from wire to body per unit length of the wire and per unit temperature difference. The heat transfer (power) from dx length of wire to the

body is therefore $h(T - T_0)\,dx$ in which T is the temperature of the wire. From previous consideration Equation (15), this power must be

$$\lambda A \frac{d^2T}{dx^2}\,dx.$$

Hence the heat balance equation is

$$\lambda A \frac{\partial^2 T}{\partial x^2}\,dx = h\,(T - T_0)\,dx \tag{30}$$

or

$$\frac{\partial^2 T}{\partial x^2} = \left(\frac{h}{\lambda A}\right)(T - T_0). \tag{31}$$

The general solution to this linear differential equation is

$$(T - T_0) = C_1 \exp\left[-x\sqrt{(h/\lambda A)}\right] + C_2 \exp\left[x\sqrt{(h/\lambda A)}\right]. \tag{32}$$

Imposing the boundary conditions that $T = T_1$ at $x = 0$ and $T = T_0$ at $x = \infty$ we get $C_2 = 0$ and $C_1 = (T_1 - T_0)$, so that

$$(T - T_0) = (T_1 - T_0) \exp\left[-x\sqrt{(h/\lambda A)}\right]. \tag{33}$$

The physical meaning of this equation is that when $x\sqrt{(h/\lambda A)} = 1$, the excess temperature of the wire has been reduced from $T_1 - T_0$ to $(T_1 - T_0)/e$. Solving for this distance x_e, we get $x_e = \sqrt{(\lambda A/h)}$. To reduce the temperature excess of the wire to $(T_1 - T_0)/10$ requires $x_{10} = (2{\cdot}303\,x_e) = 2{\cdot}303\ \sqrt{(\lambda A/h)}$ length of wire. If it is desired to bring the temperature of the wire to $(T_1 - T_0)/1000$, we must have $x_{1000} = 3(2{\cdot}303)\ \sqrt{(\lambda A/h)}$ length of wire. This type of tempering problem has application in calorimetry in a number of problems in which the heat flow can be approximated in the above manner. The heat transfer coefficient h (W cm^{-1} deg^{-1}) must be evaluated for the particular problem. In the case of a wire insulated from a tube, the cylindrical heat flow formula (Equation 27) is used to evaluate it. In the case of radiative heat transfer frequently it is sufficiently constant for design purposes so that a "radiative" h can be calculated. In case the calorimeter is used over a temperature range, sometimes the "worst case" is assumed.

There is a similar example for a *finite* length (l) of wire with the boundary conditions that $T = T_1$ at both $x = 0$ and $x = l$. In this case, the values of C_1 and C_2 satisfying the boundary conditions are

$$C_1 = \frac{(T_1 - T_0)\,[\exp(ml) - 1]}{[\exp(-ml) - \exp(ml)]} \text{ and } C_2 = \frac{(T_1 - T_0)\,[\exp(-ml) - 1]}{[\exp(-ml) - \exp(ml)]}$$

in which $m = \sqrt{(h/\lambda A)}$.

A problem that sometimes arises is to estimate the extent of tempering of a wire which cannot be treated as having an infinite length in contact

with the body. Such a case arises when a lead is brought through a body at a temperature between that of the surroundings (e.g., room temperature) and the temperature of the calorimeter. This body will supply some of the heat flowing along the wire and reduce the amount which must be supplied from the direction of the calorimeter. Equation (32) still applies, but with different boundary conditions. Neglecting heat flow from the direction of the calorimeter (a less favorable case) gives $dT/dx = 0$ at $x = 0$. The other boundary condition is obtained by equating heat flow along the external part of the wire to the total heat flow from the body to the wire, with the result that

$$C_1 = C_2 = \frac{(T_s - T_0)\sqrt{(h/\lambda A)}}{[1 - L\sqrt{(h/\lambda A)}]\{\exp[l\sqrt{(h/\lambda A)}] - \exp[-l\sqrt{(h/\lambda A)}]\}}$$

in which T_s is the temperature of the surroundings, T_0 is the temperature of the body, and L is the length of the wire between the body and the surroundings.

(8) *Tempering of Wires Carrying Current.* The problem of tempering a wire carrying current is similar to the problem of a wire with no current. If p is the power developed per unit length of wire, the heat balance equation is

$$\lambda A \frac{\partial^2 T}{dx^2} dx + p dx = h(T - T_0) dx$$

or

$$\frac{\partial^2 T}{\partial x^2} = \left(\frac{h}{\lambda A}\right)(T - T_0) - \left(\frac{p}{\lambda A}\right). \tag{34}$$

Solving this linear differential equation gives

$$(T - T_0) = C_1 \exp[-x\sqrt{(h/\lambda A)}] + C_2 \exp[x\sqrt{(h/\lambda A)}] + (p/h)$$

for the same boundary conditions that $T = T_1$ at $x = 0$ and $x = l$, and with

$$C_1 = \frac{[T_1 - T_0 - (p/h)][\exp(ml) - 1]}{[\exp(ml)] - [\exp(-ml)]}$$

and

$$C_2 = \frac{[T_1 - T_0 - (p/h)][1 - \exp(-ml)]}{[\exp(ml)] - [\exp(-ml)]},$$

in which $m = \sqrt{(h/\lambda A)}$.

(9) *Step Tempering.* Another method of tempering leads is by steps in contrast to continuous tempering. This is done by "thermal tiedowns", as used extensively in calorimeters described in *Figure 2* in Chapter 11. A thermal tiedown, as used here, is defined as a thermal connection between

a point on the wire and a small region on the body whose temperature is to be approached. For a given electrical insulation between wire and the body, this method may have an advantage in that it can give better tempering by effectively increasing the length of path of heat flow along the wire.

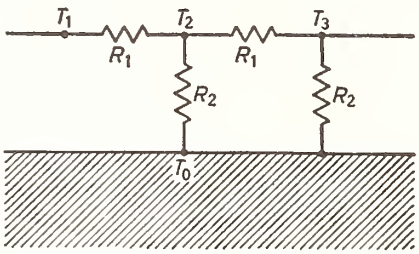

Figure 5. Principle of thermal tiedowns.

This method may also have certain other advantages, such as ease of disassembly, etc. The principle of this step tempering is shown in *Figure 5*. In this figure, T_1, T_2, and T_3 represent the temperatures along a wire (referred to the temperature T_0 of the body) in the tempering network, R_1 represents the thermal resistance of a chosen length of the wire, whereas R_2 represents the thermal resistance of the thermal tiedown. If $R_1 = 100\ R_2$, then $(T_2 - T_0) \cong 0{\cdot}01\ (T_1 - T_0)$ and $(T_3 - T_0) \cong 0{\cdot}01\ (T_2 - T_0)$, so that $(T_3 - T_0) \cong 0{\cdot}0001\ (T_1 - T_0)$. In one calorimeter described in Chapter 11, the thermal resistance R_1 was that of about 10 cm of small wire whereas R_2 (thermal tiedown) was *equivalent* in thermal resistance to about 0·1 cm length of the same wire, thus giving an attenuation factor of 0·01 for each tiedown. Details of the thermal tiedown which has proved effective even in vacuum are given in Chapter 11.

(10) *Tempering of Fluid in a Tube.* In some calorimetry, such as flow calorimetry, a fluid (liquid or gas) is brought close to the temperature (T_0) of a bath by flowing through a "tempering" tube in the bath. In designing this tempering tube, it may be advantageous to know the minimum length required to bring the temperature of the fluid sufficiently close to the bath temperature. If F is the mass rate of flow of fluid (g/sec), c is the specific heat of the fluid (J $g^{-1}deg^{-1}$), T_1 is the temperature of the fluid at $x = 0$, and h is the heat transfer coefficient ($Wcm^{-1}deg^{-1}$) between tube and fluid[12] per cm length of tube, then the heat balance equation is

$$h\,(T - T_0) = -\,cF\frac{\mathrm{d}T}{\mathrm{d}x} \tag{35}$$

or

$$\frac{\mathrm{d}T}{\mathrm{d}x} + \left(\frac{h}{cF}\right) T = \left(\frac{h}{cF}\right) T_0 \tag{36}$$

which is a linear differential equation whose solution is

$$T = T_0 + (T_1 - T_0)\ \exp\ -\,(h/cF)x. \tag{37}$$

The above solution assumes that the radial gradient in the fluid is small by comparison with the difference in temperature between fluid and tube. This type of approximation is usually adequate for design purposes. The length of tube necessary for the fluid to come to the fraction $1/e$(63 per cent) of its starting temperature difference $(T_1 - T_0)$ is cF/h.

These examples of steady-state heat flow are only a few of the many calorimetric problems that may arise. Solutions to many more complicated problems are given in Carslaw and Jaeger[6]. In most calorimetric problems, the heat balance differential equation is a *linear* differential equation so that its solution can be treated as the combination of several solutions. This is known as the Principle of Superposition, which is discussed in the following section (B).

B. Unsteady-State Heat Flow

An unsteady-state heat flow problem is one in which temperature changes with time. Although perhaps the majority of calorimetric design problems can be solved using steady-state heat flow, there are some important unsteady-state problems which arise. In general, the *complete* solution of a heat flow problem, in which temperature is a function of both distance and time, is considerably more difficult than that for the steady state. The complete solution usually consists of a "*transient*" term, which may be short-lived, and a "steady" term, which changes only owing to either change in the material physical properties or time variable boundary conditions. If the transient terms decay before the final temperature is observed, West[21] has shown that in an adiabatic calorimeter heated intermittently, heat leaks due to initial and final transients are equal and opposite in sign. It is usually advantageous, therefore, to design the calorimeter and shield with fast transients, i.e. with small "time constants". In unsteady state heat flow, in which the transient may be approximated by a single exponential term, the term "time constant" frequently is used in a manner similar to the electrical time constant RC. If a capacitor is charged to some potential difference $(E_1 - E_0)$, and then connected to the resistance, the potential difference across the capacitor will decay exponentially through the relation $\Delta E = (E_1 - E_0) \exp [-(t/RC)]$. When $t = RC$, $\Delta E = (E_1 - E_0)/e$, so that RC is called the electrical time constant (τ) defined as that time in a single exponential decay for the potential difference to come to $1/e$ of its initial value. In the analogous heat case, the capacitor corresponds to a body with a heat capacity c, which is heated to an initial temperature T_1 and then put in thermal contact through thermal resistance R with another body held at temperature $T = T_0$. This is mathematically similar to the discussion of tempering a wire in which there is a distance to bring the wire to $1/e$ of its initial temperature difference. In both cases we are considering a decay through a single exponential term. The time required to come to 1/10 the initial temperature difference is simply 2·303 (τ), the time to come to 1/100 is 2 (2·303 τ), etc. Sometimes it is desired to estimate this time constant τ from cooling experiments. In principle, this can be done from any two measurements of temperature at different times. As a simple short cut, it is sometimes convenient to measure the initial cooling rate and divide the initial temperature difference by this initial cooling rate to get the time

constant (τ). For example, if a body with a heat capacity of 1000 joules/deg C, has an initial cooling rate of 10 deg C/sec, for an initial temperature difference of 1000 deg C, then the time constant (τ) = 100 sec. If the thermal resistance is known, the time constant is merely the product of the heat capacity and thermal resistance. For example, the above case corresponds to a thermal resistance of 0·1 deg C/watt.

Although in some calorimetric design the use of a single exponential may be adequate for design purposes, the actual transient is usually not so simple. Fortunately, a variety of unsteady state heat problems have already been solved[6], and in some important cases the solution is shown graphically to facilitate its use.

Consider the case of a thin cylindrical shell similar to that treated earlier in a steady-state case. Suppose this shell has a specific heat c, thermal conductivity λ, density ρ, and length l, and the cylinder is initially at tempera ture $T = T_0$. Assume also that the thermal properties are independent of temperature. Now at time $t = 0$, start to heat one end ($z = 0$) at a constant rate β, so that $T_{z=0} = \beta t$. Putting the initial and boundary conditions into the general heat balance differential equation gives

$$\lambda \frac{\partial^2 T}{\partial z^2} = \rho c \frac{\partial T}{\partial t}. \tag{38}$$

The complete solution is given as

$$(T - T_0) = \beta t + \frac{\beta z^2}{2a} + [\text{transient term}] \tag{39}$$

in which a is thermal diffusivity ($\lambda/\rho c$). If the transient term is short-lived as it is frequently in good calorimetric design, the "steady" temperature gradient on the cylindrical shell is of primary interest. This temperature difference (after transient has died out) over the length l is $\beta l^2/2a$. Note that the average temperature is not at $z = l/2$.

Consider now a case of radial instead of linear heat flow. In terms of cylindrical coordinates, the general differential heat balance equation for a cylinder infinitely long for which the temperature is dependent only on radius r and time t, is Equation (20)

$$\frac{\partial^2 T}{\partial r^2} + \frac{1}{r}\frac{\partial T}{\partial r} = \left(\frac{1}{a}\right)\frac{\partial T}{\partial t}. \tag{40}$$

Now suppose that we have a circular disk of radius a which initially is at temperature $T = T_0$, but at time $t = 0$, the circumferential area of the disk is heated at a constant rate β so that $T_{r=a} = T_0 + \beta t$. Upon assuming that there is no heat transfer at the plane surfaces of the disk, this problem becomes the same as for a cylinder of infinite length, whose solution is

$$T - T_0 = \beta \left[t - \frac{(a^2 - r^2)}{4a}\right] + [\text{transient}]. \tag{41}$$

Although the transient in Equation (41) can be calculated[6], it is usually short-lived so that the "steady" temperature difference between $r = 0$ and $r = a$ is most important. This temperature difference is simply $\beta a^2/4\alpha$.

(1) *The Principle of Superposition.* Before consideration of thermal transients in calorimetry, the Principle of Superposition should be mentioned. This principle, which can be applied to *linear differential equations*, states that solutions to linear differential equations with linear boundary conditions may be summed to give other solutions; a complex solution can be obtained by adding the solutions to simpler problems. This method not only makes numerical solutions easier but also provides physical insight into the heat flow process in calorimetry. A concise statement of superposition theorems is given by Korn and Korn[15]. In brief, the temperature for some particular problem may be considered as a sum of terms all satisfying the heat flow equation, but separately taking account of (*i*) heat generated in the calorimeter, (*ii*) heat exchange between calorimeter and surroundings, and (*iii*) an initial temperature distribution in the calorimeter.

A problem involving two thermocouple errors will be used to illustrate the use of the principle of superposition. Suppose that the shield control in an adiabatic calorimeter is subject to errors due (*i*) to an inhomogeneity in a segment of thermocouple wire between the calorimeter and the shield and (*ii*) to a constant zero bias, which might be caused by an inhomogeneity in a region outside of the shield or simply to a zero offset in an electronic control device. Since the shield temperature is not matched to the calorimeter temperature because of these two spurious e.m.f.s, there will be a temperature gradient in the segment of thermocouple wire and an additional offset due to the effect of this gradient on the inhomogeneity†. When the calorimeter is heated, the heat flowing into the wire segment from the calorimeter and shield will have an additional effect on the inhomogeneity. The problem is to account for the two effects in the measurement process.

To set up the equations, the segment of wire is taken to be of length l, the constant heating rate $dT/dt = \beta$ deg/sec, and the constant control offset ΔT_c. Assuming negligible current in the thermocouple, the heat balance equation is

$$\alpha \frac{\partial^2 T}{\partial z^2} = \frac{\partial T}{\partial t} \qquad (42)$$

which is just Equation (17) with the power term zero. Since the solution for constant heating rate is desired, the substitution $dT/dt = \beta$ can be made at once. Equation (42) is linear either before or after the substitution, since the temperature and its derivatives appear only in the first power. (Linear equations also cannot have cross products such as $T(\partial T/\partial z)$). The boundary condition at the calorimeter end of the wire is that the temperature is rising at a constant rate and that its temperature would have been T_0 at $t = 0$

$$T = T_0 + \beta t \quad \text{at } z = 0.$$

† In adiabatic calorimetry, this secondary effect is probably negligible; however, similar reasoning applies in isothermal shield calorimetry for which the effect on the spurious e.m.f. of the temperature difference between calorimeter and shield may be appreciable.

The temperature at the shield end of the wire differs from that on the calorimeter by the constant offset ΔT_c and the effect of the inhomogeneity

$$T = T_0 + \beta t + \Delta T_c + b\,(T_1 - T_2) \quad \text{at } z = l$$

in which T_1 and T_2 represent the temperatures at the ends of the inhomogeneity and b is the ratio of the thermoelectric power of the inhomogeneity to that of the thermocouple.

The problem can be written in terms of $T - T_0 = U + V$ [noting $\partial T/\partial t = \partial\,(T - T_0)/\partial t$] in which

$$\frac{\partial^2 U}{\mathrm{d}z^2} = \frac{\beta}{\alpha}$$

$$U = \beta t \text{ at } z = 0$$

$$U = b(U_1 - U_2) + \beta t \text{ at } z = l \tag{43}$$

and

$$\lambda \frac{\partial^2 V}{\partial z^2} = 0$$

$$V = 0 \text{ at } z = 0$$

$$V = \Delta T_c + b(V_1 - V_2) \text{ at } z = l. \tag{44}$$

Evidently summing Equations (43) and (44) for U and V will result in the equation for $T - T_0$. Inspection of these two sets of equations for U and V shows that the contribution V to the temperature due to the control offset has been separated from the effect of heating the calorimeter, even with respect to the spurious e.m.f. This effect is constant and independent of the heating rate, so that it can be evaluated in separate experiments, as in fore and after rating periods, assuming only that ΔT_c is the same in both cases. The effect on U of a change in the heating rate is now easily deduced. If the rate is changed by a constant ratio to $k\beta$, then it is easily verified by substitution that kU satisfies the equations for U, including the effect of the spurious e.m.f. Any error associated with U, such as the effect of the spurious e.m.f., is directly proportional to the heating rate. It does not follow that heat leak due to U or similar functions can be detected by measuring the heat capacity of a calorimeter at various heating rates. The time required to heat through the temperature rise for which comparison is made is inversely proportional to the heating rate. Heat transfer between the calorimeter and its surroundings is proportional to the product of the time and functions like U, but the heating rate constant cancels from the product.

The more general problem of the effect of heating rates on heat exchange in adiabatic calorimeters is discussed in Chapter 9, based on detailed mathematical arguments given in the literature[21].

By contrast, the inclusion of a simple variation of the thermal conductivity

with temperature, such as $\lambda = \lambda_0 (1 + \alpha T)$, results in the following *nonlinear* equation

$$\lambda_0 \frac{\partial}{\partial x} (1 + \alpha T) \frac{\partial T}{\partial x} = \beta c, \tag{45}$$

and the substitution $T = U + V$ results in cross terms in U, V, and their derivatives. Mathematical tractability is gone, but more important is the loss of validity of the correction for the control offset. In general, of course, the thermal properties of materials are functions of temperature, so that the linear equations are approximations. The designer must keep in mind that temperature differences in the experiment should be small enough that the linear differential equation provide an adequate description. The tolerable temperature differences are greater when the temperature variations of thermal properties are small and when the total heat transfer between the calorimeter and its surroundings is small. Obviously, if the heat leak is zero, it cannot produce a temperature distribution to interact with that due to heating.

In testing an apparatus after assembly, it seems worth while to investigate the linearity by deliberately exaggerating the magnitudes of the various contributions to the temperature distribution. In the simple case of the terms U and V discussed above, different rates of rapid heating and different offset of controls might set an upper limit on permissible rates and offsets. Variable heating rates commonly used in adiabatic heat capacity calorimeters rarely reveal a corresponding variation in the observed heat capacity. One obvious interpretation is that it is not very difficult to obtain an apparatus which is adequately described by linear partial differential equations.

(2) *Transients in One-Dimensional Heat Conduction.* Transients may be important to the design of calorimeters. Calorimeters must come to equilibrium in a reasonable time so that the uncertainty in the heat leak correction remains tolerable. Transient problems are difficult, but most cases of interest for the approximate design calculations in calorimetry have been worked out[6]. A transient problem will be illustrated with a calculation of the flow in one direction (one-dimensional) with no lateral losses. This problem treats approximately the temperature distribution in a lead wire, with one end fastened to the constant temperature bath and the other heated at the rate β, with the initial temperature that of the bath. Although the problem seems restricted in scope, by the principle of superposition we can apply it also to the case for which both ends are heated and the wire has an initial temperature distribution which might be the steady state between a calorimeter at one temperature and a bath at another temperature.

The solution to this problem is given by Churchill[7]

$$T - T_0 = \beta \left[\frac{1}{6} \left(\frac{x^3}{l^3} - \frac{x}{l} \right) + \frac{xt}{l} + \frac{2}{\pi^3} \sum_{n=1}^{\infty} \frac{(-1)^{n-1}}{n^3} \right.$$
$$\left. \exp \left[(-\lambda n^2 \pi^2 t / \rho c l^2) \right] \left[\sin (n\pi x / l) \right] \right]. \tag{46}$$

The exponential series does not converge rapidly for small values of the argument, but for $\lambda t/\rho c l^2$ greater than 0·1 only the term for $n = 1$ is significant in the time required for the calorimeter to come to equilibrium. Qualitatively, in order to get rapid equilibrium in the calorimeter, we would like to have the thermal conductivity large and the length, which appears to the second power, small. For a copper wire 10 cm long at room temperature, the time constant for the first term is equal to 10 sec (time to decrease to $(1/e)$ of the initial value). For an insulated copper wire we can use the approximation that heat is conducted along the copper to the insulating material which contributes to the heat capacity but not to conduction. For a copper wire of 0·02 cm diam and 0·0025 cm thickness of insulation of approximately the same heat capacity per unit volume, the time constant is increased to 14 sec. Doubling the length increases the time constant for the insulated wire to 56 sec. The time constant is greatly increased for alloy wires. If we consider a constantan wire instead of the insulated copper wire above, the time constant is about 20 times longer or 220 sec. If such a wire has a spurious e.m.f. or sufficiently large heat capacity so that we must wait until it is within one per cent of its final value then the time required is about 2(2·3) times the time constant or 1000 seconds. If it is necessary to install long wires in the apparatus, their temperatures should be kept constant during an experiment.

If supports for a calorimeter are chosen only on the basis of low thermal conductivity, harmful lags may be introduced. A calorimeter supported on glass rods provides an example. Equation (46) applies with the thermal diffusivity $\lambda/\rho c \sim 5{\cdot}7 \times 10^{-3}$ for a glass near room temperature, and the time constant for the first term is 176 sec for a 1 cm length, and 704 sec for a 2 cm length. Of course, if the calorimeter merely rests on the glass rods, the additional thermal resistance of the contact will give a still longer time constant.

Although Equation (46) applies to the case of turning on power in a calorimeter, the same arguments apply when the power is turned off. To obtain the solution for this case we merely subtract the right hand side of Equation (46) in which we have substituted $(t - t_f)$ for t, in which t_f is the time at which the power is turned off. In the general case there will be two sets of decaying exponentials, but those in $t - t_f$ will be predominant and the equilibrium time depends on these.

When some portion of the apparatus is subjected to automatic control it is important that the transient response be rapid. The thermal conductivity should be as large as possible, the distances between heaters should be kept small and heat capacities should be kept small. These problems are discussed in detail in other chapters. The previous example of transients is for a linear heat flow. Many other problems, including transients in radial heat flow, are solved in Carslaw and Jaeger's book[6].

IV. Applications to Calorimeter Design

1. *Temperature in a calorimeter wall at constant heating rate*

One of the most important problems in accurate calorimetry results from temperature gradients in the calorimeter. In most calorimeters the heater

is not distributed in such a manner as to avoid gradients, and even if it were for one amount of filling in the calorimeter, the same condition probably would not hold for another filling.

Consider as a simple example the temperature difference in a cylindrical calorimeter wall which receives heat only at one end ($z = 0$). Assume that the wall has a length l, thickness w, radius r, thermal conductivity λ, density ρ, and heat capacity c, and that all these quantities are constant during an experiment so that each part is heating at a constant rate β. The heat balance differential equation here is $\lambda(2\pi rw)\ \partial T/\partial z = p(l - z)$ in which p is the power per unit length of cylinder necessary to heat it at a rate β. The power p is simply $p = (2\pi rw)\rho c\beta$, so that

$$\lambda(2\pi rw)\ \frac{\partial T}{\partial z} = (2\pi rw)\rho c\beta\ (l - z) \tag{47}$$

or

$$\frac{\partial T}{\partial z} = \beta\left(\frac{\rho c}{\lambda}\right)(l - z) = \frac{\beta}{a}\ (l - z) \tag{48}$$

in which a is thermal diffusivity, $\lambda/\rho c$.

Integrating between $z = 0$ and $z = l$ gives

$$(T_l - T_0) = -\frac{\beta l^2}{2a} \tag{49}$$

in which T_l and T_0 are both increasing at the rate β. This relation is the same as that given by Equation (39) after the transient. It is apparent that the largest temperature gradient occurs near the heat source, so that the assumption of linear temperature change on the surface is invalid. The average temperature (relative to T_0) over the surface can be calculated from the equation

$$(T - T_0)_{\text{av}} = \frac{\beta}{a}\frac{\int_0^l [(z^2/2) - lz]\,dz}{\int_0^l dz} = \frac{\beta}{a}\frac{l^2}{3} \tag{50}$$

However, $(T_{l/2} - T_0) = -\beta/a(3/8)l^2$, so that the difference between the average temperature and $T_{l/2}$ is about $(0{\cdot}042\ \beta/a\ l^2)$.

The example given above is for a cylindrical calorimeter wall heated at one end. In a similar manner there may be obtained the temperatures in a shell heated equally from both ends. The solution here using boundary conditions that $T = T_0$ at $z = 0$ and $z = l$ is

$$(T_{l/2} - T_0) = -\frac{\beta}{2a}\ (lz - z^2) \tag{51}$$

The minimum temperature is at $z = l/2$, and its value is $(T_{l/2} - T_0) = -(\beta l^2/8\alpha)$, so that the use of two heaters reduces the maximum gradient by a factor of four.

To avoid temperature differences on the surface, various techniques are used. Stirred liquids are used to distribute the heat in many calorimeters and in others metal vanes run from the heat source to the surface. In large calorimeters, the stirred liquid technique is usually preferable. Conduction is less attractive for large dimensions because the temperature difference increases rapidly with the distance. In the simple case described by Equation (49), the temperature increases with the square of the distance. In small calorimeters, good metallic conductors serve well and avoid the heat and mechanical problems of stirring.

2. *Uncertainty in heat leak due to temperature gradients*

It has been illustrated that for the different methods of heating the calorimeter wall the temperature gradients in the wall may be different. When the heater is located at one end of the cylindrical wall, the *average* temperature of the cylindrical surface occurs at a distance of about $(0{\cdot}43l)$ in which l is the length of cylinder. If the heat leak is entirely by radiation from the wall surface (assume constant emittance), then a single thermocouple should be located at $0{\cdot}43l$ from the end for proper accounting of radiation heat leak. If the thermocouple had been located at the middle of the cylindrical wall (at $l/2$), then the thermocouple temperature would differ from the average surface temperature. Let us examine an actual case to see the magnitude of this difference. As an unfavorable case, take a calorimeter wall of steel having length $l = 10$ cm, thermal diffusivity $\alpha = 0{\cdot}1$, and heated at a rate of 0·01 deg/sec. The temperature at its middle $(l/2)$ referred to the heated end is less by $\beta/\alpha\ [(3/8\ l^2)] = 3{\cdot}75$ deg. However, the average temperature of the surface is $\beta/\alpha\ (l^2/3) = 3{\cdot}33$ deg. Therefore, the location of the thermocouple at $l/2$ gives a heat leak error corresponding to 0·42°C over the surface. If copper were used instead of steel, the temperature difference would be about 0·04 deg.

3. *Methods of minimizing heat leak due to temperature gradients*

The previous example indicates that temperature gradients in a calorimeter or shield wall can result in errors in heat leak measurement if the thermocouple (or couples) used are not located properly to account for the temperature gradients. Where possible, one obvious solution to the problem is to design the calorimeter and shield to minimize temperature gradients. This may be done by stirring or by use of materials with high conductivity or proper distribution of heater so that heat has to flow only a short distance. This latter solution may be complicated by different relative power requirements at different times. For example, in heating experiments with most of the power going to changing the temperature, the power distribution needed in the shield will be approximately according to mass. However, at steady temperatures with the power going only to heat leak, the power distribution needed probably will be entirely different. One partial solution to this problem has been to use two separate heaters, one distributed according to mass and one according to heat leak.

Another method of minimizing temperature gradients in a shield is to minimize the power required to keep it at a given temperature. This may be accomplished with better insulation from its cooler surroundings. Generally, it is better to provide insulation with a minimum of heat capacity because of effects of time lag in the insulation. One such insulation with a minimum of lag is a number of concentric thin shells, such as discussed later in this chapter. Another method of reducing the power required in a shield, thereby reducing temperature gradients, is to provide external concentric shells, with the temperature of each independently controlled. In this manner, the power in the shield (inner shell) at a constant temperature can be negligible. An example of this is given in Chapter 11. However, use of such a system does not avoid temperature gradients on the shield while heating.

Another solution of the temperature gradient problem is to use a sufficient number of thermocouples to provide adequate information on the temperature distribution. One calorimeter (Chapter 11) used eight thermocouples on both the calorimeter and shield wall surfaces to evaluate average temperatures. In the case of heat capacity experiments, it is possible in principle to reduce errors in heat leak due to temperature gradients by using two series of experiments, a tare and a gross series. If the gradients on both calorimeter and shield are the *same* (considering each separately) in both series, then ideally the absolute heat leak errors are the same. They then cancel out when taking the difference between the tare and gross series. The effectiveness of this method for reducing heat leak errors depends upon the extent that the temperature gradients are the same. The shield gradients do not have to be the same as the calorimeter gradients. This method is used commonly with the assumption that the gradients are nearly the same in the two series. The fallacy in this assumption is that the temperature gradients in the calorimeter are necessarily changed by the change in the amount of sample, the magnitude of the change being a function of the design.

The obvious solution to this problem is to provide a calorimeter surface whose temperature is *independent* of the presence of the sample. This ideal condition can be approached in many calorimeters by a technique applied in Chapters 9 and 11. The principle of this technique is illustrated simply in *Figure 6* which shows a portion of a sample container with a heaterless

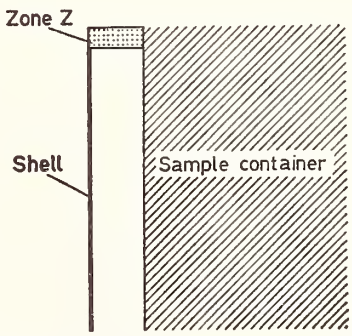

Figure 6. Method of reducing heat leak errors due to temperature gradients on sample container.

thin metal shell S thermally attached *only* at the zone Z. In heating experiments, in which it is assumed for simplicity that the calorimeter is solid metal, the heater produces a temperature gradient. After the starting transient has diminished, *all* of the calorimeter, including the ring at Z and the heaterless shell, will be heating at the rate β. This, of course, assumes constancy of λ, ρ, c, and no heat transfer except by solid conduction at zone Z. Under this condition, the heaterless shell will also have gradients. Since the gradients will be *independent* of the gradients on the calorimeter, any heat leak will also be independent of the gradients in the calorimeter. In this case, in principle, the use of the tare and gross series of experiments avoids heat leak errors *if* the temperature at the zone Z follows the same time-temperature function in the two series of experiments†. The success of this technique depends on the extent of thermal isolation of the heaterless shield S from the sample container C over the cylindrical surface. In one adiabatic calorimeter near room temperature with a single heaterless shell on the sample container, the thermal isolation was obtained by evacuation and use of polished gold surfaces. The effectiveness of this single shell can be demonstrated by considering the effect of the vertical gradient in the sample container (*Figure 6*) on the temperature of the shell. The principle of superposition can be used to separate the vertical gradient in the shell into two components, one due to heat flow through the zone Z to heat the shell at the rate β, and the other due to heat flow from the sample container directly across to the shell by radiation. For simplicity, consider only the cylindrical portions. Let h = heat transfer coefficient between the two surfaces, λ, w, r, and l the thermal conductivity, thickness, radius, and length of the heaterless cylindrical shell. Also assume there is a gradient on the sample container so that its surface temperature (referred to zone Z) is Mz^2 in which $z = 0$ at the zone Z. Also as a first approximation, assume that the resulting gradient in the shell is much smaller than the gradient on the sample container. The heat balance equation here is

$$\lambda(2\pi rw)\,\frac{\partial^2 T}{\partial z^2}\,\mathrm{d}z = -\,h\,(2\pi r\mathrm{d}z)\,(Mz^2) \tag{52}$$

in which h is the heat transfer coefficient between sample container and the shell, so that $\partial^2 T/\partial z^2 = -\,(hM/\lambda w)\,z^2$. Integrating this equation between the limits $z = 0$ and $z = l$ gives

$$\Delta T = (T_l - T_0) = -\,\frac{hM}{\lambda w}\left(\frac{l^4}{12} + C_1 l\right). \tag{53}$$

Using the boundary condition that $\partial T/\partial z = 0$ at $z = l$, gives $C_1 = -\,hMl^3/3\lambda w$ so that

$$\Delta T = -\,\frac{hM}{3\lambda w}\left(\frac{l^4}{4} - l^4\right) = \frac{hMl^4}{4\lambda w}\,. \tag{54}$$

† In general, the transient effects for the gross differ from those for the tare. The statement is valid, but depends on a more sophisticated argument which does not even require the same heating rate[21].

For an example, use $l = 5$ cm, $w = 0{\cdot}025$ cm, $\lambda = 1{\cdot}0$ W cm^{-1} deg^{-1}, and $M = 1$, giving a 25 deg temperature difference on the sample container. If the space is evacuated and the surfaces are polished gold plated, the radiative heat transfer coefficient is about 10^{-5} W cm^{-2}deg^{-1}. Substituting these values gives $\Delta T = 0{\cdot}0625$ deg C. This contrasts with the 25°C temperature difference on the sample container. The conclusion is that in this case, one heaterless shell has attenuated the effect of the sample container gradient by a factor of approximately 400. It is interesting to note the magnitude of the temperature difference in this shell due to heating the shell at a constant rate β. This temperature difference after the transient has vanished can be calculated using Equation (49), giving $(T_l - T_0) = -\beta l^2/2a$. Using $l = 5$ cm, a heating rate of 0·01 deg/sec, and $a = 1$ cm^2/sec (for copper) we get $\Delta T = 0{\cdot}125$ deg C.

With this technique of providing a calorimeter surface whose temperature is independent of temperature differences in the calorimeter, it is no longer necessary to position thermocouples on the surface of the shell in order to obtain an average surface temperature. The tare and gross experiment will have the same heat loss, independent of the location of the thermocouple. It usually is convenient to locate one or more thermocouples at the zone [22].

The use of the heaterless shell is equally valuable in experiments such as heat of vaporization for which the calorimeter temperature is not changing with time. In this case, the shell attached to the calorimeter at one zone is isothermal in spite of temperature gradients in the calorimeter due to vaporization. A similar shell attached to the inside of the shield at one zone also is isothermal, in spite of temperature gradients in the shield due to heat loss to the surroundings.

It is not always possible to obtain as low a heat transfer coefficient as there was in the evacuated space bounded by polished gold surfaces. In a high-temperature adiabatic calorimeter[22] in which the space was not evacuated, the effectiveness of an unheated shield was not so great, so that it was necessary to use several shells.

4. *The calorimetric heater lead problem*

A more complicated case in steady-state heat flow is the problem of the calorimeter heater leads between calorimeter and shield. This problem has been considered in great detail in a recent publication[9], so that it will be discussed here only briefly.

The calorimeter heater current leads must be considered differently than the other calorimeter leads because the electric current in them develops heat which must be properly accounted for and apportioned to calorimeter and shield. The other leads merely serve as heat conductors to contribute to heat leak coefficients. The calorimetric error resulting from any uncertainty in the apportionment of the heat in the current lead segment between calorimeter and shield may be made small by using current lead segments of low electrical resistance relative to the calorimeter heater resistance. The problem here is that electrical and thermal resistances are usually proportional under ordinary conditions with metal wires, so that the smaller electrical resistance gives smaller thermal resistance. In turn, this results in

a larger heat transfer coefficient which increases the heat leak uncertainty. The optimum size of lead depends on the particular calorimeter.

There is, however, a method by which any error in current lead power apportionment can be made smaller without this increased heat leak uncertainty. This method is simply to increase the relative resistance of the calorimeter heater. Accordingly, in most calorimeters at moderate temperatures, a calorimeter heater resistance of at least 100 Ω is considered desirable if accuracies approaching 0·01 per cent are desired. Sometimes at low temperatures, heaters are used which have resistances of thousands of ohms.

In accounting for the power in the current lead segments, the convention assumes that the heat developed in a current lead segment divides equally between calorimeter and shield, so that the potential lead is attached to the center of the current lead segment. It has been pointed out earlier (Equation 25) that this assumption is strictly true only when the ends of a current lead segment are at the same temperature. This condition for validity is satisfied if the calorimeter and shield are at the same temperatures and the thermal connections to the calorimeter and shield at the ends of a current lead are also the same. It has also been pointed out that even if these thermal connections are the same, the use of potential leads at mid points is valid with the calorimeter and shield at *different* temperatures only *if* a heat leak correction is made for the "apparent" heat flow along the current lead segments *assuming* their ends are at the temperatures of calorimeter and shield. This procedure is approximated in accurate calorimetry by merely measuring an overall heat transfer coefficient between calorimeter and shield when there is no current in the calorimeter heater and using this coefficient to calculate heat leak corrections, including periods when there is current through the heater lead.

The general problem of calorimeter current leads is when (*i*) the calorimeter and shield are at different temperatures (T_c and T_s), and (*ii*) the thermal connections at the ends of the current lead segments are different.

Consider calorimeter current leads, each having cross section A and length l between calorimeter and shield, and having a thermal conductivity λ. Now suppose that there is electric heat developed at a time rate p for unit length of the wire, and that all heat lost from the current lead segment is by solid conduction along the wire. Also suppose that each current lead is thermally and electrically insulated from the calorimeter or shield and that these thermal resistances per unit length between the wire and the calorimeter or shield are R_c and R_s, respectively. With these conditions a solution[9] of the heat balance equations gives the rate of heat flow P_c into the calorimeter by conduction along the current lead segment.

$$P_c = \frac{p}{2}\left[\frac{l^2 + 2l\sqrt{(\lambda A R_s)} + 2\lambda A(R_s - R_c)}{l + \sqrt{(\lambda A R_s)} + \sqrt{(\lambda A R_c)}}\right] + \left[\frac{\lambda A(T_s - T_c)}{l + \sqrt{(\lambda A R_s)} + \sqrt{(\lambda A R_c)}}\right]. \tag{55}$$

The solution is shown in the two terms to demonstrate its physical significance. The *second* term in the solution is independent of power developed in the wire and is the heat flow due to the temperature difference ($T_s - T_c$)

between shield and calorimeter. It is important to note that this second term (involving $T_s - T_c$) is usually accounted for by conventional calorimetric techniques, which experimentally measure and correct for the *overall* heat transfer coefficient between shield and calorimeter when there is no current in the leads. The first term in Equation (55) is proportional to the power developed in the current lead so that it accounts for that part of the heat flow caused by the current in the lead. The resulting overall calorimetric error resulting from this first term has been calculated[9] to be

$$\text{Calorimetric Error } (\%) = 100\, r \left[\frac{2(L_s^2 - L_c^2) + (L_s - L_c)}{1 + L_s + L_c}\right] \quad (56)$$

in which r is the ratio of electrical resistance of length l of the current lead segment to the total electrical resistance of the calorimeter heater, including leads out to the potential terminal, and

$$L_s = \frac{\sqrt{(\lambda A R_s)}}{l}, \text{ and } L_c = \frac{\sqrt{(\lambda A R_c)}}{l}.$$

The relation between these dimensionless quantities L_c and L_s and [$(1/r)$. Calorimetric error] is illustrated in *Figure 7*.

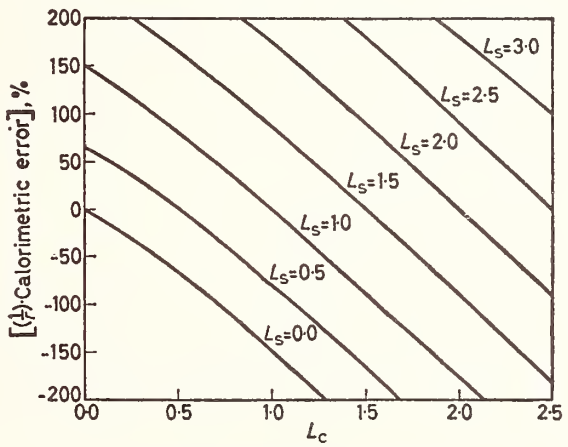

Figure 7. Calorimeter error relation.

In order to judge the practical importance of the error described above, it is necessary to calculate values of L_s and L_c and r for specific examples. Suppose that the current lead is circular, that the length l of the current lead segment is 3 cm, and that the lead is copper with o.d. = 0·02 cm Also suppose for thermal contact in the calorimeter this lead is electrically insulated by a cylindrical solid surrounding the wire to an o.d. of 0·2 cm and having a thermal conductivity of 0·002 W cm^{-1} deg^{-1} corresponding to a typical organic material. In this case, R_c = 184 $degW^{-1}$ cm^{-1} and L_c = 0·166. Now suppose that in the shield there is an air gap of 0·005 cm

between the wire and the insulation (o.d. of 0·2 cm). The resulting value of $R_s = 411$ deg W^{-1} cm^{-1} so that $L_s = 0{\cdot}238$ and $[(1/r) \cdot$ (calorimetric error)] is 9·3 per cent. If the calorimeter heater has a resistance of 10 Ω, $r = 0{\cdot}0016$ so that the calorimetric error in the power measurements due to using a potential lead at the mid point of the current lead is 0·0016 (9·3) = 0·015 per cent. This error is only significant in the most accurate calorimetry. On the other hand, it is possible to have considerably larger error in a poor design. Take a case in which R_c is reasonably small but R_s is perhaps 2000 degW^{-1} cm^{-1} due, for example, to an evacuated powder insulation. In this case, the calorimeteric error is 0·083 per cent.

In the previous discussion of calorimeter heater leads, it has been assumed that the potential leads were attached to the current lead segments at their mid points and that heat flow along these leads is negligible. If this heat flow is not negligible, consideration should be given to the location of their attachments. The mid point attachment has the disadvantage that the temperature of the mid point is a function of the current in the calorimeter heater, but the resulting heat conduction along the potential lead is not accounted for in the first term in Equation (55). Although probably an analysis for the heat flow could be obtained, since the effect is usually a small one, it is easier to change the design to avoid the error. One method which has been used[22] is to attach thermal tiedowns on the current leads close to the calorimeter and shield mechanical boundaries. If the two current leads and their thermal tiedowns are symmetrical, it is convenient to attach one potential lead at the calorimeter tiedown of one current lead and the other potential lead at the shield tiedown of the other current lead. In this way, the energy apportionment is *effectively* at the mid points of the current leads without having the problem of heat transfer along the potential leads being a function of the heater current.

V. References

[1] Barry, F., *J. Am. Chem. Soc.*, **44**, 927 (1922).
[2] Berman, R., *J. Appl. Phys.*, **27**, 318 (1956); Berman, R., and C. F. Mate, *Nature*, **182**, 1661 (1958).
[3] Brunot, A. S., and F. F. Buckland, *Trans. Am. Soc. Mech. Engrs.*, **71**, 253 (1949).
[4] Caldwell, F., *Thermocouple Materials*, Natl. Bur. Standards Monograph 40, U.S. Govt. Printing Office, Washington, D.C., 1962; *Temperature, Its Measurement and Control in Science and Industry*, Vol. I, American Institute of Physics, Reinhold, New York, 1941; Vol. III, C. M. Herzfeld, editor-in-chief, Part 1, F. G. Brickwedde, ed., Part 2, A. I. Dahl, ed., Reinhold, New York, 1962.
[5] Campbell, I. E., *High-Temperature Technology*, John Wiley and Sons, Inc., New York, 1956.
[6] Carslaw, H. S., and J. C. Jaeger, *Conduction of Heat in Solids*, Oxford University Press, London, 1959.
[7] Churchill, R. V., *Operational Mathematics*, McGraw-Hill Book Co., Inc., New York, 1958.
[8] Ditmars, D. A., and G. T. Furakawa, *J. Res. Natl. Bur. Std.*, **69C**, 35 (1964).
[9] Ginnings, D. C., and E. D. West, *Rev. Sci. Instr.*, **35**, 965 (1964).
[10] Hoge, H. J., *Rev. Sci. Instr.*, **20**, 59 (1949).
[11] Jacobs, R. B., and C. Starr, *Rev. Sci. Instr.*, **10**, 140 (1939).
[12] Jakob, M., *Heat Transfer*, Vol. I, John Wiley and Sons, Inc., New York, 1949.
[13] Jakob, M., *Heat Transfer*, Vol. II, John Wiley and Sons, Inc., New York, 1957.
[14] Kistler, S. S., and A. G. Caldwell, *Ind. Eng. Chem.*, **26**, 658 (1934).
[15] Korn, G. A., and T. M. Korn, *Mathematical Handbook for Scientists and Engineers*, McGraw-Hill Book Co., Inc., New York, 1961.
[16] Lyman, T., ed., *Metals Handbook*, 8th ed., American Society for Metals, Novelty, Ohio, 1961; *American Institute of Physics Handbook*, McGraw-Hill Book Co., Inc., New York, 1957; *International Critical Tables*, McGraw-Hill Book Co., Inc., New York, 1928.

[17] Mebs, R. W., and W. F. Roeser, *Solders and Soldering*, Natl. Bur. Standards Circular 492, U.S. Govt. Printing Office, Washington, D.C., 1950.
[18] Petree, B., and G. Ward, *Natl. Bur. Standards Technical Note* **163** (1962), U.S. Govt. Printing Office, Washington, D.C.
[19] Scott, R. B., *Cryogenic Engineering*, D. Van Nostrand and Co., Inc., New York (1959).
[20] Weills, N. D., and E. A. Rider, *Trans. Am. Soc. Mech. Engrs.*, **71**, 259 (1949).
[21] West, E. D., *J. Res. Natl. Bur. Std.*, **67A**, 331 (1963).
[22] West, E. D., and D. C. Ginnings, *J. Res. Natl. Bur. Std.*, **60**, 309 (1958).
[23] White, W. P., *The Modern Calorimeter*, The Chemical Catalog Co., Inc., New York, 1928.
[24] White, W. P., *J. Am. Chem. Soc.*, **40**, 382 (1918).

Reprinted from*

Experimental Thermodynamics
Volume I

CHAPTER 11

Calorimetry of Saturated Fluids Including Determination of Enthalpies of Vaporization

D. C. Ginnings
National Bureau of Standards, Washington, D.C., U.S.A.
H. F. Stimson
National Bureau of Standards, Washington, D.C., U.S.A. (retired)

Contents

I. Introduction

Calorimetry of saturated fluids is the measurement of the heat required for changes of state in them (liquids and vapors). The term "saturated", as used in this chapter, restricts the states of the fluid to those for which the liquid and the vapor phases are both present in equilibrium within the calorimeter. The relative amounts of the two phases, however, may differ by large factors; i.e., the calorimeter may be nearly full of liquid in a high-filling experiment or may have only a little liquid in a low-filling experiment.

In heat capacity determinations both high and low fillings can be used. Sometimes such experiments are called gross and tare experiments. The method of saturation calorimetry described in this chapter differs from calorimetric methods in some other chapters of this book in which tare experiments are made with an empty calorimeter. In 1917 Osborne[5] described his experiments on the specific and latent heats of ammonia in which he made tare experiments with an empty calorimeter. These required him to make some troublesome corrections about whose accuracy he felt somewhat

*See complete ref. on page 1-I.

uncertain. In 1924 he developed[6] the method described here, to be used for determining the thermal properties of water and steam. This method of saturation calorimetry not only simplifies the computations but also, in principle, eliminates certain errors.

In saturation calorimetry the temperatures depend only on the pressures along the vapor pressure line; thus, at any instant, the temperature at all liquid–vapor interfaces in the calorimeter is essentially uniform and depends only on the pressure of the vapor there. Enthalpy of vaporization experiments, therefore, can be performed at a constant temperature, by adding heat and withdrawing fluid from the calorimeter while controlling the flow rate to keep the pressure constant.

In heat capacity experiments, the power input can be chosen so that the temperature may be raised at essentially the same rate in both the high and the low fillings, thus making the pressure changes occur in the same way in both. This procedure has the advantage that, by taking differences, one can eliminate the correction for fluids in the filling tubes and the correction for work done by strain of the calorimeter as the pressure is raised.

By Osborne's method the enthalpy values of both the saturated liquid and the vapor can be obtained directly from three types of experiments made in one apparatus without precise knowledge of the volume in the calorimeter or other thermal properties of the fluid. This calorimetric method was first applied to water and steam[7,9,10] and later to hydrocarbons[12]. A review of the theory of this method will be given, together with experimental applications to determine some thermal properties of water in the temperature range from 0–374°C. In addition, there will be some discussion of other methods of measuring enthalpies of vaporization.

II. Theory of the Method

The method makes use of a single calorimetric apparatus. A sample (both liquid and vapor) is so isolated (in the calorimeter) that its quantity, state and energy can be accounted for. With this apparatus, a system of measurements can be made at progressively higher temperatures to determine values of enthalpy of both the liquid and the vapor, referred to values at some reference temperature such as 0°C.

The calorimeter is provided with two outlet tubes, one at the bottom for introducing or withdrawing liquid and the other at the top for withdrawing vapor. Valves on these tubes either shut the fluid in the calorimeter or control the rate at which fluids are withdrawn. Provisions are made for observing the mass of fluid put into the calorimeter, the heat added, and the temperature of the calorimeter with its contents. The calorimeter is surrounded by a shield whose temperature is controlled so as to minimize net exchange of heat between them. All experiments are made with both the liquid and vapor phases present in the calorimeter.

The essential equations involved in the method follow; for more detail on the derivations of these equations the reader is referred to Osborne's original papers[6]. First consider two heat capacity experiments with the calorimeter, (A) one with a large volume of liquid and some vapor, and (B) the other with a small volume of liquid and the rest vapor. In these two experiments the calorimeter contains the sample masses m_A and m_B,

respectively. The corresponding quantities of energy, q_A and q_B, which are necessary to heat the calorimeter and its contents from an initial temperature, T_1, to a higher final temperature, T_2, are found. From these experiments it is concluded that the difference of the energies, $q_A - q_B$, is used to heat the difference of the masses of the sample, $m_A - m_B$, from T_1 to T_2. The quotient of these differences would represent the change of the enthalpy, H, of the saturated liquid, were it not for the larger volume of vapor in experiment (*ii*). This requires a "vapor correction", $\Delta H_v[V/(V' - V)]$ in which ΔH_v is the enthalpy of vaporization and V and V' are the specific volumes of the saturated liquid and vapor respectively. The equations are

$$\Delta q/\Delta m = (q_A - q_B)/(m_A - m_B) = \Big[H - \Delta H_v[V/(V' - V)]\Big]_{T_1}^{T_2}$$
$$= [\alpha]_{T_1}^{T_2} \qquad (1)$$

The quantity in brackets, $[H - \Delta H_v[V/(V' - V)]]$, is a specific thermodynamic property of the sample itself and is *not* dependent on the calorimeter. This property, which Osborne called α, has the dimensions of enthalpy.

Equation (1) shows that this property, α, is less than H by a vapor correction term $\Delta H_v[V/(V' - V)]$ which Osborne called β and which is also a specific thermodynamic property of the sample. Hence

$$\alpha = H - \Delta H_v[V/(V' - V)] = H - \beta. \qquad (2)$$

Now consider a second type of experiment which can be used for measuring the enthalpy of vaporization ΔH_v. Let heat be supplied to evaporate liquid while withdrawing vapor. A throttle valve is operated to control the rate of withdrawal so as to keep the pressure, and consequently the temperature of evaporation, constant throughout the experiment. The vapor thus removed is essentially saturated at the temperature of the experiment. The theory shows that the heat added, Δq, divided by the mass withdrawn, Δm, is equal to the enthalpy of vaporization ΔH_v plus the same vapor correction β described above in the α experiments. The quantity $\Delta q/\Delta m$ used for this vaporization experiment, and called γ by Osborne, is also a specific thermodynamic property of the sample so that

$$\gamma = \Delta q/\Delta m = \Delta H_v + \Delta H_v[V(V' - V)] = \Delta H_v + \beta. \qquad (3)$$

Now consider a third type of experiment in which liquid is withdrawn through the lower tube as heat is added. Here it is obvious that all energy goes to producing vapor to fill the space whence liquid is removed. For unit mass of liquid withdrawn, there is $[V/(V' - V)]$, of unit mass of liquid vaporized in the calorimeter, so that

$$\Delta q/\Delta m = \Delta H_v[V(V' - V)] = \beta. \qquad (4)$$

Here then is an experiment which *directly* evaluates the vapor correction β used to obtain H and ΔH_v from the α and γ experiments.

The relations between Osborne's measured α, β, and γ, and conventional enthalpy (at saturation) are summarized by the equations 5 to 7.

$$H = \alpha + \beta \tag{5}$$

$$\Delta H_v = \gamma - \beta \tag{6}$$

$$H' = H + \Delta H_v = \alpha + \gamma \tag{7}$$

in which H' is the enthalpy of the saturated vapor.

So far these derivations have involved only the first law of thermodynamics. If the Clapeyron relation is used, which involves the second law of thermodynamics, the following equations result

$$\beta = \Delta H_v[V/(V' - V)] = VT(\mathrm{d}P/\mathrm{d}T) \tag{8}$$

$$\gamma = \Delta H_v + \Delta H_v[V/(V' - V)] = \Delta H_v[V'/(V' - V)] = V'T(\mathrm{d}P/\mathrm{d}T) \tag{9}$$

in which T is the absolute thermodynamic temperature and P is the vapor pressure. The ratio of these equations reduces to

$$\frac{\beta}{\gamma} = \frac{V}{V'} \tag{10}$$

at any temperature. From this it is seen that calorimetric measurements can lead directly to the ratio of the specific volumes of the saturated fluids. From equations (8) and (9) it is also seen that the calorimetric measurements can lead to values of the specific volumes if the vapor pressure derivative, $\mathrm{d}P/\mathrm{d}T$, is known.

In order to visualize the relative magnitudes of these specific thermal properties (α, β, γ, and H), *Figure 1* shows the formulated results of the experiments which were performed to obtain values of the thermodynamic properties of saturated water and water vapor. The α is shown starting from zero at 0°C and increasing almost linearly up to the critical point (~374°C). The γ is greatest at 0°C and decreases with increasing rapidity until its slope becomes $-\infty$ at the critical point. The β, on the other hand, is very small at 0°C, but its slope increases with temperature. Above 300°C the slope increases faster than exponentially and β meets γ at the critical point where the slope is ∞. The enthalpy of the saturated liquid, H, is the sum of α and β. The enthalpy of the saturated vapor, H', is the sum of α and γ and it meets H at the critical point. At any temperature the difference $H' - H$, which is the same as the corresponding $\gamma - \beta$, is the enthalpy of vaporization ΔH_v. The mean diameter is defined as $(\gamma + \beta)/2$.

Figure 1 shows that for water, β is relatively small except at the higher temperatures and pressures. At 100°C, the normal boiling point of water, β is only about $\gamma/1600$ and about $\alpha/300$. For liquids below their normal boiling points it is usually more accurate to calculate the values of β, by using the equation $\beta = VT(\mathrm{d}P/\mathrm{d}T)$, than to measure them calorimetrically.

The saturation enthalpy is $H = \alpha + \beta$, so that

$$(\partial H/\partial T)_S = \mathrm{d}\alpha/\mathrm{d}T + \mathrm{d}\beta/\mathrm{d}T. \tag{11}$$

For most liquids near their normal boiling points $\mathrm{d}\beta/\mathrm{d}T$ is as much as 1 per cent of $\mathrm{d}\alpha/\mathrm{d}T$ so some care must be taken there when using the Clapeyron relation for calculating β and $\mathrm{d}\beta/\mathrm{d}T$ accurately.

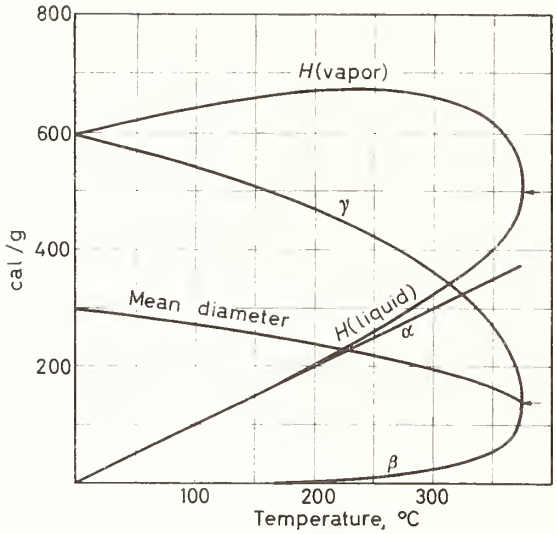

Figure 1. Thermodynamic properties of water.

Values of the specific heats, $C_S = (\partial q/\partial T)_S$ and $C_P = (\partial q/\partial T)_P$, are often needed. The value of C_S can be obtained from the relation

$$C_S = (\partial H/\partial T)_S - V(\partial P/\partial T)_S = d\alpha/dT + d\beta/dT - \beta/T. \quad (12)$$

C_P may be obtained from C_S using the relation

$$C_P = C_S + T(\partial V/\partial T)_P(\partial P/\partial T)_S. \quad (13)$$

As a general rule $(\partial H/\partial T)_S$, C_S, and C_P differ from each other by less than 0·1 per cent at temperatures below the normal boiling points.

III. General Calorimetric Design and Procedures

The design of apparatus for the calorimetry of saturated fluids depends upon such factors as the amount of the sample available, the temperature and pressure range, the accuracy desired, the thermal properties of the sample, and the state of calorimeter design at the time. In the calorimetry of Osborne and his collaborators, several general principles were adopted at the start. Some of these will now be discussed.

Early in the program it was accepted that heat leak uncertainties could be the largest item of error in accurate calorimetry and that it was necessary to minimize and evaluate the heat leaks. The solution to this problem involved three different procedures, (*i*) minimization of the heat transfer coefficient between calorimeter and surroundings, (*ii*) minimization of the temperature differences between calorimeter and surroundings, and (*iii*) measurement of all unavoidable temperature differences in order to correct for the resulting heat leak. The application of these three procedures follows.

In three of the calorimeters described in this chapter the space surrounding

the calorimeter was evacuated in order to eliminate heat leak by gaseous conduction and convection. However, in one calorimeter operating at higher temperatures at which heat leak by radiation is large, it was not convenient to evacuate, but the heat transfer was minimized by using a series of progressively larger shields, appropriately spaced. The coefficients of heat transfer by radiation were minimized also by using polished reflecting surfaces of gold or silver, which had low emittances. Minimizing the coefficient of heat transfer by solid conduction was more difficult because some metallic connections were necessary. The metal connecting tubes at the top and bottom of the calorimeter were made of alloys chosen for their low thermal conductivity, chemical inertness and mechanical strength. The dimensions of these tubes were chosen to give adequate strength and fluid conductance without excessive cross section. There was also a heat leak from the calorimeter along some of the thermocouple wires. The sizes and materials of these were chosen by giving consideration to the combination of sturdiness, thermal and electrical conductance, and thermoelectric power.

It is more difficult to make the temperature differences between the calorimeter and its surroundings small when there are temperature gradients on the surface of the calorimeter and the shield. The first step, therefore, was to minimize temperature gradients. This was accomplished in several different ways, depending upon the particular calorimeter. In two calorimeters, mechanical stirring was used to distribute heat and thus reduce the temperature differences over the surface of the calorimeter. In the calorimeter designed for higher pressures and temperatures, for which mechanical stirring would have been difficult, bubbles of vapor mixed the fluid as in a coffee percolator and heat was distributed further by conduction in a system of silver vanes. In a fourth small calorimeter, many copper vanes distributed the heat by conduction.

It is not only important to consider the temperature gradients in the calorimeter but also the gradients in its surroundings. Although it is true that calorimetric procedures usually reduce the effect of errors which are due to temperature gradients in a shield, this reduction of errors is more effective if the gradients are small and essentially independent of the environment. One calorimeter used a stirred liquid bath to distribute heat over a shield (shell) surrounding the calorimeter. In another calorimeter at higher temperatures, for which it was impractical to use a stirred liquid bath, a heavy silver shield was used to distribute heat from a heater wound on it. In still another designed for the maximum accuracy at moderate temperatures, a novel heat distribution system using a saturated vapor bath was very effective over a large surface.

In addition to minimizing heat transfer coefficients and temperature gradients, the remaining unavoidable temperature differences were recorded and summed algebraically so corrections could be made for the net amount of heat transfer. The evaluation of the overall heat leak in an experiment was performed by dividing the heat leak into four parts, (*i*) the heat leak to the shield from most of the surface area of the calorimeter, usually measured by means of a combination of thermocouples, (*ii*) the heat leak along the upper tube connecting to the calorimeter, (*iii*) the heat leak

along the lower tube and (*iv*) a heat leak called the "residual" heat leak, which is that heat leak occurring when there is no indicated temperature difference between the calorimeter and its surroundings. In order to evaluate the various heat leaks adequately, it was necessary to give systematic attention to experiments designed for this purpose. For example, the residual heat leak was usually evaluated before and after each experiment. Experiments to evaluate the various heat transfer coefficients at different temperatures were made daily by deliberately exaggerating the temperature difference and measuring the change of temperature produced in the calorimeter.

The most difficult problem in measuring and evaluating heat leak is the measurement of the effective temperature differences along the various paths for heat flow between the calorimeter and its surroundings, especially when the calorimeter is not at thermal equilibrium. One obvious solution of this problem would be to use a great many thermocouples located at representative places. In one calorimeter[9], 38 thermocouples were used to obtain information on temperature distribution. Of these, 31 had measuring junctions located on the calorimeter and its immediate surroundings. Experience had shown that the design of the attachment of a thermocouple junction to a calorimeter was vital to the validity of the temperature measurement. When the thermojunction could be soldered directly to metal, it was assumed to be in good thermal contact. In this case, if the wires were small and made of material having low thermal conductivity, the temperature of the junction would represent the temperature of the metal to which it was attached. In most cases, however, the thermocouple junctions needed to be electrically insulated from the metal so that they could be connected in series for averaging temperatures or be used for measuring temperature differences. Since most good electrical insulators are also good thermal insulators, a special type of thermocouple attachment was developed. This type of attachment, called a "thermal tie-down" and shown in *Figure 2*, was used extensively in all calorimeters developed by Osborne and his colleagues. It has been used subsequently in a calorimeter described in Chapter 9. Basically, this thermojunction tie-down consists of a gold terminal, *T*, insulated by thin mica, *M*, all pressed firmly against the metal part by a nut on a threaded stud. Two or more gold terminals were used together to connect thermocouples with each other. If the thermocouples were to be used in a region where there would be large temperature gradients and heat flow along the thermocouple wires which would affect the temperature of the thermojunctions, thermal tie-downs were used on the lead wires before they reached the thermojunction. In some calorimeters, second tie-downs were used for this purpose. This type of thermal tie-down was found to be effective even in an evacuated space. The general theory of heat tempering along wires is discussed in Chapter 4.

An alternative method of minimizing heat leak uncertainties, which avoided the use of a multitude of thermocouples, was developed for one calorimeter[12]. The principle of this method seems so important to calorimetry that some discussion will now be given. In accurate calorimetry, it is desirable to utilize the comparison method as much as possible for minimizing errors. In heat capacity calorimetry, the comparison method is used by

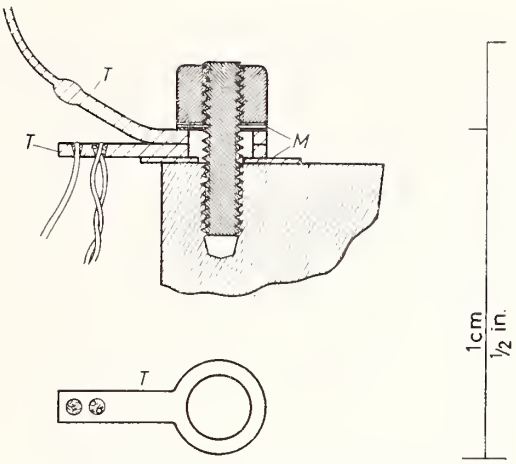

Figure 2. Details of thermal tie-downs.

making two series of experiments, one gross series with the calorimeter nearly full and one tare series with the calorimeter nearly or completely empty. If the two series of experiments are made in the same manner, the gradients on the shield (immediate surroundings) should be very nearly identical in the two series of experiments. If the gradients on the calorimeter are also the same in the two series, the heat leak will be the same. Even though its magnitude is not known, the heat leak should be balanced out by differences when the tare measurements are subtracted from the gross measurements. The difficulty with this assumption is that different amounts of the sample in the calorimeter practically always give rise to different temperature gradients in the calorimeter, so that the above assumption is not usually valid. It is possible, however, to design a calorimeter which validates this assumption reasonably. The principle of the design is to add an outer calorimeter surface whose temperature–time function is essentially independent of the contents of the calorimeter, so that temperature gradients on it are the same in the gross and tare series. This can be accomplished by providing an outer calorimeter surface which is thermally separated from the sample container except in one chosen zone whose temperature is measured. Examples of this type of construction have been given in Chapter 9. and further examples are given later in this chapter.

Another characteristic of all four of the calorimeters used by Osborne and his collaborators in the study of water and hydrocarbons was the use of a "reference block" to contain the platinum resistance thermometers which determine the temperature on the international scale. Many experimenters using a resistance thermometer place it inside the calorimeter and use its temperature at equilibrium to represent the temperature of the calorimeter. In the calorimeters used by Osborne and his collaborators, the resistance thermometers were placed in a reference block separate from the calorimeter. The block temperature was kept at about the same temperature as the calorimeter, and all temperatures on the calorimeter and its surroundings were

referred to the reference block temperature by means of thermocouples. The use of a reference block has several advantages. (*i*) The heat capacity of the empty calorimeter can be less. (*ii*) It facilitates the use of two or more resistance thermometers instead of one, so that a failure of one resistance thermometer may be detected before it invalidates the experimental results. (*iii*) By the use of a silver or copper block of appropriate dimensions, the reference block can conveniently provide an isothermal region for both the resistance thermometers and the reference junctions of thermocouples. By using thermocouples differentially so that the thermocouple wires do not pass through large temperature gradients, most of the effects of thermocouple inhomogeneities are avoided. While the use of a reference block has the above advantages, it adds two complications which may have prevented its general use. These are (*i*) that it may require a more complex design and also (*ii*) that the temperature of the reference block may have to be controlled separately, depending on the design.

IV. Calorimeters for Measuring Properties of Water

1. *Calorimeter for* 0–270°*C*

The first calorimeter described here was used to measure values of the thermodynamic properties α, β, and γ of water up to 270°C. *Figure 3* shows a diagram of the calorimeter and its accessory parts. In the bottom of the calorimeter there was a double centrifugal pump which served two functions, (*i*) to circulate liquid over almost the entire inner wall of the calorimeter and (*ii*) to flow water in a thin stream over the heater, located near the top of the calorimeter. The pump capacity was sufficient to circulate the entire contents of the calorimeter in about 5 sec, so that temperature gradients on the calorimeter surface were minimized. Furthermore, in the vaporization experiment, the use of a thin flowing layer of water over the heater, H, permitted quiet evaporation, thus producing essentially saturated vapor. The calorimeter was held in place by the upper and lower tubes, ST, inside a shell, E, whose temperature was controlled by a circulating oil bath. In the upper part of this bath was located the reference block, R, containing three resistance thermometers, T, and various reference junctions of thermocouples, J. The upper and lower tubes, connecting to the calorimeter, led to throttle valves used for controlling the flow of vapor or liquid, respectively. In the vaporization (γ) experiments, vapor flow was diverted from one receiving container to another by valves actuated by time signals. In the β experiments (withdrawal of liquid), however, only one receiving container was used, so that the flow of liquid was started and stopped during an experiment.

In this calorimeter, α experiments were made over the entire range 0–270°C, but β and γ experiments were made only over the range 100–270°C. The values of α from these experiments were converted to H, enthalpy at saturation pressure referred to 0°C, by using measured values of β above 100°C. Below 100°C, the values of β are so small that values calculated from the relation $\beta = TV\,\mathrm{d}P/\mathrm{d}T$ were better. The values of ΔH_v were obtained directly from the observed values of β and γ between 100 and 270°C. The accuracy of the derived values of H, C, and ΔH_v was usually

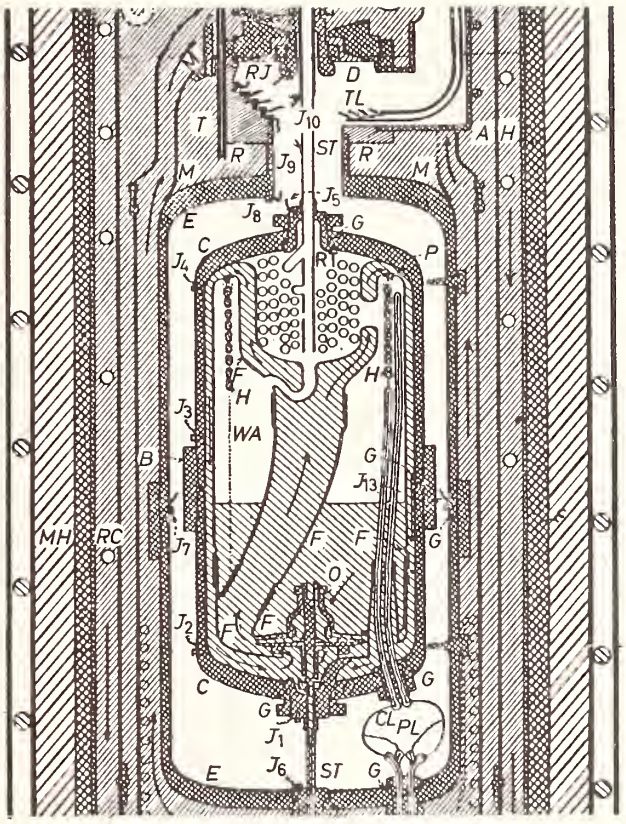

Figure 3. Calorimeter for 0–270°C

C, Calorimeter shell
E, Envelope shell (shield)
B, Threaded band
G, Gold gaskets
ST, Support tubes
I, Pump impeller
F, Pump casing
O, Ball bearings
P, Water port
H, Calorimeter heater
WA, Gauze apron
CL, Current lead
PL, Potential lead
R, Reference block
M, Mantle
J_1, J_2, etc., Measuring junctions of thermocouples
RJ, Reference junctions of thermocouples
TL, Thermocouple leads
T, Platinum resistance thermometer
AH, Auxiliary heater
MH, Main heater
RC, Refrigerating coil

better than 0·1 per cent, as confirmed by experiments with two later calorimeters.

2. *Calorimeter for* 100–374°C

This calorimeter was designed for measurements on water up to the critical temperature (about 374·1°C) and pressure (about 218 atm). Because of the higher pressure and temperature, the design required more mechanical strength and corrosion resistance. Although in the earlier calorimeter (0–270°C) a copper–nickel alloy had sufficient strength for the calorimeter

shell, it was necessary in the 100–374 °C calorimeter to use a special non-corrosive alloy steel to avoid mechanical creep at the higher temperatures. *Figure 4* shows a diagram of this calorimeter, together with some of its

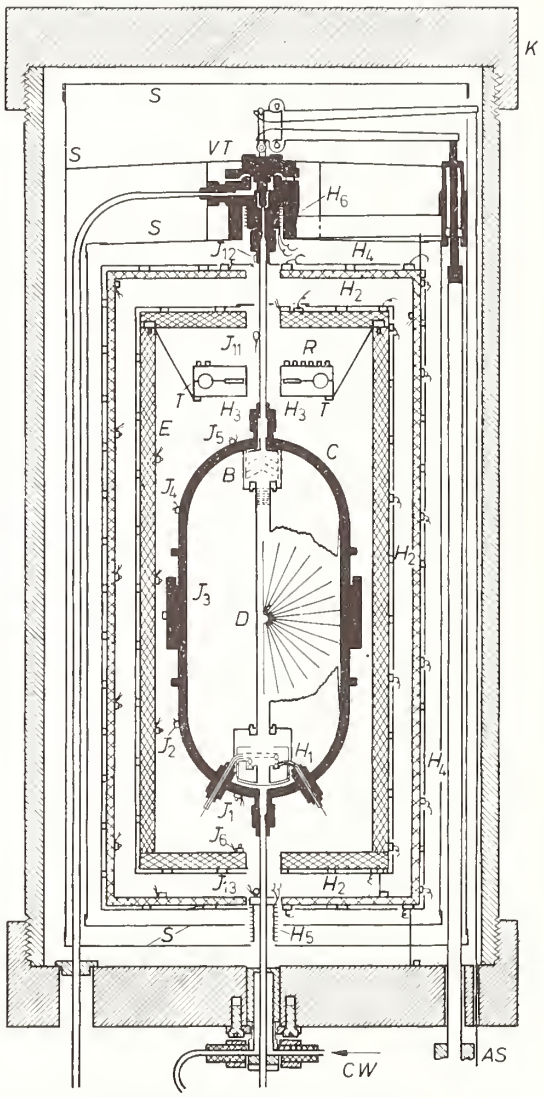

Figure 4. Calorimeter for 100–374 °C

C,	Calorimeter shell	H_2,	Shield heater
H_1,	Calorimeter heater	H_4,	Guard heater
D,	Heat diffusion system	H_5,	Lower tube heater
R,	Reference block	*CW*,	Cooling water
H_3	Reference block heater	*S*,	Aluminum radiation shields
T,	Platinum resistance thermometers	*VT*,	Vapor throttle valve
J_1, J_2, etc.	Measuring junctions of thermocouples	H_6,	Heater for valve
E,	Shield	*AS*,	Adjusting screw for valve
		K,	Outer casing

accessory parts. The calorimeter heater, H_1, was located in the bottom of the calorimeter, C, and was concentrated so as to produce bubbles of vapor for convective mixing by use of the principle of the coffee percolator. A system of radial silver vanes, D, was placed inside the calorimeter to speed thermal equilibrium and minimize temperature gradients. As in the previous example, the calorimeter was held in place by the upper and lower tubes, in a space surrounded by a shield, E, made of $\frac{1}{4}$ in. thick silver. The reference block, R, also located in this space above the calorimeter, held two platinum resistance thermometers, T, and the reference junctions of the thermocouples. In this apparatus there were 38 thermocouples, 13 located on the outer surface of the calorimeter, 12 on the inner surface of the shield ($\frac{1}{4}$ in.), 2 on the upper tube, 1 on the vapor throttle valve, VT, 3 on the lower tube and 7 on the inner surface of another silver shell ($\frac{1}{8}$ in.) which served as a guard surrounding the shield. One purpose of the guard was to supply most of the heat required at a steady state, so that essentially no heat was needed in the shield when accurate temperature measurements were made at thermal equilibrium. This procedure helped make the temperatures on various parts of the shield independent of changes in outside temperatures. The heaters, H_2 and H_4, on both the shield and guard were distributed approximately proportional to area. The guard was thermally insulated by successive thin aluminum shells, S, surrounding it to impede the loss of heat both by radiation and convection. The use of thin aluminum also minimizes thermal lag in the insulation, thereby enabling the control of guard temperature to be fast.

One feature of this calorimeter, which was believed to be important in vaporization experiments at temperatures approaching the critical temperature, was the baffle system, B, located in the vapor flow path at the exit from the calorimeter. This baffle system, made of silver gauze, was designed to catch small water drops so that they would not be carried out of the calorimeter. Evidence of the effectiveness of the baffle system was obtained by measurements at different rates of vaporization on the assumption that, if drops were formed, the amount of liquid so entrained and carried out with the vapor would vary with the rate and show differences in the results. Additional evidence on the effectiveness of the baffle system was obtained from special measurements of the specific volume of vapor, described later. In this calorimeter, vaporization experiments were successfully made up to within about one degree of the critical temperature before any evidence of entrained water droplets was found.

The apparatus was also provided with means for observing the pressure in the calorimeter, using a diaphragm-type pressure-transmitting cell in the liquid line to confine the liquid while transmitting the pressure to a pressure gauge. The use of this calorimeter for accurate measurement of the vapor pressure of water is described in a separate publication[8]. In the calorimetric experiments for β and γ, this provision for pressure measurement proved very useful. At thermal equilibrium before starting an experiment, the pressure in an outside container was made equal to that inside the calorimeter, as indicated by the null position of the diaphragm in the pressure transmitting cell. During the γ experiment, the fluid withdrawal rate was controlled so that the pressure in the calorimeter was the same as

before the experiment. In this way, the surface of the liquid in the calorimeter was maintained essentially at the starting temperature, even though most of the liquid became somewhat warmer during evaporation. The throttle valves used to control the fluid withdrawal rate were specially designed to provide continuous adjustment without back-lash.

Since this calorimeter was used for accurate pressure measurements, it was possible to provide an independent check on β and γ at high temperatures where the possibility of mixing of liquid and vapor phases might exist, even though there had been no evidence for it in the experiments changing the rate of flow. As stated earlier in section II of this chapter using the Clapeyron relation we have

$$\gamma = TV'\mathrm{d}P/\mathrm{d}T$$
$$\text{and } \beta = TV\mathrm{d}P/\mathrm{d}T.$$

If V' and V are known, values of γ and β can be calculated from the vapor pressure data. Although it was not convenient to use the calorimeter as a volume-measuring device for extensive measurements on the specific volumes of saturated liquid and vapor, a method was devised to make such measurements at 370°C in order to check the calorimetrically measured γ and β. For these measurements it was possible to establish a reasonably sharp boundary for the volume of the calorimeter, by means of the thermocouples and heater on the lower tube from the calorimeter. From a calibration of this volume it was possible to measure the specific volumes of both the saturated liquid and vapor at 370°C, and to calculate values of γ and β by using the vapor pressure data. These calculated values of γ and β agreed with the calorimetrically measured values of γ and β to within about 0·3 per cent, which could be attributed to the error of these specific volume measurements.

3. *Calorimeter for 0–100°C*

Measurements of the heat capacity of water in the range 0–100°C have special significance because water has been used for a heat capacity standard in this range. The calorimeter described here was designed to obtain as high an accuracy as possible, using the techniques available in 1938, on both heat capacity and enthalpy of vaporization. Following Osborne's method, this meant measurements of α, β, and γ. However, at temperatures below 100°C, β is so small that values calculated by using the Clapeyron relation were more accurate than values measured calorimetrically. At 100°C, β is less than 0·1 per cent of γ, and at lower temperatures it is a still smaller fraction. Therefore, no measurements of β were made with this calorimeter.

In order to strive for accuracies of 0·01 per cent for heat capacities, it was decided to use a calorimeter with a capacity larger than the earlier ones, namely almost 1200 cm³. It was thought that a large sample would be more favorable for higher accuracies for several reasons. (*i*) The mass accounting should be more reliable. (*ii*) The volume of a calorimeter of a given shape increases as the cube of the linear dimension, whereas the surface increases only as the square and hence the area subject to heat leak is proportionately less. (*iii*) A sphere has the least surface for its volume and the spherical

shape deforms less under pressure. At temperatures seldom exceeding 100°C the pressure would be moderate so the calorimeter could be thin-walled.

It was recognized that the larger surfaces of the calorimeter would cause larger temperature differences which would be less favorable for heat leak accounting, so it was decided to stir the liquid contents by using a synchronous motor for its constant speed. By these means it was possible to keep the effective heat capacity in the low-filling experiments down to less than 5 per cent of the effective sample size, which is the difference between masses of samples in high and low fillings. (With many calorimeters the empty calorimeter heat capacity is more than 20 per cent of the sample heat capacity.)

A study was made of the method of the stirring to provide the maximum amount of mixing with a minimum of pump power. The system chosen is shown in *Figure 5*. The circulating system consisted of two screw propellers on one shaft, and a system of guides to direct the water flow. The larger (upper) propeller, P_1 did most of the circulating, and the smaller (lower) propeller, P_2, was used to avoid stagnation in the extreme bottom of the calorimeter. The liquid went downward next to the wall of the calorimeter shell and was directed by radial guides, *PG*, at the bottom so that the liquid flowed without swirl past the heater, H_1, into the propeller. The water from the propellers was guided axially upward by a circulator pump casing, *PC*, and curved guide vanes served to remove the swirl imparted to the water by the propellers. A synchronous motor kept the pump speed very constant at 70 rev/min which gave adequate circulation while dissipating only about 0·004 W in the calorimeter. Such low pump power was possible in this design because the water level was not raised as it had been in the 0–270°C calorimeter. It was found, however, that even with this low power, there was a random variation in the dissipated pump power which may have been a major contribution to the variation in the experimental results.

The calorimeter shell, *C*, was made of copper, all surfaces of it and parts inside were gold-plated, and the outer calorimeter surface was polished to minimize heat transfer by radiation. A baffle, *B*, was installed near the vapor outlet tube to prevent passage of liquid drops during the vapor withdrawal experiments.

For accurate evaluation of electric power in the calorimeter, particular attention was given to the design of the calorimeter heater. The earlier calorimeter heaters had resistances of about 10 Ω with the usual four electrical leads, i.e., two current leads and two potential leads attached to the current leads at points midway between the calorimeter and its surrounding shield. This selection of points for attaching the potential terminals seemed reasonable for measuring the power to the calorimeter. The choice of size and resistance of the current leads between the calorimeter and shield was a compromise between the amount of heat developed in the leads and the heat transferred along these leads. With calorimeter heaters having 10 Ω resistance, this compromise was difficult to make when accuracies of 0·01 per cent were sought. If, however, the heater resistance was increased from 10 Ω to 100 Ω, the relative heat developed in the leads compared to that in the calorimeter heater was reduced by a factor of 10. A discussion of this problem is given in Chapter 4. The resistance of this

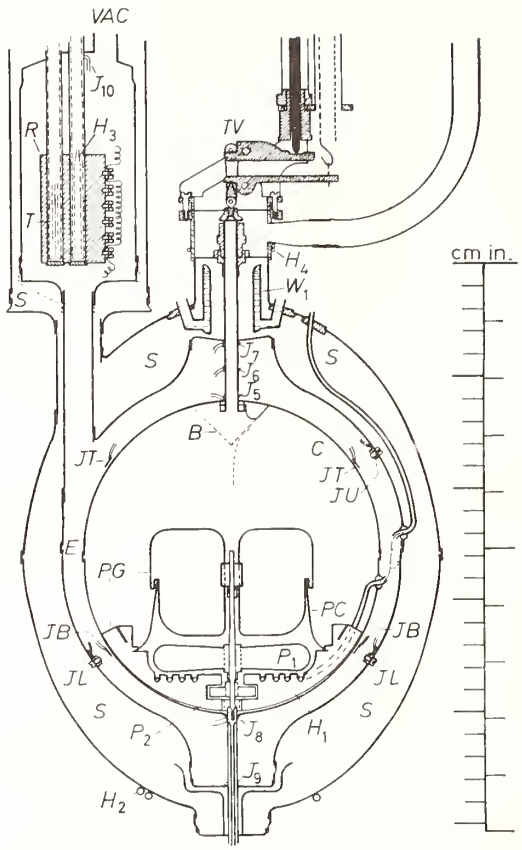

Figure 5. Calorimeter for 0–100°C

C,	Calorimeter shell	H_2,	Steam bath heater
H_1,	Calorimeter heater	*R*,	Reference block
P_1, P_2,	Pump propellers	H_3,	Heater for block
PC,	Pump casing	*T*,	Platinum resistance thermometers
PG,	Flow guides	W_1,	Condenser
B,	Gauze baffle	*TV*,	Throttle valve
JT, J_5, etc.,	Measuring junctions of thermocouples	H_4,	Heater for valve
S,	Saturated steam bath	*VAC*,	Vacuum line

calorimeter heater was made about 107 Ω so that the problem of accounting for heat developed in the leads was considerably simplified. Actually the entire heat developed in both current leads between calorimeter shell and shield amounted to only about 0·03 per cent of the heat developed in the calorimeter heater.

In this calorimeter a different method of attaching potential leads was used. The mid-points of the current leads between the calorimeter and shield became hot, so that it seemed preferable to avoid attaching potential leads to the mid-points if possible. One potential lead was attached to one current lead where it entered the calorimeter shell and the other potential

lead was attached to the other current lead where it entered the shield. If the two leads are tied down thermally to the calorimeter and the shield symmetrically, the method accounts better for the heat developed in the leads.

The shield for this calorimeter was double-walled so as to contain a saturated steam bath, S, to control its temperature. This type of temperature control has considerable advantage for large areas such as in this calorimeter. The principle of the saturated steam bath is simply that, for a metal surface covered with a thin film of liquid, the metal surface temperature is determined essentially by the pressure of the saturated vapor. If the surface is cooler than the saturation temperature, some vapor will condense to warm the surface. If, on the other hand, the surface is warmer than the saturation temperature of the vapor but is wet, some liquid will evaporate until the surface cools to the saturation temperature. This system is very effective when the surface can be kept wet with a thin film of liquid. In this apparatus, the surface of the saturated steam bath was kept wet by condensing liquid at the top and directing the condensate down over the inner wall of the shield. The outer wall of the shield was kept wet automatically because its surroundings were always kept slightly cooler. The pressure of the saturated vapor was controlled by a heater located in the liquid water at the bottom of the bath. The liquid necessary to wet the shield surface (inner saturated steam bath surface) was supplied by two condensers, one at the top of the shield and the other in the top of a part of the saturated steam bath which contained the reference block, R. In this way, the reference block temperature was maintained essentially at the shield temperature which in turn was controlled to a temperature very close to that of the calorimeter. The reference block accommodated several resistance thermometers, T, and also the reference junctions for the thermocouples.

There were eight thermocouples, JT, JB, with measuring junctions distributed in azimuth and height on the surface of the calorimeter, in an attempt to give them equal weighting for heat leak accounting. Individual leads to these thermocouples were brought out either for check of the temperature uniformity, when used individually, or for connection in series for evaluation of the average temperature. All eight were used in series to measure the temperature difference between calorimeter and reference block, or the group of eight could be opposed to eight corresponding thermocouples distributed over the inside area of the shield for maintaining adiabatic conditions. In addition to these, there were three thermocouples, J_5, J_6, J_7, on the upper tube and two thermocouples, J_8, J_9, on the lower tube. The thermocouple, J_6, located at the mid-point of the upper tube, furnished data for calculation of the temperature of the vapor leaving the calorimeter during the vaporization experiments. The thermocouples used in all the calorimeters described here were made of Chromel P versus Constantan (or their equivalent) because these materials give a high thermoelectromotive force ($\sim$60 μV/°C near room temperature) and have reasonable thermal and electrical resistivities.

Since this calorimeter was intended to give results consistent with the best techniques available in 1938, some discussion will now be given of the precautions taken to insure highest accuracy. This discussion will be in three parts as follows.

A. Accounting for Mass of Sample

Precautions were taken to insure pure samples of water and proper accounting for the masses. In the heat capacity measurements, the difference in masses of water in the calorimeter in the high and low fillings was approximately 1 kg. In all experiments, the amount initially put into the calorimeter was compared with the amount finally taken out. Usually these amounts agreed to 0·02 g, which corresponded to about 1 part in 50000 in the heat capacity experiments. When the mass accounting was not this accurate, the experimental results were discarded. In preparing the sample, precautions were taken to reduce the impurities (including dissolved gases) to a negligible amount. For transferring samples, the connecting tubes were evacuated before the transfer. In the vaporization experiments, the mass taken out in a typical experiment was about 20 g. Systematic precautions were taken to insure reproducible weighing conditions for the sample container. It is believed, therefore, that the accounting for mass was not the principal limitation on the overall accuracy of the results.

B. Accounting for Energy

The energy supplied to the calorimeter can be considered in three principal parts (*i*) the electrical energy supplied, (*ii*) the energy supplied by the circulating pump, and (*iii*) the heat leak from the calorimeter. These three parts will now be considered, with emphasis on their effects on the overall accuracies of the experiments.

(*1*) *Electrical Energy.* With modern techniques the measurement of electrical energy does not seem to be a limitation on the accuracy of calorimetric experiments. For standards of e.m.f., a group of saturated standard cells was maintained in a specially insulated aluminum box whose temperature was controlled constant within 0·01 °C[4]. These standard cells and also the resistance standards were calibrated periodically. The temperatures of both the standard cells and the standard resistors were usually checked at both the beginning and the end of the day. Two specially constructed volt boxes were used in combination so that if any part of either volt box changed resistance between calibrations, the daily check on them would detect it. A check was made at least twice a day for any change in the potentiometer factor. This check consisted essentially of comparing a given potentiometer reading (which is effectively a ratio) with the ratio of two standard resistors.

The accounting for heat developed in the current leads to the calorimeter heater has already been discussed. Another small effect which was considered was the "starting effect" of the change in calorimeter heater resistance immediately after the current was started. With the high resistance of the calorimeter heater which required a high voltage storage battery, it was not convenient to use an external resistor having the same resistance in order to minimize the effect on power of change in resistance of the heater[3]. Consequently, because of a significant change in resistance of the heater during the first 30 sec before the first power reading, the calorimeter heater power could not be extrapolated perfectly from regular periodic observations starting at 30 sec. A study was made of this starting correction, observing the change in power during the first 30 sec. The result was that a correction

was made which amounted to only 0·01 per cent of the whole energy input, even for the extreme case of a short experiment.

In addition to measurements of power, measurements of time intervals were necessary in order to calculate energies. These time interval measurements were perhaps the easiest of all measurements because they were determined by using accurate standard time signals (seconds). The time signals were used to trip a switch in the heater circuit. The time for operation of this switch was determined to be negligible.

(*2*) *Pump Energy.* As mentioned previously, the pump power in the heat capacity experiments was approximately 0·004 W which, with the pump running continuously, amounted to about 0·015 per cent of the energy put into the sample during a typical 10° heat capacity experiment. Although this is small, separate measurements of this power were made near the time of the experiment in order to estimate the correction. Even though the pump speed was very constant, the mechanical power dissipated was found to vary at random by amounts larger than could be accounted for by the uncertainty in temperature measurement. This variation, however, was usually not more than would correspond to about 0·005 per cent for the value of α.

(*3*) *Heat Leaks.* The accurate control and measurement of heat leak is vital in accurate calorimetry. Heat leaks in this calorimeter are classified, like those in earlier calorimeters, into shield heat leak, upper tube heat leak, lower tube heat leak, and residual heat leak. Measurements of these heat leaks were made daily throughout the experiments, and calibration experiments were made for determinations of the various heat transfer coefficients. In spite of the large calorimeter surface it was possible to keep the shield heat leak down to a very low value by use of the evacuated space and polished gold-plated surfaces. The use of numerous thermocouples on this surface, in addition to the effective use of the circulating pump to reduce temperature gradients, made it possible to reduce the actual shield heat leak to a small value. The residual heat leaks, such as could have resulted from imperfect weighting of the controlling thermocouples, were almost negligible and were automatically included with the pump energies in the experiments. The upper and lower tube heat leaks were small and were accurately evaluated by the thermocouples located on them. In the heat capacity experiments, the net corrections applied for all measured heat leaks averaged less than 0·001 per cent of the energy put into the sample.

C. Accounting for Change in State

The temperature of the calorimeter was determined by measurements with platinum resistance thermometers, calibrated on the International Temperature Scale, combined with thermocouple measurements. The temperature of the calorimeter was observed at essentially thermal equilibrium at the beginning and end of each experiment. For this temperature measurement, the temperature of the reference block containing the resistance thermometers was brought very close to the temperature of the calorimeter, as indicated by the eight thermocouples (in series) having measuring junctions on the calorimeter and reference junctions on the reference block. Thus, the temperature measured by the resistance thermometers was essentially the

average temperature of the calorimeter, except for a small difference which was calculated from the thermocouple readings. For this calculation, the sensitivity of the thermocouples was determined in place directly against the resistance thermometers.

In all the experiments, the change in proportion of liquid and vapor in the calorimeter is accounted for in the theory of the method as described earlier. In the vaporization experiments, the calorimeter was usually about half-full. Under this condition, the temperature of the vapor leaving the calorimeter was determined by means of the group of four thermocouples on the upper part of the calorimeter, representing its average temperature, in conjunction with the three thermocouples giving temperatures along the upper tube. During the actual vaporization and withdrawal of vapor through the upper tube, this tube was tempered by the outgoing vapor so there was no correction for upper tube heat leak during this period. In the vaporization experiments, the shield heat leak accounting was slightly less accurate than in the heat capacity experiments because of the larger temperature gradients on the calorimeter. These gradients were larger on account of the sharp temperature gradient in the liquid next to the surface where evaporation was taking place. These gradients were large even when the circulating pump speed was increased to 106 rev/min. A small correction, sometimes amounting to as much as 0·002 per cent and depending on the location of the liquid level in the calorimeter, was applied to account for the change in liquid level.

4. *Comparison of results with the three calorimeters*

Of the three calorimeters described, the 0–100°C calorimeter was designed to have the highest accuracy, probably about 0·01 per cent. It is interesting to compare the results from this calorimeter with the results from the others where measurements were made at the same temperatures. In all three calorimeters, the measurements were made of the enthalpy of vaporization at 100°C. If the vaporization results with the 0–100°C calorimeter are used as a basis for comparison at 100°C, the 0–270°C calorimeter gave a value 0·06 per cent high whereas the 100–374°C one gave a value 0·02 per cent high. Measurements of enthalpy of vaporization at 50°, 70°, and 90°C with the 0–270°C calorimeter[2] gave values averaging less than 0·02 per cent higher than the one used for 0–100°C. Heat capacities from measurements made with the 0–270°C calorimeter could also be compared with those from the one used for 0–100°C over its entire range. These values were found to be about 0·07 per cent higher.

V. Calorimeter for Hydrocarbons

As part of a program for the investigation of the properties of hydrocarbons, accurate measurements of enthalpies of vaporization at 25°C of a large number of pure samples were needed. The calorimeter described here was designed particularly for measuring these although it was used for a few times at other temperatures above and below 25°, both for vaporization and heat capacity experiments.

In designing this calorimeter, there were three principal aims. (*i*) The calorimeter shell should be made small because some of the pure hydrocarbons were available in relatively small amounts. (*ii*) The measurements

(especially vaporization) should be accurate to at least 0·1 per cent. (*iii*) The apparatus should permit relatively rapid measurements of vaporization so that a large number of materials could be investigated. Making the calorimeter small has certain other advantages besides favoring the use of small samples. In a small calorimeter, it is possible to distribute heat by conduction with a system of many copper vanes and dispense with mechanical stirring. These vanes minimized the time required for thermal equilibrium and contributed both to accuracy and ease of operation. Mechanical stirring was purposely avoided after having found in the 0–100°C calorimeter that there were unpredictable variations in the dissipated pump power. Another advantage of a small calorimeter is that it is possible to use effectively unheated metal shields for the control and evaluation of heat leak, and thus practically eliminate one common source of error in adiabatic heat capacity calorimetry. This important feature will be discussed while describing details of the apparatus.

Because measurements on most of the materials were at temperatures considerably below the normal boiling point, values of the quantity β were negligible in some cases, and in other cases small enough so that they could be calculated adequately from known thermal properties of the material. Therefore, this calorimeter was not provided with a lower tube for β experiments. All samples were vaporized into and out of the calorimeter. A schematic drawing of the apparatus is shown in *Figure 6*, and a scale drawing of essential features is shown in *Figure 7*. The calorimeter, holding approximately 100 ml of sample, had the heat distributing system shown in *Figure 8*.

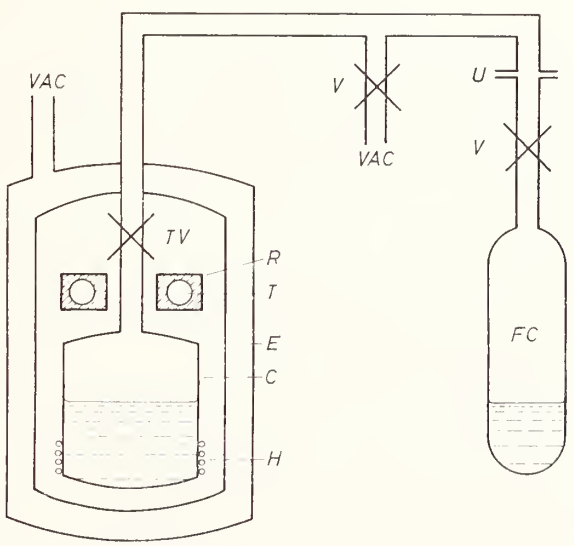

Figure 6. Schematic diagram of calorimeter for hydrocarbons

C,	Calorimeter shell	*R*,	Reference block
E,	Adiabatic shield	*T*,	Resistance thermometer
FC,	Fluid container	*TV*,	Throttle valve
H,	Calorimeter heater	*U*,	Union
V,	Valve	*VAC*,	Vacuum line

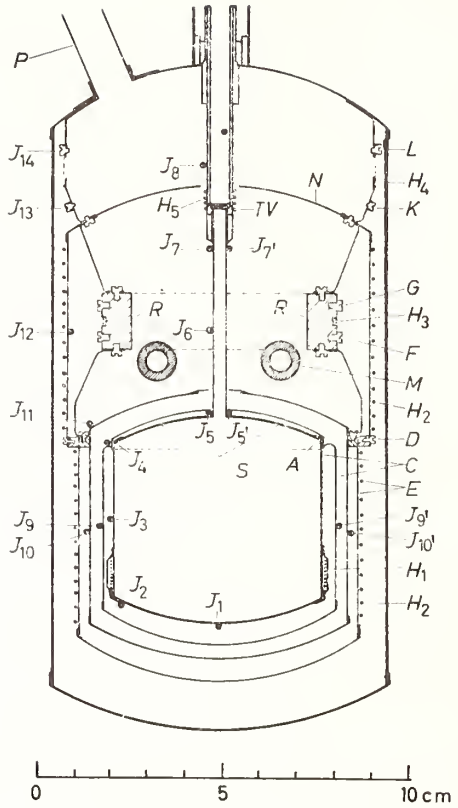

Figure 7. Scale drawing of calorimeter for hydrocarbons

A, Attachment of calorimeter shell to its shield
C, Calorimeter shell and shield
D, Attachment of adiabatic shield to its shield
E, Adiabatic shield with its shield
F, *G*, *K*, *L*, Zones of thermal attachment of thermocouples
H_1, Calorimeter heater
H_2, Adiabatic shield heater
H_3, Reference block heater
H_4, Heater
H_5, Throttle valve heater
J_1, J_2, etc., Measuring junctions of thermocouples
M, Receptacles for platinum resistance thermometers
N, Deck of adiabatic shield
P, Lead wire and vacuum duct
R, Reference block
S, Gauze baffle
TV, Throttle valve seat

The tinned copper vanes were arranged so that no point in the liquid sample was more than 3 mm from a conducting metal part. The heater, H_1, (100 Ω) was located on the bottom part of the calorimeter shell, as shown in *Figure 7*. The heater was covered with a copper sheath soldered to the calorimeter shell. Thermocouple measuring junctions, *J*, were located as shown, with reference junctions on the reference block. The calorimeter shell was provided with a thin copper 'heaterless' shell surrounding it and attached to it

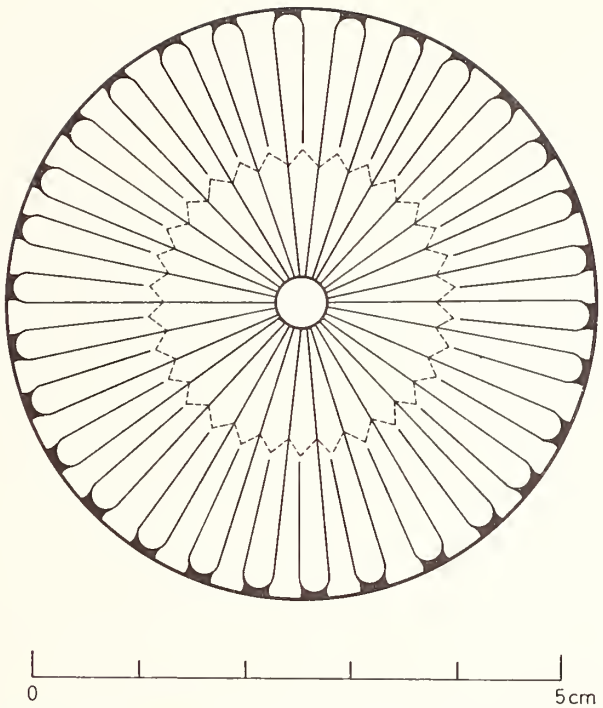

Figure 8. Heat distribution system in a calorimeter for hydrocarbons.

at one zone. Thus, so far as calorimetric experiments were concerned, this thin shell was part of the calorimeter where energy must be accounted for. The calorimeter was surrounded with an adiabatic shield, E, provided with heaters. This adiabatic shield, similar to the calorimeter shell, was also provided with a thin heaterless copper shell which was attached inside the shield at a zone at the same height as that on the calorimeter. Thus the outer calorimeter surface was one heaterless thin copper shell and the inner shield surface another. The calorimeter shell, the adiabatic shield, the heaterless copper shells and the reference block, R, were all gold plated and polished to minimize radiation emittance. The spaces between and around these parts were evacuated to eliminate gaseous conduction and convection. There were therefore two paths for heat leak from the calorimeter, one by radiation from the polished gold surface of the calorimeter heaterless thin shell, and the other by solid conduction along the upper tube and electrical leads from the calorimeter which were thermally attached to the tube. The heat leak along the upper tube was controlled and measured by means of the thermocouples $(J_7–J_5)$ and $(J_{7'}–J_{5'})$ attached to it. The heat leak from the calorimeter was controlled and measured using the thermocouples $(J_{10}–J_9)$ and $(J_{10'}–J_{9'})$.

In the vaporization experiments, even though there was a significant temperature gradient on the calorimeter shell, the heaterless copper shell attached to the calorimeter shell was nearly isothermal owing primarily to the very low heat transfer coefficient to the calorimeter at all points except

at the chosen attachment zone. The thermocouples J_9 and $J_{9'}$ measured effectively the temperature of the calorimeter surface relative to the temperature of the reference block. Similarly, in the vaporization experiments, J_{10} and $J_{10'}$ measured the temperatures of the surrounding surface.

During the heat capacity experiments, however, there were necessarily temperature gradients on both of these heaterless shells. Although the two thermocouples were located so as to represent approximately the average temperature of these two surfaces when heating, it is not necessary that they do so. When using the method of two series of heat capacity experiments, a gross series and a tare series, the only requirement is that both surfaces have the same temperature distributions at corresponding times in both series of experiments. This means that to have a valid heat leak accounting, any change in temperature gradients on the surface of the calorimeter shell itself must not affect the temperature distribution on its heaterless shell. With the design shown, the temperature distribution on this heaterless shell was essentially independent of any temperature gradients on the calorimeter shell due to either the presence of the sample or the type of experiment conducted.

Similarly, the temperatures on the heaterless shell which was attached to the adiabatic shield were independent of the temperature gradients on the adiabatic shield. Thus with this design in the heat capacity experiments, the thermocouples (J_{10}–J_9) were not required to measure the true heat leak in any experiment, although these thermocouples probably did so.

It is believed that the above principle of design is vital to all calorimetry and that many of the differences in results in accurate calorimetry can be attributed to the effects on heat leak caused by temperature gradients in the calorimeter and by changes in these gradients between the gross and tare series in heat capacity experiments. A much more comprehensive discussion of this and related questions is given in Chapter 9.

Since further details of the apparatus can be obtained from the original publication, further discussion will be limited to significant points in its use and the accuracies obtained. The effectiveness of the overall heat accounting was remarkable. It was proved possible to use this calorimeter for accurate vaporization experiments with samples of less than 3g in the calorimeter. In various vaporization experiments, temperature differences on the calorimeter varied by about 1°, depending upon liquid level and rate of vaporization. In spite of this there was no evidence of change in measured enthalpy of vaporization due either to liquid level or to rate of vaporization. This latter independence is also evidence of the withdrawal of essentially saturated vapor, rather than of either superheated vapor or vapor containing liquid droplets. The independence of the measured enthalpies of vaporization upon temperature differences in the calorimeter shell was evidence of the effectiveness of the method using unheated shields.

Possibly the most convincing evidence of the accuracy of this calorimeter is the comparison of results on the same material used both in this calorimeter and the earlier 0–100°C calorimeter. For this purpose, vaporization measurements at 25°C were made on water before, during, and after the series of experiments on 59 hydrocarbons. The average of the measurements, with the present calorimeter, for enthalpy of vaporization at 25°C differed

by about 0·001 per cent from the tabulated value in the previous work[11], and the average deviation of values from individual experiments from this tabulated value was about 0·01 per cent.

It is interesting to note that this calorimeter was used also on materials having relatively low vapor pressures, such as *n*-oetane. With this material, the mass rate of withdrawal was limited to about 0·15 g/min. In spite of these unfavorable conditions, it is believed that the results justify the estimate of accuracy of 0·1 per cent in the vaporization experiments, which was made when the calorimeter was designed.

Although the heat capacity experiments with this calorimeter were incidental to the vaporization experiments, it is interesting to examine the heat capacity results for evidence of their accuracy. Here again, possibly the best evidence lies in a comparison of results on water used to check the performance of the calorimeter. Heat capacity measurements with water were made at the beginning and near the end of this series of experiments. It was found that the 30 experiments with water gave results about 0·025 per cent different from the previous results in the 0–100°C calorimeter. Additional evidence was also available in the measurements on *n*-heptane, because some experiments were made on a sample of heptane in the 0–100°C calorimeter. In spite of the use of a sample from a different source, heat capacity measurements in the range 10–35°C gave an average deviation of 0·037 per cent from a least-square formulation of the results with the 0–100°C calorimeter. It is of interest that these earlier experimental measurements gave an average deviation of 0·028 per cent from the same formulation. The evidence from the results seems to indicate that the hydrocarbon calorimeter, although intended for vaporization experiments, is capable of an accuracy better than 0·1 per cent for heat capacity experiments in its temperature range.

VI. Other Calorimetric Methods for Measuring Enthalpy of Vaporization

The calorimeters described have been used in vaporization measurements in the range 0–374°C and at pressures up to 218 atm. No attempt will be made to describe other vaporization calorimeters which use similar methods in this temperature range. At temperatures below 0°C heat capacity calorimeters have also been used for vaporization measurements. Some of these are described in Chapters 5 and 6. At high temperatures at which accurate direct measurements of enthalpy of vaporization are very difficult or impossible, indirect measurements can be made by using the Clapeyron relation $\Delta H_v = T(\mathrm{d}P/\mathrm{d}T)\,(V' - V)$. For this evaluation the determination of $\mathrm{d}P/\mathrm{d}T$ is probably the most difficult.

In the direct methods described, the heat required to vaporize the liquid has usually been supplied by electrical heaters because of the convenience and accuracy of the electrical measurements. Some measurements, mostly of historic value, have measured the heat of condensation, rather than that of vaporization.

Another direct method which has proved useful in certain vaporization measurements is the transpiration method, sometimes known as the carrier gas method. In this method, which has application mostly below the normal boiling temperatures of liquids, vapor is removed from the calorimeter

with an inert carrier gas. Measured electric power is usually used to evaporate the liquid. An advantage of this method is the relative ease in controlling the rate of vaporization by controlling the rate of flow of the carrier gas; no elaborate throttle valve is required for this control. A recent example of the application of this method at 25°C is the work of Wadsö[13], who measured enthalpies of vaporization of samples as small as 0·15 g to an accuracy better than 0·5 per cent. His calorimeter was designed for samples having vapor pressures at 25°C in the range 1–100 mm Hg.

In the transpiration method there are several precautions that should be considered in addition to the usual heat leak measurement. As in the method used by Osborne and colleagues it is necessary, in principle, to make a β vaporization correction, that is, to correct for the vaporization into the space occupied by the liquid evaporated. As pointed out earlier, this vaporization correction is small and sometimes negligible at temperatures below the normal boiling point. Another possible correction, which is usually small, allows for departures from the ideal process of evaporation at saturation pressure, such as might occur at large rates of gas flow.

Another interesting vaporization calorimeter using the transpiration method is that of Coon and Daniels[1]. They made measurements on small samples of carbon tetrachloride incidental to its use as a refrigerating material in microcalorimetry. By using twin calorimeters and compensating unknown heat with the vaporization of carbon tetrachloride they were able to measure exothermic reactions at room temperature which gave heat rates of about 4 J/h.

VII. Summary

Discussion has been mainly of calorimetry of saturated fluids, as carried out at the National Bureau of Standards over the period 1928–1942. From these experimental measurements values of enthalpy of vaporization, heat capacities and derived thermodynamic quantities were obtained. Four calorimeters have been described, three for water to pressures of 218 atm in the temperature range 0–374°C, and one for hydrocarbons near 25°C. An effort has been made to discuss the advantages and disadvantages both of method and various experimental features. Although in general this calorimetry was carried out with as high an accuracy as the "state of the art" permitted at the time, it must be remembered that the calorimeters were developed about three decades ago. With advances in technology since that time, and with the benefit of the experience with these calorimeters, it seems certain that improvements could now be made in both design and operation.

VIII. References

[1] Coon, E. D., and F. Daniels, *J. Phys. Chem.* **37**, 1 (1933).
[2] Fiock, E. F., and D. C. Ginnings, *J. Res. Natl. Bur. Std.* **8**, 321 (1932).
[3] Hoge, H. J., *J. Res. Natl. Bur. Std.*, **36**, 111 (1946).
[4] Mueller, E. F., and H. F. Stimson, *J. Res. Natl. Bur. Std.*, **13**, 699 (1934).
[5] Osborne, N. S., *Bu. Stds. Bull.*, **14**, Scientific Papers 301, 313, and 315 (1917).
[6] Osborne, N. S., *J. Opt. Soc. Am.*, **8**, 519 (1924); *J. Res. Natl. Bur. Std.* **4**, 609 (1930); *Trans. Am. Soc. Mech. Engrs.*, **52**, 221 (1930).
[7] Osborne, N. S., H. F. Stimson, and E. F. Fiock, *J. Res. Natl. Bur. Std.* **5**, 411 (1930); *Trans. Am. Soc. Mech. Engrs.*, **52**, 191 (1930).

[8] Osborne, N. S., H. F. Stimson, and D. C. Ginnings, *J. Res. Natl. Bur. Std.*, **10**, 155 (1933); *Mech. Eng.*, **54**, 118 (1932).
[9] Osborne, N. S., H. F. Stimson, and D. C. Ginnings, *J. Res. Natl. Bur. Std.*, **18**, 389 (1937).
[10] Osborne, N. S., H. F. Stimson, and D. C. Ginnings, *J. Res. Natl. Bur. Std.*, **23**, 197 (1939).
[11] Osborne, N. S., H. F. Stimson, and D. C. Ginnings, *J. Res. Natl. Bur. Std.*, **23**, 261 (1939).
[12] Osborne, N. S., and D. C. Ginnings, *J. Res. Natl. Bur. Std.*, **39**, 453 (1947).
[13] Wadsö, I., *Acta Chem. Scand.*, **14**, 566 (1960).

U. S. Department of Commerce National Bureau of Standards

RESEARCH PAPER RP1693

Part of Journal of Research of the National Bureau of Standards, Volume 36, February 1946

HEAT CAPACITY OF A TWO-PHASE SYSTEM, WITH APPLICATIONS TO VAPOR CORRECTIONS IN CALORIMETRY

By Harold J. Hoge

ABSTRACT

A formula is derived that gives the heat capacity of a system composed of solid or liquid in equilibrium with saturated vapor in terms of the specific heat of the condensed phase and certain auxiliary data. This formula is valid throughout the entire range from 0 to 100 percent of vapor, and at the latter extreme reduces to a well-known relation between the specific heats of saturated liquid and saturated vapor.

The formula is applied to the calculation of vapor corrections in calorimetry. Its advantage lies in the fact that the correction is expressed as a single term that may be readily transformed with Clapeyron's equation, yielding two alternative correction formulas.

Vapor corrections to the heat capacity and to the heat of fusion are summarized and tabulated for four different experimental procedures in calorimetry.

CONTENTS

I. INTRODUCTION

A solid or liquid having an appreciable vapor pressure will partially vaporize when placed in a closed calorimeter. The presence of vapor, which changes both in volume and density as the temperature is changed, makes it necessary in such cases to apply a vapor correction to heat-capacity data. The size of the correction varies with the degree of filling of the calorimeter. In practice it seldom exceeds 3 or 4 percent of the heat capacity of the solid or liquid, but under unusual conditions has been reported to be as large as 20 percent [1].*

Osborne and Van Dusen [2] appear to have been the first to give a detailed mathematical treatment of the problem of vapor corrections. Their equations are given in the Handbuch der Experimentalphysik [3] and seem to have been widely adopted. In 1924 Osborne [4, 5] gave a new treatment of the problem of vapor corrections based on the practice of making duplicate calorimetric runs, one with a large and the other with a small amount of material in the calorimeter. He appears to have been the first to use this method, which has

* Figures in brackets indicate the literature references at the end of this paper.

several advantages, among which are the elimination both of the effect of material in the filling tube and the effect of strain on the heat capacity of the calorimeter. Others who have discussed vapor corrections, either incidentally or in detail include Babcock [6], Awbery and Griffiths [7], and Bennewitz and Splittgerber [8].

All the correction formulas given by these authors are mathematically and physically correct, but some are unnecessarily complicated. Nowhere has it been clearly brought out that the correction can always be expressed in two alternative forms, one of which is in terms of latent heats, the other in terms of vapor pressures. The present paper is an attempt to clarify the situation, and to present in their simplest form the equations needed for making the vapor correction in any ordinary calorimetric experiment. It is thought that these correction formulas may help to eliminate the unnecessary work that is sometimes done when vapor pressure data are first used to compute latent heats, the latent heats then being used in a vapor correction formula. In such a calculation the specific volume of the vapor appears twice, once in Clapeyron's equation, and again in computing x, the fraction of the material in the vapor phase. If incorrect vapor volumes are used, incorrect latent heats are obtained, but this error is exactly compensated by the error in x, so that the vapor correction is independent of the assumed vapor volume. It seems unlikely that investigators have been generally aware of this fact.

The starting point in the derivation given below is an equation for the entropy of a two-phase system. This considerably shortens the derivation as compared with the conventional approach of accounting for all the energy supplied, and yields the results directly in the desired form without the necessity of combining terms. The suggestion that the problem be treated from the entropy standpoint was made by Harold W. Woolley, and it was this point of view that led to equation 5.

II. HEAT CAPACITY OF A TWO-PHASE SYSTEM

Consider a mass M [1] of material confined in a volume, V, and partially vaporized, so that there are M_g grams of gas in equilibrium with M_c grams of condensed phase, which may be either solid or liquid. This system has a definite heat capacity, provided the volume, V, is a definite function of temperature, for if this is the case, the state of the system is completely defined by the temperature. The pressure in the system is always the vapor pressure of the material. We wish to find an expression for the heat capacity of this system. This is most easily done by finding an expression for the total entropy of the system, and finally converting this expression by differentiation into an equation giving the desired heat capacity.

Let s_g and s_c be the entropies per unit mass of saturated vapor and saturated condensed phase, respectively. Then the total entropy of the system is

$$\begin{aligned} S &= M_c s_c + M_g s_g \\ &= M s_c + M_g (s_g - s_c). \end{aligned} \tag{1}$$

[1] Symbols are defined as they appear, and a table of symbols used is given at the end of this paper.

Since $s_g - s_c$ is the entropy of vaporization per unit mass it is equal to l/T, where l is the heat of vaporization per unit mass, so that

$$S = Ms_c + M_g l/T. \tag{2}$$

The quantity $M_g l/T$ may be considered an "excess" entropy, since it represents the difference between the entropy of the actual system and that of the corresponding system with no vapor phase. Putting $S' = M_g l/T$ we have

$$S = Ms_c + S' \tag{3}$$

and differentiating with respect to T

$$\frac{dS}{dT} = M\frac{ds_c}{dT} + \frac{dS'}{dT}. \tag{4}$$

Now for any reversible absorption of heat $dS = \delta Q/T = CdT/T$. Hence we may substitute $dS/dT = C/T$ and $ds_c/dT = c_c/T$, where C is the heat capacity of the two-phase system and c_c is the heat capacity of unit mass of saturated condensed phase. This gives

$$C = Mc_c + T\frac{dS'}{dT}, \tag{5}$$

which is the basic formula for the heat capacity of a two-phase system.

The next problem is to evaluate $S' \equiv M_g l/T$. The mass of vapor, M_g, can be expressed in terms of the total mass, M, the total volume, V, and the specific volumes of vapor and condensed phase, v_g and v_c, as follows:

$$\begin{aligned} V &= M_c v_c + M_g v_g \\ &= Mv_c + M_g(v_g - v_c), \end{aligned}$$

whence

$$M_g = \frac{V - Mv_c}{v_g - v_c}. \tag{6}$$

The excess entropy is therefore

$$S' \equiv \frac{M_g l}{T} = \frac{l}{T}\frac{V - Mv_c}{v_g - v_c}. \tag{7a}$$

The quantity $l/[T(v_g - v_c)]$ is by Clapeyron's equation equal to dp/dT, the slope of the vapor-pressure curve. This substitution gives an alternative expression for excess entropy.[2]

$$S' = \frac{dp}{dT}(V - Mv_c). \tag{7b}$$

Equations 5, 7a, and 7b, permit c_c, the specific heat of saturated condensed phase to be calculated from C, the heat capacity of the two-phase system, and certain auxiliary data, which may be either l, V, v_g, and v_c; or dp/dT, V, and v_c. When these formulas are used to make vapor corrections they will ordinarily be applied to systems whose vapor fraction, or dryness ($=M_g/M$) is between 0 and 10 per-

[2] A shorter but less obvious method of getting equations 7a and 7b is to note that S' is the change in entropy when the volume occupied by the material is increased from Mv_c to V at constant temperature, so that $S' = (\partial S/\partial V)_T(V - Mv_c)$. Since, by Maxwell's relation $(\partial S/\partial V)_T = dp/dT$, we have 7b at once and 7a may be obtained from 7b by use of Clapeyron's equation.

cent. They are valid, however, throughout the whole range from 0 to 100 percent dryness. For the limiting case of 100 percent dryness, 5 and 7a yield a well-known relation between the heat capacities of saturated vapor and saturated liquid. For this particular case, $V=Mv_g$, so that S' is simply Ml/T, and 5 is

$$C=Mc_g=Mc_c+T\frac{d}{dT}\left(\frac{Ml}{T}\right),$$

where c_g is the heat capacity per gram of saturated vapor. Since M is independent of T, this reduces to the usual form

$$c_g-c_c=T\frac{d}{dT}\left(\frac{l}{T}\right). \tag{8}$$

III. VAPOR CORRECTION TO THE HEAT OF FUSION

When a melting point or other first-order transition is encountered in a two-phase system, special formulas are needed for making the vapor correction. The simplest way to obtain these is to start with equation 3, the equation for the entropy of the two-phase system, $S=Ms_c+S'$. Let the subscript "a" refer to the system just before the transition starts (solid-gas) and let the subscript "b" characterize it at the end of the transition (liquid-gas). The change in entropy during melting is, by equation 3,

$$S_b-S_a=M(s_{cb}-s_{ca})+S'_b-S'_a. \tag{23}$$

If Q is the measured quantity of heat supplied during the process, then $Q/T=S_b-S_a$. Likewise, $s_{cb}-s_{ca}$, the difference in specific entropies of the two condensed phases, is l_f/T, where l_f is the heat of fusion per gram. Making these substitutions and multiplying by T gives

$$Q=Ml_f+T(S'_b-S'_a). \tag{24}$$

The excess entropies may be evaluated with the formulas previously developed. If 7a is used,

$$S'_b-S'_a=\left[\frac{(V-Mv_c)}{(v_g-v_c)}\right]_a^b, \tag{25}$$

while if 7b is used,

$$S'_b-S'_a=\left[\frac{dp}{dT}(V-Mv_c)\right]_a^b \tag{26}$$

When evaluating these expressions it should be remembered that the only quantities having the same value at both limits are V, M, T, and v_g.

The vapor correction to the heat of fusion may be considered to be made up of two parts. One part is due to the fact that M_g is not zero, and hence not all of the total mass M takes part in the process of melting. The other is due to the fact that M_g generally changes a little one way or the other owing to a difference between v_{ca} and v_{cb}. This causes the absorption or liberation of the heat of vaporization of a small amount of material.

IV. APPLICATION TO CALORIMETRY

Use of the formulas derived above in making vapor corrections is a straightforward procedure that need not be discussed in detail. The vapor correction is not made until after the calculation of the gross, tare, and net heat capacities. In calculating both the gross and the tare heat capacities it may be necessary to apply a curvature correction [reference 9, p. 79]. After this correction has been applied it is convenient to tabulate the gross and tare heat capacities at 5-degree intervals and to subtract one table from the other to obtain the net heat capacity. The vapor correction is then applied to the net heat capacity.

The working formulas for this purpose depend on the type of experiment. Four different types of experiment may be considered, characterized by the presence or absence of a filling tube that contains a small part of the calorimetric charge, and by whether the tare charge is zero or a mass of material M_2, which is small compared to the gross charge M_1 but sufficient to fill the system with saturated vapor at all temperatures.

In the next section the appropriate formulas for each of the four types of experiment are tabulated. The quantities which must be known in order to evaluate the formulas are also listed. These are divided into two groups: the basic data, which are required regardless of the vapor correction; and the auxiliary data, which are needed only to evaluate the vapor correction. For one type of experiment, formulas are given which contain M_t, the mass of material in the filling tube. These formulas may be derived by treating the vapor in the tube as an ideal gas. The problem is essentially the same as that of correcting for the gas in the capillary of a gas thermometer [10]. In order that the filling tube shall contain only vapor, it is of course necessary that no part of it shall have a temperature lower than that of the calorimeter proper.[3]

In calculating the vapor correction, the derivative $d\bar{E}'/dT$ must always be calculated, and in many cases the derivative dp/dT also. A procedure which has been found satisfactory for this purpose is to tabulate $\bar{E}'$ (or p) at 5-degree intervals and to calculate $\Delta\bar{E}'/\Delta T$ for each interval. The values of $\Delta\bar{E}'/\Delta T$ are ordinarily sufficiently good approximations to the values of $d\bar{E}'/dT$ at the midpoints of the intervals. Where greater accuracy is desired, formulas such as that of Rutledge [11], which are based on polynomial approximations of higher degree may be used.

The author acknowledges valuable discussions with M. S. Van Dusen, of the Bureau's Pyrometry Section.

[3] Osborne and his coworkers have for certain experiments used a filling tube that is at all times filled with liquid. This requires the opposite condition—that no part of the tube shall have a temperature higher than that of the calorimeter proper.

V. SUMMARY OF FORMULAS AND REQUIRED DATA

For definitions of terms and symbols, see section VI.

Type 1. Gross charge: M
Tare charge: 0
Filling tube: No

$$\begin{cases} c_c = \dfrac{C_{net} - T dS'/dT}{M} \\ \\ l_f = \dfrac{Q - T(S'_b - S'_a)}{M} \\ \\ \text{Basic data: } C_{net},\ M,\ T,\ Q \end{cases}$$

$$\begin{cases} S' = \dfrac{l}{T}\dfrac{V - Mv_c}{v_g - v_c} \\ \\ \text{Auxiliary data: } l_a,\ l_b,\ V,\ v_{ca},\ v_{cb},\ v_g \end{cases}$$

or

$$\begin{cases} S' = \dfrac{dp}{dT}(V - Mv_c) \\ \\ \text{Auxiliary data: } (dp/dT)_a,\ (dp/dT)_b,\ V,\ v_{ca},\ v_{cb}. \end{cases}$$

Type 2. Gross charge: M_1
Tare charge: M_2
Filling tube: No

$$\begin{cases} c_c = \dfrac{C_{net} - Td(S'_1 - S'_2)/dT}{M_1 - M_2} \\ l_f = Q_{net} - T\dfrac{[(S'_1 - S'_2)_b - (S'_1 - S'_2)_a]}{M_1 - M_2} \\ \text{Basic data: } C_{net},\ M_1 - M_2,\ T,\ Q_{net}, \end{cases}$$

$$\begin{cases} S'_1 - S'_2 = -\dfrac{l}{T}\dfrac{(M_1 - M_2)v_c}{v_g - v_c} \\ \text{Auxiliary data: } l_a,\ l_b,\ v_{ca},\ v_{cb},\ v_g. \end{cases}$$

or

$$\begin{cases} S'_1 - S'_2 = -\dfrac{dp}{dT}(M_1 - M_2)v_c \\ \text{Auxiliary data: } (dp/dT)_a,\ (dp/dT)_b,\ v_{ca},\ v_{cb}. \end{cases}$$

Type 3. Gross charge: M_1
Tare charge: M_2
Filling tube: Yes

The temperature distribution in the tube must be the same in the tare run as in the gross run. With this precaution, the quantities M_t and dM_t/dT drop out of the working equations, which become identical with those for an experiment of type 2.

Type 4. Gross charge: M
Tare charge: 0
Filling tube: Yes

$$\begin{cases} c_c = \dfrac{C_{net} - TdS'/dT - ldM_t/dT}{M - M_t} \\ l_t = \dfrac{Q - T(S'_b - S'_a)}{M - M_t} \\ \text{Basic data: } C_{net},\ M,\ T,\ Q. \end{cases}$$

$$\begin{cases} S' = \dfrac{l}{T}\dfrac{V - (M - M_t)v_c}{v_g - v_c} \\ \text{Auxiliary data: } l_a,\ l_b,\ V,\ v_{ca},\ v_{cb},\ v_g \end{cases}$$

or

$$\begin{cases} S' = \dfrac{dp}{dT}[V - (M - M_t)v_c] \\ \text{Auxiliary data: } (dp/dT)_a,\ (dp/dT)_b,\ V,\ v_{ca},\ v_{cb} \end{cases}$$

also

$$\begin{cases} M_t = p\dfrac{W}{R}\sum_i \dfrac{V_i}{T_i} \\ \dfrac{dM_t}{dT} = \dfrac{W}{R}\left[\dfrac{dp}{dT}\sum_i \dfrac{V_i}{T_i} + p\dfrac{d}{dT}\sum_i \dfrac{V_i}{T_i}\right] \\ \text{Auxiliary data: } p,\ V_t,\ T_t,\ dp/dT. \end{cases}$$

VI. DEFINITIONS AND SYMBOLS

Calorimeter.—That part of the apparatus which contains the material and participates in absorbing the measured power input.
Charge.—Mass of material in the calorimeter and filling tube.
Filling tube.—Tube extending from the calorimeter to outside the apparatus. Contains a small part of the total charge during measurements.
Gross heat capacity.—Heat capacity of calorimeter plus a large charge M_1.
Tare heat capacity.—Heat capacity of calorimeter with no charge, or with a small charge M_2.
Net heat capacity.—Gross heat capacity minus tare heat capacity.

C=heat capacity
c=specific heat (heat capacity per unit mass)
l=heat of sublimation, vaporization or fusion per unit mass
M=mass of charge contained in calorimeter and filling tube
p=pressure, equal to vapor pressure of material at temperature T
Q=heat absorbed during a transition such as melting
R=gas constant
S=entropy
S'=excess entropy of a system, as compared with the same mass of saturated condensed phase
s=entropy per unit mass
T=absolute temperature of calorimeter and contents
V=volume of the calorimeter

v=volume per unit mass
W=molecular weight of the material
x=fraction of the material in the vapor phase, sometimes called dryness.

SUBSCRIPTS

a=pertaining to the form stable below a transition
b=pertaining to the form stable above a transition
c=condensed phase, solid or liquid
f=pertaining to fusion
g=gaseous phase
i=pertaining to the ith element of volume of the filling tube
t=pertaining to the filling tube
1=corresponding to the gross charge M_1
2=corresponding to the tare charge M_2.

VII. REFERENCES

[1] A. Eucken and E. Schröder, Low temperature caloric measurements on a few fluorides (BF_3, CF_4, SF_6), Z. physik. Chem. [B] **41,** 307–319 (1938).
[2] Nathan S. Osborne and Milton S. Van Dusen, Specific heat of liquid ammonia, Bul. BS **14,** 397–432 (1918) S313.
[3] A. Eucken, Hand. Experimentalphysik **8,** part 1, p. 291–294 (1929).
[4] Nathan S. Osborne, Calorimetry of saturated fluids, J. Opt. Soc. Am. & Rev. Sci. Instr. **8,** 519–540 (1924).
[5] Nathan S. Osborne, Calorimetry of a fluid, BS J. Research **4,** 609–629 (1930) RP168.
[6] Henry A. Babcock, The specific heat of ammonia, Proc. Am. Acad. Arts Sci. **55,** 323–409 (1920).
[7] J. H. Awbery and Ezer Griffiths, The specific heat of liquid CH_3Cl, Proc. Phys. Soc. **52,** 770–776 (1940).
[8] K. Bennewitz and E. Splittgerber, Investigations in the critical region. I. Specific heat of CO_2 near the critical point, Z. physik. Chem. **124,** 49–65 (1926).
[9] N. S. Osborne, H. F. Stimson, T. S. Sligh, Jr., and C. S. Cragoe, Specific heat of superheated NH_3 vapor, BS Sci. Pap. **20,** 65–110 (1925) S501.
[10] Harold J. Hoge and Ferdinand G. Brickwedde, Establishment of a temperature scale for the calibration of thermometers between 14° and 83° K, J. Research NBS **22,** 351–373 (1939) RP1188.
[11] George Rutledge, A reliable method of obtaining the derivative function from smoothed data of observation, Phys. Rev. **40,** 262–8 (1932).

Washington, October 24, 1945.

Offprinted from the *Transactions of The Faraday Society*,
No. 489, Vol. 59, Part 9, September, 1963

Heating Rate as a Test of Adiabatic Calorimeters and the Heat Capacity of α-Alumina*

By E. D. West

Heat Division, National Bureau of Standards, Washington, D.C.

Received 14*th January*, 1963

The constancy of heat capacities measured in an adiabatic calorimeter at different heating rates does not demonstrate the absence of heat leak errors due to departures of the surface temperature from the "isothermal" condition. On the contrary, the total heat exchange between the calorimeter and its shield is virtually independent of the heating rate. The tests tend to obscure a real source of error due to the variation in the total heat exchange between experiments with the empty and the full calorimeter.

Edwards and Kington [1] have recently described a low-temperature adiabatic calorimeter together with measurements of the heat capacity of α-alumina. Their data, in common with other sets of data discussed in their paper, were generally higher than the results of Furukawa *et al.*,[2] and of West and Ginnings.[3] As a possible explanation, Edwards and Kington considered heat loss: "One possible explanation might be offered in terms of a non-isothermal surface on the calorimeter or radiation shield. This effect has been investigated by using different calorimeter heating rates. At slower rates of heating there is a greater chance of attaining a near-isothermal surface on the calorimeter and shield." Their experiments at different heating rates revealed no significant effect and they concluded, "Thus no explanation can be found from this source for the difference between the present results and those of Furukawa *et al.*"

The variation of heating rate is commonly used to test calorimeters, although the effects to be revealed by the variation usually are not specified. It will be shown below that the variation should not be expected to detect the heat exchange due to non-isothermal surfaces on the calorimeter and adiabatic shield.

In an adiabatic calorimetric apparatus, the calorimeter is surrounded by an adiabatic shield. Usually the temperatures of the outer surface of the calorimeter and the inner surface of the shield are sensed by a thermocouple (or a thermopile) and the two temperatures (or average temperatures) are controlled to be equal. During the heating period, the heat flow (energy per unit time) from the respective heaters sets up temperature gradients with the result that the effective temperatures of the surfaces of the calorimeter and shield differ from the temperatures at the thermocouple junctions. The result is, in general, a net heat flow to or from the calorimeter.

Edwards and Kington argue that, at lower heating rates, the calorimeter and shield surfaces will be more nearly isothermal. There can be no disagreement with this statement, nor with the implication that the rate at which heat flows between the calorimeter and shield will be smaller at lower heating rates. In fact, in most adiabatic calorimeters, temperature differences on either of the surfaces and the corresponding heat flow between them are, to a good approximation, directly proportional to the heating rate except for transients.

* with special reference to *Trans. Faraday Soc.*, 1962, **58**, 1313.

The continuous heating method for adiabatic calorimetry minimizes transient effects in the heat exchange between calorimeter and shield. After the calorimeter heater has been on for a sufficient time, the temperature distribution in an adiabatic calorimeter reaches a quasi-steady state in which the temperature at all points in the calorimeter and shield is rising at the same rate and the temperature difference between any two points is constant and proportional to the heating rate. If one of the points is that at which the temperature for shield control is taken, it is apparent that the average temperature difference of the other points on the calorimeter is proportional to the heating rate. A similar argument applies to the shield relative to the control point on it. The heat flow resulting from these deviations from isothermal surfaces is therefore proportional to the heating rate.

For calorimeters using alternate heating and equilibration periods, the transients due to turning the power on and off confuse the problem of heat flow. With the approximation implicit in most calorimetry that the heat flow equations are linear, the principle of superposition can be used to express the temperature as a sum of terms satisfying various boundary and initial conditions.* The temperature difference between the control point and an arbitrary point on the surface of the calorimeter or on the surface of the shield can be expressed as a sum of three terms: (i) the quasi-steady state distribution, satisfying exactly the same equations as in continuous heating, but taken to be zero outside the heating period; (ii) a transient at the beginning of the heating period to allow for the fact that the quasi-steady state is not set up instantaneously; and (iii) a final transient after the end of the heating period to allow for the gradual decay of the quasi-steady state after the heater is turned off. Assuming no geometrical changes during the heating period, as from melting or mechanical motion, the same heat flow equations and boundary conditions apply to both the beginning and final transient terms. At the beginning of the heating period, the temperature gradient due to heating is zero, but the quasi-steady state term used to describe heat flow during the heating period is independent of time as in continuous heating calorimetry. The " initial " condition is therefore imposed on the beginning transient term that it must be equal and opposite to the quasi-steady state term. When the calorimeter is turned off, the quasi-steady state term is set to zero and its decay is described by the final transient. The " initial " condition on the final transient is therefore imposed that it be equal to the quasi-steady state term. The transients are therefore equal and opposite for equal increments of time (see footnote). If the final temperature of the calorimeter is taken after the transients become negligible, the sum of the time integrals of the heat flow due to the transients is also negligible. The heat exchange between the calorimeter

* There are two sources of heat in the apparatus: the calorimeter heater and the shield heater. Some of the shield heater power flows to the surroundings, assumed to be at some constant temperature, and some goes to raise the temperature of the shield during the heating period. The effect of the first part of the shield proper is to set up a gradient in the shield which causes a temperature mismatch and an exchange of heat between the calorimeter and the shield throughout the experiment. Heat leak observations at equilibrium can be used to correct for this heat leak. The remaining shield power and the calorimeter power are present only during the heating period, so that no observations of heat leak can be made independent of heat capacity measurements. However, by putting the shield-to-environment temperature difference in the boundary conditions for the heat leak at equilibrium, we obtain homogeneous boundary conditions on the terms describing the gradients in the calorimeter and shield during heating. From the equal and opposite magnitude of the initial conditions on the transients, it follows that they are equal and opposite for equal increments of time. (If y is a solution to a homogeneous differential equation, with homogeneous boundary conditions, then ky is also a solution, where k is any constant, including $k = -1$ as required by our initial condition.) The mathematics have been worked out in detail for an accurately defined physical model.[4]

and the shield due to heating the calorimeter can now be treated as due to the same quasi-steady state gradients in the calorimeter and shield as in continuous heating; that is, an adiabatic calorimeter should give the same observed heat capacities by either method. For intermittent as well as continuous heating, it follows that the average temperature of the calorimeter or shield surface differs from the temperature at the control point and that this difference and the corresponding heat flow are proportional to the heating rate.

It does not follow that the rate of heating affects the observed heat capacity. The effect of heat flow between calorimeter and shield on the observed heat capacity is due to the total heat exchanged, not to the rate at which the exchange takes place; i.e., the length of the heating period must be taken into account. The effect of the heat exchanged is apparent from the following argument:

If the power P generated in the calorimeter is subject to no other appreciable effect than the one under consideration (or has been corrected), then, from conservation of energy, one obtains the relation

$$C\Delta T = (P+P_L)\Delta t,$$

where C is the heat capacity, P_L is the small quasi-steady state heat flow between the calorimeter and the shield, Δt is the time interval, and ΔT is the temperature interval for an experiment. It was shown above that $P_L = kP$, where k may be a positive or negative constant depending on the apparatus. Substituting in the equation above and rearranging gives the result,

$$P\Delta t/\Delta T = C/(1+k).$$

Although various combinations of P and Δt may be taken to give the temperature increase over which comparison is made, the observed heat capacity based on these quantities is wrong by the constant ratio $1/(1+k)$. Evidently, the observed heat capacity, in this somewhat simplified view, could not be expected to vary with the heating rate. This conclusion is bolstered by observations with a high-temperature adiabatic calorimeter.[3] For heating rates different by a factor of two, the observed heat capacities agree to about one part in 10,000, although the calorimeter surface temperature varies up to 0·1° from the temperature at the location of the control thermopile. The heat loss from the calorimeter corresponding to this temperature gradient is about 36 times the reproducibility of the measurements.

Since the heat capacity experiments at different heating rate do not reveal the effects of the heat exchange during heating, it must be admitted as a possibly significant quantity in the work of Edwards and Kington, as well as in the work of other groups. It is suggested here that the differences in heat capacity obtained by various groups are due in part to differences in the unknown heat exchange in experiments with the full and empty calorimeter.

Edwards and Kington remark that three independent sets of authors report positive deviations from the work of Furukawa *et al.* Two other sets of data may be considered. Martin [5] reports heat capacities at room temperature 0·2 to 0·3 % higher than those of Furukawa *et al.*, but 0·4 to 0·5 % below those of Edwards and Kington. West and Ginnings report agreement with the room temperature data of Furukawa *et al.* to $\pm$0·02 %. In the design of the calorimeter used in the latter measurements considerable care was taken to make the surface temperature distributions the same for the empty and the full calorimeter. The analysis presented here does not, however, explain the predominantly positive deviations from the work of Furukawa *et al.*, and of West and Ginnings. As Edwards and Kington point out, the cause of such generally positive systematic deviations is worth further investigation.

The question of which calorimeter gives the best data for the heat capacity of Al_2O_3 cannot be answered unequivocally. To analyze heat flow in each apparatus completely is not possible from information given in publications. Too many additional details of construction are required. Even with these details, probably only rough estimates are possible. A major problem in accurate adiabatic calorimetry is to develop methods to demonstrate experimentally that no changes are made in the surface temperature distribution and in the thermal contact of the control thermocouple when the sample is introduced. Evidently, data for the heat capacity of Al_2O_3 of more generally accepted accuracy would be of value.

It may be pointed out that the systematic error due to the unknown heat exchange will, in general, differ from one sample to another, depending on thermal properties. Even if exact values were available for the heat capacity of Al_2O_3, it would not necessarily follow that a calorimeter which reproduced those values would give comparable data for other materials.

[1] Edwards and Kington, *Trans. Faraday Soc.*, 1962, **58**, 1313.
[2] Furukawa, Douglas, McCoskey and Ginnings, *J. Res. Nat. Bur. Stand.*, 1956, **57**, 67.
[3] West and Ginnings, *J. Res. Nat. Bur. Stand.*, 1958, **60**, 309.
[4] West, *J. Res. Nat. Bur. Stand.*, 1963, *67A*, 331.
[5] Martin, *Can. J. Physics*, 1962, **40**, 1166.

A Two-Body Model for Calorimeters with Constant-Temperature Environment

Estal D. West and Kenneth L. Churney

National Bureau of Standards, Washington, D. C.

(Received 18 March 1968)

Equations are derived describing a model of an isoperibol calorimeter in which the calorimeter proper consists of two parts thermally connected, one surrounding the other and exchanging heat with the constant-temperature environment. These solutions provide insights into the behavior of real calorimeters. Inferences are drawn relative to the effect of the locations of the thermometer and heat source on the energy equivalent of the calorimeter and some possible errors are pointed out. Macleod's application of the two-body theory of King and Grover to high-temperature enthalpy measurements is discussed and weaknesses in theory and experiment are pointed out. Procedures having a better theoretical basis are outlined.

INTRODUCTION

Isoperibol calorimeters[1]—those in which the temperature of the calorimeter varies and the temperature of the surroundings is constant—are in common use for solution calorimetry, for combustion calorimetry, for heat-capacity measurements, and for the determination of enthalpy changes between high temperatures and standard temperatures. They are of both stirred water and aneroid types. The theory of operation of these calorimeters has not been worked out in detail from the laws of thermodynamics and heat transfer, probably because of the difficulty of describing the apparatus in mathematical terms. Instead, only very simple theoretical models have been discussed for which rigorous mathematical solutions can be obtained.

The simplest theoretical model of an isoperibol calorimeter represents the calorimeter by a single body having a geometrically uniform but time-dependent temperature, and exchanging heat with an environment at a uniform, constant temperature. This single-body model fails for accurate calorimetry because it neglects the temperature gradient and the changes in the gradient with time in both the calorimeter and its environment.

White[2] considers isoperibol calorimeters in a more comprehensive way. He summarizes the effect of temperature gradients in what he terms "the general law of lag." This "law" is frequently expressed by the quotation from White: "When the calorimeter is calibrated, it is calibrated, lag effects and all." He restricts this statement to "constant" lags. In another part of his book (p. 36) he notes that a systematic error may occur if the location of a heat source is different from the location of the calibrating heater. White's treatment is inadequate because he does not state clearly what assumptions he makes about the calorimeter which lead to "the general law of lag." For this reason, it is difficult to judge whether a calorimeter satisfies the conditions under which White's conclusions about lags are valid.

A two-body model of an isoperibol calorimeter, consisting of two bodies, each having a geometrically uniform, but time-dependent temperature, is the simplest model in which effects of temperature differences in the calorimeter can be considered in explicit mathematical terms. Equations derived for this model illustrate some of the deficiencies of the one-body model and some of the conditions under which "the general law of lag" is valid.

A two-body model is especially attractive for treating the problems encountered in measuring relative enthalpies at high temperatures. This experiment requires that a hot body be placed in the calorimeter where the heat given up on cooling is compared to a known energy. The thermal resistance between the hot body and the calorimeter is large compared to the thermal resistances between other parts of the calorimeter, so that it is logical to treat the calorimeter during the rating periods as consisting of two heat capacities with a thermal resistance between them. This approximation is similar to the lumped constant treatment of an electrical network of two capacitors and a resistance connected by wires of negligible resistance and capacitance.

The two-body model is treated by King and Grover,[3] but they do not explore the general implications and reach some wrong conclusions. Jessup[4] extends the treatment, criticizing the results of King and Grover, pointing out the errors, especially as they relate to bomb calorimetry.

King and Grover[3] use the two-body model to develop a method for treating data from high-temperature enthalpy experiments. This method represents a radical departure from established methods because it assumes a particular form for the heat flow between the hot body and the calorimeter. Macleod[5] applies the method to actual calorimetric data, with the claim that it is more accurate than other methods. Such a claim affects a great deal of thermodynamic data obtained by iso-

[1] O. Kubaschewski and R. Hultgren, in *Experimental Thermochemistry*, H. A. Skinner, Ed. (Interscience Publishers, Inc., London, 1962), Vol. 2, p. 351.

[2] W. P. White, *The Modern Calorimeter* (Reinhold Publishing Corp., New York, 1928), p. 88.

[3] A. King and H. Grover, J. Appl. Phys. **12**, 557 (1941).

[4] R. S. Jessup, J. Appl. Phys. **13**, 128 (1942).

[5] A. C. Macleod, Trans. Faraday Soc. **63**, 289 (1967).

peribol calorimetry and therefore warrants careful examination of its bases.

THE TWO-BODY HEAT-FLOW PROBLEM

The two-body model for an isoperibol calorimeter is represented schematically in Fig. 1. The calorimeter consists of two bodies—an inner body having a uniform temperature Θ and heat capacity K_2 completely enclosed by an outer body with a uniform temperature θ and heat capacity K_1.[6] The calorimeter is completely enclosed by surroundings having a uniform constant temperature θ_j. The fundamental relationship for the calorimeter is obtained by application of the first law of thermodynamics. For an infinitesimal time interval dt, we equate the increase in enthalpy to the net heat to (or work done on) the calorimeter:

$$K_1(d\theta/dt)+K_2(d\Theta/dt)=(dQ_1/dt)+(dQ_2/dt) -h_1(\theta-\theta_j)+P_s. \quad (1)$$

In (1), Q_1 and Q_2 are heats developed in the outer and inner bodies, respectively; P_s is the stirring power[7] in the outer body; and h_1 is the constant coefficient for heat transfer between the outer body and the surroundings.

In the usual manner, we consider a calorimetric experiment consisting of three time intervals—an initial rating period, a main period, and a final rating period. The main period includes the time during which heat is generated in the calorimeter; the rating periods are chosen before and after the main period when dQ_1/dt and dQ_2/dt have been zero long enough to have negligible effects on θ and Θ. Experimentally, this criterion means that the observed temperature is a single exponential function of time.

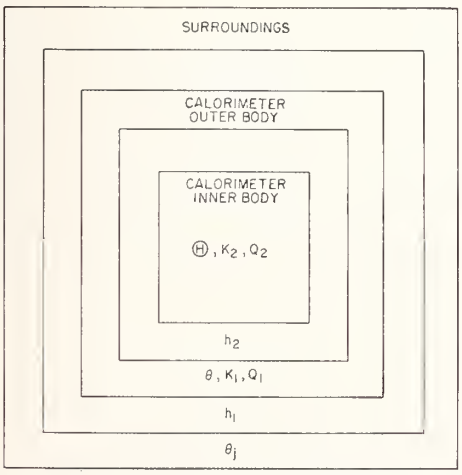

FIG. 1. Schematic cross section showing the inner body at temperature Θ enclosed by an outer body at temperature θ and both bodies of the calorimeter enclosed by the surroundings at the constant temperature θ_j.

[6] Where possible, the notation of King and Grover[3] and Jessup[4] have been retained to facilitate intercomparisons.

[7] If the stirring work is done on the inner body, the convergence temperature will be different for the two bodies. We do not consider this case.

We now define the convergence temperature θ_k of the calorimeter in the usual way: $\theta_k=\theta_j+P_s/h_1$. Substituting in Eq. (1) and integrating between a state $(\theta_0, \Theta_0, t_0)$ in the initial rating period and a state $(\theta_1, \Theta_1, t_1)$ in the final rating period, assuming K_1, K_2, and h_1 are independent of temperature, we obtain the following equation:

$$K_1(\theta_1-\theta_0)+K_2(\Theta_1-\Theta_0)=Q_1+Q_2-h_1\int_{t_0}^{t_1}(\theta-\theta_k)\,dt. \quad (2)$$

Physically, Eq. (2) equates the increase in enthalpy of the calorimeter to the net heat added to the calorimeter for the time interval t_1-t_0.[8] In an actual calorimeter, K_1, K_2, and h_1 change slowly with temperature, so that the temperature range is restricted for real calorimeters.

Only one temperature is measured in actual experiments. To impose this condition in (2), we need an additional relationship which will let us write the entire equation in terms of either Θ or θ alone. If the temperature is measured in the outer body, then we need only express Θ_1 and Θ_0 in terms of θ_1 and θ_0, respectively, *during the rating periods* in order to make comparisons of different Q's—electrical energy and a heat of combustion, for example.

During the rating periods $\Theta-\theta$ will be small and the heat flow between the two bodies can be described by Newton's Law of Cooling. Applying the first law of thermodynamics to the inner body alone, we obtain

$$K_2 d\Theta/dt=-h_2(\Theta-\theta). \quad (3)$$

In Eq. (3) h_2 is the heat-transfer coefficient between the inner and outer bodies. Subtracting (3) from (1) for the rating period when $Q_1=Q_2=0$, we obtain

$$K_1 d\theta/dt=h_2(\Theta-\theta)-h_1(\theta-\theta_k). \quad (4)$$

It is important, especially if the inner body is a hot capsule as in high-temperature enthalpy measurements, that no restriction has yet been made on the heat transfer between the inner and outer bodies during the main period. Solution of the simultaneous Eqs. (3) and (4) gives the results of Jessup[4]:

$$\theta-\theta_k=Ae^{-\epsilon t}+B\exp[-(2p-\epsilon)t], \quad (5)$$

$$\Theta-\theta_k=[a/(a-\epsilon)]Ae^{-\epsilon t} +[aB/(a-2p+\epsilon)]\exp[-(2p-\epsilon)t], \quad (6)$$

where a, p, q, and ϵ are defined in Table I, and A and

[8] In an electrical calibration, Q_1 or Q_2 will represent electrical work done on the system calorimeter plus contents, and the integral term is the heat transferred to the system from the surroundings. In a combustion experiment, for example, Q_1 or Q_2 represents the heat of combustion, so the net increase in enthalpy of the system is the left-hand side of (2) less Q_1 or Q_2. Equation (2) permits determination of an unknown heat effect in terms of electrical units; it remains to translate the unknown heat effect into thermodynamic quantities.

Table I. Symbols.

θ	temperature of inner body $\dot{\theta}=d\theta/dt$
Θ	temperature of outer body
θ_j	temperature of surroundings
θ_k	$=\theta_j+P_s/h_1$, the convergence temperature
P_s	constant power sources—stirring, thermometer, etc., in outer body
t	time
K_1	heat capacity of outer body
K_2	heat capacity of inner body
Q_1	heat generated in a finite time in outer body
Q_2	heat generated in a finite time in inner body
h_1	coefficient for heat transfer between outer body and surroundings
h_2	coefficient for heat transfer between inner and outer bodies
a	$=h_2/K_2$, $b=h_2/K_1$, $c=h_1/K_1$
$2p$	$=h_2/K_2+h_2/K_1+h_1/K_1=a+b+c$
q	$=h_1h_2/K_1K_2=ac$
ϵ	$=p-(p^2-q)^{1/2}=h_1/[K_1+aK_2/(a-\epsilon)]$

B are constants to be determined from values of θ and Θ at a particular time in the appropriate rating period. These equations are derived from two first-order equations, so there can be only two undetermined constants. From the definition of p and q, it may be shown that $p^2>q$ and $p>(p^2-q)^{1/2}\gg 0$. Thus, ϵ and $2p-\epsilon$ are always real and positive. In good design, h_1/K_1 should be small compared to h_2/K_2; that is, equilibrium within the calorimeter is attained more rapidly than equilibrium with the environment. In this case $(2p-\epsilon)\gg\epsilon$ and the second exponential terms in (5) and (6) decay relatively rapidly. After the second exponentials become negligible, the following relationships, valid only during rating periods, are easily derived[9];

$$d\theta/dt=-\epsilon(\theta-\theta_k), \tag{7}$$

$$d\Theta/dt=-\epsilon(\Theta-\theta_k), \tag{8}$$

$$\Theta-\theta_k=[a/(a-\epsilon)](\theta-\theta_k). \tag{9}$$

The relations (7) or (8) are statements of the usual exponential behavior of the observed temperature of an isoperibol calorimeter during the rating periods.

THERMOMETER ON OUTER BODY

If the thermometer is located on the outer body, θ is the measured temperature and Θ in (2) must be expressed in terms of θ using (9) and the definitions of ϵ, p, and q, in Table I. On rearranging, we obtain the equation in the form commonly used in isoperibol calorimetry:

$$[K_1+aK_2/(a-\epsilon)]\left[\theta_1-\theta_0+\epsilon\int_{t_0}^{t_1}(\theta-\theta_k)\,dt\right]=Q_1+Q_2. \tag{10}$$

In (10), $K_1+aK_2/(a-\epsilon)$ is an energy equivalent, multiplying a corrected temperature rise. Several significant points are contained in (10). The energy equivalent is independent of the *form* of the time–temperature curve, in agreement with the "general law of lag." The energy equivalent has the dimensions of heat capacity, but it is *not* the sum of the heat capacities. To calculate the energy equivalent even for this simple model would require knowing h_1, h_2, K_1, and K_2 separately. This illustrates a reason for preferring the experimental determination of energy equivalents to calculation.

Equation (10) does not discriminate between Q_1 and Q_2. That is, when the temperature is measured on the outer body, an electrical calibration with the heater on either body determines the proper energy equivalent for measurements of some unknown heat developed in either body (but see the next section).

According to (7) and (8), ϵ can be determined by measurements on either body. We emphasize, in agreement with Jessup,[4] that the cooling constant $\epsilon=h_1/[K_1+aK_2/(a-\epsilon)]$ is exactly the one desired, and not the ratio h_1/K_1 as recommended by King and Grover.[3] This point is discussed in detail below.

There is no restriction in (10) on the rate at which heat is developed nor on the duration of heating, so that different heating rates in electrical calibrations must give the same energy equivalent, a result deduced earlier for adiabatic calorimeters.[10]

THERMOMETER ON INNER BODY

If the thermometer is located on the inner body, Θ is the temperature measured and θ in (2) must be expressed in terms of Θ.

To obtain the desired relation, we again substitute into (2) from (9), but we must also substitute for θ in the integrand. Since the integral must be taken over the heating period, the expression for Θ must be valid during the heating period. We again assume, as in (3), that the heat transfer is proportional to the temperature difference, which restricts our description to experiments in which $\Theta-\theta$ is small. Applying the first law of thermodynamics to the inner body, we obtain

$$K_2(d\Theta/dt)=-h_2(\Theta-\theta)+(dQ_2/dt). \tag{11}$$

Dividing by h_2 and adding $(\Theta-\theta_k)$ to both sides, we obtain

$$\theta-\theta_k=(K_2/h_2)(d\Theta/dt)-(1/h_2)(dQ_2/dt)+\Theta-\theta_k. \tag{12}$$

Substituting (12) into the integral in (2) and using (9) to express θ_1 and θ_0 in terms of Θ_1 and Θ_0, we obtain after rearrangement

$$\left(K_1+\frac{K_2a}{a-\epsilon}\right)\left[\Theta_1-\Theta_0+\epsilon\int_{t_0}^{t_1}(\Theta-\theta_k)\right]=Q_1+\frac{h_1+h_2}{h_2}Q_2. \tag{13}$$

[9] In our derivation, we take Eqs. (1) and (3) to describe the calorimeter and derive (4) and (7)–(10). The argument can be made in another way. Equation (7) states a commonly observed phenomenon and can be used with (1) to derive the other equations.

[10] E. D. West, J. Res. Natl. Bur. Std. 67, 337 (1963).

This equation states that the energy equivalent determined by supplying a known amount of heat Q_1 to the outer body is not applicable to determinations of heat generated in the inner body Q_2 when the temperature is measured on the inner body. This result illustrates a limitation of the general law of lag and emphasizes White's warning that electric heat produced in a part of the calorimeter different from the part where other heat is produced, may cause a systematic error.

For a thermometer on the inner body, as in the preceding section, ϵ is exactly the cooling constant required.

THE TWO-BODY ANALYSIS OF KING AND GROVER

Since the results of the two preceding sections are in conflict with statements of King and Grover,[3] and since, despite Jessup's[4] treatment, some confusion about the problem apparently remains, it appears worthwhile to consider in detail just where their analysis[3] is at fault. They state that "The heating period has been considered to end when the time–temperature curve begins to obey...a pure exponential relation. Our analysis of this problem indicates that this assumption is not valid." This statement is contrary to our Eqs. (10) and (13), which are exact, providing that the end of the experiment is taken when the time–temperature curve *does* obey a single exponential relation. We consider their analysis in some detail to point out the errors which lead to their statement.

The first difficulty with King and Grover's analysis is in connection with their Eq. (6):

$$d\theta/dt = F(t) - c(\theta - \theta_k), \qquad \text{(KG6)}$$

where $c = h_1/K_1$ and $F(t)$ is the "heating function," representing the heat flowing from the inner body divided by the heat capacity of the outer body. This equation is an alternate, but less specific version of our Eq. (1). They integrate this equation with the restriction that $F(t) = 0$ during rating periods. Comparing (KG6) with Eq. (1), which is just the application of the first law in a two-body calorimeter, we identify

$$F(t) = (1/K_1)[d(Q_1+Q_2)/dt] - (K_2/K_1)(d\Theta/dt). \quad (14)$$

Since Q_1 and Q_2 are zero in rating periods, their restriction that $F(t) = 0$ in rating periods means that either $d\Theta/dt = 0$ or $K_2 = 0$. If $d\Theta/dt = 0$, then $\Theta = \theta = \theta_k$ and we have the trivial case of zero temperature rise. If $K_2 = 0$, there is no inner body. Hence, (KG6) and related equations [their (7)–(26)] apply to a calorimeter consisting of a single body at uniform temperature. In this case, of course, c would be the cooling constant.

The same type of error occurs in connection with their Eq. (27), which is the same as (KG6) with the additional restriction that $F(t)$ is, "...a constant over a limited time (the heating period) and zero otherwise." This equation was intended to apply to electrical calibrations. It suffers from the same defect as (KG6) and an additional defect during the heating period. This additional defect can be seen from the following. Again comparing with (1), but for the heating period, then the heating rate $d(Q_1+Q_2)/dt$ must be adjusted to compensate for the change in $d\Theta/dt$, which is a practical absurdity, or K_2 must again be zero.

The burden of this criticism is that their concept of a "limited heating period" with $F(t) = 0$ in rating periods is not compatible with a meaningful two-body problem. In the resulting one-body problem, no time is needed for equilibration. This rough approximation is used in their Eq. (29) which takes the final temperature reading at the end of the heating period.

A practical objection can be made to this identification of the end of the experiment with the end of the heating period [e.g., their Eqs. (9) and (29)]. This identification follows from their disguised one-body problem; it is wrong for the next more-subtle model, the two-body problem, and certainly goes contrary to experience with actual calorimeters.

Their further treatment of the two-body problem beginning with their Eq. (33) does treat the case where K_2 is finite, but $Q_1 = Q_2 = 0$. However, they still identify the constant $c = h_1/K_1$ as the cooling constant (p. 563). To illustrate the fallacy of this identification by a physical example, we consider a large block as the inner body, so that K_2 is very large, surrounded by a a thin shield, so that K_1 is very small. If the temperature of the shield is measured and the heat is generated by a source located on the shield, then, when the heat supplied by the source is stopped, e^{-ct} goes to zero almost instantaneously. If c were really the cooling constant, the temperature of the shield would have to revert to θ_k very soon after the supply of heat is stopped. Actually, of course the heat flow to the shield from the inner body would maintain the temperature of the shield above the temperature of the surroundings.

One further precaution is necessary if their Eq. (4) is used for experimental data. It is derived from their (39) which follows directly from the equation of mixtures (see their footnote 20). We rewrite their (39), using the identity $b(a+b) = K_2/(K_1+K_2)$:

$$(K_1+K_2)(\theta_\infty{}^* - \theta_0) = K_2(\Theta_0 - \theta_0). \qquad (15)$$

The right-hand side is the total energy given up by the inner body in cooling from Θ_0 to θ_0. The energy equivalent appropriate to the corrected temperature rise defined in this way is therefore K_1+K_2. A basic flaw of this definition and the associated procedure is that no isoperibol method will determine K_1+K_2 because different parts of the calorimeter undergo different temperature rises. (In fact, K_1+K_2 is an energy equivalent only for a two-body adiabatic calorimeter, as the definition implies.)

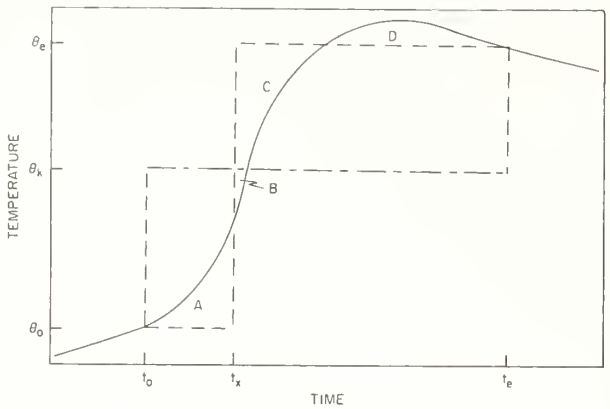

FIG. 2. Illustration of Dickinson's method for the case that the final temperature θ_e is above the convergence temperature θ_k. The time t_x is chosen so that $A+D=B+C$.

DICKINSON'S GRAPHICAL METHOD

Dickinson's graphical method[11] for evaluating the temperature–time integral in isoperibol calorimetry was based on the experimental fact that the rate of change of the calorimeter temperature during rating periods is proportional to the thermal head as in (7) and (8). For the two-body model, as well as for real calorimeters, the rating periods must, therefore, begin some time after the end of the heating period to permit decay of other exponentials. The discussion of Dickinson's method by King and Grover is wrong because they take the final temperature at the end of the heating period. Macleod[5] selects the maximum temperature for use in Dickinson's method.

Because of this evidence of improper use and because the method is sometimes poorly described, it is instructive to derive the method in connection with the two-body problem. It should be pointed out that, for real calorimeters, Dickinson's method requires only that heat transfer between calorimeter surface and surroundings be proportional to the observed temperature difference and that (7) and (8) hold during rating periods. We treat the case where $\theta_1>\theta_k$, because that seems to cause the most trouble.

In Fig. 2 a hypothetical temperature–time curve is represented for which the integral in (1) must be evaluated. This is done by finding two rectangles of equal area. From the figure, the integral is expressed in terms of two rectangles and the areas A, B, C, and D:

$$\int_{t_0}^{t_e}(\theta_k-\theta)\,dt=(\theta_k-\theta_0)(t_x-t_0)-A+B-[(\theta_e-\theta_k)(t_e-t_x)-C+D]. \quad (16)$$

If t_x is found so that $A+D=C+B$, and substitution is made from (7) and (8), the form given by Coops *et al.*[12] is obtained in terms of experimental quantities:

$$\epsilon\int_{t_0}^{t_e}(\theta_k-\theta)\,dt=\left(\frac{d\theta}{dt}\right)_e(t_e-t_x)+\left(\frac{d\theta}{dt}\right)_0(t_x-t_0). \quad (17)$$

For either the one- or the two-body model, Dickinson's method is a theoretically exact evaluation of the integral. Any approximations occur in the application to experimental data.

Roth and Becker[13] present an alternative method for evaluating the time–temperature integral. The two methods give exactly the same corrected temperature rise but the values of t_x obtained by one method must not be used with the other method. Jessup[4] has used the Roth and Becker method, but has erroneously ascribed it to Dickinson.

ISOPERIBOL CALORIMETRY FOR HIGH-TEMPERATURE ENTHALPY MEASUREMENTS

An isoperibol aneroid "receiving" calorimeter for use in high-temperature enthalpy measurements presents problems of data reduction which can be analyzed by means of a two-body model of the calorimeter. In these measurements, a hot body at a high temperature is dropped into the calorimeter at the end of the initial rating period and allowed to cool. The final rating period is taken with the added body still in the calorimeter. Since the calorimeter has a different energy equivalent and therefore a different cooling constant in the two rating periods, the usual isoperibol methods for determining the cooling constant and the convergence temperature do not apply exactly. In addition, the difference between the final observed calorimeter temperature and the temperature of the added body must be taken into account.

Various experimental procedures have been used. The experiment will be analyzed in some detail to indicate advantages of particular procedures and methods of estimating some of the errors involved.

The analysis on the basis of the two-body model is related to the real problem in about the same way that a one-body model relates to a combustion or solution calorimeter. The one-body model—a single body with temperature varying in time but uniform in space—predicts the correct formula for calculating the corrected temperature rise for real calorimeters providing that the energy equivalent and cooling constant are determined experimentally and that initial and final temperatures are taken after the temperature in the rating periods can be represented by a single exponential function of time. These provisions take care of most of the differences between the simple model and real calorimeters. The energy equivalent and cooling constant of a receiving calorimeter can be determined experimentally

[11] H. C. Dickinson, Bull. Bur. Std. **11**, 189 (1915).

[12] J. Coops, R. S. Jessup, and K. Van Ness in *Experimental Thermochemistry*, F. D. Rossini, Ed. (Interscience Publishers, Inc., New York, 1956), Vol. 1.

[13] W. A. Roth and F. Becker, *Kalorimetrische Methoden zur Bestimmung chemischer Reaktionswärmen* (Frederick Vieweg und Sohn, Brunswick, Germany, 1956).

so that dependence on theory is confined to the effect of adding the relatively small heat capacity of the dropped body to the large energy equivalent of the calorimeter.

The basic relationship is derived from application of the first law to the system calorimeter plus dropped body by equating energy measured by the calorimeter to the decrease in the enthalpy of the dropped body $H_f - H_1$ less the small heat Q_L "lost" in dropping:

$$K_1\left[\theta_1-\theta_0+c\int_{t_0}^{t_1}(\theta-\theta_k)\,dt\right]=H_f-H_1-Q_L. \quad (18)$$

Since we are now treating real calorimeters, the quantity K_1 is the energy equivalent determined by calibration. In (18) H_f is the enthalpy of the dropped body at the temperature of the furnace, H_1 is its enthalpy at the final temperature of the calorimeter, and Q_L allows for heat lost in transferring the body from the furnace to the calorimeter, for heat radiated directly from the furnace into the calorimeter during the transfer, and any other small heat quantities associated with the transfer operation. In careful work Q_L is usually accounted for by experiments made with a capsule and a capsule plus sample in such a way that Q_L is the same for both experiments and their difference is a thermodynamic property of the sample. In our analysis of the calorimetric part of the experiment, it is sufficient to note that the right-hand side is the sum of an unknown heat Q_L and a thermodynamic quantity $H_f - H_1$, which we may treat in accord with thermodynamic theory.

The enthalpy of the dropped body H_1 is, in general, not constant during the final rating period because the temperature is changing. The temperature of the dropped body and, consequently its enthalpy, must also change as long as the calorimeter temperature changes. One way to avoid this problem is to make $\theta_1=\theta_k$ as suggested by Jessup.[4] Another way which may be easier experimentally is suggested below.

The inconstancy of the enthalpy of the dropped body and of the corrected temperature rise may be the source of the idea of the "unlimited heating period" of King and Grover. The inconstancy is eliminated by the procedure suggested below and is therefore more a matter of data treatment than of inherent difficulty in the experiment.

The difficulty is overcome merely by treating the calorimeter by the two-body model in which the inner body is the dropped body. Using (9), we write the increase in enthalpy of the dropped body between the initial and final states of the calorimeter in terms of the observed initial and final temperatures:

$$K_2(\theta_1-\theta_0)\,a/(a-\epsilon)=H_1-H_0, \quad (19)$$

where H_0 is the enthalpy that the dropped body would have at time t_0, if it were present in the calorimeter during the initial rating period. Adding (19) to (18) and rearranging, we obtain

$$\left(K_1+\frac{aK_2}{a-\epsilon}\right)\left[\theta_1-\theta_0+\epsilon\int_{t_0}^{t_1}(\theta-\theta_k)\,dt\right]=H_f-H_0-Q_L. \quad (20)$$

Equation (20) has the virtue that the right-hand side does not depend on the final temperature of the calorimeter. The corrected temperature rise must therefore be constant and its constancy can be used as a criterion for deciding when the experiment is complete. We have found this criterion useful in data analysis.

The cooling constants and the convergence temperature required in (18) and (20) cannot, in principle, be determined directly from the experimental data because the dropped body is absent during the initial rating period but present during the final rating period. For some work, it may be adequate to ignore the change in cooling constant due to the dropped body and proceed by ordinary isoperibol methods. For more accurate work with a given calorimeter, the change in cooling constant can be accounted for. We proceed to develop methods for obtaining the constants from the data. The formulas developed can also be used to estimate the error in using ordinary isoperibol methods.

The relation between the cooling constants is evident from their definitions in Table I:

$$c/\epsilon=1+[aK_2/(a-\epsilon)K_1]. \quad (21)$$

We solve (21) for ϵ, substitute into (7), and rearrange to obtain an expression for the final rating period in terms of c ($\dot\theta\equiv d\theta/dt$):

$$[1+aK_2/(a-\epsilon)K_1]\dot\theta_1=-c(\theta_1-\theta_k). \quad (22)$$

For the initial rating period without the dropped body, we can write

$$\dot\theta_0=-c(\theta_0-\theta_k). \quad (23)$$

Subtracting (23) from (22) gives an expression for the cooling constant c required in Eq. (18):

$$c=\frac{[1+aK_2/(a-\epsilon)K_1]\dot\theta_1-\dot\theta_0}{\theta_0-\theta_1}. \quad (24)$$

An expression for the cooling constant ϵ required in Eq. (20) is obtained by substituting for c from (21) into (23) and subtracting (7) for the final temperature θ_1:

$$\epsilon=[1/(\theta_0-\theta_1)]\{\dot\theta_1-\dot\theta_0/[1+aK_2/(a-\epsilon)K_1]\}. \quad (25)$$

The temperatures and time derivatives of temperatures in (24) and (25) can be obtained from initial and final rating periods; K_1 is obtained by electrical calibration and K_2 from known weights and heat capacities in the literature. The contribution of a suspension wire to K_2 can usually be neglected. The ratio $a/(a-\epsilon)$ is close to one; $1/a$ is the time constant for the dropped body cooling to the calorimeter and should be about 10 min or less; $1/\epsilon$ is the time constant for the calorimeter con-

taining the dropped body cooling to the environment jacket and is typically about 500 min. It is usually sufficient therefore to take $a/(a-\epsilon)$ to be one, although the time constant $1/a$ should doubtless be calculated for other reasons. If the apparatus is arranged so that an experiment for a furnace temperature 1000° above the calorimeter temperature causes a 3° increase in the latter, then K_2/K_1 is approximately 1/300. The quantity $aK_2/(a-\epsilon)K_1$ in (24) and (25) is therefore about 0.003 and need not be known accurately for the determination of the cooling constant. In fact, this uncertainty can be made very small by making the final temperature near the convergence temperature in (24) as suggested by Jessup,[4] or by making the initial temperature near the convergence temperature in (25). Other reasons for such experimental arrangements are discussed below.

If (20) is to be used for data reduction then the energy equivalent must be determined with the dropped body in place or a suitable correction made. Ordinarily, only K_1 is measured and the question is whether $aK_2/(a-\epsilon)$ can be calculated with sufficient accuracy. If $K_1=300\ K_2$ and an uncertainty in the energy equivalent of 1/10 000 is permissible, then a value of $aK_2/(a-\epsilon)$ is required, good to about 3%. The heat capacity K_2 can usually be calculated with sufficient accuracy from data in the literature, and the calculation hinges on knowing $a/(a-\epsilon)$ with sufficient accuracy.

Several methods might be used to obtain a value for $a=h_2/K_2$. Calculation from first principles may be adequate, especially if one is sure that $a\gg\epsilon$. A few comparisons with measured energy equivalents should give a good test of the calculation. Curve fitting (5) might give useful values of $2p-\epsilon$, which is a good approximation to $a(K_1+K_2)/K_1$. Measurement of the cooling constants in the final rating period both with and without the dropped body give the ratio of energy equivalents, but this procedure does not appear to be accurate enough. Electrical calibration with and without the dropped body together with K_2 calculated from known weights and heat capacities should give a good value for h_2, but this value may be considerably different for an empty capsule and for one filled with a powder, for example.

In applying any of these refinements, one must keep in mind that the theory treats two bodies, each at a uniform temperature. Calibration takes care of lags in the calorimeter, but large departures from uniform temperature occur in a capsule filled with an evacuated powder, for example.

Once either cooling constant is known with sufficient accuracy, the convergence temperature θ_k can be determined in the usual way from data for one of the rating periods.

The remaining problem in connection with data analysis by either (18) or (20) is that the reference temperature of the dropped body is not in general the same as the corresponding observed temperature of the calorimeter. The desired relation is obtained by subtracting $\theta-\theta_k$ from both sides of (9):

$$\Theta-\theta=[\epsilon/(a-\epsilon)](\theta-\theta_k). \tag{26}$$

The ratio $\epsilon(a-\epsilon)$ is approximately ϵ/a which is on the order of 0.02. The error in taking the observed temperature as the reference temperature of the dropped body can be made as small as desired by making the final calorimeter temperature near the convergence temperature for (18) or making the initial temperature near the convergence temperature for (20). These are just the conditions required for the best determinations of the cooling constants in (24) and (25). Substitution from (7) into (26) gives an alterative form in terms of the rate of change of the temperature.

The procedure suggested by King and Grover[2] has a weakness not present in either of the procedures suggested here: the heat flow from the dropped body to the calorimeter is assumed to follow Newton's law of cooling (3) from the moment it enters the calorimeter. They recognize the nature of the approximation: "Actually the rate is undoubtedly a more complicated function of $\Theta-\theta\cdots$." For a hot capsule, it is likely that the initial rate is nearly proportional to the fourth power of its absolute temperature, which would give an algebraically greater correction to the temperature rise. It might be argued that, since heat leak accounts for only about one percent of the total energy, their approximation for the heating period may be adequate. It does appear to be adequate for some work. Even so, there appears to be no compelling reason to use the inferior theory.

MACLEOD'S COMPARISON OF PROCEDURES

Macleod[5] set out to test the adequacy of the King and Grover procedure with actual experimental measurements. He presents the experimental data for an electrical calibration and an enthalpy experiment in his isoperibol calorimeter and compares the corrections to the temperature rises calculated by various methods.

His thesis is that the method of King and Grover for isoperibol data analysis is superior to Dickinson's method, which is essentially equivalent to the methods we have advanced. His basic arguments are (1) that data treated by the method of King and Grover agree with data taken by the adiabatic method in the same calorimeter, and (2) that these data yield enthalpies for aluminum oxide in better agreement with values in the literature.

In Macleod's calibration experiment, the calorimeter initially comes to a constant temperature so that the initial temperature is equal to the convergence temperature. Electrical energy is supplied for 46 min and the calorimeter temperature passes through a maximum at 48.5 min. After 185 min, the calorimeter temperature decreases exponentially with time.

The corrected temperature rise calculated according to the left-hand side of Eq. (18) is shown in Table II.

The corrected temperature rise decreases by 0.2% between 48.5 and 100 min and then increases. From 185 to 275 min the corrected temperature rise is constant to about one part in 14 000. If the simple one-body model is an adequate representation of Macleod's calorimeter, the corrected temperature rise will be the same for all temperatures after the end of the heating period. The model fails to describe the calorimeter by about 0.2%.

If the final temperature is taken during the final rating period, the corrected temperature rise calculated by Dickinson's method is 1427.38 μV, which is 0.11% less than Macleod's value of 1428.03 μV calculated by the method of King and Grover. The latter is 0.06% less than our value at 48.5 min in Table II. The discrepancy appears to be due to his use of a trapezoidal approximation in calculating the time integral of $\theta-\theta_k$.

Our analysis of the enthalpy experiment shows a significant discrepancy between the values Macleod used for c and ϵ. For the two-body model of King and Grover, which is the basis of Macleod's recommended procedure, Eq. (21) holds exactly and is probably a good approximation for real calorimeters. To use (21), we need the ratio $a/(a-\epsilon)$. We have shown in the preceding section that this ratio is close to unity. We can show an equivalent result from Macleod's data. He does not determine a value of a, but it may be calculated from his value of $a+b=aK_1/(K_1+K_2)$ if K_2/K_1 can be estimated. From the size of his graphite capsule described in his companion paper,[14] assuming a density of 1.8 and a volume of 2.5 cm^3 for the sample, we calculate $K_2=1.25$ cal/°K. He gives $K_1=2215$ cal/°K, from which we calculate $a=0.9994(a+b)=0.10552$, whence $a/(a-\epsilon)=1.0052$. Using these values in (21) we obtain $c/\epsilon=1.00056$, which contrasts with the ratio of Macleod's values of 1.0862.

From another point of view, not restricted to any simple model, the ratio c/ϵ is just the ratio of the energy equivalent with the dropped body to that without, assuming only that the coefficient for heat transfer to the surroundings does not change. The experimental ratio of $c/\epsilon=1.0862$ requires us to believe that the addition of a heat capacity of 1.25 cal/°K adds 8.6% to an energy equivalent of 2215 cal/°K.

At least part of the difficulty lies in attempting to determine the cooling constant from a single rating period. Although a good fit to the data can be obtained, goodness of fit is not an adequate criterion for the accuracy of the cooling constant. We can demonstrate this point by using the *same* cooling constant to fit the data of both the initial and final rating periods. In Table III we compare differences between the observed data and equations of the form

$$\theta=\theta_0+(\theta_k-\theta_0)(ct+c^2t^2/2),$$

in which a value for θ_0 is determined to give the best average fit. For one set, we have used Macleod's values of c, ϵ, and θ_k; for the other set, we have determined θ_k and a single cooling constant by usual isoperibol techniques.[12] It is evident that the set using the single cooling constant, in conformity with our conclusion that the effect of the capsule is small, represents the data as well as the set using two cooling constants.

[14] A. C. Macleod, Trans. Faraday Soc. **63**, 300 (1967).

Table II. Macleod's electrical calibration experiment.

t_1(min)	Corrected temp. rise[a], (μV)	t_1(min)	Corrected temp. rise[a] (μV)
48.5	1428.98	185	1427.56
52	1428.34	195	1427.22
60	1426.79	205	1427.21
80	1424.22	215	1427.27
100	1424.10	225	1427.29
120	1425.41	235	1427.31
140	1425.31	245	1427.48
160	1426.03	255	1427.28
170	1428.17	265	1427.24
		275	1427.16

[a] Heater off at 46 min; $h_1/K_1=6.006$ min^{-1} (calc. by Macleod); $\theta_k=6180.18$ μV; $t_0=0$ min.

Macleod calculates the corrected temperature rise to be 1422.06 μV by the method of King and Grover and 1420.32 by "Dickinson's" method, using the maximum temperature, which occurs ahead of the final rating period. Our value for the corrected temperature rise obtained by (25), using our value of c (or ϵ) and θ_k given in Table III and a final temperature at 120 min later is 1423.88 μV, some 0.13% higher than that given by Macleod by the method of King and Grover.

CONCLUSIONS

The two-body model of an isoperibol calorimeter shows several interesting features:

(1) The location of the thermometer is critical for satisfying a necessary condition for isoperibol calorimetry that the energy equivalent be the same for both calibration and unknown experiments. For the thermometer located in the outer body the energy equivalent for a heat source in the outer body is the same as the energy equivalent for a heat source in the inner body; for the thermometer in the inner body, the energy equivalent for a heat source in the outer body is greater than the energy equivalent for a source in the inner body. We cannot deduce from the simple two-body model all the restrictions on the locations of thermometer and heat sources in real calorimeters, but, for the model, the problem arises when one of the sources to be compared is located in a body outside the body where temperature is measured. White's statement, quoted above, about cancellation of lags must therefore be restricted to heat sources which have the same energy equivalent associated with them. For the two-body model, the criterion for sources to have the same energy equivalent is that no source shall be located outside the thermometer.

TABLE III. Comparison of fitting drift-period data.

Initial drift period			Final drift period		
Time (min)	Macleod obs.-calc.[a] (μV)	Authors obs.-calc.[b] (μV)	Time (min)	Macleod obs.-calc.[c] (μV)	Authors obs.-calc.[d] (μV)
−60	+0.02	+0.02	120	−0.23	−0.02
−50	+0.01	0.00	130	−0.13	+0.05
−40	+0.01	−0.01	140	−0.04	+0.10
−30	+0.02	−0.01	150	+0.05	+0.16
−20	−0.03	+0.02	160	+0.06	+0.13
−10	−0.02	0.00	170	+0.04	+0.07
0	−0.04	0.00	180	+0.02	+0.01
			190	+0.03	−0.01
			200	+0.02	+0.02
			210	+0.04	−0.08
			220	+0.06	−0.09
			230	+0.07	−0.13
			240	+0.07	−0.13

[a] $\theta_k = 1395.86$ μV; $\theta_0 = 463.37$ μV; $c = 0.5998 \times 10^{-4}$ min^{-1}.
[b] $\theta_k = 1426$ μV; $\theta_0 = 463.37$ μV; $c = 0.582 \times 10^{-4}$ min^{-1}.
[c] $\theta_k = 1395.86$ μV; $\theta_0 = 1894.67$ μV; $\epsilon = 0.5522 \times 10^{-4}$ min^{-1}.
[d] $\theta_k = 1426$ μV; $\theta_0 = 1894.46$ μV; $\epsilon = 0.582 \times 10^{-4}$ min^{-1}.

(2) The energy equivalent is *not* the sum of heat capacities but may be either greater or less than the sum. This fact may have implications for heat capacity measurements. If (10) is used for heat-capacity measurements by determining the heat capacity K_1 of the outer body alone and then with the inner body (sample), what is actually obtained by the difference of the two experiments is $[K_1 + aK_2/(a-\epsilon)] - K_1$. If $a \gg \epsilon$, as it would be for the calorimeter in vacuum at low temperatures, then $a/(a-\epsilon)$ is very close to one and a good value of K_2 is obtained from the difference in the two measurements. At some higher temperature, where radiation from the outer body is appreciable $a/(a-\epsilon) > 1$ and the apparent heat capacity is too large. Real calorimeters are probably too complicated for even this qualitative conclusion to apply, but the general idea that they are subject to systematic error which increases with the heat leak appears to be valid. A discussion of this problem is given by Cole *et al.*[15] in their section on "Correction for Thermal Gradients within the Calorimeter."

(3) The corrected temperature rise multiplied by the proper energy equivalent gives the quantity of heat exactly, even though the energy equivalent is not a sum of heat capacities. This result illustrates the reason for experimental calibrations. Calibrations with standard materials are especially useful because they are more likely to produce the calibrating heat in the same place as the heat to be measured.

(4) The same cooling constant will be observed during rating periods regardless of the thermometer location, although the temperatures are not the same.

(5) The cooling constant is the heat-transfer coefficient divided by the energy equivalent determined with the same thermometer. It is *not* the heat-transfer coefficient divided by the sum of heat capacities. The cooling constant determined by experiment is therefore just the constant required to multiply the temperature-rise correction.

The first treatment of the two-body problem by King and Grover suffers from the imposition of a mathematical condition which is not possible physically and leads to the conclusion that the final temperature in an experiment can be taken at the end of a heating period. The correct two-body model predicts a waiting period after the end of the heating period before the temperature–time curve becomes a single exponential function of time. This prediction checks experience.

Their second treatment assumes a particular form for the temperature–time curve during the heating period. In effect, the practical use of this theory requires that the two-body model be an adequate model of the real calorimeter. Alternate procedures suggested, which avoid this assumption, are preferable on theoretical grounds.

When Macleod's experimental data are analyzed by our Eq. (20), the corrected temperature rise becomes independent of the time taken for the end of the experiment. There is, therefore, no compulsion to consider experiments with "unlimited" heating periods, as suggested by King and Grover.

Macleod concludes that the method of King and Grover is superior to Dickinson's method for treating data from isoperibol calorimeters because (1) it gives agreement with data from an adiabatic method, and (2) it gives more acceptable values for the enthalpy of Al_2O_3. Apart from his dependence on an inadequate theory, the agreement he found between methods may depend on small compensating errors. The corrected temperature rise calculated by the method of King and Grover is too small. The corrected temperature rise for the calibration experiment is larger than that obtained by more accurate methods, and therefore the energy equivalent he used should be too small.

[15] A. G. Cole, J. O. Hutchens, R. A. Robie, and J. W. Stout, J. Am. Chem. Soc. **82**, 4897 (1960).

The effect of these various errors on the enthalpy of Al_2O_3 is not clear to us. The error in the corrected temperature rise may be partly accounted for when the energy found for the empty capsule is subtracted from the energy found for the full capsule. The error in the energy equivalent might possibly be compensated by an error in placement of potential leads for the calibrating heater. Not enough information is given on the lengths of leads, location of potential taps, and thermal contacts of the leads for an independent judgment to be made.

Regardless of any small errors, Macleod is evidently right that the heat-exchange correction can contribute errors of several tenths of a percent in high-temperature enthalpy measurements. Papers which fail to describe the method of making the correction are therefore suspect at this level of accuracy. It is unfortunate that many papers are vague on this point.

ACKNOWLEDGMENTS

We are grateful to Ward N. Hubbard and Donald R. Fredrickson of the Argonne National Laboratory for discussions of the practical aspects of this problem.

Reprinted from Journal of Applied Physics, Vol. 39, No. 9, 4206–4215, August 1968

Electrical Resistances of Wires of Low Temperature Coefficient of Resistance Useful in Calorimetry (10°–380°K)

G. T. Furukawa, M. L. Reilly, and W. G. Saba

Heat Division, National Bureau of Standards, Washington, D. C.

(Received 20 June 1963)

THE resistance of some alloy wires was measured in the range 10° to 380°K as a part of the program in the low temperature calorimetry laboratory of the National Bureau of Standards to simplify and to improve the accuracy in determining the electric power introduced into the resistance heater of adiabatic calorimeter vessels. The goal is to achieve regularly an accuracy of 0.001% in the determination of power. The total energy introduced is the time integral of the product of instantaneous voltage across the heater and current through the heater. In practice, the energy is calculated from the discrete values of voltages observed during the heating period, so that to obtain the highest accuracy, the voltage and current, and therefore the heater resistance, must remain as constant as possible between readings.

Constantan and manganin are used fairly extensively as heater wires in low temperature calorimetry and, in the range above about 250°K, have a very small temperature coefficient of resistance. (See Fig. 1.) Below about 250°K, however, both constantan and manganin wires show large changes in resistance, manganin more so than constantan. A survey was made, therefore, to find a wire of smaller temperature-coefficient of resistance at the lower temperatures. The resistances of promising wires were measured from 10° to 380°K, the range in which heat measurements are made in low temperature calorimetry. The wires were wound on a cylindrical copper block which was installed within one of the laboratory calorimeters in the position normally occupied by the calorimeter sample vessel. The resistances were measured at various selected temperatures maintained constant by means of the adiabatic shield.[1] The temperatures were determined by means of a platinum resistance thermometer installed in the copper block.

Table I. Composition and room temperature resistance of wires tested.

Wire	Nominal composition weight percent	Nominal specific resistance at 20°C $\mu\Omega$cm	Supplier
Manganin	Cu 84, Mn 12, Ni 4	48	Driver–Harris Co.
Constantan (Advance)[a]	Cu 57, Ni 43	49	Driver–Harris Co.
Karma[a]	Ni 76, Cr 20, Fe, Al	133	Driver–Harris Co.
Evanohm[a]	Ni 75, Cr 20, Al 2.5, Cu 2.5	134	Wilbur Driver Co.

[a] Trade name of the respective suppliers.

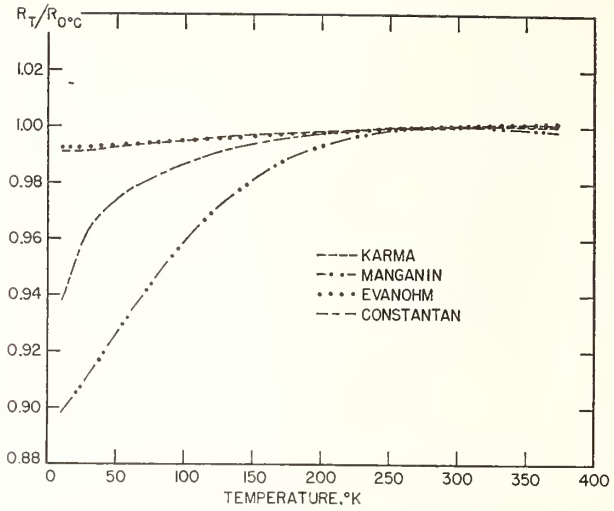

Fig. 1. Ratio of resistances of various wires at low temperatures to resistance at 273°K.

The resistance of two alloy wires Evanohm and Karma was found from the results of the measurements to change considerably less than constantan or manganin wire below 250°K. (For constantan, a wire of comparable composition sold under the trade name Advance was investigated.) Above 250°K, all four wires have comparable low temperature-coefficient of resistance suitable for calorimeter heaters. The ratios of the resistances to that at 273°K (0°C) of the four wires are compared in Fig. 1. The nominal chemical composition and the resistivity at 20°C of the wires as given in the literature supplied by the respective manufacturers are summarized in Table I. The total changes in resistance over the temperature range of measurements were 6% and 10% for constantan and manganin, respectively. On the other hand, the resistance of Evanohm and Karma wires changed by only about 0.9%. When applied to heat capacity measurements with the usual heating rate of one degree per minute, these newer heaters will change in resistance on the average only about 0.002% to 0.003% per min. With this small rate of change, interpolations should be possible between power readings at one-min intervals to better than 0.001%, using, for example, a constant current power supply, which is now generally available with 0.001% stability or better.

[1] G. T. Furukawa and M. L. Reilly, J. Res. Natl. Bur. Std. **56**, 285 (1956).

Reprinted from The Review of Scientific Instruments, Vol. 35, No. 1, 113–114, January 1964

Techniques in Calorimetry. I. A Noble-Metal Thermocouple for Differential Use

E. D. West
National Bureau of Standards, Washington, D. C.
(Received April 4, 1960)

A PROBLEM which arises frequently in calorimetry is the observation and control of the temperature of one body at or near the temperature of another. The temperature difference is frequently detected with one or more thermocouples. In selecting from the usual thermocouple materials for operation at temperatures above a few hundred degrees Celsius, a choice must be made between the better sensitivity of base metals and the good corrosion resistance and ease of construction of noble metals. Although alloys of gold and palladium have been used to make thermocouples of greater sensitivity than those of platinum and rhodium, such couples have been less stable and less reproducible.[1]

These disadvantages are of far less consequence when the thermocouple wires are used directly between surfaces at elevated temperatures with more stable leads through the large temperature gradients to the observation and control apparatus. For example, if the temperature difference between a body at 1000° and one at 1001°C is measured by two thermocouples brought out to cold junctions, an uncertainty of 0.1% in one of them would be as large as the temperature difference to be measured; but, if the alloy wires are kept in the hot region, the same percentage variation is small compared to the difference measured. The accuracy of the measurement can thus be made to depend mostly on the wires used for leads.

In the process of rebuilding an adiabatic calorimeter for use up to 600°C,[2] it was desirable to replace the Chromel-Alumel thermopiles, which frequently broke at the silver-soldered junction in the original assembly, with a corrosion-resistant combination of comparable sensitivity. Since the region in which the thermopiles are located is virtually isothermal, it appeared that gold-palladium might be useful. An alloy of 60% gold and 40% palladium (Au-Pd) of commercial purity was obtained at a nominal cost, without specifying close tolerances on the composition. A check was made of the emf of a couple of Au-Pd and platinum-10% rhodium (Pt-Rh) by welding a length of Au-Pd wire to a couple of platinum and Pt-Rh and heating in a tube furnace. The emf of the Au-Pd versus Pt-Rh thermocouple determined in this way is given in Fig. 1 together with the first derivative with respect to temperature. The curves are close to the calculated values for gold-35.11%-palladium versus Pt-Rh[1] and gold-40% palladium.[3] For comparison, a curve is included for Chromel-Alumel.

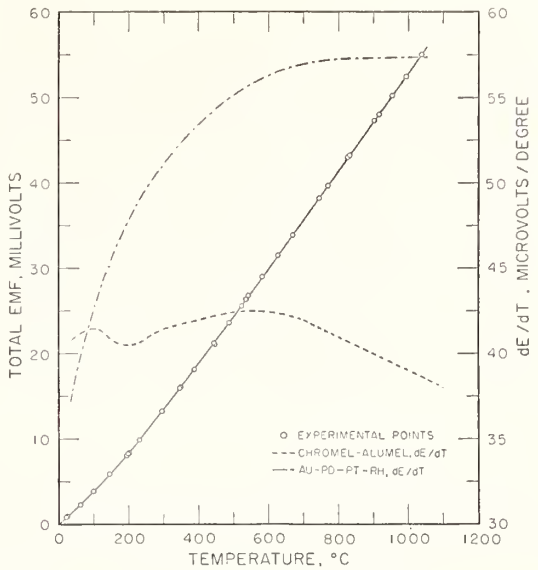

FIG. 1. Electromotive force of a thermocouple of gold-40% palladium and platinum-10% rhodium.

The thermopile junctions were made up by inserting No. 36 alloy wires through two small holes about 1 mm apart in gold "tiedown" tabs and brazing them simultaneously with silver. A 20-junction thermopile was installed in the calorimeter with gold leads out to a cold junction. The calorimeter has since been used intermittently for about a year. The thermopile is calibrated in place as a regular part of the calorimetric procedure in terms of heat flow per microvolt. At 50°C the heat leak from the calorimeter is 0.4 joules/hr for an indicated "zero" difference. Although the design of the calorimeter is such that a heat leak of about this magnitude will be present at zero temperature difference, ascribing the observed heat leak to uncertainty in the thermopile results in a calculated uncertainty of about 0.3 μv (0.4 millidegree C). The "zero" heat leak is greater by a factor of several at 350°C, but most, if not all, of this increase is due to the increase in the radiation heat transfer coefficient.

The Au-Pd is stiffer and more difficult to handle than wire ordinarily used for thermocouples, but this disadvantage is more than offset by the ease of soldering or welding. Since broken wires of Au-Pd and Pt-Rh can be repaired without flux and solder, no uncertainty is introduced in the weight of the calorimeter.

[1] A. A. Rudnitskii, *Termoelektricheskie svoistva blagorodnykh Metallov i ikh splavov* (Isdatel'stvo Akademii Nauk SSSR, Moscow, 1956). Available as translated document AEC-tr-3724 from Office of Technical Service, Department of Commerce, Washington 25, D. C. A good summary of data on many possible and practical thermocouple materials.

[2] E. D. West and D. C. Ginnings, J. Research Nat. Bureau Standards **60**, 309 (1958).

[3] *International Critical Tables* (McGraw-Hill Book Company, Inc., New York, 1929), vol. VI.

Reprinted from THE REVIEW OF SCIENTIFIC INSTRUMENTS, Vol. 31, No. 8, 896-897, August, 1960

Journal of Research of the National Bureau of Standards Vol. 50, No. 2, February 1953 Research Paper 2392

Calorimetric Determination of the Half-Life of Polonium

D. C. Ginnings, Anne F. Ball, and D. T. Vier [1]

The heats of radioactivity of four samples of polonium have been measured with a Bunsen ice calorimeter over a period of about seven months. With samples ranging in initial powers from 0.17 to 1.4 watts, the half-life values calculated from these measurements were found to agree within 0.1 percent, or the equivalent of 0.0003 watt, whichever was the larger. The results with the sample with the largest power gave a half-life value of 138.39 days, with an uncertainty of 0.1 percent (0.14 day). This is in agreement with the value of 138.3 days (±0.1 percent) reported by Beamer and Easton, who used a different calorimetric method.

1. Introduction

Of all published determinations of the half-life of polonium, probably the most accurate is that by Beamer and Easton [1],[2] who used a calorimetric method and observed a sample for as long as 97 days. Their method consisted in measuring the temperature difference between a container with the sample of polonium and an identical container that was empty. Both containers were surrounded by an isothermal jacket, and the relation between temperature difference and power was determined by means of electric calibration experiments. The value of the half-life was found to be 138.3 days (±0.1%). A Bunsen ice calorimeter is also suitable for measuring radioactive power (and half-life) of radioactive materials. Because this method is entirely different from that used by Beamer and Easton, and because much larger samples of polonium were available, it seemed worth while to measure the half-life of several samples that were suitable for measurements with the ice calorimeter.

The Bunsen ice calorimeter seems ideally suited for several reasons to the measurement of the heat evolved by curie or multicurie quantities of alpha, weak beta, and with modification [2], other radioactive materials. First, the heat leak is small (perhaps 0.0002 w). Second, the calorimeter requires very little attention during the measurements, usually a few minutes every hour or two for ice-bath replenishment. Third, no electrical or temperature measuring instruments are required because the measurement of heat requires only weighing of mercury. Fourth, the calibration factor of the ice calorimeter is a fundamental physical constant, which has been determined to about 0.01 percent by electrical calibration experiments [3].

On the other hand, the ice calorimeter in its present application has an inherent variation, or error, which is comparable with its heat leak. While this does not limit the precision of experiments involving about 1-w power, it would limit the precision of measurements of much smaller powers. Other ice calorimeters designed specifically for small radioactive powers [2] have proved sensitive to as little as 0.00003 w. An improved ice calorimeter has been in use at the National Bureau of Standards for some time in the measurement of heat capacities at high temperatures [3]. Although this calorimeter was not intended for measurements of radioactive power, it seemed suitable for measurements on certain samples of polonium (alpha emitter) furnished by the Los Alamos Scientific Laboratory, which initially developed powers in the range of 0.17 to 1.4 w. By measuring the decay of radioactive power of a sample of polonium over time intervals comparable with its half-life, values were obtained of its half-life.

2. Experimental Details

The ice calorimeter used in these experiments is shown in figure 1. It is the same calorimeter previously described [3]. An ice mantle (I) was frozen around the central calorimeter well (A) on a system of copper vanes (F) designed to increase the area of contact of the central well with the ice. The sample was suspended in the bottom of this well by a small wire that was pushed over against one side of the well by the gate G. The heat developed in the sample melted some of the ice, thereby decreasing the volume of the ice-water system and causing mercury to be forced into the calorimeter from beaker B. A small flow upward of dry helium in the calorimeter well was maintained to prevent condensation of water vapor from the room in the calorimeter and also to increase thermal contact between the sample and the calorimeter.

The polonium samples were sealed in glass or metal containers, which were enclosed in brass outer containers made to fit closely to the central well of the ice calorimeter. Because the radiation from polonium is essentially all of the alpha type, the containers were completely effective in converting all the radioactive energy into heat within the container. A sample was lowered into the calorimeter (with the two platinum shields above it, as described elsewhere [4]), and about 10 or 15 min was allowed for it to come to essentially a steady temperature, the valve V being open. Then the mercury meniscus was adjusted to the upper part of the scale, C, by partly evacuating reservoir R. Valve V was immediately closed, thereby causing the meniscus at C to start to move downward due to the heat input to the calorimeter. The time was

[1] Los Alamos Scientific Laboratory, University of California.
[2] Figures in brackets indicate the literature references at the end of this paper.

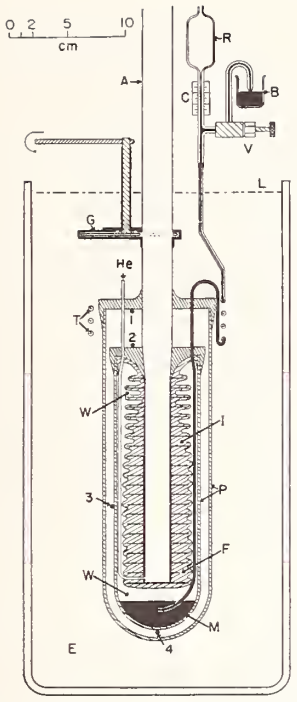

FIGURE 1. *Schematic diagram of ice calorimeter.*

A, calorimeter well; B, beaker containing mercury; C, glass capillary; E, ice bath; F, copper vanes; G, gate; I, ice mantle; M, mercury; P, Pyrex containers; R, mercury reservoir; T, mercury "tempering" coil; V, needle valve; W, water; 1, 2, 3, and 4, thermocouple junctions.

recorded when the meniscus passed an arbitrary zero on this scale, the beaker of mercury (B) was replaced by a weighed beaker of mercury, and valve V opened again. At the end of an experiment, the valve was closed again and the time recorded when the meniscus again passed its zero. The difference in the weights of the beaker gave the weight of mercury sucked into the calorimeter in a measured time. A small correction (perhaps 1 joule) was made for heat leak. The corrected mass of mercury was converted to energy by use of the calibration factor of the ice calorimeter as previously determined [3], 270.46 abs j/g of mercury for the "ideal" calorimeter or 270.47 abs j/g for the actual calorimeter used. From the duration of the experiment (difference in times at which the mercury meniscus passed the arbitrary zero), the energy was converted into average power.

The values of power calculated in the manner described would be correct if the sample and all other parts in thermal contact with the calorimeter did not change temperature during the experiment. However, as heat is put into the calorimeter, the thickness of the water layer between the ice and the central well with its vanes increases, and as there is flow of heat across this water layer, the temperature drop across this water layer must increase. As a result, the temperatures of the central well and vanes, and the sample with its container, all increase slightly during an experiment, so that part of the heat produced by the sample does not melt ice. This amount of heat depends on the power of the sample, the heat capacities of the various parts, and on the thickness of the water layer at the beginning of the experiment. The analysis of the correction for this heat is given as follows.

Consider a system (such as the radioactive sample plus metal calorimeter well with vanes) separated from ice by a layer of water. Consider also that the thermal contact between sample and calorimeter does not change during an experiment. Let

Q=the total amount of heat (joules) that has been introduced into the ice calorimeter at any particular time,
P=the power (j/sec) developed by the sample,
H=the heat capacity (j/deg C) of the system (sample plus calorimeter well with vanes),
A=the effective area of contact of the system with ice, cm^2,
K=the thermal conductivity of water at 0° C, 0.0052 w cm^{-1}deg^{-1},
m=the average thickness of the water layer, cm,
F=the heat of fusion of ice, 333 j/g.

Then the grams of ice melted $=Q/F=Q/333$.

The volume of water between the ice and the vanes is the same as the volume of ice melted because any void created by the difference in density of ice and water is filled almost instantaneously by water outside the mantle passing through and around the cracks in the ice mantle. Hence, the volume of water layer formed=(specific volume of ice) $(Q/333)$ $=(1.09)$ $(Q/333)=0.0033Q$; $m=0.0033(Q/A)$; and the temperature difference across the water film$=$ $Pm/(0.0052)A=(0.0033/0.0052)(PQ/A^2)=0.63(PQ/A^2)$. Thus the heat stored in the system after Q joules have been introduced (assuming no temperature gradient in the metal system)$=(0.63H)$ (PQ/A^2), and the heat stored in the water after Q joules have been introduced (assume linear temperature gradient across the film)$=(4.18)$ $(0.0033Q)$ $(0.63/2)$ $(PQ/A^2)=$ 0.0043 (PQ^2/A^2), and the total heat stored$=(P/A^2)$ $(0.63HQ+0.0043Q^2)$. If we start an experiment with Q_1 joules of heat already put into the calorimeter and a steady state of heat flow from the sample to the ice mantle, and end the experiment with Q_2 joules of heat in the calorimeter, and the same steady state of heat flow, then the difference in heat stored $=(P/A^2)[0.63H(Q_2-Q_1)+0.0043(Q_2^2-Q_1^2)]$.

The relative error, E, is

$$E=\frac{P}{A^2(Q_2-Q_1)}\,[0.63H(Q_2-Q_1)+0.0043(Q_2^2-Q_1^2)],\ \text{or}$$

$$E=\frac{P}{A^2}\,[0.63H+0.0043(Q_2+Q_1)].$$

If E is plotted against (Q_2+Q_1), the slope of the resulting straight line is

$$\text{Slope}=0.0043\,\frac{P}{A^2},$$

and the intercept of this line with the E axis is

$$\text{Intercept}=0.63\,\frac{HP}{A^2}.$$

This analysis shows that for any given power P of the sample, the slope of this line is dependent only on the effective area of contact (A) of the metal vanes with the ice. This effective area depends, of course, on the length of the sample. The intercept of this line with the relative error axis depends not only upon the area A but also upon the heat capacity, H of the sample-plus-vane system.

For any given sample with a known heat capacity and length, values of A and H can be calculated, using the dimensions and heat capacity of the corresponding portion of the calorimeter well and its system of vanes. It is believed that a better evaluation of A and H can be obtained by electrical calibration experiments, putting in known quantities of electric heat into the calorimeter over a length equivalent to the radioactive samples to be measured. If the heat is distributed in the electrical experiments the same as in the experiments with the radioactive samples, the value of A obtained from the electrical experiments should also be the same. However, the value of H obtained from the electrical experiments differs from that for the radioactive experiments by the difference in heat capacities of the electric heater and the radioactive samples.

The results of the electric calibration experiments are indicated by the circles in figure 2, which shows the relative error, E, plotted against (Q_1+Q_2). The best straight line through these circles is labeled "Electric Experiments" and was determined by the method of least squares to be $E=0.000633+2.992\times 10^{-8}(Q_1+Q_2)$, where Q_1 and Q_2 are expressed in joules. The electric calibration experiments were made with a power of about 1.4 w to correspond approximately to the initial radioactive power of sample 4, which was the largest of the four samples and therefore had the largest correction for the water layer. The slope of the solid line (electric experiments) indicated that the effective area of contact (A) between the ice and the source of heat was about 420 cm². This is roughly equivalent to a 9-cm length of the calorimeter well, as compared to an actual length of the electric heater of about 7 cm.

While the value of A obtained from the electric calibration experiments agreed as well as expected with that estimated from the dimensions, the value of heat capacity H (after correction for the heat capacity of the heater) corresponded to about a 17-cm length of the calorimeter well, which is considerably more than expected. Some of this difference may be due to the assumption in the theory that the temperature gradient in the copper vanes is negligible. If the position of the line had been calculated entirely on the basis of a 9-cm length of the calorimeter well, it would have the same slope as the line given by the electric experiments but would be shifted to decrease E by almost 0.0003. Because it is believed that the electric calibration experiments give more reliable values of the effective A and H, the solid line in figure 2 was used as basis for the corrections for the experiments with the radioactive samples. The dashed lines shown in the figure for sample 4 were calculated on this basis, as well as corresponding lines (not shown) for the other samples. Values of apparent calibration factor (which is equivalent to 270.47 $(1+E)$) were read from the dashed lines for the corresponding values of (Q_1+Q_2).

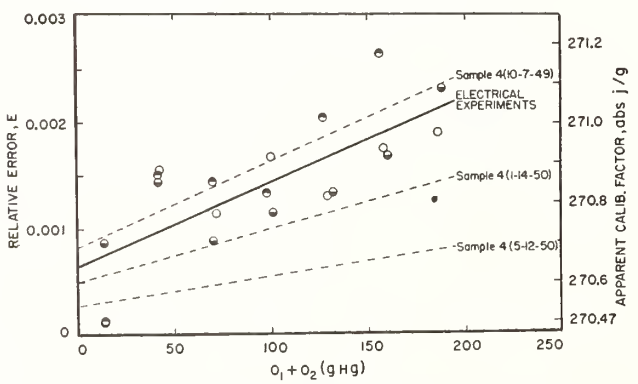

FIGURE 2. *Corrections for water layer in calorimeter.*
Electrical experiments: ◓, 10-11-49; ◒, 10-12-49; ○, 10-14-49.

3. Results

The results of the measurements with the four samples are given in table 1. The mean time of experiment is given, so that all experiments in one group can be corrected for the radioactive decay to bring them all to the same time (noon, EST) on the reference date. The mass of mercury was corrected for the effect of heat leak between the calorimeter and its surroundings (this effect is usually only a few milligrams of mercury). The quantities Q_1 and Q_2 are as previously described. Using the quantity Q_1+Q_2, the apparent calibration factor of the ice calorimeter was obtained from figure 2, from the curve for the appropriate sample. The product of this factor and the mass of mercury, divided by the duration of the experiment, gives the power at mean time of experiment. Using an approximate value of the half-life of polonium, this power was converted to power at noon (EST) on the reference date. The deviations from mean power are the deviations of the results of the individual experiments from the mean power of the group of experiments. The values of half-life given in the last column are based on the mean powers and reference dates, and the values indicated in parentheses are the authors' estimated uncertainties of the half-life based on both accidental and systematic errors.

It will be noted that more measurements were made with sample 4 than with the other three samples. This was because sample 4 had the highest power of the four samples, and it was believed that the highest relative calorimetric accuracy could be obtained with this sample, resulting in the best determination of the half-life of polonium. The power of sample 1 was so low that calorimetric errors could account for the low value of half-life calculated. The uncertainty in heat leak of the calorimeter was believed to be about 0.0002 w. This uncertainty, when compared with the power measured for sample 1 on May 14, 1950 (0.05698 w), could explain most of the discrepancy with the results with the other

TABLE 1. *Results of experiments*

Date of experiment	Mean time of experiment EST	Duration of experiment	Mass of mercury	O_1	O_2	Apparent calorimeter factor $270.47(1+E)$	Power at mean time of experiment	Power at noon (EST) on reference date	Reference date	Deviations from mean power	Mean power	Half-life
Sample 1												
		sec	*g*	*g* Hg	*g* Hg	*j g*$^{-1}$	*abs w*	*abs w*		*percent*	*abs w*	*Days*
10-3-49	3:24 p. m.	3 557.8	2.3048	0	2	270.49	0.17523	[a] 0.17451		+0.16		
	6:36 p. m.	12 367.2	7.9892	2	10	270.49	.17474	.17411		−0.07		
10-4-49	12:32 p. m.	9 928.0	6.3924	10	17	270.50	.17417	.17419	10- 4-49	−0.02	0.17423	
	3:20 p. m.	10 126.5	6.5205	17	23	270.50	.17418	.17430		+0.04		
5-3-50	1:14 p. m.	20 354.0	4.5269	24	29	270.48	.06016	.05694		+0.07		137.7
5-4-50	1:19 p. m.	19 440.0	4.2913	29	34	270.48	.05971	.05680		−0.32		[b] (±1.0)
5-14-50	2:16 p. m.	21 909.5	4.6221	0	5	270.48	.05706	.05709	5-14-50	+0.19	0.05698	
	7:14 p. m.	13 948.0	2.9396	5	8	270.48	.05700	.05709		+0.19		
Sample 2												
10-5-49	11:10 a. m.	6 168.5	9.1630	23	32	270.56	0.40190	0.40183		+0.04		
	12:45 p. m.	5 224.0	7.7486	32	40	270.57	.40133	.40139	10- 5-49	−0.06	0.40165	
	2:15 p. m.	5 478.0	8.1294	40	48	270.58	.40154	.40173		+0.02		138.52
4-27-50	1:48 p. m.	16 514.9	8.8470	24	33	270.50	.14491	.14425		+0.18		[b] (±0.4)
4-28-50	1:00 p. m.	17 999.8	9.5623	33	43	270.50	.14370	.14373	4-28-50	−0.18	0.14399	
Sample 3												
10-8-49	1:24 p. m.	5 134.4	12.2025	0	12	270.58	0.64306	0.64323		+0.02		
	2:45 p. m.	5 207.5	12.3623	12	24	270.61	.64241	.64278	10- 8-49	−0.05	0.64312	
	4:06 p. m.	4 576.2	10.8695	24	35	270.63	.64280	.64335		+0.04		
4-19-50	1:49 p. m.	12 692.3	11.4817	0	11	270.51	.24471	.24358		−0.01		138.52
4-20-50	11:35 p. m.	10 313.6	9.2898	11	20	270.52	.24367	.24365	4-20-50	+0.02	0.24361	[b] (±0.2)
	2:31 p. m.	10 808.6	9.7279	20	30	270.52	.24347	.24360		0.00		
Sample 4												
10-6-49	12:55 p. m.	2 634.7	14.0020	28	42	270.84	1.43937	1.43307		−0.01		
	1:35 p. m.	2 766.9	14.7066	42	57	270.91	1.43994	1.43382		+0.04		
	1:28 p. m.	2 622.8	13.8785	0	14	270.72	1.43251	1.43296		−0.02		
	2:07 p. m.	2 676.2	14.1607	14	28	270.78	1.43279	1.43345		+0.01		
	2:57 p. m.	2 733.6	14.4582	28	42	270.84	1.43249	1.43338	10- 7-49	+0.01	1.43327	
10-7-49	3:43 p. m.	2 717.2	14.3735	42	57	270.91	1.43306	1.43423		+0.07		
	4:28 p. m.	2 736.5	14.4643	57	71	270.97	1.43226	1.43361		+0.02		
	5:14 p. m.	2 689.3	14.1840	71	86	271.03	1.42948	1.43105		−0.15		138.39
	6:00 p. m.	2 879.7	15.2113	86	101	271.10	1.43202	1.43382		+0.04		[b] (±0.14)
1-14-50	11:00 a. m.	3 170.1	10.2320	10	20	270.64	0.87353	0.87335		+0.05		
	11:54 a. m.	3 345.9	10.7884	20	31	270.67	.87274	.87272		−0.03		
	12:50 p. m.	3 359.8	10.8281	31	42	270.70	.87242	.87257		−0.04		
	1:44 p. m.	3 067.7	9.8837	42	52	270.73	.87225	.87256	1-14-50	−0.04	0.87294	
	2:35 p. m.	3 115.1	10.0448	52	62	270.74	.87302	.87349		+0.06		
	3:28 p. m.	3 178.3	10.2384	62	72	270.78	.87228	.87292		+0.00		138.40
5-12-50	10:04 a. m.	8 282.3	14.8070	3	18	270.56	.48370	.48350		+0.00		[b] (±0.18)
	12:25 p. m.	8 395.9	15.0148	18	33	270.58	.48389	.48393		+0.10		
	2:46 p. m.	8 534.5	15.2193	33	48	270.61	.48257	.48284		−0.12		
	5:00 p. m.	7 439.2	13.2613	48	61	270.63	.48243	.48293	5-12-50	−0.10	0.48342	
	6:55 p. m.	6 260.2	11.1775	61	72	270.64	.48322	.48391		+0.09		
	8:43 p. m.	6 947.3	12.3852	72	85	270.66	.48252	.48339		0.00		

[a] Experiment weighted one-third because of short duration of experiment.
[b] Figure given for uncertainty based upon authors' estimate of both accidental and systematic errors.

samples having higher power because it would require an increase of only 0.0003 w in the value observed on May 14 to agree with the other samples.

It is interesting to note the corresponding effects of an uncertainty of 0.0003 w on the other samples having higher powers. With samples 2 and 3, this uncertainty in the May values would result in half-life uncertainties of about 0.21 percent (0.29 day) and 0.12 percent (0.17 day), respectively. With sample 4, however, the same power uncertainty in the values on January 14 results in only 0.04 percent (0.06 day) uncertainty in the over-all half-life. The uncertainty in heat leak is probably the largest error in the measurements with samples 1, 2, and 3. With sample 4, however, the heat leak uncertainty is probably comparable with all other errors. In addition, sample 4 was observed at an intermediate date (0.7 half-life) in an effort to detect any change in the decay constant with time.

The measurements with the four samples agree within ±0.1 percent, or 0.0003 w, whichever is the larger. The slightly different half-life values on sample 4 for the two different periods are not significant because the difference is much less than the experimental error. There is no significant evidence, therefore, of a change in the decay constant, such as would occur either if the polonium was contaminated with radioactive impurities having values of half-life different from polonium, or if some secondary chemical or nuclear reaction produced heat that was not

directly proportional to the radioactive energy of the polonium sample. In addition, the polonium samples used were of a purity that should have precluded the possiblity of appreciable contamination by other radioactive elements. The polonium had been purified both by distillation and by electrodeposition on platinum foils from dilute nitric-acid solution of polonium nitrate. Of course, the stable lead isotope formed from the decay of polonium was present but could not affect the results of this investigation.

The best value of the half-life of polonium was estimated from the two values for sample 4, giving more weight to the earlier value, where the sample had a larger power. On this basis, the authors believe that the best value of the half-life derived from these measurements is 138.39 days. It is believed that the calorimetric uncertainties (based upon both accidental and systematic errors) in the experiments may result in an error in this value of ± 0.1 percent (0.14 day).

The results of these measurements are in agreement with the value reported by Beamer and Easton [1] of 138.3 days ± 0.1 percent, determined calorimetrically by another method.

4. References

[1] William H. Beamer and William E. Easton, J. Chem. Phys. **17,** 1298 (1949).

[2] Swietoslawski, Microcalorimetry, p. 66 (Reinhold Publishing Corporation, New York, N. Y., 1946).

[3] Defoe C. Ginnings, Thomas B. Douglas, and Anne F. Ball, J. Research NBS **45,** 23 (1950) RP2110.

[4] D. C. Ginnings and R. J. Corruccini, J. Research NBS **38,** 593 (1947) RP1797.

Washington, July 15, 1952.

JOURNAL OF RESEARCH of the National Bureau of Standards—A. Physics and Chemistry
Vol. 69A, No. 3, May–June 1965

Heats of Transformations in Bismuth Oxide by Differentia Thermal Analysis

Ernest M. Levin and Clyde L. McDaniel

(January 5, 1965)

DTA was chosen as a convenient method for resolving differences in the reported heat of transition and heat of fusion of Bi_2O_3. The heat of the low to high transition of K_2SO_4 (at 583 °C) and the heat of fusion of Ag (at 960.8 °C) were used as internal standards. These standards were mixed directly with the Bi_2O_3 in three weight ratios. The heating schedule for each weight ratio was 3°/min, 9°/min, and 3°/min. For evaluating internal consistency, DTA determinations were made for mixtures of the two standards. Linearity was obtained within limits between the weight ratio of Bi_2O_3 and standard and the corresponding ratio of peak areas. The heat of transition of Bi_2O_3 (mon$\xrightarrow{730\ °C}$ cubic was found to be 9.9 ± 0.5 kcal/mole and the heat of fusion (cubic$\xrightarrow{825\ °C}$liq.) 3.9 ± 0.2 kcal/mole. The uncertainties are estimated limits of error, based on internal consistency and on the values of the standards.

1. Introduction

By application of the Clausius-Clapeyron equation to the liquidus curve of the Bi_2O_3–PbO system [1],[1] K. K. Kelley determined the heat of fusion of Bi_2O_3 to be 6.8 kcal/mole [2]. This value is listed in tables of thermodynamic data [3, 4]. Levin and McDaniel [5] applying the same Clausius-Clapeyron equation to the Bi_2O_3–B_2O_3 system obtained a heat of fusion value of 2.0_5 kcal/mole. Gattow and Schröder [6] and Gattow and Schütze [7] have used these two values in conjunction with differential thermal analysis (DTA) data to calculate the heat of transition of monoclinic- to cubic-bismuth oxide (see table 1). They found that the area of the peak representing the monoclinic to cubic transition was 4.10 ± 0.11 times the area of the peak representing the cubic to liquid transformation; and, consequently, the heat of transition should be 4.10 × the heat of fusion.

TABLE 1. *Heats of transformations in bismuth oxide*

Investigator	Method	Heat of transformation	
		Transition (mon → c)	Fusion (c → liq)
		kcal/mole	*kcal/mole*
K. K. Kelley (1936) [2]	Bi_2O_3–PbO liquidus [1]		6.8
Levin and McDaniel (1962) [5]	Bi_2O_3–B_2O_3 liquidus		2.0_5
Gattow and Schröder (1962) [6]	DTA[a]	27.9 ± 1.0	
Gattow and Schütze (1964) [7]	DTA[b]	8.4 ± 0.3	
Levin and McDaniel (1964)	DTA[c]	9.9 ± 0.5	3.9 ± 0.2

[a] Heat of transformation = (4.10 ± 0.11) × heat of fusion (6.8 kcal/mole).
[b] Heat of transformation = (4.10 ± 0.11) × heat of fusion (2.05 kcal/mole).
[c] Using K_2SO_4 and Ag as internal standards.

[1] Figures in brackets indicate the literature references at the end of this paper.

The two reported values for the heat of fusion of Bi_2O_3 differ by a factor of about three. The value of 6.8 kcal/mole obtained from the Bi_2O_3–PbO diagram is suspect for two reasons: First, a reinvestigation of the Bi_2O_3–PbO system [8] has shown Belladen's simple liquidus diagram to be incorrect, inasmuch as PbO exists in solid solution with Bi_2O_3 at the liquidus Second, the sum of the reported entropy of transitior and of fusion, $\left(\frac{6800}{1098}+\frac{27900}{1003}\Big/5\right)$, is about 7 cal/°K/ξ atom, an abnormally high value.

Because of the increasing importance of Bi_2O_3 in the electronics and ceramics industries, it is desirable to verify the basic thermodynamic data. As equipment for direct calorimetric measurement was not available, differential thermal analysis, using internal standards, was selected as a convenient, independent method for determining heats of transformation.

2. Equipment

The differential thermal analysis equipment was built in the laboratory and is of conventional design. The furnace heating element consists of a ceramic core 10 in. long × 2⅜ in. o.d., wound with 20 gage, 80 percent Pt: 20 percent Rh, wire. Linear temperature rise with time is accomplished by means of a program controller and a pneumatically activated variable autotransformer. Heating rates of 3°/min and 9°/min are obtained by controlling the percentage of time during which the set point is driven. Using a multipoint recorder, the emfs of the sample thermocouple and of the differential thermocouple are plotted as a function of time. Determinations are made at overall sensitivities of 14 μV/in.

To minimize errors that might be caused by poor thermal diffusivity, a special holder assembly is used.

The two thermocouples (Pt – 90 percent Pt:10 percent Rh) from the holder assembly are welded, near the bottom, to Pt containers. The containers are made from Pt tubing and measured 16 mm long × 2.6 mm i.d. × 3.0 mm o.d. The tubes contain a total of 0.2 to 0.4 g of material, depending on the substances and weight ratios studied. To reduce the effect of air currents in the furnace, the Pt tubes are covered with thin ceramic thimbles.

3. Method

The usual procedure for measuring heats of transformation by DTA depends on calibration of the equipment with a known weight of a standard, e.g., benzoic acid, $AgNO_3$, KNO_3 [9, p. 111] and [10, 11]. The calibration can be expressed in terms of calories per unit of integrated peak area, in the differential temp.-time curve representing the transformation. Assuming approximate constancy of the calibration factor, the unknown heat of transformation for a substance can be determined from the peak area in its differential temp.-time curve.

The method depends on conditions that are seldom closely realized. First, the geometry of the physical arrangement and other operating conditions should be exactly the same for the determination of the unknown as for the calibration with the standard. Second, and even more unlikely, such thermal properties as conductivity, diffusivity, and specific heat should be essentially identical for the two samples.

A method using internal standards avoids the problems inherent in a separate calibration method. Therefore, several high-purity chemicals, with appropriate temperatures and heats of transformations were tried, in a search for internal standards.

Two substances were found satisfactory for calibrants: (1) Finely ground crystalline K_2SO_4 with a heat of transition ($\alpha \xrightarrow{583\ ^\circ C} \beta$) of 2.14 kcal/mole [3, 12]. (2) Fine, precipitated Ag powder with a heat of fusion ($s \xrightarrow{960.8\ ^\circ C}$ liq.) of 2.61 kcal/mole [2] [13]. The transformation temperatures in these two substances bracket the transition temp. of Bi_2O_3 (monoclinic $\xrightarrow{730\ ^\circ C}$ cubic) and the fusion temp. of Bi_2O_3 (cubic $\xrightarrow{825\ ^\circ C}$ liquid). Two additional substances, NaCl and Li_2SO_4, were found to be unsatisfactory as internal calibration standards.

DTA experiments were carried out for $Bi_2O_3 : K_2SO_4$ mixtures in wt. ratios of 3.46 : 1, 1.72 : 1, and 1.00 : 1; and for Bi_2O_3 : Ag mixtures in wt ratios of 4.32 : 1, 2.16 : 1, and 2.00 : 1. Mixtures were made in 2g batches by shaking in a mechanical mixer accurately weighed amounts of dried starting materials. As will be shown below under "Derivation of Equations" the heat of transformation calculations are not based on the actual weights of the two substances in the sample holder but only on the formulated ratios.

Each mixture was given a preliminary heat-cycling treatment by heating the mixture at 12 °C/min to about 775 °C (above the transition of K_2SO_4 and Bi_2O_3 but below the melting point of Bi_2O_3) and then cooling to room temperature. The preliminary heat treatment was followed by three successive cycles of heating to above the mp of Bi_2O_3 in K_2SO_4 mixtures and above the mp of Ag in Ag mixtures. The heating and cooling rates for the three cycles were 3°/min, 9°/min, and 3°/min, respectively. Only the peak areas in heating curves were considered, as previous work, using both DTA and high-temperature x-ray techniques [14], had shown that the stable high-temperature cubic phase is supercooled below the equilibrium transition temperature of 730 °C; and at about 650 °C a metastable tetragonal and/or body-centered cubic phase is formed, which in turn, transforms back to the stable monoclinic form.

To check on the internal consistency of the method and to evaluate the accuracy, DTA determinations were made with mixtures of the two standards, at the same heating rates and at weight ratios of K_2SO_4 : Ag of 1.36:1 and 4.00:1.

It should be noted that a number of investigators [9] have used internal standards for quantitative estimation of a phase. Barshad [11] has proposed using "indicators" either mixed with the sample or in separate layers, for direct temperature calibration of a DTA curve. However, the use of internal standards for heat of reaction measurements as herein proposed has not been previously reported, according to the best knowledge of the authors.

An obvious and valid à priori criticism of the internal-standard method is the possibility of obtaining erroneous results if reaction occurs between the bismuth oxide and the standards during the heat-cycling treatments. This possibility was foreseen and was shown to be minimal by a number of observations.

(1) The ratio of the areas under the peaks representing the monoclinic to cubic transition and the cubic to liquid transformation for pure Bi_2O_3 could be compared with the corresponding ratio when standards were mixed with the Bi_2O_3.

(2) Ratios of corresponding areas for successive heat cycles could be compared with each other, and any discrepancies noted.

(3) At the conclusion of each series of determinations for a given weight ratio, the mixture was examined by x-ray powder diffraction techniques to check for any new phases that might have formed by reaction of the starting materials.

(4) Finally, experimental results could be checked for conformance to theory.

By the criteria listed above, it was possible to evaluate the individual experimental data and to eliminate the few values which were obviously in error. However, even in these instances, the evidence did not indicate chemical reaction of the Bi_2O_3, but pointed to physical factors.

4. Derivation of Equations

It can be shown that to a close approximation [9, p. 111] the total heat of reaction in a DTA determination

[2] The literature values reported for the heats of transformations in K_2SO_4 and Ag vary over a range of about 10 percent. The values selected here are shown later in this paper (see Internal Consistency) to be self-consistent.

is given by:

$$\Delta H = \frac{cK_s}{g}\int ydt = \frac{cK_s}{g}\cdot A \qquad (1)$$

where, H = heat of transformation per g

c = geometrical shape constant

K_s = thermal conductivity of the sample

g = mass of reactive component in sample

$\int ydt = A$ = peak area for the transformation.

If two substances, designated by subscripts 1 and 2, are considered in a mixture, eq (1) may be applied to each substance. Assuming no reaction between the substances, constancy in c, and approximate constancy in K_s (now the combined thermal conductivity of the mixture), the following expression is readily obtained:

$$\frac{\Delta H_1}{\Delta H_2} = \frac{A_1 g_2}{A_2 g_1}. \qquad (2)$$

As ΔH_1 and ΔH_2 are constants, g_2/g_1 is the weight ratio of the binary mixture, as formulated, and A_1/A_2 is the experimentally measured peak area ratio of the two transformations, the basic equation for an unknown heat of transformation becomes:

$$\Delta H_1 = \Delta H_2 \left(\frac{g_2}{g_1}\right)\left(\frac{A_1}{A_2}\right). \qquad (3)$$

It may be noted that eq (3) is a straight line that passes through the origin and with slope, m, equal to $(A_1/A_2)/(g_1/g_2)$. Thus, over the range that the assumptions made in the derivation hold true, a linear relationship should exist between the formulated weight ratios and the corresponding measured peak area ratios.

If the heat of transformation is desired directly in kcal/mole rather than on a gram basis, eq (3) may be transformed to:

$$L_1 = L_2 \left(\frac{M_1}{M_2}\right)\left(\frac{A_1}{A_2}\right)\Big/\left(\frac{g_1}{g_2}\right) \qquad (4)$$

where, L_1 and L_2 are the heats of transformation of substances 1 and 2, respectively, in kcal/mole, and

M_1 and M_2 are the corresponding molecular weights.

Applying eq (4) to the specific case of $Bi_2O_3 : K_2SO_4$ mixtures:

$$L_{Bi_2O_3} = 2.14 \left(\frac{465.96}{174.27}\right)\left(\frac{A_{Bi_2O_3}}{A_{K_2SO_4}}\right)\Big/\left(\frac{g_{Bi_2O_3}}{g_{K_2SO_4}}\right) = 5.722 m_1 \qquad (5)$$

where, $L_{Bi_2O_3}$ refers to the heat of transformation (transition or fusion), in kcal/mole;

2.14 = the heat of transition of K_2SO_4, from the α to β form, in kcal/mole;

465.96/174.27 = the molecular weight ratio of Bi_2O_3 to K_2SO_4; and

m_1 = the slope of the line obtained by plotting as ordinate the ratio of the peak areas representing the particular transformation of Bi_2O_3 to the transition of K_2SO_4 ($A_{Bi_2O_3}/A_{K_2SO_4}$) and plotting as abscissa the corresponding weight ratio of Bi_2O_3 to K_2SO_4 ($g_{Bi_2O_3}/g_{K_2SO_4}$).

Applying eq (4) to the case of Bi_2O_3: Ag mixtures:

$$L_{Bi_2O_3} = 2.61 \left(\frac{465.96}{107.87}\right)\left(\frac{A_{Bi_2O_3}}{A_{Ag}}\right)\Big/\left(\frac{g_{Bi_2O_3}}{g_{Ag}}\right) = 11.274 m_2 \qquad (6)$$

where, 2.61 = the heat of fusion of Ag, in kcal/mole,
465.96/107.87 = the molecular weight ratio of Bi_2O_3 to K_2SO_4, and m_2 is the slope of the line obtained by plotting $\frac{A_{Bi_2O_3}}{A_{Ag}}$ as ordinate versus $\frac{g_{Bi_2O_3}}{g_{Ag}}$ as abscissa.

Applying eq (4) to the case of mixtures of the two standards, K_2SO_4 and Ag:

$$L_{K_2SO_4} = 2.61 \left(\frac{174.27}{107.87}\right)\left(\frac{A_{K_2SO_4}}{A_{Ag}}\right)\Big/\left(\frac{g_{K_2SO_4}}{g_{Ag}}\right) = 4.217 m_3 \qquad (7)$$

where, $L_{K_2SO_4}$ = the heat of transition of K_2SO_4, in kcal/mole;
2.61 = the heat of fusion of Ag, in kcal/mole
174.27/107.87 = the molecular weight ratio of K_2SO_4 to Ag; and
m_3 = the slope of the line obtained by plotting $\frac{A_{K_2SO_4}}{A_{Ag}}$ as ordinate versus $\frac{g_{K_2SO_4}}{g_{Ag}}$ as abscissa.

Inasmuch as DTA determinations were made in binary combinations of the three substances, Bi_2O_3, K_2SO_4, and Ag, it is possible to evaluate the internal consistency of the method. From eqs (5), (6), and (7), where m_1, m_2, and m_3 are given in terms of the specific ratios, it follows that any one ratio can be determined independently from the other two, for example:

$$\frac{\frac{A_{Bi_2O_3}}{A_{Ag}}\cdot\frac{g_{Ag}}{g_{Bi_2O_3}} = \frac{A_{K_2SO_4}}{A_{Ag}}\cdot\frac{g_{Ag}}{g_{K_2SO_4}}}{\frac{A_{Bi_2O_3}}{A_{K_2SO_4}}\cdot\frac{g_{K_2SO_4}}{g_{Bi_2O_3}}} \qquad (8)$$

or $m_2/m_1 = m_3$. (9)

5. Results and Discussion

5.1. General

Figure 1 shows a reproduction of the DTA curve for one of the $Bi_2O_3 : K_2SO_4$ mixtures. The various transformations within the phases are labeled. Peak areas were obtained by tracing the curve on millimeter ruled graph paper and averaging several counts. The modification of the sample holder in conjunction with the amplification of the equipment was found to be sensitive to heat of reaction effects. In a 1 : 1 mixture of $Bi_2O_3 : K_2SO_4$, for example, 0.1192 g K_2SO_4 absorbed a calculated 1.4635 calories of heat at the transition and produced an area under the peak of 208 mm², or about 0.007 cal/mm². No corrections were applied to the area data for change in thermocouple (Pt-90 percent Pt : 10 percent Rh) sensitivity with temperature. Attempted corrections did not improve the results; furthermore, the use of two standards whose transformation temperatures bracketed those of Bi_2O_3 provided automatic compensation.

The experimentally determined transformation ratios for pure Bi_2O_3 and the binary mixtures between Bi_2O_3, K_2SO_4, and Ag are given in table 2. Transformation ratios as a function of weight ratios are plotted in figures 2, 3, and 4. Slopes of the lines and standard deviations of the slopes were determined by the method of least squares for lines passing through the origin. If the assumptions used previously in deriving the linear relationships hold, then the origin constitutes a valid fixed point, for obviously as $g_{Bi_2O_3}$ in the mixture approaches 0, so does $A_{Bi_2O_3}$ and consequently so do the ratios $g_{Bi_2O_3}/g_{K_2SO_4}$ and $A_{Bi_2O_3}/A_{K_2SO_4}$.

Examining the transformation ratios (table 2) as a function of the 3°/min and 9°/min heating rates or as a function of the heating cycle (1st, 2d, or 3d), no overall trend of statistical significance can be discerned. The average ratios of the Bi_2O_3 transformations ($M \rightarrow c / c \rightarrow l$) of 2.54 and 2.52 for the $Bi_2O_3 : K_2SO_4$ mixtures and of 2.53 for the Bi_2O_3 : Ag mixture (4.32 : 1) are in good agreement with each other and with that for pure Bi_2O_3, 2.46. However, the ratios of 3.20 and 2.80 for the Bi_2O_3 transformations in the Ag mixtures (2.16 : 1 and 2.00 : 1) appear high. The heat of fusion of Bi_2O_3 is 2/5 that of the heat of transition, and the shape of the fusion peak tends to be low and flat (see fig. 1). Therefore, as the amount of Bi_2O_3 decreases in the mixture, the peak area for fusion becomes less defined and broader tending to give a low area count.

It may be noted in figure 2 for the $Bi_2O_3 : K_2SO_4$ mixtures that the curves deviate from linearity above a 2:1 wt ratio of $Bi_2O_3 : K_2SO_4$. This deviation is not due to any significant reaction between Bi_2O_3 and K_2SO_4 but to poor thermal properties of the Bi_2O_3 mixture. For the mixtures containing Ag, which is a good thermal conductor and which has been used to improve thermal transfer [9, 15], linearity extends beyond the 4:1 ratio of substance to Ag (fig. 3 and 4). Therefore, the area ratios for the 3.46 to 1 wt ratio of Bi_2O_3 to K_2SO_4 were not used in computing the slopes.

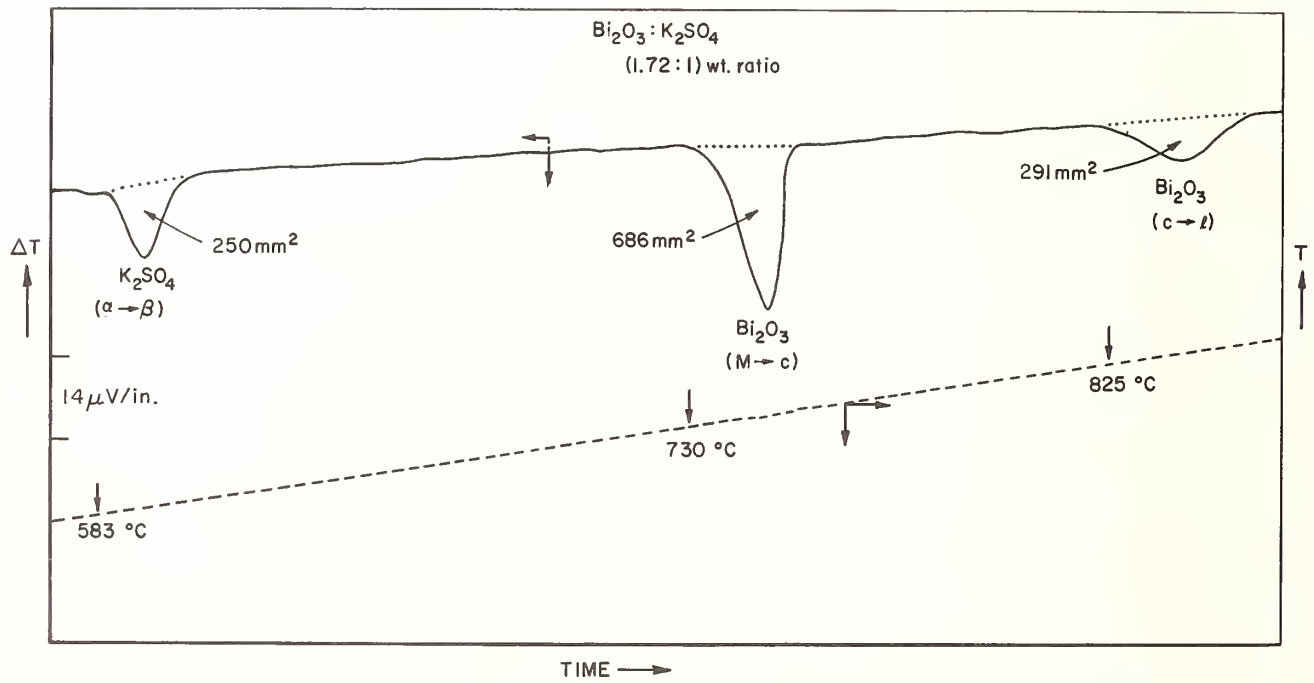

FIGURE 1. *Differential thermal analysis curve for third cycle of heat treatment of* $Bi_2O_3 : K_2SO_4$ *mixtures of weight ratio 1.72 : 1.*

Approx. 0.2 g of sample in Pt tube was heated in air at 3°/min. The temperature of sample container was measured with Pt—90 percent Pt:10 percent Rh thermocouple; reference material was compacted alumina powder. Areas under peaks were obtained by counting squares in tracings of the peaks on millimeter ruled graph paper.
$\alpha \rightarrow \beta$ = transition of K_2SO_4
$M \rightarrow c$ = monoclinic to cubic transition of Bi_2O_3
$c \rightarrow l$ = fusion of cubic Bi_2O_3.

TABLE 2. *Ratio of peak areas between transformations in* Bi_2O_3 *and in binary mixtures of* Bi_2O_3, K_2SO_4, *and* Ag, *as a function of heating rates and weight ratios**

Composition wt. ratio	Transformation ratios [a] A_1/A_2	Ratio of peak areas at heating rates: 3°/min	9°/min	3°/min	Average
Bi_2O_3 (pure)					
	$\frac{M \rightarrow c}{c \rightarrow l}$	2.47	2.57	2.33	2.46
Bi_2O_3 : K_2SO_4 mixtures					
77.6 Bi_2O_3 / 22.4 K_2SO_4 (3.46 : 1)	$\frac{M \rightarrow c}{c \rightarrow l}$	2.86	2.18	2.58	2.54
	$\frac{M \rightarrow c}{\alpha \rightarrow \beta}$	4.67	4.87	4.57	4.70
	$\frac{c \rightarrow l}{\alpha \rightarrow \beta}$	1.63	2.23	1.92	1.93
63.3 Bi_2O_3 / 36.7 K_2SO_4 (1.72 : 1)	$\frac{M \rightarrow c}{c \rightarrow l}$	2.51	2.70	2.36	2.52
	$\frac{M \rightarrow c}{\alpha \rightarrow \beta}$	3.03	2.94	2.74	2.90
	$\frac{c \rightarrow l}{\alpha \rightarrow \beta}$	1.21	1.09	1.16	1.15
50.0 Bi_2O_3 / 50.0 K_2SO_4 (1.00 : 1)	$\frac{M \rightarrow c}{\alpha \rightarrow \beta}$ [b]	1.61	1.61	1.62	1.61
Bi_2O_3 : Ag mixtures					
81.2 Bi_2O_3 / 18.8 Ag (4.32 : 1)	$\frac{M \rightarrow c}{c \rightarrow l}$	2.56	2.52	2.51	2.53
	$\frac{M \rightarrow c}{s \rightarrow l}$	3.91	3.82	3.96	3.90
	$\frac{c \rightarrow l}{s \rightarrow l}$	1.52	1.51	1.58	1.54
68.35 Bi_2O_3 / 31.65 Ag (2.16 : 1)	$\frac{M \rightarrow c}{c \rightarrow l}$	3.10 [c, d]	3.29 [d]	.....	3.20 [d]
	$\frac{M \rightarrow c}{s \rightarrow l}$	2.14 [c]	1.68	.....	1.91
	$\frac{c \rightarrow l}{s \rightarrow l}$	0.69 [c]	0.51	.....	0.60
66.7 Bi_2O_3 / 33.3 Ag (2.00 : 1)	$\frac{M \rightarrow c}{c \rightarrow l}$	.....	2.80	.....	2.80 [d]
	$\frac{M \rightarrow c}{s \rightarrow l}$	1.99	1.72	.....	1.86
	$\frac{c \rightarrow l}{s \rightarrow l}$	.....	0.61	.....	0.61
K_2SO_4 : Ag mixtures					
57.7 K_2SO_4 / 42.3 Ag (1.36 : 1)	$\frac{\alpha \rightarrow \beta}{s \rightarrow l}$	0.637	0.638	0.604	0.626
80.0 K_2SO_4 / 20.0 Ag (4.00 : 1)	$\frac{\alpha \rightarrow \beta}{s \rightarrow l}$	2.27	2.16	2.07	2.17

*Sample weights varied from 0.2 to 0.4 g, depending on the particular mixtures. Samples were contained in Pt tubes and heated in air. Sensitivity on the differential temperature scale was 14 μv/in.

[a] Refers to ratio of peak areas between the indicated transformations:
$M \rightarrow c$, monoclinic to cubic transition of Bi_2O_3 phase at 730 °C
$c \rightarrow l$, cubic to liquid transformation of Bi_2O_3 phase at 825 °C
$\alpha \rightarrow \beta$, low to high transition of K_2SO_4 phase at 583 °C
$s \rightarrow l$, solid to liquid transformation of Ag phase at 960.8 °C.

[b] No values for $\frac{M \rightarrow c}{c \rightarrow l}$ and $\frac{c \rightarrow l}{\alpha \rightarrow \beta}$ ratios as $c \rightarrow l$ transformation of Bi_2O_3 is not well defined.

[c] 12°/min heating rate.

[d] Area for $c \rightarrow l$ transformation of Bi_2O_3 appears low.

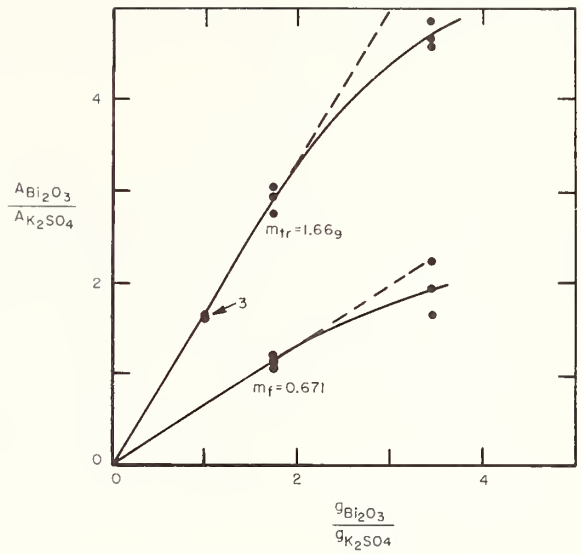

FIGURE 2. *Peak area ratios versus weight ratios for mixtures of* Bi_2O_3 *and* K_2SO_4.

$g_{Bi_2O_3}/g_{K_2SO_4}$ refers to the weight ratio. $A_{Bi_2O_3}/A_{K_2SO_4}$ for slope of line m_{tr} refers to area under transition of Bi_2O_3 ÷ area under transition of K_2SO_4. $A_{Bi_2O_3}/A_{K_2SO_4}$ for slope of line m_f refers to area under fusion of Bi_2O_3 ÷ area under transition of K_2SO_4. Slopes calculated by method of least squares.

$L_{Bi_2O_3} = 5.722 m_1$ (see eq (5), in text).
$L_{tr}Bi_2O_3 = 5.722 \times 1.66_9 = 9.5_5$ kcal/mole. S.D. $m_{tr} = 0.031$.
$L_fBi_2O_3 = 5.722 \times 0.671 = 3.8_4$ kcal/mole. S.D. $m_f = 0.020$.

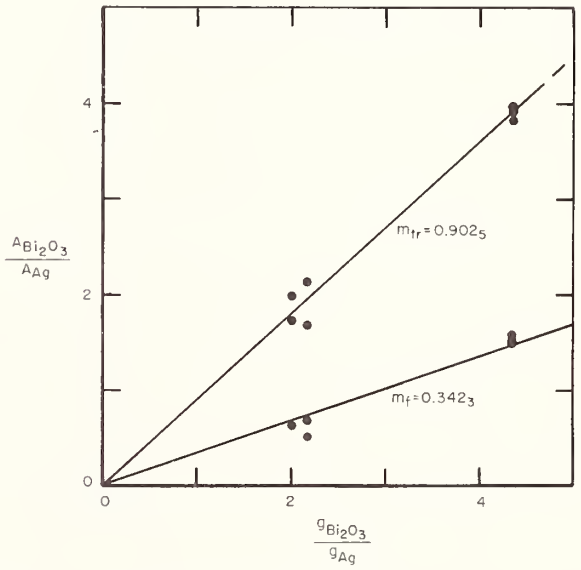

FIGURE 3. *Peak area ratios versus weight ratios for mixtures of* Bi_2O_3 *and* Ag.

$g_{Bi_2O_3}/g_{Ag}$ refers to the weight ratio. $A_{Bi_2O_3}/A_{Ag}$ for slope of line m_{tr} refers to area under transition of Bi_2O_3 ÷ area under fusion of Ag. $A_{Bi_2O_3}/A_{Ag}$ for slope of line m_f refers to area under fusion of Bi_2O_3 ÷ area under fusion of Ag. Slopes calculated by method of least squares.

$L_{Bi_2O_3} = 11.274 m_2$ (see eq (6), in text).
$L_{tr}Bi_2O_3 = 11.274 \times 0.902_5 = 10.1_7$ kcal/mole. S.D. $m_{tr} = 0.019$.
$L_fBi_2O_3 = 11.27 \times 0.342_3 = 3.8_6$ kcal/mole. S.D. $m_f = 0.015$.

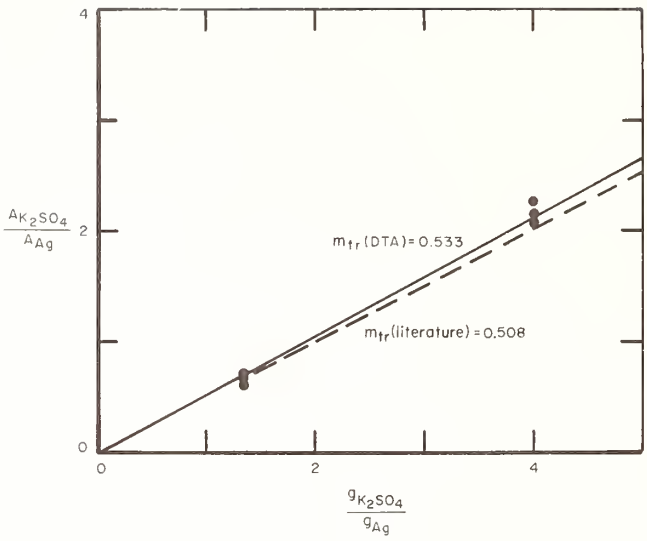

FIGURE 4. *Peak area ratios versus weight ratios for mixtures of* K_2SO_4 *and* Ag.

$g_{K_2SO_4}/g_{Ag}$ refers to the weight ratio. $A_{K_2SO_4}/A_{Ag}$ for slope of line m_{tr} (DTA) refers to the area under the transition of K_2SO_4 ÷ area under the fusion of Ag. Slope for solid line calculated by method of least squares; slope for dashed line calculated from literature values.
$L_{K_2SO_4} = 4.217 m_3$ (see eq (7), in text).
$L_{tr}K_2SO_4 = 4.217 \times 0.533 = 2.2_5$ kcal/mole. S.D. $m_{tr} = 0.014$.
$L_{tr}K_2SO_4$, from literature [3. 12] = 2.14 kcal/mole.

5.2. Heats of Transformations

By application of eq (5) to the slopes in figure 2:

$$L_{tr}Bi_2O_3(M \rightarrow c) = 5.722 \times 1.669 = 9.5_5 \text{ kcal/mole}$$

$$\text{S.D. } m_{tr} = 0.031 \text{ (0.30 kcal/mole)}$$

$$L_f Bi_2O_3(c \rightarrow l) = 5.722 \times 0.671 = 3.8_4 \text{ kcal/mole}$$

$$\text{S.D. } m_f = 0.020 \text{ (0.08 kcal/mole)}$$

Similarly, by application of eq (6) to the slopes for the Bi_2O_3 : Ag mixtures (fig. 3):

$$L_{tr}Bi_2O_3(M \rightarrow c) = 11.274 \times 0.9025 = 10.1_7 \text{ kcal/mole}$$
$$\text{S.D. } m_{tr} = 0.019 \text{ (0.19 kcal/mole)}$$

$$L_f Bi_2O_3(c \rightarrow l) = 11.274 \times 0.3423 = 3.8_6 \text{ kcal/mole}$$

$$\text{S.D. } m_f = 0.015 \text{ (0.06 kcal/mole).}$$

The standard deviations of the slopes for the Bi_2O_3 : Ag mixtures are somewhat lower than for the Bi_2O_3 : K_2SO_4 mixtures because of the additional data, for the high weight ratio, that could be used in the calculations. Certainly, the difference in the heat of fusion of Bi_2O_3 obtained from the two standards is not statistically significant. The difference in values for the heat of transition is of questionable significance.

5.3. Accuracy

The linear relationship between area ratios and weight ratios for mixtures of the two standards can be seen in figure 4. The experimentally determined slope (0.533) is 4.7 percent greater than the theoretical slope (0.508) derived from the literature values. The difference between slopes is about twice the standard deviation of the experimentally determined slope. The agreement is good considering that the binary mixture of standards presents the most extreme in physical conditions of the three binary mixtures. In the K_2SO_4 : Ag mixtures, the area of the solid-solid transition of K_2SO_4 at 583 °C is compared to the area of the solid-liquid transformation of Ag at 960.8 °C.

Substituting in eq (7) the slope of the transformation ratio shown in figure 4 (0.533) gives a value of 2.25 kcal/mole for the heat of transition of K_2SO_4, compared to 2.14, the literature value. The agreement between these two values, as well as for the slopes, tends to substantiate the standard values used in the calculations, namely, 2.61 kcal/mole for L_f of Ag and 2.14 kcal/mole for L_{tr} of K_2SO_4. Attempts to correct for the change in thermocouple sensitivity with temperature or the use of other literature values for the heats of transformation of the standards has a detrimental effect on the agreement.

5.4. Internal Consistency

As shown in the development of eqs (8) and (9), it is possible to check the internal consistency of the results through a calculation which does not involve any heat of transformation values. From eqs (8) and (9):

$$\frac{m_2}{m_1} = m_3 = \frac{A_{K_2SO_4}}{A_{Ag}} \cdot \frac{g_{Ag}}{g_{K_2SO_4}}.$$

Substituting the values for the slopes m_1, m_2, and m_3, as given in figures 2, 3, and 4, respectively: For transition data, $\frac{0.902_5}{1.66_9} = 0.541$ (calc.) versus 0.533 (expt.). For fusion data, $\frac{0.342_3}{0.67_1} = 0.510$ (calc.) versus 0.533 (expt.).

The internal consistency calculations give deviations between the experimentally determined slope, m_3, and the calculated one, m_2/m_1, of +1.5 percent, for the transition data and −4 percent for the fusion data. The average of the two calculated slopes agrees to better than 1.5 percent with the experimentally determined one.

5.4. Conclusion

Consideration of the three criteria, namely, standard deviation of the slopes, internal consistency, and accuracy, as determined with the binary mixtures of standards, indicate an overall uncertainty of about 5 percent.

Averaging the results for the heats of transformation of Bi_2O_3 obtained from the mixtures with K_2SO_4 and Ag, yields:

$$L_{tr}Bi_2O_3(M \rightarrow c) = 9.9 \pm 0.5 \text{ kcal/mole}$$

$$L_f Bi_2O_3(c \rightarrow l) = 3.9 \pm 0.2 \text{ kcal/mole}$$

The sum of the entropy of transition and of fusion equals $\left(\frac{9900}{1003} + \frac{3900}{1098}\right) \Big/ 5 = 2.7$ cal/°K/g atom, a reasonable value [3].

6. Summary

To avoid problems inherent in a separate heat of reaction calibration of DTA equipment, a technique was developed which makes use of internal standards.

Binary mixtures of Bi_2O_3 and two standards, K_2SO_4 and Ag, were formulated in three weight ratios and subjected to three cyclic heat treatments, in the DTA equipment. Small amounts of mixtures, 0.2 to 0.4 g in total weight, were heated in platinum tubes which were isolated from the tubes containing the reference material, Al_2O_3. Thermocouples, Pt-90 percent Pt:10 percent Rh, of fine wire were welded to the outside of the tubes. The modification of the sample holder and overall sensitivity of the equipment was found to respond to heat effects equivalent to 0.007 cal per mm^2 of the area under the peak.

A number of criteria were employed to check on possible reaction between Bi_2O_3 and the standards and to eliminate erroneous date. These criteria were as follows: Comparison of corresponding transformation ratios in successive heat cycles; comparison of the transformation ratio $(M \rightarrow c/c \rightarrow l)$ in the Bi_2O_3 phase of mixtures with that in pure Bi_2O_3; x-ray powder analysis of mixtures at the completion of a determination; and, finally, observing the adherence of the data to linearity as prescribed by theory.

Except for the high weight ratio of Bi_2O_3 to K_2SO_4 in the 3.46:1 mixture, plots of ratios of transformation areas versus corresponding weight ratios were linear and passed through the origin. The presence of Ag in the Bi_2O_3:Ag and the K_2SO_4:Ag mixtures contributed to thermal transfer, and linearity was observed for all the weight ratios.

The data were analyzed according to (1) standard deviation of the slopes, (2) internal consistency, which is independent of the heat of transformation of the standards, and (3) agreement between calculated and selected literature value when one standard is mixed with the other. The heat of transition of Bi_2O_3 was found to be 9.9 ± 0.5 kcal/mole and the heat of fusion, 3.9 ± 0.2 kcal/mole. The uncertainties are estimated limits of error, based on internal consistency and on the values of the standards.

The authors express their sincere appreciation to Joan R. Rosenblatt of the Statistical Engineering Section, who was consulted on the statistical analysis of the data.

7. References

[1] L. Belladen, Il sistema Bi_2O_3-PbO (The System Bi_2O_3-PbO), Gazz. chim. ital. **52,** II, 160–164 (1922).

[2] K. K. Kelley, Contributions to Data on Theoretical Metallurgy: V, Heats of Fusion of Inorganic Substances, U.S. Bur. Mines Bull., No. 393, 166 pp. (1936); p. 26; Ceram. Abstr. **16** [5] 162 (1937).

[3] O. Kubaschewski and E. LL. Evans, Metallurgical Thermochemistry, 426 pp, 3d ed., rev. (Pergamon Press, New York, 1958).

[4] F. D. Rossini, D. D. Wagman, W. H. Evans, S. Levine, and I. Jaffee, Selected Values of Chemical Thermodynamic Properties, NBS Cir. 500, (1952) 1268 pp.

[5] E. M. Levin and C. L. McDaniel, The System Bi_2O_3-B_2O_3, J. Am. Ceram. Soc. **45** [8] 355–360 (1962).

[6] G. Gattow and H. Schröder, "Über Wismutoxide, III, Die Kristallstruktur der Hochtemperaturmodifikation von Wismut (III)-oxid (δ-Bi_2O_3)", Z. anorg. allg. Chem. **318** [3–4] 176–189 (1962).

[7] G. Gattow and D. Schütze, Über Wismutoxide, VI, Über ein Wismut (III)-oxid mit höherem Sauerstoffgehalt (β-Modifikation), Z. anorg. allg. Chem. **328,** [1–2] 45–67 (1964).

[8] E. M. Levin and R. S. Roth, Polymorphism of bismuth sesquioxide. II. Effect of oxide additions on the polymorphism of Bi_2O_3, J. Res. NBS **68A** (Phys. and Chem) No. 2, 197–206 (1964).

[9] W. J. Smothers and Yao Chiang, Differential Thermal Analysis: Theory and Practice, 444 pp (Chemical Publ. Co., Inc., New York, 1958).

[10] F. C. Kracek, The polymorphism of potassium nitrate, J. Phys. Chem. **34,** 225–47 (1930).

[11] Isaac Barshad, Temperature and heat of reaction calibration of the differential thermal analysis apparatus, Am. Mineral. **37** [7&8] 667–694 (1952).

[12] K. K. Kelley, Contributions to the Data on Theoretical Metallurgy. XIII. High-Temperature Heat-Content, Heat-Capacity, and Entropy Data for the Elements and Inorganic Compounds, U.S. Bur. Mines Bull. 584, 1960. 232 pp.

[13] (a) Cavallaro, Atti Real. Acad. Ital., Rend. Class Sci., Fiz., Mat. et Nat. **[4–5]** 520–526 (1934). (b) F. E. Wittig, Z. Elektrochem. **54,** 288 (1950). (c) W. Oelson, Arch. Eisenhüttenw. **28,** 1–6 (1957).

[14] Ernest M.Levin and Robert S. Roth, Polymorphism of bismuth sesquioxide. I. Pure Bi_2O_3, J. Res. NBS **68A** (Phys. and Chem.) No. 2, 189–195 (1964).

[15] C. J. Penther, S. T. Abrams, and F. H. Stross, Semi-automatic Thermal Analysis Apparatus, Anal. Chem. **23,** 1459–66 (1951).

(Paper 69A3–342)

2. Cryoscopic Measurements

COMPARISON OF CRYOSCOPIC DETERMINATIONS OF PURITY OF BENZENE BY THERMOMETRIC AND CALORIMETRIC PROCEDURES

by

A. R. GLASGOW, Jr., G. S. ROSS, A. T. HORTON, D. ENAGONIO, H. D. DIXON AND C. P. SAYLOR

Pure Substances Section of the Chemistry Division

and

G. T. FURUKAWA, M. L. REILLY, AND JEANETTE M. HENNING

Thermodynamics Section of the Heat and Power Division, National Bureau of Standards, Washington, D.C. (U.S.A.)

I. INTRODUCTION

For some time, workers at the National Bureau of Standards have been embarassingly aware of the discordant results sometimes yielded by the two methods upon which we principally depend to assay the purity of nearly pure compounds. Almost always the thermometric method, by which a stirred sample is frozen at nearly constant rate, had indicated larger impurity than the calorimetric method, by which an adiabatically controlled frozen sample is melted in stages by the addition of accurately controlled increments of energy. The fundamental physical principles and assumptions are the same in both cases, and the analysis depends upon the measurements of temperature. The discordances in assays by the two methods were dramatically laid bare when CINES[1] and MATHIEU[2] published comparisons of results obtained at the National Bureau of Standards using a thermometric method with those obtained at the U.S. Bureau of Mines employing the calorimetric procedure.

In general, we have tended to assume that the much more elaborate calorimetric method provides truer results, for reasons that do not need to be elaborated here. Neither method can be considered free of its own pitfalls, however, and it was decided to attempt a rigorous and objective comparison of the two methods. This depended on deliberate contaminations of an unusually pure sample, division of the contaminated samples in such manner that the compositions would not be altered, and independent determinations of purities by the two methods.

Fortunately for the independence of this comparison, the group at the National Bureau of Standards who use the calorimetric procedure work in a different building, in a different division, and under different supervisors from those who use the thermometric procedure. As a consequence, it was possible to plan a coordinated system of comparison in which each group of workers would be unaware of the results being achieved by the other and for both to be totally uninformed about the extent of the deliberate contaminations that had been made.

References p. 79

For the sake of objectivity, an elaborate scheme was employed so that no one could know the real measure of contamination until all results by both procedures had been reported. Thus the *n*-heptane with which a highly purified sample of benzene was to be contaminated was measured by three workers into 6 different weighed glass vessels. After they had been filled, the vessels were weighed by another worker who kept a private record of his results. Volumetric amounts of *n*-heptane were determined by still another participant. The vessels containing contaminant were entrusted to another worker, a young woman who did not otherwise participate in the study. When requested, she selected the sealed tubes of contaminant that were broken into the liquid benzene by another group of workers who alone knew the amount of the benzene to which the *n*-heptane was added. Only after all measurements and calculations had been completed were the scattered bits of information assembled from which it was possible to calculate the actual degree of contamination.

In the actual performance of analyses we felt that there was no reason to use any techniques except those presently believed to give the most accurate results. Consequently refinements of procedure were employed that can be mentioned here only in the most cursory fashion. It was stipulated that each method would be utilized in the manner believed by its practitioners to be the most dependable. In this there was just one limitation. Although it is our custom when using the thermometric method to determine both freezing and melting curves and to base judgments on the data obtained each way, it was decided in this instance to utilize for the official computations only those data obtained during freezing.

II. PREPARATION OF SAMPLES

1. *Selection of materials*

Benzene was chosen as the major constituent with knowledge that it had a number of disadvantages. Thus, in the fully dried state, it is an extreme desiccant. There is a long record of difficulties in determining its true melting point or triple point. On the other hand, its triple point is conveniently close to the triple point of water. Further, it was believed that some of the anomalies of its properties might be resolved during the investigation.

The choice of *n*-heptane as the contaminant was largely based upon the extreme difficulty of separating it from benzene by regular distillation. Although the boiling points of *n*-heptane and benzene are 18° apart, the boiling points of benzene and the azeotrope, which contains 0.7% of *n*-heptane, differ by only 0.1°C. All samples for the investigation were prepared to lie between benzene and the azeotrope. For this reason the fractionation of the samples even in an efficient still would be practically impossible. It can be totally neglected in connection with the transfers employed in this study. *n*-Heptane was chosen also because of a belief that its solution in liquid benzene would be ideal within the range of the measurements while it would be insoluble in frozen benzene.

2. *Preparation of a "pure" benzene*

As starting material, 2 liters of "ACS Reagent Grade" benzene, claimed by its producers to be "thiophene-free" and found to be of good quality, was chosen. This was further purified by 5 treatments with concentrated sulfuric acid lasting about 20 hours, and leachings with 5 portions of distilled water.

References p. 79

The benzene was transferred to a 2-liter distillation flask fitted by standard unlubricated glass joints to a Widmer column, condenser, adapter, and receiving flask. After about 250 ml of benzene and water had been slowly distilled, and without interruption of the boiling, the condenser, adapter, and receiver were replaced by a similar assembly of a dry condenser, adapter, and the ampoule D illustrated in Fig. 1. After 800 ml were distilled into the ampoule, the ampoule was disconnected from the condenser and stoppered.

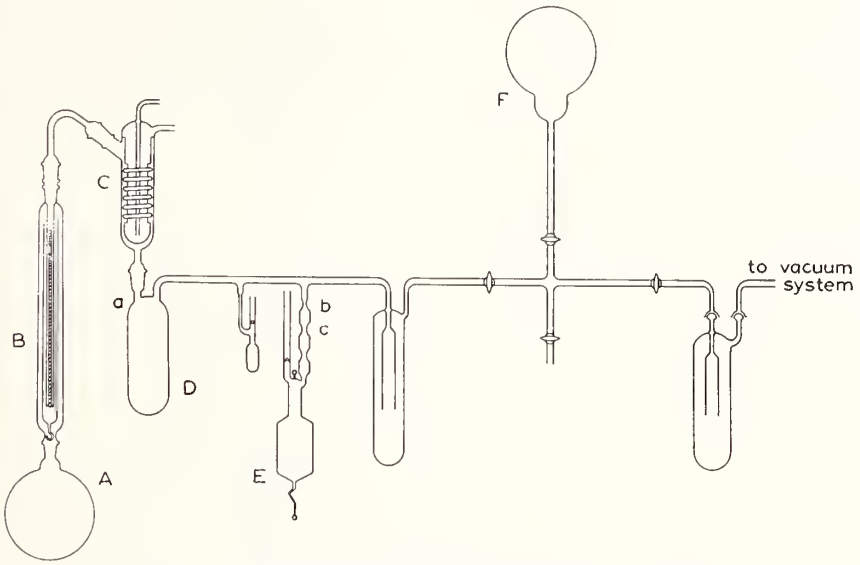

Fig. 1. Apparatus for filling the crystallization ampoule.

As the first stage of removing gases and water, the benzene in the ampoule D was frozen with a bath of solid carbon dioxide. During freezing, the pressure in the system was kept reduced by intermittent pumping. When the benzene was completely frozen, the system was sealed at *a* in Fig. 1. The benzene was then melted and refrozen slowly. The gases, including water, which were evolved during freezing, were pumped off from time to time by opening the ampoule to the ballast bulb F. When the ballast bulb was not open to the freezing benzene, the pressure in it was maintained at approximately 10^{-6} mm Hg by means of a mercury diffusion pump. After the benzene was completely solidified, it was subjected to the direct pumping of the diffusion pump for about half an hour during which time the glass of the system, wherever feasible, was heated with a soft flame. The benzene was melted and was refrozen while pumping in the same fashion as before. The benzene was again melted. The desired amount of benzene was transferred to ampoule E, by chilling the ampoule. This benzene was slowly frozen and degassed as before, chilled with liquid nitrogen and subjected to the direct action of the pump while the glass was again heated with a flame. The ampoule with its break-bulb was then sealed. Resinous ethylene glycol phthalate, which is considered as insoluble in benzene, was used on the stopcocks. Two samples of about 500 ml each were prepared as outlined.

References p. 79

Greatest reliance for the purification of the benzene was placed upon the growth of single crystals by a method developed by HORTON[3] and derived from that of TAMMANN or of BRIDGMAN. In HORTON's apparatus, Fig. 2, the large glass tube contains two immiscible liquids. Since convection occurs within each liquid but not across the

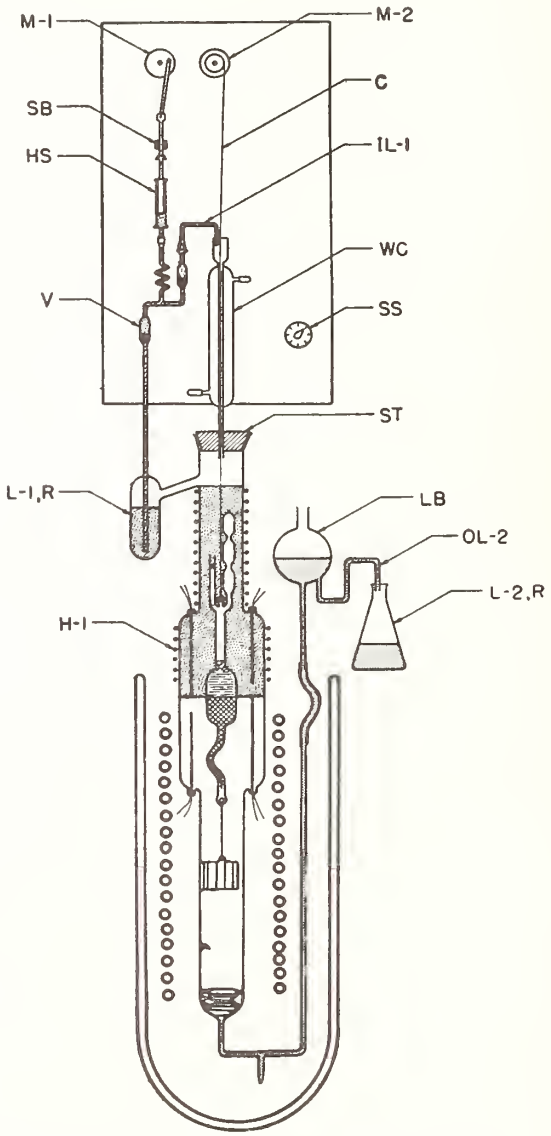

Fig. 2. Apparatus for growing single crystals of benzene.

interface, we were able to maintain a difference in temperature of approximately 60° across the interface of the two liquids, although the temperature distribution within each liquid was nearly uniform. The upper liquid was kept at about 30°C

References p. 79

by a coil of heating wire wound around the tube, and the lower liquid cooled to about —28°C by immersion in a refrigerated bath contained in a Dewar-type flask. During a period of about 10 days, the ampoule of benzene was lowered across the interface between the upper and lower liquids, the slow movement being controlled by a clock mechanism. Fig. 3 is a diagram of the apparatus. At the end of the 10 days, all but about 15 ml of the benzene had frozen. The ampoule was removed from the bath and clamped in an inverted position. Upon warming the surface of the vessel with the hands, the surface of the crystal and all of the solid in the crooked capillary melted and drained into one of the seal-off bulbs *b* of Fig. 1. Here it was chilled to the temperature of liquid nitrogen and sealed off from the rest of the sample. A second crystal was grown in the other ampoule. We believe the impurity in the two crystals of these samples to be less than can be disclosed by thermal analysis.

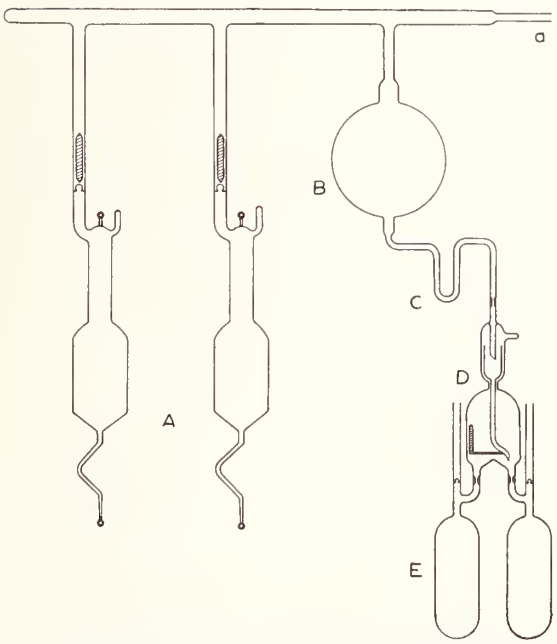

Fig. 3. Apparatus for mixing the two samples of purified benzene and distributing the mixture into smaller sample vessels.

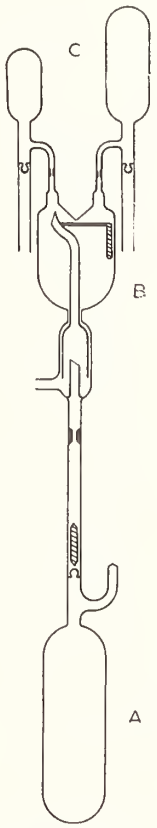

Fig. 4. Apparatus for the partitioning of samples for analysis (also used for introducing contaminant).

The material in these two ampoules was combined and divided into 4 parts. To do this, the ampoules were sealed into the system shown in Fig. 4. Over a period of several hours the system was evacuated with a diffusion pump while, from time to time, the glass was heated with a flame. The system was then closed by sealing off at *a*.

References p. 79

Liquid nitrogen was placed at trap C and solid carbon dioxide packed around the bulb B. The samples from separate single-crystal growing operations were combined in the bulb by opening the ampoules at the break-bulbs with a magnetic hammer. The major part of benzene distilled into the bulb, that which condensed in the trap serving as a form of stopcock. Finally, the benzene in the bulb was allowed to melt, the liquid nitrogen bath was removed from around trap C, and the benzene was allowed to flow through the magnetically controlled distributor D into ampoules. The ampoules were chilled with liquid nitrogen and sealed off. Four ampoules containing approximately 250 ml each were prepared.

3. Partition and contamination of the portions

The 4 ampoules prepared as described were divided, either with or without intentional contamination. The final samples were subsequently subjected to the thermometric and calorimetric methods of analysis. The contaminations and partitions were performed in the following manners. In one instance a group of thin-wall glass tubes about 10 cm long and somewhat less than 1 mm in bore was washed by putting them upright in a column in which dry, reagent-grade benzene was refluxed for about an hour. The tubes were then dried in a heated vacuum system. The internal diameters at both ends of the tubes were measured with a microscope and filar-micrometer eyepiece. Tubes selected for uniformity in diameter were weighed on a micro balance. NBS Standard Sample No. 216a *n*-heptane was introduced into 3 of these tubes by means of a micro-buret. The ends containing the *n*-heptane were then cooled with compact solid carbon dioxide; the tubes were exhausted and sealed off with a flame. The portion of the tube containing the *n*-heptane and the portion removed in sealing were weighed. The length of the liquid in each tube was measured with a travelling microscope, the sealed end of the tube and the meniscus of the liquid having nearly the same conformation. Thus two measurements were made of the amount of *n*-heptane in each tube. For a more highly contaminated sample, *n*-heptane was introduced in 3 of the fragile sample bulbs that are used in combustion calorimetry. The determination of the amount of contaminant was based solely on the comparative weights.

Apparatus shown in Fig. 5, is similar to that used to partition the original purified benzene, and was used to divide and contaminate the samples. The tube or bulb selected by the young woman not otherwise participating in the work was placed above the break-bulb of the ampoule. The system was pumped and flamed for about 2 hours before sealing. The tube or bulb of *n*-heptane and the break-bulb were broken by the same magnetic hammer. After steps were taken to assure thorough incorporation of the *n*-heptane into the benzene, the apparatus was inverted and each sample partitioned into ampoules containing 40, 80, and 100 ml by means of the magnetically controlled distributor. These ampoules were then sealed and removed in the usual fashion. One of the samples was divided without contamination. For simplicity of identification the uncontaminated sample was given the designation A, the first contaminated sample the designation B, and the second contaminated sample the designation C.

III. THERMOMETRIC ANALYSIS

1. Apparatus

The apparatus used in the determination of the purity of benzene from time-temperature freezing and melting curves is similar to the one developed by GLASGOW AND

References p. 79

TENENBAUM[4]. The cell and the completely assembled apparatus are shown in Figs. 6 and 7. The seeding devise was not used because preliminary experiments had shown that, in general, the small degree of undercooling exhibited by benzene made it unnecessary.

In order to minimize errors in the experiments, all components used in temperature measurement were carefully calibrated. The Meyers bifilar, helical, platinum resistance thermometer and the 10-ohm standard resistance used in the calibration of the Mueller G-2 bridge were calibrated at the National Bureau of Standards. During the course of the experiments, the thermometer was periodically checked against the triple point of pure water.

The triple-point cell was of the type used for calibrating thermometers, and the depth of immersion of the thermometer in the cell was 13 inches. A comparison of the triple point of water in this cell was made with that observed in the cell shown in Fig. 5 with 40 ml of water and with a depth of immersion of the thermometer of 2.8 inches. The results of this comparison are given in Table VIII.

Resistance readings were taken every minute. In addition to these manual readings the temperature was recorded in two fashions. The first consisted of amplifying the off-balance signal from the bridge by passing it through a DC high-gain amplifier (Liston-Becker Model No. 14). This amplified signal was fed into a Brown 10 millivolt recording potentiometer. In order to obtain both a manual and a printed continuous record of the same experiment, the signal from a copper-constantan thermocouple junction was balanced out by a Rubicon potentiometer to within 0.01 millivolt of the total signal generated at the freezing point. The residual signal was fed through the DC amplifier and into the recorder. The sensing junction of the couple was placed in the middle of the length of the platinum coil, between the glass case of the thermometer and the thermometer well. A triple-point water cell was used as the reference point. This cell was equipped with radiation shielding and insulated at the top with glass wool to stabilize it as much as possible. The entire potentiometer was thermally insulated so as to minimize thermal e.m.f.'s. Under these conditions it was possible to record to a precision of approximately 0.0001°C. This precision has been checked by using a triple point cell of diphenyl ether and one of water. The apparent overall drift over a period of 1 hour was found to be less than 0.00005°C.

The data, as given in this paper, were handled both by the methods given by TAYLOR AND ROSSINI[5] and by SCHWAB AND WICHERS[6]. Other procedures were employed by SAYLOR. Portions of these results will be reported in another paper.

2. *Experimental details*

Extreme care was exercised during the filling of the cell. The cell was cleaned with chromic acid, and carefully washed with distilled water. It was then evacuated with a mercury diffusion pump and subsequently heated to 150°C for a period of 24 hours. All samples were introduced by breaking the break-off tip of the containing ampoule and pouring the contents directly into the tube. In order to prevent any accidental contamination of the cell between runs, additional break-off tips were included in the manifold so that other samples could be introduced into the cell and investigated without letting air into the cell between runs. The samples were run in the following order: (1) two samples of A, (2) one of sample B, and (3) one of sample C.

The original size of sample was 50 ml. However, for a sample of this size, the freezing

References p. 79

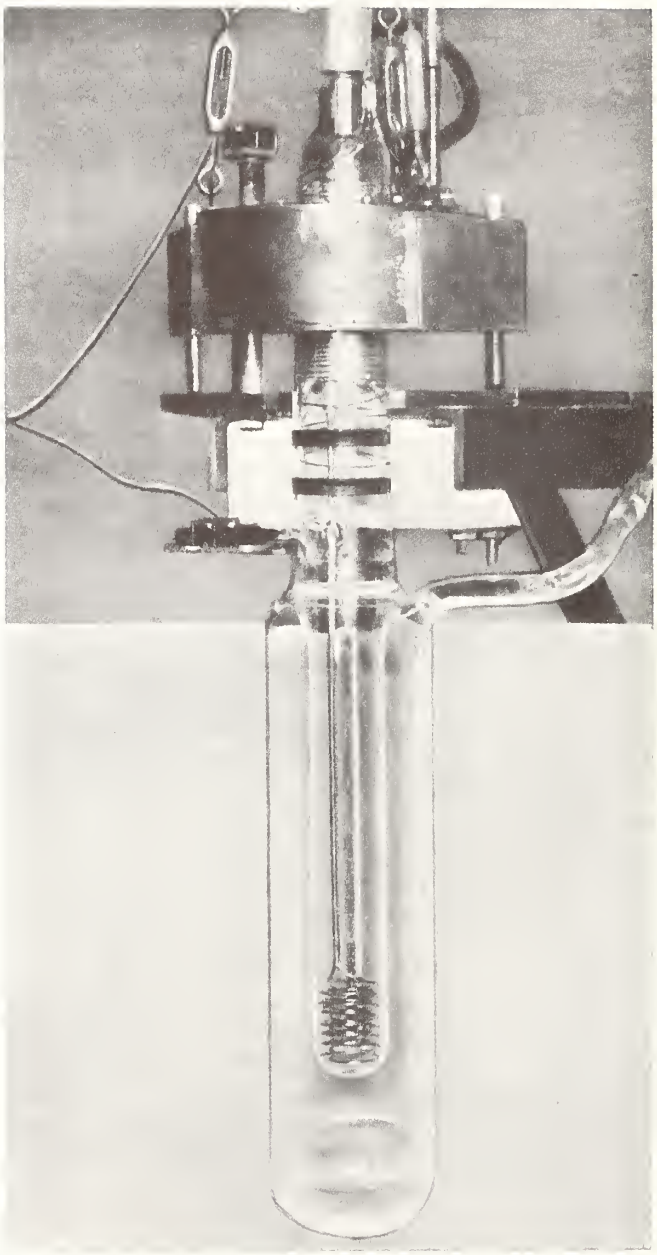

Fig. 5. Modified thermometric cell (silvering of the glass surface of the double-walled jacket, confining the evacuated space, was removed to show stirrer, thermometer well, and sample holder)

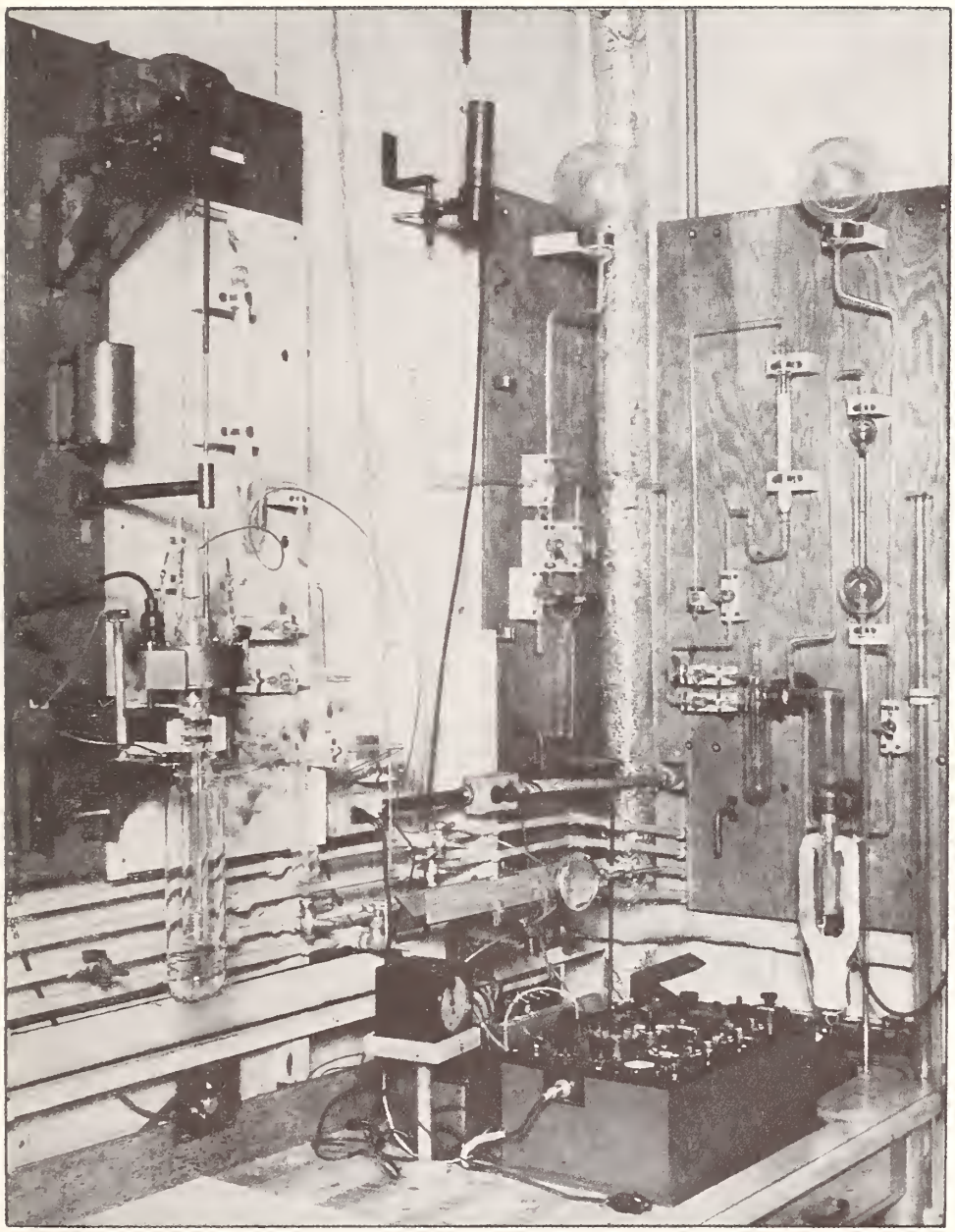

Fig. 6. Complete apparatus used in the measurement of purity by the thermometric method.

TABLE I

RESULTS OF THERMOMETRIC ANALYSIS OF BENZENE, SAMPLE A-1[1]

Expt.	T_f^{tp}	$T_{f_0}^{tp}$	ΔT	N_2*
1	278.6106	278.6188	0.0082	0.00012
2	278.6072	278.6090	0.0018	0.000027
3	278.6107	278.6366	0.0259	0.00039
5	278.6138	278.6391	0.0253	0.00039
6	278.6104	278.6325	0.0221	0.00034
7	278.6108	278.6400	0.0292	0.00044
8	278.6126	278.6367	0.0241	0.00037

$\overline{T}_f^{tp} = 278.6109 \pm 0.0020°K$ $\quad \overline{T}_{f_0}^{tp} = 278.6304 \pm 0.0113°K$

Variance $= 423 \cdot 10^{-8}$ $\quad$ Variance $= 13918 \cdot 10^{-8}$

Standard deviation $= \pm 0.0021$ $\quad$ Standard deviation $= \pm 0.0118$

Purity[a] $= 99.97_0 \pm 0.02$ mole %

Purity[b] $= 99.90_5 \pm 0.006$ mole %

[1]Melting experiments on 50-ml sample.

experiments exhibited peculiarities which made analysis impossible. The sample would recover rapidly from undercooling, but then the observed temperature would

TABLE II

RESULTS OF THERMOMETRIC ANALYSIS OF BENZENE, SAMPLE A-2[1]

Expt.	T_f^{tp}	$T_{f_0}^{tp}$	ΔT	N_2*
1	278.6690	278.6708	0.0018	0.000027
2	278.6686	278.6721	0.0035	0.000053
3	278.6682	278.6696	0.0014	0.000021
4	278.6670	278.6683	0.0013	0.000020
7	278.6683	278.6706	0.0023	0.000035
8	278.6693	278.6744	0.0051	0.000078
9	278.6680	278.6708	0.0028	0.000043
10	278.6679	278.6702	0.0023	0.000035

$\overline{T}_f^{tp} = 278.6683 \pm 0.0006°K$ $\quad \overline{T}_{f_0}^{tp} = 278.6709 \pm 0.0014°K$

Variance $= 54 \cdot 10^{-8}$ $\quad$ Variance $= 254 \cdot 10^{-8}$

Standard deviation $= \pm 0.0007$ $\quad$ Standard deviation $= \pm 0.0016$

Purity[a] $= 99.99_6 \pm 0.002$ mole %

Purity[b] $= 99.99_3 \pm 0.002$ mole %

[1]Melting experiments on 50-ml sample.

rise steadily, although slowly, until the sample could no longer be stirred. For this reason, Table I shows only melting experiments. When the "melting" bath was placed around the cell the temperature was observed to fall very rapidly before commencing to rise. This erratic freezing behavior was suspected to be related to the size of the benzene sample, so auxiliary experiments were conducted in another similar cell with reagent grade benzene. The behavior was identical to the more pure benzene. Successive experiments were run wherein 10 ml fractions of the sample were removed. When the sample size approached 40 ml, a normal freezing behavior was noted.

References p. 79

The freezing curves, as obtained with this type of apparatus, are generally considered to be more reliable than the melting curves, and all subsequent measurements on the benzene consisted of freezing curves only, using a sample size of 40 ml. However, a comparison of Table II with Table III shows that there is no appreciable difference between the data obtained from melting experiments employing 50 ml of sample and freezing experiments employing only 40 ml of benzene.

As shown in Table I, the purity of the supposedly "pure" benzene is not appreciable high. We suspected that in some unexplained fashion we had contaminated the sample. We therefore removed this sample and introduced another identical sample into our cell, without allowing air to enter the cell at any time. Tables II and III show the results. Further investigation showed that the first sample was probably contaminated by water from the cell walls. This water could be considered as "chemi-adsorbed" in contrast to the "physi-adsorbed" water removed by the heating and pumping technique. In view of the relatively large surface area of the cell and the manifold, the observed lowering in temperature is not unduly large if attributed to water. From this experience,

TABLE III

RESULTS OF THERMOMETRIC ANALYSIS OF BENZENE, SAMPLE A-2[1]

Expt.	T_f^{tp}	$T_{f_0}^{tp}$	ΔT	N_2^*
1	278.6684	278.6745	0.0061	0.000093
2	278.6684	278.6718	0.0034	0.000052
3	278.6699	278.6732	0.0033	0.000050
4	278.6692	278.6744	0.0052	0.000079
5	278.6689	278.6734	0.0045	0.000068
6	278.6696	278.6714	0.0018	0.000027
7	278.6692	278.6718	0.0026	0.000040
8	278.6709	278.6736	0.0027	0.000041
9	278.6691	278.6716	0.0025	0.000038
10	278.6697	278.6729	0.0032	0.000049

$\bar{T}_f^{tp} = 278.6693 \pm 0.0005$°K
Variance $= 56 \cdot 10^{-8}$
Standard deviation $= \pm 0.0007$

$\bar{T}_{f_0}^{tp} = 278.6729 \pm 0.0008$°K
Variance $= 133 \cdot 10^{-8}$
Standard deviation $= \pm 0.0012$

Purity[a,b] $= 99.99_4 \pm 0.002$ mole %

[1]Freezing experiments on 40-ml sample.

one might suspect that the benzene in the form of the large single crystal was much purer than the sample measured and could have been contaminated during the partition process. The partitioning of the samples were done after careful evacuation and "flaming" of all glass parts at approximately 350-400°C.

This higher temperature could account for the smaller contamination. When sample A-1 was transferred from the ampoule to the cell, the cell and manifold were dried by heating to 150°C while evacuating the system with a mercury diffusion pump backed by an oil mechanical fore-pump. However, the inclusion of several break-off tip seals in the permanent part of the manifold assemble attached to the cell made possible the introduction and removal of all subsequent samples without allowing the cell and permanent manifold to be open to the air. In this fashion, owing to the order in which

References p. 79

the samples were run, the cell was in each case "conditioned" or purged by material of a higher purity than the sample being tested.

The portion of the manifold between the particular break-off tip being used and the new sample being introduced was thoroughly cleaned and dried by first heating and pumping, followed by a purging of this section with dry benzene. After the removal of this benzene, the break-off tips of the ampoule and the cell manifold were broken and the sample was poured into the cell. This technique of purging the entire system with benzene before introducing the next sample is thought to be necessary in order to assure non-contamination of the sample in the cell itself. All handlings of the samples were preceded by the distillation of a dry sample of benzene, using the manifold as a reflux column and condenser.

The data given in Table IV are those obtained from the analysis of the recorded thermocouple e.m.f. The curves indicate that much of the "randomness" exhibited by the

TABLE IV

RESULTS OF THERMOMETRIC ANALYSIS OF BENZENE, SAMPLE C[1]

Expt.	T_f^{tp}	$T_{f_0}^{tp}$	ΔT	N_2*
2	278.6288	278.6798	0.0510	0.000777
5	278.6325	278.6784	0.0459	0.000699
6	278.6386	278.6874	0.0488	0.000743
7	278.6342	278.6549	0.0207	0.000315
8	278.6342	278.6630	0.0288	0.000439
9	278.6346	278.6719	0.0373	0.000568
11	278.6364	278.6692	0.0328	0.000499
12	278.6366	278.6643	0.0277	0.000422
14	278.6360	278.6634	0.0274	0.000417
15	278.6358	278.6545	0.0187	0.000285

$\overline{T}_f^{tp} = 278.6348 \pm 0.0019°K$ $\quad$ $\overline{T}_{f_0}^{tp} = 278.6687 \pm 0.0024°K$

Variance $= 719 \cdot 10^{-8}$ $\quad$ Variance $= 1166 \cdot 10^{-8}$

Standard deviation $= \pm 0.0027$ $\quad$ Standard deviation $= \pm 0.0034$

Purity[a] $= 99.94_8 \pm 0.004$ mole %

Purity[b] $= 99.94_2 \pm 0.002$ mole %

[1] These freezing experiments on a 40-ml sample were machine recorded with a thermocouple as the sensing element. They were also manually recorded with a platinum thermometer as the sensing element. The manually recorded results on the same experiments are shown in Table VII.

TABLE V

RESULTS OF THERMOMETRIC ANALYSIS OF BENZENE, SAMPLE B[1]

Expt.	T_f^{tp}	$T_{f_0}^{tp}$	ΔT	N_2*
1	278.6512	278.6575	0.0063	0.000096
2	278.6505	278.6566	0.0061	0.000093

$\overline{T}_f^{tp} = 278.6509°K$ $\quad$ $\overline{T}_{f_0}^{tp} = 278.6570°K$

Purity[a] $= 99.99_1$ mole %

Purity[b] $= 99.96_6$ mole %

[1] These freezing experiments on 40 ml of benzene were machine recorded with a platinum resistance thermometer as the sensing element.

References p. 79

manual recording of points is not random. Since the thermocouple is small and lies next to the thermometer well, it is more sensitive to local changes, and the departures as shown by the recorded trace are larger in magnitude than those manually recorded. The divergence of the two curves, as increasing amounts of sample are frozen, is considered to arise from the difference between local effects sensed by the thermocouple and the larger overall effect sensed by the thermometer. Since the thermocouple was not accurately calibrated, the data in Table IV give only a relative comparison. Table V, which shows the results of recording the resistance of the platinum thermometer itself does not have this restraint, and may be directly compared with values as given in the manually recorded experiments. The fluctuations observed on the machine-recorded data can readily be shown to be real changes. The true fitting of these recorded curves should give better accuracy and precision, since a fit of the manually recorded values is limited by the necessary assumption that the scatter is random.

3. Correlation and explanation of data

In order to reduce individual errors a rather large number of experiments have been run on each sample. In these, the freezing bath was always a solid carbon dioxide slush. The bath immersion was kept constant throughout all experiments. The rate of cooling of the liquid benzene was varied between 0.3° and 0.5° per minute. The warming bath used in the melting experiments was water maintained at 25°C. These melting experiments took place over a longer period of time and the liquid warming rate was varied between 0.1° and 0.3° per minute.

All curves which were capable of mathematical analysis are given. Some freezing curves exhibited the peculiarity of having a constant slope, and since these are not capable of mathematical interpretation they are not included. Five experiments on sample A and four on sample B exhibited this tendency.

TABLE VI

RESULTS OF THERMOMETRIC ANALYSIS OF BENZENE, SAMPLE B[1]

Expt.	T_f^{tp}	$T_{f_0}^{tp}$	ΔT	N_2*
1	278.6564	278.6594	0.0030	0.000046
2	278.6488	278.6562	0.0074	0.000113
3	278.6526	278.6819	0.0293	0.000446
4	278.6559	278.6697	0.0138	0.000210
5	278.6534	278.6794	0.0260	0.000396
6	278.6527	278.6810	0.0283	0.000432
7	278.6518	278.6733	0.0215	0.000327
8	278.6553	278.6936	0.0383	0.000583
9	278.6550	278.6732	0.0182	0.000277
10	278.6524	278.6607	0.0083	0.000126
11	278.6514	278.6901	0.0387	0.000589
12	278.6488	278.6640	0.0152	0.000231

$\overline{T}_f^{tp} = 278.6529 \pm 0.0016$°K
Variance $= 628 \cdot 10^{-8}$
Standard deviation $= \pm 0.0025$

$\overline{T}_{f_0}^{tp} = 278.6735 \pm 0.0077$°K
Variance $= 14528 \cdot 10^{-8}$
Standard deviation $= \pm 0.0120$

Purity[a] $= 99.96_9 \pm 0.014$ mole %
Purity[b] $= 99.97_0 \pm 0.004$ mole %

[1] Freezing experiments on 40-ml sample.

References p. 79

In Tables I-VII, purity is calculated using two different $T_{f_0}{}^{tp}$'s. When the purity is listed as "purity^a", this signifies that the $T_{f_0}{}^{tp}$ used is that obtained by averaging the calculated $T_{f_0}{}^{tp}$'s for the group of experiments listed in the table above the value. The "best" or most probable value of $T_{f_0}{}^{tp}$ is considered to be the average of the experiments listed in Table III, and purity, as calculated using this value, is listed as "purity^b". The value of the cryoscopic constant A, $\frac{\Delta H_f}{RT_{f_0}{}^2}$, which was used in this calculation is the A.S.T.M. value of 0.01523 degrees^{-1}. The minor difference in the value as reported in the following section of this paper is not enough to change the purity values listed herein.

The calculation of the mole fraction of the total amount of impurity present in each sample, N_2*, was made by using the following equation:

$$N_2{}^* = A(T_{f_0}{}^{tp} - T_f{}^{tp}) \quad \ldots \ldots \ldots \ldots \ldots \ldots \quad (1)$$

This simplified equation was derived on the assumption that it is valid only when the total mole fraction of impurity is small and only when all the impurity remains in the liquid phase during crystallization and forms an ideal solution with the major component.

TABLE VII

RESULTS OF THERMOMETRIC ANALYSIS OF BENZENE, SAMPLE C[1]

Expt.	$T_f{}^{tp}$	$T_{f_0}{}^{tp}$	ΔT	$N_2{}^*$
1	278.6311	278.6551	0.0240	0.00036
2	278.6327	278.7313	0.0986	0.00150
3	278.6341	278.6727	0.0386	0.00059
4	278.6339	278.6655	0.0316	0.00048
5	278.6341	278.6650	0.0309	0.00047
6	278.6331	278.6548	0.0217	0.00033
7	278.6356	278.6606	0.0250	0.00038
8	278.6336	278.6595	0.0259	0.00039
9	278.6339	278.6645	0.0306	0.00047
10	278.6351	278.6674	0.0323	0.00049
11	278.6364	278.6771	0.0407	0.00062
12	278.6337	278.6628	0.0291	0.00044
13	278.6331	278.7041	0.0710	0.00108
14	278.6329	278.6478	0.0149	0.00023
15	278.6344	278.6631	0.0287	0.00044
16	278.6332	278.6566	0.0234	0.00036

$\bar{T}_f{}^{tp} = 278.6338 \pm 0.0007°K$ $\quad$ $\bar{T}_{f_0}{}^{tp} = 278.6692 \pm 0.0112°K$

Variance $= 153 \cdot 10^{-8}$ $\quad$ Variance $= 43415 \cdot 10^{-8}$

Standard deviation $= \pm 0.0012$ $\quad$ Standard deviation $= \pm 0.0208$

Purity^a $= 99.94_6 \pm 0.018$ mole %

Purity^b $= 99.94_0 \pm 0.002$ mole %

[1] Freezing experiments on 40-ml sample.

The data is tabulated showing the purity and delta temperature as calculated for each experiment as well as a purity value determined by the average $T_{f_0}{}^{tp}$ and the $T_{f_0}{}^{tp}$ obtained on the second sample of A which is considered to be the best value. The

References p. 79

calculation of the variance and standard deviation is straightforward. The uncertainty is given in terms of each sample and indicates the probable percision (95% confidence level) as calculated by usual statistical methods. All temperatures are given in terms of degrees Kelvin and were obtained by adding the constant 273.16 to the $T_f{}^{tp}$ and $T_{f_0}{}^{tp}$ values originally calculated in terms of degrees Celsius.

There is no readily apparent explanation for $T_{f_0}{}^{tp}$ as calculated from these experiments being lower than previously reported values.

TABLE VIII

CALIBRATIONS AND RELIANCE LIMITS OF RESULTS GIVEN IN TABLES I-VII

H_2O (triple-point measurements)

(A) In normal triple point cell (13-inch immersion)

(1) at time of sample A-1
$R = 25.4818_{37} \pm 0.000010$ abs. ohms
(2) at time of sample A-2
$R = 25.4818_{04} \pm 0.000010$ abs. ohms
(3) at time of sample B
$R = 25.4818_{62} \pm 0.000010$ abs. ohms
(4) at time of sample C
$R = 25.4818_{42} \pm 0.000010$ abs. ohms

(B) 40 ml distilled and degassed H_2O in freezing point apparatus (2 experiments performed after running sample C)

(1) $R = 25.4818_{00} \pm 0.000018$ abs. ohms
(2) $R = 25.4818_{11} \pm 0.000016$ abs. ohms

Bridge and thermometer calibrations

(A) For ice triple point — $(N-R)/2$ varies between limits of 0.002207 and 0.002246 abs. ohms with average of 0.0022_{19}.
(B) For benzene samples — $(N-R)/2$ varies between limits of 0.02221 and 0.02269 with average of 0.02245.
(C) The change in the bridge calibration between start and finish of these experiments is not known, but, in view of previous calibrations, the change is probably less than —0.000030 abs. ohms. Such a change is of the same order as the precision in a single calibration.

Reliability of reported T_{f_0}'s and T_f's of benzene samples

(A) Assuming an accumulative propagation of error, the absolute value of the $T_{f_0}{}^{tp}$ of benzene should be $5.51_{29} \pm 0.002$°C.
(B) In terms of the above, the absolute values of the $T_f{}^{tp}$'s reported would also have the same limits of accuracy.
(C) The errors as expressed above are of the order of magnitude necessary to account for the standard deviations obtained in those experiments relating to sample A-2.

IV. CALORIMETRIC ANALYSIS

1. *Method*

The calorimetric method for determining the chemical purity of benzene involved the measurements of liquid-solid equilibrium temperatures at various precisely known liquid to solid ratios evaluated from the total heat input, heat of fusion, and heat capacity. The measurements of liquid-solid equilibrium temperatures were made under

References p. 79

conditions of saturation vapor pressure of benzene. The method requires considerably more equipment than the thermometric method but offers an advantage in that the equilibrium temperature can be measured at one's leisure. If temperature equilibrium is not indicated, then a longer time can be allowed, within reason, until a temperature equilibrium is attained. Recently, the calorimeters of this laboratory have been provided with automatic adiabatic controls which conveniently permit long equilibrium times. Previously, when the calorimeters were controlled manually to attain the adiabatic condition, the maximum conveniently allowable equilibrium time was about 2 hours. In the experiments described in this paper, at least 16 hours have been allowed per measurement in order to attain more closely the liquid-solid equilibrium conditions.

For a substance of high purity, the relation for thermodynamic equilibrium between the pure crystal and the liquid containing mole fraction impurity N_2 may be given by the simplified equation:

$$N_2 = A(T_{f_0}^{tp} - T_{obs}) \quad \ldots\ldots\ldots\ldots\ldots\ldots \quad (2)$$

where

A = $\triangle H_{f_0}/R[T_{f_0}^{tp}]^2$, the cryoscopic constant,
$\triangle H_{f_0}$ = the heat of fusion at $T_{f_0}^{tp}$,
R = the gas constant,
$T_{f_0}^{tp}$ = the triple-point temperature of the pure substance, and
T_{obs} = the observed liquid-solid equilibrium temperature.

When this high-purity substance containing total mole fraction N_2* of liquid-soluble, solid-insoluble impurity is partially crystallized, the concentration of the impurity in the liquid phase is greater by the ratio $1/F$, where F is the fraction melted. The mole fraction impurity of the solution in equilibrium with the crystal is then given by:

$$N_2 = N_2^*(1/F) \quad \ldots\ldots\ldots\ldots\ldots\ldots \quad (3)$$

and when equations (2) and (3) are combined,

$$(N_2/A) = (N_2^*/A)(1/F) = T_{f_0}^{tp} - T_{obs} \quad \ldots\ldots\ldots\ldots \quad (4)$$

Equation (4) shows that the plot of T_{obs} with respect to $1/F$ is a straight line and that, when $1/F = 0$, $N_2 = 0$ and the temperature intercept is the triple-point temperature of the pure material. The slope (N_2^*/A) of the line determines the total mole fraction impurity of the material.

2. *Apparatus*

Determinations of the purity of benzene were made in an adiabatic calorimeter designed for heat-capacity measurements in the range 10° to 300°K on substances that can be readily transferred by vaporization[7]. Fig. 7 shows a schematic drawing of the calorimeter.

The sample container, suspended in the calorimeter by a thin-walled monel filling tube, was constructed chiefly of copper with a capacity of about 106 ml. In order to provide as uniform a distribution of energy as possible to the enclosed sample, tinned copper vanes were arranged radially from the central re-entrant well, containing a heater and an encapsulated platinum-resistance thermometer, to the outer wall of the

Reerences p. 79

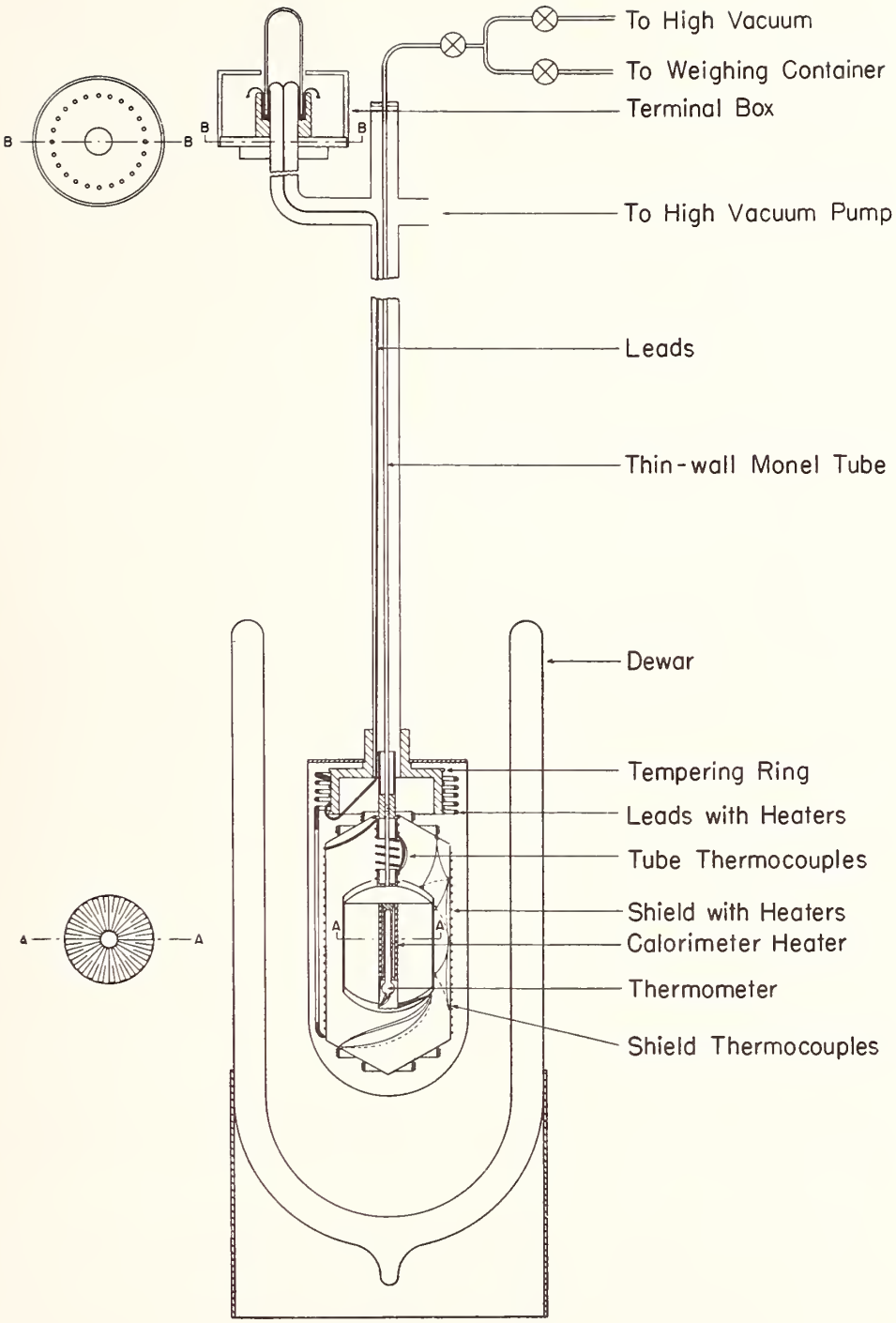

Fig. 7. Adiabatic calorimeter for volatile substances.

container. The vanes were held in place by means of a thin coating of pure tin applied to the interior surfaces of the container and so spaced that the maximum separation was about 4 millimeters. The tin afforded an inert surface to benzene.

A thin copper thermal shell attached to the upper periphery of the container afforded a nearly isothermal surface, regardless of any localized temperature differences on the surface of the container, to the adiabatic shield surrounding the container and the shell. Electronic control equipment was used to adjust the currents in the several shield heaters so that the temperature of the shield could be automatically maintained at the same temperature as that of the shell. Sensitive thermocouples placed between the shield and the shell controlled the operation of the electronic system. The outer surface of the container, the inner and outer surfaces of the shell, and the inner surface of the adiabatic shield were gold-plated and polished to minimize heat transfer by radiation. A high vacuum (10^{-6} mm Hg) was maintained in the space surrounding the sample container and the adiabatic shield.

The resistance of the platinum thermometer, having the ice-point resistance of about 25.5 ohms, was measured by means of a special Mueller bridge designed for the range of 0.00000 to 422.11110 ohms. The platinum-resistance thermometer was calibrated in accordance with the 1948 International Temperature Scale[8]. The temperatures in degrees Kelvin were obtained by adding 273.1600 degrees to the temperatures in degrees Celsius*.

The electrical input energy was determined from the measurements of the current and potential across the 100 ohm Constantan wire heater and the time interval of heating. The heater current and potential were determined by means of a Wenner potentiometer in conjunction with a standard resistor and a volt box. The time-interval of heating was measured by means of a precision interval timer operated on a standard frequency of 60 cycles furnished by the Time Laboratory of the Bureau. The timer has been compared periodically with standard second signals and found to vary not more than ± 0.02 second per heating period, which was never less than 6 minutes. All electrical instruments have been calibrated in terms of the standards maintained at the National Bureau of Standards.

3. *Experimental procedure*

Oil-diffusion vacuum pumps were used in conjunction with suitable mechanical vacuum pumps to evacuate the calorimeter and the various accessory equipment. The vacuum manifolds contained liquid nitrogen traps to prevent back diffusion of oil into the apparatus being evacuated. The general procedure for evacuating an apparatus was to maintain it for at least 24 hours at 100°C and at 10^{-6} mm Hg as registered at the vacuum manifold. Although the resistance to gaseous flow was minimized, some of the equipment necessarily contained valves and small diameter tubulations, particularly the weighing flasks and the calorimeter container.

---

* The temperatures given are believed to be accurate to ± 0.01 degree Kelvin. Wherever temperatures are given to four decimal figures, the last two digits are significant only in the measurement of small temperature differences.

At the Tenth General Conference held in 1954, the General Conference on Weights and Measures adopted a new definition of the thermodynamic temperature scale by assigning the temperature 273.16°K to the triple-point temperature of water. For details regarding the adoption of this new scale, see reference[9].

References p. 79

Each sample of benzene was vacuum-distilled directly from the ampoule, in which it was received, into a separate weighing container fitted with a valve. After weighing, the container was attached to the calorimeter transfer manifold and the entire sample vacuum-distilled into the sample container. When the purity of the uncontaminated sample (sample A), which was investigated first, was found to be 99.99_{37} mole %, a purity considerably lower than anticipated, the weighing containers and all transfer manifolds were thoroughly purged with portions of the sample A and then pumped to a high vacuum before transferring the subsequent samples. The evacuation of the system for 24 hours at 100°C and at 10^{-6} mm Hg at the vacuum manifold was considered to be still insufficient when working with extremely pure substances. Repeated purging and evacuation were thought to be helpful in cleaning the system. Since another sample of the purest material was not available, tests could not be made to determine whether the sample A had been contaminated during the transfer to the calorimeter.

The experimental procedure for making the purity measurements was the following. The heat capacity of the system containing the sample was determined in the range from about 250° to 290°K. Then, the heat of fusion was determined by introducing a known quantity of electrical energy sufficient to raise the temperature of the system from just below to just above the triple point and making corrections for the heat capacity and for the premelting due to the presence of impurity.

The liquid-solid equilibrium temperatures were determined as follows. To avoid local concentration of the impurities, which was considered possible by slow cooling methods, the sample was rapidly crystallized either in part or in whole, taking the precaution to maintain the filling tube temperature considerably above the melting point of the sample so that the sample would not condense in the tube. When the sample was partially crystallized, it was allowed to equilibrate by bringing the adiabatic shield into automatic control. When the sample was totally crystallized, it was heated electrically under adiabatic control to the desired liquid-solid ratio and allowed to equilibrate. It was convenient to allow the sample to equilibrate over-night and to observe the liquid-solid equilibrium temperatures during the morning of the following day. After the liquid-solid equilibrium temperature was established, a known quantity of electrical energy was added sufficient to raise the temperature of the sample to just above the triple point. If Q is the electrical energy that was added, then $Q - \int C\mathrm{d}T$ is the energy required to melt the material from the observed equilibrium temperature. The term $\int C\mathrm{d}T$ is the heat-capacity correction. Then,

$$1/F = \frac{L_f}{L_f - (Q - \int C\mathrm{d}T)} \quad \ldots\ldots\ldots\ldots\ldots\ldots \quad (5)$$

where L_f is the total heat of fusion. In this method any small heat leak that may occur during the prolonged equilibrium interval would not affect the $1/F$ value.

4. Results

The results of the measurements of heat of fusion on the benzene samples are given in Table IX. The results compare favorably with the selected value (9837 abs j mole^{-1}) given by Rossini *et al.*[10]. Since sample B was somewhat larger than generally used in the calorimeter, it was felt that a small amount of the sample could have been condensed in the tube during the heat-of-fusion measurements. When measurements on all the

References p. 79

TABLE IX

HEAT OF FUSION OF THE BENZENE SAMPLES

Molecular weight = 78.1140 g; °K = °C + 273.16°

Temperature interval of heating °K	*Total energy input* abs j	*Corrections* heat capacity abs j	*Corrections* premelting abs j	L_f Total abs j	ΔH_f abs j mole^{-1}
Sample A, mass of sample = 76.6591 g					
274.9985 to 282.2772	11005.6	1357.1	10.6	9659.1	9842.4
275.8612 to 281.2168	10650.4	998.4	13.9	9665.9	9849.3
275.7011 to 280.8662	10611.4	961.2	13.1	9663.3	9846.7
275.6013 to 282.2809	10899.3	1247.8	12.7	9664.2	9847.5
271.1321 to 281.4924	11556.2	1907.9	5.1	9653.4	9836.6
		Mean			9844.5
		Standard deviation of the mean[a]			±2.3
Sample B, mass of sample = 90.3655 g					
260.7869 to 281.5943	15601.4	4214.2	4.5	11391.7	9847.2
Sample B, mass of sample = 76.0445 g					
261.1786 to 282.3869	13401.5	3824.8	3.9	9580.6	9841.3
		Mean			9844.2
		Standard deviation of the mean			±3.0
Sample C, mass of sample = 86.3014 g					
268.5729 to 281.0443	13345.9	2499.7	35.6	10881.8	9849.4
257.9009 to 280.7212	15296.1	4452.5	16.7	10860.3	9830.0
271.6529 to 281.3753	12785.3	1957.0	52.0	10880.3	9848.1
		Mean			9842.5
		Standard deviation of the mean			±6.3

[a] Standard deviation of the mean as used above is defined as $[\Sigma' d^2/n(n-1)]^{1/2}$; where d is the difference between a single observation and the mean, and n is the number of observations.

TABLE X

LIQUID-SOLID EQUILIBRIUM TEMPERATURES OF BENZENE, SAMPLE A

$1/F$	*Treatment of sample*[a]	T_{obs}[b] °K	T_{calc} °K	$T_{obs} - T_{calc}$ °K
8.844	*H*	278.6450	278.6445	0.0005
7.703	*C*	278.6486	278.6492	—0.0006
5.051	*C*	278.6603	278.6601	0.0002
3.165	*C*	278.6672	278.6679	—0.0007
2.221	*H*	278.6718	278.6718	0.0000
2.088	*C*	278.6720	278.6723	—0.0003
1.287	*C*	278.6762	278.6756	0.0006
1.000			278.6768	

Triple-point temperature, 278.6809°K or 5.5209°C.
Slope, —0.00411F°K.
Impurity, 0.0063 ±0.0010 mole %[c].

[a] The symbol *C* indicates that the sample was rapidly crystallized and the symbol *H* indicates that the sample was rapidly crystallized and heated to the $1/F$ values given.

[b] These temperatures were obtained from the relation °K = °C + 273.1600° and are believed to be accurate to ±0.01°K. The last two decimal places are significant only in the measurement of small temperature differences.

[c] The uncertainty was estimated by examining the imprecision of the measurements and all known sources of systematic error. The system was assumed to follow the ideal solution law and to form no solid solution with the impurity.

References p. 79

samples were completed, the heat-of-fusion measurements were repeated using about 84 % of the original sample B. The results indicate that a negligible amount, if any, was in the tube during the first measurements.

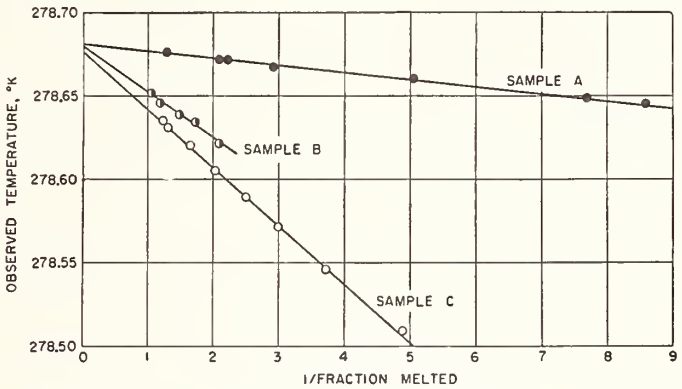

Fig. 8. Liquid-solid equilibrium temperatures of the benzene samples at various $1/F$ values.

The observed liquid-solid equilibrium temperatures and the corresponding $1/F$ values are summarized in Tables X, XI, and XII, for the benzene samples A, B and C, respectively, and are plotted together in Fig. 8. The values of temperatures given in column 4 of these tables were calculated from equation (4) using the values of N_2* and $T_{f_0}{}^{tp}$ as determined from a linear equation fitted to the experimental data by the method of least squares. The comparison of calculated and observed liquid-solid equilibrium temperatures gives an indication of thermodynamic equilibrium, of ideality of the solution, and of formation of solid solution in the range of the experiments.

The cryoscopic constant used in the various calculations was $0.01525(°K)^{-1}$, based on the triple-point temperature, $T_{f_0}{}^{tp}$, and the mean heat of fusion obtained on the

TABLE XI

LIQUID-SOLID EQUILIBRIUM TEMPERATURES OF BENZENE, SAMPLE B

$1/F$	*Treatment of sample*[a]	T_{obs}[b] °K	T_{calc} °K	$T_{obs} - T_{calc}$
2.100	*H*	278.6212	278.6221	—0.0009
1.735	*H*	278.6339	278.6322	0.0017
1.484	*H*	278.6387	278.6391	—0.0004
1.187	*H*	278.6458	278.6473	—0.0015
1.047	*H*	278.6518	278.6511	0.0007
1.000			278.6525	

Triple-point temperature, 278.6799°K or 5.5199°C.
Slope, —0.0275F°K.
Impurity, 0.042 ±0.005 mole %[c].

[a] See footnote a, Table X.
[b] See footnote b, Table X.
[c] See footnote c, Table X.

References p. 79

purest sample A. The values obtained with sample A are considered to be the most nearly accurate. The $T_{f_0}{}^{tp}$ value 278.6809°K, when reconverted to degrees Celsius, becomes 5.5209°C. Considering the imprecision of the measurements and the various sources of errors, the uncertainty in the value of 5.5209°C for the triple-point temperature of pure benzene was estimated to be ±0.0050°C including the uncertainty of ± 0.0030°C in the determination of the temperature. MATHIEU[11] reported the value 5.524°C for the triple-point temperature of pure benzene.

The samples were allowed to equilibrate at least 16 hours, and the temperatures observed during the next 4 hours did not change in any instance by more than 0.0002 degree. The prior treatment of the sample, whether it was partially crystallized rapidly or totally crystallized rapidly and melted to the desired $1/F$ value, did not seem to give any definite trend in the results. The deviations of the observed liquid-solid equilibrium temperatures from the calculated values are scattered and are somewhat larger than those observed in previous investigations in which successive liquid-solid temperatures were observed during a single day by melting the same crystal stepwise and allowing shorter time intervals (about 1 to 2 hours) for equilibrium [12,13]. The measurements of the temperature using the same bridge and thermometer over a relatively short

TABLE XII

LIQUID-SOLID EQUILIBRIUM TEMPERATURE OF BENZENE, SAMPLE C

$1/F$	Treatment of sample[a]	T_{obs}[b] °K	T_{calc} °K	$T_{obs} - T_{calc}$ °K
4.905	*C*	278.5092	278.5072	0.0020
3.733	*H*	278.5461	278.5476	—0.0015
2.998	*C*	278.5716	278.5729	—0.0013
2.492	*H*	278.5891	278.5903	—0.0012
2.040	*H*	278.6054	278.6059	—0.0005
1.651	*H*	278.6201	278.6193	0.0008
1.321	*C*	278.6312	278.6307	0.0005
1.226	*C*	278.6350	278.6340	0.0010
1.000			278.6418	

Triple-point temperature, 278.6764°K or 5.5164°C.
Slope, —0.0346F°K.
Impurity, 0.053 ±0.005 mole %[c].

[a] See footnote a, Table X.
[b] See footnote b, Table X.
[c] See footnote c, Table X.

range of temperature, are considered to be reproducible within about 0.0002° from day to day. The observed deviations greater than these amounts may arise from the differences in the crystallization process[14], although the crystallization was thought to be well controlled, and the non-equilibrium conditions even after 16 hours. Since the calorimeter was operated at a temperature very close to room temperature, a small amount of benzene and *n*-heptane may have condensed in the filling tube during the long equilibrium period. Both benzene and *n*-heptane have sufficient vapor pressure at 5°C to condense on the tube if any portion of the tube is colder than the sample container. The contribution to the deviation from this source, however, is considered

References p. 79

to be fairly small, unless there is a preferential condensation of *n*-heptane, which is unlikely.

A series of controlled experiments is required to resolve these small differences. Continuous measurements of the liquid-solid equilibrium temperatures could be made at various $1/F$ values by successively melting a crystal formed by both rapid crystallization and by slow crystallization. These measurements could be made at equilibrium times equivalent to those involved in manually controlled measurements and at the prolonged equilibrium times possible in automatic controlled measurements. At the writing of this report sufficient data have not been accumulated on these measurements for presentation.

V. CONCLUSIONS

The analyses by thermometric and calorimetric procedures can now be compared with the anticipated purities based upon the methods of preparing the three samples A, B, and C. For this, the assumptions are made that the uncontaminated benzene was pure beyond any power of either method to disclose the impurity and that the contaminations had proceeded exactly in accord with the plans and calculations.

Table XIII shows two effects that were unexpected before the final assemblage of data. These effects can serve as valuable guides to future work, however. First, the large divergence between the thermometric and the calorimetric analyses that had characterized earlier comparisons, both in our own laboratories and elsewhere, is not displayed. The differences between the analyses on all three samples are roughly of the order of the statistically estimated uncertainties of the averages and less than deviations between individual experiments by one method. The inherent evidences of accuracy are good and both groups of workers completed their tasks with a sense of confidence. Second, both forms of analysis gave results that differed significantly from values computed by the amount of contaminant that had been added.

TABLE XIII

COMPARISON OF THE RESULTS FROM THERMOMETRIC AND CALORIMETRIC ANALYSES WITH THE VALUES COMPUTED FROM CONTAMINATION

Sample	*Purity, mole %*			*Excess of purity computed from amount of deliberate contamination above average of analysis by thermometric and calorimetric processes*
	Computed from contamination	*Thermometric analysis*	*Calorimetric analysis*	
A	100[a]	$99.99_4 \pm 0.002$	99.9937 ± 0.0010[b]	0.006
B	99.9964	$99.97_0 \pm 0.004$	99.958 ± 0.005[b]	0.032
C	99.9610	$99.94_0 \pm 0.002$	99.947 ± 0.005[b]	0.017

[a] The "pure" sample was assumed to be pure beyond the sensitivity of the methods of analysis employed.

[b] See footnote c, Table X.

It should not be too surprising that the earlier differences between the methods should have become much reduced. Both sets of analyses were performed under the conditions mentioned in the introduction — "that each method would be utilized in the manner believed by its practitioners to be most dependable." The result is that

References p. 79

there were significant modifications of procedure or interpretation of data by both groups.

In the thermometric experiments the greatest change, except for refinements of temperature measurement were modifications of the means of interpreting data. It has been known that, when $T_{f_0}{}^{tp}$ is calculated by the method of TAYLOR AND ROSSINI, the values become progressively higher as purer samples are employed. In the present work, although the same fundamental method is used, slightly modified criteria were employed to select the usable portion of a freezing curve and for calculation both of ideal and actual points of initial freezing.

In the calorimetric analyses the principle changes were experimental, there being two important changes of technique. The time of equilibration was greatly increased both to attain temperature stability and to allow diffusion of impurities within the liquid phase. Furthermore, the thermal history of each run was changed in such ways that very little separation of the impurities from the rest of the sample could occur.

On the second point, the difference between the analyses and the assumed purity of the samples as prepared and contaminated, an important clue is found in data of Table I. The first two runs were made on a Friday after the benzene had been introduced into the freshly heated and exhausted apparatus. The sealed apparatus remained unused until the following week when the other runs were made and a much larger amount of impurity was disclosed. On this basis subsequent runs were made by conditioning the interior of the apparatus with benzene of high purity. This can account for the difference between Table I and those that follow. Observing, both on the assumed "pure" sample and on the several contaminated samples, that the impurities found exceeded those anticipated more or less in relation to the number of times that a benzene sample had been introduced into a flamed and exhausted glass vessel without contact with air, it is beguiling to infer that flaming with exhaustion does not adequately prepare glass to receive benzene without contaminating it.

In the body of the paper it was suggested that chemi-sorbed water might be a source of contamination. This inference was drawn before the assemblage of data disclosed the difference between assumed and determined purities. Whether it is true or not may possibly be disclosed by experiments now in progress, but in any event the evidence is strong that it is difficult to manipulate benzene in glass in such manner as to preserve a state of high purity. The results of this investigation strongly indicate that additional series of closely controlled experiments need be performed to determine (a) the source of discrepancies previously found between the thermometric and calorimetric methods of analysis and (b) the sources of contamination during the handling of the benzene samples.

SUMMARY

Workers at the National Bureau of Standards and elsewhere have been conscious of the discordant results sometimes yielded by two methods for determining purity employing the same physical principle. A comparison was made on samples of benzene by the thermometeric method, by which a stirred sample is frozen at nearly constant rate, and by the calorimetric method, by which a frozen sample is melted in stages by the addition of accurately controlled increments of energy under adiabatic conditions.

Benzene, purified by single crystal formation and of very high purity, was contaminated in known amounts by *n*-heptane and samples of the same level of purity determined by both procedures. Great care was taken to submit samples of the same composition to the different groups employing the two different methods. Further, the actual degree of contamination of the benzene was unknown to both groups until final values of the purity were submitted.

References p. 79

Results of this comparison showed that the large divergence between the two methods that had characterized earlier comparisons is not displayed. The differences between the analyses on all three samples are roughly of the order of the statistically estimated uncertainties of the averages and less than deviations between individual experiments by one method.

Comparison of the methods with absolute values of purity could not be made because of contamination of the highly purified sample of benzene with supposedly chemically adsorbed water from the borosilicate glass walls.

RÉSUMÉ

Des chercheurs au Bureau National des Étalons des États Unis et ailleurs se sont rendu compte du fait que l'on obtient parfois des résultats discordants lorsque l'on détermine une pureté par deux méthodes basées sur le même principe physique. Dans ce mémoire on décrit une comparaison de déterminations de puretés d'échantillons de benzène d'une part par la méthode thermométrique au cours de laquelle un échantillon agité est congelé à une vitesse à peu près constante et, d'autre part, par la méthode calorimétrique où l'on fait fondre un échantillon congelé en étappes en lui fournissant des portions d'énergie exactement réglées sous des conditions adiabatiques.

Du benzène purifié par formation de cristaux et d'une très haute pureté a été contaminé par des quantités connues de *n*-heptane et des échantillons d'un même degré de pureté ont été examinés par les deux procédés. L'on a pris grand soin de soumettre des échantillons de même composition aux différentes équipes employant les deux méthodes différentes. De plus, les vrais degrés de contaminations du benzène étaient inconnus aux deux équipes jusqu'à ce que les valeurs définitives de puretés furent soumises.

Les résultats de cette comparaison ont montré que les grandes divergences entre les deux méthodes qui avaient caractérisé les comparaisons plus anciennes ne se produisaient pas. Les différences entre les résultats des analyses de tous les trois échantillons sont, approximativement, de l'ordre des incertitudes des valeurs moyennes estimées statistiquement; elles sont inférieures aux déviations entre les expériences individuelles par une seule méthode.

Une comparaison des méthodes donnant des valeurs de pureté absolues n'a pas pu être faite à cause de la contamination des échantillons hautement purifiés de benzène par de l'eau que l'on suppose être adsorbée chimiquement à partir du borosilicate des parois de verre.

ZUSAMMENFASSUNG

Forscher im ,,National Bureau of Standards'' und anderswo waren sich davon bewusst, dass man manchmal nicht übereinstimmende Resultate erhält wenn man den Reinheitsgrad mit zwei verschiedenen Methoden, die sich auf dasselbe physikalische Prinzip gründen, bestimmt. Ein Vergleich solcher Bestimmungen an Benzolproben wurde nun angestellt, und zwar einerseits mit Hilfe der thermometrischen Methode bei der eine gerührte Probe mit nahezu konstanter Geschwindigkeit zum Gefrieren gebracht wird, andererseits mit der kalorimetrischen Methode bei welcher eine gefrorene Probe in Etappen durch Zuführen genau geregelter Energiemengen unter adiabatischen Bedingungen geschmolzen wird.

Durch Einzelkristallbildung gereinigtes Benzol von hohem Reinheitsgrad wurde mit bekannten Mengen *n*-Heptan verunreinigt und Proben von gleichem Reinheitsgrade wurden nach beiden Verfahren geprüft. Es wurde besonders darauf geachtet, dass die verschiedenen Arbeitsgruppen, die die verschiedenen Verfahren anwendeten, Proben von gleicher Zusammensetzung erhielten. Ausserdem war der wirkliche Verunreinigungsgrad des Benzols beiden Gruppen solange unbekannt, bis die endgültigen Reinheitswerte mitgeteilt waren.

Die Ergebnisse dieses Vergleiches zeigten, dass die grossen Abweichungen zwischen den beiden Methoden, welche frühere Vergleiche kennzeichneten, nicht auftreten. Die Unterschiede zwischen den Analysen aller dreier Proben waren im grossen und ganzen von der Grössenordnung der statistisch geschätzten Unsicherheiten der Mittelwerte; sie waren kleiner als die Abweichungen zwischen den einzelnen mit einer selben Methode ausgeführten Versuchen.

Ein Vergleich der Methoden mit absoluten Reinheitswerten konnte nicht gemacht werden, weil das hoch gereinigte Benzol durch wahrscheinlich chemisch adsorbiertes Wasser aus dem Borosilikat der Glaswände verunreinigt wird.

ACKNOWLEDGEMENT

The authors wish to acknowledge the assistance of Marthada V. Kilday, H. B. Lowey, L. A. Machlan, Patricia B. Nalls, and O. T. Termini for their help in the various phases of this work.

References p. 79

REFERENCES

1 M. R. Cines, *Physical Chemistry of the Hydrocarbons*, Vol. I, Academic Press Inc., New York, 1950, p. 315.
2 M.-P. Mathieu, *Acad. roy. Belg., Classe sci., Mém.*, 28 (1953) Fasc. 2, No. 1639.
3 A. T. Horton, *U.S. Patent No.* 2, 754, 180, July 10, 1956.
4 A. R. Glasgow, Jr. and M. Tenenbaum, *Anal. Chem.*, 28 (1956) 1907
5 W. J. Taylor and F. D. Rossini, *J. Research Natl. Bur. Standards*, 32 (1944) 197.
6 F. W. Schwab and E. Wichers, *Temperature, its Measurement and Control in Science and Industry*, Reinhold Publishing Corp., New York, 1941, p. 256.
7 R. B. Scott, R. D. Rands, Jr., C. H. Meyers, F. G. Brickwedde and N. Bekkedahl, *J. Research Natl. Bur. Standards*, 35 (1945) 39.
8 H. F. Stimson, *J. Research Natl. Bur. Standards*, 42 (1949) 209.
9 H. F. Stimson, *Am. J. Phys.*, 23 (1955) 614.
10 F. D. Rossini, K. S. Pitzer, R. L. Arnett, R. M. Braun and G. C. Pimentel, *Selected Values of Physical and Thermodynamic Properties of Hydrocarbons and Related Compounds*, Carnegie Press, Pittsburgh, 1953.
11 M.-P. Mathieu, *Bull. soc. chim. Belges*, 61 (1952) 683.
12 G. T. Furukawa, D. C. Ginnings, R. E. McCoskey and R. A. Nelson, *J. Research Natl. Bur. Standards*, 46 (1951) 195.
13 T. B. Douglas, G. T. Furukawa, R. E. McCoskey and A. F. Ball, *J. Research Natl. Bur. Standards*, 53 (1954) 139.
14 J. P. McCullough, paper presented at the *Eleventh Calorimetry Conference, Johns Hopkins University, September 14 and 15, 1956.*

13253—U.S. Dept. of Comm—DC—1957

Received April 23rd, 1957

Reprinted from Analytica Chimica Acta
Vol. 17, Nr. 1, July, 1957

Journal of Research of the National Bureau of Standards Vol. 52, No. 5, May 1954 Research Paper 2493

A Cryoscopic Study of the Solubility of Uranium in Liquid Sodium at 97.8° C

Thomas B. Douglas

The equilibrium temperatures, at various stages of melting, of three samples of sodium were measured with a standard deviation of 0.001 degree. One sample contained uranium in compact form, and one contained finely divided uranium. Impurities lowered the freezing points of all the samples by approximately 0.035 degree, but the sodium containing finely divided uranium was found to have a freezing point higher than those of the other two samples by 0.005 degree, an effect that may be due to a partial purification of the sodium by the uranium. After extrapolation to no impurity, the freezing points of the three samples agree within 0.001 degree. Allowing for errors, it is concluded that the solubility of uranium in liquid sodium at 97.8° C probably does not exceed 0.05 percent by weight and may actually be many times smaller.

1. Introduction

One of the most sensitive and convenient methods commonly used to estimate the concentration of a dilute solution is the comparison of its liquidus temperatures (freezing points) with that of the pure solvent, if the solid phases are immiscible. This method was applied in an attempt to estimate the solubility of uranium in liquid sodium at 97.8° C, the triple point of the latter element. The equilibrium temperatures at intervals from 70- to 100-percent completion of fusion of the sodium were observed.

2. Experimental Procedure

Three samples were prepared, each containing 6½ g of sodium from a batch that had been purified by distillation. In addition to the sodium, the sample designated as A contained no uranium, sample B contained 2 g of a solid section of uranium, and sample C contained 2 g of finely divided uranium prepared by hydride decomposition. The samples were sealed, by induction welding in an oxygen-free inert atmosphere, in small cylinders of stainless steel type 347. Subsequent tests at room temperature and at 150° C indicated leakage through the seals to be no greater than 4×10^{-12} cm³ of helium per second, a rate not taken to indicate a real leak.

The apparatus for the cryoscopic measurements is shown in figure 1. Each sample was suspended by a No. 32 nichrome wire in air inside a vertical furnace, whose core maintained a highly uniform environmental temperature because it was surrounded by a silver pipe 10 in. long and of ½-in. wall thickness. The temperature of the silver was measured by a platinum resistance thermometer whose ice point remained constant to within an amount equivalent to ±0.0005 deg throughout the measurements. Heat was supplied to the sample at will by a constantan heater imbedded in a gold-plated copper jacket that surrounded the sample container at an average distance of 0.002 in. A four-junction differential thermocouple (chromel P versus constantan), calibrated in place against freezing sodium, enabled precise measurement of the temperature difference between the silver pipe of the furnace and the sample.

A detailed systematic procedure was followed in an effort to make the systematic errors constant and thereby to secure accurate differences in temperature among the three samples. With the individual runs numbered chronologically, runs 1, 5, and 9 were on sample A; runs 2, 3, and 4 were on sample C; and runs 6, 7, and 8 were on sample B. Run 10 was on a fourth sample of sodium, taken from a different batch prepared 2 years earlier. Each run was made on a different day.

With the sample in place, the furnace was heated to a temperature at which melting of the sodium would just begin, and was then held at approximately this temperature for the next 3 hr. The sample was then heated for separated intervals of time until fusion was clearly complete. Thus at any stage of the fusion process the fraction of the total fusion heat that had entered the sample could be taken as a measure of the fraction of the sodium then present as liquid. After each such interval of heating, the equilibrium temperature was measured in the following way. The temperature of the furnace was held constant (within ±0.0005 deg) at a temperature no more than 0.003 deg higher or lower than the prevailing sample equilibrium temperature,[1] until the thermocouple reading appeared to be changing by less than 0.0001 deg/min. This furnace control was accomplished by means of a 0.7-w variable auxiliary heater inside the silver. When the sodium was all crystalline or all molten, the difference between its temperature and that of the furnace decreased by 15 percent per minute owing to heat conduction through the intervening air spaces. However, during melting the error introduced in this way was negligible because of the large magnitude of the heat of fusion and the ease of maintaining then a small temperature difference.

To each equilibrium temperature found was added 0.012 deg, as the thermocouple reading was found to approach −0.012 deg when the temperatures of its junctions were known to be rapidly approaching

[1] Reversal of the sign of this temperature difference was used to prove that the thermocouple read the unbiased relative temperature of the sample.

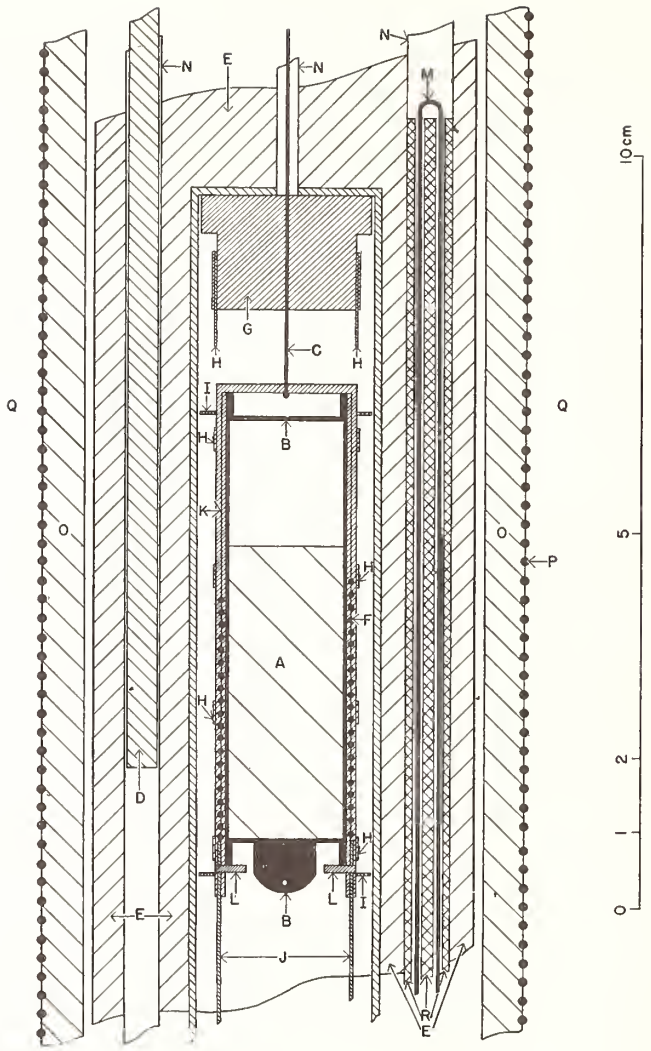

FIGURE 1. *Apparatus for cryoscopic measurements.*

A, Sodium sample (with or without uranium); B, sealed container for sample (stainless steel type 347); C, suspension wire (Nicbrome V); D, platinum resistance thermometer; E, isotbermal jacket (silver); F, heater for sample (glass-covered constantan); G, tbermocouple reference block (gold-plated copper); H, thermocouple junctions (copper bands or tabs); I, spacers (nichrome V wire); J, heater leads (copper); K, jacket for sample container and beater cover (gold-plated copper); L, pins for supporting sample container; M, auxiliary heater for silver jacket (platinum); N, Inconel tubing; O, alundum tube; P, main furnace beater (platinum); Q, furnace insulation (silica powder); R, porcelain tube.

equality. In addition, 0.003 deg also was added to correct for the error due to the estimated azimuthal temperature gradient in the silver pipe.

3. Results and Conclusions

The variation of temperature as the impure sodium melts may be predicted from Raoult's law. For very small proportions of impurities entirely insoluble in the solid solvent (sodium), this law may be written in the approximate form

$$t = t_0 - (RT_0^2/L_f)(x_1 + x_2). \qquad (1)$$

In this equation the total mole fraction of all solutes in solution in the liquid sodium has been divided into two parts. x_1 designates that part due to solute that, if present at all, is sufficient in amount to maintain the liquid sodium saturated with it. (This solute will be assumed to be uranium only.) x_2 designates that part due to any solute at all times entirely in solution in whatever liquid sodium is present; t is the equilibrium temperature (in deg C); t_0 is the freezing (triple) point of pure sodium (also in deg C, the corresponding value in deg K being T_0); R is the gas constant; and L_f is the molal heat of fusion of sodium.

It is evident that as fusion of the sodium progresses, the increasing amount of liquid available as solvent leads to a decrease of x_2 but not of x_1. x_2 may be replaced by its equivalent, x_2'/f, where f is the fraction of the sodium present as liquid when the temperature is t, and x_2' is then the value of x_2 when f is unity. Equation (1) then becomes

$$t=t_0-RT_0^2x_1/L_f-(RT_0^2x_2'/L_f)(1/f). \qquad (2)$$

Substituting numerical values for the known constants (R=8.314 j mole^{-1} deg K^{-1}, T_0=371.0° K, and L_f=2603 j mole^{-1}),[2] eq (2) may be written in the present specific case as follows:

$$t=t_0-440x_1-440x_2'(1/f). \qquad (3)$$

The points in figure 2 show for various stages of fusion the individual observed equilibrium temperatures. The chronological number of each run is shown beside its respective points. It may be seen that for the same sample there is, in general, more variation from one run to another than in the systematic deviations from linearity of the points of one run. This is due partly to the errors in the calculated fractions melted, these errors arising chiefly from the difficulty of determining accurately when in each run fusion began and ended. The solubility of the steel container in the liquid sodium [3] should have caused a constant error of less than 0.001 deg. This error has been ignored. Temperatures recorded when fusion was less than 70 or more than 98 percent complete were always decidedly too high to be in line with the others and were discarded. It seems likely that these latter discrepancies resulted partly from lack of the expected thermal and composition equilibrium, under these less favorable conditions, as the samples were neither shaken nor stirred. Also, the solubility of unidentified impurity may have been exceeded until a large fraction of the sodium had become molten.

Equation (3) predicts that as fusion progresses, the temperature will increase linearly with the decrease in $1/f$. In figure 2 the straight line for each sample was obtained from the observed points by the method of least squares. The corresponding numerical values of the coefficients of eq (3), together with their standard deviations (precision), are shown in table 1. Several conclusions may be drawn from these values.

TABLE 1. *Coefficients of equation (3) for three samples*

Sample	t_0-440x_1	$440x_2'$
	°C	°C
A	97.8199 (±0.0056)	0.0349 (±0.0048)
B	97.8208 (±0.0033)	.0379 (±0.0028)
C	97.8202 (±0.0025)	.0297 (±0.0021)

[2] D. C. Ginnings, T. B. Douglas, and A. F. Ball, J. Research NBS **45**, 23 (1950) RP2110.
[3] L. F. Epstein (private communication).

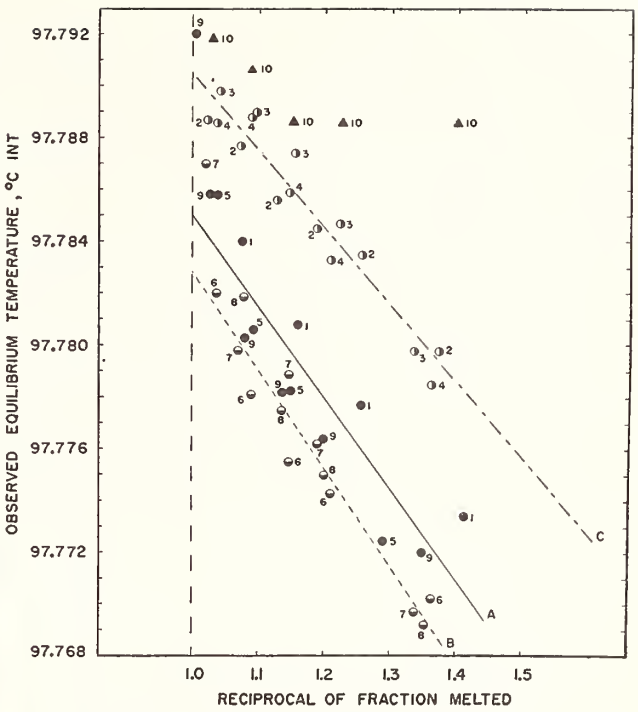

FIGURE 2. *Observed equilibrium temperatures.*

●——————, sample A (sodium); ◒- - - - - - - - - - - -, sample B (sodium plus bulk uranium); ◑– – – – – – – – – –, sample C (sodium plus finely divided uranium); ▲, sample D (an earlier sodium sample).
The run numbers given with the points are in chronological order.

From consideration of the details of purification of the sodium, it appears that the impurity with respect to which the liquid sodium was unsaturated may well have been largely sodium oxide, Na_2O. The values of the third column of table 1 give immediately the corresponding values of x_2', the mole fraction of this type of impurity in the whole sample. This averages 8×10^{-5} for samples A and B. This value corresponds to 0.02 percent of Na_2O by weight,[4] a reasonable amount of impurity from this source as it corresponds to the order of magnitude of the solubility of Na_2O in liquid sodium at this temperature. The corresponding quantity for sample C is somewhat lower than that for sample A, the difference having a standard deviation equal to the difference itself. It is possible that sample C actually contained substantially less impurity of this type, for the large surface of the finely divided uranium in this sample may have led to the removal of a considerable amount of the original impurity. Such a hypothesis is supported by the known ability of uranium to remove oxygen from Na_2O at higher temperatures.

If it be assumed that sample A, into which no uranium had been introduced, was free of all other "saturated" solutes, the value of t_0-440x_1 for this sample from table 1 gives 97.82° C as the triple point of pure sodium, and from a consideration of the

[4] If the effective molecular weight of Na_2O be taken equal to its formula weight.

various likely instrumental errors, this value is estimated to have an absolute accuracy of ± 0.02 deg. Earlier measurements on another sample of sodium, using a less stable copper resistance thermometer, had similarly yielded $97.80 \pm 0.03°$ C (see footnote 2).

The differences among the three values of the second column of table 1 will now be examined. Unless the uranium in samples B and C was completely protected from the sodium by some insoluble surface film, the values for these two samples should be lower than that for sample A by amounts $(440x_1)$ corresponding to the solubility of uranium in liquid sodium at this temperature.[5] These differences, with their standard deviations, are as follows: For sample B, $440x_1 = -0.0009° \pm 0.0067°$; and for sample C, $440x_1 = -0.0003° \pm 0.0058°$. These differences are thus zero within the precision of their measurement. The probability that the real differences exceed 0.02 deg is very small. This figure would correspond to a value of x_1 of 5×10^{-5}, equivalent to 0.05 percent by weight of uranium dissolved in the liquid sodium if the dissolved uranium is monatomic. It is accordingly concluded from these measurements that the solubility of uranium in liquid sodium at 97.8° C probably lies between 0.00 and 0.05 percent.

It seems likely that a radioactive tracer method would furnish a more definite value for this solubility.

[5] It seems very unlikely that uranium is appreciably soluble in solid sodium.

This work was supported by the Atomic Energy Commission. The author thanks C. E. Weber, of the Knolls Atomic Power Laboratory, Schenectady, N. Y., for supplying the sealed samples, and D. C. Ginnings, of the Bureau, for advice in designing part of the apparatus.

Washington, December 31, 1953.

3. Low Temperature Calorimetry

Continuously Operating He^3 Refrigerator for Producing Temperatures down to $\frac{1}{4}$°K

E. Ambler and R. B. Dove
National Bureau of Standards, Washington 25, D. C.

(Received January 13, 1961)

A continuously acting, portable, He^3 refrigerator is described. The He^3 is recirculated in a system that operates without mechanical pumps. The throttling of the returning liquid is accomplished by means of a porous plug. Good regulation is obtained by using a system that allows the pressure across the porous plug to vary with the circulation rate. The lowest temperature reached while circulating is 0.26°K at zero "external" heat input, and 0.40°K at 2mw.

It is well known that the relatively high vapor pressure at any given temperature and absence of film flow in He^3 constitute considerable practical advantages over He^4 for producing very low temperatures by evaporation under reduced pressure. Although a lowest temperature[1,2] of 0.71°K has been reached with He^4, a more usual limit for convenient operation is in the range 1° to 0.8°K. With He^3, temperatures down to 0.35°K can be reached very easily, while a practical limit could be taken to be 0.25°K. A number of He^3 cryostats have been described,[3–6] most of which have been discussed and compared in a review article[7] on He^3. We wish to describe a cryostat in which the lowest temperature reached comes close to what might be considered a lower practical limit, and which can, with good temperature regulation, cope with rather large heat inputs. Novel features in the design consist of an automatic device for throttling the liquid He^3 returning to the evaporator, and the use of a mercury ejector pump (without mechanical backing pump) for circulating the He^3.

The cryostat was designed in connection with experimental work on nuclear reactions with oriented nuclei, and in this connection it is worth noting a fact that has been realized for some time, viz., that at the temperatures obtainable with a He^3 refrigerator a significant degree of nuclear orientation can be obtained with a number of nuclei (e.g., Ho, Tb, U, Np), without further cooling (i.e., by magnetic cooling). It was desirable that the refrigerator have the following features:

(a) It should be continuously operating; therefore, a refluxing system for the He^3 is used.

(b) It should be portable and self-contained in order to be movable from one particle accelerator to another.

(c) It should be fast, i.e., it should be possible to recycle from the lowest temperature to 1°K, or higher, quickly. In this way measurements can be done alternately with oriented and unoriented nuclei.

Before describing the apparatus, we should like to mention one fact that is of importance for the detailed design of targets refrigerated to such low temperatures in this way, viz., that allowance must be made not only for the relatively low thermal conductivity of liquid He^3, but also for the Kapitza thermal boundary resistance.[7] We shall discuss these points in a later paper on the detailed design of a scattering chamber. For the present we shall give details of the refrigerator only.

The cryostat is shown schematically in Fig. 1. The overall diameter of the cryostat, which is about 10 cm exclusive of helium and nitrogen Dewars, is determined by

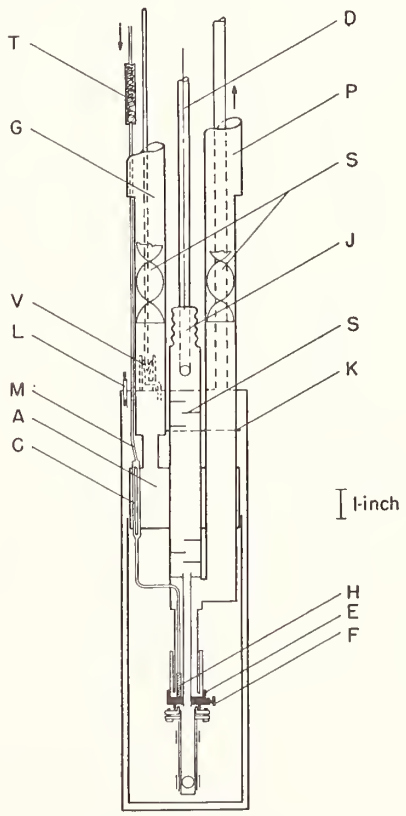

Fig. 1. Schematic diagram of the He^3 cryostat. The He^4 Dewar and nitrogen Dewar are not shown.

[1] W. H. Keesom, Communs. Kamerlingh Onnes Lab. Univ. Leiden No. 219(a), 1 (1932); Proc. Roy. Acad. (Amsterdam) **35**, 136 (1932).
[2] B. G. Lasarev and B. N. Eselson, J. Exptl. Theoret. Phys. U.S.S.R. **12**, 549 (1942).
[3] S. G. Sydoriak and T. R. Roberts, Phys. Rev. **106**, 175 (1957).
[4] G. Seidel and P. H. Keesom, Rev. Sci. Instr. **29**, 606 (1958).
[5] H. A. Reich and R. L. Garwin, Rev. Sci. Instr. **30**, 7 (1959).
[6] V. P. Peshkov, K. N. Zinov'eva, and A. I. Filimonov, J. Exptl. Theoret. Phys. U.S.S.R. **36**, 1034 (1959) [translation: Soviet Physics —JETP **9**, 734 (1959)].
[7] V. P. Peshkov and K. N. Zinov'eva, Repts. Progr. in Phys. **22**, 504 (1959).

the diameter of the pumping tubes required, i.e., 2 cm at liquid helium temperatures, 4 cm at liquid nitrogen temperatures, and 10 cm at room temperature. The over-all length of 100 cm is determined by the allowable evaporation rates of the refrigerant liquids. The He^4 Dewar has a capacity of about $1\frac{1}{2}$ liters, and starting from liquid nitrogen temperature, may be filled by taking $4\frac{1}{2}$ liters from the transport Dewar. The average evaporation rate allows an operational time of about 15 hr, although, of course, by repeated transfers the cryostat can operate indefinitely. A separately pumped He^4 space A, which is filled from the He^4 Dewar through a needle valve V, is incorporated to allow a low temperature to be reached (0.82°K) with smaller, more portable,[8] pumps than normally required when the helium Dewar is pumped directly. A lower temperature at A yields a smaller heat influx into the He^3 evaporator E, both through heat conduction and by the refluxing liquid He^3.

The vapor pressure of He^3 at the temperature of A is about 3 mm Hg, so that by placing there the He^3 condenser C, a system is obtained that will operate with a maximum pressure in the He^3 system slightly in excess of this. Thus the vapor is condensed from a pressure well below the backing pressure of many mercury ejector pumps, and a system can be constructed without using mechanical pumps of any kind. This gives a simple, quiet, fast system which can be made vacuum tight very easily, and which requires, furthermore, a minimal amount of He^3. No special measurement was made to see how little was needed for operation, although the 2 cm^3 of liquid He^3 available to us proved to be more than sufficient. Since most of this is used in filling the "dead volume" of the condenser and associated tubes, it is felt that by suitable minor modifications, it should be possible to operate with a significantly smaller amount of liquid He^3.

Although we should like to emphasize that the mercury ejector pump used[9] would have been adequate by itself, an oil diffusion pump with a nominal speed of 300 liters/sec was also incorporated in series. This enabled us to use a previous pumping and circulating system,[10] originally designed for use with another less suitable type of ejector pump. The oil pump was used without trap or baffle. Apart from liquid nitrogen cooled traps on both sides of the mercury pump and a very small trap T packed with copper wire and placed in the He^4 Dewar, no special cleaning of the He^3 is done.

[8] We used a Welch mechanical pump, type 1397, and a Consolidated oil diffusion pump, type MCF 300.

[9] We used an Edwards high vacuum pump, type 2M4

[10] Preliminary measurements show, however, that changing the temperature of the space A through the interval 0.8° to 1°K does not alter significantly the overall performance of the He^3 refrigerator. It appears, therefore, that both oil diffusion pumps, i.e., that used in pumping the He^3 and that used in pumping the He^4, may be omitted. This leaves an extremely simple and compact arrangement, involving only one mechanical pump for pumping the He^4, and one ejector pump for pumping the He^3.

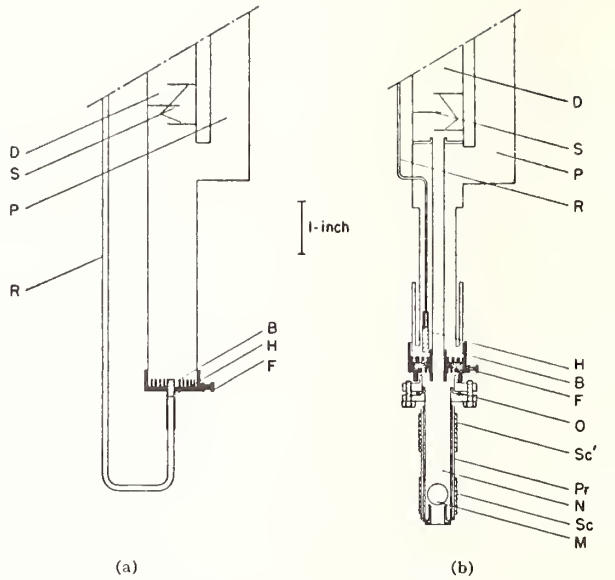

FIG. 2. Details of two different types of evaporator used in the He^3 cryostat.

The throttle H which allows the liquid He^3 to expand into the evaporator consists of a plug of porous stainless steel.[11] The plug is swaged inside a copper tube which is in turn connected thermally to the evaporator [see Fig. 2(a)]. The pressure across the plug adjusts automatically to the circulation rate, by a rise in the discharge pressure of the ejector pump. With this arrangement there is no possibility of troublesome vapor locks forming on the one hand; and on the other hand, regulation is achieved with quite a small net change of liquid He^3 in the evaporator. The minimum pressure across the throttle is approximately equal to the vapor pressure at 0.82°K, i.e., about 3 mm Hg, and the maximum pressure is equal to the largest tolerable discharge pressure of the ejector pump ($\simeq$35 mm Hg). The maximum heat input (2mw) at which the refrigerator will operate at present is governed by the pressure, at the discharge side of the ejector pump, rising above this value. At this heat input, the circulation rate is about the maximum that can be carried by the pumps.

The use of a storage container with a large volume enables the He^3 gas to be stored very simply after the experiment at the discharge pressure of the ejector pump. Other components shown in Fig. 1 are the tube G, for pumping the He^4 bath, the tube P, for pumping the He^3 bath, and the tube D, for measuring the He^3 vapor pressure. S's are radiation baffles, L is a platinum to soft glass seal for bringing electrical leads into the vacuum case, and J is a fitting that may be interchanged, as required, for the performance of different experiments. The copper link K connects thermally all tubes in the vacuum case to the

[11] We found that a cylinder, $\frac{3}{8}$ in. long, $\frac{1}{8}$ in. diam., of Micrometallic Corporation, type H porous stainless steel to be suitable.

He^4 pumping tube in such a way that maximum use[12] is made of the latent heat in the He^4 film creeping up G. The volume available for experiments at He^3 temperatures is about 500 cm^3 with the present arrangement.

Measurements have been made with two types of evaporator shown in detail in Fig. 2(a) and (b). The temperature was determined by means of the He^3 vapor pressure[3] transmitted on a static line (0.386 cm radius) and measured on a McLeod gauge. Corrections were applied for thermomolecular pressure.[13] An electrical resistance F is used to provide a heat input, when required, and is used both to check the performance of the refrigerator and to recycle the temperature rapidly by evaporating off the liquid He^3. Copper fins B are included to give a large surface area for heat transfer.

The results obtained with the apparatus shown in Fig. 2(a) are given in Fig. 3, where we have plotted vapor pressure and temperature against the heat dissipated in F. We should point out that the pressure at the intake of the He^3 pump remained low throughout the run so that the pressure given in Fig. 3 is for all practical purposes the pressure drop down the pumping tube.

The lowest temperature reached was computed to be 0.26°K. Since the thermomolecular pressure corrections at these temperatures were very large, it was decided to verify these measurements by using a magnetic thermometer, calibrated only at the higher and more certainly established temperatures. In order to do this it was necessary, for practical reasons, to alter the apparatus to the form shown in Fig. 2(b). The vapor pressure bulb N is sealed with a gold O-ring O, and contains a $\frac{1}{2}$ in. diam sphere of chromic methylammonium alum M. The change in susceptibility of the salt was determined ballistically, using a niobium primary Pr, and copper secondary Sc, with compensator Sc′ wound around N. From the vapor pressure measurements we computed the temperature as before, and plotted the reciprocal against the ballistic throw δ in Fig. 4. Since it is known that the susceptibility of the salt shows little deviation from Curie's Law in this temperature range, this plot should give a straight line. It can be seen that this is so except for the points at the lowest temperatures, where there appears to be a small deviation. This deviation is thought to arise through the evaporator being at a temperature slightly lower than the salt space, and the vapor pressure indicated of course being that of the coldest part of the system, viz., the evaporator. On assuming this to be the correct explanation, we can conclude from Fig. 4 that the salt cools to nearly 0.27°K and the evaporator to 0.26°K; the latter figure is in good agreement with the measurement using the evaporator shown in Fig. 2(a).

Finally we should point out that an important advantage of an arrangement of the type shown in Fig. 2(b) over that shown in Fig. 2(a) lies in the fact that in the former case a completely enclosed He^3 system can be built, which need not be broken into on changing specimens or setting up a different kind of experiment.

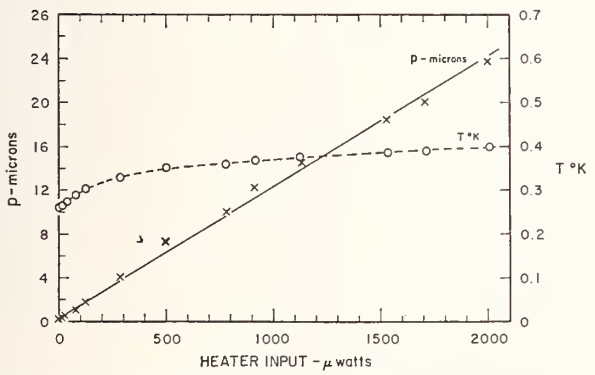

FIG. 3. Performance of the He^3 cryostat using evaporator shown in Fig. 2(a). The abscissa is the heat input, the right-hand scale of the ordinate refers to the temperature reached, and the left-hand scale to the pressure in the evaporator.

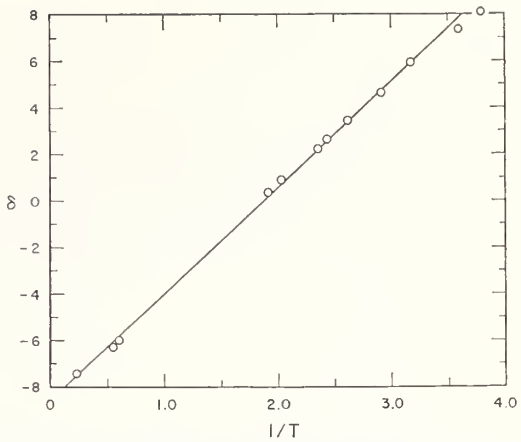

FIG. 4. Throw of ballistic galvanometer δ against $1/T$, where T is the temperature determined from vapor pressure measurements, obtained using the apparatus shown in Fig. 2(b).

[12] E. Ambler and N. Kurti, Phil. Mag. **43**, 1307 (1952).
[13] T. R. Roberts and S. G. Sydoriak, Phys. Rev. **102**, 304 (1956).

Reprinted from THE REVIEW OF SCIENTIFIC INSTRUMENTS, Vol. 32, No. 6, 737–739, June, 1961

JOURNAL OF RESEARCH of the National Bureau of Research—Engineering and Instrumentation
Vol. 65C, No. 4, October–December 1961

Apparatus for Determination of Pressure-Density-Temperature Relations and Specific Heats of Hydrogen to 350 Atmospheres at Temperatures Above 14 °K*

Robert D. Goodwin

(June 20, 1961)

Method and apparatus are designed for more rapid determination of accurate, closely-spaced, PVT and specific heat data than realized by previous procedures. A sequence of pressure-temperature observations at nearly constant density is made by a modified Reichsanstalt method. Temperatures of the essentially adiabatic piezometer are regulated by electric heating under control of the measuring thermometer. Instruments for measurement and control are integrated with a high-pressure calorimeter for compressed liquid and fluid. Calorimetric experimentation is accelerated by use of an electronic battery for the calorimetric heat supply and of a d-c power regulator developed for automatic shield control. Details are given of the PVT calibrations, adjustment computations, and comparisons with independent data.

1. Introduction

The high-density physical properties of hydrogen are needed for technological applications [5, 10]. Thermodynamic functions may be computed from certain thermal data combined with a wide range of precise mechanical properties (PVT) and vapor-pressure data [1, 2, 3, 9]. The purpose of this paper is to describe the essential features of apparatus used to obtain PVT data for parahydrogen from 16 to 100 °K and from 2 to 350 atm, and to obtain specific heats of compressed liquid and fluid in the same range. Advent of high-speed digital computers renders practical the handling of a large quantity of data, produced by closely-spaced observations with accelerated methods to be described.

2. Experimental PVT Method

The PVT method and its numerous calibrations are emphasized in preference to the better-known calorimetric techniques, outlined below. The popular Burnett method for PVT determinations [17] is not suitable for compressed liquids [9]. That of Holborn and coworkers [20, 21, 22], termed the Reichsanstalt method [2], involves essentially direct measurement of each variable. As employed by Michels and coworkers, a sample of fluid of known PVT behavior at normal temperature is confined in the piezometer and pressure gage system at that temperature. Pressure of the sample then decreases rapidly with temperature of the piezometer [25]. In the Ohio State University modification for gaseous states, adjustments for obnoxious volumes of capillary and gage were eliminated by placing a valve in the cryostat. This necessitated an independent determination of the amount of sample following every P–T determination [24]. For liquid states they employed a boiling hydrogen thermostat. Successive small portions of the sample were released from the piezometer or "pipet" to obtain a series of isothermal P–v determinations from a given filling, each P–v point again requiring an independent volumetric determination [23].

Average time per determination is greatly reduced in the present method. Temperature of the nearly adiabatic pipet is varied to obtain a series of P–T determinations at nearly constant density. Temperatures are automatically controlled at exact, integral values, to permit handling the data as isotherms. Only one determination of the amount of sample is required following each experimental "pseudo-isochore". The portion of the total sample which was in the pipet during each P–T determination is calculated by subtracting the computed amounts residing simultaneously in capillary and diaphragm cell under those conditions. For this small adjustment, the known and estimated PVT behavior of normal hydrogen is employed.

With reference to figure 1, a sample of the experimental fluid is confined by valve C–4 to the following system: the heavy-walled copper pipet, the stainless "transition" capillary tube in the cryostat, the capillary tubes and valves at room temperature, and the pressure-sensitive diaphragm cell (N. P. D.). Volumes of these elements are calibrated independently. The latter transmits pressure of the fluid to the oil of a piston-type, deadweight gage. With reference to figure 2, liquid hydrogen refrigerant resides in the tank. The pipet is cooled strongly as required by liquid hydrogen reflux action from hydrogen gas introduced to the thin-walled, stainless steel "reflux" tube supporting the pipet. For automatic temperature regulation by electric heating, under control of

*Contribution from the Cryogenics Engineering Laboratory, National Bureau of Standards, Boulder, Colo.

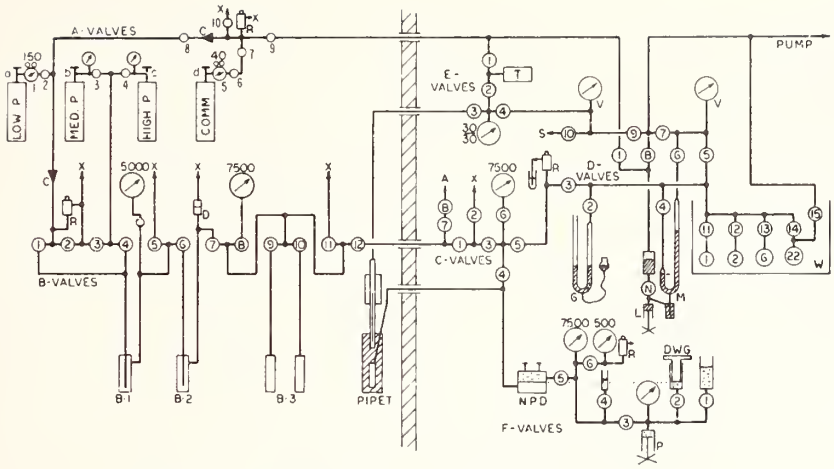

FIGURE 1. *Pneumatic apparatus for PVT determinations.*

A, Connection to thermal conductivity analyzer.
B–1, Absorbent bomb at 76 °K.
B–2, Iron-oxide, ortho-para catalyst bomb at 19.6 °K.
B–3, Thermal pump bombs.
C, Check valves
COMM., Commercial hydrogen.
D, Bursting disk.
DWG, Dead weight gage.
G, Gas buret.
L, Mercury leveling screw.
M, Precision manometer.
NPD, Null pressure detector.
P, Oil press.
R, Relief valves.
S, Sampling connection.
T, Reflux gas dose tank.
V, Philips vacuum gauges.
W, Water-bath thermostat.
X, Exterior vent lines.

the platinum resistance measuring thermometer, gas pressure in the reflux tube is reduced to provide controlled cooling by gas convection, aided by a copper rod suspended in this tube.

An experimental run consists of measurement of a sequence of pressure versus temperature points, beginning at the lowest temperature. The total quantity of confined fluid then is determined by releasing it as gas into volumetric system *D* of figure 1 and measuring P, V, and T at about normal conditions, accounting also for the gas remaining in all obnoxious volumes and in the pipet at this pressure. Experimental time required for filling and emptying the pipet is greatly reduced through capability of the commercial, null-pressure diaphragm instrument to withstand high-pressure imbalance without damage. About 30 points on a pseudo-isochore are determined routinely in 8 hr by 2 or 3 men.

3. Sample Preparation, Handling, and Analysis

By mass-spectral analysis, electrolytic hydrogen in clean steel cylinders at 2,000 psig contains less than 5 ppm helium and 100 ppm air, respectively. The preparation system on the left of figure 1 has three functions. Impurities are absorbed at 76 °K in B–1 on 20 ml of 1.6 mm diam extrusions of "molecular sieve" silica [71]. The paramodification of hydrogen is produced catalytically in B–2 at 19.6 °K on 10 ml of "30–100 mesh" particles of an iron oxide, batch 48–C, used in activity studies [72]. Small disks of sintered stainless steel retain the fine solids in their containers. Two stainless steel bombs, B–3, each of about 20 ml capacity, may be immersed in liquid nitrogen to provide a two-stage, thermal pump for boosting the parahydrogen pressure. Solidification of hydrogen at the catalyst is avoided by placing the catalyst ahead of these pumps in the train. The hydrogen cylinders, preparation system, liquid hydrogen transport Dewar, cryostats and vacuum pumps are separated from the instrument room by an explosion-proof wall. Valve manifold C in the instrument room uses a bourdon gage as a doser for filling the pipet to selected densities and for controlling release of the pipet sample to the gasometer system *D*.

Systems B and C of figure 1 are assembled with $\frac{1}{16}$-in. o. d. stainless steel tubing and high-pressure midget valves with solid stems and polytetrafluoroethylene O-ring packings. Shop-fabricated gage connectors force a small, drilled, metal cone against a conical recess on the gage stem. This special fitting is necessary to avoid contamination of the gas. Bourdon gages for hydrogen must be phosphor-bronze, beryllium-copper, or type 316 stainless steel [75].

Analysis for parahydrogen is performed on gas bled from valve C–8 at 100 ml NTP/min through a thermal conductivity instrument [58]. Calibration depends upon parahydrogen produced independently. In preliminary studies the rate of conversion of para- to orthohydrogen in the pipet at pressures up to 4,500 psi was in the order of one percent per day at 76 °K and 25 to 30 percent per day at 275 to 300 °K. The vapor pressure of parahydrogen was measured at the beginning of a number of PVT runs [66]. Following one of the routine, 8-hr PVT determinations, the presence of parahydrogen again was confirmed by a vapor pressure measurement.

4. Cryostat and Piezometer

Descriptions and summaries of low temperature techniques are available [11, 12, 13, 14, 38, 46].

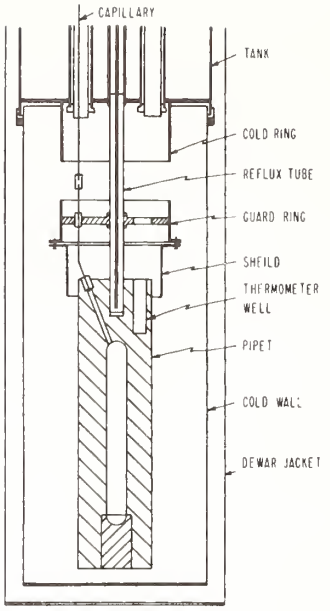

FIGURE 2. *Piezometer region of PVT cryostat.*
(Shield is misspelled in the above figure.)

Figure 2 shows a cross section of the lower portion of the cryostat. A 25-ml pipet sample cavity, 5/8-in. diam, is bored into a two-in. diam, solid copper cylinder 8.5-in. long. To avoid oxidation, the plug is brazed with helium in the cavity. Metal stress is about one half the internal pressure. Helical grooves on the cylinder carry a 32-gage, 500 Ω constantan wire heater. The platinum thermometer is tinned and cast into the pipet with Rose's alloy. Above the pipet on the supporting, thin-walled, stainless steel tube, a guard ring thermally tempers electric wires leading to and wound on the pipet; the ring is automatically controlled at pipet temperature by a gold-cobalt versus copper thermocouple [40, 44] and a 36-gage, 100 Ω constantan wire heater. A cold ring, integral with the refrigerant tank, tempers electric wires entering from room temperature. Before it was mounted and wound in the cryostat, the bundle of 36-gage, low-level wires was constructed as a unit with all wires lightly varnished together parallel in a plane to insure good thermal contact on the rings. The levels of cooling through the reflux tube which do not disturb the temperature-versus-pressure relationships are determined experimentally. About 10 milliwatts cooling normally is used.

An evacuable copper can, soldered to the tank with Rose's alloy, encloses the pipet. A Dewar vacuum jacket immersed in an open Dewar of liquid nitrogen protects the can and the tank. A permanent liquid hydrogen transfer line with built-in valves enters the cryostat refrigerant tank through an O-ring seal, with the amount of refrigerant in the tank shown by an electronic level-indicator instrument. Suitable valves and safety devices on the vent from the tank permit the use of a rotary oil pump to attain the triple-point temperature of the refrigerant.

5. Measurement of Sample Volume

5.1. Normal Pipet Volume

This volume is required for computation of density. By ignoring the adjustments contained in eqs (10.1–1) and (10.3–1) there is obtained the rough approximation for sample density,

$$\sigma \approx (P_m/RT_b)(V_g/V_o), \qquad (5.1\text{–}1)$$

where P_m, T_b and V_g refer to the gasometry system and V_o is pipet volume. Whereas the ratio V_g/V_o dominates the computation of eq (10.3–1), it is a practical convenience to perform absolute calibrations.

The pressure and temperature-dependent volume of the pipet is required. Connection to the pipet cavity is made with a 3-in. length of 0.35 mm stainless capillary brazed to the pipet drill hole, figure 2. The pipet was briefly tested to 8,000 psi. A midget valve was attached to the capillary, the pipet evacuated, and freshly boiled water admitted to the pipet. The three determinations yielded an adjusted volume of 25.83 ± 0.016 cm^3 at 25 °C. Volume at room temperature after mounting in the cryostat was determined by expanding hydrogen from the pipet at about 1,000 psi into the gasometer system of section 6. Seven determinations yielded adjusted volume 25.854 ± 0.037 cm^3 at 25 °C. Following two series of high-density experiments for PVT data to 5,400 psi, low-density experimental results violated general, low-density, limiting gas behavior. Six redeterminations of pipet volume by gas expansion yielded normal volume 25.913 ± 0.009 cm^3 relative to the gasometer volumes, in agreement with deductions from low-density behavior. The first series of PVT experiments is rejected, and the increase of molal volume by factor 1.00263 is applied to all other data. The annealed pipet is thus assumed to have deformed in use. With this correction, the estimate of error in normal pipet volume is 0.5 parts per thousand.

5.2. Elastic Stretching of Pipet

Circumferential and longitudinal stresses in a closed-end cylinder are, respectively,

$$S_c = kP/(R-1) \text{ and } S_l = P/(R^2-1), \qquad (5.2\text{–}1)$$

where P is excess internal pressure, R is the ratio of external to internal diameters, and k incorporates both end-effects and relative behavior of thick walls. With modulus of elasticity E, relative diameters, lengths, and volumes are, respectively,

$$D/D_o = 1 + kP/E(R-1) \qquad (5.2\text{–}2)$$

$$L/L_o = 1 + P/E(R^2-1) \qquad (5.2\text{–}3)$$

$$V/V_o - 1 = (P/E)[(R^2-1)^{-1} + 2k(R-1)^{-1}]. \qquad (5.2\text{–}4)$$

The temperature-dependence of E from [73] in T °K is

$$E=1.15\cdot 10^{6}[1-4.35\cdot 10^{-4}T],\ \text{atm}, \quad (5.2\text{–}5)$$

and the behavior of k by comparison with [70, 74, 79] is

$$k=a(R-1)[(R^{2}+1)/(R^{2}-1)+m]=1.11 \quad (5.2\text{–}6)$$

by introducing $R=3.2$, $a=1/3$ for end-effect and $m=0.3$ for Poisson's ratio. Within the accuracy of above estimates, therefore,

$$\lambda\equiv V/V_{o}=1+1\cdot 10^{-6}[1+4.35\cdot 10^{-4}T]\cdot P_{\text{atm.}} \quad (5.2\text{–}7)$$

5.3. Thermal Contraction of Pipet

Thermal expansivity of copper [78] in the form $a\equiv(L_{o}-L)/L_{o}$ as a function of temperature is used to compute a table of V/V_{o} versus temperature. For use with computing machines, this is fitted by a quadratic polynomial on the Kelvin temperature scale,

$$V/V_{o}=a+bT+cT^{2},$$

$$V_{o}=25.913\ \text{cm}^{3};\ a=0.990069;\ b=1.667\cdot 10^{-6};$$

$$c=1.317\cdot 10^{-7}. \quad (5.3\text{–}1)$$

6. Measurement of Amount of Sample

6.1. The Gasometer

The fluid contained in the pipet, the capillary, and the diaphragm cell is released into the gasometer system D (fig. 1). This is a set of spherical glass standard volumes in a precision water-bath thermostat, and a valve manifold with precision mercury manometer [48] in a circulating-air cabinet. Elevation of each arm of the leveled manometer is read to ±0.05 mm by a highly reproducible lightbeam and photocell arrangement. A standard volume is selected such that the pressure is in the upper range of the manometer; i.e., 500 mm or greater. The instrument room temperature is controlled to about ±0.5 °C. To compromise between low obnoxious volumes and adequate pumping speeds, the manifolds are ¼-in. copper tubing of 0.19-in. diam bore. For leak-free behavior, bellows-sealed valve seats and gaskets are a plasticized vinyl chloride polymer. Bellows volume increase per single turn is 0.15 cm³. This adds to standard volumes of 10 liters or more used for most determinations. Ionization gages serve for vacuum leak testing.

6.2. Gasometer Calibration

Volumes of the 1- and 2-liter spherical glass flasks are determined by weighing them with water on a 3-kg analytical balance against class Q weights. The 6-liter flask is weighed on a 20-kg single-beam platform balance against calibrated weight slugs. Adjustment is made for air buoyancy, water density, and thermal expansion of the borosilicate glass [76]. Volumes at 300 °K are given by the second column of table 1.

TABLE 1. *Calibration of gasometer flask volumes*

Nominal volume	Water weighing	Gas expansion	Assigned
	ml	*ml*	*ml*
1 L	994.48	(994.48)	994.11
2 L	2,036.35	2,037.5±0.7	2,036.7
6 L	6,429.1	6,427±3.0	6,427
22 L		21,226±3.0	21,226
Ratio, 2 L/1L	2.0477	2.0488	

After determination of all manifold volumes including the manometer, the 2-liter flask is calibrated by gas expansion relative to the 1-liter flask; each successive flask then is calibrated relative to the sum of all smaller flasks. With all adjustments the results shown in the third column are obtained. Absolute volume standard is selected as the sum of volumes of the 1- and 2-liter flasks by water weighing, and the ratio of these two volumes by gas expansion is selected for assigning the values shown in the last column. Pressure-dependence of the flask volumes was computed from physical dimensions and mass of the individual flasks and the modulus of elasticity [76]. The nearly uniform results were confirmed experimentally upon a flask filled with water extending into a capillary neck,

$$(1/V)(dV/dP)=1\cdot 10^{-4}\ \text{atm}^{-1}. \quad (6.2\text{–}1)$$

6.3. Adjustment for Capillary and Cell

The amount of sample in the pipet is the total amount behind valve 4 of figure 1, determined by gasometry, less amounts in capillaries and in the diaphragm cell under conditions of measurement for each P–T point. The rapid experimental method is justified provided these latter amounts can be estimated with sufficient accuracy. This is attained with a diaphragm cell volume which is small relative to the pipet, and by utilizing known and estimated gas-imperfection behavior of normal hydrogen.

A volume of 0.655 cm³ for capillary tubing and diaphragm-cell exterior to the top of the cryostat and up to the pipet valve C–4 is obtained by weighing mercury out of the tubing and by finding differences with suitable gas-expansion methods. The quantity of hydrogen in these obnoxious volumes is computed from their temperatures, the pressure, and the compressibility factor for normal hydrogen [65].

The volume of the 71-cm-long, transition capillary from the top of the cryostat to the guard ring is $V_{c}=0.0672$ cm³, or 0.26 percent of pipet volume. The amount of fluid in the capillary is computed by calculating the temperature T_{z}, corresponding to any position at a fraction x of capillary length from the ring at pipet temperature T_{o} to the top of the cryostat at room temperature T_{1}, from thermal conductivity K of stainless steel [77] by the relation,

$$x=\left[\int_o^{T_x} KdT-\int_o^{T_o} KdT\right]\cdot\left[\int_o^{T_1} KdT-\int_o^{T_o} KdT\right]^{-1} \tag{6.3-1}$$

The number of gram moles of fluid in the capillary is

$$N_c=(PV_c/RT_o)\theta \tag{6.3-2}$$

where

$$\theta\equiv T_o\int_o^1 dx/T_xZ_x. \tag{6.3-3}$$

Indices o refer to the ring or pipet, x to relative position along the capillary, and $Z\equiv Pv/RT$ where v=molal volume. By known [23, 64, 68, 69] and extrapolated [3] data for Z, the capillary factor θ for hydrogen is determined at a sufficient number of sensitive points for smoothing, taking note of liquid-vapor discontinuities; results are summarized by figure 3. The ratio of amount of fluid in the transition capillary to amount in the pipet is necessary for an estimate of required accuracy. This ratio is $(V_c/V_o)\cdot\phi$, where $\phi\equiv Z_o\theta$ is summarized by figure 4. Due to the small value of V_c/V_o, a ten percent error in ϕ would correspond to a relative error well under 0.03 percent in density of the pipet sample at temperatures $\leq$100 °K.

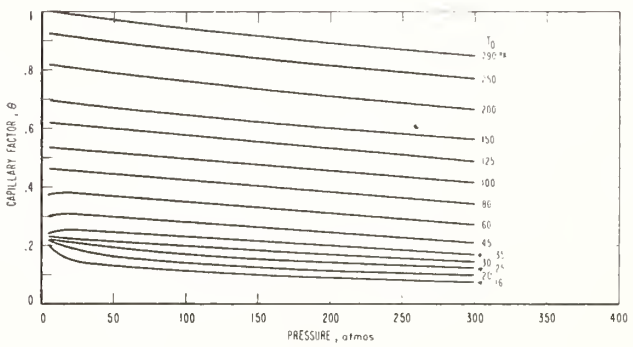

FIGURE 3. *Capillary factor, θ.*

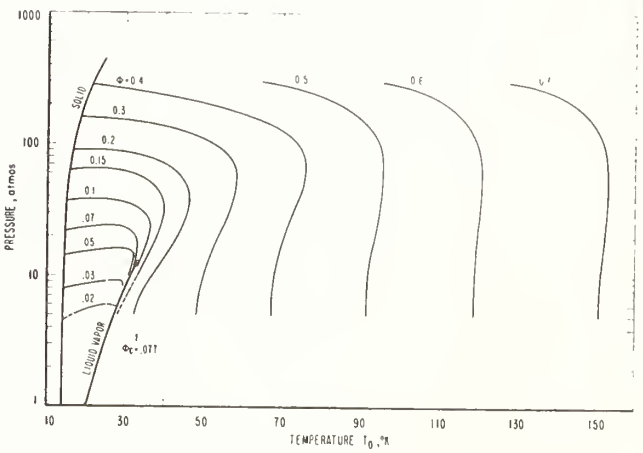

FIGURE 4. *Capillary relative content, ϕ_c.*

7. Measurement of Pressure

7.1. Piston Gage and Diaphragm Cell

The commercial, dual-range, precision, dead-weight gage and null-detector operate in the oil-filled F-manifold, figure 1 [52, 53, 57, 59]. The diaphragm, with adjustable electric contacts to indicate null position, is centered by use of an open-tube manometer. The oil pressure is adjusted to the experimental gas pressure with the screw-type oil press P. Prior to placing weights on the piston gage, the approximate pressure is read from bourdon gages.

Piston diameters of about 0.182 and 0.407 in. are measured with a light-wave micrometer to $\pm$5 millionths of an inch. Tolerance on the weights, determined by comparison with class S standards [54], decreases from 0.05 percent on the 1 psi weight to 0.002 percent on the 1000 psi weights. Adjustments to gage readings are made for temperature, pressure, acceleration of gravity, and barometric pressure. Observed sensitivity of pressure measurement with the small piston varies from under $\pm$0.05 psi below 500 psi to under $\pm$0.5 psi at 5000 psi.

As compared with known diaphragm-detectors [49, 61], the commercial instrument used here withstands extreme pressure imbalance without damage, but exhibits temporary hysteresis effects up to about $\pm$0.05 psi. A measured shift of null-point with absolute pressure is applie l by the relation

$$P_{\text{gas}}=P_{\text{barom}}+(1.00002)P_{\text{oil}}. \tag{7.1-1}$$

Table 2 summarizes estimates of accumulated errors at different pressures.

TABLE 2. *Estimates of accumulated pressure errors*

Gage pressure, atm	2	20	200
	Error, atm×10³		
Barometer	0.50	0.50	0.50
Diaphragm cell	4.00	4.00	4.00
Piston-cylinder diameter	0.06	0.60	6.00
Calibration of weights	.67	1.52	4.07
	5.23	6.62	14.57
Relative error $(\delta P/P)\cdot 10^3$	2.6	0.33	0.073

Thermal equilibrium of the fluid sample, following a step-increase of temperature, is found by pressure observations to be established nearly as rapidly as the heating rate of the massive pipet. Occasional pressure balances are taken an hour apart to confirm this inference from the steady behavior of single observations.

7.2. Adjustment for Capillary Column

The column of cold fluid standing in the transition capillary tube produces an additional pressure P_c at the pipet,

$$P_c/P=JML_c\theta/RT_0$$

using symbols of section 6.3, pressure conversion factor J, molecular weight M, and capillary length L_c=71 cm. Since JML_c/R=1.68 · 10^{-3} °K for hydrogen, the adjustment for capillary column pressure is negligible.

8. Measurement of Temperature

8.1. Method and Instruments

The potentiometric method of figure 5 is employed with a 25-ohm platinum resistance thermometer calibrated by the NBS Temperature Physics section and a six-dial microvolt potentiometer [41, 42, 46]. The low-impedance, unsaturated standard cells are protected from occasional extreme temperatures of the laboratory by two concentric boxes of 1/2-in. aluminum in a plywood case [43]. The upper potentiometer current supply is stabilized by placing a lead-acid battery across an isolated, rectified, and filtered a-c source [60]. A 25-v, 200 amp-hr, thermally insulated and shielded battery, of a similar, low internal-discharging type, supplies the stable thermometer currents which flow in the calibrated precision standard resistors. The microvolt switch is wired so that the thermometer potential connections to the potentiometer can be reversed when the thermometer current is reversed. Microvolt galvanometer amplifiers with floating input circuits are coupled to 50-μa panel galvanometers in suitable damping and range-changing circuits. To minimize spurious effects in the thermometer and thermocouple potential circuits, the continuous copper wires from the pipet in the cryostat are joined by a special solder [45] to untinned, copper cable wires near the cryostat on copper lugs in an iron-shielded, heavy aluminum box. The cryostat wires and shielded cables run in iron conduits. The cryostat and all electrical instruments are interconnected and grounded to the earth with heavy copper conductors.

8.2. Procedure and Calibration

When the instrument room air conditioner is started, spurious potentials up to ±0.1 microvolt arise in the galvanometer circuit. These potentials are observed by use of an internally-shorted emf position on the potentiometer and are bucked out at the galvanometer amplifier. When the cryostat is cooled with liquid hydrogen, a 0.35-μv spurious potential, which is nearly independent of pipet temperatures up to 40 °K and increases with higher temperatures, appears across the thermometer potential leads in the absence of thermometer current. Potential measurements with reversed thermometer currents show the effect to be independent of current.

Thermometer currents are adjusted to exact integral milliampere values. To a corresponding, tabulated, thermometer potential is added the spurious thermometer potential to obtain a potentiometer dial setting yielding an automatically-controlled, integral-valued temperature. A thermometer current of 5 ma is used at temperatures below 35 °K; 2 ma, from 35 to 75 °K; and 1 ma, at 75° and above. Thermometer heating by the 5 ma current produces an error of 0.0007 °K at 40 °K. All measurements occur in the low range of the potentiometer.

The specified error limit of the potentiometer low range is 0.01 percent of reading plus 0.02-μv. The calibrated value of the 1-ohm standard resistor is 0.99999±0.00001 ohms. Apparently satisfactory agreement was found between the platinum thermometer calibration tables and measurements with above procedures for the ice-point and for vapor pressures of high-purity nitrogen and of parahydrogen, as described in section 11.

The accuracy of temperature measurements is summarized by table 3. It is based on the thermometer characteristic and currents, the potentiometer specifications, and a latitude of 0.05 μv for bucking out spurious potentials. Thermometer calibration uncertainties are not included.

TABLE 3. *Estimates of accumulated temperature errors*

T, °K	Thermometer			Potentiometer error, μv	Errors, δT, °K · 10^3		δT/T, ×10^6
	i, ma	R, Ω	dR/dT		Potentiometer	External ±0.05 μv	
15	5	0.049	0.0074	0.045	1.22	1.35	170
20	5	.112	.017	.076	0.89	0.58	74
40	2	1.07	.075	.234	.62	.13	19
76	1	4.65	.109	.485	.89	.09	13
100	1	7.25	.109	.745	1.37	.09	15

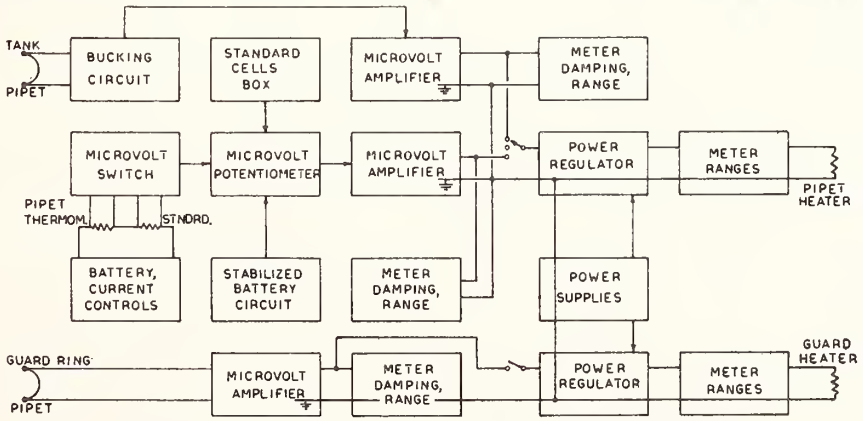

FIGURE 5. *Temperature measurement and control methods.*

9. Regulation of Temperature

Precisely controlled electric heating compensates for crudely adjusted, spontaneous cooling (section 4). The pipet temperature can be controlled [29] from a thermocouple, relative to the temperature of the refrigerant tank (upper left of figure 6), by a wide range microvolt bucking circuit, a microvolt amplifier [56] and a d-c power-regulator [50]. For all PVT measurements the pipet temperature is controlled from the platinum resistance thermometer and potentiometer. There is no perceptible noise at 0.0002 °K sensitivity. The accuracy of controlled temperature is equivalent to the described accuracy of measurement. To maintain a steady temperature during other operations with the potentiometer, the power regulator input signal switch is opened and the steady-state heating carefully adjusted by the power regulator control before undertaking such operations. If required, the above thermocouple control can be used. The guard ring temperature is controlled with similar instruments.

10. Computation of PVT Observations

10.1. Gasometry

The number, N, of gram moles of hydrogen contained behind pipet valve C–4 is calculated by the relation,

$$RN/P_m=[(EV_g+V_w)/T_w+V_a/T_a+V_b/T_b]/Z_{w,m}+V_o/T_oZ_{o,m}, \quad (10.1\text{–}1)$$

where P_m is mercury manometer pressure in atmospheres,

R=82.057 cm³ atm/g mol deg K,

$$P_m=KgDL_m, \quad (10.1\text{–}2)$$

K=0.986923.10^{-6} atm cm²/dyne [4],

g=979.615 dyne/gram in this laboratory room,

$$D=13.5948-0.00245 \cdot t_m,\ g/\text{cm}^3\ [4], \quad (10.1\text{–}3)$$

t_m=manometer mercury temperature, °C,

L_m=manometer mercury height, cm (brass scale),

$$E=\text{glass volume/pressure coefficient}=1+10^{-4}(P_m-0.825), \quad (10.1\text{–}4)$$

T_a=air-bath manifold temp, °K,

T_b=NPD temp, °K,

T_o=pipet temp, °K,

T_w=water-bath temp, °K,

V_a=vol of air-bathed manifold and manometer, 59.66 cm³,

V_b=vol of lines, gasometer to C-valves, including gage, 22.37 cm³,

V_g=vol of glass bulbs used, cm³,

V_w=vol of water-bath manifold, 13.00 cm³,

V_o=vol of pipet, cm³,

$$V_o/T_o=25.913[0.990069/T_o+1.667.10^{-6}+1.317.10^{-7} \cdot T_o], \quad (10.1\text{–}5)$$

$$Z_{w,m}\ (\text{at } T_w \text{ and } P_m)=1.000044+0.000555P_m, \quad (10.1\text{–}6)$$

$$Z_{o,m}\ (\text{at } T_o \text{ and } P_m)=1.0007-1055/T_o^3 \text{ for } T_o \geq 40\ °\text{K}. \quad (10.1\text{–}7)$$

10.2. Pressure

The pipet fluid pressure P in international atmospheres is

$$P=0.0680457P_g+P_b \quad (10.2\text{–}1)$$

where

P_g=deadweight oil gage pressure in psig,

P_b=barometric pressure in atm,

$$P_g=k(g/g_s)[1-2.4 \cdot 10^{-5}(t_g-20\ °\text{C})]\ [1+4.2 \cdot 10^{-8}P_g] \cdot [\text{Nominal wt psi}]. \quad (10.2\text{–}2)$$

k=1.00002, eq (7.1–1),

(g/g_s)=979.615/980.665,

t_g=deadweight gage temperature, °C,

$$P_b=KgD \cdot L_b \text{ as in eq (10.1–2)}, \quad (10.2\text{–}3)$$

L_b=barometer height, cm,

t_b=barometer temp, °C.

10.3. Density

Density, σ, g moles cm³, is calculated by

$$\sigma V_o=N-(P/R)[V_c\theta/T_o+V_d/Z_dT_d] \quad (10.3\text{–}1)$$

where

T_d=temperature NPD, °K,

T_o=pipet temperature, °K,

$$V_o=25.913\ \lambda[0.990069+1.667 \cdot 10^{-6}T_o+1.317 \cdot 10^{-7}T_o^2], \quad (10.3\text{–}2)$$

V_c=0.0672 cm³,

V_d, volume of NPD and warm capillary=0.655 cm³,

Z_d, for gas at P and room temperature in V_d is

$$Z_d=0.99990+0.000623447\ P, \quad (10.3\text{–}3)$$

λ, eq (5.2–7),

θ, eq (6.3–3) and figure 3.

11. Checks on PVT Calibrations

11.1. Thermometry Fixed Points

Vapor pressures of a commercial, high-purity nitrogen and of parahydrogen were measured prior to the PVT experiments. Examination of experimental technique later revealed failure to compensate some of the spurious potentials. Determination of these potentials provided adjustments, estimated accurate within 0.005 °C, which have been applied in preparing table 4.

TABLE 4. *Thermometry fixed point observations**

P, mm [a]	T_{obs}	T_{lit}	ΔT
Vapor pressure of nitrogen [b]			
625.05	75.732	75.730	−0.002
625.42	75.741	75.735	−0.006
626.03	75.744	75.743	+0.001
631.75	75.825	75.816	+0.009
631.68	75.826	75.815	+0.011
Vapor pressure of parahydrogen [c]			
626.33	19.639	19.632	+0.007
626.72	19.645	19.634	+0.011
626.90	19.650	19.635	+0.015
628.18	19.656	19.642	+0.014
629.12	19.656	19.646	+0.010

*All temperatures in deg K on NBS 1955 scale.
[a] Mercury column height reduced to 0 °C at standard gravity.
[b] G. T. Armstrong, 1954.
[c] Hoge and Arnold, 1951.

11.2. Elevated Vapor Pressures

Initial PVT points of several runs were taken at saturation conditions to check instrumentation. If the substance is nearly pure parahydrogen, the observed pressure-temperature relations should agree with those of Hoge and Arnold. Table 5 presents

TABLE 5. *Elevated vapor-pressures observations*

P_{obs}, atm			Data from Hoge and Arnold [a]	
T °K	II	III	P, atm	dP/dT
22	----------	1.612	1.614	0.417
23	----------	2.069	2.071	.498
24	----------	----------	2.614	.587
25	----------	3.246	3.249	.685
26	3.978	3.983	3.985	.790
27	4.832	4.829	4.832	.904
28	5.785	5.792	5.795	1.026
29	----------	6.886	6.889	1.162
30	----------	----------	8.121	1.304
31	9.499	9.502	9.500	1.459
32	11.051	----------	11.047	1.643
32	11.051	----------	11.047	1.643
32	11.052	----------	11.047	1.643

[a] Data of Hoge and Arnold interpolated to NBS 1955 temperature scale.

observed vapor pressures of parahydrogen from the series II compressed liquid runs and from the series III low-density runs in the vapor and gaseous region. Data of Hoge and Arnold are interpolated to the NBS 1955 temperature scale of the present work. Temperature deviations corresponding to pressure deviations in series II range from 0.0098 deg at 28 °K to 0.0030 deg at 32 °K. The series III range is from 0.005 deg at 22 °K to 0.003 deg at 32 °K.

11.3. PVT Data for Normal Hydrogen

The first PVT run was made with normal hydrogen for comparison with known data, table 6. The

TABLE 6. *PVT observations on normal hydrogen*

T, °K	P, atm	v, cm³/mol	Z_{exp}	$1.0026 \cdot Z_{exp}$	Z_{lit}
28	30.869	30.443	0.4090	0.4101	0.4093[a]
30	45.357	30.460	.5612	.5627	.5616[a]
32	59.738	30.476	.6933	.6952	.6945[a]
36	88.443	30.508	.9134	.9160	.914*[b]
40	116.969	30.538	1.0883	1.0911	1.0902[b]
45	151.884	30.574	1.2576	1.2609	1.259*[b]
50	186.213	30.607	1.3892	1.3928	1.3928[b]

[a] Friedman and Hilsenrath, private communication.
[b] Johnston and White, Trans. ASME **72**, 785 (1950).
*Nonlinear interpolation.

known data have been interpolated linearly except where indicated. Present results for Z in column 4 are multiplied by 1.0026 in column 5 as an adjustment for the pipet deformation which occurred at an unknown time during the experiments. Deviations of the former results are within 0.07 to 2.6 parts per thousand; of the latter within 0.00 to 2.2 parts per thousand.

11.4. Virial Coefficients

Corresponding to the virial equation,

$$Z \equiv Pv/RT = 1 + B/v + C/v^2 + \cdots, \quad (11.4\text{–}1)$$

the data function,

$$\phi \equiv RT(Z-1)v = RTB + RTC/v + \cdots, \quad (11.4\text{–}2)$$

exhibits satisfactory linear dependence on density at each temperature when the recalibrated pipet volume, $V_0 = 25.913$ cm³ is used for computation of experimental densities below critical. Unsmoothed values of RTB and RTC, determined by least squares, are given by table 7. These new data are equivalent to an equation of state for parahydrogen at densities up to 9 g mol/liter. For comparison are given values for normal hydrogen calculated from the smoothed table 19 of H. W. Woolley et al. [69], and values for RTB only, smoothed by us from the "smoothed" table CIV of A. S. Friedman [19]. Negative third virial coefficients in the latter table below 50 °K suggest that corresponding second virial coefficients are too small in absolute value. Our closely-spaced data suggest a so-called lambda-point maximum in the third virial coefficient at the critical temperature. The criteria of its validity have not been investigated. Concerning comparison of results, it recently has been shown that second virial coefficients for parahydrogen may be about 1 percent smaller in absolute value than for normal hydrogen at liquid hydrogen temperatures, in

agreement with these results [63]. Quantitative study of the ϕ-density behavior before and after correction of the pipet volume suggests accuracy of volumetric calibrations within one part per thousand.

TABLE 7. *Virial coefficients, parahydrogen*

Units of cm³, g mol, atm, deg K

	$-RTB\cdot10^{-5}$			$RTC\cdot10^{-6}$	
T, °K	*Exp*	(a)	(b)	*Exp*	(a)
24	2.229*	2.247	2.20	3.053*	----
25	2.185*	----	----	3.432*	----
26	2.139‡	2.159	2.11	3.273‡	----
27	2.098	----	----	3.519	----
28	2.059	2.075	2.02	3.647	----
29	2.023	----	----	3.826	----
30	1.987	1.996	1.95	3.938	----
31	1.952	----	----	4.021	----
32	1.917	1.921	1.88	4.096	----
33	1.883	----	----	4.124	----
34	1.848	1.849	1.81	4.110	4.171
35	1.814	----	----	4.103	----
36	1.780	1.781	1.75	4.073	4.089
37	1.747	----	----	4.043	----
38	1.714	1.715	1.70	4.020	4.020
39	1.683	----	----	3.998	----
40	1.651	1.653	1.64	3.966	3.962
42	1.591	1.591	1.59	3.934	3.914
44	1.533	----	----	3.920	----
46	1.478	1.473	1.49	3.922	3.846
48	1.423	----	----	3.929	----
50	1.369	1.360	1.40	3.926	3.811
55	1.239	1.224	1.28	3.971	3.804
60	1.116	----	1.16	4.074	----
65	0.992	----	----	4.143	----
70	.873	----	0.94	4.232	----
75	.762	----	----	4.414	----
80	.647	----	.65	4.514	----
85	.531	----	----	4.587	----
90	.417	----	.40	4.688	----
95	.310	----	----	4.849	----
100	.205	----	.14	5.007	----

[a] H. W. Woolley et al., J. Research NBS **41**, 379 (1948) RP1932, normal H_2.
[b] A. S. Friedman, Ohio State dissertation (1950), normal H_2.
*Based on only two data points.
‡Based on only three data points.

12. Comments on Overall PVT Accuracy

Requests for a statement of overall accuracy of data in the form $Z \equiv Pv/RT$ are commonplace. This accuracy depends not only on calibrations, but also on all the adjustment computations and the particular conditions defining the state of the fluid. The relative error in Z is the sum of relative errors in experimental variables,

$$\frac{\delta Z}{Z} = \frac{\delta P}{P} + \frac{\delta v}{v} - \frac{\delta T}{T}.$$

Estimation of pressure errors is indicated by section 7.1. and table 2. The complexity of error estimates for molal volume, v, is appreciated by reference to eq (10.3–1). In view of sections 5 and 6, table 1, and the unpublished details of calibration and adjustment of obnoxious volumes, we venture the experimentalist's opinion that error in v generally is under two parts per thousand. Temperature errors, in view of tables 3, 4, and 5, are within 0.02 °C except near 14 °K, comparable to uncertainty in the low temperature scale [38]. Value of the gas constant used for present computations is $R = 82.057$ cm³ atm/g mol deg. It may be noted that at high densities, any isotherms of pressure as a function of density are highly sensitive to errors in density, due to the relatively incompressible state of the fluid, a situation giving spurious indications of low precision in the measurement of pressure.

13. Calorimetric Apparatus

13.1. Introduction

Measurements of the volume, mass, and temperature of a fluid sample are necessary to define the state corresponding to each specific heat determination. For high pressures the PVT pipet must be massive so that its volume will be calculable. The PVT data are obtained first because they are used for calibration of the volume of the thin-walled calorimeter as a function of temperature and pressure. Calorimetric methods have been reviewed [29] and the calorimetry of some compressed fluids described [28, 30, 33, 34, 35, 36]. The purpose of this section is to provide a brief description of some improved instrumentation and of the integration of calorimetric with PVT apparatus. Calorimetric calibrations will accompany the publication of results.

13.2. Cryostat and Calorimeter

The calorimeter resides in an additional cryostat of basic construction identical with that for the PVT pipet, with the high-pressure hydrogen capillary, vacuum, and liquid-transfer plumbing in parallel through suitable valves. Alternation of experiments requires no dismantling. Figure 6 is the calorimeter region of the cryostat, and figure 7 is the calorimeter section. All parts are copper except for

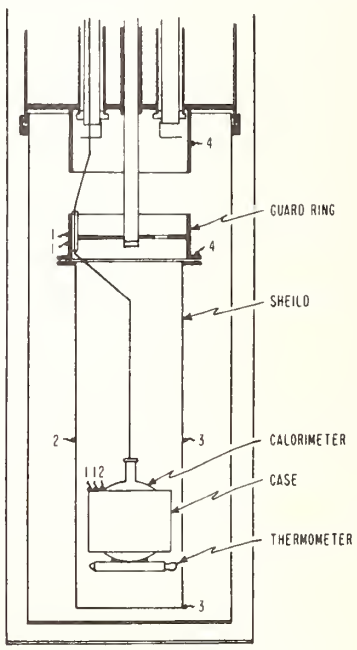

FIGURE 6. *Calorimeter region of calorimeter cryostat.*
(Shield is misspelled in the above figure.)

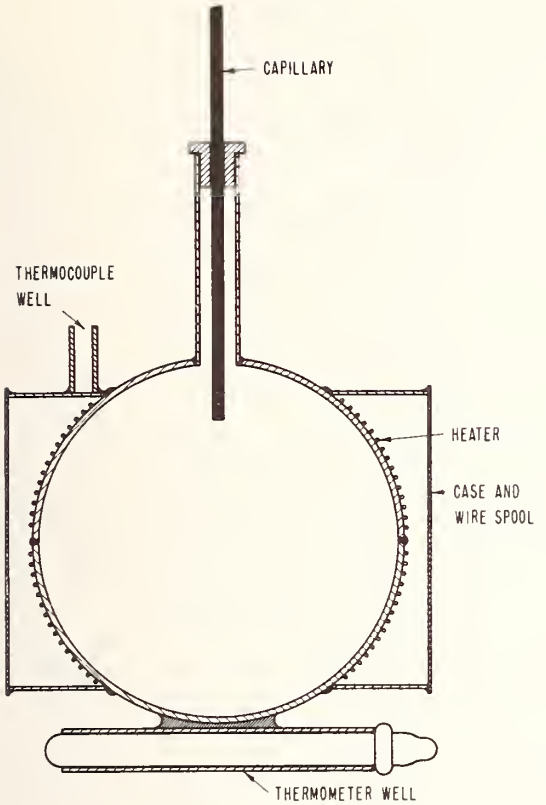

FIGURE 7. *Calorimeter section.*

sphere, capillary tube, and the guard-ring support tube. The 2-in. diam, type 316 stainless steel, spherical calorimeter has a nominal wall thickness of 0.06 in. It is fabricated from spun hemispheres, welded together, with addition of a 1-in.-long neck of ¼-in. tubing. The spherical shape is improved by expansion with water pressure. Yielding to a permanent volume increase of 10 percent was observed with a pycnometer surrounding the calorimeter. It occurred at pressures from 5,000 to 6,400 psi, corresponding to metal stress roughly 8.3 times these values. Elastic behavior following this deformation was $\Delta V/V\Delta P = 1.59 \cdot 10^{-5}$ atm^{-1}, corresponding roughly to a circumferential modulus $(3d/4t)$ $V\Delta P/\Delta V = 23 \cdot 10^6$ psi, where d is diameter and t is wall-thickness. After electroplating copper inside and outside to about 0.2 mm thickness, avoiding sulfate electrolytes, the normal volume is 72.35 cm^3, determined by gas expansion from the calorimeter in the cryostat. The 100-ohm, constantan wire heater is varnished directly onto the sphere, and shielded by the lightweight calorimeter case, which serves also as the wire spool for thermally anchoring thermocouple and thermometer lead-wires. The 1/16-in. o.d. stainless steel capillary has a bore diameter of 0.0345 cm. This relatively large bore is essential for rapid filling and emptying of the calorimeter. Volume of this capillary, including a valve at the head of the cryostat, is 0.080 cm^3.

Adiabatic shielding is in two parts: the guard ring, and attached, lightweight shield can. The ring tempers all electric wires, pressed into individual, longitudinally machined grooves. These wires lead from similar grooves in the cold ring and lead to the calorimeter case. Separate heaters are wound on the guard ring, the cylindrical surface of the shield and as a plane spiral on the bottom of the shield can. The two shield heaters operate in a divider circuit from a single regulator. These heaters are automatically controlled from thermopile *1* and thermocouple *2* respectively of figure 6. Thermocouple *3* serves for manual adjustment of the side-to-bottom heat divider. Thermocouple *4* serves for automatic temperature control of shields and calorimeter, during gas-expansion calibrations of the calorimeter volume, with reference to the refrigerant tank temperature.

To facilitate control of the calorimeter temperature during some calibrations, a small heat leak is introduced to the present apparatus. Thermal contact between electric wires and tempering ring is reduced to obtain the calorimeter cooling drift described in section 13.4 The calorimetric method therefore may be described as quasi-isothermal.

13.3. Control and Measurement of Heat

The control circuits for calorimetric heating are indicated by figure 8. Although they are conventional in principle, a useful simplification is application of an electronic battery: a 0.5 amp, transistorized, d-c power supply, continuously adjustable to 0.02 v from 0 to 32 v, with regulation and stability better than 0.002 v. The rms ripple is 0.001 v. The battery source impedance, R_b of the figure, is readily adjusted equal to the calorimeter heater resistance when the battery potential indicated by P–1 is twice the heater potential indicated by P–2 [31]. To provide time for potentiometric measurements of the heater power, and for shield temperature adjustments, a temperature rise of about 2° in a fixed interval of 10 min at all temperatures is realized by adjusting the battery potential. This adjustment does not affect R_b, in contrast to behavior with conventional batteries and rheostats. Relay coils are operated with direct current to reduce induction of spurious a-c effects in the low-level circuits.

Potentials are measured with the 6-dial microvolt potentiometer and with a type K–3 universal potentiometer, each indicating through an electronic galvanometer [56], as in figure 5. Potentials to be measured are connected to each potentiometer by high-quality, commercial, microvolt selector switches. Four measurements of heater potential and current are made in 10 min. Heater power is constant to better than 1 part in 10,000. The standard electric, clutch-type, synchronous stopclock utilizes local, 60 c/s, powerline frequency for the time standard. The NBS Time Standards Section finds that this frequency usually is accurate and constant to well within 0.03 percent.

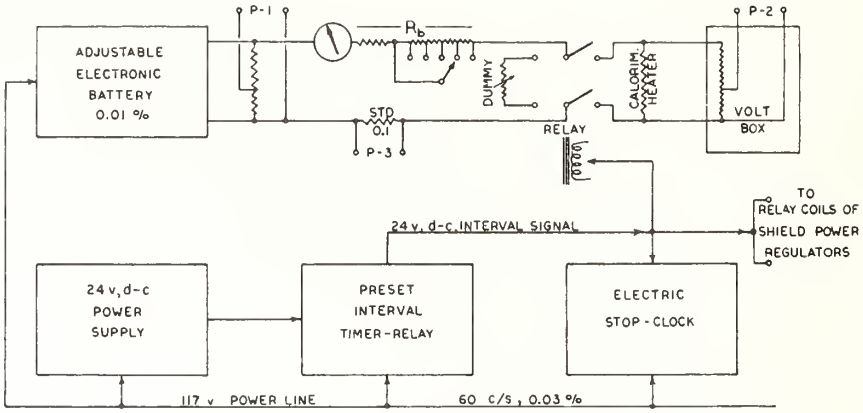

FIGURE 8. *Calorimetric heat control methods.*

13.4. Measurement of Temperatures

The calorimeter platinum resistance thermometer is calibrated and the thermometric technique checked as described for PVT determinations. Imperfections of adiabatic shielding yield empty calorimeter drift rates from −0.0009°/min at 20 °K to −0.0019°/min at 100 °K. These are linear in time.

Five temperature observations in 5 min precede a heating interval. Nonlinear equilibration following the interval requires a few minutes, and is observed with a recorder. Five similar temperature measurements follow. Temperature-time behaviors are extrapolated to mean time of the heating interval, by a least-squares computer program, at which time is taken the calorimetric temperature increment.

13.5. Control of Shield Temperatures

The different methods, isothermal and adiabatic shielding, are useful for different purposes [37]. The adiabatic method is selected here for rapid adjustments in the range 20 to 100 °K where thermal transport is almost entirely conductive. Gold-cobalt versus copper thermocouples indicate temperature differences between the calorimeter and the guard ring and shield respectively. An individual regulating system is employed for each of the latter. An improvement of present instrumentation, indicated by the bottom row of figure 5, is its simplicity relative to current practices [27]. Control instruments are the microvolt amplifier [56] and the power regulator [50]. Two factors contribute to satisfactory operation. (1) Thermocouples are so placed on shields as to give rapid but average response. The heater windings and powers are designed to match the areas and masses of metal to be controlled. (2) The power regulator contains a solenoid relay, operated by the heating interval signal, figure 8, which automatically boosts the shield heating to a manually pre-set level. This eliminates the delay otherwise required for development of the temperature difference normally utilized for automatic control. The booster circuit does not affect the low output impedance of this regulator, thereby avoiding the loss of power-gain and temperature-regulation otherwise suffered when resistances or other impedances are inserted in the heater circuit for boosting control. Because automatic resetting instruments are not necessary for the present work, the normal steady-state heating also is manually adjusted at the power regulator. For calibration work, the shield versus calorimeter temperature differences may be recorded from the microvolt amplifier output signals by means of simplified strip-chart instruments. A typical chart shows that, with routine error in adjustment of the boost heat level, the guard ring-versus-calorimeter temperature difference peaks at 0.001 °C at the start of an interval and decays to within 0.0001° in 20 sec. The same behavior with opposite sign follows the ending of an interval. Relative change in the steady heat-leak over the copper wire bundle between guard ring and calorimeter is negligible during a heating interval.

The numerous machined parts for the cryostats were made in the NBS, Boulder shop under S. Landis. The skillful assembly and silver-soldering of these parts as well as the construction of the liquid transfer and hard vacuum systems by Cryogenic Division instrumentalist W. R. Bjorklund greatly advanced the project. D. E. Diller placed all of the small electric wiring in the cryostats, intercalibrated the gasometer glass volumes, performed the gas-expansion calibrations of the pipet, checked fixed-points of the platinum thermometer, and measured null-point shift of the diaphragm cell in addition to other important contributions. L. A. Weber assisted with the many details of placing the PVT apparatus in final operating condition. B. A. Younglove determined mechanical properties of the calorimeter and with D. E. Diller placed the calorimetry in successful operation. Hans M. Roder, in programing the computer work, devised subsidiary equations presented in sections 5.3 and 10. Continuing encouragement from Robert J. Corruccini and Russell B. Scott have been essential in bringing this long task to completion.

14. References

14.1. General

[1] Stanley H. Bransom, Applied thermodynamics (D. van Nostrand Co., Ltd., London, 1961).
[2] F. Din, editor, Thermodynamic functions of gases, 1 (Butterworths Scientific Publications, London, 1956).
[3] B. F. Dodge, Chemical engineering thermodynamics (McGraw-Hill Book Co., Inc., New York, N.Y., 1944).
[4] W. E. Forsythe, Smithsonian physical tables, Ninth revised ed. (Smithsonian Institution, Washington, D.C., 1956).
[5] Lawrence Lessing, The master fuel of a new age, Fortune **63** (5), 152 (1961).
[6] A. Michels, High pressure research, Research **9**, 99 (1956).
[7] A. Michels, J. C. Abels, C. A. Ten Seldam, and W. deGraff, Polynomial representation of experimental data; application to virial coefficients of gases, Physica **26**, 381 (1960).
[8] J. B. Opfell and B. H. Sage, Application of least-squares methods, Ind. Eng. Chem. **50**, 803 (1958).
[9] J. S. Rowlinson, The properties of real gases, Handbuch der Physik, vol. **XII**, S. Fluegge, ed. (Springer-Verlag, Berlin 1958).
[10] R. B. Scott, Liquid hydrogen for chemical and nuclear rockets, Discovery **21** (2), 74 (1960).

14.2. Cryogenic Technique

[11] J. G. Aston and H. L. Fink, Application of low temperatures to chemical research, Chem. Revs. **39**, 357 (1946).
[12] F. Din and A. H. Cockett, Low temperature techniques (Geo. Newness, Ltd., London, 1960).
[13] R. B. Scott, Cryogenic engineering, D. van Nostrand, Co., Ltd., London (1959).
[14] G. K. White, Experimental techniques in low-temperature physics (Clarendon Press, 1959).

14.3. PVT Methods

[15] E. P. Bartlett, H. C. Hetherington, H. M. Kvalnes, and T. H. Tremearne, The compressibility isotherms of hydrogen, nitrogen and a 3:1 mixture of these gases at temperatures of −70, −50, −25 and 20° at pressures up to 1000 atmospheres, J. Am. Chem. Soc. **52**, 1363 (1930).
[16] J. A. Beattie, The apparatus and method used for the measurement of the compressibility of several gases in the range 0° to 325°C. Proc. Am. Acad. Arts. Sci. **69**, 389 (1934).
[17] E. S. Burnett, Compressibility determinations without volume measurements, J. Appl Mechanics **3**, 136 (1936).
[18] D. Cook, The second virial coefficient of carbon dioxide at low temperatures, Can. J. Chem. **35**, 268 (1957).
[19] A. S. Friedman, Pressure-volume-temperature relationships of gaseous hydrogen, nitrogen and a hydrogen-nitrogen mixture, Thesis, The Ohio State University, (1950).
[20] L. Holborn and H. Schultze, On the pressure balance and the isotherms of air, argon and helium between 0 and 200°, Ann. der Physik **47**, 1089 (1915).
[21] L. Holborn and J. Otto, On the isotherms of helium, nitrogen and argon below 0°, Z. Physik **30**, 320 (1926).
[22] L. Holborn and J. Otto, The isotherms of helium, hydrogen and neon below −200°, Z. Physik **38**, 359 (1926).
[23] H. L. Johnston, W. F. Keller, and A. S. Friedman, The compressibility of liquid normal hydrogen from the boiling point to the critical point at pressures up to 100 atm., J. Am. Chem. Soc. **76**, 1482 (1954).
[24] H. L. Johnston and D. White, Pressure-volume-temperature relationships of gaseous normal hydrogen from its boiling point to room temperature and from 0–200 atmospheres, Trans. ASME **72** (6), 785 (1950).
[25] A. Michels, T. Wassenaar, and Th. N. Zwietering, The experimental determination of the equation of state of gases at temperatures between 0° and −180° C, Physica **18**, 67 (1952).

14.4. Calorimetric Methods

[26] J. G. Aston and M. L. Eidinoff, The low temperature precision adiabatic calorimeter adapted to condensed gases from 10 °K. to room temperature, J. Am. Chem. Soc. **61**, 1533 (1939).
[27] W. J. Cooper, R. H. Forsythe, J. F. Masi, and R. E. Pabst, Low temperature adiabatic calorimeter with automatic shield control, Rev. Sci. Instr. **30**, 557 (1959).
[28] A. Eucken, On the thermal behavior of some compressed and condensed gases at low temperatures, Verh. deut. Phys. Ges. **18**, 4 (1916).
[29] R. W. Hill, Low-temperature calorimetry, Progress in Cryogenics, vol. **1**, K. Mendelssohn, ed. (Heywood and Co., Ltd., London, 1959).
[30] H. J. Hoge, Heat capacity of a two-phase system, with applications to vapor corrections in calorimetry, J. Research NBS **36**, 111 (1946) RP1693.
[31] H. J. Hoge, Circuits for minimizing transient effects on energy measurements in calorimetry, Rev. Sci. Instr. **20**, 59 (1949).
[32] Hugh M. Huffman, Low-temperature calorimetry, Chem. Revs. **40**, 1 (1947).
[33] O. V. Lounasmaa, Specific heats at low temperatures, Thesis, University of Oxford, Brasenose College, 1958. (Helium C_v and PVT.)
[34] A. Michels and J. C. Strijland, The specific heat at constant volume of compressed carbon dioxide, Physica **18**, 613 (1952).
[35] E. B. Rifkin, E. C. Kerr, and H. L. Johnston, Condensed gas calorimetry. IV. The heat capacity and vapor pressure of saturated liquid diborane above the boiling point, J. Am. Chem. Soc. **75**, 785 (1953).
[36] P. A. Walker, The equation of state and the specific heat of liquid argon, Thesis, Queen Mary College, Univ. of London (1956).
[37] D. M. Yost, C. S. Garner, D. W. Osborne, T. R. Rubin, and H. Russell, Jr., A low temperature adiabatic calorimeter. The calibration of platinum resistance thermometers, J. Am. Chem. Soc. **63**, 3488 (1941).

14.5. Thermometry

[38] Anonymous, Symposium on Temperature, Its Measurement and Control in Science and Industry (Columbus, Ohio, March 27, 1961), Abstracts, 116 pp., $5.00, American Institute of Physics, 335 E. 45th St., New York, N.Y.
[39] T. M. Dauphinee and H. Preston-Thomas, A copper resistance temperature scale, Rev. Sci. Instr. **25**, 884 (1954).
[40] N. Fuschillo, A low-temperature scale from 4 to 300 °K in terms of a gold-cobalt vs. copper thermocouple, J. Phys. Chem. **61**, 664 (1957).
[41] F. K. Harris, Electrical Measurements (John Wiley & Sons, Inc., New York, N.Y., 1952).
[42] H. J. Hoge and F. G. Brickwedde, Establishment of a temperature scale for the calibration of thermometers between 14° and 83 °K, J. Research NBS **22**, 351 (1939) RP1188.
[43] E. F. Mueller and H. F. Stimson, A temperature-control box for saturated standard cells, J. Research NBS **13**, 699 (1934) RP739.
[44] R. L. Powell, M. D. Bunch, and R. J. Corruccini, Low-temperature thermocouples—I. Gold-cobalt or constantan versus copper or "normal" silver, Cryogenics **1** (3), 139 (1961).
[45] Bruce K. Smith, Low thermal soldering procedures for copper junctions, Electronic Design **7** (25), 52 (1959).
[46] H. F. Stimson, Precision resistance thermometry and fixed points, Temperature, vol. **2**, H. C. Wolfe, editor (Reinhold Publ. Corp., New York, N.Y., 1955).
[47] H. F. Stimson, Heat units and temperature scales for calorimetry, Am. J. Phys. **23**, 614 (1955).

14.6. Instruments

[48] W. G. Brombacher, D. P. Johnson, and J. L. Cross, Mercury barometers and manometers, NBS Mono. 8 (1960).

[49] D. O. Coffin, High-pressure gas-to-liquid transducer, Rev. Sci. Instr. **29,** 896 (1958).
[50] R D. Goodwin, An improved d.c. power regulator, Advances in cryogenic engineering, vol. **5,** K. D. Timmerhaus, ed. (Plenum Press, New York, N.Y., 1960).
[51] P. C. Hoell, Low-level d.c. amplifier with whole-loop feedback, Rev. Sci. Instr. **29,** 1120 (1958).
[52] D. P. Johnson and D. H. Newhall, The piston gauge as a precise pressure-measuring instrument, Trans. ASME **75,** 301 (April 1953).
[53] F. G. Keyes, High-pressure technic, Ind. Eng. Chem. **23,** 1375 (1931).
[54] T. W. Lashof and L. B. Macurdy, Precision laboratory standards of mass and laboratory weights, NBS Circ. 547 (1954).
[55] L. LeBlan, The precise measurement of pressures, Chimie et ind. **61,** 235; 349 (1949).
[56] M. D. Liston, C. E. Quinn, W. E. Sargeant, and G. G. Scott, A contact-modulated amplifier to replace sensitive suspension galvanometers, Rev. Sci. Instr. **17,** 194 (1946).
[57] A. Michels, Calibration of pressure-balance in absolute units, Proc. Kon. Ak. Amsterdam **35,** 994 (1932).
[58] J. R. Purcell and R. N. Keeler, Sensitive thermal conductivity gas analyzer, Rev. Sci. Instr. **31,** 304 (1960).
[59] H. H. Reamer and B. H. Sage, Experience with piston-cylinder balance for pressure measurements, Rev. Sci. Instr. **26,** 592 (1955).
[60] E. E. Watson, Constant current supply for the potentiometer, Am. J. Phys. **27,** 404 (1959).
[61] D. White and J. Hilsenrath, A pressure-sensitive diaphragm-type null detector, Rev. Sci. Instr. **29,** 648 (1958).

14.7. Fluids Properties

[62] G. T. Armstrong, Vapor pressure of nitrogen, J. Research NBS **53,** 263 (1954) RP2543.
[63] J. J. M. Beenakker, F. H. Varekamp, and H. F. P. Knapp, The second virial coefficient of ortho and para hydrogen at liquid hydrogen temperatures, Physica **26,** 43 (1960).
[64] A. S. Friedman and J. Hilsenrath, The thermodynamic and transport properties of liquid hydrogen and its isotopes (private communication).
[65] Joseph Hilsenrath et al., Tables of thermal properties of gases, NBS Circ. 564 (1955).
[66] H. J. Hoge and R. D. Arnold, Vapor pressures of hydrogen, deuterium, and hydrogen deuteride and dew-point pressures of their mixtures, J. Research NBS **47,** 63 (1951) RP2228.
[67] V. J. Johnson, editor, A compendium of the properties of materials at low temperature. Part I, Properties of fluids. Part II, Properties of solids, WADD Technical Report 60–56, Office of Technical Services, U.S. Dept. Commerce, Washington 25, D.C.
[68] R. B. Stewart and V. J. Johnson, A compilation and correlation of the P-V-T data of normal hydrogen from saturated liquid to 80 °K, Advances in Cryogenic Engineering, vol. **5,** K. D. Timmerhaus, ed. (Plenum Press, New York, N.Y., 1960).
[69] H. W. Woolley, R. B. Scott, and F. G. Brickwedde, Compilation of thermal properties of hydrogen in its various isotopic and ortho-para modifications, J. Research NBS **41,** 379 (1948) RP1932.

14.8. Solids Properties

[70] J. H. Faupel and A. R. Furbeck, Influence of residual stress on behavior of thick-walled closed-end cylinders, Trans. ASME **75,** 345 (April 1953).
[71] M. J. Hiza, Cryogenic impurity adsorption from hydrogen, Chem. Eng. Progr. **56** (10), 68 (1960).
[72] R. N. Keeler and K. D. Timmerhaus, Poisoning and reactivation of ortho-parahydrogen conversion catalyst, Advances in Cryogenic Engineering, vol. **4,** K. D. Timmerhaus, ed. (Plenum Press, New York, N.Y., 1960).
[73] R. M. McClintock, D. A. vanGundy, and R. H. Kropschot, Low-temperature tensile properties of copper and four bronzes, ASTM Bull. No. 240, p. 47 (TP 177) (Sept. 1959).
[74] A. Michels, The behavior of thick-walled cylinders under high pressures, Proc. Kon. Ak. Amsterdam **31,** 552 (1928).
[75] R. L. Mills and F. J. Edeskuty, Hydrogen embrittlement of cold-worked metals, Chem. Eng. Prog. **52** (11), 477 (1956).
[76] G. W. Morey, The properties of glass (Reinhold Publ. Corp., New York, N.Y., 1954).
[77] R. L. Powell and W. A. Blanpied, Thermal conductivity of metals and alloys at low temperatures, NBS Circ. 556 (Sept. 1, 1954).
[78] T. Rubin, H. W. Altman and H. L. Johnston, Coefficients of thermal expansion of solids at low temperatures, J. Am. Chem. Soc. **76,** 5289 (1954).
[79] S. Timoshenko, Strength of materials II, 2d ed., eq. (208) (D. van Nostrand Co., Inc., New York, N.Y., 1941).

(Paper 65C4–76)

JOURNAL OF RESEARCH of the National Bureau of Standards—C. Engineering and Instrumentation
Vol. 69C, No. 1, January–March 1965

Detection and Damping of Thermal-Acoustic Oscillations in Low-Temperature Measurements

David A. Ditmars and George T. Furukawa

(June 8, 1964)

The spontaneous thermal-acoustic oscillations in nonisothermal columns of helium, hydrogen, nitrogen, argon, and oxygen gas have been investigated. The pressure fluctuations were measured with a barium titanate transducer and the particle displacements observed by a smoke technique. The observed pressure oscillations were often nonsymmetrical and of sufficient amplitude to indicate the necessity for a nonlinear approach in a theoretical treatment of the oscillations. An adjustable "Helmholtz resonator" attached at the warm end of the oscillating column was found to damp completely the oscillations and eliminate the energy transfer which they caused.

1. Introduction

Spontaneous pressure oscillations in gaseous columns, along which there is a temperature gradient, often hamper cryogenic work. An excellent review of this oscillation phenomenon has been given by Wexler [6].[1] While there are at least three reports of such oscillations having been used to advantage [1,2,3], they are most often undesirable. They can introduce errors in vapor-pressure measurements and sometimes make the measurements impossible to obtain [1,4]. Frequently, the oscillations cause a large uncontrollable energy transfer from hot to cold regions, making calorimetric measurements difficult or impossible.

Experience gained with a calorimeter at the National Bureau of Standards confirmed Wexler's observation [6] that the energy transfer due to gas oscillation from the room temperature region to the 4 °K region can be as much as 1000 times greater than the energy transfer by thermal conduction. It was decided to investigate the possibility of damping the oscillations by some device added externally.

Experiments with a simple auxiliary apparatus showed this solution to be promising. This apparatus was then used to investigate further the factors affecting the cause and suppression of the oscillations. In the course of this investigation, an adjustable "Helmholtz resonator" attached at the warm column end proved to be a reliable and effective damper.

2. Apparatus

The auxiliary apparatus shown in figure 1 consists basically of a tube T extending down into a Dewar containing a cryogenic liquid boiling at atmospheric pressure. The lower end of the tube T was always open and the upper end was closed by a pressure transducer and a device used to suppress the gaseous oscillations.

The Dewar, of two-liter capacity, was generally used with less than a liter of liquid. When the liquid was helium, the Dewar was immersed in a liquid nitrogen bath.

Temperatures along the tube T were occasionally measured with thermocouples. Typical temperature gradients along the tube ranged from 1 to 2 °C per mm when the Dewar contained 1 liter of liquid. The only means of changing the temperature gradient along the tube was to add or withdraw cryogenic liquid in the Dewar, keeping the same apparatus dimensions.

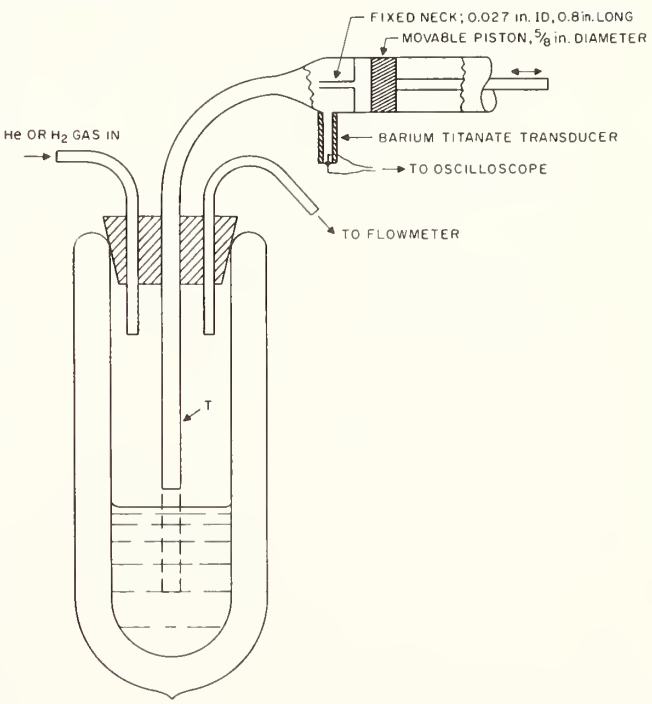

FIGURE 1. *Auxiliary apparatus for studying thermal-acoustic oscillations.*

[1] Figures in brackets indicate the literature references at the end of this paper.

A barium titanate tube, cemented onto the upper end of T, served as a pressure transducer. This transducer (2 in. long, ⅜ in. o.d. with a 1/16 in. wall) was silvered on the inside and outside and polarized through the wall thickness. A static pressure calibration showed that the transducer had a sensitivity of 7 mV/torr[2] differential pressure across its walls. This potential was measured with a vibrating reed electrometer and was a linear function of pressure in the range covered, 0 to 30 torr. The sensitivity should be independent of frequency at the low frequencies involved in these experiments (less than 60 Hz). The transducer output was fed directly to a sensitive oscilloscope. Because of the low impedance of the oscilloscope, the trace, at low frequencies (2 to 10 Hz), represented more nearly the time derivative of the average pressure fluctuations inside the transducer than the pressure itself. Additional circuitry or a dynamic calibration of the transducer-oscilloscope system would be necessary to interpret the trace directly as a pressure at low frequencies.

Some direct visual observations of the wave motion were made when T was a glass tube by introducing a smoke of finely divided TiO_2 particles into the tube. In the case of oscillations over liquid helium, that part of the energy dissipated in the liquid by the oscillating gas column was measured by passing the gas evolved from the Dewar through a flowmeter.

Pressure and net mass flow of gas in the tube were not controlled in these experiments. The mean pressure in the tube was always within a few torr of atmospheric and the net gas flow in the tube was zero. This is not to imply that oscillations occur only under these conditions. For instance, in the calorimeter referred to above, oscillations have been detected at pressures below 400 torr and also in tubes through which a net helium gas flow existed.

3. Results

3.1. Generation and Observation of Oscillations

The literature contains only references to oscillations in helium or hydrogen gas columns over baths of liquid helium or hydrogen, respectively. The present work has shown the phenomenon to be of a more general nature. For instance, gaseous columns can also be made to oscillate over baths of liquid nitrogen or oxygen. Columns of helium, hydrogen, nitrogen, argon, or oxygen gas were readily made to oscillate over a liquid oxygen bath. Evaporation caused by oscillation energy transfer to nitrogen or oxygen baths in the present experiments was small and could not be distinguished from evaporation due to other sources of heat leak to the baths. Two conditions had to be met, however, for the oscillations to occur with the higher temperature baths: (a) The open tube end had to extend several tube diameters beneath the bath surface, and (b) the Dewar volume above the surface had to be flooded with helium or hydrogen gas. This

[2] 1 torr = 1/760 normal atmosphere = 133.322 N/m².

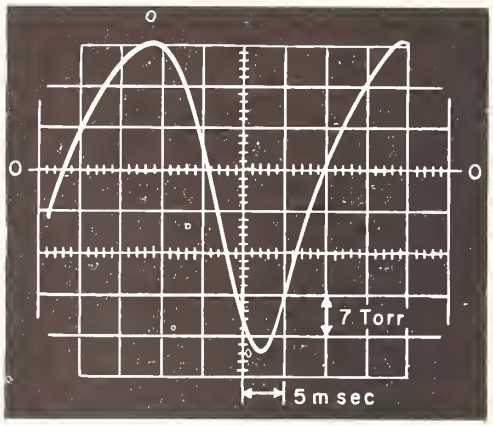

FIGURE 2. *Pressure oscillation at closed end of He gas column.* Open end 1.5 cm above liquid He surface. "O" indicates sweep position without oscillation.

is in distinction to helium or hydrogen gas columns which oscillate in tubes whose open end is either above or below the surface of a liquid helium or hydrogen bath respectively. Probably the most important effect of the flooding was the increase in the surface heat-transfer coefficient [14] at the exterior tube wall. This also altered the bath composition and the tube temperature gradient. Experiments performed, in which these latter effects were eliminated or produced independently of any change in the heat transfer coefficient, showed that helium or hydrogen gas had to be present for oscillations to be sustained.

To obtain a column of a gas other than that of the bath species, the tube T, removed from the Dewar, was first flushed by introducing the desired gas through an opening in the upper tube end. The tube was then lowered into the Dewar until its lower (open) end was beneath the bath surface and the gas flow gradually reduced to zero. This procedure was followed, for instance, to obtain a column of helium gas above liquid nitrogen. The amplitude and period of the ensuing oscillation were recorded as soon as they reached stable values in order to minimize the effect of contamination of the helium gas column with nitrogen. The observed frequency was always several times that of a nitrogen gas column oscillating under the same condition—as much as eight times in one instance. By way of comparison, a similar gas column resonating in its lowest acoustic mode with helium would normally exhibit a frequency which is about three times that when resonating with nitrogen in the same mode. A helium column oscillating with the open tube end below the bath surface displayed approximately equal frequencies with baths of helium or nitrogen though the amplitude over the helium bath was several times that over the nitrogen bath.

At low amplitudes the pressure oscillations appeared sinusoidal, but with either increasing amplitude or increasing temperature gradient, a nonsymmetrical distortion appeared (fig. 2). The time between a pressure maximum and the following pressure minimum exceeded half the period.

Using the smoke technique referred to above, observations were made with a glass tube of 2 mm i.d. and 0.8 mm wall thickness, containing a nitrogen gas column oscillating at about 5 Hz over a liquid nitrogen bath. No displacement nodes were observed other than at the closed end. The displacement amplitude of the smoke particles increased monotonically along the tube length and was as great as ± 8 mm near the open (cold) tube end. The amplitude of this oscillation was 5 to 10 times less than typical amplitudes of helium gas oscillations over liquid helium in which a large energy transfer occurred. When direct observation of the liquid meniscus in the tube T was possible (i.e., with glass tubes), the mean position of the meniscus was below the bath level, indicating a net positive pressure within the tube during oscillation.

3.2. Damping the Oscillations

Reported attempts to damp or eliminate thermal-acoustic oscillations fall into three main categories:

(1) Changes in apparatus geometry such as employing tubes of greater diameter or closing tubes at the cold end when possible [2,7].

(2) Insertion of objects such as wire, wire mesh or knotted threads into the oscillating column [5,8,13].

(3) Thermal isolation of the oscillating column [2,4]. None of these methods was practical to apply to the calorimeter referred to above. It was possible to control the oscillations in the auxiliary apparatus (fig. 1) at any desired amplitude or to eliminate them completely with an adjustable Helmholtz resonator attached at the warm end of the oscillating column. The same technique permitted the control of the oscillations in the calorimeter. The effect of the resonator dimensions on its efficiency as a damper was then investigated using the auxiliary apparatus.

Resonator neck diameters from 0.014 in. to 0.058 in. and lengths up to 2 in. were tried. The neck dimensions were found to be critical and the best results were obtained with the neck dimensions indicated in figure 1. Necks whose diameters or lengths varied from the indicated neck dimensions by as little as a factor of two provided poor damping. Oscillations in helium and nitrogen gas columns ranging in frequency from 2 to 60 Hz and causing heat leaks of up to 7 W were successfully damped with the resonator. A typical set of damping curves obtained for helium gas oscillating over liquid helium is given in figure 3. The distance of the tube end above the liquid surface was kept constant along any curve. Larger values of the relative pressure amplitude correspond to lesser values for this distance. These curves varied considerably in shape with different oscillating gas columns and different neck dimensions. They exhibited, however, the common characteristic of a continual decrease in pressure amplitude (and associated energy transfer) with increasing piston extension.

Piston extensions up to three times the minimum length required for complete damping were investigated and in no instance did the oscillation ever reappear. No correlation was discovered between

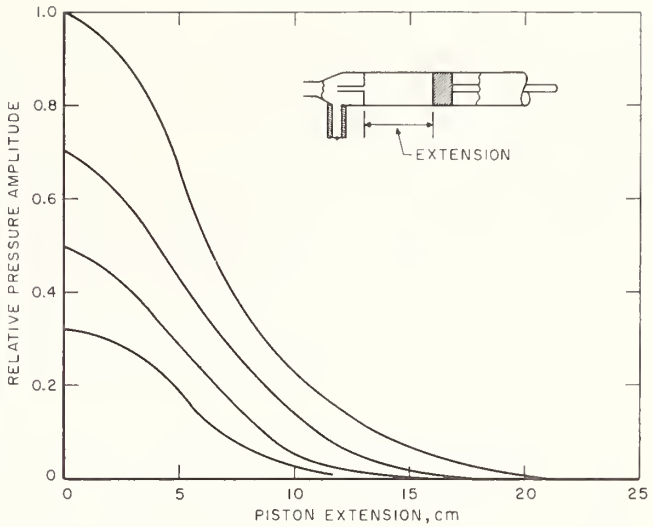

FIGURE 3. *Effect of piston extension on pressure amplitude.*
Pressure amplitude increased by decreasing distance between cold tube end and liquid surface.

the piston diameter and the minimum piston extension required to damp an oscillation of given amplitude; neither was the natural acoustic frequency of the damper related in any obvious way to its effectiveness as a damper. Piston diameters from 3/8 in. to 1 in. have been used successfully at extensions not exceeding 50 cm to damp oscillations in the entire amplitude and frequency range attainable in the auxiliary apparatus with the combinations of gas columns and liquid baths mentioned earlier.

The damper illustrated in figure 1, together with the oscillating column, constitutes a variable volume system. Equivalent results were also obtained by fixing the position of the piston and moving the neck assembly. In this case, the neck was mounted on a thin piston which was attached to a rod extending through a seal in the fixed piston.

In one series of experiments a porous tissue plug was substituted for the neck assembly. The damping of some oscillations was possible with this arrangement.

4. Discussion

The neck assembly is the vital part of the damper shown in figure 1. Since oscillations cannot be sustained in a tube open at the warm end, one could, in principle, attach a large closed volume onto the end of any tube to simulate an open end condition and thus damp the oscillations without use of the neck assembly. In practice, the volume required is often rather large and cumbersome. Damper experiments performed with the neck assembly removed have shown that the volume changes alone caused by retraction of the piston have little effect on the oscillation amplitude.

The resonator damper has several advantages. No modification of apparatus design in the cold region and no obstruction in the oscillating tube is required. This is an important consideration if a pumping tube is oscillating. Connections can be

provided so that the damper can be removed and it can be designed to be vacuum or pressure tight if the gas column is oscillating at a mean pressure considerably different from atmospheric. In the application to the above calorimeter, the piston was designed to be vacuum tight.

The coupling between the damper and oscillating system is not fully understood. Several workers [9,10] have investigated the nonlinear impedance of a Helmholtz resonator at large amplitudes and have tried to correlate it with energy dissipation in vortices near the resonator neck. The flow pattern near the neck of a damper used in the present experiments was observed by the smoke technique and appeared to be a pulsating jet similar to those described in [9].

A number of variables, probably not all independent of one another, determine whether or not a given system will perform sustained oscillations and if so, what the wave form and associated energy transfer will be. With a given temperature distribution throughout the system, the essential requirements seem to be that the gas column have a diameter small enough (usually less than ½ in.), that the cold tube end be open to a volume whose characteristic dimensions are large compared to the tube diameter, that the warm end be terminated with a high acoustic impedance, and that the tube be in good thermal contact with its surroundings. This contact need not be due to a conducting gas but can be provided by metal contact with heat sources or sinks along the tube length as was observed in the above calorimeter.

Kramers [15] has attempted to treat the gas oscillations analytically assuming small amplitudes of vibration. This linear approach did not account for the observed phenomena, a result which is plausible considering the oscillation amplitudes encountered in the present work. The possible existence of such oscillating states of a thermal system has been treated in some detail from an energy standpoint by Milne [11]. Milne's theory predicts periodic fluctuations with just the asymmetry observed in these experiments. Squire [12] has speculated that the occurrence of the Boyle temperature in the oscillating column may play a role in initiating the oscillations. Since a column of helium gas readily oscillates over liquid nitrogen, this evidently need not be a decisive role.

Since thermal-acoustic oscillations so often hamper low temperature experiments, the need for a fuller understanding of them is great. It is felt that an apparatus specifically designed to reproduce known temperature gradients would be valuable in future experimental investigation.

5. References

[1] K. W. Taconis, J. J. M. Beenakker, A. O. C. Nier, and L. T. Aldrich, Physica **15,** 733 (1949).
[2] J. R. Clement, Proc. 1954 Cryogenic Engineering Conf. (1954).
[3] D. Ter Harr, Proc. Paris Conference on Low Temperature Physics, p. 347 (1955). (See appended discussion.)
[4] F. E. Hoare and J. E. Zimmerman, Rev. Sci. Instr. **30,** 184 (1959).
[5] O. V. Lounasmaa, Ann. Univ. Turku, **A1,** No. 39 (1959).
[6] A. Wexler; in F. E. Hoare, L. C. Jackson, and N. Kurti (Eds.), Experimental Cryophysics, p. 155 (Butterworths, London, 1961).
[7] A. Van Itterbeek and W. H. Keesom, Comm. Leiden 209C.
[8] R. B. Scott, Cryogenic Engineering, p. 118 (D. Van Nostrand Co., Inc., 1959).
[9] U. Ingård and S. Labate, J. Acoust. Soc. Am. **30,** 211 (1950).
[10] F. Barthel, Frequenz **12,** 72 (1958).
[11] E. A. Milne, Quart. Journ. of App. Math. **4,** 258 (1933).
[12] C. F. Squire, Low Temperature Physics, p. 23 (McGraw-Hill Book Co., Inc., New York, N.Y., 1953).
[13] H. Plumb, private communication.
[14] M. Jakob, Heat Transfer, **I** (John Wiley & Sons, Inc., New York, N.Y., 1949).
[15] H. A. Kramers, Physica **15,** 971 (1949).

(Paper 69C1–183)

4. High Temperature Calorimetry

Reprinted from*

Experimental Thermodynamics
Volume I

CHAPTER 8

High-temperature Drop Calorimetry

THOMAS B. DOUGLAS
National Bureau of Standards, Washington D.C., U.S.A.
EDWARD G. KING
Albany Metallurgy Research Centre, Bureau of Mines, Albany, Oregon, U.S.A.

Contents

*See complete ref. on page 1-I.

I. Introduction

The determination of accurate high-temperature enthalpies provides a valuable tool in the study of materials and processes at elevated temperatures. As interest in high-temperature research increases, impetus is given to experimental methods that will extend the temperature range of measured enthalpies.

The enthalpies of the simpler, ideal gases can be determined much more accurately from spectroscopic data than by measurement. Calculation methods may also be accurately applied for less simple gases with molecules in a single electronic state and without internal rotations. In these cases molecular-constant data must be available, *i.e.*, molecular-structure and vibrational-frequency data.

At present, enthalpies of solids and liquids must be determined experimentally; and most of the accurate data for solids and liquids, above 100°C, have been provided by drop calorimetry. With this method a sample is heated to a known temperature and is then dropped into a calorimeter (usually operating near room temperature), which provides measurement of the heat evolved by the sample in cooling to the calorimeter temperature.

Currently the major applications of enthalpy and enthalpy-related data are to problems in microstructure, heat transfer, and chemical thermodynamics. In particular, the last application is of great importance. If room-temperature values of enthalpy, Gibbs energy, or entropy have been obtained by other means, the values may be extended to the limit of the high-temperature measurements. In many cases equilibrium vapor pressures can be calculated more accurately than they can be directly measured. If vapor pressure measurements do exist, the measured enthalpies and derived data can be used in a complementary way.

1. *General requirements*

The general requirements for drop-calorimetry operation of high accuracy may be considered in terms of (*i*) the sample, (*ii*) the furnace, and (*iii*) the calorimeter.

(*i*) The substance measured must not change irreversibly to a significant extent during the measurements. Such a change can occur through decomposition, reaction with the container, or deterioration caused by container

leakage. In passing from the higher (furnace) temperature to the lower (calorimeter) temperature, the amount of heat evolved by the sample is meaningful only if the forms of the sample at the two temperatures are defined.

(*ii*) The accurate determination of the average temperature of the sample referred to some well defined temperature scale (usually the International Practical Temperature Scale) is the most important requirement of the furnace. The heat lost by the sample as it drops through the region between the furnace and the calorimeter must cancel out through empty-container measurements. This requirement dictates a high and reproducible rate of fall (most easily accomplished by a close approximation to free fall) and constancy of surface emissivity, because these factors strongly affect radiation losses which predominate at high temperatures.

(*iii*) The calorimeter must be capable of measuring the heat delivered by the sample with high accuracy, a requirement which entails the accurate determination of the heat losses from the calorimeter itself.

In designing calorimetric apparatus for high accuracy and choosing materials of construction, intuition is a poor substitute for relatively simple calculations, even ones which may be in error by as much as a factor of two or three. This is especially true of questions involving heat transfer. For considerably lower requirements in accuracy, a much simpler furnace and type of calorimeter can replace those subsequently described in this chapter; in this case, simple calculations or tests may indicate an otherwise unsuspected degree of simplification in construction and operation which may be safely adopted.

2. *Advantages and disadvantages of the drop method*

Advantages and disadvantages of the drop method compared with other calorimetric methods are discussed in Chapter 1, Section V. Perhaps the greatest advantage of the drop method over the adiabatic method is that the precise calorimetric measurements are made at or near room temperature where suitable conditions are most easily maintained. Above 500 °C or so the drop method at present excels applications of the adiabatic method in accuracy as well as simplicity. With high-temperature adiabatic and isothermal-jacket calorimeters there is considerable difficulty in temperature control and in accounting for heat losses by radiation.

With the drop method, enthalpies of transition and fusion are obtained by the difference between two measured quantities of heat. If these quantities are large, the errors in the enthalpies of transition or fusion may be correspondingly large. This may be regarded as a weakness of the drop method; however, this effect is partially cancelled by systematic procedure.

A. Cases for which the Drop Method is Unsuitable

The success of the drop method depends upon complete return to the same, defined, thermodynamic reference state after each measurement. The method inherently involves the rapid cooling of the sample. Sometimes, during cooling, a sample fails to complete a solid–solid transition or fails to completely crystallize upon returning from a fused state. If the calorimeter is normally precise, such cases will usually make themselves known through

lack of precision or through continued heat evolution to the calorimeter over a longer period of time than usual (sometimes over a period of many hours). If the time is too long or the results inconsistent, the drop method is unsuitable and must be abandoned. If the behavior is consistent and measurable, the difficulty may be resolved through use of auxiliary calorimetry such as solution calorimetry by which enthalpies are referred to a desired reference state.

Particularly uncertain are drops from the liquid state if the solid-composition line is not vertical. Changes of composition of solid phases will occur upon cooling, with resultant indefinite final states. Such cases can usually be predicted if phase diagrams are available.

II. The Furnace

Invariably the furnace involves a vertical cylindrical core surrounding the sample. Sometimes the core is heated by means of its own electrical resistance, but more commonly through the electrical resistance of one or more suitable wire windings on it. Sometimes at the higher temperatures inductive heating is used instead.

Reference may be made to published descriptions of some of the furnaces designed specifically for drop calorimetry. Important contributions to precision in operation were made by White[36, 37]. Southard[33] described a wire-wound furnace suitable for use up to 1500°C. His design has been used and described more fully by Kelley, Naylor, and Shomate[19], and its essential features have been adopted by numerous other investigators, such as Ginnings and Corruccini[16] The U.S. National Bureau of Standards[6] improved the temperature profile of a furnace for use to 900°C by means of thick silver tubes surrounding the core. Nickel was used for the same purpose by Oriani and Murphy[28], Dworkin and Bredig[3], Gilbert[7], and others. Graphite was used for this purpose for the temperature range 900–1650°C by Lucks and Deem[24]. Douglas and Payne[2] have presented design calculations for a furnace operating up to 1500°C. Fomichev, Kandyba, and Kantor[5] used a solid tube of platinum as a resistance heater, and nickel tubes to equalize the temperature. These last workers also describe a vacuum furnace for the range 900–3000°K with a graphite heater, together with a system of coaxial graphite and metal shields. Levinson[23] used a graphite resistance furnace for measurements in the range 1000–2400°C. Olette's[27] furnace follows the design of Southard's[33], but gives measurements to as high as 1900°C. The furnace of Kirillin, Sheindlin, and Chekhovskoi[20, 21] is heated by tungsten windings and has been used up to 2400°C. Hoch and Johnston[12] have described a furnace in which the sample is heated by radio frequency induction in the temperature range 700–2700°C.

1. *Furnace design and operation*

In designing and constructing a furnace, ease of operation and ready access for repairs are certainly important (along with superior performance) if the purpose of the undertaking is a satisfactory rate of production of a body of data. For example, the ability to easily swing or hoist the furnace away from the calorimeter is an advantage. It is convenient to be able to exchange heater windings and thermocouples without disturbing other parts. Easy and

rapid return of the specimen from the calorimeter to the furnace and readying conditions for a succeeding measurement deserve consideration.

A. General Type of Furnace Most Commonly Used

Most accurate drop calorimetry to date has been performed with wire-wound, resistance-heated furnaces at temperatures of 1500°C or lower. The cross-section of such a furnace is diagrammed in *Figure 1* and may be considered typical. However, the following discussion will present several alternative features.

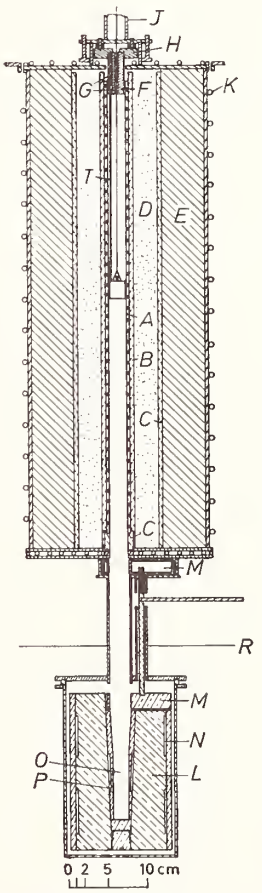

Figure 1. Diagram of furnace and copper-block calorimeter

A, Alumina winding tube
B, Alumina tube
C, Mullite
D, Alumina powder
E, Magnesia brick
F, Refractory plug
G, Porcelain tube
H, Stainless steel holder
J, Brass dropping tower
K, Copper cooling coil
L, Copper block
M, Gates
N, Resistance thermometer
O, Receiving "well"
P, Heater
R, Oil level
T, Thermocouple

(*1*) *Materials of Construction.* For operation up to 1500°C, the furnace core (or cores, if there are two or more coaxial ones) is usually a tube of alumina. The core, *A*, shown in *Figure 1* (inside diameter 2·5 cm, wall thickness 0·5 cm, length 58 cm) is a porous tube made of alumina. It is sometimes desirable to pass an inert gas through the core, partly to prevent oxidation of the heater winding, sample container, or suspension wire. This protection is not essential when platinum (or platinum–rhodium alloy) is used throughout for these purposes.

The top and bottom plates of the furnace shown are of ordinary steel plate. The outside boundaries of the furnace are water-cooled through use of copper tubing. This is mainly for convenience, so metal sheet all around should be satisfactory. If metal sheet is used, stainless steel is recommended. The furnace pictured is disengaged from the calorimeter by means of a hand-operated, geared hoist (not shown).

The bottom of the alumina core fits into a short section of mullite tube which in turn fits into a recess in the bottom plate of the furnace. This arrangement serves to center the core. No centering device is used for the top of the furnace; the furnace packing material serves to hold it in place. However, some workers have found it convenient to silver-solder stainless steel rings to the top and bottom plates.

Surrounding the alumina core and fitting closely to it is a second tube of alumina, *B*, 0·6 cm thick. About midway in the insulation space is located a tube of refractory mullite, *C*, and the space inside it is packed with pure alumina powder. The repair and replacement of the furnace winding is easily accomplished with this arrangement. The space outside the mullite tube is filled with magnesia brick.

As an alternative, the insulating space between the core and the outside container may be occupied by several concentric, highly polished metal cylinders which serve as radiation shields.

(*2*) *The Heaters.* Although a furnace may be heated by passing an electric current through a conducting core, the electrical resistance of the core must be relatively high unless very large currents are used, requiring unusually large or water-cooled leads. This difficulty is usually avoided by passing the heating current through a wire which may be wound on the furnace core.

The main requirement of the heater is that it surround the sample with a region whose temperature varies as little as possible so that the mean temperature of the sample may be ascertained accurately. Constancy of furnace temperature implies a steady state in which the heat losses are balanced by the output of the heaters. A variation of the heating current by 1 per cent will vary the steady-state temperature of the furnace by approximately 20° in the neighborhood of 1000°C, an example which illustrates the fact that approximate constancy of furnace temperature depends more upon the thermal inertia (large heat capacity) of the furnace than is often realized.

The furnace power is nearly always supplied by one or more heaters wound on the core, which may be purchased with grooves on the outside for uniform heater spacing. Frequently more power is supplied to the ends of the core than the middle to compensate for the heat losses from the top and bottom of the furnace. This may be accomplished by shunting part of the

current from the center portion of a single winding or by having three separate windings with independent controls. In practice, the center heater usually extends over the middle 65–80 per cent of the core. Care must be taken that the temperature profile of the furnace does not have or develop unwanted humps or hollows. Although a single winding has a narrower constant-temperature zone, it is free from this defect.

When massive cores are employed *within* the main heaters, additional secondary heaters are advisable to prevent temperature lags and to aid in controlling the core temperature. These heaters may be wound around a separate core immediately surrounding the sample, or if the massive core is a sufficiently good heat conductor, be located within the conductor itself. The use of the secondary heaters can be more important if automatic temperature control is employed.

Power is conveniently supplied by means of variable autotransformers. If more than one heater section is used, it is advisable to feed each section by its own transformer.

Nichrome (Ni–Cr 80:20) wire is used most often for heater windings at lower temperatures. It has a fairly low temperature coefficient of resistivity, but cannot be used in air much above 1000°C because of excessive oxidation. Platinum–rhodium windings are suitable for continuous use up to about 1500°C, but in air they deteriorate rather rapidly above this temperature. Platinum containing 10 per cent rhodium has about three times the resistivity at 1500°C as at room temperature, but this is no real disadvantage. Platinum containing 20 per cent rhodium is sufficiently flexible for winding on the core if annealed; its advantage is mainly a slightly higher melting point. For still higher temperatures a more refractory winding is needed. Lucks and Deem[24] used molybdenum windings up to 1650°C, surrounding the wire with a protective atmosphere. Main heater wire should not be too fine, because of decreased mechanical strength and shorter life. A diameter of from 0·05–0·1 cm has been commonly used. Care should be taken to wind the heaters firmly and uniformly.

The single-winding heater used in the furnace shown in *Figure 1* is made up of 58 ft. of *B* and *S* No. 18 (diameter, 0·1 cm) platinum containing 20 per cent rhodium on the spirally grooved alumina core. AC power is supplied by means of a voltage stabilizer and two 7·5 kVA variable autotransformers in series. This scheme permits sensitive manual control. The power consumption at 1500°C is about 1700 W.

(*3*) *Heat Transfer and Temperature Gradients*. Despite the practical importance of enthalpy measurements at high temperatures and the simplicity of the drop method, the results of different investigators on the same materials have often varied by several per cent. This type of calorimetry is thus seen to be less developed than techniques at low temperatures. The principal reason for disagreement undoubtedly lies in measuring the sample temperature in the furnace. The singly wound furnace shown in *Figure 1* provides an axial temperature gradient of less than 0·1 per cent of the temperature (Celsius) per inch over the range 100–1500°C. Refinement may be made to improve and lengthen this 'hot zone'. The use of multiple heaters (Ginnings and Corruccini[10]) provided a few tenths of a degree per inch at 1100°C in a furnace 46 cm long. The use of innermost, heat-distributing tubes of

silver provided the U.S. National Bureau of Standards[6] with virtually no temperature gradient within the masses of silver. This furnace is fully described in a subsequent section. Fomichev *et al.*[5] used nickel tubes and obtained a precision of measurement of 0·1° up to 1500°K.

It is desirable to reduce the temperature difference between the inner furnace wall and the sample as much as possible. This is particularly important if the temperature of the sample is measured by means of a thermocouple whose junction is attached to the wall. Also, the presence of a gas surrounding the sample (a few mm Hg suffices) will minimize the wall-to-sample gradient, as will fusing the sample in its container if this is possible. Heat transfer between the container and wall is increased by reducing the gap between them. Consideration should be given also to the heat-transfer coefficient of the gas to be used in the furnace. When the conditions are favorable and the nearly isothermal part of the core is not too short, the sample will radiate an insufficient amount of power from the bottom of the furnace to invalidate its temperature measurement.

B. Furnaces with a Good Heat-Conducting Core

A good heat-conducting core is provided by a material of high thermal conductivity and by using a large cross-section of the material. The result is an unusually large total heat capacity. The major consequences in the performance of the furnace compared with that described in Section II-1-A are, first, that axial temperature gradients and errors in measuring the sample temperature can be made smaller or alternatively that they can be made equally small with considerably less effort, and second, that the inertia of the furnace to temperature change becomes so large that the temperature can easily be kept constant to 0·01° or better by simple control by hand.

A few examples of such furnaces and their major differences from the more commonly used type will be discussed. The U.S. National Bureau of Standards[6] constructed a furnace having a core of silver, which is resistant to corrosion, has the highest thermal conductivity of any metal, and can be used up to its melting point, 962°C. A cross-section of the furnace is shown in *Figure 2*. The main furnace heater was made in three separate sections corresponding in elevation to the three silver cylinders, *J*, *K*, and *L*, which were located inside the alumina. The silver cylinders are supported and separated by porcelain spacers, *Y*, having a far lower thermal conductivity than silver, so that the end silver cylinders, *J* and *L*, need to be maintained at a temperature no less than a few tenths of a degree of that of the central silver cylinder, *K*, for the gradients in cylinder *K* to be negligible. Coaxially with the silver and porcelain cylinders are Inconel tubes which enclose the sample container, *D*, with its suspension wire and shields, *S*. Helium flows upwards past the container and escapes from a small orifice at the top. (Care must be taken that cold air cannot fall into the lighter helium in the furnace.)

Figure 2 shows some of the vertical holes, *N*, drilled through the silver and porcelain and placed 90 degrees apart azimuthally. These holes contain the platinum resistance thermometer, the platinum–rhodium thermocouple, and the differential thermocouples between the end silver cylinders, *J* and *L*, and the central cylinder, *K*. In one of these holes are placed three small

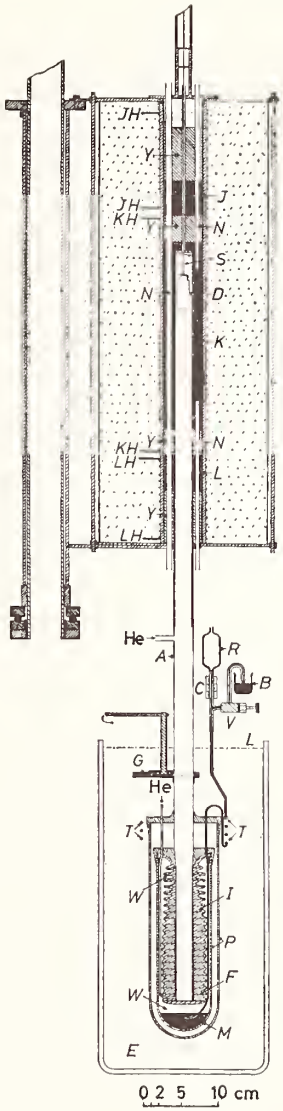

Figure 2. Diagram of silver-core furnace and ice calorimeter

A, Calorimeter "well"
B, Beaker of mercury
C, Glass capillary
D, Sample container
E, Ice bath
F, Copper vanes
G, Gate
I, Ice mantle
M, Mercury
N, Inconel tubes
P, Pyrex vessels
R, Mercury reservoir
S, Platinum shields
T, Mercury "tempering" coil
V, Needle valve
W, Water
Y, Porcelain spacers
JH, KH, LH, Furnace heater leads
J, K, L, Silver cylinders

secondary heaters, running parallel to the axis of the furnace and located at the elevations of the three silver cylinders. The temperature of the silver responds to sudden changes in the main-heater currents in 3–6 min, but to changes in the secondary-heater currents almost completely within 1 min. For furnace insulation, powdered silica (Silocel) is used.

The operation of the furnace is normally limited to 900°C, to provide a margin of safety against melting the silver, and a thermocouple-reading meter (Sym-ply-trol) monitors each silver cylinder to shut off the heating current automatically should the temperature accidentally become a few degrees higher. A fourth such monitoring device shuts off the heating currents if the platinum resistance thermometer is in place and the furnace temperature exceeds about 625°C.

Some investigators have accomplished the same objectives by using copper instead of silver. Pure copper has a higher melting point (about 1083°C, but it has been reported that dissolved oxygen can lower the melting point by as much as 20°); however, at all except relatively low temperatures the copper must be protected by an inert atmosphere. Other investigators have replaced the silver by nickel, which has only about 20 per cent of the thermal conductivity of silver but still provides a similar advantage; the nickel has a still higher melting point, but must of course be protected from excessive oxidation. Lucks and Deem[24] have used a silver furnace of the above design up to 900°C, separating the silver cylinders by alumina spacers. From 900–1650°C they used a similar furnace in which the silver was replaced by graphite and the alumina by refractory brick; the graphite was protected from oxidation by an atmosphere of 95 per cent argon–5 per cent hydrogen.

C. Furnaces Operating Above 1500°C

Although a relatively small amount of enthalpy data above 1500°C has been reported, designs of several calorimeters have been published for measurement to as high as 3000°K. The furnaces for two of these calorimeters will be described briefly.

Hoch and Johnston[12] have designed a furnace to be used in drop calorimetry to 3000°K. The sample is heated inductively, the radio frequency being supplied by a 20 kW General Electric RF generator through a "work coil" consisting of water-cooled, 0·25 in copper tubing. The sample, heated in the center of this "work coil", is suspended by means of a tantalum wire. The tantalum wire is attached to an iron cylinder which is held in place by an external electromagnet. This arrangement provides a dropping mechanism for the sample. Thus, the furnace is essentially a vacuum-tight shell containing the coil and sample. The sample temperature is measured by sighting holes in the sample container with a disappearing-filament optical pyrometer. The furnace and attached calorimeter are sealed vacuum tight with O-rings and the system is evacuated with an oil diffusion pump. A small amount of helium is introduced after dropping the sample to facilitate heat distribution. The furnace walls are wound on the outside with copper tubing. The tubing is used to help degas the furnace when heated by steam and then to cool it during a run. The furnace is about 34 cm long and 25 cm in diameter.

Fomichev *et al.*[5] describe a furnace for use at 1000–3000°K. Heating is

accomplished by means of a graphite tube with an internal diameter of 4·5 cm, a length of 60 cm, and a wall thickness of 0·3 cm. Electrical contact is made with water-cooled flanges of copper or brass. These flanges are attached to springs to allow for expansion of the graphite tube. The heater is surrounded by nine coaxial shields; the first is made of graphite, the second and third of tantalum, the fourth, fifth and sixth of molybdenum, and the remaining three of stainless steel. All outer surfaces of the furnace are water-cooled. In addition, two water-cooled screens are provided above the top and below the bottom of the central furnace openings. These screens can be moved to one side by means of bellows. Temperature is measured by optical pyrometry, utilizing a reflecting prism which is located along the central axis and between the sample and the calorimeter. The prism is moved out of the way with a bellows. All parts of the apparatus are vacuum-tight, and different parts may be sealed off so that samples may be placed in the furnace without disturbing the furnace temperature. The sample is suspended in the furnace by a 0·1 mm tungsten wire which is melted to release the sample. An inert gas (at a pressure of 10–20 mm Hg) is used during the measurements, as it improves the general performance. Power is supplied through stepdown transformers. At 3000°K the power consumption is 40 kW.

D. Automatic Temperature Control of the Furnace

The two furnaces illustrated by *Figures 1* and *2* use manual control of heaters. The resulting temperature fluctuations are well within the limits of other uncertainties involved in the measurement of the sample temperature. Manual control satisfactorily provides for the "over-shooting" necessary for overcoming the thermal lag of the furnace parts, thus providing a quicker approach to thermal equilibrium. Automatic controls have been found to be of limited value for these furnaces.

The detailed treatment of automatic-control instrumentation can be found elsewhere. Specific applications to calorimetry are discussed in Chapters 5 and 9. A few general comments may be made here relating to automatic stabilization of furnaces in drop calorimetry.

The important point is to have the response time between the sensing element and the heater it controls as small as practicable. This sensing element may reflect the temperature of a point or the temperature of a region. The former may be sensed by a single-junction thermocouple, the latter by a multiple-junction thermocouple or an element whose electrical resistance varies sufficiently with temperature. When the furnace winding is of platinum–rhodium, the temperature coefficient is such that its resistance may be used as the temperature-sensing element.

Furnaces with low thermal inertia, such as those using reflection shields, are more sensitive to small current changes and are best served by automatic control devices. Furnaces with massive metal inner tubes are very sluggish to temperature change and will benefit least from automatic controls.

The response of the best controls on the market is dependent on three factors. Briefly, they are: how far the temperature differs from the desired value, how long it has been so, and how fast it is changing. If the refinements of control are adequate for the time-lag of response, the major remaining

problem is likely to be securing a wide enough range of control to handle all likely variations in heater power and furnace heat losses.

2. *Temperature measurement*

A. The Thermocouple

The most common temperature-measuring device up to 1500°C has been the thermocouple. Some base-metal thermocouples (such as Chromel–Alumel and iron–constantan) have the appeal of large sensitivities. However, with modern potentiometers reading to one microvolt or less, this sensitivity is not needed, and for the most accurate work, the base-metal thermocouples are not preferred over the more stable Pt *versus* Pt–Rh thermocouple.

Thermocouples of 94 Pt–6 Rh *versus* 70 Pt–30 Rh[38] and 80 Pt–20 Rh *versus* 60 Pt–40 Rh[15] have the advantage of maintaining their calibrations for comparable periods of time at temperatures some 300° higher than the conventional Pt *versus* 90 Pt–10 Rh couple. Additional investigation of these and other thermocouples particularly adapted to high temperatures may recommend them for measurement in calorimetry. At the present time the reliable Pt *versus* 90 Pt–10 Rh thermocouple (or the Pt *versus* 87 Pt–13 Rh thermocouple) is the best for accurate work. This couple shows very little change up to 1200°C, and can be used up to about 1500°C with frequent calibrations. Roeser and Wensel[34] have stated that with favorable calibration the uncertainty in interpolated values of temperature should be as small as 0·3° near 1100°C and 2° near 1500°C.

(1) *Calibration.* Details of thermocouple calibration *outside* the furnace are dicussed in Chapter 2. The ideal Pt *versus* 90 Pt–10 Rh thermocouple is completely homogeneous and free from strains so that its reading depends solely on the temperatures of its junctions. As the thermocouple is used, the e.m.f. changes are mainly due to diffusion through the junction and to oxidation. These effects can be made negligible if the working couple is frequently calibrated *in situ* in the furnace. Calibration below the point of thermocouple deterioration (about 1500°K) may be accomplished by comparison with a calibrated thermocouple. A special method of calibration makes the comparison with the hot junction of a "standard" thermocouple firmly attached (preferably in a well) to the sample container which is hanging in place in the furnace.

Otherwise calibration *in situ* at one temperature is generally made by melting a short length of gold wire (at least 1 mm) welded between the elements of the thermocouple. The e.m.f. at the melting point corresponds to the halt in the temperature rise. The assumed temperatures of all fixed points used for thermocouple calibration should be stated because such information has sometimes permitted later revision of old data to a basis closer to the true thermodynamic temperature scale. Roeser and Wensel[34] report that in most cases curves of differences between actual thermocouples and standard reference tables are linear over the entire range 0–1700°C.

The use of Pt *versus* 90 Pt–10 Rh thermocouples above about 1500°K necessitates frequent recalibrations. It has been found that, in typical circumstances, the rates of change per 3 h of heating in an oxidizing atmosphere are about 0·2° at 1600°K, 0·4° at 1700°K, and 1·0° at 1800°K.

(2) *Common Sources of Thermocouple Error.* The temperature measurement of the sample suspended in the furnace requires that the thermocouple junction and the sample be at the same temperature. Further, the temperature gradient of the thermocouple along the leads to the junction should be small. In the furnace shown in *Figure 1*, the thermocouple leads are brought into the furnace through a 5 cm-long refractory plug, *F*, by means of porcelain tubes, *G*. The plug is made of zirconium silicate tubing for high thermal shock resistance. The porcelain tubes are fixed in position with alumina and cement. The thermocouple leads run along near the furnace wall to the sample container. The junction touches the top wall of the suspended container at temperatures below 800°K, and it is placed within 1 mm of the top above this temperature to prevent welding or other interaction between the two surfaces. Proximity of the leads to the solid parts of the furnace is highly desirable to prevent conduction into or away from the junction; a similar result can be achieved by welding the junction to a band of a highly conducting metal such as platinum which lies firmly against the inside wall of the furnace. The problem here is the difficulty in making frequent calibrations of the couple. If, as is normally to be expected, heat is being conducted *away* from the junction, an error from this effect will result in an enthalpy that is too high. This error is equivalent to associating the net enthalpy of the sample with a furnace temperature that is too low, and in this sense the same effect in the empty-container run affords no compensation. The furnace of *Figure 2* has its thermocouple tubes inserted directly into the thick inner wall of silver.

A possible source of error in thermocouple readings may arise if there is electrical leakage from the heaters. The heaters are usually operated with a.c. to minimize this, but such errors might arise from some rectifying effect in the insulator materials. Momentary shutting off of the furnace power is the standard technique for testing this source of error. Other sources of error are contamination through container leakage and contamination from impurities in the insulating inlet tubes.

When differential thermocouples are used, leads to the outside should be of platinum rather than platinum–rhodium to avoid changes of composition arising from passage through regions of large temperature gradients.

B. Use of Other Temperature-Measuring Instruments

Even at the lowest furnace temperatures, the error in temperature measurement with a thermocouple may easily be as much as 0·1°C. The platinum resistance thermometer defines the International Practical Temperature Scale up to 630·5°C and, because an accuracy between 0·01° and 0·1°C is not difficult to obtain with it, may be substituted in this temperature range. If the thermometer uses mica for insulation, as has been customary in the past, it cannot be used for higher temperatures. The thermometer must be encased in some material which does not soften at the highest temperatures of use and at the same time allows a snug fit inside a solid part of the furnace so that conduction along the leads is not a source of appreciable error. Such a mica-insulated thermometer, encased in 90 per cent Pt–10 per cent Rh, has been used in the silver-core furnace at the U.S. National Bureau of Standards[6]. This thermometer had an ice-point resistance of about the

conventional 25Ω, which is better than thermometers of much lower resistance that have been constructed. Periodic reading of the ice-point value, particularly after the thermometer has been to its highest temperatures, is highly desirable to detect the need for recalibration. If the resistance element becomes stretched, readings at all temperatures should be displaced by the same percentage as at the ice point. However, if other changes occur, *e.g.* through contamination of the platinum, the readings at all temperatures may tend to be changed by more nearly the same *amounts* as at the ice point.

If a platinum resistance thermometer and thermocouple are both used in the furnace, it becomes possible not only to calibrate the thermocouple by the thermometer (up to 630°C) or to compare their independent calibrations, but also to compare them regularly as a means of detecting any large, otherwise unsuspected, change in the calibration of either measuring instrument. Compared with a thermocouple, a platinum resistance thermometer has the disadvantages of slower response to temperature changes (offset by the temperature sluggishness of a massive core), and difficulty in construction, particularly in mounting and insulating the long fine wire.

The optical pyrometer is usually used to measure furnace temperatures above the range of Pt–Rh thermocouples. It affords less precision than the Pt *versus* 90 Pt–10 Rh thermocouple, but has the advantage that it defines the International Practical Temperature Scale above 1063°C.

3. *The sample in the furnace*

A. The Container

(1) *Choice of Material.* The choice of a suitable container material is usually not difficult at lower temperatures, but it well may be the greatest single factor hindering the extension of data to higher temperatures. Important considerations for container materials are mechanical strength, melting point, emissivity, reactivity, and reproducibility of their thermodynamic states.

The most common factor limiting the choice of a suitable container material is reactivity with the sample, through either chemical reaction or miscibility. If the container is exposed to an oxidizing atmosphere, this is also a factor. A useful generalization is that a metallic sample is more likely to be inert to a non-metallic container and vice versa. Since reactivity often varies greatly with temperature, a calculation or estimation of the free energy changes of all possible reactions is often useful. Platinum–rhodium (10 or 20 per cent) most generally satisfies the requirements for a metallic container to about 1500°C. Gold and silver have similar advantages below their melting points (1063° and 962°C). The high purity and reproducible state attainable with these metals allow container replacement with no appreciable change in enthalpies. If a non-metallic container is needed silica glass has frequently been used. Devitrification to cristobalite above 1300°C limits its use to about 1450°C.

Measurements above 1500°C are sparse, so that container information is also lacking. Tantalum has been used to 2600°C and tungsten to 2500°C. Graphite, surrounded by a shell of metal to improve the radiation characteristics or to afford an extra seal against possible escape of the sample, could sometimes be used. It must be recognized that in many cases a high container enthalpy will have to be tolerated.

In the absence of any suitable container material, the problem has been solved by using the sample itself in mechanically cohesive form. In this case the heat lost in the dropping process must be estimated or else determined by varying the ratio of mass to the surface exposed. Beryllium oxide was measured to 2200°K[16] by using a sintered sample of BeO surrounded by a 0·2 mm-thick sheath of molybdenum metal which protected the sample from excessive heat loss and provided a hollow for temperature measurement.

Many laboratories have adopted transition-metal or base-metal containers for use to moderately high temperatures. The ready availability and workability of these metals and alloys have made them a logical choice. However, it is wise to avoid the use of alloys that undergo transitions during cooling. If the degree of transformation and the consequent heat evolved are the same in measurements when empty and when full, the transition cannot cause any error. However, with a full container the slower rate of cooling *can* result in the evolution of more of the heat of transition. The net heat attributed to the sample is consequently too high. Ginnings[8] has critically examined three sets of drop calorimetry data involving containers of Nichrome V (80 Ni–20 Cr) and stainless steel, types 430 and 446, all of which undergo transitions between 500° and 700°C. He detected abrupt increases in the enthalpy–temperature functions derived for the samples from the measurements and showed that, by attributing the effect to the above cause, the data above the transition temperature became much smoother. The enthalpy correction in these cases ranged from 0·05–1·8 cal/g of sample and lowered the calculated heat capacities by 0·3 to several per cent.

(2) *Container Design; Enclosing the Sample.* The container is usually cylindrical and has a capacity of the order of 10 cm^3. The capacity is determined primarily by the requirements of the receiving medium after the drop. The wall thickness of metal containers is usually 0·2–0·3 mm, but a thicker wall is needed for non-metallic containers.

Five designs of sample containers are shown in *Figure 3*. *Figure 3*(*a*) shows a single cylinder with snug-fitting end caps. When made of a base metal, the edges can be sealed by induction welding if gas-tightness is needed, with the sample remaining cold and surrounded by any desired gas. If the container is of noble metal (Pt–Rh, Au, or Ag) the edges can be welded with a gas–oxygen torch. *Figure 3*(*b*) shows a variation used by the U.S. Bureau of Mines in which the top is connected to a narrow neck. After the sample has been introduced, the container may be evacuated and filled with helium gas. The neck may be pinched shut near the top and sealed gas-tight by gas–oxygen welding. A container sealed in this manner will usually remain so to 1500°C. If volatility during welding is a problem, the neck can be sealed shut by gold soldering; this, of course, limits the measurements to temperatures below the melting point of gold. In extreme cases of volatility, placing the container in a shallow dish of water keeps the temperature down during the soldering process.

Figures 3(*c*) and *3*(*d*) show two containers closed by hard metal cones against gold gaskets. These have been used extensively at the U.S. National Bureau of Standards, container in *Figure 3*(*c*) being of Nichrome V, and container in *Figure 3*(*d*) being of Monel for measuring hydrocarbons up to 20 atm vapor pressure. The threads of the screw cap are pre-oxidized to

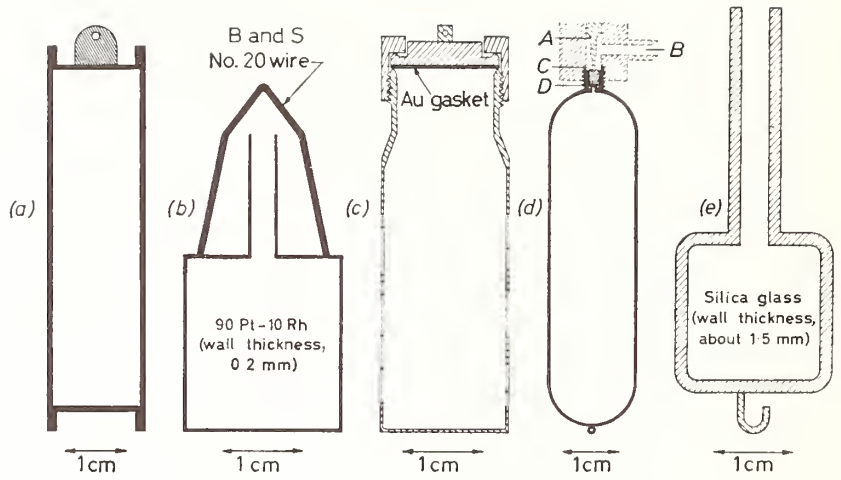

Figure 3. Designs of sample containers
a, Of base or noble metal and with welded end-caps
b, Of 90% Pt–10% Rh, sealed by welding or soldering
c, Of Nichrome V (80% Ni–20% Cr), sealed by a gold gasket
d, Of Monel, sealed by a gold gasket *D* (for volatile liquids) (filling device: *A*, screw driver; *B*, filling tube; *C*, tin gasket)
e, Of silica glass, sealed by welding

prevent sticking by self-welding at high temperatures. Such mechanical closure is convenient, but gas-tight seals are difficult to maintain.

Figure 3(e) shows a type of silica glass container. Upon filling, the tube is attached to a vacuum pump and "pulled off" with a hydrogen–oxygen torch close to the body of the container, retaining the vacuum inside.

Accurate knowledge of the masses of sample and container materials is especially important because the series of runs could have a high inter-consistency that would not reveal large constant or systematic errors in mass. A simple test for a gas leak in the container is to pump around it, then surround it with air one time and helium (or hydrogen) another; with a few cubic centimeters of gas space inside, the difference in weight when there is a leak is easily detectable.

B. Suspending and Dropping the Sample

(1) *Suspension and Dropping Mechanisms.* The sample is suspended in the furnace by means of a suitable wire, the kind and diameter of which depend upon the temperature and the load. Platinum–rhodium (10 or 20 per cent) has commonly been used up to 1500°C. Diameters range between 0·1 mm and 0·4 mm. Tungsten and tantalum have been used at higher temperatures. Southard[33] and many later investigators left the suspension wire attached to the container as it fell into the calorimeter, enabling easy return of the sample to the furnace. The enthalpy of the wire is assumed to cancel out in the measurements of the container when full and when empty. The other common procedure is to melt or cut the wire. One investigator used a magnetic release[12]. Another had an arrangement whereby the wire was made to slip off the container[4].

The presence of two or three thin circular disks of bright platinum attached to the suspension wire just above the sample will reduce radiation losses out of the top of the furnace. In the furnace shown in *Figure 2* such shields are more important in preventing serious heat losses by convection from the hot sample out the calorimeter[10], because there is only one gate and it must be outside the calorimeter proper to dissipate radiation from the furnace. However, in the furnace shown in *Figure 1* the lower gate is inside the calorimeter and therefore prevents such losses of heat from the sample.

If the sample falls unattached into the calorimeter, the impact with the calorimeter may be cushioned by falling on to a deformable body. Southard's procedure of leaving the entire suspension wire attached includes the use of a heavy metal plunger which, attached to the suspension wire, falls through a vertical tube above the furnace. Through the use of holes in the tube there is nearly free fall until the plunger reaches a position corresponding to the point where the sample has entered the calorimeter, when it is slowed by an air cushion. The air escapes through a small hole in the tube near the bottom of the plunger travel. The entire fall (including deceleration) takes less than 0·5 sec. To minimize stretching of the suspension wire, Douglas and Payne[2] arranged for the container to decelerate uniformly at the end of the fall by stretching a pre-set spring that had a stop at the end of the fall.

The addition of weights to the plunger when the empty container is used (to keep the total falling mass constant) will help to prevent a systematic error between the full and empty experiments. It is more important to minimize friction within the plunger tube in order to approach as nearly as possible the acceleration of free fall. Ginnings and Corruccini[10] have estimated that in free fall at 900°C, a typical container with sample would lose not more than one calorie more than the empty container.

(2) *Time in the Furnace.* The length of time that the sample is in the furnace is important and varies with the conductivity and size of the sample. A simple test for temperature equilibrium is to compare several experiments with different times in the furnace and then to select a time which is clearly adequate. Under conditions such that the sample is heated mainly by conduction, it may be shown that approximately

$$k = t/\log_{10}[q_0/(q_0 - q)] \qquad (1)$$

in which q is the heat found with time t in the furnace, q_0 is the heat when the time is adequate for reaching virtual equilibrium, and k is a constant representing the time for the temperature difference between the furnace and sample to be reduced to 10 per cent of the original value. A time in the furnace can then be adopted of at least $4k$, since according to equation (1) this time brings heat transfer to the sample to within 0·01 per cent of completion. Actually, the contribution of radiation to the heating of the sample increases rapidly with temperature, with the result that the use of equation (1) gives an upper limit to the time required in the furnace at higher temperatures.

Additional factors, such as proximity to temperatures of melting, transition, or other complex structural changes, may make equation (1) unsuitable.

III. The Calorimeter

1. *The isothermal calorimeter*

An isothermal calorimeter absorbs or evolves heat without a change in temperature, and the amount of heat is measured by an accurately measurable change in some quantity such as volume. Although calorimeters involving vaporization are more sensitive, those involving fusion (particularly of ice) have been more commonly used in drop calorimetry. If the volume change is determined from the mass of displaced mercury, the ratio of heat absorbed to the mass of mercury (K, the calibration factor of the calorimeter) is given by

$$K = \Delta H_m/(v' - v)d_{\mathrm{M}} \tag{2}$$

in which ΔH_m is the enthalpy of fusion of the melting substance per unit mass, v' and v are its specific volumes in the less and more dense states respectively, and d_{M} is the density of mercury (all at the calorimeter temperature).

Compared with other calorimeters, the isothermal type has certain advantages and disadvantages well exemplified by the ice calorimeter. Its calibration factor is a universal constant, no temperature or electrical measurements are required in its operation, and when surrounded by an ice bath the heat leak can be made very small and quite constant. However, such a calorimeter is restricted to use at a fixed temperature and must be completely leak-free and so rigid that its volume capacity is extremely constant. The isothermal type of calorimeter is not inherently more precise nor more accurate than the best of the other types, and its construction for accurate work requires a fair amount of time and care; but once properly built, it can yield measurements rapidly and accurately by relatively simple operation.

In this chapter detailed discussion of the isothermal calorimeter will be limited to the ice calorimeter. Isothermal calorimeters employing organic liquids in place of water have also been used. The diphenylether calorimeter, which has been applied to the determination of the enthalpy of metals[14] as well as in reaction calorimetry, differs from the ice calorimeter principally in operating at a higher temperature (26·87 °C), expanding during absorption of heat, and being over three times as sensitive.

A. Design of the Ice Calorimeter

A cross-sectional diagram of an ice calorimeter which has been in use in high-temperature drop calorimetry at the U.S. National Bureau of Standards for many years[6] is shown in the bottom half of *Figure 2*. The calorimeter "well", A, which receives the sample from the furnace, is constructed of some low-thermal-conductivity metal such as Nichrome, with a wall thickness of approximately 0·25 mm. (The slight taper in the tube shown in *Figure 2* is really unnecessary.) The hot sample comes to rest near the bottom of the well, and conduction of unmeasured heat out of the well is negligible. Dry gas (He) flows slowly up the well at all times to keep out moisture, and the top of the well is stoppered loosely when not attached and sealed to the furnace.

The well is really in two sections joined by a gate, *G*, which is opened briefly to admit the sample but otherwise shields the calorimeter from radiation from the hot furnace. The gate is a tinned copper disk with a hole and a wide-angle slot which moves the sample and its suspension wire to the side of the well when the gate is closed after dropping in the sample.

Around the bottom end of the calorimeter well are two coaxial cylindrical vessels, *P*, the inner one enclosing the "calorimeter proper" and the outer one constituting the calorimeter jacket. These vessels are commonly of Pyrex glass to permit visual observation as ice is being frozen; however, to reduce somewhat the heat transfer by radiation between them, some experimenters have silvered the surfaces except for a narrow vertical strip.

The two glass vessels are attached at their tops to metal "caps". At the U.S. National Bureau of Standards the outside top of each glass vessel was first ground to true roundness, and the seal to the metal was then made with a thin intervening layer of Apiezon W wax. If the wax layer is too thick, the calorimeter may sag or fall apart when allowed to warm up, but the thickness of the hard wax must be several times the difference in shrinkage of the glass and the metal when cooled. In one case[2], the wax gap was successfully reduced to 0·15 mm by using a low-expansion iron alloy called "Therlo" (29 per cent Ni, 17 per cent Co, 0·3 per cent Mn), which, however, must be protected against corrosion. Some experimenters have replaced the wax joints by less fragile seals. Leake and Turkdogan[22] interposed a winding of string impregnated with Araldite synthetic resin, with compression by a screw collar outside the metal flange. Glass-to-metal seals[28] and O-rings have also been used.

Figure 2 shows a series of horizontal copper disks or vanes, *F*, which provide good heat paths inside the calorimeter vessel. These disks are conveniently separated by short metal sleeves. In soldering this assembly to the well and subsequently tinning or silver-plating the surfaces to render them inert to water, it is believed desirable to avoid all narrow crevices which might be filled to an irreproducible extent by the water in the calorimeter.

Several experimenters have provided the top metal cap of the calorimeter vessel with a filling tube to introduce the water or replace it. Such a tube (necessarily closed at the top) entails the danger that during the freezing of an ice "mantle", *I*, the water in it may freeze solid at the level of the cap and burst the tube owing to the expansion accompanying freezing. The use of only one opening to the outside (the "mercury inlet tube"), which normally is completely filled with mercury, obviates this danger. This inlet tube connects the mercury pool, *M*, in the calorimeter with the mercury accounting system (*C*, *B*, *V* and *R*) outside. The center portion, *T*, of this tube, wound around the outside of the outer metal cap, has preferably a capacity for as much ice-cooled mercury (perhaps 10 cm^3) as will ever enter the calorimeter in a single run. The ends of the tube, however, should be of smaller bore, partly to minimize the effect of varying room temperature on the volume of the mercury outside the ice bath. Since solder which would dissolve in the mercury must be avoided, one can use a single tube and draw down its ends.

The mercury-accounting system has two glass capillary branches, one

leading through a valve, *V*, to a weighed beaker of mercury, *B*, and the other (a capillary, *C*, of 0·6 mm bore which is preferably calibrated after assembly) being provided with a scale for observing small volume changes when the valve is closed. The capillary is sealed to a mercury reservoir, *R*, above. For the valve, a hard-steel needle seating *precisely* on soft steel gives satisfactory closure, but a rotationless stem and a softer seat (platinum or Kel-F) may be preferable[2]. Oriani and Murphy[28] substituted a precision-bore glass stopcock. The capacity of the valve must be small and reproducible because one cubic millimeter of mercury is equivalent to almost one calorie of heat.

The calorimeter heat leak can be made so small that it does not require frequent or accurately timed readings. The scale for the capillary outside the calorimeter is located some 20 cm above the mercury level inside the calorimeter so that the pressure head on the water in the calorimeter lowers its freezing point to approximately that of the air-saturated water in the ice bath outside, the heat leak therefore being conveniently small. Some investigators have evacuated the jacket space of the ice calorimeter to reduce heat leak. However, keeping the space filled with a *dry* gas (such as CO_2) at atmospheric pressure has the advantages of decreasing the net downward force on the inside (calorimeter) vessel and of making the volume capacity of the latter nearly independent of changes in atmospheric pressure.

In designing rigid mechanical supports for the calorimeter (not shown in *Figure 2*), some compromise must be made between low flexibility and low-conduction heat paths from the room to the calorimeter. It is also wise to provide sufficient adjustability to facilitate making the calorimeter well and the furnace core coaxial and strictly vertical.

Although modern techniques of thermoregulation permit control of the temperature of a bath to $\pm 0{\cdot}001\,^{\circ}C$, a simple ice bath, *E*, accomplishes the same result with no necessary temperature fluctuations and no instrumentation. If wax seals are present, it is convenient to replace the ice bath by circulated cold water during idle periods, but such a bath is likely to be inadequate to preserve any ice mantle present in the calorimeter.

B. Assembly

The two glass vessels are attached and tested for the slightest leak; a helium leak detector is convenient. Pure gas-free water, *W*, which must be kept in a closed system to prevent absorption of air, is then allowed to fill, by gravity, through the mercury inlet tube if no special filling tube has been incorporated, the dry and thoroughly evacuated inner glass vessel. Unless freezing is begun immediately, some mercury is then drawn into the reservoir to seal the calorimeter water from air.

A suitable amount of mercury is next substituted for an equal volume of water in the calorimeter by alternately freezing ice to expel water and melting the ice to draw in mercury in its place. A closed-bottom tube inserted into the calorimeter well can serve to hold crushed 'Dry Ice' (solid CO_2) to freeze an ice mantle or to contain a stream of warm water to melt it.

When the mercury level inside the calorimeter is above the bottom of the mercury inlet tube, one more ice mantle must be frozen, and this must be large enough to expel a combined volume of water and mercury equal to

the inlet-tube capacity plus the largest amount (30 cm^3 or more for the calorimeter shown in *Figure 2*) that will be expelled in freezing any future ice mantle. Owing to a lens effect, the ice mantle will soon appear to occupy the entire cross section inside, even when it is far from doing so, and an estimate of the total volume (and hence average diameter) of the ice present is far more reliably provided by the total volume of mercury that has been expelled.

High purity of the water inside the calorimeter is essential for calorimetric accuracy for two reasons. First, any dissolved gas forced out of solution by freezing would tend to redissolve slowly and in so doing vitiate the accurate volume determinations. Second, if the water is impure the calorimeter will absorb, without measuring, heat of the order of a calorie for every 0·001 °C that the calorimeter temperature rises as the ice melts. It is believed possible, however, to remove as much as 99·9 per cent of the dissolved air by a single fractional distillation of the water, and tests of electrical conductivity can be used to detect electrolytic solutes. The mercury used should be of very high purity. As long as the mercury is kept out of contact with metals which it dissolves, it can be separated from surface impurities by the usual process of fractional filtering and can be reused repeatedly in the calorimeter.

C. Calibration Factor

The calibration factor used for the ice calorimeter should not be a value calculated by substitution into equation (2), but one determined by direct electrical measurement. Nevertheless, the same calibration factor should be applicable to all precise ice calorimeters. The following electrically-determined values are "ideal" in the sense that they have been corrected to the basis of no pressure change through a change in the mercury level inside the calorimeter when heat is absorbed.

Ginnings and Corruccini[9], in an extensive investigation of optimum conditions, found 270·42 $\pm$ 0·06 abs. J/g Hg; and later Ginnings, Douglas, and Ball[11], using an improved ice calorimeter and more favorable conditions, found from about 100 determinations a mean value which, with a slight correction[6], is 270·48 $\pm$ 0·03 abs. J/g Hg. (The tolerances stated are estimates of absolute accuracy.) Leake and Turkdogan[22] later obtained a value of 270·54 abs. J/g Hg, with a standard deviation of $\pm$ 0·17. These values agree within their uncertainties, but the value of Ginnings, Douglas, and Ball is believed to be the most reliable.

D. General Procedure of Operation

For heat measurements, the first step is to freeze an ice mantle. There is usually more or less supercooling, so that the first ice appears suddenly, and may branch out so as to *appear* to fill the calorimeter. For precise calorimetry it is recommended that most of this initial ice be melted. A thin layer of ice in the top region of the calorimeter is needed to trap small amounts of heat that might otherwise escape. If the calorimeter is to be operated the same day, a very small layer of ice on all the metal surfaces should be deliberately melted first. The inside of the well is then wiped dry and the entire ice bath is replenished (to the level, *L*, in *Figure 2*). Since ice–water interfaces in the bath must be kept close to the calorimeter,

freshly ground clear ice is used, and the interstices are filled with pure water. When the heat leak becomes "normal" and steady (usually within 2 h), enthalpy measurements may begin.

It is believed that ice mantles may be used in accurate heat measurements up to several days after they are frozen, provided the melting of ice at the top of the ice bath during periods of standing (especially overnight) has not allowed much of the upper, protective part of the ice mantle to melt. To maintain a constant heat leak when the calorimeter is in actual operation, it sometimes proves necessary to pack occasionally a little fresh ice in close contact with the emerging calorimeter well. If the ice bath is well insulated (Styrofoam of a few cm thickness serves excellently), one packing of ice in the bath should be sufficient for 12 h or so if the top few cm of ice are replenished often enough. Once an ice mantle is partly melted, it is considered mechanically safer to melt all the ice attached to the inside calorimeter surfaces before freezing a new ice mantle.

When the beaker of mercury is removed from the submerged tip, the mercury in the latter should not recede owing to the presence of air in the valve. If the packing of the stem in the mercury valve is not airtight, it may be necessary to replace the air in the valve with mercury daily. Keeping the inside surfaces of the glass capillary and mercury reservoir clean may prove troublesome, but a few mm of water above the mercury meniscus helps to maintain its proper shape. Oriani and Murphy[28] used a precision-ground glass taper-joint on the capillary to permit easy removal for cleaning. The top part of the mercury in the capillary, where foreign particles tend to accumulate, may be periodically removed by suction. Before each reading of the mercury meniscus, it is advisable to apply enough pressure to the reservoir to depress the mensicus slightly (about 1 mm) so that it will rise to a reproducible level.

To allow mercury from the weighed beaker to enter the calorimeter in a heat measurement, the valve may simply be opened and checked against possible clogging. However, at first, some samples deliver heat to the calorimeter so rapidly that the meniscus would fall below the capillary and allow air to enter the calorimeter unless the pressure in the reservoir were first lowered sufficiently. An alternative procedure is to draw more than enough mercury for the experiment from the weighed beaker into the reservoir and then close the valve. (One of the important precautions in using the ice calorimeter is to avoid introducing heat to the well, even from an object at room temperature, unless the inlet tube is connected to a supply of mercury in the accounting system.) The gate of the calorimeter is then opened long enough to admit the sample.

E. A Typical Experiment

The data and calculations involved in a typical enthalpy measurement with an ice calorimeter are given in *Table 1* and *Figure 4*. Examples of calorimeter misbehavior and numerous small corrections are introduced to show how they are handled.

In this example, a sample of aluminum oxide in a 90%Pt–10%Rh container was measured. (The empty container, also with air sealed in at 600°C and 1 atm, had already been measured in separate runs.) In *Figure 4*

Table 1. Data and calculations for a typical drop calorimetry experiment with a platinum resistance thermometer and ice calorimeter

Sample ("Al_2O_3")		*Furnace Temperature*	
weight	16·8299 g	*Time*	*Thermometer ohms*
buoyancy correction	+0·0026	10:55	77·9094
0·14% SiO_2 by analysis	−0·0236	10:57	77·9083
		11:01	77·9078
mass, pure Al_2O_3	16·8089 g	Mean:	77·9085 (found)
			−77·8733 (=600°C)
			0·0352
		dR/dT=0·0802 Ω/deg at 600°C	
		600+0·0352/0·0802=600·44°C (sample temperature)	

Heat measurement

+126·9382 g	(weight of beaker + Hg before drop)
−74·0812	(weight of beaker + Hg after drop)
−13·6333	(corrected mass of Hg, empty container, 600·44°C)
−0·0027	[buoyancy correction for net Hg (sample + container)]
+0·0069	[offset correction, g Hg (see *Figure 4*)]
−0·0006	(correction for 0·0021 g Pt − 10% Rh extra with sample, g Hg)†
+0·0035	(correction for air, 600°C and 1 atm, displaced by sample, g Hg)†
−0·0524	(correction for SiO_2 in sample, g Hg)†
−0·0324	(correction to exactly 600°C, g Hg)†
39·1460 g	(corrected mass of Hg for sample at 600°C)

Enthalpy calculation

$(H_{600°C} - H_{0°C})$ (final, pure Al_2O_3)
= (39·1460) (270·48 + 0·01‡)/16·8089.
= 629·94 abs J/g
(÷4·1840 = 150·56 defined cal/g)

†Computed from reference 17.
‡Calculated correction for rise of mercury level in this calorimeter.

the mercury capillary readings taken when the valve was closed are plotted against time, with a new line through the points whenever the mercury valve was opened and the capillary meniscus reset. (The initial abnormal steepness was traced to moisture in the well that had to be removed.)

The temperature of the furnace was read frequently, just before the drop, with a platinum resistance thermometer. The sample had too much thermal inertia to follow the small short-time drift indicated by the three readings in *Table 1*, so the average was taken.

Eight minutes after the sample was dropped, the mercury valve was closed and the meniscus read, but the negative slopes up to 11:30 suggested that the sample was still evolving heat. The decreased slope after 12:00 was traced to a failure to keep the ice bath well packed on top, and illustrates the error that would have resulted had this later part of the graph been extrapolated back to the time of the drop. The "reset" correction was computed from an empirical calibration factor of 6·3 mg Hg/scale mm, and was subtracted algebraically from the *loss* of mercury in the beaker. To show readily their importance relative to the precision of duplicate

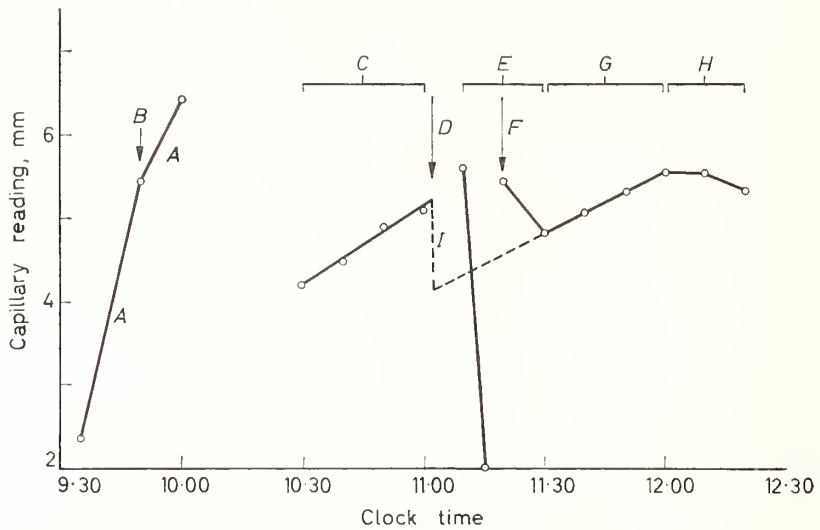

Figure 4. Ice-calorimeter heat leak and reset correction in a typical experiment
A, Calorimeter "well" wet
B, Gas flow through well reduced
C, Normal heat-leak rate before drop
D, Time of sample drop
E, Sample not at thermal equilibrium with calorimeter yet
F, Valve opened and capillary meniscus reset
G, Near-normal heat-leak after drop
H, Ice-bath packing deficient
I, Reset correction = −1·1 mm.

experiments, which was of the order of 5 mg of mercury, it was convenient to express the corrections in terms of mass of mercury.

In applying the correction for the impurity (SiO_2), it was assumed on the basis of the high-temperature preparation of the sample that the silica was present in the form of an aluminum silicate, and the correction was accordingly computed by subtracting from the enthalpy[17] of Al_2SiO_5 that of an equivalent amount of Al_2O_3.

F. Tests for Accuracy

Overall checks of the accuracy of a particular ice calorimeter used in high-temperature drop calorimetry are afforded by comparing enthalpy measurements on a suitable material with the best published values. Highly pure α-Al_2O_3 (corundum) is currently considered the best single material for comparisons up to above 1500°C; the published values have been referenced and reviewed recently by Kelley[17], and more recent values by Hoch and Johnston[13] (up to 2000°C) are probably the most accurate available at the highest temperatures. However, the use of such differences to establish an empirical calibration of a new apparatus is not recommended in work of high accuracy.

Several comparisons of enthalpy changes obtained by precise drop and adiabatic calorimetry have been made at the U.S. National Bureau of Standards. Values for water over the range 0–250°C agreed within an

average of 0·05 per cent by the two methods[6], whereas the results for aluminum oxide over the range 25–107 °C were about 0·2 per cent higher by the drop method than by low- and high-temperature adiabatic calorimeters[6]. (The two adiabatic calorimeters agreed with each other to 0·01 per cent on the average[35].) At these relatively low temperatures the adiabatic calorimeters were believed to be several times as accurate as the drop method apparatus. At somewhat higher temperatures the precision of adiabatic calorimetry decreases considerably because of increased radiation effects, and for this reason the two methods were believed to give comparable accuracy at these higher temperatures; however, for the range 242–416 °C the difference found for aluminum oxide averaged only 0·05 per cent[35]. At still higher temperatures, the drop method is the more accurate.

G. Hunting Causes of Trouble

The possible causes behind a perplexing symptom of trouble are often numerous. If the cause is likely to be a single one, it is economical to eliminate from initial consideration those causes which can produce effects only of the opposite sign or of a different order of magnitude from that observed. If the only symptom is unsatisfactory precision or accuracy of the enthalpy values, it may not be immediately clear whether the sample, the furnace, or the calorimeter is responsible. Errors arising from the sample and the furnace are discussed elsewhere in this chapter.

When the trouble is in the ice calorimeter itself, one source of error and poor precision is the melting of a hole in the ice mantle. This allows unmeasured heat to escape, but fortunately, such a hole can usually be observed visually, or at least it is usually manifest by an abnormally slow equilibration after the drop. (Occasionally two successive runs have relatively large errors of comparable magnitude but opposite sign, presumably because of a slight irreproducible collapse of the calorimeter like that of the bottom of an oil can.)

A large positive or negative heat-leak rate of the ice calorimeter, apart from its indication of a condition which is likely to be highly variable, is too great to be followed accurately. If there is apparently a large heat leak *into* the calorimeter (falling meniscus), there may be a hole in the ice mantle, the ice bath may need more careful packing, further time may be required for the calorimeter to equilibrate with respect to heat and volume changes, or there may be air bubbles in the calorimeter which are slowly dissolving in the water. (In the last case the compressibility of the calorimeter may be found to have increased considerably.) On the other hand, if there is apparently a large heat leak *out* of the calorimeter (rising meniscus), the calorimeter well may be wet, or so large an ice mantle may have been frozen that some water has replaced mercury in the inlet tube (causing an abnormally high calorimeter temperature).

There are other possible causes of an apparently abnormal heat leak. Fluid leaks of the calorimeter deserve special mention. If water is leaking out of the top of the inner glass vessel, this will be visible in time but will immediately cause a falling (or more rapidly falling) mercury meniscus. On the other hand, if there is leakage at a level higher than the meniscus, fluid will be entering the calorimeter and the meniscus will tend to rise.

Fluid leaks may be verified by standard procedures. A time-consuming procedure is to follow the meniscus readings of a thoroughly temperature-steady ice-free calorimeter. A more rapid method involves brief evacuation above the mercury meniscus (when the mercury column will break), but prolonged evacuation may lead to volume hysteresis which simulates a fluid leak.

2. *The isothermal-jacket, block-type calorimeter*

The isothermal-jacket, block-type calorimeter absorbs or evolves heat with a change of temperature, the change usually not exceeding 4–5°. Although block calorimeters have been designed to operate adiabatically[23], the usual type employs isothermal surroundings. The following discussion is limited to a model of this type.

A. Design and Construction

The block calorimeter shown in *Figure 1* is the one designed by Southard[33], and is being used at present by the U.S. Bureau of Mines. It is essentially a cylindrical block of copper, *L*, 12·6 cm in diameter and 20·3 cm high. The mass is large enough that the largest heat absorption does not cause a temperature rise of greater than about 5°. Aluminum blocks have been used successfully in place of copper. The block shown is gold-plated and rests on plastic knife-edges that are glued to the bottom of the surrounding jacket. The interior surface of the jacket is also gold-plated and both jacket and block are kept polished to minimize the heat interchange between them. A brass tube (2·5 cm diameter) through which the sample drops, connects the jacket to the furnace. The top of the jacket is removable and is flange-connected to the lower part with machine screws and a Tygon gasket. The jacket and calorimeter are immersed to level *R* in a stirred oil bath maintained at 29·70 $\pm$ 0·005°C. It is more convenient to maintain the temperature of a bath by heating than by cooling or a combination of the two; thus, if room temperature conditions are such, the bath may be more conveniently maintained at a reference temperature higher than the standard temperature of 25°C.

The receiving "well", *O*, is a removable, tapered copper plug bearing a 100Ω manganin wire heater, *P*, which is used in the electrical calibration of the heat capacity of the calorimeter. The well is covered by a circular copper gate, *M*, about 2 cm thick. The gate (solid, except for a 2·5 cm hole) is closed except for the brief interval necessary for dropping the capsule. The bottom surface is machined to fit into a similarly machined recess in the block itself, thus providing good thermal contact and guarding against heat losses by convection. The gate rotates on a shaft eccentric with the center line of the receiving well and is operated manually. The shaft is also connected to a similar, but hollow, gate located just under the furnace. This gate is cooled by a slow stream of water, preventing the intrusion of heat into the calorimeter from the furnace. Both gates have a thin slot of the proper radius to allow the suspension wire to pass through when the gate is closing.

A slow stream of CO_2 (about 50 cm^3/min) is introduced at the bottom of the jacket and flows continually around the calorimeter and through the furnace. The procedure prevents condensation of atmospheric moisture

on the calorimeter and furnace refractory. It also maintains an oxidizing atmosphere around the furnace thermocouple, which is located within the furnace core. The heat exchange rates between the block and jacket are reduced by the CO_2 to about 60 per cent of those in air. This rate is about 0·002°/min for a temperature difference of one degree between the block and the jacket and is reproducible to about 1 per cent. There is a slight departure from this figure for large temperature rises. This variation is taken into account in the calculations.

The calorimeter resistance thermometer, wound on recess *N*, is of the transposed bridge type described by Maier[25]. The thermometer is wound so as to cover about one-half of the outer surface of the block and is coated with Bakelite varnish. The winding is then covered by a tapered copper sleeve that makes a driving fit on to the similarly tapered block. It consists of four windings, two of copper and two of manganin wire alternately arranged in the bridge. The two copper coils are wound together in one operation, as are the two manganin coils. The current passing through the thermometer is then exactly divided at all temperatures and the bridge is in balance at only one temperature. The four windings are approximately 210Ω each and have a balance-point at 20·8°C.

The use of this kind of thermometer reduces the number of decades of a potentiometer—in this case three—necessary for temperature measurements, and provides greater temperature sensitivity than a single winding. In this particular case the temperature coefficient is 410 μV/deg with a current of 1 mA. The use of a Leeds and Northrup White 100000 μV potentiometer with a high-sensitivity galvanometer gives a precision of 0·03 μV or about 0·0001°C. Heat is generated by the thermometer at 0·003 cal/min, which is a negligible quantity. (If a singly wound resistance thermometer of either platinum or copper is used, a bridge such as the Leeds and Northrup G-2 type Mueller bridge should be used for comparable precision.) The voltage drop across the thermometer is 3860 μV at 30·00°C. The heat capacity of the block is 3.691 defined calories per microvolt change in the thermometer. There is a small heat capacity change of the block with temperature.

B. Additional Measuring Equipment

The same potentiometer and galvanometer are used in the electrical calibration of the calorimeter and in measuring the resistance of the manganin heater. Two standard resistances are used, both calibrated by the U.S. National Bureau of Standards. A 0·1Ω resistance is used in the energy-measuring circuit, and a 100Ω resistance is used in determining, and in periodically checking, the resistance of the manganin heater. The standard cell used with the potentiometer is checked periodically against several standard cells used only for this purpose.

The potentiometer working cells and the cell for supplying the thermometer current are 200 ampere-hour lead cells of the charge-retaining type. The energy source for heating the block is composed of a battery of 23 Edison cells with taps to use any number. Experience has shown that the lead cells and Edison cells are equally suited to any of these three uses.

Energy input is made by using a stop watch which is checked at regular

intervals against a standard chronometer. If electrical timing is used, care should be taken to see that the line frequency is maintained at 60 cycles; otherwise a proper correction must be applied. Time for attainment of thermal equilibrium by the calorimeter is around 10 min for a calibration and 10–60 min for a calorimetric measurement, depending mainly upon the thermal conductivity of the sample.

C. A Typical Experiment

A typical experiment will serve to illustrate the method of operation of the calorimeter and the calculations involved. During the time that the container and contents are coming to thermal equilibrium in the furnace, the block is set at some desired temperature. This is conveniently done with dry ice and the heater used in the calibration measurements. During the last 20 min or so preceding the drop, the temperature of the calorimeter is read at two-minute intervals and the furnace temperature is checked for constancy. The gates are then momentarily opened and the plunger falls, dropping the sample into the calorimeter. This operation takes about 2 sec and correction is made for the radiation into the calorimeter from the furnace. (This heat gain is negligible below 750°C and does not exceed 0·1 per cent at higher temperatures.) During the time that the calorimeter is heated, its temperature is observed, first at one-minute intervals and then at longer intervals, until equilibrium is established. Finally, readings are taken again at two-minute intervals. *Table 2* gives the record of a typical experiment.

The sample temperature in the furnace is given by the thermocouple reading at 23 min and 23·5 min after the start of the experiment—just prior to dropping the capsule. The constant resistance thermometer current of 1000 μA is checked several times during the warming and cooling rate periods. Adjustment is made with a resistance box connected in series with the thermometer to provide constancy to $\pm$ 0·01 μA. During the equilibration period the change of current is more rapid, necessitating a significant adjustment before the final equilibrium cooling period.

Correction for heat interchange of the block with the thermostat is made with the equation $R = \mathrm{d}T/\mathrm{d}t = -0{\cdot}002027\ (T - 3734)$. In this equation, $\mathrm{d}T/\mathrm{d}t$ is the measured rate in microvolts per minute, $-0{\cdot}002027$ is Newton's constant, T is the calorimeter temperature in microvolts, and 3734 is the temperature, also in microvolts, at which the heat interchange rate is zero. The magnitude of Newton's constant depends mainly upon the heat capacity of the block, the thermal conductivity of the gas and metal leads between the block and jacket, the exposed area of the block or jacket, and the distance between them.

The remaining calculations of *Table 2* are for the most part self-explanatory. The conversion from microvolts to joules is made by using the heat capacity of the calorimeter (15·445 J/μV) as determined by separate calibration measurement. The conversion from electrical units to defined calories is made by using the relation 1 cal = 4·1840 J. The heat value of the experiment is corrected from the equilibrium temperature (3823 μV) to 30°C (3860 μV) by using 1°C = 410 μV. The heat capacity value of 1·23 cal/deg. for the container and contents is taken from Kelley and King[18]. The enthalpy of the container was obtained from a separate series of measurements. The

Table 2. Data and calculations for a typical drop-calorimetry experiment with a thermocouple and copper block calorimeter (Sample, La_2O_3)

Thermostat temperature	29·70 ± 0·005°C
Wt. of La_2O_3 (corrected to vacuum)	10·4440 g
Wt. of Pt–10% Rh container (corrected to vacuum)	10·9640 g
Time in furnace (at temperature) before start of experiment	1 h
Resistance thermometer maintained at	1000 ± 0·01 μamp

Record of Experiment

Time (min)	*T or RT e.m.f.*† (μV)	*Time* (min)	*T or RT e.m.f.*† (μV)	*Time* (min)	*Resistance thermometer e.m.f.* (μV)
0	9976 (T)	22	3443·78‡(RT)	38	3822§
2	3431·75‡(RT)	23	9980(T)	42	(3823·21)¶
4	3432·93‡(RT)	23·5	9980(T)	44	3822·87¶
6	3434·04‡(RT)	24	(3444·98)*(RT)	46	3822·52¶
8	3435·39‡(RT)	24·5	3613§(RT)	48	3822·15¶
10	3436·57‡(RT)	25	3685§(RT)	50	3821·81¶
12	3437·78‡(RT)	26	3749§(RT)	52	3821·48¶
14	3439·07‡(RT)	27	3781§(RT)	54	3821·15¶
16	3440·19‡(RT)	28	3799§(RT)	56	3820·75¶
18	3441·36‡(RT)	30	3814§(RT)	58	3820·40¶
20	3442·55‡(RT)	34	3821§(RT)	60	3820·02¶
				62	3819·68¶

Calculations

Temperature of container and contents in furnace (9980μV)	1308·5°K
Final resistance thermometer e.m.f.	3823·21μV
Initial resistance thermometer e.m.f.	3444·98μV
Thermometer rise	378·23μV
Correction for time gates were open	−0·20μV
Correction for heat interchange with thermostat, by using e.m.f. *vs.* time plot for equilibration period, as indicated below	2·27μV

Time interval (min)	*Resistance thermometer e.m.f.* (μV)	*Heat interchange rate* (μV/min)	*Correction* (μV)
24–24·5	3542	0·390	0·195
24·5–25	3652	0·167	0·084
25–26	3720	0·029	0·029
26–27	3766	− 0·064	− 0·064
27–28	3790	− 0·113	− 0·113
28–30	3807	− 0·147	− 0·294
30–34	3818	− 0·170	− 0·680
34–42	3822	− 0·178	− 1·424
			Total − 2·27

Corrected temperature rise	380·30μV	
Conversion to calories $\frac{(380{\cdot}30 \times 15{\cdot}445)}{4{\cdot}1840}$	1403·86	cal
Correction to 30·00°C $\frac{[(3860 - 3823)1{\cdot}23]}{410}$	− 0·11	cal
Enthalpy of empty container	− 419·61	cal
Net enthalpy of La_2O_3	984·14	cal
Enthalpy per mole $\frac{(984{\cdot}14 \times 325{\cdot}82)}{10{\cdot}4440}$	30 700	cal
Correction to 25°C (5 × 25·9)	130	cal
Final value, La_2O_3 $(H_{1308{\cdot}5} - H_{298{\cdot}15})$	30 830	cal/mole

*Drop Capsule
†T = Thermocouple, RT = Resistance thermometer
‡Warming rate, $R_1 = 0{\cdot}601$ μV/min
§Period of equilibration
¶Cooling rate, $R_2 = -0{\cdot}176$ μV/min

final correction of the La_2O_3 enthalpy from 30°C to 25°C utilizes the room temperature heat capacity data of Kelley and King[18]. If this datum is not available from some compilation such as the one cited, the measured enthalpy data must be extrapolated. Very little error results from this procedure.

D. Calibration Factor

The calibration factor of the block calorimeter described here has remained substantially unchanged for several years. A single calibration is made for each substance, and its constancy serves as an overall check on the precision measuring equipment.

A block calibration experiment is conducted in the same manner as the run, except that measured electrical energy is supplied in place of the heat from the container. This heat is supplied through the calibrated manganin heater coil, *P*, surrounding the receiving well. The current passing through the heater is measured on the White potentiometer by measuring the voltage drop across a standard resistor (0·1Ω) in series with the heater. These readings are made alternately with those of the resistance thermometer. A substitute external resistance of the same magnitude as the heater is used to "exercise" the energy battery for about an hour before introducing energy into the block. This procedure provides a total change in current during a calibration of about 0·03 per cent, so that the current values may be averaged to determine the energy input. In case a precision bridge is used to measure temperature, a less precise potentiometer such as the Leeds and Northrup type K-3 is entirely suitable for the measurement of the energy of calibration.

As can be seen from the sample experiment, there is no need to convert from microvolts to degrees. Calibrations are calculated in terms of joules per microvolt and applied to the experiment in that form.

IV. Treatment of the Data

1. *Correcting to standard conditions*

A. Correction to a Basis of a Pure Sample

Frequently a sample contains from several tenths to several per cent of impurities. The thermal behavior of these impurities can be the source of significant error if ignored. A spectrographic analysis will identify and estimate the orders of magnitude of the elements of these impurities if they are different from those of the main sample. An X-ray diffraction analysis will show the crystal form and indicate impurities, including uncombined compound constituents, usually to the extent of about 1 per cent or more. Microscopic examination also is an aid in determining the presence of an impurity phase, particularly amorphous content if this possibility exists. In most cases a quantitative chemical analysis is highly desirable to determine the chemical composition with certainty.

(1) *Correcting for Insoluble Impurities.* For all impurities which are completely immiscible with the sample the thermal corrections are strictly additive. Sometimes such an impurity will melt or undergo transition in the measured range. Proper enthalpy correction removes the resulting apparent discontinuity of enthalpy of the main sample. At high temperatures substances

usually become more miscible, so that a misjudgement based on assumed immiscibility may result in significant error. This consideration stresses the need for taking pains to secure samples of high purity.

Some compilation such as that of Kelley[17] is useful in computing corrections for insoluble impurities.

(2) *Correcting for Soluble Impurities.* Enthalpy corrections for impurities that are wholly or partly in solution in the main substance are almost never strictly additive. There is a variety of combinations which can occur regarding the states of the impurity and the main sample, as well as the solubility of the impurity at the two temperature extremes of the measurement. Corrections for the heat effects involved are often relatively small and frequently neglected, because they are difficult even to estimate. The heat corrections are most important when the impurity is in liquid solution only at the upper temperature. If no heat-of-solution data are available, a good approximation is to apply a correction based on the heat of fusion of the impurity at its melting point. Other cases are estimated by treating the impurity as though it were insoluble. If the correction needs to be refined, special information is required, *i.e.*, information that provides the degree of solubility at the two temperatures of the measurement and the accompanying heat effects.

When impurities are dissolved in a sample that melts in the range of measurements, they cause a lowering of the melting point often called "pre-melting". This subject is discussed at some length in other chapters of this volume. If the amount of dissolved impurities is low, the solution may be considered ideal. In this case the enthalpy correction is approximately

$$\Delta H_{\text{corr}} = -N_2 R T\, T_m/(T_m - T), \tag{3}$$

in which N_2 is the total mole fraction of impurities, R is the gas constant, T is the absolute temperature in question, and T_m is the melting point of the pure sample. If the solution is not ideal so that equation (3) is not applicable, or if the analysis for the proportion of impurities cannot be relied on, the value of N_2 in equation (3) is better determined empirically as the value that will give corrections to make the enthalpy–temperature relation the most plausible one.

This matter of judgement often introduces considerable uncertainty in the corrections and the resulting corrected heat of fusion, even for samples as pure as 99·5 per cent. A sensitive way to examine the results for pre-melting effects is to plot mean heat capacities for successive intervals of furnace temperature and then to look for excessive upturn in the curve below the melting point. The heat capacity–temperature curves of some pure solids show an upward turn as the melting point is approached. This upward curvature can be attributed to lattice vacancies or anharmonic vibrations, but this effect is more gradual than that due to pre-melting. If the empirical application of equation (3) leads to a curve which shows a heat capacity decreasing with temperature, the value chosen for N_2 is too great.

B. Correcting for Vaporization Inside the Container; Correcting to a Different Pressure

If even a small fraction of the sample or one of its components vaporizes

inside the sample container in the temperature range of the measurements, the heat involved in the vaporization process may be an appreciable fraction of the total heat measured, and correction for it is usually desired. If the necessary subsidiary information is available, the total correction can be computed from an exact thermodynamic relation given by Osborne[29].

$$[mH]_1^2 = [q]_1^2 + [PV]_1^2 - [(V - mv)\,L/(v' - v)]_1^2. \qquad (4)$$

In equation (4) the superscript 2 and the subscript 1 indicate the value of the bracketed quantity at the higher temperature less that at the lower temperature; m is the total mass of sample, including the vapor; H is the enthalpy, per unit mass, of the condensed phase (solid or liquid) at pressure P, which is its vapor pressure; $[q]_1^2$ is the heat evolved by the sample (after correction for the container and its parts); V is the inside volume of the container; L is the heat of vaporization (or sublimation, if solid) per unit mass at the temperature in question; and v' and v are the volume per unit mass of the vapor and condensed phase, respectively. It is usually more convenient to make a substitution in equation (4) from the exact Clapeyron equation, to obtain

$$[mH]_1^2 = [q]_1^2 + [PV]_1^2 - [(V - mv)\;T\,\mathrm{d}P/\mathrm{d}T]_1^2. \qquad (5)$$

If the vapor pressure and its temperature coefficient are known with sufficient accuracy (which must be high if P and consequently $\mathrm{d}P/\mathrm{d}T$ are large), it is sufficient to apply equation (5) to measurements on a single sample, with the precaution to minimize the gas space $(V - mv)$ (after due allowance for thermal expansion of the sample) in order to minimize the last correction term. However, an alternative procedure is available if the vapor pressure data are not sufficiently reliable. The most uncertain quantity in equation (5) can be eliminated by making heat measurements on both a "high" and a "low" filling of the container and applying the equation to each. Sufficient sample must be used in the "low filling" experiments to ensure that not all the condensed phase is evaporated.

As an example, Douglas *et al.*[1] measured the enthalpy (relative to 0°C) of *n*-heptane at 250°C, at which temperature the vapor pressure is about 21 atm, using "high" and "low" fillings in which the liquid occupied 83 per cent and 27 per cent of the container, respectively. Although in the case of the "low" filling experiments the net correction calculated from equation (5) amounted to about 12 per cent of the total heat measured (the correction was far smaller for the "high" filling), the two separately corrected liquid enthalpies differed by only 0·1 per cent. Each value was the mean from several duplicate experiments.

If the pressure on the sample varies with temperature either because of a rapidly changing vapor pressure or because inert gas is sealed in at some temperature and pressure, it may be desirable to correct the enthalpy increment for the condensed sample, calculated from equation (4) or (5), to the basis of a given fixed pressure, such as a standard state of 1 atm. The correction may be computed for both terminal temperatures from the exact thermodynamic relation

$$(\partial H/\partial P)_T = V - T(\partial V/\partial T)_P \qquad (6)$$

in which V and H apply to the same quantity of sample. For large pressure differences, equation (6) requires integration if the thermal expansion data are accurate enough to justify it. For a change of pressure of only a few atmospheres, however, the correction is very small (less than 0·1 per cent). The calculation of C_V from C_P, which are thermodynamically related by

$$C_P - C_V = \alpha^2 VT/\beta \tag{7}$$

in which α is the volume coefficient of thermal expansion and β is the compressibility, is a special case of correction to different pressures.

2. *Smoothing and representing enthalpy values*

Measurements of relative enthalpies over a range of temperature may be presented by graph, equation, or tabulation.

A. Graphing

Although graphing is not generally considered to be a satisfactory way to represent the final data, it is a good aid in smoothing the data and finding a suitable form of empirical equation or its coefficients. For these purposes it is not suitable to graph the enthalpy data directly; instead, functions of enthalpy are plotted. These function plots must be sensitive enough to show deviations from smooth continuity which are within the precision attained by the measuring technique.

Generally, some form of heat capacity function is most convenient for plotting the measured data. This procedure not only provides a good basis for smoothing the data, but also shows continuity with any existing low-temperature heat capacity data directly and provides a precise means of comparison with other work.

The heat capacity curve derived from the smoothed enthalpy data is often plotted together with unsmoothed heat capacity values corresponding to mean heat capacities given directly by $\Delta H/\Delta T$ for pairs of successive furnace temperatures. If the heat capacity does not vary linearly with temperature, a curvature correction is needed to convert mean values to true heat capacities; the curvature correction is given by the infinite series according to Osborne *et al.*[30]

$$C - (q/\Delta T) = -(\partial^2 C/\partial T^2)(\Delta T)^2/24 - (\partial^4 C/\partial T^4)(\Delta T)^4/1920 - \ldots \tag{8}$$

in which C is the true heat capacity, q is the heat interval for the sample over the temperature interval ΔT, and C and its derivatives apply at the mean temperature of this interval. Even for a temperature interval as large as 100°C, the first term of the right-hand side of equation (8) is normally only a very small fraction of the total heat capacity and the remaining terms are completely negligible. If this is not true because the curvature is unusually great, measurements should be made at one or more intervening temperatures. If the enthalpy–temperature relation is represented analytically, it is convenient to compute the derivatives in equation (8) from that relation. If the heat q is that for the sample at constant pressure, q may be replaced by ΔH and C by C_P.

Another method is to plot the quotients of the individual enthalpies

divided by the corresponding temperature intervals of the measurements. The value of the ordinate is the mean heat capacity between the furnace temperature and the standard reference temperature. Thus if 298°K is the reference temperature, the ordinate of this curve at 298°K is the true heat capacity at this temperature. Any existing low-temperature data can easily be calculated in this form to show continuity with these data. This comparison is important, because almost always the low-temperature heat capacity data are more accurate than the high-temperature data. If $(H_T - H_{298})/(T - 298)$ is the mean heat capacity as defined here, then the true heat capacity is given by the relation

$$C_P = (H_T - H_{298})/(T - 298) + (T - 298)\mathrm{d}\,[(H_T - H_{298})/(T - 298)]/\mathrm{d}T. \qquad (9)$$

(1) *Choice and Treatment of Measurements.* In the process of smoothing data, the choice of the number of measurements over the same temperature interval requires some decision as to how such duplicates will be handled. It is the usual practice to repeat measurements for which agreement is unsatisfactory. This raises the question as to which individual measurements to discard, and of those remaining, which will receive the most weight. Statistical methods have been developed to show when a single measurement can be discarded objectively. Most of these methods depend upon the assumption that the probability of encountering a single measurement with such a large deviation from the mean is small. This mean can be considered as the mean value of several duplicate experiments or as a smooth curve such as the heat capacity curves discussed. Of the measurements remaining for each temperature range, it is a good procedure to treat them equally in getting the mean value, and then to treat these mean values equally in deriving smooth values or an empirical equation to represent them. Additional measurements for any one temperature range should be chosen primarily so as to give statistical precision to the mean value of enthalpy or its derivatives. However, the existence of systematic errors usually makes a large number of repetitive experiments of limited value.

B. Representation by Equations

(1) *Theoretical and Semi-Theoretical Equations.* For the crystalline state, the Debye treatment for intermolecular vibrations is often coupled with the Einstein treatment for intramolecular vibrations. This procedure has given a representation of the C_V–temperature curve so closely approximated by experimental results for many substances as to be useful, especially at low temperatures for which the difference between C_P and C_V is generally small. However, the limiting value $(3R)$ of the Debye and Einstein functions is generally exceeded over the high-temperature range. In this case calculations of heat capacities are so complicated by such factors as anharmonic vibrations, electronic heat capacity, and the difference between C_P and C_V that such calculations are seldom made.

(2) *Empirical Equations.* Empirical equations for enthalpy may necessitate more labor in obtaining values at odd temperatures than from tables, and

they are usually less precise than the smooth values given in tables; but they have the advantage of affording an easy means of deriving related thermodynamic properties such as heat capacity and entropy increments. In addition, if the form of the enthalpy equation is the standard one suggested by Maier and Kelley[26], the constants in the calculation of chemical reactions may be expeditiously combined. This equation is

$$H_T - H_{298\cdot15} = aT + bT^2 + cT^{-1} + d \tag{10}$$

A procedure for evaluating the constants of this equation was given by Shomate[31]. If the heat capacity at 298·15°K was accurately known from low-temperature calorimetry, Shomate used the following equations

$$C_{P,298\cdot15} = a + 596\cdot30b - c/(298\cdot15)^2 \tag{11}$$

$$0 = 298\cdot15a + (298\cdot15)^2b + c/298\cdot15 + d \tag{12}$$

$$[(H_T - H_{298\cdot15}) - C_{P,298\cdot15}\,(T - 298\cdot15)]\;T/(T - 298\cdot15)^2 = bT + c/(298\cdot15)^2 \tag{13}$$

The function on the left side of equation (13) is evaluated for each measured high-temperature enthalpy value (or for evenly spaced, smooth-curve values), and the results are plotted against T. The slope and intercept of what is judged to be the best straight line give values for b and c respectively. If c is nearly zero, the line is sometimes drawn to make it exactly so. The other constants are then supplied by equations (11) and (12). If the substance has a melting point or transition in the measured temperature range, the same procedure can be applied above and below the temperature of discontinuity. Otherwise, four simultaneous equations are used to determine the constants. Frequently the equation form can be simplified above a temperature of discontinuity. This is particularly true if the discontinuity is above about 600°K.

The general adoption of equation (10) for all substances has the advantage of fitting data reasonably well while minimizing the number of terms. In addition, the error in using the equation to extrapolate the data to higher temperatures, while generally considerable, is often less than with many other forms of equation. However, there are the disadvantages that in many cases this equation form does not fit the precise data at all temperatures within the precision of the measurements or does not give weight to the temperature derivative of C_P at 298·15°K indicated by precise low-temperature calorimetry.

A better fit of an equation to the data may be obtained for many specific cases by choosing a different temperature function with the same or a greater number of constants. The number of constants should not be increased to the extent that implausible points of inflexion appear. The labor of fitting coefficients of an empirical equation by the least squares method is greatly reduced by the present-day availability of high-speed electronic computers and the ability to develop general-use codes, each of which includes any

desired combination of temperature terms. A least squares method has the advantage of mathematical objectivity, but loss is encountered through the difficulty of selecting the temperature range of "best fit".

Unless an equation is found which fits the enthalpy measurements within their precision at all temperatures, tabular values should be used for the most precise calculations.

C. Treatment of Fusions and Transitions

After correcting for any pre-melting, the enthalpy of a pure substance as a function of temperature is extrapolated to the melting point for both the solid and the liquid. If the enthalpies of both the solid and the liquid are expressed relative to the same state at the same temperature, the difference is the heat of fusion. The accuracy of the heat of fusion so obtained will depend upon the uncertainties of these extrapolations, the correction for "pre-melting", and the melting point. Since the heat capacities of the solid and liquid are not too far different at the melting point, an error of several degrees in the melting point has little effect on the resulting heat of fusion.

Unless the melting point is already known, it may be determined directly in the furnace by the cooling curve method, or by using the enthalpy data as a basis. In the latter case the melting point is taken as the lowest temperature at which the enthalpy measurement of the pure material falls on the liquid curve.

Solid–solid transitions are classed as first and second order according to whether, at equilibrium, they are abrupt and isothermal or gradual over a range of temperature. A first order transition is sometimes so sluggish that it is difficult to distinguish between the two types by drop calorimetry. These cases are spread out as an enhanced heat capacity. Sluggish heats of transition may sometimes be assigned arbitrarily as isothermal transitions for convenience in deriving the empirical equations. In any case, if the range of interest is above the range of transition, the enthalpies will be unaffected by the interpretation of the transition range, and the entropy calculations are likely to suffer little error. In efforts to measure enthalpies of substances in the neighborhood of either transition points or melting points, it may be necessary to greatly increase the length of time in the furnace. Also it is sometimes necessary to "overshoot" the temperature of transformation and then lower the temperature in order to increase the rate of transformation.

If a latent heat of transition is quite small, its existence may be hard to detect. An enthalpy-function plot such as the $\Delta H/\Delta T$ *vs* T plot mentioned earlier is of considerable value in detecting and defining them. Shomate[32] describes another type of plot used for this purpose; it is based on equation (13).

3. *Derivation of other thermodynamic properties from relative enthalpy*

The following common thermodynamic functions can be readily derived by the indicated mathematical operations on the enthalpy equation; the values are those at temperature T unless otherwise indicated

$$C_P^\circ = [\partial(H^\circ - H^\circ_{298.15})/\partial T]_P \qquad (14)$$

$$S^\circ = \int_{T'}^{T} (C_P^\circ/T)\mathrm{d}T + S_{T'}^\circ \qquad (15)$$

$$-(G^\circ - H^\circ_{298\cdot15})/T = S^\circ - (H^\circ - H^\circ_{298\cdot15})/T. \qquad (16)$$

Sometimes $(H^\circ_{298\cdot15} - H^\circ_0)$ is known from low-temperature calorimetry; in such cases the enthalpy and free-energy functions are often expressed relative to 0° instead of 298·15°K. For high-temperature thermodynamic applications, however, it is much more important to be able to substitute into equation (15) an accurate value of the integration constant $S_{T'}^\circ$ (at some temperature T' within the range of the high-temperature enthalpy measurements). In this case, equation (16) will yield free-energy functions, the use of which predicts equilibrium relations at high temperatures without the need for their direct measurement. A value for $S^\circ_{298\cdot15}$ is often available from low-temperature calorimetry on the substance in question and assumption of the Third Law of Thermodynamics.

If for some reason the enthalpy is represented only approximately by an empirical equation, the deviations of the unsmoothed values from the equation may be plotted and an empirical curve drawn through them. A smooth value of enthalpy at any temperature in the range can then be obtained by adding algebraically the ordinate of the deviation plot to the value given by the equation. A value of the heat capacity can also be obtained by adding the slope of the deviation plot to the temperature derivative of the (approximate) enthalpy equation. A variation for determining heat capacity is given by equation (9). Usually the contribution of the second term is only a few per cent of the first term, and the error in its graphical determination thus contributes only a small percentage error to the C_P so evaluated.

Kelley[17] describes a correction in the calculation of entropy based on the standard equation form. The corrections are applied incrementwise every 100°C as $q/T_{av.}$, in which q is the enthalpy deviation of the equation from the smooth values for the temperature interval, and $T_{av.}$ is the mean temperature of the interval.

4. *Precision and accuracy*

Values derived from drop measurements are often given accompanied by tolerance figures, but it is sometimes not clear whether precision or estimated accuracy is meant. In drop calorimetry the systematic errors are the important ones, so that the precision, as calculated by standard statistical procedures, is not as large as the absolute uncertainty of the results. Some estimate of the systematic error should be made to combine with the precision in arriving at a value of estimated uncertainty. Examples of experimenters who have presented such detailed analysis of their errors are Ginnings and Corruccini[10], Furukawa *et al.*[6], and Hoch and Johnston[12]. Particular sources of error are measurement of the temperature of the sample; calibration of the calorimeter and other instruments such as standard cells, potentiometers, thermometer bridges, thermocouples, and pyrometers; the calorimetric measurement, including allowance for heat leak corrections; sample impurities and mass changes; empty-container measurements; and

the loss of unmeasured heat by the sample during the drop and in the calorimeter.

Some investigators will combine possible errors statistically and then multiply the result by some arbitrary factor such as two, whereas others will combine possible errors with the signs taken to give the largest overall error. Comparison with work of different laboratories is an aid in error estimation.

The uncertainty of the heat capacity is difficult to estimate. The process of differentiation of enthalpy may multiply the percentage uncertainty characteristic of the enthalpy by a factor of two to much more if the heat capacity itself is changing rapidly with temperature. The uncertainty of the derived entropy may be calculated from the equation

$$S_T - S_{298.15} = (H_T - H_{298.15})/T + \int_{298.15}^{T} [(H_T - H_{298.15})/T^2]\, dT. \quad (17)$$

By substituting in the uncertainties of the enthalpy measurements and integrating the second part graphically, the entropy uncertainty may be determined. It is a close approximation to assume the same percentage uncertainty for the entropy increment as for the measured enthalpy increment.

Precise calorimetric data gain maximum value not only when the uncertainties can be estimated and stated, but also when the results are reported in sufficient detail to permit future corrections to less arbitrary procedures of data treatment or to more accurate physical constants.

V. References

[1] Douglas, T. B., G. T. Furukawa, R. E. McCoskey, and A. F. Ball, *J. Res. Natl. Bur. Std.*, **53,** 139 (1954).

[2] Douglas, T. B., and W. H. Payne, in S. F. Booth, ed., Natl. Bur. Standards Handbook 77, *Precision Measurement and Calibration*, Vol. II, *Selected Papers on Heat and Mechanics*, U.S. Govt. Printing Office, Washington, 1961, pp. 241–276.

[3] Dworkin, A. S., and M. A. Bredig, *J. Phys. Chem.* **64,** 269 (1960).

[4] Ferrier, A., *J. Sci. Instr.* **39,** 233 (1962).

[5] Fomichev, E. N., V. V. Kandyba, and P. B. Kantor, *Izmeritel. Tekhn.* **1962,** No. 5, 15.

[6] Furukawa, G. T., T. B. Douglas, R. E. McCoskey, and D. C. Ginnings, *J. Res. Natl. Bur. Std.*, **57,** 67 (1956).

[7] Gilbert, R. A., *J. Chem. Eng. Data*, **7,** 388 (1962).

[8] Ginnings, D. C., *J. Phys. Chem.*, **67,** 1917 (1963).

[9] Ginnings, D. C., and R. J. Corruccini, *J. Res. Natl. Bur. Std.*, **38,** 583 (1947).

[10] Ginnings, D. C., and R. J. Corruccini, *J. Res. Natl. Bur. Std.*, **38,** 593 (1947).

[11] Ginnings, D. C., T. B. Douglas, and A. F. Ball, *J. Res. Natl. Bur. Std.*, **45,** 23 (1950).

[12] Hoch, M., and H. L. Johnston, *J. Phys. Chem.*, **65,** 855 (1961).

[13] Hoch, M., and H. L. Johnston, *J. Phys. Chem.*, **65,** 1184 (1961).

[14] Hultgren, R., P. Newcombe, R. L. Orr, and L. Warner, *N.P.L. Symposium* No. 9 (1958), *Met. Chem.*, H.M.S.O. (1959), p. 1H.

[15] Jewell, R. C., E. G. Knowles, and T. Land, *Metal Ind. (London)* **87,** 217 (1955).

[16] Kantor, P. B., R. M. Krasovitskaya, and A. N. Kisel, *Fiz. Metal. i Metalloved.* **10,** No. 6, 835 (1960).

[17] Kelley, K. K. "Contributions to the Data on Theoretical Metallurgy. XIII. High-Temperature Heat-Content, Heat Capacity, and Entropy Data for the Elements and Inorganic Compounds", *U.S Bur. Mines Bull.* 584 (1960).

[18] Kelley, K. K., and E. G. King, "Contributions to the Data on Theoretical Metallurgy. XIV. Entropies of the Elements and Inorganic Compounds", *U.S. Bur. Mines Bull.* 592 (1961).

[19] Kelley, K. K., B. F. Naylor, and C. H. Shomate, *U.S. Bur. Mines Technical Paper*, No. 686 (1946).
[20] Kirillin, V. A., A. E. Sheindlin, and V. Y. Chekhovskoi, *Dokl Akad. Nauk SSSR* **135,** No. 1, 125 (1960).
[21] Kirillin, V. A., A. E. Sheindlin, and V. Y. Chekhovskoi, *Dokl. Akad. Nauk SSSR*, **139,** No. 3, 645 (1961).
[22] Leake, L. E., and E. T. Turkdogan, *J. Sci. Instr.*, **31,** 447 (1954).
[23] Levinson, L. S., *Rev. Sci. Instr.*, **33,** 639 (1962).
[24] Lucks, C. F., and H. W. Deem. "*Thermal Properties of Thirteen Metals*", ASTM Special Technical Publication No. 227, American Society for Testing Materials, Philadelphia, Pa. (1958).
[25] Maier, C. G., *J. Phys. Chem.*, **34,** 2860 (1930).
[26] Maier, C. G., and K. K. Kelley, *J. Am. Chem. Soc.*, **54,** 3243 (1932).
[27] Olette, M., *Compt. rend.*, **244,** 1033 (1957).
[28] Oriani, R. A., and W. K. Murphy, *J. Am. Chem. Soc.*, **76,** 343 (1954).
[29] Osborne, N. S., *Bur. Std. J. Res.* **4,** 609 (1930).
[30] Osborne, N. S., H. F. Stimson, T. S. Sligh, and C. S. Cragoe, *Bur. Standards Sci. Pap.*, **20,** 65 (1925).
[31] Shomate, C. H., *J. Am. Chem. Soc.* **66,** 928 (1944).
[32] Shomate, C. H. *J. Phys. Chem.* **58,** 368 (1954).
[33] Southard, J. C., *J. Am. Chem. Soc.*, **63,** 3142 (1941).
[34] Wensel, H. T. and W. F. Roeser. In *Temperature, Its Measurement and Control in Science and Industry*, Vol. I, American Institute of Physics, Reinhold Publishing Corp., New York, 1941, pp. 284–314.
[35] West, E. D., and D. C. Ginnings, *J. Res. Natl. Bur. Std.*, **60,** 309 (1958).
[36] White, W. P., *The Modern Calorimeter*. Chemical Catalog Co., New York, 1928.
[37] White, W. P., *J. Am. Chem. Soc.*, **55,** 1047 (1933).
[38] Wisely, H. R., *Thermocouples for Measurement of High Temperature*, Ceramic Age, Newark, N.J. (1955).

A Calorimetric Determination of the Enthalpy of Graphite from 1200 to 2600°K

E. D. West and S. Ishihara

National Bureau of Standards
Washington, D. C.

Abstract

Measurements are reported of the increase in the enthalpy of high-purity graphite between room temperature and 1200 to 2600°K. A new apparatus is described briefly. Methods of operation are developed which eliminate some systematic and random errors and are especially advantageous at high temperatures. The enthalpy data fit the equation

$$H_T - H_{298.15} = 28.9004T - 1.045 \times 10^{-4}\ T^2 - 16{,}126.2 \log_{10} T/313.15 - 8907.3$$

where H is in absolute joules per gram atomic weights and T in degrees Kelvin.

Introduction

Spence [1] has pointed out deficiencies in the data on the heat capacity of graphite. As one of the tests of a preliminary version of a new high-temperature apparatus, we have made measurements of the enthalpy of graphite which overlap the work of McDonald [2] from 1200°K to 1700°K and extend to 2600°K.

Specimen

The specimen was a solid cylinder machined from a larger piece of grade CCH graphite (National Carbon Company) density 1.6 g/cm^3. According to the supplier, this grade is purified by the same treatment used for spectroscopic grades. After machining, it was heated in our furnace at temperatures up to 2700°K for several hours before measurements were begun.

The specimen was weighed before and after each group of experiments at each furnace temperature. The average observed weight was 2.4023 g and the maximum variation was 0.2 mg. The calculations were nevertheless made with the observed weight for that experiment, so that the data include the random errors of weighing.

Spectrographic analysis of the sample showed traces of Al and Si (less than 0.001 per cent and faint traces of B, Ca, and Mg (less than 0.0001 per cent).

Apparatus

The apparatus will be described briefly to indicate several novel features; a detailed description will be deferred until improvements indicated by these preliminary measurements have been incorporated and tested.

The apparatus, shown schematically in Fig. 1, consists essentially of a furnace in which the capsule, with or without the sample, is held at a constant temperature and a calorimeter to which it is lifted for measurement of the quantity of heat. The furnace core is a hollow graphite cylinder heated by induction. The induction coil has a higher turns density near the ends to produce a greater field and

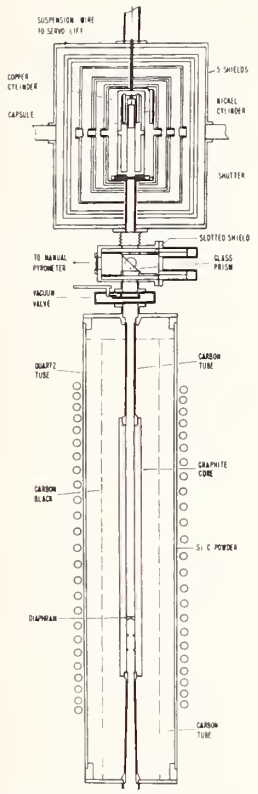

FIG. 1 DIAGRAM OF THE APPARATUS FOR ENTHALPY MEASUREMENTS.

more heat near the ends of the core, in contrast to the usual uniform solenoid which produces the maximum field at its center.

To reduce the power requirement and the accompanying temperature gradient, the graphite core is supported by thin carbon tubes and insulated by successive layers of carbon black and silicon carbide powder. The furnace operates in about 0.1 atm of purified argon, and can be held at 2500°K with 980 W, including coil losses. It is heated to 2500°K in about an hour with 5 kW power input.

The furnace is controlled directly by sensing the temperature of a graphite diaphragm located four inches inside the furnace core with a Leeds and Northrup automatic optical pyrometer sighted into the bottom of the furnace. The observed temperature of the diaphragm is held constant within ± 0.2°K throughout the experimental range. Two different instruments were used in different phases of this work.

The temperature is also observed after each lift with a visual optical pyrometer focussed on the diaphragm at the bottom of the region which was occupied by the sample. The currents in the pyrometers are calculated from the voltage across one-ohm standard resistors measured with a Wenner potentiometer. The automatic pyrometers tend to give a temperature reading a few degrees lower than the visual pyrometer, indicating a significant temperature gradient in the furnace (or a difference in the calibrations). The calibration for the automatic optical pyrometer was not appreciably better than that for the visual pyrometer at the time these measurements were undertaken. The temperature of the latter was therefore taken as more indicative of the temperature of the capsule without appreciable sacrifice of the accuracy of the measurements. A calculation exaggerating the effect of the gradient has been made assuming the temperature of the furnace core is uniformly 5 degrees different from that of the diaphragm. This calculation shows that the effect on the temperature measurement of the gradient in the graphite core is small compared to other temperature uncertainties discussed below.

The heat is measured with an adiabatic calorimeter operating between 30 and 65 C. The calorimeter proper consists of a hollow nickel cylinder surrounded by a hollow copper cylinder which is enclosed by thin gold-plated copper shields similar to an earlier calorimeter used in this laboratory [3]. The total heat capacity is about 2400 J/C. The main heat capacity of the calorimeter is made up of two coaxial parts which are separated by a 4.8 mm (3/16 in.) annular space except for an annular metallic contact midway along the axis. This construction introduces a time constant of about a minute, which eases the problem of adiabatic control of the surrounding shield. This time constant is short compared to the time constant for equilibration between the capsule and the calorimeter, so that the experiment is not lengthened appreciably. In the upper part of the temperature range corrections are still necessary for shield control deviations, equivalent to 0.1 per cent of the heat evolved by the full capsule at 2360°K. After the last alteration of the calorimeter, two electrical calibration experiments were made of its heat capacity by usual techniques over each five-degree interval. From these data the pooled estimate of the standard deviation of the mean over each interval is 0.01 per cent.

The heat capacity and temperature range of the calorimeter limit the number of lift experiments to six per day at low furnace temperature and four per day above 2100°K.

When the capsule is in the calorimeter, the bottom of the calorimeter is closed by a "shutter" consisting of two gold-plated copper radiation shields which reflect most of the radiation from the hot capsule back into the nickel block. These radiation shields have a large area of thermal contact with the copper block so that any excess heat they absorb from the radiation may be returned to the copper block with only a small thermal head.

Located between the furnace and the calorimeter are a vacuum valve, a sliding support for a prism for

temperature observations, and a sliding radiation shield, with a slot to accommodate the suspension wire. This shield reduces the radiation heat transfer when the capsule is in the furnace so that the measurement of the initial temperature of the calorimeter can be made more accurately, and so that the correction for radiation into the calorimeter will not depend critically on timing.

The sample is lifted from the furnace into the calorimeter by a servo-mechanism which imposes constant acceleration (or deceleration) on the capsule, avoiding the large forces of the usual jerky stops. The tension in the suspension wire is thus kept small, an important consideration for small wires at high temperatures. We have used 800 cm sec^2 for both acceleration and deceleration. The time for the capsule to cross the "cold" region between the top of the graphite tube in the furnace and the boundary of the calorimeter is 0.16 sec. The period of acceleration (= 1/2 the lift time) is measured in each experiment with an electronic counter-timer. This observed time did not vary more than 1 ms from 312 ms.

The capsule is machined from grade AUC graphite. It is 4 cm long and 1 cm in diameter with a 1.5 mm wall. It is fitted with a screw cap having a tantalum wire hook for attaching to the suspension wire. The capsule wall thickness is calculated from the thermal diffusivity of graphite to give no cooling of the inner wall during the short exposure time in the "cold" region. This technique has the advantage that the presence of the sample cannot increase the heat loss during the lift by maintaining the outer surface at a higher average temperature than in the corresponding empty capsule experiment.

As a check on the apparatus, we determined the enthalpy of a solid cylinder of single crystal sapphire (Al_2O_3) at 1179.2°K which is in the temperature range of earlier National Bureau of Standards measurements with another apparatus. The average result of three measurements each on the empty and full capsule is $H_{1179.2} - H_{313.15} = 99134$ J/mole, about 0.14 per cent below the data of Furukawa, *et al.* [4], as corrected by Ginnings [5]. This agreement is well within the estimated maximum uncertainty of 3 to 4°K in the calibration of the pyrometer.

Method of Operation

The experiments are carried out so that a day's work provides all the data required for calculating the enthalpy at one furnace temperature. Four to six experiments are carried out in a day – two or three each on the empty and full capsule. This method of operation has several advantages over the more usual practice of making one series of measurements on the empty capsule and another series on the full capsule. An important practical advantage is that subsequent minor disasters, such as breaking a suspension wire or chipping the capsule, do not affect the validity of results for other days. This method also eliminates the systematic error due to the slow changes in the emittance of the surface of the capsule between two series of measurements with the empty and full capsule and the corresponding change in the radiative heat loss in the lift. Often, no estimate is made of this error, presumably because other uncertainties are relatively large, but in one case the error was estimated to be less than 0.1 per cent in work at 1200°K [4]. Without this method of operation, much larger errors might be expected in our temperature range. From an alternate point of view, it permits the use of different capsules, different samples and different suspension wires to suit the temperature range.

At each furnace temperature the last experiment duplicates the first – if the first is on the empty capsule, so is the last. This technique affords the considerable advantage of averaging out most of the effect of gradual changes which occur during the day, such as changes in the emittance of the capsule or in its weight due to evaporation, or changes in temperature gradients in the furnace. The latter were found to be significant at the higher temperatures where a large furnace power was used in a one-hour heat-up period before stabilizing the furnace with the automatic control.

Although the first experiment is made three hours after the heat-up period, the gradient continues to decrease somewhat during the day. Making the first and last experiments on the empty capsule for example, will partially compensate for the effects of the change in gradient when the observations are averaged.

The experimental procedure is designed so that the small amount of radiation from the furnace to the calorimeter is the same for all experiments at the same furnace temperature. This procedure makes it unnecessary to measure the radiation to the calorimeter under the various conditions of shielding and temperature.

To start an experiment, the calorimeter heat leak rate is observed for ten minutes with the shutter closed and with the vacuum valve and the prism blocking radiation from the furnace. (Either the valve or the prism is sufficient to block the radiation.) The prism is removed, the capsule lowered to a position just above the vacuum valve and the slotted shield is positioned around the suspension wire. The vacuum valve is then opened and the capsule lowered slowly into the furnace so as not to disturb its temperature control. After about 15 minutes, the initial calorimeter temperature is observed. The subsequent operations are in a timed sequence starting 85 sec after the temperature measurements and requiring 10 sec to complete: the slotted shield is removed,

the lift mechanism is actuated, the shutter closed and the prism moved into position for temperature measurements. The time the capsule is in the furnace is adequate as shown by the experiments on aluminum oxide near 1200°K, where radiation is least and the time constant therefore longest. Data taken after 15 and 20 minutes in the furnace were not significantly different at this temperature.

The temperature is then observed with the visual pyrometer, usually eight readings by two observers. The final calorimeter temperature is taken when its rate of change is constant, about 25 min after the lift for the empty and 35 min for the full capsule. In the experiments with aluminum oxide, the equilibration time was 50 min, reflecting the higher heat capacity at the calorimeter temperature and the correspondingly longer time constant for equilibration.

Results

The experimental results are shown in Table I. The heat delivered to the calorimeter has been corrected to a calorimeter temperature of 313.15°K and to the average observed furnace temperature, using the integral of the heat capacities over the small temperature intervals.

The validity of these corrections depends on the following argument: the heat Q delivered to the calorimeter is equal to the enthalpy of the capsule (and contents) at the furnace temperature, H_F, decreased by the enthalpy at the calorimeter temperature, H_C, and by the heat loss Q_L during the lift, and increased by the heat Q_R radiated from the furnace between the time of the initial calorimeter temperature measurement and blocking the radiation with the shutter and prism. In our experiments the Q's as defined are always positive quantities. The difference in the heat delivered to the calorimeter for two experiments is given by

$$Q_1 - Q_2 = H_{F1} - H_{C1} - Q_{L1} + Q_{R1} - H_{F2} + H_{C2} + Q_{L2} - Q_{R2}. \qquad (1)$$

If the temperatures of the furnace differ by only a few degrees, then, since Q_L and Q_R are already small, the differences $Q_{L1} - Q_{L2}$ and $Q_{R1} - Q_{R2}$ can be neglected. The right-hand side of (1) then reduces to $(H_{F1} - H_{F2}) - (H_{C1} - H_{C2})$ which can be computed from heat capacities and weights of materials in the capsule and specimen. The remaining differences are the random errors of the experiment.

Corrections at the calorimeter temperature range up to 0.6 per cent of the observed heat. Corrections for small variations in the observed furnace temperature do not exceed 0.1 per cent of the observed heat. To some extent, they reflect random errors in the visual pyrometry. The corrections are so small that the effect of uncertainties in the heat capacity data used in making them [6]-[8] is negligible.

The enthalpy may be represented by the following equation for the range 1200 to 2600°K:

$$H_T - H_{298.15} = 28.9004T - 1.045 \times 10^{-4}\, T^2 - 16{,}126.25 \log_{10} \frac{T}{313.15} - 8907.3 \qquad (2)$$

where H is in absolute Joules per gram atomic weight and T in degree Kelvin. The heat capacity is given by

$$C_p = 28.9004 - 2.090 \times 10^{-4}\, T - 7003.54/T. \qquad (3)$$

Eq. (2) was obtained by a least squares fit of the enthalpies in Table I. Per cent differences between these observed values and those calculated from the equation are shown just below the observed values. Above 2200°K, where the effect of the temperature gradient in the furnace is greatest, the order of taking the data alternated – empty capsule first at 2263 and 2462 and full capsule first at 2364 and 2576 C – in order to exaggerate the effect of the change in gradient. The data at 2034 C, lacking the final empty capsule data, would be expected to lie above the smooth curve. Data at 2576 C, also incomplete, would be expected to lie below the smooth curve because the first experiment was made with the full capsule. These two sets of data were not used in computing (2).

The estimated standard error for the enthalpy calculated from (2) is not more than 0.14 per cent. Systematic errors in measuring the furnace temperature are estimated to be not more than 0.3 per cent due to the pyrometer calibration and not more than 0.4 per cent due to the difference between the observed temperature and the average temperature of the capsule.

Discussion

In the case of carbon, two questions must be considered in a presentation of the thermodynamic properties of the standard state: 1) Are the data sufficiently accurate in themselves? 2) Do they refer to a standard crystalline form of carbon?

Enthalpy differences calculated from (2) lie consistently about 0.7 per cent below the smooth data of McDonald for spectroscopic grade SPK graphite (density 1.9). They agree with recent reviews of older data, maximum deviations being 1 per cent below Dergazarian, *et al.* [8] at 1200°K and 0.7 per cent above Evans [7] at 2500°K. The heat capacity data derived from (3) are well within the scatter of the observations and the estimated accuracy of Rasor and

McClelland [9] in the range 1500-2600°K. Since the older experimental work includes measurements on natural graphite, this consensus supports reasonable confidence that the enthalpy and heat capacity are known to a few per cent from ambient to 2600°K.

Regarding the second question, there is experimental evidence to indicate differences in the heat capacity of different graphites. DeSorbo [10] reports enthalpies at 298.15°K for Ceylon natural graphite and an Acheson graphite which differ by 88 J/gfw, almost twice the tolerance on the heat of formation of CO_2 set by Rossini and Jessup [11] in their paper recommending graphite as the standard state for carbon. The corresponding difference in heat capacity might be expected to extend at least to somewhat higher temperatures. There are obvious systematic trends amounting to several per cent in the high temperature data for the four samples of Rasor and McClelland, but they state that these differences are not significant. The difference between our measurements and those of McDonald on Al_2O_3 near 1200°K is about 0.3 per cent. Taking this to represent the systematic difference between the two methods, we have 0.5 per cent difference between smoothed values at 1200°K to ascribe to random errors of measurement or to a difference in the samples. Considering our standard error of 0.14 per cent and a slightly larger value for McDonald's data, the 0.5 per cent difference is too large to claim no significant difference in samples, but too small to be reasonably sure of a significant difference.

TABLE I

EXPERIMENTAL DATA FOR GRAPHITE*

Furnace Temperature and Date	Heat to Calorimeter at 313.15°K	$H_T - H_{313.15}$ and % above Eq. (2)	Furnace Temperature and Date	Heat to Calorimeter at 313.15°K	$H_T - H_{313.15}$ and % above Eq. (2)
	4148.3 J	15884 J/gfw		8544.1 J	33397 J/gfw
	4148.6			8559.7	
1191.3	7327.5	0.00	1920.2	15248.7	+0.09
7-2-64	7325.6		7-1-64	15234.1	
	7329.6			15245.5	
	4152.0			8578.2	
	4682.3	17957		9311.4	36269
	4681.0			9323.0	
1281.4	8277.2	+0.02	2034.2	16576.7	+0.16
6-23-64	8271.9		6-12-64	16574.0	
	8277.7			16571.6	
	4684.9				
				10210	40198
	5974.0	23051	2191.2	18259	+0.10
	5975.4		7-15-64	18246	
1498.2	10593.3	-0.04		10207	
6-25-64	10582.2				
	10591.4			10605	41989
	5980.6		2263.2	19031	+0.02
			7-17-64	19040	
	6950.7	26927		10663	
	12349.2				
1659.7	12352.3	-0.12		20087	44398
6-30-64	6968.4		2364.7	11247	-0.36
	6970.3		7-20-64	11249	
				20176	
	7280.3	28231			
	7290.4			11872	47138
1710.9	12935.0	+0.08	2462.1	21300	+0.21
6-19-64	12935.8		7-27-64	21339	
	7289.3			11906	
			2576.4	22652	49869
			7-29-64	12677	-0.19

* At. wt. 12.01115

Acknowledgment

The authors are grateful to Mrs. E. K. Hubbard of the National Bureau of Standards Spectrochemical Analysis Section for the analytical work on the graphite specimen.

References

[1] G. B. Spence, Technical Report WADD-TR-61-72, Vol. XLI to the Air Force Materials Lab., Wright-Patterson AFB, Ohio, 1963.

[2] R. A. McDonald, private communication. Smoothed data are given by H. Prophet and D. R. Stull, *J. Chem. Eng. Data*, Vol. 8, 1963, p. 78.

[3] E. D. West and D. C. Ginnings, *J. Res. Natl. Bur. Stds.*, Vol. 60, 1958, p. 309.

[4] G. T. Furukawa, T. B. Douglas, R. E. McCoskey, and D. C. Ginnings, *J. Res. Natl. Bur. Stds.*, Vol. 57, 1956, p. 67.

[5] D. C. Ginnings, *J. Phys. Chem.*, Vol. 67, 1963, p. 1917.

[6] G. T. Furukawa and M. A. Krivanek, to be published.

[7] W. H. Evans, private communication.

[8] T. E. Dergazarian, N. J. Dumont, L. A. du Plessis, W. E. Hatton, S. Levine, F. L. Oetting, H. Prophet, G. C. Sinke, D. R. Stull, and C. J. Thompson, "JANAF Interim Thermochemical Tables," The Dow Chemical Co., Midland, Michigan; March 31, 1961.

[9] N. S. Rasor and J. D. McClelland, *J. Phys. Chem. Solids*, Vol. 15, 1960, p. 17; Wright Air Development Command Tech. Report 56-400, 1956.

[10] W. De Sorbo and W. W. Tyler, *J. Chem. Phys.*, Vol. 21, 1953, p. 1660. W. De Sorbo, *J. Amer. Chem. Soc.*, Vol. 77, 1955, p. 4713.

[11] F. D. Rossini and R. S. Jessup, *J. Res. Natl. Bur. Stds.*, Vol. 21, 1938, p. 491.

Reprinted from "Advances in Thermophysical Properties at Extreme Temperatures and Pressures," 1965, The American Society of Mechanical Engineers, 345 East 47th Street, New York, N. Y. 10017.

Dynamic Measurement of Heat Capacity and Other Thermal Properties of Electrical Conductors At High Temperatures

A. Cezairliyan and C. W. Beckett

Most measurements of heat capacity at high temperatures (above 1000 K) use the "drop method" in which the specimen is heated in a furnace to a known temperature and then dropped into a calorimeter near room temperature which measures the heat given up (enthalpy) by the specimen as the latter cools to the ambient temperature. A series of such experiments yields the relative enthalpy of the specimen from which heat capacity can be derived.

When this technique is extended to very high temperatures (above 2000 K) many problems are created as the result of increased heat transfer, chemical reactions, evaporation, diffusion, mechanical strength, etc., which limit the application of the method. Consequently, it has become necessary to develop a dynamic method which allows the heating of the specimen and the measurement of the pertinent quantities in a time so short the contribution of most of the phenomena, which limit the application of the conventional methods to very high temperatures, become negligible.

In dynamic measurements of heat capacity, the tubular specimen (electrical conductor) is heated from room temperature to near its melting point by a single heavy-current pulse of subsecond duration (heating rate is approximately 10 °K/ms). During this period, current flowing through the specimen, voltage drop across the specimen, and its temperature are measured at 0.4 ms intervals. The measurement of current is achieved by measuring the potential difference across a standard resistance placed in series with the specimen. Temperature measurements are made with a high-speed photoelectric pyrometer, which permits 1200 evaluations of the specimen temperature per second. A small hole drilled in the wall of the tubular specimen provides blackbody conditions. A bank of heavy-duty batteries constitutes the pulse-power source.

Dynamic recording of the pertinent variables is made with a high-speed digital data acquisition system which has a full-scale resolution of one part in 8000. The recording system consists of a multiplexer, analog-to-digital converter, a core memory, together with control and interfacing equipment. The output of the system consists of a teletypewriter which is connected to a time-sharing computer. Thus, the recording system allows the automatic digitization and storage of data during the dynamic experiment, and their computerized processing after the experiment.

The method described above provides considerable versatility in the measurements and the computational techniques. Heat capacity and electrical resistivity are calculated from data obtained during the heating period. Because of the short duration of the experiments, the only significant heat loss is that due to thermal radiation, which in most cases is less than five percent of the input power. Data taken during the initial free cooling period enables one to compute hemispherical total emittance and thus apply a correction to heat capacity. By conducting separate dynamic experiments—where the pyrometer is aimed at the outer surface of the specimen instead of the hole—one can obtain sufficient data to compute normal spectral emittance. Melting point of the specimen can be determined by allowing the heavy pulse current to flow until the specimen undergoes partial melting.

Preliminary results on molybdenum in the range 1800–2800 K yield standard deviations of 0.3, 0.1, and 2 percent for the precision of heat capacity, electrical resistivity, and hemispherical total emittance, respectively. It is believed that the accuracies of these measurements are comparable or better than the accuracies of other measurements of these properties at high temperatures.

Manuscripts related to the construction and operation of the various components of the dynamic measurements system, and the final results on molybdenum are in preparation.

The Vapor Pressure, Vapor Dimerization, and Heat of Sublimation of Aluminum Fluoride, Using the Entrainment Method[1]

by Ralph F. Krause, Jr., and Thomas B. Douglas

National Bureau of Standards, Washington, D. C. 20234 *(Received May 1, 1967)*

The vapor pressure P of anhydrous aluminum fluoride was measured at eight temperatures between 1194 and 1258°K by an entrainment method. The standard deviation of P from a least-square fit was 0.15%, and possible systematic errors of 0.5% in P and 1° in T were estimated. Smoothed values of P and dP/dT at 1225°K were determined. Considering P as the sum of the ideal monomeric and twice the dimeric vapor pressure, the other two thermodynamic properties necessary to define (1) $AlF_3(c) \rightleftharpoons AlF_3(g)$ and (2) $2AlF_3(g) \rightleftharpoons Al_2F_6(g)$ were taken as (a) $\Delta S°(1)$, derived from published spectroscopic and crystalline heat capacity data, and (b) $2\Delta H°(1) + \Delta H°(2)$, reported in a recent mass spectrometric study. The derived results at 1225°K along with their estimated uncertainties were $\Delta H°(1) = 67.0 \pm 0.4$ kcal, $\Delta S°(1) = 43.0 \pm 0.4$ eu, and $\Delta G°(2) = -7 \pm 1$ kcal.

Introduction

As part of a program of research to determine accurately the thermodynamic properties of substances that are important to high-temperature applications like chemical propulsion, a new apparatus was constructed to apply the entrainment method for measuring equilibria between solid and vapor. The high stability of anhydrous aluminum fluoride AlF_3 and the ease of obtaining a sample of fairly high purity made it suitable for precise measurements. Also, interpretation of current work in this laboratory on subliming AlF_3 in the presence of $AlCl_3$ vapor demands precise data for AlF_3.

Even though several investigators[2-13] had measured the vapor pressure of AlF_3, predominantly from 890 to 1100°K or from 1370 to 1570°K, most of their results were too imprecise to contribute to an evaluation of the composition of the saturated vapor. Each had derived a $\Delta H°$ for

$$AlF_3(c) \rightleftharpoons AlF_3(g) \qquad (1)$$

by assuming the vapor to be completely monomeric.

A mass spectrometric study by Porter and Zeller[14] indicated that the saturated vapor at 1000°K sustains perceptible dimerization

$$2AlF_3(g) \rightleftharpoons Al_2F_6(g) \qquad (2)$$

Also, the mole fraction of dimer in the saturated vapor increases with temperature because a mass spectrometric study by Büchler[15] showed that $\Delta H°$ of reaction 1 is less than that for

$$2AlF_3(c) \rightleftharpoons Al_2F_6(g) \qquad (3)$$

If each of the preceding vapor pressure measurements were considered to reflect the presence of both the monomer and the dimer, a corrected $\Delta H°$ of reaction 1 could be shown to be less than a second-law value, derived by assuming the vapor to be completely monomeric, and greater than a corresponding third-law value; moreover, the difference between these uncorrected second- or third-law values and the true ones would increase with temperature. Nevertheless, an inspection of all of these uncorrected values showed no such trend, but rather a scattering.

(1) This work was supported by the Advanced Research Projects Agency under Order No. 20 and by the Air Force Office of Scientific Research under Contract No. ISSA-65-8.

(2) W. Olbrich, Dissertation, Technische Hochschule, Breslau, 1928.

(3) O. Ruff and L. LeBoucher, *Z. Anorg. Allgem. Chem.*, **219**, 376 (1934).

(4) I. I. Naryshkin, *Zh. Fiz. Khim.*, **13**, 528 (1939).

(5) P. Gross, C. S. Campbell, P. J. C. Kent, and D. L. Levi, *Discussions Faraday Soc.*, **4**, 206 (1948).

(6) W. P. Witt, Thesis, Oxford University, Cambridge, 1959.

(7) W. P. Witt and R. F. Barrow, *Trans. Faraday Soc.*, **55**, 730 (1959).

(8) A. M. Evseev, G. V. Pozharskaya, A. N. Nesmeyanov, and Ya. I. Gerasimov, *Zh. Neorg. Khim.*, **4**, 2196 (1959).

(9) M. M. Vetyukov, M. L. Blyushtein, and V. P. Poddymov, *Izv. Vysshikh Uchebn. Zavedenii, Tsvetn. Met.*, **2**, 126 (1959).

(10) D. L. Hildenbrand and L. P. Theard, Aeronutronic Report No. U-1274, Newport Beach, Calif., June 1961.

(11) D. L. Hildenbrand and N. D. Potter, personal communication, 1964.

(12) P. E. Blackburn, Arthur D. Little Report, Cambridge, Mass., May 1965.

(13) H. C. Ko, M. A. Greenbaum, J. A. Blauer, and M. Farber, *J. Phys. Chem.*, **69**, 2311 (1965).

(14) R. F. Porter and E. E. Zeller, *J. Chem. Phys.*, **33**, 858 (1960).

(15) A. Büchler, Arthur D. Little Report, Cambridge, Mass., Sept 1962.

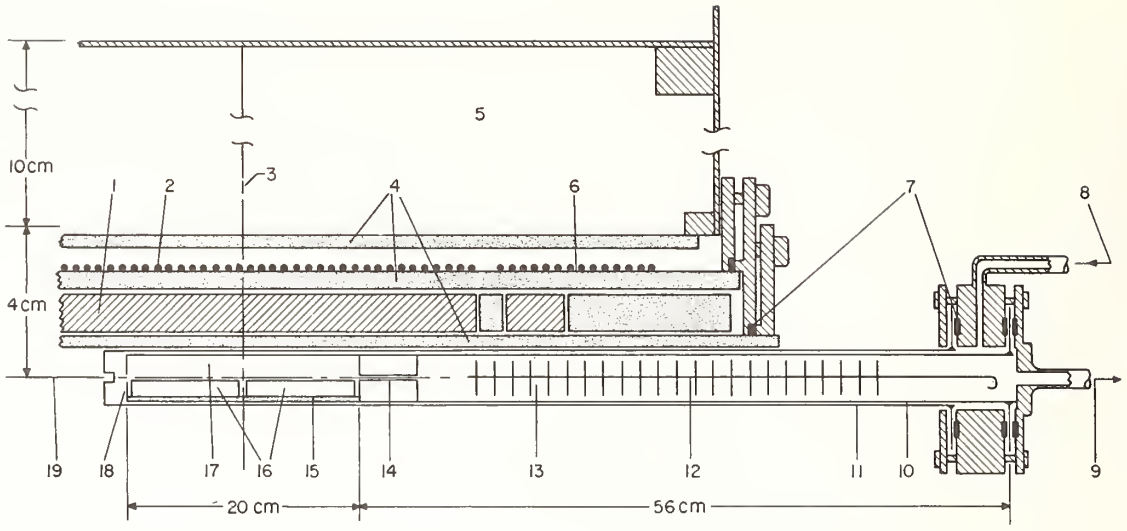

Figure 1. Diagram of entrainment tubes in the cylindrical furnace: (1) nickel core, (2) Pt–20% Rh main heater, (3) cross-sectional center, (4) alumina tubes, (5) insulation, (6) an end heater, (7) Teflon gaskets, (8) argon input, (9) argon output, (10) Pt–10% Rh composite tube, (11) Pt–20% Rh housing, (12) perforated disks, (13) condenser, (14) capillary tube, (15) alumina sled, (16) sample boats, (17) vapor cell, (18) detachable entrance cap, and (19) longitudinal axis. Note that vertical and horizontal scales differ.

The aim of this paper is to show how far the use of our precise sublimation data can go toward defining the thermodynamic properties of sublimation and dimerization of AlF_3 at temperatures where the vapor pressure is appreciable.

Entrainment Method

The entrainment method used in this work involved the flowing of argon gas through a high-temperature vapor cell, holding a sample of anhydrous AlF_3. The sublimed sample was condensed downstream, while the carrier gas was collected in a tank. Saturation was closely approximated by using an appropriate geometry of the vapor cell and flow of the gas mixture.

The vapor cell and condenser were separate sections of the same Pt–10% Rh composite tube as shown in Figure 1. The detachable cap prevented accidental spilling of the sample from the cell. The exit of the cell was connected to the condenser by a capillary tube of 5-cm length and 1-mm i.d. The application of Merten's[16] diffusion study to this system indicated negligible diffusion of the sample vapor through the capillary tube at the gas flows employed in this work.

The crystalline sample of anhydrous AlF_3 had been sublimed preliminarily at 1050° in a nickel retort. A spectrographic analysis reported 0.01 to 0.1% Mg; 0.001 to 0.01% Ca, Cu, Fe, Mn, Ni, and Si; and 10^{-4} to 10^{-3}% Cr and V. Triplicate chemical analyses reported from 67.61 to 68.00% F and from 32.13 to 32.17% Al, compared to the theoretical value of 32.130% Al. The mass of sublimed sample, roughly 200 mg, was taken as the mean of the condenser gain and the sample loss. The sample loss was the weight change of the loaded boats minus 11–16 mg of the weighed sample accidentally spilled in the cell. Since the sample loss was observed to be less than 0.2 mg for several experiments at zero gas flow, no correction for diffusion or distillation of the sample was warranted. While the condenser gain was consistently less than the above mean by an average 0.3%, apparently due to a weight loss of the composite tube itself, this difference was near the weighing uncertainty of this 137-g tube.

Preliminary to the argon flow, the atmosphere of air which was held in the vapor cell prior to its installation in the furnace was reduced to 10^{-4} torr while the vapor cell was being heated to 500°. Next, 99.996% pure argon, dried by anhydrous $Mg(ClO_4)_2$, was carefully introduced into the flow path until its pressure was equal to barometric pressure. Finally, after the vapor cell was heated to its operational temperature, an additional 3–4 hr at zero gas flow was required to attain a steady temperature. The total pressure of the gas mixture in the vapor cell was taken as the time average of the continuously recorded barometric pressure plus a head pressure of 0.6–1.2 torr. The volume of argon was measured with an accuracy of 10 ml by a calibrated gasometer which was immersed in a high-vacuum-pump oil saturated with argon and whose displacement of 14–28 l. was corrected for differences in the initial and final barometric pressure and room temperature.

Vapor Cell Temperature

Usually being the greatest single source of error in vapor pressure measurements, the temperature of

(16) U. Merten, *J. Phys. Chem.*, **63**, 443 (1959).

the vapor cell was measured with special care,[17] using Pt—Pt–10% Rh thermocouples. As shown in Figure 1, a nickel core in an atmosphere of nitrogen served to reduce any temperature gradient in the vapor cell, which was centered within an alumina tube of a wire-wound resistance furnace. Three thermocouples were inserted longitudinally into the walls of the nickel core; two had fixed differential junctions and the third had variable immersion to observe the temperature profile. A fourth was inserted along the furnace axis with its junction in the well near the vapor-cell entrance. A fifth was placed aside to check periodically the stability of the others. The thermocouples were calibrated by the NBS temperature section to an accuracy of ±0.5° at 1000°.

Some preliminary experiments showed that if the temperature gradient were negative in the direction of the gas flow through the vapor cell, the sample vapor would condense prematurely and plug the capillary tube. To prevent this deposit, each of three heaters was adjusted manually by an autotransformer to give the same temperature at the entrance and exit of the vapor cell and at the exit of the capillary tube. Instead of a zero-temperature gradient, however, a steady profile was observed to decrease about 2° for the first 5 cm along the length of the vapor cell, to increase linearly about 2° for the remaining 15 cm of the cell, and to be close to zero through the capillary tube. Besides, the axis temperature was observed to be 0.05–0.3° lower than that in the nickel core at the same cross section.

The temperature of an experiment was taken as the time average of the vapor-cell exit, the temperature of which drifted 1 or 2° during an 8–16-hr flow. An automatic recorder registered continuously the thermocouple emf relative to that of a Diesselhorst potentiometer with a precision equivalent to 0.05°. A possible systematic error of 1° in T was estimated and was considered to be nearly constant over the entire range of our measured temperatures.

Test for Saturation

Since diffusion of the sample vapor through the capillary tube was shown to be negligible, a test for saturation would be the linearity, extrapolated through the origin, of the flow of sample mass q *vs.* the average flow, v, of the gas mixture at a given cell temperature. When v was varied by a factor of 2, this test was satisfied, within accidental error, as shown by the very close agreement of each of the four successive pairs in the sixth column of Table I.

Another test for the degree of saturation was applied by considering the mass of sample lost in each of two successive boats in the vapor cell with a temperature gradient. The ratio of the weight loss of the second boat to that of the first was observed as 0.03 ± 0.005 for v near 120 ml/min and 0.04 ± 0.005 for v near 60 ml/min; the uncertainty resulted from accidently spilling some sample from either boat for each assembly. The partial pressure p of the sample was assumed to increase with the distance x beyond the start of the first boat at a given v according to

$$dp/dx = k(P - p) + AD(d^2p/dx^2)/v \qquad (4)$$

where k is a constant, P is the vapor pressure at x, A is the cross-sectional area, and D is the interdiffusion coefficient of the gas mixture. If there were no temperature gradient and p were zero at zero x, integration of eq 4 would yield a degree of unsaturation at the exit of the vapor cell less than 0.1%. Since we observed a temperature gradient $b = dT/dx$, P was assumed to be represented by

$$P \doteq P_0(1 + bcx) \qquad (5)$$

where P_0 is the vapor pressure at $x = 0$ and $c = dP/PdT$. Assuming the observed b and c, integration of eq 4 combined with eq 5 yielded a degree of unsaturation less than 0.4%.

Preliminary Assumption

If the sample vapor under the conditions of this work were assumed to be wholly monomeric and ideal, the vapor pressure P could be calculated from

$$P = P_T/(1 + (nM/w)) \qquad (6)$$

in which P_T is the total gas pressure, n is the number of moles of collected argon, w is the mass of sublimed AlF_3, and M is the molecular weight of its monomer. The resulting P's at eight independently measured temperatures are tabulated in Table I.

Second-law values of $\Delta H°(1)$[18] and $\Delta S°(1)$, which are listed in Table I, were determined by a least-square fit of our entrainment data with

$$R \ln P = \Delta S°(1) - (\Delta H°(1)/T) + \Delta C_p°[\ln (T/T') + (T'/T) - 1] \qquad (7)$$

in which the published value of $\Delta C_p° = -2.67R$ at $T' = 1225$°K was assumed constant over our temperature range. Such a fit gave standard deviations of 0.15% in P, 0.07 kcal in $\Delta H°(1)$, and 0.06 eu in $\Delta S°(1)$. A possible systematic error of 1° in T would give an additional 0.01 kcal in $\Delta H°(1)$ and 0.05 eu in $\Delta S°(1)$.

A third-law value of $\Delta H°(1)$ at $T' = 1225$°K was determined for each vapor pressure measurement according to

$$\Delta H°(1) = T[(-(\Delta G° - \Delta H°_{T'})/T) - R \ln P] \qquad (8)$$

whose mean $\Delta H°(1)$ and deviations from this mean

(17) W. F. Roeser and H. T. Wensel, *J. Res. Nat. Bur. Stand.*, 14, 247 (1935).

(18) Hereafter, a specific reaction will be indicated by the number in parentheses, and 1 cal = 4.1840 joules.

Table I: Preliminary Results for Reaction 1 by Assuming Wholly Monomeric Vapor

No.[a]	T, °K	q_{obsd}, mg/min	v_{obsd}, ml/min	P, matm	$(P - P_{calcd})/P_{calcd}$, %: II law	III law
1	1194.0	0.1441	112.1	1.500	0.07	−1.8
2	1194.7	0.0781	59.90	1.523	−0.10	−1.9
3	1212.1	0.2385	122.5	2.311	0.11	−0.6
4	1217.5	0.1342	61.00	2.619	0.00	−0.4
5	1236.9	0.3875	115.1	4.070	−0.3	0.4
6	1233.8	0.1948	51.65	3.810	0.09	0.6
7	1252.5	0.5869	124.3	5.778	0.08	1.7
8	1257.5	0.3226	62.23	6.441	0.03	1.9
	1225			$\Delta H°(1) = 68.49 \pm 0.1$[b]		66.73 ± 0.4 kcal
				$\Delta S°(1) = 44.44 \pm 0.1$[b]		43.0 ± 0.4 eu[c]

[a] Chronological sequence: 3, 7, 5, 1, 4, 8, 6, and 2. [b] This uncertainty was taken to be the sum of the random and possible systematic errors. [c] See ref 19, 20, and 24.

are listed in Table I. Each $-(\Delta G° - \Delta H°_{T'})/T$, the third-law $\Delta S°(1)$, and $\Delta C_p°$ of eq 7 were evaluated from the literature which is discussed in the next section.

A comparison of the preceding second- and third-law values reveals that our entrainment data appear incompatible with this preliminary assumption. The second-law $\Delta H°(1)$ in Table I is appreciably greater than the mean third-law $\Delta H°(1)$. Neither the experimental uncertainty of the entrainment data nor a reasonable estimate of the uncertainty of the third-law $\Delta S°(1)$ appears sufficient to overlap these discrepant values. Incidentally, the third-law values exhibit the characteristic temperature trend which is consistent with the concept of dimerization as shown by the two previously mentioned mass spectrometric studies. Although its magnitude has doubtful significance, the trend itself reflects the precision of our work.

Entropy of Sublimation

Of course, a possible cause for the trend and discrepancy of the preliminary assumption might be the third-law value of $\Delta S°(1)$. More importantly, however, its value and uncertainty were examined closely to evaluate the extent of dimerization whose reliability would depend upon the accuracy of $\Delta S°(1)$ despite the relatively high reliability that we believe our entrainment data have. Since $\Delta S°(1)$ was last evaluated for the JANAF tables,[19] more recent studies led us to make two revisions.

The first revision is that suggested by Douglas and Ditmars,[20] who measured the relative enthalpy of the crystal from 273 to 1173°K. Their work is in good agreement with a similar measurement by O'Brien and Kelley[21] and invalidates Frank's[22] adjustment of the latter's temperature scale. The assumed uncertainty in the entropy of the crystal arises from estimated uncertainties of 0.08 eu/mol from the high-temperature enthalpy measurements and of 0.08 eu/mol from King's[23] measurement of the low-temperature heat capacity.

The second revision is that suggested by Snelson's[24] infrared spectrum of AlF_3 by matrix isolation which is considered by most spectroscopists to yield more precise locations of band centers than a direct high-temperature technique. Both Büchler[25] and McCory, *et al.*,[26] performed the latter, which was a basis of the latest JANAF table.[19] Snelson observed spectra of saturated AlF_3 vapor in matrices of neon, argon, and krypton down to 200 cm^{-1} and assigned the strong absorption features to the three infrared-active frequencies of the AlF_3 molecule, which has a planar configuration of D_{3h} symmetry, analogous to BF_3. His assignment of the two doubly degenerate frequencies was confirmed by the matrix environment appearing to remove the degeneracy of these modes. Weaker absorption features of the saturated vapor were attributed to the dimer molecule Al_2F_6; the spectrum of the superheated vapor gave further support to this assignment, since only the strong absorption features remained. Another matrix spectrum reported by Linevsky[27] is in good agreement with Snelson's observed spectra, but Snelson noted that frequency shifts in his three matrices showed a regular trend. Following the procedure described in an earlier paper,[28] he estimated the gas-phase frequencies from the values

(19) D. R. Stull, *et al.*, "JANAF Thermochemical Tables," Dow Chemical Co., Midland, Mich., 1965.

(20) T. B. Douglas and D. A. Ditmars, *J. Res. Nat. Bur. Stand.*, **71A** 185 (1967).

(21) C. J. O'Brien and K. K. Kelley, *J. Am. Chem. Soc.*, **79**, 5616 (1957).

(22) W. B. Frank, *J. Phys. Chem.*, **65**, 2081 (1961).

(23) E. G. King, *J. Am. Chem. Soc.*, **79**, 2056 (1957).

(24) A. Snelson, *J. Phys. Chem.*, **71**, 3202 (1967).

(25) A. Büchler, Arthur D. Little Report, Cambridge, Mass., June 1962.

(26) L. D. McCory, R. C. Paule, and J. L. Margrave, *J. Phys. Chem.*, **67**, 1086 (1963).

(27) M. J. Linevsky, Space Science Laboratory Report, Philadelphia, Pa., Nov 1964.

(28) A. Snelson, *J. Phys. Chem.*, **70**, 3208 (1966)

...ve observed in the neon matrix to be $\nu_2 = 300$, $\nu_3 = 965$, and $\nu_4 = 270$ cm^{-1} with a probable accuracy of 10 cm^{-1}. Using the formulas given by Herzberg,[29] ν_1 was calculated to be 660 cm^{-1}. If the uncertainties of these assignments were all added in the same direction, this would contribute 0.3 eu/mol to the entropy of the monomeric gas established by applying the harmonic-oscillator, rigid-rotor approximation to the published spectroscopic data.

Two other sources of uncertainty were considered. First, an electron-diffraction study of AlF_3 by Akishin, *et al.*,[30] was considered to have an uncertainty of 0.03 Å in the Al–F bond distance which would contribute 0.1 eu/mol to the entropy of the gas. Second, we attempted to realize an error due to the neglect of anharmonicity and stretching. The formula derived by Mayer and Mayer[31] for diatomic molecules gives +0.1 eu correction to AlF at 1000°K. Assuming comparable anharmonicity and stretching for AlF_3 gave us a rough estimate of +0.2 eu, which may be several times larger than a true correction.

Applying the previous revisions to the JANAF[19] value at 1225°K yielded $\Delta S°(1) = 43.0 \pm 0.4$ eu.[32] Incidentally, the second-law value of $\Delta S°(1)$, derived from our entrainment data by assuming the dimer content of the saturated vapor to be zero, set an upper limit which is 1.5 eu higher than the above adopted value.

Correction for Dimerization

The previously mentioned mass spectrometric studies[14,15] and the infrared spectra by matrix isolation,[24,27] besides the results of our preliminary assumption, indicate that the saturated vapor of AlF_3 can be interpreted by taking into account the occurrence of some dimerization.

Two of the four thermodynamic properties necessary to define reactions 1 and 2 at 1225°K, near the midpoint of our observed temperature range, were derived solely from our entrainment data. They are the smoothed values $P = (3.115 + 0.072t)10^{-3}$ atm and $dP/dT = (7.154 + 0.165t)10^{-5}$ atm/deg derived from the least-square fit with eq 7, as discussed previously. The parameter $t = T_{true} - T_{obsd}$ was introduced to reflect the effects of a possible systematic error in our temperature measurements on P and dP/dT. A value of $t = 1°$ corresponds to an error in P of 2.3%, which makes a possible systematic error of 0.5% in P from eq 6 negligible. Having to look elsewhere for the other two properties, we chose $\Delta S°(1)$, discussed earlier, and $\Delta H°(3)$.

Since P was determined by the monomeric vapor assumption of eq 6, its resolution into the partial pressures of monomer and dimer is approximated very closely by

$$P = P_m + 2P_d \qquad (9)$$

where P_m and P_d are assumed to be related to properties of reactions 1 and 3, respectively, by

$$P_i = \exp[(\Delta S°/R) - (\Delta H°/RT)] \qquad (10)$$

The relationship among reactions 1, 2, and 3 is obviously exemplified by

$$\Delta H°(3) = 2\Delta H°(1) + \Delta H°(2) \qquad (11)$$

To make temperature conversions of $\Delta H°(2)$ and $\Delta S°(2)$ between 1000 and 1225°K, $\Delta C_p°(2)$ was assumed as $2R$ from the equipartitional heat capacities of the gas species involved. Combining eq 9, 10, and 11 allows P and dP/dT to be expressed as functions of $\Delta S°(1)$, $\Delta H°(1)$, $\Delta G°(2)$, and $\Delta H°(3)$ at 1225°K.

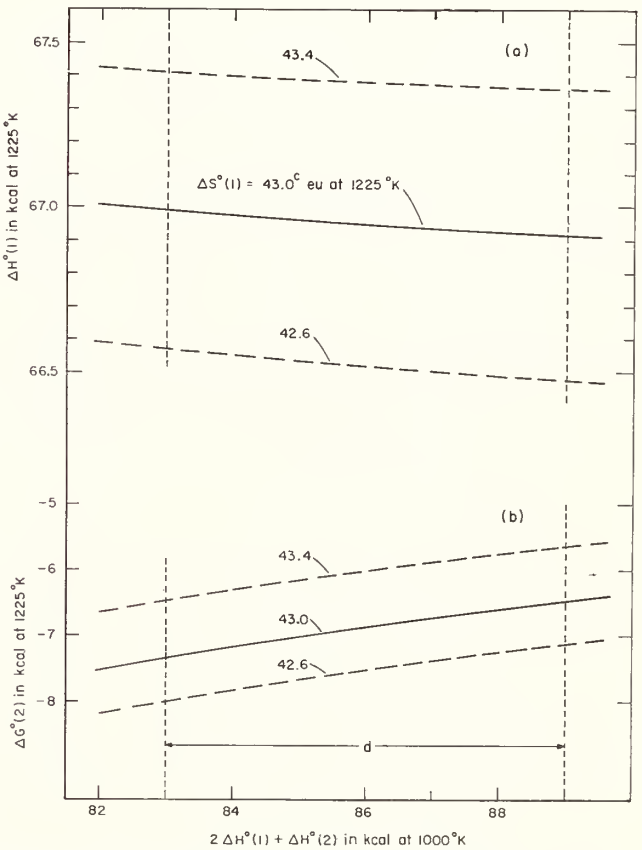

Figure 2. Hypothetical values of (a) $\Delta H°(1)$ and (b) $\Delta G°(2)$ calculated from P and dP/dT of this work and selected values of $\Delta S°(1)$ and $2\Delta H°(1) + \Delta H°(2)$ for reactions (1) $AlF_3(c) = AlF_3(g)$ and (2) $2AlF_3(g) = Al_2F_6(g)$. A possible systematic error of 1° in our observed T would contribute 0.05 kcal to $\Delta H°(1)$ and $\Delta G°(2)$. The superscript c in part a refers the reader to ref 19, 20, and 24, and the d at the bottom of part b, to ref 15.

(29) G. Herzberg, "Infrared and Raman Spectra of Polyatomic Molecules," D. Van Nostrand Co., Inc., New York, N. Y., 1945, p 177.
(30) P. A. Akishin, N. G. Rambidi, and E. Zasorin, *Kristallografiya*, 4, 186 (1959).
(31) J. E. Mayer and M. G. Mayer, "Statistical Mechanics," John Wiley and Sons, Inc., New York, N. Y., 1940, p 165.
(32) This uncertainty was taken to be the root of the sum of the several independent uncertainties squared.

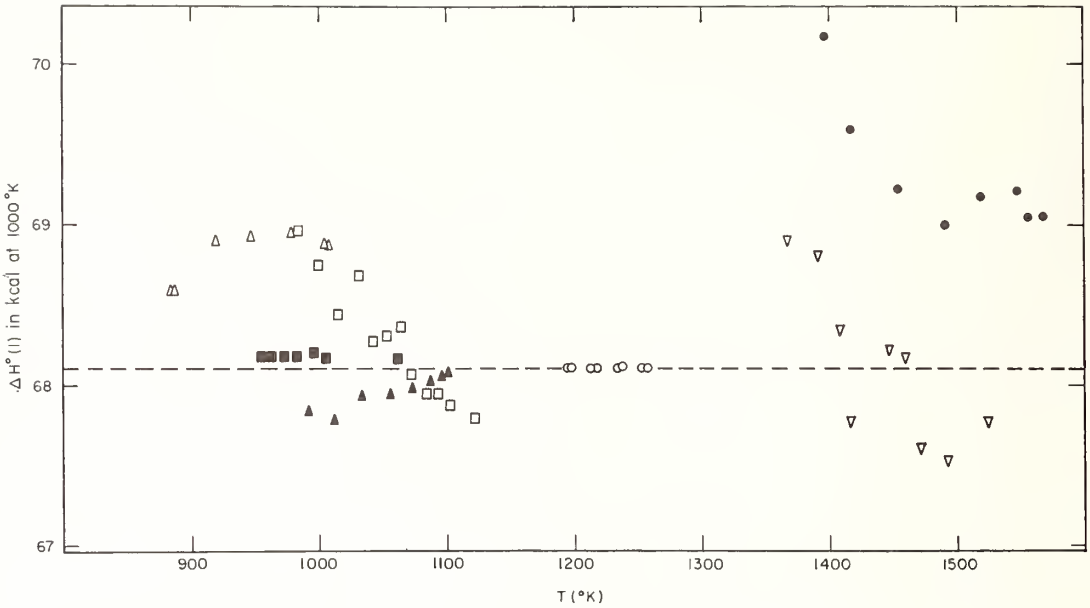

Figure 3. Third-law values of $\Delta H°(1)$ for $AlF_3(c) = AlF_3(g)$ from several vapor pressure measurements corrected for dimerization: Olbrich,[2] ●; Ruff and LeBoucher,[3] ▽; Witt,[6] ■; Evseev, *et al.*,[8] □; Hildenbrand and Theard,[10] ▲; Blackburn,[12] △; and this work, ○. Hildenbrand and Potter[11] reported 108 other values from 949 to 1128°K, which gave a 0.2-kcal standard deviation and whose mean $\Delta H°(1) = 67.5$ kcal. Note that $\Delta H°(1)$ was derived using $\Delta S°(1) = 43.0$ eu at 1000°K.

In this way, we generated hypothetical values of $\Delta H°(1)$ and $\Delta G°(2)$, calculated from P and dP/dT of this work and selected values of $\Delta S°(1)$ and $\Delta H°(3)$. An iterative method was used with a digital computer programed in BASIC.[33]

Derived Values

Figure 2 indicates values of $\Delta H°(1)$ and $\Delta G°(2)$ which are simultaneously in agreement with our precise entrainment data and reasonable choices of $\Delta S°(1)$ and $\Delta H°(3)$ of eq 11. Note that a $\Delta H°(1)$ which is associated with a given $\Delta S°(1)$ is nearly constant over a reasonable range of $\Delta H°(3)$. In view of our adopted value of $\Delta S°(1)$ and Büchler's[15] $\Delta H°(3)$, the foregoing analysis leads us to $\Delta H°(1) = 67.0 \pm 0.4^{32}$ kcal and $\Delta G°(2) = -7 \pm 1^{32}$ kcal at 1225°K. The effects on these values of small errors in the data used to derive them are shown explicitly by

$$\Delta H°(1) = 66.9_5 + 1.1s - 0.01h + 0.05t \quad (12)$$

$$\Delta G°(2) = -6.9 + 2s + 0.1h + 0.05t \quad (13)$$

where s, h, and t represent any variations from the values that we have assumed for $\Delta S°(1)$, $\Delta H°(3)$, and our observed T, respectively.

The above values derived from this work are given in Table II to compare with several values resulting from previously published investigations. Although Porter and Zeller[14] reported a value of $\Delta H°(2)$ which depends upon $\Delta S°(2)$ assumed by analogy with other halides, their measurement of P_d/P_m may be represented independently of this assumption by

$$\Delta G°(1) + \Delta G°(2) = -RT \ln (P_d/P_m) \quad (14)$$

Our evaluation of the extent of dimerization implicit in our entrainment data substantiates Porter and Zeller's mass spectrometric measurement.

The precision of our entrainment data is demonstrated by its comparison with that of some other investigations.[2,3,6,8,10-12] After each reported vapor pressure was corrected for dimerization, $\Delta H°(1)$ at 1000°K was calculated by eq 8 and plotted in Figure 3 at the temperature of its measurement. The consistency of our points contrasts with the scattering of most of the others. Only the results of Witt[6] agree rather closely with ours, except for a systematic discrepancy equivalent to about 1° in measuring temperature. Although his data have a precision similar to ours, they could do much less toward evaluating dimerization, whose extent is much smaller over his temperature range than ours. We found the mole per cent of dimer in the saturated vapor to be 4.6 ± 1.4 at 1225°K while Porter and Zeller[14] reported it to be near 1 at 1000°K.

There are numerous other substances besides aluminum fluoride for which the status of the data available for evaluating the thermodynamics of evaporation and vapor association is similar. Invariably, the various types of data are related complexly, and hence inconsistencies among them are not easy to evaluate. We believe that such parametric plots as Figure 2 offer perhaps the clearest and most objective means of

(33) J. G. Kemeny and T. E. Kurtz, "BASIC," Dartmouth College, Hanover, N. H., 1965.

Table II: Thermodynamic Values for Reactions 1 and 2

T, °K	Property	Previous work		This work[a]
1225	$\Delta H°(1)$, kcal			67.0 ± 0.4
	$\Delta S°(1)$, eu			43.0 ± 0.4[b]
	$\Delta G°(2)$, kcal			-7 ± 1
1000	$2\Delta H°(1) + \Delta H°(2)$, kcal	85.8 ± 3	[c]	
	$\Delta H°(1)$, kcal	67.3 ± 3	[c]	68.1 ± 0.4
	$\Delta H°(2)$, kcal	-48 ± 4	[d]	-50 ± 3
	$\Delta S°(2)$, eu	-32 ± 3	[d]	-35 ± 3
	$\Delta G°(1) + \Delta G°(2)$, kcal	8.6 ± 0.6	[d]	9 ± 1

[a] Derived by assuming $2\Delta H°(1) + \Delta H°(2) = 86$ kcal at 1000°K. [b] References 19, 20, and 24. [c] Reference 15. [d] Reference 14. See eq 14 for conversion of observed P_d/P_m, the uncertainty of which was taken to be twice its standard error.

establishing what the inconsistencies are, how sensitive they are to errors in the various types of data, and whether there are one or more sets of fundamental thermodynamic quantities which appear to fit all the available data within the respective experimental reliabilities.

Acknowledgments. The initial development of the entrainment apparatus was carried out by A. Ç. Victor. We thank E. J. Maienthal and R. A. Paulson for their chemical analyses of the sample and appreciate the helpful advice of D. R. Lide, Jr., and S. Abramowitz in evaluating the spectroscopic data. George Long, of the Aluminum Company of America, kindly supplied the sample.

[Reprinted from the Journal of Physical Chemistry, **72**, 475 (1968).]

5. Reaction Calorimetry

UNITED STATES DEPARTMENT OF COMMERCE · Frederick H. Mueller, *Secretary*
NATIONAL BUREAU OF STANDARDS · A. V. Astin, *Director*

Precise Measurement of Heat of Combustion With a Bomb Calorimeter

R. S. Jessup

National Bureau of Standards Monograph 7

Issued February 26, 1960

For sale by the Superintendent of Documents, U.S. Government Printing Office, Washington 25, D.C. - Price 25 cents

237-I

Contents

Precise Measurement of Heat of Combustion With a Bomb Calorimeter [1]

R. S. Jessup

This Monograph gives detailed descriptions of apparatus and methods which are used at the National Bureau of Standards for precise determinations of heats of combustion of liquid hydrocarbon fuels. Numerical examples are given of methods of calculating results of measurements from observed data. The technique of making and filling glass bulbs to contain samples of volatile liquid fuels is described.

The accuracy of the methods described is about 0.1 percent. This is intermediate between the accuracy of 0.01 or 0.02 percent attained in certain measurements on pure compounds, and the accuracy of several tenths of one percent obtainable with published standard procedures for measurements on fuels.

1. Introduction

Standard methods of moderate precision for bomb-calorimetric measurement of heats of combustion of solid and liquid fuels are published by the American Society for Testing Materials [1,2].[2] These methods can be used to measure heat of combustion with an accuracy of several tenths of one percent. Apparatus and methods for measurements of heat of combustion with an accuracy of 0.01 or 0.02 percent have been described in the literature [3]. The attainment of such accuracy involves the use of rather laborious and time-consuming procedures. In some applications of fuels the heat of combustion is required with an accuracy of approximately 0.1 percent, which is probably not attainable with the standard methods referred to [1, 2], but can be attained with less expenditure of time and effort than is required in the most precise measurements.

This Monograph describes methods and apparatus used at the National Bureau of Standards in connection with several series of investigations of heats of combustion of aircraft fuels [4, 5, 6, 7]. The restrictions of the treatment to a particular set of apparatus, and a particular experimental procedure involves some loss of generality, but this is not believed to be serious. Most precise measurements of heats of combustion of materials containing essentially only the elements carbon, hydrogen, nitrogen, and oxygen have been made in apparatus of similar design, to which the same procedures are applicable. Descriptions of other equally satisfactory apparatus for this purpose will be found in reference [3] and the references there cited. There will also be found in some of these references descriptions of apparatus and procedures suitable for measurements on materials containing considerable amounts of such elements as sulfur and halogens. The apparatus and methods described in this Monograph are not suitable for measurements on such materials.

Although the apparatus described in this Monograph is suitable for measurement of heat of combustion with an accuracy of 0.01 or 0.02 percent, the procedure in measurements on fuels is such that a considerable saving in time was achieved at the cost of a somewhat lower precision. This lower precision resulted from several factors as follows:

(1) As a rule only two experiments were made on each fuel, as compared with six or more experiments where the highest possible accuracy is desired; (2) an approximate method was used to obtain the corrected temperature rise of the calorimeter, i.e., the temperature rise corrected for heat of stirring and heat transfer between calorimeter and surroundings; (3) because some liquid fuels are quite volatile there may be an appreciable loss of lighter components in handling. In spite of these effects the results of measurements even on the most volatile fuels (gasolines) are, in general, precise to about 0.05 percent. The results contain a nearly constant systematic error of approximately 0.03 percent (for hydrocarbon fuels) due to neglect of the Washburn correction [18] which takes account of the difference between heats of combustion in oxygen under a pressure of about 30 atm and at a pressure of 1 atm.

(If desired, this error can be approximately corrected, in the case of hydrocarbon fuels only, by reducing the observed heat of combustion by 0.03 percent.)

In other respects the methods described are applicable in measurements of the highest precision, and may serve as a useful guide to persons interested in such measurements.

1.1. Definitions of Terms

a. Heat Units

The heat units used in connection with measurements of heats of combustion of fuels are the IT calorie [3] and the Btu. These units are here defined as follows:

[1] The preparation of this Monograph was supported in part by the Air Force Ballistic Missiles Division, Air Research and Development Command, U.S. Air Force.

[2] Figures in brackets indicate the literature references on page 16.

[3] IT calorie is an abbreviation for International Steam Tables calorie. This calorie was adopted by the International Steam Table Conference held in London in July 1929 [12], and is in fairly general use in engineering practice both in this country and abroad.

1 IT calorie=4.1868 absolute joules
1 Btu=1055.07 absolute joules.

The definition of the Btu was obtained from that of the IT calorie by means of the relations

1 pound (avoirdupois)=453.5924 grams
1 IT calorie per gram=1.8 Btu per pound.

b. Heats of Combustion

The quantity directly measured in a bomb-calorimetric experiment is generally referred to as the "total (or gross) heat of combustion at constant volume"; this quantity is represented by the symbol Q_v (gross) in this Monograph. A precise definition of this term requires a specification of the initial states of the reactants (oxygen and fuel) and of the final states of the products of combustion. For most purposes the following definition is sufficient: *The total (or gross) heat of combustion at constant volume of a liquid or solid fuel containing only the elements carbon, hydrogen, oxygen, nitrogen and sulfur is the quantity of heat liberated when unit weight of the fuel is burned in oxygen in an enclosure of constant volume, the products of combustion being gaseous* CO_2, N_2, *and* SO_2 *and liquid* H_2O, *with the initial temperature of fuel and oxygen and the final temperature of the products of combustion at 25° C.*

Although the total heat of combustion is the quantity directly measured in a bomb-calorimetric experiment, the quantity required in many practical applications is the "net heat of combustion at constant pressure." This quantity is designated by the symbol Q_p (net), and may be defined as follows: *The net heat of combustion at constant pressure of a liquid or solid fuel containing only the elements carbon, hydrogen, oxygen, nitrogen, and sulfur is the quantity of heat liberated when unit weight of the fuel is burned in oxygen (or air) at a constant pressure of one atmosphere, the products of combustion being* CO_2, N_2, SO_2, *and* H_2O, *all in the gaseous state, with the initial temperature of fuel and oxygen and the final temperature of products of combustion at 25° C.*

For the most fuels to which these definitions apply the elements oxygen, nitrogen, and sulfur will be minor constituents if present at all. The methods described in this Monograph are not suitable for accurate measurements on materials containing more than about 2 percent sulfur.

2. General Discussion of Bomb-Calorimetric Measurements

A bomb calorimeter consists essentially of a calorimeter vessel containing a measured amount of water, in which are immersed (1) a thermometer for measuring the temperature of the water, (2) a stirring device for maintaining the water at a uniform, and therefore definitely measurable temperature, and (3) a "bomb" of constant volume in which combustible materials can be burned in oxygen under pressure. In order to control heat transfer between the calorimeter and its environment ("thermal leakage") the calorimeter vessel is enclosed by a "jacket" which is separated from the vessel by an air space about 1 cm thick, and which for a majority of precise calorimeters, is kept at constant temperature by means of a thermostat.

A schematic diagram of a bomb calorimeter and its jacket is shown in figure 1. The calorimeter vessel is made in the form shown in order to facilitate stirring of the calorimetric liquid. The effectiveness of a screw propeller stirrer is greatly increased by enclosing it in a tube which extends from near the top to near the bottom of the calorimeter vessel. Putting the tube outside of the main part of the calorimeter vessel, as shown in figure 1(b), reduces the total volume of the calorimeter necessary for a bomb of given size.

In principle, a measurement of the heat of combustion of a given material consists in comparing the corrected temperature rise of the calorimeter in an experiment in which a known quantity of energy is supplied to it, with that produced in another experiment by combustion in the bomb of a weighed sample of the given material. The temperature rise in both experiments should be as nearly as possible over the same temperature range from a standard initial temperature to a standard final temperature. This method of using the corrected temperature rise of the calorimeter to compare an unknown with a known quantity of energy eliminates some of the systematic errors of calorimetric measurements, in particular those associated with uncertainty as to the exact location of the boundary of the

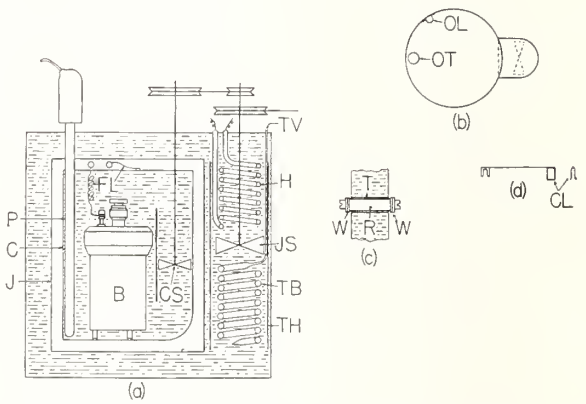

FIGURE 1. *Schematic diagram of a bomb calorimeter.*

(a) Assembled calorimeter with jacket: B, bomb; C, calorimeter vessel; J, jacket wall; P, resistance thermometer; FL, firing leads; CS, calorimeter stirrer; JS, jacket stirrer; TV, tube to thermostat valve; H, jacket heater; TB, thermostat bulb; and TH, tubular housing. (b) Top view of calorimeter vessel OL, opening for firing lead; and OT, opening for thermometer. (c) Firing lead through jacket T, tube; R, rod; and W, washers. (d) Firing lead to calorimeter vessel CL, clip.

calorimeter, and those associated with various kinds of lag, by virtue of which different parts of the calorimeter are at different temperatures when the temperature is changing.

Experiments to determine the corrected temperature rise of the calorimeter when a known quantity of energy is supplied to it are generally called calibration experiments, and the mean result of a series of such experiments expressed as energy supplied per unit of corrected temperature rise is called the "energy equivalent" of the calorimeter. The product of the energy equivalent and the corrected temperature rise of the calorimeter in an experiment in which a material of unknown heat of combustion is burned in the bomb gives the energy liberated in the combustion reaction plus any side reactions which may occur.

Calibration experiments are conveniently carried out by burning in the bomb weighed samples of a standard material, such as benzoic acid (NBS Standard Sample 39), the heat of combustion of which is accurately known. If the calorimeter is to be used for measurements of heats of combustion of volatile liquids, such as gasolines, it is desirable to supplement the calibration experiments with benzoic acid by making a series of measurements on NBS Standard Sample 217 of 2,2.4-trimethylpentane, which is a volatile liquid with a certified value for its heat of combustion. The difference between the measured and certified values of heat of combustion will give an overall check on the accuracy of the measurements, and in particular, on the effectiveness of precautions taken to eliminate effects of volatility.

Since a measurement of heat of combustion involves the comparison of two nearly equal changes in temperature covering the range from a standard initial temperature to a standard final temperature, the temperature scale used in the measurement is not important. Thus temperatures can be expressed in terms of the resistance in ohms of a given platinum resistance thermometer with the energy equivalent of the calorimeter in calories per ohm, or in Celsius degrees with the energy equivalent in calories per degree.

3. Factors Affecting Accuracy in Bomb-Calorimetric Measurements

The overall error in the result of a bomb-calorimetric measurement is the algebraic sum of individual errors contributed by various factors. Some of the individual errors may be positive and others negative, so that to some extent they may be expected to cancel. However, the extent to which cancellation may take place is uncertain, and may vary from one experiment to another, so that the percentage contribution of each individual error should be kept well below the permissible overall error of the determination. In the present Monograph the permissible difference between duplicate determinations is taken as 0.05 percent. In order to attain this precision, the error contributed by each of the various independent factors should be kept below 0.01 percent so far as possible.

The factors which may affect the accuracy of a bomb-calorimetric determination may be divided roughly into two classes, (1) side reactions which may take place in the bomb, the effect of which cannot be readily evaluated, and (2) the experimental techniques used in making the various individual measurements. These two classes of factors are discussed in sections 3.1 and 3.2, respectively.

3.1. Undesirable Side Reactions

These include (a) formation of carbon monoxide, carbon, or other products of incomplete combustion of the samples; (b) oxidation of the crucible in which combustion of the fuel sample takes place, or oxidation of other parts of bomb or fittings; (c) reaction of acids formed in combustion with the material of the bomb; (d) oxidation of combustible impurities such as hydrogen or hydrocarbon gases in the oxygen used.

a. Incomplete Combustion

In tests of volatile liquid fuels which must be enclosed in glass bulbs to prevent loss by evaporation, incomplete combustion sometimes occurs as a result of breakage of the bulb before ignition of the sample. In such cases large amounts of carbon will usually be formed, and the results of such tests should be discarded. Normally a bulb containing a volatile liquid sample does not break before ignition of the sample, and in such cases there is generally little or no evidence of incomplete combustion. It occasionally happens that globules of glass remaining in the crucible after combustion are gray or black in color. This may be due to metal oxides formed in combustion of the fuse wire, or to inclusion of a small amount of carbon in the glass while it is molten. Determinations of carbon dioxide in the products of combustion of pure liquid hydrocarbons which were enclosed in soft glass bulbs indicate that the amount of carbon in such glass globules does not exceed 0.01 percent of the carbon in the sample.

Incomplete combustion of solid materials, such as benzoic acid, is very likely to occur if these materials are placed in the crucible in powdered form. For this reason, such materials should be compressed into pellets. For samples of non-volatile liquid fuels which are not enclosed in glass bulbs, and for pelleted samples of benzoic acid, incomplete combustion almost never occurs in apparatus such as that described in the appendix.

b. Oxidation of Crucible and Fittings

Oxidation of the crucible and its support and other fittings exposed to the direct action of the flame can be avoided by using platinum crucibles and fittings (see appendix).

c. Reaction of Acids with Bomb Material

Reaction of acids formed in combustion with the material of the bomb can be made negligible by the use of suitable corrosion-resistant material for the bomb. The bomb described in the appendix has been found satisfactory in this respect. Bombs provided with gold or platinum linings have also been found to be satisfactory.

d. Combustible Impurities in Oxygen

Combustible impurities in the oxygen used may introduce very serious errors into the results of bomb-calorimetric measurements. Oxygen prepared by electrolysis of water may contain enough hydrogen to cause errors of 1 percent or more. The possibility of error from this source is eliminated by passing the oxygen over copper oxide at 500° C before admitting it to the bomb (see appendix).

3.2. Experimental Techniques of Individual Measurements

The most important of the individual measurements which go to make up a bomb calorimetric determination include measurements of (a) the weight of the sample of combustible; (b) the weight of the calorimeter plus water; and (c) the temperature rise of the calorimeter, including correction for thermal leakage and heat of stirring. A given percentage error in any one of these measurements introduces an equal percentage error into the final result of the experiment. Other individual measurements which determine relatively small correction terms and which can be easily made with the necessary precision include measurements of (d) the quantity of energy used to fire the charge of combustible; (e) the amounts of oxygen and other materials in the bomb; and (f) the amounts of nitric and sulfuric acid formed in the combustion reaction.

a. Weight of Sample of Combustible

The sample of combustible (0.8 to 1.5 g) is weighed with a precision of about 0.02 mg using an undamped semimicro balance with a keyboard arrangement for adding and removing the smaller weights (see appendix). Calibrated high grade (class M) weights are used, and the corrections to the weights given on the calibration certificate are applied in determining the weight of the sample. If weighings are made in the ordinary manner with weights and object weighed on opposite pans of the balance, the balance should be tested to determine whether the balance arms are of equal length. If the arms are found to differ in length by a significant amount a correction for this difference will be necessary.

The necessity for such a correction can be eliminated by using the method of weighing by substitution. This consists in placing on the left-hand pan a fixed weight or "tare," somewhat greater in weight than the heaviest object to be weighed, then placing the object to be weighed on the right-hand pan together with sufficient weights, including rider adjustment, to balance against the tare. The object being weighed is then removed and weights and rider again adjusted to obtain balance. The difference in the weights required in the two cases is the desired weight of the object. In addition to eliminating the effect of any difference in length of the balance arms, this method also eliminates any change in sensitivity with load, since the load is constant. The following description of the procedure is for this method of weighing by substitution.

Each half of the balance beam from the center knife edge to the outer knife edge is graduated in 100 equal divisions, so that if a 1 mg rider were used a change in position of the rider by one division on the scale would correspond to a change in weight of 0.01 mg. However, it may be inconvenient to use such a small rider because of the likelihood of its being deformed or lost. Instead, a 10 mg rider may be used so that one division on the scale corresponds to 0.1 mg in weight, and hundredths of a milligram obtained from the deflection of the pointer, as described below.

Weighings are normally made with the weights to the nearest milligram on the right-hand pan of the balance, and the 10 mg rider so placed (between 0 and +10 divisions on the beam scale) that the tare weight on the left-hand pan is balanced to the nearest 0.1 mg. The equilibrium position of the pointer with reference to the zero of the index scale is then determined by observing the turning points of the pointer in an odd number of swings (3 or 5).

The procedure in using the balance will be illustrated by an example of the weighing of a sample of benzoic acid. All weighings are made after time has been allowed for temperature equilibrium to be established, and for air currents set up when the balance case was open to die out. To determine when equilibrium has been established, the apparent weight is observed from time to time until no change has been observed during a period of about 10 min.

The following observations were made in determining the weight of a pellet of benzoic acid, the first set of observations were made with the empty crucible, and the second with the crucible containing the pellet:

Crucible empty:		
Weights	12.493 g	Turning points of swings:
Rider	0.0002	−2.6 2.0
Pointer deflection ×2, −0.55×0.07×10−3	− .00004	−2.5
Total weights	12.49316	−2.55 2.0
		2×pointer deflection=−0.55
Crucible plus pellet:		
Weights	10.971	Turning points of swings:
Rider	0.0003	−2.3 2.6
Pointer deflection ×2, 0.45×0.07×10−3	.00003	−2.0
Total weights	10.97133	−2.15 2.6
		2×pointer deflection=+0.45
Observed weight of pellet	1.52183	
Weight correction [a]	+ .00005	
Corrected weight of pellet	1.52188	

[a] The weight correction is the algebraic sum of the certificate corrections to the individual weights used with the empty crucible minus the algebraic sum of the corrections to the weights used with crucible plus pellet.

In the above example the weight corresponding to the pointer deflection from the zero of the index scale was obtained by multiplying twice the average deflection (in divisions on the scale) by one-half of the sensitivity reciprocal of the balance, in this case $0.07=1/2\times0.14$ mg per scale division. (The same result would be obtained, of course, if the average deflection were multiplied by the sensitivity reciprocal, e.g., for the first weighing of the above example the average pointer deflection $=-0.28$ and $-0.28\times0.14=-0.04$ mg).

The same procedure is followed, for example, in weighing a sample of a volatile liquid which must be enclosed in a glass bulb to prevent loss by evaporation, except in this case it is not necessary to include the crucible in either weighing. The empty bulb is first weighed against the tare, and then the filled bulb together with glass removed in sealing is weighed against the tare. It should be emphasized that the balancing weight against the tare with only the weights on the right-hand pan should be determined in weighing both the empty bulb and the filled bulb. The use of a fixed value for the balancing weight against the tare with only the weights on the right-hand pan would introduce errors if the rest point of the balance changes between the times of weighing the empty and filled bulbs. This is likely to occur if a considerable length of time elapses between the weighings with the bulb empty and filled. The use of a fixed value for the balancing weight with the empty crucible on the right-hand pan is ruled out by the fact that the crucible is subject to changes in weight in use.

b. Weight of Calorimeter Plus Water

The calorimeter plus water (3,700 g total weight)[4] is weighed on a magnetically damped balance having a capacity of 5 kg and a sensitivity of 0.5 mg (see appendix). The procedure in this weighing is as follows: The calorimeter is filled with approximately the desired quantity of water, the temperature of which is adjusted to a value such that after assembly of the calorimeter its temperature will be a few tenths of a degree below the desired initial temperature in the experiment. The choice of the temperature to which the water is to be brought before weighing will depend upon a number of factors, including room temperature, the desired initial temperature in the calorimetric experiment, and the relative heat capacities of calorimeter vessel, water, and bomb. No definite rule can be given for this choice, but the operator will learn by experience how to select the proper temperature under the conditions of his particular laboratory and apparatus.

After adjustment of the temperature the calorimeter is placed on one pan of the balance with the desired weights (see footnote 4) on the other. The amount of water in the calorimeter is adjusted so that the total weight of calorimeter plus water exceeds slightly that of the weights on the opposite balance pan, and the balance case is closed. Because of evaporation of water the weight of calorimeter plus water decreases slowly, and the pointer on the balance gradually moves toward the zero of the index scale. When the pointer reaches the scale zero the balance beam is arrested, the case is opened, and the calorimeter is removed from the balance and placed in position in its jacket preparatory to making a calorimetric experiment.

It is not feasible in weighing the calorimeter to wait for it to come to temperature equilibrium with the air, partly because this would require a very long time and partly because the desired initial temperature in the calorimetric experiment will usually differ from room temperature. Any difference in temperature between calorimeter and the air in the balance case will cause convection currents which will affect the observed weight. The effect of this will partially cancel if the difference between the temperature of calorimeter and the air in the balance case when the calorimeter is weighed is the same in all experiments, including both calibration experiments and measurements of heat of combustion.

The change in weight of the water in the calorimeter due to evaporation after weighing will affect the energy equivalent of the calorimeter, but the effect of this is small and will cancel if the

[4] The weight should correspond to an amount of water in the calorimeter such that when the bomb is immersed in the water the calorimeter cover can be put in place with its lower side in contact with the water.

procedure in placing the calorimeter in its jacket and completing the assembly of the system is carried out in the same manner and in the same length of time in the calibration experiments as in measurements of heat of combustion.

In addition to the water in the calorimeter vessel, 1 cm^3 of water is placed in the previously dried bomb before each experiment to insure that the space in the bomb is saturated with water vapor at the beginning of the experiment as well as at the end, when water formed in combustion will be present in any case. This water is introduced into the bomb by means of a buret or pipet accurate to about 0.01 cm^3, immediately before introducing the sample of combustible.

c. Temperature Measurements

The temperature rise of the calorimeter in a combustion experiment is approximately 3° C, and must be measured with an accuracy of 0.0003° if the error in temperature measurement is to contribute not more than 0.01 percent to the result of the calorimetric experiment. Measurements of temperature differences with this precision can be made conveniently with a suitable 25 ohm platinum resistance thermometer, and a Mueller bridge of the type commonly designated as G–2.

In precise measurements of temperature with a resistance thermometer it is customary to eliminate the resistance of the thermometer leads completely by making two resistance readings, with the commutator set first in the N position and then in the R position. In bomb calorimetric measurements where only a small temperature difference is to be measured and where time for making the temperature measurements is limited, it is permissible to omit changing the commutator setting. However, if this procedure is followed it is very important that all measurements in all experiments be made with the same commutator setting, since the change in observed resistance per degree change in temperature may be different for the N and R positions of the commutator. The possibility of error due to change in the commutator setting may be eliminated by permanently disconnecting one of the current leads (c or t) of the thermometer from the bridge. The thermometer is then effectively a 3-lead thermometer and the bridge can be operated with only one setting of the commutator.

It is also important that the thermometer be immersed to the same depth in all experiments, so that its contribution to the energy equivalent of the calorimeter will be the same in all experiments, and so that the temperature distribution along the leads will be the same.

The observations of the temperature of the calorimeter in a bomb-calorimetric experiment must be made in such a manner as to provide data from which can be derived a value for the temperature rise corrected for thermal leakage and heat of stirring. The following procedure is for a calorimeter with the jacket maintained constant at a standard temperature.[5]

Temperatures of the calorimeter are measured at definite times during three periods: (1) An initial period of 6 to 10 min during which the temperature change results solely from thermal leakage and heat of stirring; (2) a middle period of about 12 min, at the beginning of which the charge in the bomb is fired, and during which the temperature change is due partly to thermal leakage and heat of stirring but mostly to the heat liberated by the combustion reaction in the bomb—this period continues until the rate of change of temperature has become constant; and (3) a final period of 10 min or more, during which the temperature change is again due solely to thermal leakage and heat of stirring. It is desirable to choose the initial temperature of the calorimeter so that its final temperature will be slightly below that of the jacket. This reduces the total thermal leakage during the middle period and eliminates heat transfer by evaporation of water from the calorimeter and condensation on the jacket wall which would occur if the temperature of the calorimeter exceeded that of the jacket.

During the initial and final periods the resistance of the thermometer should be measured with the highest possible accuracy, since the overall accuracy of the determination depends directly upon the accuracy of these temperature measurements. During the middle period, because of the very rapid rate of temperature rise, it is not possible to make readings as accurately as during the initial and final periods, but this is not important because the readings of the middle period are used only for calculating the relatively small correction for thermal leakage and heat of stirring.

With a G–2 bridge and a thermometer having a resistance of approximately 25.5 ohms at 0°C, one step in the last dial of the bridge (0.0001 ohm) corresponds to approximately 0.001°C in temperature. Readings of the bridge are made to the nearest 0.00001 ohm (0.0001°) by interpolating between two adjacent settings of the last dial of the bridge. This interpolation is accomplished by observing the deflection of the galvanometer as follows: The galvanometer is located about 2 meters from a ground glass scale graduated in millimeters, which is so placed as to be conveniently observable by the operator of the bridge. In front of the galvanometer mirror is placed a lens of such focal length that the reflected image of the vertical filament of a light source is focused on the ground-glass scale.[6] The bridge current is adjusted so that with constant thermometer resistance a change of 0.001 ohm in the bridge

[5] The NBS calorimeter is located in an air-conditioned laboratory, the temperature of which is maintained at about 25° C. The jacket temperature is always maintained constant at 28° C and the calorimetric experiments cover the range from 25° to 28° C. If room temperature is not controlled the standard temperature of the jacket should be taken high enough so that it will be above room temperature at all seasons. A jacket temperature below that of the room is undesirable as it may result in the condensation of water on the calorimeter, the initial temperature of which is 3° C below that of the jacket.

[6] Lamp and scale devices for indicating galvanometer deflection are available commercially, and are as satisfactory as the device described here.

setting causes a galvanometer deflection corresponding to a 2.5 cm displacement[7] of the filament image on the scale. This is equivalent to a displacement of 2.5 mm per step in the last dial of the bridge, i.e., to 2.5 mm per millidegree. This sensitivity is doubled by reversing the current through the bridge and observing the resulting change in position of the filament image. The sensitivity is such that when the bridge current is reversed a displacement of the filament image by 0.5 mm corresponds to 0.00001 ohm (0.0001°). Reading the bridge by observing the deflection of the galvanometer when the bridge current is reversed not only increases the sensitivity but also reduces the effect of changes in the galvanometer zero. The reversal of the bridge current is conveniently made by means of a double-pole double-throw toggle switch connected in the battery circuit.

The above discussion of the deflection of the galvanometer when the bridge current is reversed tacitly assumes that the resistance of the thermometer remains constant during this operation. In an actual calorimetric experiment the resistance of the thermometer is usually changing with time; in the initial period for example the resistance of the thermometer is increasing at a rate of approximately 0.0007 ohm/min. (0.007° C/min). During this period readings are made once per minute in such a manner as to give the resistance of the thermometer to the nearest 0.00001 ohm at intervals of exactly 1 min. These readings are made as follows: The switch for reversing the bridge current is thrown in the direction such that as the temperature of the calorimeter rises the image of the filament of the galvanometer light source moves toward the observer's right. The bridge dials are adjusted occasionally so as to keep the filament image slightly to the left of its zero position. The time is observed by means of a stop watch, or preferably by means of a combination of stop watch and audible second signals from a standard clock. The position of the filament image is observed to the nearest 0.5 mm at a time 4 sec before the even minute and the reversing switch is thrown immediately. The position of the image is observed again at 4 sec after the even minute[8] and the switch is then thrown back to its original position in preparation for later readings. If the second position of the filament image is exactly the same as the first, then the galvanometer deflection on the even minute was zero, and the reading of the bridge is correct with zero in the next place after the reading of the last dial. If the second position of the filament image is x mm to the left (or right) of the original reading, then the reading of the bridge should be increased (or decreased) by $0.00002x$ ohm to obtain the reading corresponding to the even minute. For example, if the reading of the bridge is 27.3956 ohms and the upper and lower arrows in figure 2(a) represent the initial and final positions, respectively, of the filament image, then the corrected reading of the bridge at the even minute would be 27.39563 ohms. On the other hand the situation represented in figure 2(b) for the same setting of the bridge dials would correspond to a corrected bridge reading of 27.39556 ohms.

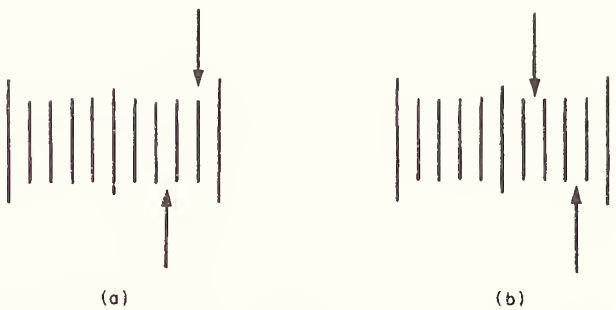

FIGURE 2. *Diagram to illustrate use of galvanometer deflections in reading bridge.*

With a little practice an observer can learn to anticipate each bridge reading fairly closely after the first one or two of a series, and to preset the bridge dials for each subsequent reading so that the change in galvanometer deflection upon reversal of the current will not exceed 2.5 mm (0.00005 ohm or 0.0005° C).

As a result of the preliminary adjustment of the temperature of the water in the calorimeter before weighing it as described in section 3.2.b., it is to be expected that after assembling the calorimeter the temperature will be a few tenths of a degree below the desired initial temperature. The temperature should then be raised to about 0.05° (0.005 ohm) below the temperature at which the initial period is to start, and allowed to drift up to this temperature as a result of thermal leakage and heat of stirring. The observations of the initial period are then made as described above.

The heating of the calorimeter to 0.05° below the starting temperature is most conveniently done by means of an electric heater which is a permanent part of the calorimeter system. Another method which is frequently used is to place a heated brass rod (½ in. × 2 in.) on top of the calorimeter cover. The rod is inserted through a hole in the jacket cover which is normally closed by a brass plug. Care is taken to avoid having the heated rod come in contact with the jacket and thereby upset the control of its temperature.

[7] With the particular combination of bridge, thermometer, galvanometer, and galvanometer to scale distance used, the bridge current of 6.8 ma (thermometer current of 3.4 ma) gives the sensitivity indicated. Much higher bridge current is undesirable because of the increased heating of the thermometer and the consequent increased variation of thermometer resistance with slight variations in bridge current. A 6-volt low-discharge storage battery is a convenient source of bridge current.

[8] The time which should elapse between the two observations of the galvanometer deflection depends upon the free period of the galvanometer. The reading time of an underdamped galvanometer with a relative damping constant of 0.8 or 0.9 is roughly equal to the free period [19].

The above instructions may be illustrated by an example. The calorimeter temperature before weighing was adjusted to a value such that after assembly of the calorimeter the thermometer reading was 20.5+7.420 ohms.[9] By means of the heated rod referred to above, the temperature was raised until the reading of the bridge was 20.5+7.465 ohms. The rod was then removed, the plug replaced in the hole in the jacket, and the calorimeter temperature allowed to drift upward until the bridge reading was 20.5+7.4701 ohms when the readings of the initial period were begun. These are made once per minute as indicated previously.

Immediately after the observations of the initial period are completed the charge of combustible in the bomb is ignited by means of an electric fuse, the sensitivity of the galvanometer is reduced by reducing the bridge current to about one-third of its original value, and the observations of the middle period are begun. These must be made so rapidly that there is no time for reversing the bridge current for each observation. The observations are made by setting the bridge dials successively at certain predetermined readings and observing the times at which the galvanometer deflection becomes zero. After about 3 min the rate of temperature rise has decreased to such an extent that the bridge current can be increased to its original value and the precise readings of resistance each minute are resumed. These precise readings are continued until the rate of temperature change has been constant for at least 10 min. The observations made after the rate of temperature change has become constant constitute those of the final period.

TABLE 1. *Observations of time and thermometer resistance during a bomb-calorimetric experiment*

Time minutes	Resistance minus 27.5 ohms	Difference $\times 10^5$	Time minutes	Resistance minus 27.5 ohms	Difference $\times 10^5$
0	0.47015		7.614	0.7000	
1	.47078	63	7.747	.7100	
2	.47142	64	7.922	.7200	
3	.47206	64	9	.75050	870
4		128 (64)	10	.75920	350
5	.47334	63 (64)	11	.76270	140
6	.47397		12	.76410	60
6.528	.4900		13	.76470	29
6.621	.5100		14	.76499	16
6.682	.5300		15	.76515	10
6.754	.5500		16	.76525	9
6.820	.5700		17	.76534	6
6.894	.5900		18	.76540	6
6.970	.6100		19	.76546	7
7.066	.6300		20	.76553	7
7.170	.6500		21	.76560	6
7.320	.6700		22	.76566	20 (7)
7.399	.6800		23		(6)
7.496	.6900		24		(7)
			25	.76586	6
			26	.76592	7
			27	.76599	7
			28	.76606	

[9] The bridge has a 20.5-ohm coil in addition to the 10-, 20-, 30-ohm coils, etc., in the 10x10-ohm decade (see appendix).

Bridge readings made during the course of a typical bomb calorimetric experiment are given in table 1, and are shown graphically in figure 3. The values given for resistance represent the observed resistance of the thermometer minus 27.5 ohms. The initial period extends from $t=0$ to $t=6$ min, the middle period from $t=6$ to $t=18$ min, and the final period from $t=18$ to $t=28$ min. The constancy of the differences between consecutive readings in the initial and final periods is an indication that the system has attained a steady state. This is a necessary condition for the applicability of the method given in section 5 for calculating the corrected temperature rise.

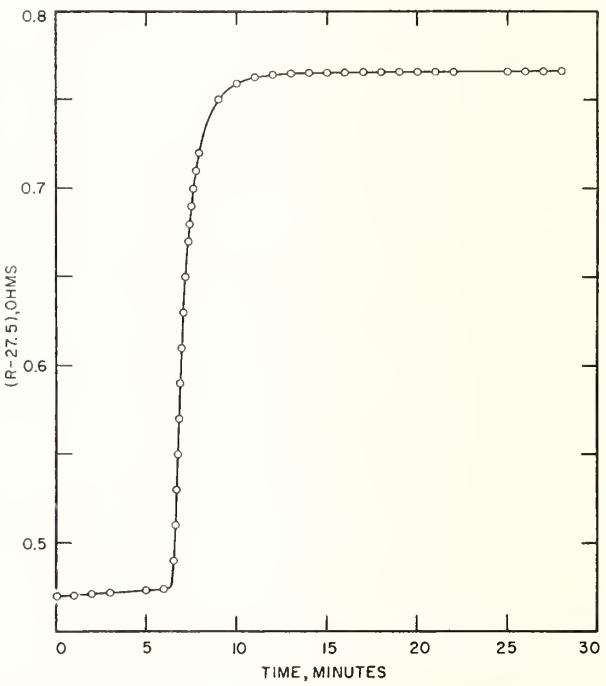

FIGURE 3. *Bridge readings versus time in a bomb calorimetric experiment.*

In the particular experiment illustrated in table 1 and figure 3 the time readings during that part of the middle period from $t=6$ to $t=9$ min were made by means of an electric timer which prints the time at which the operator presses a button when he observes the galvanometer deflection to pass through zero. This instrument is a convenience and would be an important part of the equipment in measurements of extremely high precision. It is not a necessary part of the apparatus for measurements of the precision aimed at in the procedures described in this Monograph. For such precision it is also not necessary to obtain as many readings in the middle period. It is sufficient to make three or four measurements in the range from 55 to 70 percent of the total temperature rise, and to read the time to the nearest second (or the nearest 0.01 min) by means of a stopwatch.

The corrected temperature rise for the experiment illustrated in table 1 and figure 3 is calculated in section 5.

d. Firing Energy

The quantity of energy used to fire the charge is the sum of the electric energy used to ignite the fuse plus the heat of combustion of the amount of fuse wire burned. The current for igniting the fuse is obtained from a small transformer with a secondary voltage of about 10. The total firing energy can be determined in a series of blank experiments in which only the fuse wire is burned. In such experiments the temperature rise of the calorimeter is very small, and the initial temperature of the calorimeter should be very near that of the jacket. The rate of change of temperature in the initial and final periods will then be small, and the correction for thermal leakage will also be small.

When a 2-cm length of fuse wire is used in the manner described in the appendix it has been found that if the wire is burned completely [10] the firing energy is constant and equal to 5.2 cal. No appreciable error will result from using this value in any case where the same type of fuse is used, i.e., a 2-cm length of Parr fuse wire wound into a helix and attached to platinum leads. The firing energy in this case is only 0.05 percent of the energy normally produced in a combustion experiment, and any error in the value 5.2 cal will largely cancel if this same value is used for both calibration experiments and measurements of heats of combustion, and if the temperature rise is about the same in the two kinds of experiment.

The most serious error likely to be encountered in accounting for the firing energy is that which may result from a short-circuit between the firing electrode and the bomb, either because of failure of the insulation around the electrode or because of moisture getting into the mica insulation inside of the bomb. This mica normally is wet by the acid solution formed in combustion and by the water introduced in washing the interior of the bomb after each experiment. It should be dried thoroughly before each experiment, and the insulation should be tested before attaching the fuse to its platinum leads. An insulation resistance of less than 10^6 ohms usually indicates either moisture in the insulation or some other failure of the insulating material which needs to be corrected. A "megger" or volt-ohmeter or other similar instrument may be used for testing the insulation resistance.

[10] Combustion of the fuse wire may not be complete in all blank experiments to determine the firing energy, although it is practically always complete when a sample of fuel is burned in the bomb. Blank experiments in which combustion of the fuse wire is incomplete should be rejected, or else a correction for the unburned wire should be applied.

e. Materials in Bomb

A calibration of the calorimeter yields a value for the energy equivalent E of the system as actually used, consisting of calorimeter vessel, stirrer, water, thermometer, bomb, and contents of the bomb at the beginning of the experiment. The calorimeter vessel, stirrer, mass of water, thermometer, and bomb will ordinarily be unchanged from one experiment to another, and the crucible and amount of water placed in the bomb will also be constant. However, the mass of the platinum leads to the fuse, the mass of oxygen, and the mass and kind of combustible material may change from one experiment to another. The heat capacity of the largest amount of platinum wire in the bomb amounts to only 0.001 percent of the total energy equivalent of the system, so that variations in the amount of platinum wire are entirely negligible. The mass of oxygen in the bomb is inversely proportional to absolute temperature and directly proportional to absolute pressure. The temperature is measured to about 0.5° C at the time the oxygen is admitted to the bomb, by means of a mercurial thermometer with its bulb near the bomb. The pressure of the oxygen (about 30 atm=450 psi) is measured to the nearest 0.1 atm (1.5 psi) by means of a calibrated Bourdon gage.

The values of the energy equivalent E obtained in calibration experiments are reduced to the energy equivalent E_s of a standard calorimeter system consisting of the calorimeter vessel with cover, the standard mass of water, stirrer, thermometer, and bomb containing 1 ml of water, the crucible, and oxygen under an absolute pressure of 30.0 atm at 28.0° C but no combustible material. In a measurement of heat of combustion the energy equivalent E_s of the standard calorimeter system is corrected for any excess of the oxygen pressure at 28° C over 30 atm and for the heat capacity of the charge of combustible.

The reduction of the observed E to the corresponding value of E_s, and vice versa, is discussed in section 5 on calculation of results.

f. Acids Formed in Combustion

Nitric acid is normally formed in the combustion reaction from nitrogen either in the fuel sample itself or present as an impurity in the oxygen. If sulfur is present in the fuel, oxides of sulfur will be formed. These are entirely converted to sulfuric acid if nitric acid is also formed. For this reason, if the fuel is known or suspected to contain a significant amount of sulfur, the air initially present in the bomb should not be flushed out with oxygen at the time oxygen is admitted to the bomb. The sulfur will then be all converted to aqueous sulfuric acid, and therefore to a determinate final state.

The total acid formed in combustion is deter-

mined by washing the inner surface of the bomb with distilled water and titrating the washings against 0.1 N sodium hydroxide, using methyl orange as the indicator.

If both nitric and sulfuric acids are formed the total acid is determined by titration as before, and the sulfur is determined by analyzing the bomb washings after titration, using the procedure described in ASTM Designation D129–58 [14]. The correction for nitric acid is 14.0 kcal/mole of acid formed. If sulfur is present in the fuel the total acid is corrected for as if it were all nitric acid, and an additional correction of 1,400 cal/g of sulfur is applied.

4. Summarized Directions for a Bomb-Calorimetric Experiment

Summarized directions will now be given for carrying out a bomb-calorimetric experiment with benzoic acid to determine the energy equivalent of the calorimeter. Following these directions there will be a brief discussion of the differences in procedure in an experiment to determine the heat of combustion of a fuel.

4.1. Preliminary Adjustment of Apparatus

Observe the temperature of the oxygen purifier and if necessary bring its temperature to 500° C. (Caution: The temperature and oxygen pressure should never be allowed to exceed values consistent with safety with respect to the possibility of explosive failure of the purifier. The manufacturer's recommendations regarding safety precautions should be adhered to rigidly.) Add water, if necessary, to fill the calorimeter jacket bath, bring its temperature to the desired standard value and put the thermostat into operation (see sec. 3.2.c.).

4.2. Preparation and Weighing of Sample of Benzoic Acid

Weigh out approximately an amount of benzoic acid somewhat in excess of 1.52 g [11] and compress it into a pellet. Weigh the pellet on a balance sensitive to about 0.01 g and adjust the weight, if necessary, to 1.52 ± 0.01 g (see footnote 11) by scraping the pellet. Carefully remove any powdered benzoic acid from the pellet by brushing. Weigh the crucible on the semimicro balance, first empty and then after placing the pellet of benzoic acid into it, following the procedure described in section 3.2.a.

4.3. Preparation of Bomb

Test insulation resistance. If less than 10^6 ohms, dry mica or replace cone insulator.

Attach fuse wire to platinum leads as described in the appendix.[12] Measure 1.00 cm^3 of distilled water into the bomb by means of a buret or pipet. Attach the crucible to its support in such a manner that the fuse is nearly touching the pellet of benzoic acid and assemble the bomb. Connect the bomb to the oxygen cylinder through the purifier and admit oxygen to a pressure of approximately 30 atm. The oxygen should be admitted slowly so as not to cool the copper oxide in the oxygen purifier below the temperature at which it will oxidize combustible impurities in the oxygen. Close the valve in the oxygen line and open the needle valve on the bomb, allowing the oxygen to escape until the pressure is reduced to atmospheric. This procedure removes about 97 percent of the nitrogen in the air initially in the bomb. Refill the bomb to the pressure of approximately 30 atm, read and record the temperature and pressure, and disconnect the bomb from the oxygen tank. Attach the binding post (fig. 6(b)) with the lead wire to the terminal nut on the bomb.

4.4. Weighing of Calorimeter Plus Water

Fill the calorimeter with water, adjust temperature of water, and weigh calorimeter plus water as described in section 3.2.b.

4.5. Assembly of Calorimeter

Immediately after the calorimeter is weighed carry it to the jacket and place it in its proper position in the jacket space. Place the bomb in the calorimeter,[13] put the calorimeter cover in place and press it down until its lower surface is in contact with the water. These operations should be performed rapidly and as nearly as possible in the same manner and in the same length of time in all experiments. Complete the firing circuit by connecting the lead to the bomb electrode to the binding post provided for this purpose (fig. 1.(c)) and connect the other lead (already attached to the other binding post) to the calorimeter vessel by means of the clip shown in figure 1.(d) (see appendix). Close the jacket cover and connect the calorimeter stirrer to its driving shaft. Measure the jacket temperature to 0.001° C (0.0001 ohm) by means of the bridge and resistance thermometer, then remove the thermometer from the jacket bath, dry it, and put it in place in the calorimeter.

[11] The standard mass of benzoic acid should be such as to give a temperature rise of approximately 3° C. The mass used should be within 0.01 g of the standard mass.

[12] It may be convenient to do this while waiting for the attainment of temperature equilibrium in the balance case in connection with weighing the sample of combustible.

[13] The bomb should be lowered into the calorimeter without touching the water with the fingers. This can be done by using some sort of hook on which the bomb can be hung and which can be removed after the bomb is in place. A hook made of a piece of brass or nichrome rod about $\frac{1}{16}$ in. in diameter and bent into the form shown in fig. 6(f) has been found satisfactory for this purpose with the Parr bomb. The hooked ends of the rod are inserted into holes on opposite sides of the screw cap of the bomb, and are easily removed after the bomb is in place. The amount of water which adheres to the hook when it is withdrawn from the calorimeter is negligible.

4.6. Adjustment of Initial Temperature of Calorimeter

Adjust the calorimeter temperature to 0.05° (0.005 ohm) below the starting temperature of the initial period, and allow it to drift up to the starting temperature as described in section 3.2.c. The starting temperature (in calibration experiments) always has the same value, which is so chosen that the final temperature of the calorimeter after combustion will be at, or preferably a few hundredths of a degree below, the temperature of the jacket.

4.7. Observation of Temperature and Ignition of Sample

After the temperature of the calorimeter has been allowed to drift up to the starting temperature, make and record the readings of time and temperature of the initial period each minute as described in section 3.2.c. Immediately after the last reading of the initial period fire the charge by closing the circuit through the fuse in the bomb. Observe the ammeter in this circuit when the charge is fired. The reading of the ammeter should rise abruptly to about 5 amp and then drop almost instantly to zero. Failure of the current to drop immediately indicates a short circuit, and the charge will probably not be ignited, or if it is ignited the result of the experiment will be in error by an unknown amount because of the excess electrical energy. If the ignition takes place normally, make and record the observations of the middle and final periods as described in section 3.2.c. After the end of the final period remove the thermometer from the calorimeter, insert it in the jacket bath and measure the temperature of this bath to 0.001°. If the temperature control equipment has been operating properly the jacket temperature should remain constant to 0.005° or better during an experiment.

4.8. Analysis of Contents of Bomb

Remove the bomb from the calorimeter, dry it, open the needle valve and allow the gas to escape at a rate such as to reduce the pressure to atmospheric in not less than 1 min. Then open the bomb and examine the interior for unburned carbon, which would indicate incomplete combustion. If more than a slight trace of unburned carbon is found the experiment should be rejected. If no appreciable amount of unburned carbon is found wash all interior surfaces of the bomb with distilled water and collect the washings quantitatively in a beaker. The quantity of the washings should preferably not exceed 150 ml. Titrate the washings against a 0.1 N solution of NaOH using methyl orange as the indicator. Calculate the correction for nitric acid as described in section 5 on calculation of results.

The procedure in a measurement of heat of combustion follows the same steps outlined in paragraphs 4.1 to 4.8, with certain differences in individual steps as indicated below.

4.2.a. Preparation and Weighing of Sample of Fuel

If the material whose heat of combustion is to be determined is a sufficiently nonvolatile liquid, weigh the empty crucible by the method of substitution as described previously, decrease the weights on the pan with the crucible by the desired weight of sample,[14] and add the liquid drop-wise from a pipet until the weights plus sample plus crucible balance the tare weight on the opposite pan. Ordinarily this procedure will add more than the desired weight of sample, and the excess may be removed, for example, by dipping the end of a fine glass capillary into the liquid. Great care should be taken during the introduction of the sample into the crucible and making the final adjustment of the weight to avoid getting any of the sample on the outside of the crucible. The final weighing of crucible plus sample is carried out as described in section 3.2.a.

If the material whose heat of combustion is to be determined is a volatile liquid, the enclosure of the sample in a glass bulb (as described in the appendix) and the determination of its weight (as described in sec. 3.2.a.) will ordinarily have been done prior to the beginning of the calorimetric measurements. It is then only necessary to place the bulb in the crucible before starting the procedure described in section 4.3. and 4.3.a.

4.3.a. Preparation of Bomb

The procedure here is the same as that described in section 4.3 except that if the sample contains sulfur the air initially in the bomb is not flushed out before filling the bomb with oxygen. If the sample does not contain sulfur the air should be flushed out as described in section 4.3 by filling the bomb with oxygen to 30 atm, allowing the gas to escape until the pressure is reduced to atmospheric, and then refilling the bomb to 30 atm. Where the sample is enclosed in a glass bulb, premature breakage of the bulb when the pressure is first raised to 30 atm can sometimes be detected by the odor of the fuel in the escaping gas when the pressure is released.

4.6.a. Adjustment of Initial Temperature of Calorimeter

In the case of a nonvolatile liquid where the weight of sample is such as to give a temperature rise equal to that in a calibration experiment the adjustment of the initial calorimeter temperature is carried out in the same manner as described in section 4.6.

[14] The weight of sample should be such as to give approximately the same temperature rise of the calorimeter as in the calibration experiments.

In the case of volatile samples it is difficult to make the glass sample-bulbs sufficiently uniform in capacity to give the same temperature rise of the calorimeter in all experiments. Select the initial temperature for each experiment so that the mean of the initial and final temperatures of the calorimeter will be the same as in the calibration experiments.

4.8.a. Analysis of Contents of Bomb

If the sample contains no sulfur follow procedure described in section 4.8. If the sample contains sulfur titrate the bomb washings to determine total acid is described in section 4.8. After this titration analyze the bomb washings for sulfur using the procedure described in ASTM Designation D129–58 [14].

5. Calculation of Results

5.1. Calibration Experiment

Calculate a value for the energy equivalent E from the data of each calibration experiment, using the following formula:

$$E=\frac{Q_c\times m_s+c_1+c_2}{\Delta t}$$

where Q_c=heat of combustion of benzoic acid in IT calories per gram under the conditions of the experiment.
m_s=weight in air, in grams, of sample of benzoic acid burned.
c_1=correction for firing energy, in calories.
c_2=correction for nitric acid, in calories.
Δt=corrected temperature rise of calorimeter, in degrees Celsius (or ohms).

The value of E will be in calories per unit of the temperature scale used, e.g., in calories per deg C, or calories per ohm.

a. Heat of Combustion of Benzoic Acid

The certified value for the heat of combustion of the present standard sample (39h) of benzoic acid under the standard conditions of the bomb process is 6318.3 IT cal/g weight in air.[15] The standard conditions are:

A. The combustion reaction is referred to 25° C.

B. The sample is burned in a bomb of constant volume in pure oxygen at an initial pressure of 30 atm at 25° C.

C. The number of grams of sample burned is equal to three times the internal volume of the bomb in liters.

D. The number of grams of water placed in the bomb before combustion is equal to three times the internal volume of the bomb in liters.

If the conditions in the experiment differ from the standard conditions A, B, C, and D above, the value of Q_c for the heat of combustion of benzoic acid under the actual conditions of the experiment will be obtained from the following approximate equation, which was derived in accordance with the procedure recommended by Washburn [18]:

$$Q_c=6318.3\left\{1+10^{-6}\left[20\left(P-30\right)+42\left(\frac{m_s}{V}-3\right)+30\left(\frac{m_w}{V}-3\right)-45\left(t-25\right)\right]\right\}$$

where P=initial absolute pressure of oxygen, in atmospheres, at the temperature t,
m_s=weight of sample, in grams,
m_w=weight in grams, of water placed in bomb before combustion,
V=internal volume of bomb in liters,
t=temperature to which the combustion reaction is referred, in degrees C.

The temperature to which the reaction is referred is here taken as the final temperature of the calorimeter. The value of the energy equivalent E obtained from eq (1) is then that of the initial calorimetric system at the mean temperature of the calorimeter. By the initial calorimetric system is meant the system before combustion of the benzoic acid, i.e., it includes the benzoic acid, water, and oxygen in the bomb before combustion takes place.

For example let the following data be given:

Volume of bomb, V = 0.380 liter
Weight of benzoic acid, m_s = 1.522g; m_s/V=4.01g/liter
Weight of water in bomb, m_w = 1.00g; m_w/V=2.63g/liter
Initial oxygen pressure = 30.8 atm gage at 25.5° C = 31.8 atm abs at 298.7° K
Final temperature of calorimeter, t=28.00° C=301.2° K
Oxygen pressure at 28.00° C, $P=31.8\times\frac{301.2}{298.7}$ = 32.1 atm absolute

Substituting in eq (2) we obtain

$$Q_c=6318.3\{1+10^{-6}[20(32.1-30)+42(4.01-3)+30(2.63-3)-45(28.00-25.00)]\}$$

=6317.9 cal/g in air.

[15] The value for the heat of combustion of benzoic acid is given here in IT calories per gram weight in air against brass weights, the densities of air, brass, and benzoic acid being taken as 0.00116, 8.4, and 1.320 g/cm³, respectively.

b. Correction Terms c_1 and c_2

The correction c_1 for firing energy is preferably determined in a series of blank experiments as described in section 3.2.d. The use of the value $c_1=5.2$ cal will not lead to a significant error if the fuse is a 2-cm length of Parr fuse wire wound into a helix and attached to platinum leads. In some cases a greater length (5 cm or more) of fuse wire is attached to electrodes which are located a short distance away from the crucible. In such cases the fuse may not all burn, and the firing energy will be different in different experiments depending upon the length of wire burned. If this procedure is followed, the length of wire burned in each experiment must be determined and the correction c_1 may be taken as $2.6\times L$ calories, where L is the length of wire burned, in centimeters.

The correction c_2 for nitric acid is 14.0 kcal/mole of nitric acid formed, or 14.0 N cal/cm^3 of sodium hydroxide solution of normality N required to neutralize the acid. Thus if 2.4 cm^3 of 0.0987 N sodium hydroxide is required to neutralize the nitric acid formed, $c_2=2.4\times14.0\times0.0987=3.3$ cal.

c. Corrected Temperature Rise

The calculation of the corrected change in resistance of the thermometer in a bomb calorimetric experiment will be illustrated by carrying out the calculations for the experiment in which the data given in table 1 were obtained. As stated in section 3.2.c. the initial, middle, and final periods in this experiment extend from $t=0$ to $t=6$, $t=6$ to $t=18$, and $t=18$ to $t=28$ min, respectively. The observed change in resistance of the thermometer is taken as the difference between the bridge readings at $t=6$ and $t=18$ min, namely, $0.76540-0.47397=0.29143$ ohm. This difference is to be corrected for thermal leakage and heat of stirring. Correct methods for calculating this correction will be found in reference [3] and in a number of the references there cited. For the accuracy aimed at in this manual it is sufficient to use the following procedure which has been found empirically to give correct results within about 0.01 percent of the total resistance change. We first calculate the average rates of change of resistance r_1 and r_2 in the initial and final periods, respectively. These are seen to be

$$r_1=\frac{0.47397-0.47015}{6}=\frac{0.00382}{6}=0.000637 \text{ ohm min}$$

$$r_2=\frac{0.76606-0.76540}{10}=\frac{0.00066}{10}=0.000066 \text{ ohm min.}$$

Next we calculate from the data of the middle period the time t_m at which 63 percent of the observed resistance change has taken place. The resistance at t_m is given by that at the final reading of the initial period (at $t=6$), 0.47397, plus 63 percent of the observed resistance change. In other words

$$R_m=0.47397+0.63\times0.29143=0.65757 \text{ ohm.}$$

Referring to table 1 it is seen that this resistance is reached at a time intermediate between 7.17 and 7.32 min, and by interpolation we obtain $t_m=7.227$ min. The corrected initial and final resistances, R_i (corr.) and R_f (corr.), are then obtained by applying corrections to the observed resistance at $t=6$ and $t=18$ min as follows:[16]

$$R_i \text{ (corr.)}=R_6 \text{ (obs)}+r_1(t_m-6)$$
$$=0.47397+0.000637\times1.227=0.474752 \text{ ohm,}$$

$$R_f \text{ (corr.)}=R_{18} \text{ (obs)}-r_2(18-t_m)$$
$$=0.76540-0.000066\times10.773=0.764689 \text{ ohm.}$$

The change in resistance corrected for thermal leakage and heat of stirring is then

$$R_f \text{ (corr.)}-R_i \text{ (corr.)}=0.764689-0.474752=0.289937 \text{ ohm.}$$

Practically the same result would have been obtained if only three readings had been taken during the period of very rapid temperature rise, say at $R=0.6300$, 0.6600, and 0.6900 ohm.

This result must be corrected for errors in the bridge coils by applying a correction equal to the algebraic sum of the certificate corrections to the coils used in obtaining R_{18} (obs) less the algebraic sum of the corrections to the coils used in obtaining R_6 (obs.). It is evident that it is not necessary in this calculation of the change in resistance to include corrections to coils which enter into both R_6 (obs) and R_{18} (obs). In this case such coils include one of 20.5 ohms and one of 7 ohms. The bridge correction in the experiment under consideration was +0.000029 ohm, making the corrected resistance change $\Delta R=0.289966$ ohm.

Resistance of the thermometer can be converted to temperature with the aid of the formula or tables accompanying the NBS certificate for the thermometer. It is somewhat more convenient, however, to compute a table of factors $\Delta t/\Delta R$ which when multiplied by the corrected change in resistance ΔR will give the desired change in temperature Δt. Such a table may be calculated as follows. First the temperatures corresponding to certain given resistances, say $R=27.5000$, 27.6000, . . . – 28.5000. . . , are calculated, using the data in the certificate for the thermometer. These temperatures are then substituted into the formula

$$\frac{\Delta t}{\Delta R}=\frac{1}{R_0\alpha\left[1+\frac{\delta}{100}-\frac{2\delta t}{10000}\right]} \qquad (3)^{17}$$

[16] Resistances are read to 1 in the fifth decimal. The calculations are carried one place farther to avoid errors from rounding off.

[17] Strictly speaking, eq (3) gives the derivative dt/dR. This is exactly equal to $\Delta t/\Delta R$ for a finite interval ΔR, provided it is calculated for the *mean temperature* of the interval. If, as is customary, the value of dt/dR corresponds to the *mean resistance* of a finite interval, then dt/dR is not exactly equal to $\Delta t/\Delta R$, but the error is entirely negligible.

where R_0, α, and δ are constants given in the calibration certificate for the particular thermometer. The values of R and corresponding values of $\Delta t/\Delta R$ calculated from the above formula are tabulated. The value of $\Delta t/\Delta R$ to use in calculating the corrected temperature rise in a given experiment is that corresponding to the mean of the corrected initial and final values of R for the experiment. This value of $\Delta t/\Delta R$ is obtained from the table, by interpolation if necessary. For example, in the example given above the value of $\Delta t/\Delta R$ used should be that corresponding to the mean of $27.5+R_i$ (corr.) and $27.5+R_f$ (corr.) or

$$27.5+(0.47475+0.76469)/2=27.5+0.6197$$
$$=28.1197 \text{ ohms.}^{18}$$

It is found that $\Delta t/\Delta R$ increases by about 0.03 percent for an increase in temperature of 1 deg C (0.1 ohm).

It is not necessary, however, to convert resistance to temperature. If desired, the resistance change can be taken as the measure of the temperature change, with the energy equivalent E expressed in caloreis per ohm. The corrected resistance change ΔR (ohms) in a measurement of heat of combustion would then be multiplied by E (calories per ohm) to give the energy (calories) produced in the combustion reaction. One disadvantage of this procedure is that E in calories per ohm changes more for a given change in the mean temperature of the experiment than does E in calories per degree. For a typical bomb calorimeter it has been calculated that the change in the value of E for an increase of one degree (0.1 ohm) in the mean temperature of the experiment is about +0.03 percent if E is expressed in calories per ohm, but is less than 0.01 percent if E is expressed in calories per degree. Hence if temperatures are expressed in ohms, then for a precision of 0.01 percent, the mean temperature of the calorimeter should be kept within about 0.2 degree (0.02 ohm) of some fixed value, or else the value of E_s in each calibration experiment should be corrected to some standard temperature, and the mean value of E_s for this standard temperature should be corrected to the actual mean temperature of each measurement of heat of combustion. The greater change with temperature of E_s expressed in calories per ohm is due to the fact that the resistance of the thermometer is not a linear, function of temperature, i.e., the fact that $\Delta t/\Delta R$ is not constant.

A convenient check on the behavior of the calorimeter and the correctness of the temperature measurements may be obtained by calculating the "cooling constant," k, of the calorimeter. This is defined by

$$k=-\frac{r_2-r_1}{R_2-R_1}$$

where r_1 and r_2 are the average rates of change of resistance in the initial and final periods, respectively, and R_1 and R_2 are the observed resistances at the mid-points of these periods. Thus, using the data of table 1 at the beginning of this section (5.1c):

$$k=\frac{0.000637-0.000066}{0.76573-0.47206}=0.001944.$$

This quantity is a constant of the calorimeter and should remain constant to better than one percent in different experiments.

d. Example Illustrating the Calculations of E and E_s

The calculation of E may be illustrated by an example, using the following data taken from preceding sections as indicated.

Weight benzoic acid, $m_s=1.52188$ g (sec. 3.2 a)
Heat of combustion of benzoic acid, $Q_c=6317.9$ cal/g (sec. 5.1.a)
Firing energy (2 cm fuse wire), $c_1=5.2$ cal (sec. 5.1.b)
Correction for nitric acid, $c_2=3.3$ cal (sec. 5.1.b)
Corrected resistance change, $\Delta R=0.289966$ ohm (sec. 5.1.c)
Corrected temperature change, $\Delta t=2.87462$ deg C ($\Delta t/\Delta R=9.91364$)
Oxygen pressure at 28.0°, $P=32.1$ atm abs (sec. 5.1.a)

Substituting the above values in eq (1), the value of E is found to be

$$E=\frac{1.52188\times6317.9+5.2+3.3}{0.289966}=33188.7 \text{ cal/ohm}$$

$$=\frac{1.52188\times6317.9+5.2+3.3}{2.87462}=3347.78 \text{ cal/deg.}$$

To reduce the above values of E to the corresponding values of E_s, the energy equivalent of the standard calorimeter system, it is only necessary to subtract the heat capacity of the sample of benzoic acid, and of the amount of oxygen in excess of that required to fill the bomb to 30 atm absolute at 28° C, as follows:

	cal/° C	cal/ohm
Observed value of E	3,347.78	33,188.7
Heat capacity of excess oxygen=(32.1−30.0)×0.077	0.16	1.6
Heat capacity of benzoic acid=1.522×0.29=	0.44	4.4
Value of E_s	3,347.18	33,182.7

The factor 0.077 used in calculating the correction for excess oxygen is the increase in heat capacity (in calories per degree) per atmosphere

[18] Strictly speaking, the corrections to all the coils used should be applied in calculating the mean value of the resistance. In many cases, however, these corrections are too small to be significant in this calculation and may be neglected.

increase in pressure in the bomb used, which has an internal volume of 0.380 liter. For a bomb of volume V the corresponding factor is $0.077\ V/0.380$. The factor 0.29 used in correcting for the benzoic acid is the specific heat of benzoic acid in calories per gram degree Celsius. Both factors are greater by a factor of 10 if E is in calories per ohm (for a thermometer having a resistance of 25.5 ohms at 0° C).

5.2. Calculation of Heat of Combustion

Calculate a value of total (or gross) heat of combustion at constant volume from the data of each measurement, using the following formula.

$$Q_v\ (\text{gross}) = \frac{E \times \Delta t - c_1 - c_2 - c_3}{m_s}, \qquad (4)$$

where:

Q_v (gross) = total heat of combustion at constant volume at the final temperature of the experiment, in IT calories per gram.

E = energy equivalent of the calorimeter as used, in IT cal/deg (or IT cal/ohm)

Δt = corrected temperature rise of calorimeter in degrees (or ohms)

m_s = mass of sample, in grams

c_1 = firing energy, in calories

c_2 = correction for energy of formation of nitric acid, in calories

c_3 = correction for energy of formation of sulfuric acid, in calories.

a. Energy Equivalent of Calorimeter as Used

The calorimeter as used differs from the standard calorimeter because it contains the sample of fuel and because, in general, the absolute pressure of the oxygen at 28° differs from 30.0 atm. The energy equivalent E of the calorimeter as used is obtained by adding to the energy equivalent E_s of the standard calorimeter the heat capacity of the charge of combustible and the heat capacity of the oxygen in excess of that required to fill the bomb to 30.0 atm absolute at 28° C. The calculation is illustrated as follows, taking the sample of combustible as 0.92231 g of gasoline, and the oxygen pressure at 28.0° as 29.0 atm absolute:

	cal/°C	cal/ohm
Energy equivalent of standard calorimeter, E_s =	3,347.18	33,182.7
Heat capacity of excess oxygen, $(29.0-30.0)\times 0.077$ =	−.08	−0.8
Heat capacity of sample, 0.922×0.51 =	+.47	+4.7
Energy equivalent of calorimeter as used, E =	3,347.57	33,186.6

The factor 0.51 used in calculating the heat capacity of the sample is the specific heat of gasoline [19] at 26.5°C in cal/g°C. The factor 0.077 used in calculating the heat capacity of the excess oxygen is defined in section 5.1.d. Both factors are greater by a factor of 10 if E_s is in calories per ohm (for a thermometer having a resistance of 25.5 ohms at 0°C). The heat capacity of the glass bulb (less than 0.1 g) used to enclose the sample of gasoline may be neglected.

b. Corrected Temperature Rise

Directions for calculating the corrected temperature rise are given in section 5.1.c. The value to be used in the example to be given later may be taken as 0.309617 ohm or 3.06943°C.

c. Corrections c_1, c_2, c_3

The correction c_1 for firing energy with a 2-cm length of fuse wire may be taken as 5.2 cal. The corrections c_2 and c_3 are calculated as follows: The correction c_2 is calculated as if all the acid found by titration were nitric acid, as described in section 5.1.b. Thus if it required 14.2 ml of 0.0987 N sodium hydroxide to neutralize the total acid the correction c_2 would be given by $c_2 = 14.2\times 14.0\times 0.0987 = 19.6$ cal. If the test for sulfur showed 0.0042 g sulfur present in the bomb washings the correction for sulfuric acid, as given in section 3.2.f., would be $c_3 = 1400\times 0.0042 = 5.9$ cal.

d. Calculation of Q_v (gross)

Substituting the values of E in calories per degree (or calories per ohm), Δt (or ΔR), c_1, c_2, c_3, and m_s given in sections 5.2.a., b., and c. into formula (4) yields:

$$Q_v\ (\text{gross}) = \frac{3347.57\times 3.06943 - 5.2 - 19.6 - 5.9}{0.92231}$$

or

$$Q_v\ (\text{gross}) = \frac{33186.6\times 0.309617 - 5.2 - 19.6 - 5.9}{0.92231}.$$

Both of these expressions yield the value 11107.4 cal/g weight in air for the total (or gross) heat of combustion of the liquid gasoline at constant volume. The corresponding value in terms of engineering units is

$$Q_v\ (\text{gross}) = 11107.4\times 1.8 = 19993\ \text{Btu/lb}.$$

The method of calculation is such that the value obtained for Q_v (gross) is referred to the final temperature of the calorimeter, in this case 28.1° C. The observed value may be reduced to the standard temperature of 25° by means of the following formula:

[19] Taken from NBS Miscellaneous Publication M97 [15] for a gasoline having an API gravity of 70. Values of heat capacity of petroleum products given in this publication for a temperature of 80° F range from 0.42 to 0.52 for API gravities ranging from 10 to 80.

$$Q_v \text{ (gross, } 25° \text{ C)} = Q_v \text{ (gross, } t° \text{ C)} + A(t-25) \quad (5)$$

Where the value of the factor A is given in the following table.[20]

Q_v (gross)	A	Q_v (gross)	A
Btu/lb	*Btu/lb° C*	*Btu/lb*	*Btu/lb° C*
18,500	0.68	19,600	1.14
18,600	.72	19,700	1.18
18,700	.76	19,800	1.22
18,800	.80	19,900	1.26
18,900	.85	20,000	1.30
19,000	.89	20,100	1.35
19,100	.93	20,200	1.39
19,200	.97	20,300	1.43
19,300	1.01	20,400	1.47
19,400	1.05	20,500	1.51
19,500	1.09	20,600	1.55

Substituting the value of Q_v (gross, 28.1° C)= 19993 Btu/lb and the corresponding value $A=1.30$ from the above table in eq (5) we obtain

$$Q_v \text{ (gross, } 25° \text{ C)} = 19993 + 1.30 \times 3.1 = 19997 \text{ Btu/lb.}$$

[20] The values of A were calculated using the specific heats of liquid petroleum fuels, of gaseous oxygen and carbon dioxide, and of liquid water. The masses of oxygen consumed and of carbon dioxide and water formed in combustion of unit mass of fuel were obtained from an empirical relation between Q_v (gross) and hydrogen content. See reference [5]. In general, the change in Q_v gross (Btu/lb) with temperature for any fuel may be calculated from the relation dO_v (gross)$/dt = K_v$ (reactants) $- K_v$ (products).

Here K_v (reactants) denotes the heat capacity at constant volume of 1 lb of fuel plus the oxygen consumed in its combustion, and K_v (products) denotes the heat capacity of the products of combustion of one pound of fuel, including gaseous carbon dioxide and liquid water. In calculating K_v the heat capacities of solids and liquids may be taken as heat capacities at constant pressure.

e. Calculation of Q_p (net)

If the hydrogen content of the fuel is known the value of the net heat of combustion, Q_p (net, 25°), can be calculated from that for Q_v (gross) by means of the following formula [4]:

$$Q_p \text{ (net, } 25° \text{ C)} = Q_v \text{ (gross, } 25° \text{ C)} - 91.23 \text{ (\%H)} \quad (6)$$

Thus if Q_v (gross, 25° C)=19997 Btu/lb and (%H)=13.9, we obtain

$$Q_p \text{ (net, } 25° \text{ C)} = 19997 - 91.23 \times 13.9 = 18729 \text{ Btu/lb.}$$

If the hydrogen content of the fuel is not known, an approximate value for Q_p (net, 25° C) can be calculated from the following empirical relation:

$$Q_p \text{ (net, } 25° \text{ C)} = 4310 + 0.7195\, Q_v \text{ (gross, } 25° \text{ C).} \quad (7)$$

Substituting the value Q_v (gross, 25° C)=19997 Btu/lb in this equation we obtain

$$Q_p \text{ (net, } 25° \text{ C)} = 4310 + 0.7195 \times 19997 = 18698 \text{ Btu/lb (approximate)}$$

Equation (6) is preferable to eq (7) for calculating net from gross heat of combustion, since the latter equation is purely empirical. A fairly accurate value of (%H) is required in eq (6), since an error of 0.1 in this quantity introduces an error of about 0.05 percent in Q_p (net).

6. References

[1] ASTM Method D 240–57T. ASTM Standards **7,** 143, (1958).

[2] ASTM Method D 271–58, ASTM Standards, **8,** 999 (1958).

[3] F. D. Rossini, Experimental thermochemistry (Interscience Publishers, New York, N.Y., 1956), and the references there cited.

[4] R. S. Jessup and C. S. Cragoe, Nat. Advisory Comm. Aeronaut. Tech. Note No. 996 (1945) (copies not available).

[5] S. Rothberg and R. S. Jessup, Ind. Eng. Chem. **43,** 981 (1951).

[6] R. S. Jessup and J. A. Cogliano, ASTM Bull. No. 201 (Oct. 1954).

[7] G. T. Armstrong, R. S. Jessup, and T. W. Mears, Chem. Eng. Data Ser. **3,** 20 (1958).

[8] H. C. Dickinson, Bul. BS **11,** 189 (1914) S230.

[9] N. S. Osborne, H. F. Stimson, and T. S. Sligh, Bul. BS **20,** 119 (1925) S503.

[10] C. H. Meyers, J. Am. Chem. Soc. **45,** 2135 (1923).

[11] T. W. Richards and F. Barry, J. Am. Chem. Soc. **37,** 993 (1915).

[12] H. N. Davis, Mech. Eng. **51,** 791 (1929).

[13] See for example:
(a) N. Irving Sax, Handbook of dangerous materials (Reinhold Publishing Corp., New York, N.Y., 1951).
(b) Manufacturing Chemists Association, General Safety Committee, Guide for safety in the chemical laboratory (D. Van Nostrand and Co., New York, N.Y., 1954).
(c) National Safety Council, Accident prevention manual for industrial operations (Chicago, Ill., 1951).
(d) National Board of Fire Underwriters, National electrical code (Chicago, Ill., 1940).

[14] ASTM Method D 129–58, ASTM Standards **8,** 81 (1955).

[15] C. S. Cragoe, Thermal Properties of Petroleum Products, NBS Misc. Publ. M97 (this paper is out of print but may be found in many public libraries).

[16] E. J. Prosen and F. D. Rossini, J. Research NBS **27,** 289 (1941) RP1420.

[17] J. Coops, D. Mulder, J. W. Dienske, and J. Smittenberg, Rec. trav. chim. **66,** 153 (1947).

[18] E. W. Washburn, J. Research NBS **10,** 525 (1933) RP546; see also chapters 5 and 6 of reference [3].

[19] F. K. Harris, Electrical measurements, p. 57 (John Wiley & Sons, Inc., New York, N.Y., 1951).

[20] E. J. Prosen, W. H. Johnson, and Florence Y. Pergiel, J. Research NBS **62,** 43 (1959) RP2927.

7. Appendix

7.1. Apparatus

The major items of apparatus used in bomb-calorimetric measurements on fuels at the National Bureau of Standards are listed in table 2. On the basis of prices listed in manufacturers' catalogs at the present time (1959), the estimated total cost of replacement of the equipment listed is in the neighborhood of $15,000.

TABLE 2. *Major items of equipment used in measurement of heats of combustion of liquid fuels at the National Bureau of Standards*

Mueller bridge.	Set of weights for above.
Resistance thermometer.	Oxygen purifier.
Galvanometer.	Temperature controller for oxygen purifier.
Calorimeter, jacket, and thermostat.	Laboratory table for bridge.
Combustion bomb.	Laboratory bench.
Platinum crucibles and fittings.	Pellet press.
Balance.	Reducing valve.
Set of class M weights for above.	Julius suspension.
Heavy duty balance	

The approximate arrangement of the calorimeter and accessory apparatus is shown in figure 4. The reading station R provides support for the lamp L and ground glass scale S, as well as for some electrical equipment for measurements not covered in this Monograph. It also contains a convenient "desk" for use in recording the data of bomb calorimetric experiments. The arrangement of the equipment for purifying oxygen and admitting it to the bomb is shown schematically in figure 5.

The arrangements shown in figures 4 and 5 are not necessarily the best under all circumstances. For example, the bench BE (fig. 4) is considerably larger than necessary for the calorimeter alone, as part of this table is used for other purposes.

The essential features of the various items of apparatus are described below. Items not obtainable commercially, and modifications of commercial items are described in considerable detail.

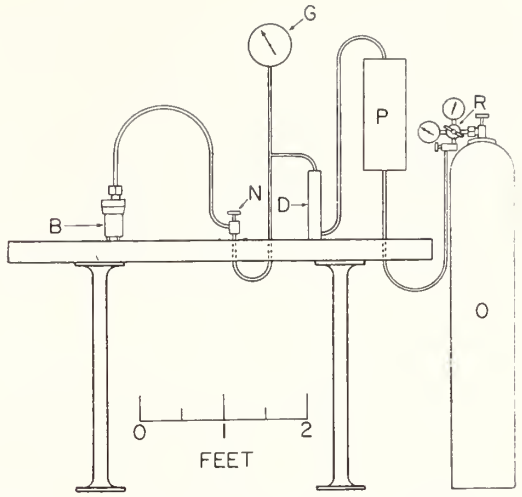

FIGURE 5. *Arrangement of apparatus for admitting oxygen to bomb.*

B, bomb; D, dryer; G, pressure gage; N, needle valve; O, oxygen cylinder; P, oxygen purifier; and R, reducing valve.

a. Bridge

The bridge used is a special Mueller bridge designed especially for bomb-calorimetric measurements. It is substantially equivalent to the commercially available bridge designated as G–2. In addition to the usual 10-, 20-, 30-ohm coils of the 10×10-ohm decade this bridge has a 20.5-ohm coil. Such a coil is useful in bomb-calorimetric measurements, where the change in resistance of the thermometer in an experiment is of the order of 0.3 ohm, since it makes it possible to avoid a change in setting of the dial of the 10×1-ohm decade which would otherwise be necessary in certain circumstances. Thus if the initial and final resistances of the thermometer are 27.8721

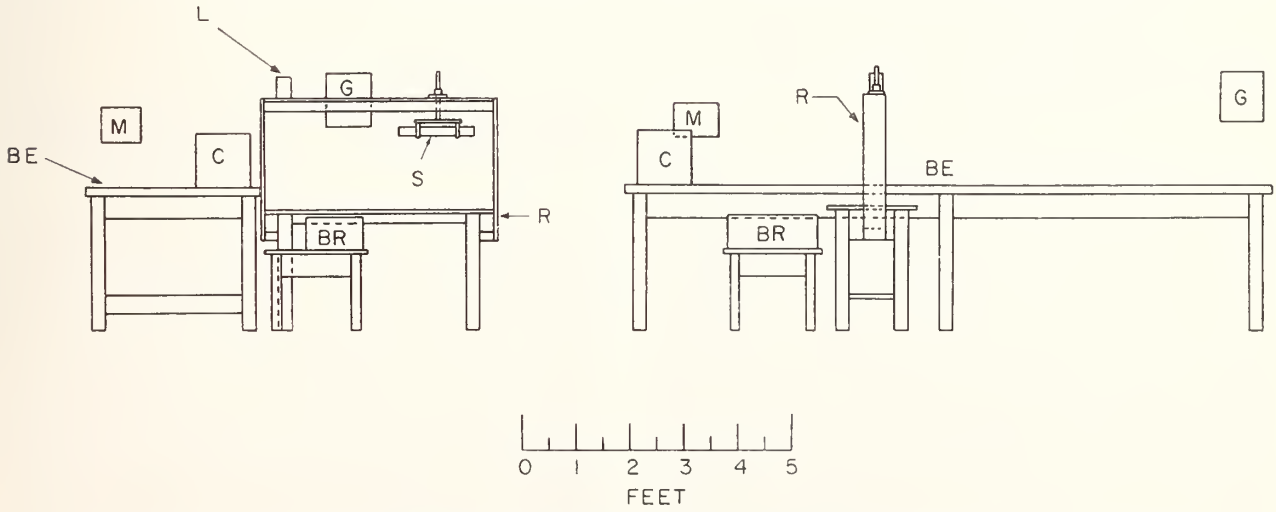

FIGURE 4. *Arrangement of calorimetric apparatus.*

BE, bench; C, calorimeter; BR, bridge; G, galvanometer; L, light source; M, stirring motor; R, reading station; and S, ground glass scale.

and 28.1806, the corresponding dial settings with the 20.5-ohm coil would be 20.5+7.3721 and 20.5+7.6806 and the change in dial setting would involve only the 10×0.1-ohm and lower decades. If no 20.5-ohm coil were available, it would be necessary to change the dial setting of the 10×1-ohm decade from 7 to 8 at a time when the temperature of the calorimeter was rising very rapidly. This would greatly increase the difficulty of following the temperature of the calorimeter during the period of rapid temperature rise, and might also involve a larger correction to the observed change in resistance of the thermometer.

b. Thermometer

The platinum resistance thermometer has a resistance of approximately 25.5 ohms at 0° C. It is of the strain-free type with coil windings very close to the wall of the enclosing glass tube. It was purchased under a specified requirement that the temperature of the coil with a current of 1 ma flowing through it should not exceed that of the bath in which the thermometer is immersed by more than 0.0003° C. Calorimetric resistance thermometers enclosed in metal sheaths are available commercially. These are less subject to breakage than glass-enclosed thermometers, but are subject to damage from bending the metal sheath. Such damage might not be obvious on casual examination, but could be detected by periodic determination of the ice point of the thermometer.

c. Galvanometer

The galvanometer has a sensitivity of about 0.2 μv/mm at 1 m, an external critical damping resistance of 40 ohms and a period of about 5 sec. The damping resistance used is so chosen that the galvanometer is slightly underdamped. The galvanometer is protected from air currents and abrupt changes in temperature by an enclosure made of cork pipe covering (for 6 in. pipe) about 10 in. in outside diameter. The galvanometer is supported by a Julius suspension, which is very effective in reducing the effect of vibrations.

d. Bomb

The combustion bomb [21] is made of a corrosion-resistant alloy (Illium). It is provided with a check valve for admitting oxygen and also with a needle valve for releasing the gases contained in it. It is sealed by a self-sealing neoprene gasket. The original bomb has been modified by replacing the three supporting feet furnished with it by new ones of monel metal about 12 mm in height. This permits freer circulation of water under the bomb.

The base-metal electrode inside of the bomb, and the crucible-support rod were cut off leaving lengths of about 3 cm from the point at which they enter the lock nuts. To the shortened electrode was hard soldered a 1/16 in. platinum rod about 3 cm in length. To the shortened crucible-support rod was hard soldered a 5-cm length of 1/8 in. o.d. platinum tube having a 0.01 in. wall. The arrangement of electrode, crucible support, crucible, electric fuse and 0.3 mm platinum leads thereto is shown in figure 6(a) (valves not shown). An enlarged view of the platinum crucible is shown at (c) figure 6. The crucible is put in place by sliding the split tube (5/32 in. o.d.) shown at the right of figure 6(c) over the end of the 1/8 in. platinum crucible-support tube referred to above until the fuse is nearly in contact with the sample of combustible. The split tube may be deformed slightly with the fingers to make it fit the 1/8 in. tube tightly enough to be held in place by friction. The length of the crucible-support, and the position of the crucible on this support should be such that the crucible cannot come in contact with the water in the bottom of the bomb when the bomb is assembled. If the crucible should come in contact with the water, combustion will be incomplete.

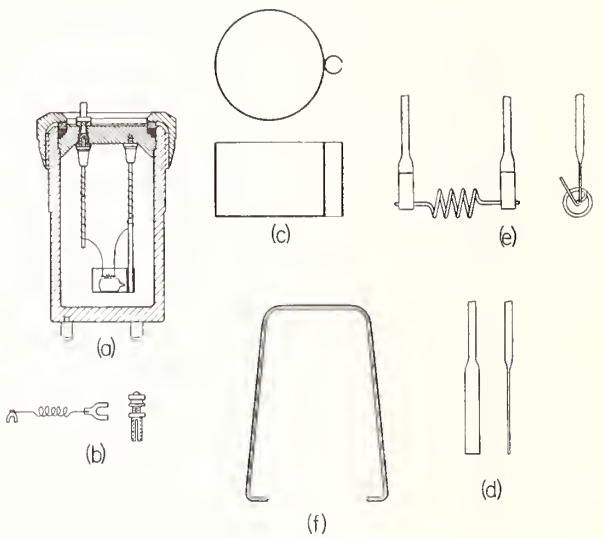

FIGURE 6. *Bomb and accessories.*

(a) Bomb, showing arrangement of crucible, crucible support, electrode, etc. (Valves not shown, see fig. 1); (b) Binding post and lead wire; (c) Enlarged view of crucible; (d) Platinum lead flattened at end; (e) Fuse wire attached to platinum leads; and (f) Hook for handling bomb.

A supply of platinum lead wire is wound around the electrode and crucible support rods as shown, and a sufficient amount of this to reach down to the crucible is unwound for each experiment. The electric fuse is a 2-cm length of Parr fuse wire (No. 34 AWG chromel C) which is formed into a small helix by winding it around a rod about 0.04 in. in diameter. The method of attaching the fuse to the platinum leads is illustrated at (d) and (e), figure 6. The ends of the lead wires are first flattened by hammering as shown at (d). The flattened ends are then bent and the fuse inserted as shown at (e), after which the turned-up ends

[21] Parr Instrument Company Catalog No. 1101.

of the lead wires are hammered down with a small hammer or squeezed together with pliers to clamp the ends of the fuse wires.

The terminal nut attached to the electrode outside of the bomb was replaced by one of the form shown at (a), figure 6. The binding post shown at (b), figure 6, has a split tube at its lower end which can be slipped over the upper part of the terminal nut, where it fits tightly so as to make good electrical contact. The lead wire shown at (b), figure 6, connects this binding post to one on the calorimeter jacket which is connected in the firing circuit. This wire is soldered to spade-type terminals at each end, the larger of which normally is permanently attached to the binding post shown at (b). This wire should be so insulated as to avoid any electrical contact with the calorimeter vessel. With alternating current the contact of the lead wire and bomb electrode with the water in the calorimeter does not result in any appreciable electrical leakage, provided actual metallic contact with the calorimeter vessel is avoided.

e. Calorimeter and Jacket

The calorimeter now used for fuel testing is of the type described by Dickinson [8]. The calorimeter vessel is of the form shown at (a) and (b), figure 1. The calorimeter cover is in the form of a flat circular disk with vertical wall about 1 cm in height at the edge. The holes OT and OL (fig. 1(b)) are surrounded by metal collars about 1 cm high. The cover fits tightly enough inside of the calorimeter vessel so that it is held in place by friction. Its lower surface is in contact with the water of the calorimeter. The calorimeter vessel is supported inside of the jacket by pins of stainless steel, in the manner described by Dickinson [8].

The Dickinson type calorimeter was constructed in the NBS shops. There is a commercially available "submarine" calorimeter, [22] based on a design developed at the National Bureau of Standards [20], which has been found to be substantially equivalent in performance to the Dickinson calorimeter. The submarine calorimeter is supplied without a thermostat for the jacket bath, so that a thermostat for controlling the bath temperature to a few thousandths of a degree must be purchased or constructed.

The thermostat [23] used with the particular Dickinson type calorimeter used for fuel testing is similar to one previously described by Osborne, Stimson, and Sligh [9]. It consists of a "bulb" filled with toluene and connected to a glass capillary U-tube (1.5 mm i.d.) containing mercury. Expansion of the toluene as a result of rising temperature causes the mercury to make contact with a needle closing an electrical circuit through an electronic relay [24] which shuts off the current in the electric heater in the jacket bath. The "bulb" *TB* (fig. 1) consists of about 3 m of 3/16 in. copper tubing with 0.01 in. wall thickness wound into a helix and so located in the same tubular housing as the jacket bath stirrer that the water flows over the bulb immediately after leaving the stirrer. The glass U-tube and attached valve for admitting or removing toluene are shown in figure 7. The valve has tubular openings at the top and bottom for attaching the reservoir *B* and the capillary U-tube as described below.

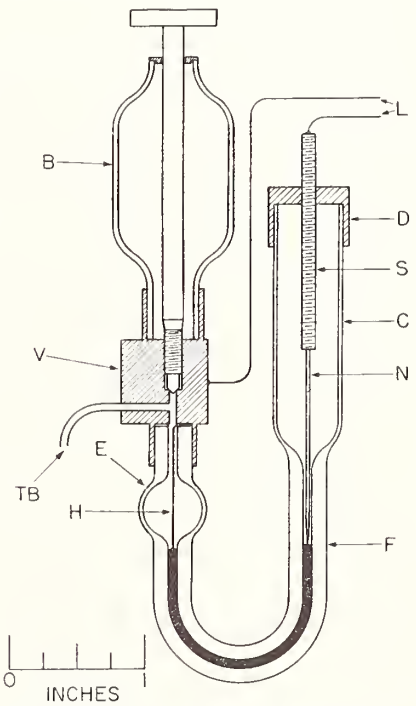

FIGURE 7. *Valve and glass parts of thermostat.*

V, valve; TB, tube to thermostat bulb; B, toluene reservoir; F, capillary U-tube; E, enlargement in capillary; H, platinum wire; L, leads to relay; C, Pyrex tube; D, brass cap; S, screw; and N, steel needle.

The Pyrex reservoir *B* contains a supply of toluene which is separated from that in the "bulb" *TB* (fig. 1) by the valve *V* when it is closed. This valve is opened when the calorimeter is shut down thus permitting toluene to flow from the reservoir into the bulb as the bath cools. Failure to open the valve when the bath cools usually results in air being drawn into the system through the capillary *F* (fig. 7). The Pyrex bulb *C* (fig. 7) also contains toluene which protects the mercury surface in the capillary from oxidation. The enlargement *E* in the capillary is larger in volume than the mercury in the capillary so that no mercury will be drawn into the metal parts of the system if the valve *V* is inadvertently left closed when the calorimeter is shut down.

[22] Catalog No. 63090, Precision Scientific Co., Chicago, Ill. This calorimeter embodies an improved method of supporting the calorimeter vessel inside of the jacket [20].

[23] Temperature-control units for which a control accuracy of 0.001° C. is claimed are available commercially. Numerous other temperature-control devices are described in the literature. See for example the papers cited in reference [3]. For any temperature-control unit it is important that the relative locations of heater, stirrer, and temperature-sensing element should be as shown in figure 1, that is, the bath liquid should flow from the heater, through the stirring propeller, and over the temperature-sensitive element by the shortest path possible.

[24] American Instrument Company Catalog No. 4-5301.

Electrical connection between the Valve V and the mercury in the capillary U-tube is provided by a platinum wire H, long enough to reach from the top of the capillary to near the bottom of the U. The upper end of the wire is flattened and bent at a right angle to the rest of the wire so as to insure electrical contact with the valve.

The glass reservoir B and the capillary glass U-tube are soldered into the tubular openings in the brass valve V with pure tin following the procedure described by Meyers [10].

To fill the thermostat with toluene the tube C (with cap D removed) is connected to a large bulb G above C (at least 250 cm^3, not shown in fig. 7) by means of a short piece of Tygon tubing. Somewhat more than enough toluene to fill the thermostat is placed in the bulb G, and some is also placed in the reservoir B. Air can be removed from the thermostat system by heating the "bulb" (TB, fig. 1) to about 100° C and repeatedly evacuating the bulb G above the toluene and then admitting air. To test for air in the system, air is admitted above the toluene in G, the valve V is opened, the toluene meniscus is brought into the capillary at F, and the valve is closed. If the system is free of air, moderate air pressure applied by mouth above the toluene will not cause a movement of the meniscus in the capillary of more than 0.2 or 0.3 mm. The removal of air from the system should be done before introducing mercury into the capillary. If air is inadvertently admitted to the system after mercury has been introduced into the capillary, the mercury should be removed before attempting to remove the air.

In preparing for a calorimetric experiment the jacket is first heated to the desired temperature, the heating current is reduced to slightly more than enough to maintain the temperature constant, and the valve V is closed. Final adjustment of the temperature can be made by moving the needle N up or down by rotating the cap D relative to the screw S (fig. 7). The heating current should be adjusted so that the on and off periods are about equal in length.

The method of bringing the firing leads through the jacket is illustrated in figure 1(c).[25] Two metal rods, one of which is shown at R, are cemented with wax into tubes T which pass through the jacket, so that the rods are insulated from the jacket. Each rod is drilled and tapped at each end for a 4–40 brass screw, which is used to clamp the terminal of the lead wire between the two washers, W, thus forming a binding post at each end of the rod. The terminal at the left end of the lead wire shown in figure 1(d) is attached permanently to one of the inner binding posts and the clip at the other end of the wire (d) is slipped over the edge of the calorimeter vessel when it is assembled preparatory to making an experiment. The other lead wire, from the binding post on the bomb (see fig. 6(b)), is attached to the other inner binding post after the bomb has been put in the calorimeter and the calorimeter cover has been put in place. The two outer binding posts are connected through an ammeter and a switch to a small transformer having a secondary voltage of 8 or 10. The switch should be of the momentary contact push-button type normally open except when held closed by the operator.

[25] This method is not applicable to some types of calorimeters, for example, submarine calorimeters. The important feature of the method is that the leads are in good thermal contact with the jacket, but are electrically insulated from it.

f. Balance for Weighing Samples

The balance used for weighing samples of combustibles is an undamped semimicro balance (capacity 100 g) having a sensitivity reciprocal of 0.14 mg per division on the index scale. The balance is provided with a keyboard arrangement for adding and removing weights from 1 to 100 mg. Temperature gradients parallel to the balance beam are reduced by covering the walls of the balance case inside and out with aluminum foil, and by locating the balance where temperature gradients in the room are small. It has been found, however, that best results are obtained with the balance when there is a vertical temperature gradient such that the top of the balance case is warmer by 0.03 to 0.1° C than the bottom.

The weights used with the balance are high-grade one-piece (class M) weights and were calibrated in the Mass and Scale Section of the National Bureau of Standards.

For most purposes a good analytical balance would be satisfactory if provided with high grade calibrated weights, and properly used.

g. Balance for Weighing Calorimeter

This is a magnetically damped heavy duty balance having a capacity of 5 kg and a sensitivity of about 0.5 mg. The tantalum-plated weights used with this balance are of good quality but are not calibrated. Calibration was considered unnecessary since the purpose of weighing the calorimeter is not to determine its absolute weight, but to reproduce the same weight of calorimeter plus water for each experiment. For this purpose it is important that the weights remain constant in value, and that the same weights be used at all times, but the actual masses of the weights used need not be known accurately.

h. Oxygen Purifier

Combustible impurities in the oxygen are removed by passing it through a cylinder containing cupric oxide maintained at a temperature of 500° C (932° F). The purifier[26] consists essentially of a heavy-walled alloy-steel cylinder having inside dimensions of approximately 1 in. diameter by 10 in. length, and capable of withstanding a pressure of at least 2500 psi at 500° C. The cylinder is provided with an electric heater. It

[26] American Instrument Company 1942 Catalog No. 406-31.

has inlet and outlet at opposite ends, and a well for inserting a thermocouple for measurement of temperature. The cylinder is filled with wire-form cupric oxide. The temperature and oxygen pressure in the purifier should not be allowed to rise above values consistent with safety. The manufacturers recommendations regarding safety precautions should be adhered to rigidly. The strength of materials decreases rapidly with increasing temperature.

The temperature of the purifier can be controlled by means of a "Fail safe" controller. Such controllers are available commercially.[27] The pressure is easily controlled by a reducing valve attached to the oxygen cylinder.

i. Laboratory Table for Bridge

This table should be large enough to accommodate the bridge comfortably, and of a height which will afford convenience in the manipulation of the bridge dials. A table 22 in. square by 18 in. high is convenient for use with a G–2 bridge as it allows space for batteries, etc

j. Pressure Gage

The Bourdon pressure gage used has a 6 in. dial and is graduated from 0 to 800 psi in steps of 10 psi, so that it can be read to about 1 or 2 psi. The gage was calibrated in the Mechanical Instruments Section of the NBS and was set so as to read correctly at 450 psi.

7.2. Glass Sample Bulbs

For measurements of heat of combustion of kerosenes, gasolines, or other volatile liquids it is necessary, in order to permit accurate weighing of the sample and to insure that it is all in the liquid state until it is ignited in the bomb, to enclose the sample in a thin-walled glass bulb, so constructed and filled that it will not break under the pressure of the oxygen. The type of bulb[28] used in testing of volatile fuels at the National Bureau of Standards, and the method of making such bulbs are illustrated in figure 8. Attempts to obtain bulbs of this type from manufacturers of glass laboratory apparatus have been unsuccessful to date, and such bulbs are therefore made in our own laboratory. A brief description of the method of making the bulbs will be given below. It should be recognized, however, that it is virtually impossible to describe the method in such detail as to enable an inexperienced worker to make bulbs successfully on his first attempt. The best that can be done is to outline the method, and to depend upon the individual worker to develop the necessary techniques by trial. It is to be expected that in the early attempts failures will far outweigh successes, and that a reasonable degree of skill can be acquired only by long and patient practice.

[27] For example American Instrument Company Catalog No. 49-9570. Arthur S. Lapine and Company Catalog No. 357–70.

[28] Bulbs of this type were first described by Richards and Barry [11].

The starting material for making bulbs is soft glass tubing 4 to 6 mm in outside diameter.[29] Approximately 2 cm of such a tube is heated in a moderately hot air-gas flame of an ordinary laboratory blast burner. When the glass becomes soft it is removed from the flame and drawn down to a fine capillary having a minimum outside diameter of about 1 mm. This procedure is then repeated in such a manner as to leave a short section of the same diameter as that of the original tube, as shown at figure 8(a). The two capillaries are then broken at about their midpoints, leaving a piece such as that shown at figure 8(b). The remaining glass-working operations are carried out with an air-gas micro blast burner capable of producing relatively small flames. Using such a micro burner the piece illustrated at (b), figure 8, is rotated and heated by a small hot flame at the point indicated by the arrows, and is then drawn down to 1 mm outside diameter. This procedure is repeated on the other side of the enlargement in the tube, the final product being as illustrated at (c), figure 8. This piece is then rotated and heated by a small sharp flame at the center of the enlargement as indicated by the arrow at (c), and the two halves of the piece are pulled apart as shown at (d), figure 8, where the enlarged end of the piece at the left has been reduced in size by removal of surplus glass. This removal of surplus glass is accomplished by heating the end of the enlargement until it softens, and then pulling off small filaments of glass until an enlargement of the proper size remains. After such removal of surplus glass from both of the pieces shown at (d) a spherical bulb, not greater than 14 mm in diameter, is blown on each piece (fig. 8(e)). The spherical bulb is then flattened on one side by holding the bulb above a small soft flame (no primary air) about ¼ in. in diameter by ¼ in. high, and gradually lowering it until the glass on the under side of the bulb softens and flattens. This procedure is then repeated so as to flatten the opposite side of the bulb. The final form of the bulb is shown at figure 8(f). The operations of bringing the bulb down on to the flame and removing it after flattening is complete should be done gradually, since too rapid heating or cooling of the bulb may cause it to break.

The most difficult part of the procedure just described is that of blowing a bulb of the proper size. Success in this operation depends in part upon having the proper amount of glass on the end of the tube (fig. 8 (d)) and in part upon the type of flame used, as well as upon the procedure followed in blowing the bulb. A flame which has been found to be satisfactory is one about ¼ in. in diameter by ⅝ in. in height with just enough primary air so that there is a small yellow tip in the flame. The end of the tube (fig. 8(d)) on which the bulb is to be blown is heated in the

[29] Pyrex glass has been found unsatisfactory for this purpose, as unburned carbon is usually found on such glass after a combustion. This may be related to the fact that the Pyrex glass does not melt completely when the sample is burned, as does soft glass, and therefore partially retains its original form, thus inhibiting access of oxygen to the fuel.

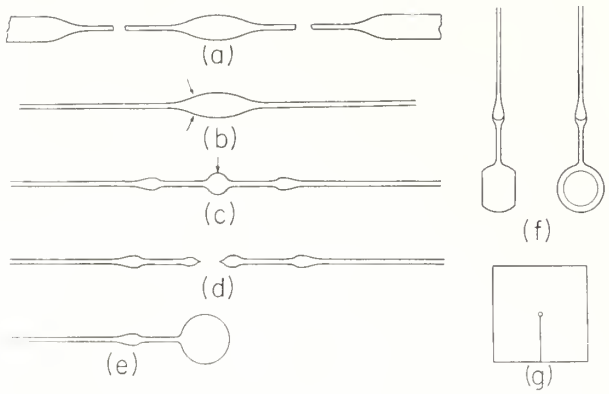

FIGURE 8. *Steps in making sample bulbs.*

flame until sufficiently hot, and is then removed from the flame and the bulb blown immediately. In order to prevent sagging of the end of the tube when heated, the tube is held at an angle of about 30° to the vertical and is rotated about its axis continuously. Usually the first few attempts to blow a bulb will be unsuccessful because the initial size of the bulb is so small that a relatively high pressure will be required to overcome surface tension and the viscous resistance to flow of the glass. If the pressure is not high enough the bulb will expand so slowly at first that the glass will harden before the desired size is reached. If the pressure is high enough to expand the bulb at a sufficiently high initial rate, the bulb may suddenly expand to too large a size before the glass hardens. The ideal procedure would be to blow very hard at first and then less so as the bulb becomes larger. This is very difficult to do because the whole operation must be carried out in a very short time before the glass hardens. It is therefore usually more successful to repeat several times the procedure of blowing the bulb to a diameter of 4 or 5 mm and then shrinking it by heating, before attempting to blow the bulb to the required size. This procedure also serves to provide a somewhat more uniform distribution of glass in the final bulb.

Too large an amount of glass in the bulb and too hot a flame are both conducive to too large size of the bulb. Too small an amount of glass and too low a flame temperature have the opposite effect. Success in blowing a suitable bulb of the proper size depends upon the proper combination of flame temperature, amount of glass and technique of blowing.

The spherical bulb should be not more than 14 mm in diameter, and the completed bulb should not contain more than about 1.3 cm^3 nor less than 0.7 cm^3 of liquid. The flat sides of the bulb should be thin enough to deflect visibly, but not so thin as to break, under moderate air pressure applied by mouth. The weight of the glass in the bulb after sealing off the stem near the bulb should be between 0.05 and 0.10 g. The outside diameter of the capillary adjacent to the bulb should be between 1.0 and 1.3 mm. The inside diameter should be at least 0.5 mm and preferably a little larger in order to permit easy insertion of a No. 27 hypodermic needle (0.4 mm diam.) in filling the bulb. The appearance of the flat sides of a completed bulb will give some indication as to whether it will be satisfactory. Usually the flat sides present a scalloped appearance, although if the amount of glass in the bulb is greater than normal they may be nearly plane. If the scallops are very fine, say 1 mm or less apart, the bulb is probably too thin and fragile to be satisfactory.

Samples of liquid fuel can be conveniently introduced into the previously weighed glass bulbs by means of a hypodermic syringe fitted with a No. 27 needle. The liquid should be introduced into the bulb slowly in order to permit escape of the air initially present without undue increase in pressure. The bulb should be filled completely so that the liquid extends up into the enlargement in the stem as indicated at figure 8(f). Usually a small bubble will be trapped in the bulb at the point where it joins on to the stem, but such a bubble can usually be removed without too much difficulty with the aid of the hypodermic needle or a piece of wire. In filling the bulbs the usual safety precautions for the handling of volatile organic solvents should be taken, particularly if the fuel contains tetraethyl lead [13].

In filling bulbs with very volatile liquid fuels such as gasolines, great care should be taken to avoid loss of material by evaporation, as this causes fractionation of the material with a consequent change in heat of combustion. The container should be kept tightly closed at all times except when withdrawing a sample with the hypodermic syringe. The sample can be withdrawn more quickly if the needle is detached from the syringe. In replacing the needle after withdrawal of the sample care should be taken to avoid contact of gasoline with the hands, particularly if it contains tetraethyl lead.

After the bulb is filled, the capillary is sealed off so as to leave a stem about 3 or 4 mm long attached to the bulb. In order to do this the bulb must be cooled so as to draw the liquid out of the capillary, and the bulb must be protected from the flame during the sealing operation. To protect the bulb from the flame a small piece of asbestos paper with a hole in the center and with a cut between the hole and the edge (fig. 8(g)) is slipped over the capillary via the cut so that the capillary goes through the hole, and the piece of asbestos paper is in contact with the bulb. The bulb is then cooled by placing it on a mass of shaved ice in a beaker, or on a copper plate in contact with ice, and when the meniscus in the capillary disappears below the asbestos paper, the capillary is sealed off with a small hot air-gas flame and removed from the bulb. The bulb should then be removed promptly from the ice to avoid possible breakage due to

excessive contraction of the liquid. The filled bulb is conveniently handled by the short projecting capillary by means of forceps of the type ordinarily used for handling balance weights. Particles of asbestos which may adhere to the bulb should be removed by means of a camel's hair brush. Any liquid remaining in the capillary detached from the bulb in sealing it should be removed before weighing the filled bulb together with this detached capillary. If the liquid is sufficiently volatile it can be removed by flaming the capillary several times with the micro-burner flame. The flame should be applied first to the closed end of the capillary, and moved gradually to the open end in such a manner as to avoid softening the glass. If the liquid is of low volatility, it should be washed out with a volatile solvent, such as benzene or petroleum ether, introduced into the capillary by means of a hypodermic syringe before flaming as described above.

When first sealed, the bulb may contain a small bubble of air. This will dissolve in the liquid after a time leaving the bulb completely filled with liquid. Bulbs prepared in the manner described should withstand changes in room temperature of 10° C or more, and pressures of at least 30 atm (450 psi) without breaking.

Glass sample bulbs of different types have been described by a number of workers [16, 17].

Washington, April 14, 1959.

U. S. Department of Commerce
National Bureau of Standards

Research Paper RP1968
Volume 42, March 1949

Part of the Journal of Research of the National Bureau of Standards

Heat of Isomerization of the Two Butadienes

By Edward J. Prosen, Frances W. Maron, and Frederick D. Rossini

The heat of isomerization of 1,3-butadiene to 1,2-butadiene, in the gaseous state at 25° C was determined by measurement of the ratio of their heats of combustion in oxygen to form carbon dioxide and water. The combustion of the gaseous hydrocarbon occurred in a flame at constant pressure in a glass calorimetric reaction vessel of improved design. A complete description of the new calorimetric reaction vessel is given.

The following experimental value is reported for the reaction of isomerization:

1,3-butadiene(gas) = 1,2-butadiene(gas), $\Delta H°$ at 25° C = 12.78 ± 0.16 kcal/mole.

Using the value for the heat of formation of 1,3-butadiene previously reported, the following calculated values are given for the reactions of formation and combustion of 1,2-butadiene:

4C(solid, graphite) + 3H_2(gas) = C_4H_6(1,2-butadiene, gas), $\Delta H°$ at 25° C = 39.53 ± 0.28 kcal/mole.

C_4H_6(1,2-butadiene, gas) + 5½ O_2(gas) = 4CO_2(gas) + 3H_2O(liquid), $\Delta H°$ at 25° C = −620.69 ± 0.28 kcal/mole.

I. Introduction

This work, sponsored by the Office of Rubber Reserve, is part of a thermochemical investigation of monomeric compounds of importance in the national synthetic rubber program, and is also a part of the work of the thermochemical laboratory of this Bureau on the determination of the heats of formation of compounds of importance to industry and science.

Calorimetric measurements have been made that yield a value for the difference in the heats of combustion at constant pressure of 1,3-butadiene and 1,2-butadiene in the gaseous state at 25° C. Combination of this value, which is the heat of isomerization in the gaseous state at 25° C, with the previously reported value for the heat of formation of 1,3-butadiene [1],[1] yields values for the heats of formation and combustion of 1,2-butadiene.

II. Unit of Energy, Molecular Weights, Uncertainties

The unit of energy upon which values reported in this paper are based is the absolute joule, derived from mean solar seconds, and absolute ohms and volts, in terms of which certification of standard resistances and standard cells is made by this Bureau. For conversion to the conventional thermochemical calorie, the following relation [2,3] is used:

1 calorie = 4.1840 absolute joules.

The atomic weights were taken as O = 16.0000, H = 1.0080, and C = 12.010 from the 1947 table of international atomic weights [4].

The uncertainties assigned to the various quantities dealt with in this paper were dervied, where possible, by the method previously described [5].

III. Method

The aim of this investigation was to determine as precisely as possible the heat of isomerization of 1,3-butadiene (gas) to 1,2-butadiene (gas) at constant pressure and 25° C. This was done by determining the ratio of the heats of combustion of these isomers [6]. The value of the difference between this ratio and unity, multiplied by an accepted value for the heat of combustion of 1,3-butadiene, gives the heat of isomerization of 1,3-butadiene to 1.2-butadiene. In principle, the

[1] Figures in brackets indicate the literature references at the end of this paper.

ratio of the heats of combustion of these isomers was determined as the inverse ratio of the masses of carbon dioxide, whose formation in the combustion of the respective isomers produced identical increases in temperature in the standard calorimeter system, measured as increases in resistance of the platinum resistance thermometer as determined on the given resistance bridge. With this procedure, the energy equivalent of the calorimeter system or the heat of combustion of one of the isomers need be known only approximately, and other systematic errors tend to cancel out.

The method of reducing the experimental observations was as follows: Let

ΔR_c=the corrected increase in temperature of the calorimeter system, expressed as the increase in resistance in ohms of the given platinum thermometer at a mean temperature of 25° C, as measured with the given resistance bridge;

m_{CO_2}=the mass of carbon dioxide formed in the combustion of the hydrocarbon, in grams;

E_s=the energy equivalent, over the 'standard" interval of temperature, of the "standard" calorimeter system, obtained as the ratio of a given quantity of electric energy to the value of ΔR_c produced by it, expressed as joules per ohm;

q_i=the energy introduced into the calorimeter in the "ignition" process, consisting of sparking, igniting the flame, and extinguishing the flame, but not including any part of the heat of combustion, expressed in joules;

q_g=the energy introduced into the calorimeter by gases entering or leaving at a temperature different from 25° C.

q_v=the energy (negative) introduced into the calorimeter by the process of evaporating such water as leaves or remains in the calorimeter in the gaseous state.

q_c=the energy introduced into the calorimeter by the "standard calorimetric process" of combustion.

The total energy, q, introduced into the calorimeter by the actual combustion process in an experiment is

$$q=E_s\Delta R_c=q_c+q_g+q_v+q_i. \quad (1)$$

Letting

$$B=\frac{q_c}{E_s m_{CO_2}}, \quad (2)$$

we obtain the following relation from which B is calculated for any given experiment:

$$B=\left(\frac{\Delta R_c}{m_{CO_2}}\right)\left[1-\frac{(q_g+q_v+q_i)}{E_s\Delta R_c}\right]. \quad (3)$$

For any two isomers, the ratio of the heats evolved per gram of carbon dioxide is equal to the ratio of their heats of combustion per mole. If the subscripts a and b refer to 1,3-butadiene and 1,2-butadiene, respectively, and $-\Delta Hc°$ is the heat evolved in the standard combustion of one mole of the hydrocarbon, then

$$B_b/B_a=(-\Delta Hc°)_b/(-\Delta Hc°)_a, \quad (4)$$

and

$$(-\Delta Hc°)_a-(-\Delta Hc°)_b=(-\Delta Hc°)_a(1-B_b/B_a). \quad (5)$$

For the reaction of isomerization,

$$1,3\text{-butadiene (gas)}=1,2\text{-butadiene (gas)}, \quad (6)$$

the standard heat of isomerization is

$$\Delta H°(\text{isomerization})=-(-\Delta Hc°)_a(1-B_b/B_a). \quad (7)$$

It may be seen from eq 3 and 7 that the heat of isomerization derived by this procedure is not sensitive to the value of E_s or of $(-\Delta Hc°)_a$. The total amount of energy in one experiment is about 60,000 j, and the largest variation in the value of $q_v+q_g+q_i$ is about 150 j. Therefore, an error of 1 percent in the value of E_s, used in eq 3, would cause an error of not more than 0.002 percent in the value of B_b/B_a. This corresponds to an error of 0.01 kcal/mole in the value of $\Delta H°$ (isomerization). Similarly, an error of 0.1 percent in the value of $(-\Delta Hc°)_a$ used in eq 5 would cause an error of 0.01 kcal/mole in the value of $\Delta H°$ (isomerization).

IV. Apparatus

1. Calorimeter Assembly and Thermometric System

The calorimeter assembly used in this investigation was similar to that used in other investiga-

tions in this laboratory [6, 7], with some improvements added. The jacket of the calorimeter was maintained near 27.00° C, at a temperature constant within ±0.002° C, by means of an automatic regulator. In all experiments, the calorimeter uniformly contained 3627.56 ±0.02 g of water, together with the stirrer, platinum resistance thermometer, calorimeter heater, and the glass reaction vessel with its metal support. The stirrer was operated at a substantially constant speed of 276 rpm with a belt drive from a synchronous motor.

The calorimeter heater consisted of about 65 ohms of enameled constantan resistance wire, No. 30 AWG, wound on a Pizein-coated, thin, copper cylinder, the whole covered with Pizein [7].

The thermometer system consisted of a platinum resistance thermometer No. 262,214 and Mueller resistance bridge No. 404 [8].

2. Reaction Vessel

An improved glass reaction vessel was designed and made for this and subsequent investigations involving combustions in a flame at constant pressure. The new reaction vessel is shown in figure 1.

In the combustion of hydrocarbons other than methane and ethane in a flame in a glass reaction vessel, it is necessary to mix some "primary" oxygen with the combustible gas before it reaches the flame, in order to prevent deposition of unburned carbon in the burner tube. For a given rate of flow of the combustible gas, the flame velocity is required to be such that the flame will neither flash back inside the burner tube, nor blow off from the burner tip. For a given combustible gas burning in an atmosphere of oxygen, the position of the flame at the burner tip is determined largely by the amount of "primary" oxygen mixed with the combustible gas. In the previous design of reaction vessel [7], the admixture of primary oxygen was determined largely by the size of the Bunsen openings at the base of the burner tip. The size of the Bunsen openings could be changed only by cutting the reaction vessel apart. As changes were always required for different types of hydrocarbons, this was a cumbersome arrangement. In the new design, the primary oxygen is introduced through a sep-

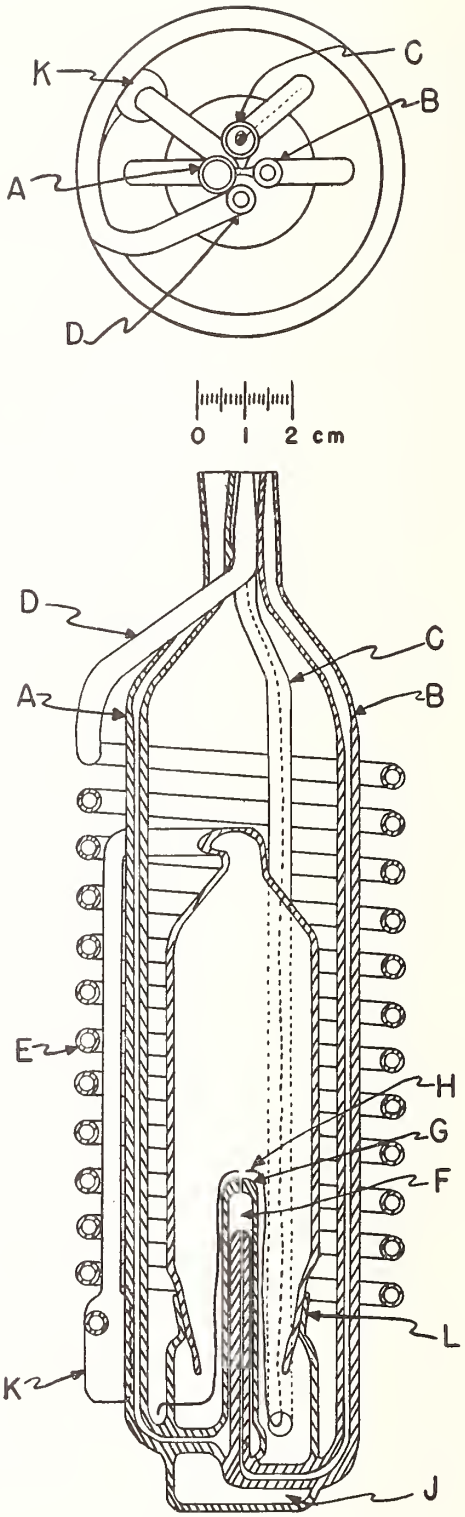

FIGURE 1. *Diagram of the reaction vessel.*

arate line, and the fraction of primary oxygen in the combustible mixture reaching the flame at the burner tip is easily controlled by regulating separately the rate of flow of the combustible gas and of the oxygen.

In the present investigation, a rate of flow of butadiene equal to 29 ml/min (or 0.0012 mole/min) was found to be satisfactory. The primary oxygen was adjusted to produce a blue flame with a sharp inner cone. The primary oxygen supplied about 30 percent of the oxygen requried for complete combustion of the hydrocarbon. The total oxygen (primary plus secondary) was about 150 percent of that required for complete combustion. (In order to avoid possible damage to the glass reaction vessel, preliminary tests of the amount of primary oxygen required for the satisfactory combustion of a given hydrocarbon, at given rates of flow, were made with a similar burner tube made of brass and provided with a glass chimney.)

The method of operation of the new reaction vessel is as follows: The hydrocarbon enters through inlet tube *A*, the primary oxygen through *B*, and the secondary oxygen through *C*. The hydrocarbon and primary oxygen mix in the chamber *F* and emerge through a hole (about 0.5 mm diameter) in the quartz tip *G*. Sparking across the platinum wires *H*, above the tip, ignites the mixture, which burns in a steady flame in the atmosphere of secondary oxygen supplied through the inlet *C*. One of the platinum wires enters through the secondary oxygen inlet tube *C;* the other is grounded to the calorimeter can. The gap between the platinum wires is about 3 mm. The gaseous products of combustion leave the combustion chamber at the top, are cooled to the temperature of the calorimeter in their passage through the glass spiral *E*, and leave the calorimeter through the outlet *D*. Most of the water vapor condenses to liquid, which collects at the bottom of the vessel at *J*, or in the bulb *K*, at the bottom of the spiral. The vessel is constructed to come apart at the joint *L*, to facilitate adjusting the spark gap and cleaning the vessel.

3. Sparking System

A new sparking system was assembled for this investigation. It consisted of a high-tension coil (Delco-Remy 538-z), a condenser having a capacity of 0.2 microfarad, and breaker points operated by a hexagonal cam driven by a synchronous motor having a speed of 1,800 rpm. Four dry cells were used as a source of energy. The spark gap at the burner tip was about 3 mm, and the normal time of sparking was 15 sec.

V. Chemical Procedure

1. Source and Purity of the Butadienes

The sample of 1,3-butadiene used was from a lot of 1,3-butadiene labeled Research Grade, Phillips Petroleum Co. The purity of this material, sampled from the vapor phase, was determined by measurements of freezing points by A. R. Glasgow, Jr. to be 99.83 ± 0.06 mole percent [9].

The 1,2-butadiene used was a sample from the API–NBS series of highly purified hydrocarbons, which are being prepared through a cooperative undertaking of the American Petroleum Institute and the National Bureau of Standards. It was made available through the American Petroleum Institute Research Project 44 at the National Bureau of Standards on "Data on properties of hydrocarbons" and was purified at the National Bureau of Standards by the American Petroleum Institute Research Project 6 on the "Analysis, purification, and properties of hydrocarbons" from material supplied by the Standard Oil Development Co. through W. J. Sweeney. A complete description of the purification and purity of this compound is given by Streiff, Murphy, Zimmerman, Soule, Sedlak, Willingham, and Rossini [10], who reported the purity by measurement of freezing points, to be 99.94 ± 0.05 mole percent.

It is calculated that in the extreme case, the heat of combustion would be affected by less than the following amounts because of the impurities: 0.012 percent for impurities in 1,3-butadiene; and 0.003 percent for impurities in 1,2-butadiene.

The butadiene was withdrawn in the vapor phase from its container, passed through a tube of anhydrous calcium sulfate followed by a small amount of anhydrous magnesium perchlorate to remove traces of water, and fed directly into the reaction vessel in the calorimeter for the combustion.

2. Purification of the Oxygen Used for Combustion

The oxygen used for combustion, including both the primary and secondary streams, was commer-

cial oxygen that was freed of combustible impurities by passage through copper oxide at about 550° C. The oxygen in both lines was freed of carbon dioxide and water before entering the calorimeter by passage through tubes containing, successively, ascarite, magnesium perchlorate, and phosphorus pentoxide.

3. Purity of the Reaction of Combustion

As a check on the purity of the reaction of combustion, both the water and carbon dioxide formed in the combustion were collected and the masses determined for each experiment. In eight combustion experiments with 1,3-butadiene, the mean value of the ratio, r, of one-fourth of the number of moles of carbon dioxide to one-third of the number of moles of water, was found to be 1.00024, with a standard deviation of ± 0.00022. Similarly for six experiments with 1,2-butadiene, the mean value of r was found to be 0.99994, with a standard deviation of ± 0.00019.

Samples of the products of combustion were analyzed for carbon monoxide by the Gas Chemistry Section of this Bureau [11]. In no case was the total amount of carbon monoxide greater than 0.004 percent of the amount of carbon dioxide formed in the combustion.

The effect of any possible incomplete combustion during the ignition or extinction of the flame was eliminated by the procedure, described below, of determining the "ignition" energy in separate experiments in which the flame was allowed to burn only long enough to produce a steady flame, and then was extinguished. With this procedure, the heat of combustion was in reality determined from the portion of the combustion when the flame was in a steady state, any constant errors associated with the ignition and extinction of the flame cancelling out.

4. Determination of the Amount of Reaction

For each calorimetric combustion experiment, the amount of reaction was determined from the mass of carbon dioxide formed, taking 1 mole or 44.010 g of carbon dioxide as equivalent to one-fourth mole of butadiene.

VI. Calorimetric Procedure

1. Calorimetric Combustion Experiments

The following procedure was followed in preparing the calorimeter for all experiments: The calorimeter jacket was brought to temperature, near 27.00° C, where it was automatically maintained constant, within about ± 0.002° C, throughout the whole experiment. The standard mass of water, 3627.56 ± 0.02 g, was weighed into the calorimeter can on the pan of a 5-kg balance, having a sensitivity at this load of 0.008 g per scale division, using the same weights in all experiments. The calorimeter can was placed in the calorimeter jacket, the dry reaction vessel with the heater around it was lowered into the can, the cover was placed on the can, the jacket was covered, the stirrer was connected, and the platinum resistance thermometer inserted into the calorimeter can through the hole in the jacket cover. The hydrocarbon and primary and secondary oxygen lines were connected to the reaction vessel through flexible glass spirals. The weighed absorption tubes for water and carbon dioxide, a guard tube containing magnesium perchlorate and ascarite, a sampling bulb, and a flowmeter were connected to the outlet side of the reaction vessel through a three-way stopcock near the vessel. This stopcock permitted oxygen to bypass the reaction vessel at the end of a combustion to flush any water and carbon dioxide in the lines into the absorption tubes. The calorimeter was brought to near the starting temperature by electrical heating, and a period of about 20 min was allowed for equilibrium to be established. The calorimetric observations were begun when the calorimeter reached the selected starting temperature. The standard temperature rise was about 4 degrees for the combustion experiments, and the final temperature was slightly below the jacket temperature.

The calorimetric observations during an experiment consisted of: (a) a fore period of 20 min during which the reaction vessel, containing oxygen at atmospheric pressure, remained closed, and readings of the resistance of the platinum thermometer were taken every 2 min; (b) a "reaction" period during which the reaction took place, with a period allowed for equilibrium to be reestablished in the calorimeter, and during which readings of the resistance of the platinum thermometer were taken about every 15 sec or every minute, depending on the shape of the time-temperature curve; and (c) an after period of 20 min during which the reaction vessel remained closed, the calorimeter temperature was slightly

below the jacket temperature, and readings of the resistance of the platinum thermometer were taken every 2 min.

The manipulation of the apparatus controlling the reaction during a combustion experiment was as follows: Before the calorimetric experiment, the two absorption tubes for water and carbon dioxide were flushed with hydrogen and weighed by a method previously described [12, 13, 14]. The hydrocarbon inlet tube was flushed with helium to remove oxygen from this line and the rest of the reaction vessel then flushed and left filled with oxygen at atmospheric pressure. During the fore period, the rates of flow of the primary and secondary oxygen and gaseous hydrocarbon were regulated through bypass flowmeters. At the end of the fore period, the three-way stopcock outlet on the reaction vessel was opened to the absorption tubes, the primary and secondary streams of oxygen were turned into the vessel, the spark was turned on, and the hydrocarbon was then turned into the vessel. The sparking was continued for 15 sec, or until the flame was started, as indicated by the flowmeter at the end of the line. The flame was allowed to burn until a final temperature slightly below the jacket temperature was reached, when the flame was extinguished by turning off the hydrocarbon. The time of combustion was usually about 22 min. The primary and secondary streams of oxygen were left on for an additional 10 min and then cut off. The reaction vessel was closed by setting the three-way stopcock at the outlet such that the oxygen would bypass the reaction vessel but would flow through the absorption tubes. Thus, all the water vapor not in the calorimetric reaction vessel was swept into the absorption tube. An additional period of about 6 min was allowed for equilibrium to be established before starting the after period. After the experiment, the absorption tube for water was flushed with hydrogen and weighed to obtain the amount of water carried out of the calorimeter as vapor. The absorption tubes were replaced on the train and the reaction vessel flushed with oxygen overnight to carry all the water and carbon dixoide into the absorption tubes. Both tubes were then flushed with hydrogen and weighed. The mass of carbon dioxide produced was used to determine the amount of reaction, and the stoichiometric ratio of the masses of carbon dixoide and water was used to check the purity of the reaction of combustion.

The corrected increase in temperature of the calorimeter system, ΔRc, expressed as the increase in resistance in ohms of the given platinum thermometer at a mean temperature of 25° C, was taken as the difference in the resistance of the thermometer between the beginning of the after period and the end of the fore period, corrected for heat of stirring and thermal leakage [15].

2. Determination of the "Ignition" Energy

Experiments to determine the energy associated with the ignition and extinction of the flame ("ignition" energy experiments) were performed in the same manner as the regular combustion experiments, except that the flame was allowed to burn only long enough to be sure a steady flame was attained. The flame was usually left burning for about 40 seconds. The initial temperature in these experiments was a fraction of a degree below the jacket temperature, and the rise of temperature was about 0.1 deg. Experiments were also performed in which only sparking energy was added to the calorimeter.

The mean value for the "ignition" energy, which is the energy associated with the process of ignition and extinction of the flame, but not including any part of the heat of combustion, obtained from seven experiments with 1,3-butadiene and two experiments with 1,2-butadiene, with an average of 0.0005 mole of butadiene burned in each experiment, was found to be 33.1 j, with a standard deviation of ± 2.8 j. In separate experiments in which no hydrocarbon was burned and sparking alone for the standard time occurred, the sparking energy was found to be 31.1 j with a standard deviation of ± 0.8 j. In making these calculations, the value of E_s, the standard energy equivalent, was taken as 154,446 abs j/ohm.

For the present experiments, the ignition energy for the standard time (15 sec) of sparking was taken as the weighted mean of the foregoing values, 31.3 j with a standard deviation of 0.8 j.

3. Reduction to the Standard Calorimetric Process

The process that actually takes place in the calorimetric reaction vessel during a combustion experiment is the following:

$$n\mathrm{C_4H_6(gas,\ 1\ atm}, t_r)+(m_1+m_2+m_3)\mathrm{O_2}$$
$$(\mathrm{gas,\ 1\ atm}, t_r)=[r\mathrm{CO_2}+m_2\mathrm{O_2}+b\mathrm{H_2O}]$$
$$(\mathrm{gas,\ 1\ atm}, t_m)+[m_3\mathrm{O_2}+c\mathrm{H_2O}](\mathrm{gas,\ 1\ atm}, t_f)+$$
$$(a-b-c)\mathrm{H_2O(liq,\ 1\ atm},\ t_f). \quad (8)$$

The energy evolved in this reaction and including the ignition energy is $q=E_s\Delta R_c$. In the foregoing equation, t_r is the temperature of the room; t_m and t_f are the mean and final temperatures, respectively, of the calorimeter; n is the number of moles of hydrocarbon entering the calorimeter; $(m_1+m_2+m_3)$ is the number of moles of oxygen entering the calorimeter; $m_1=\frac{11}{2}n$ is the number of moles entering during the actual combustion period and being used in the combustion; m_2 is the excess number of moles entering during the actual combustion period and leaving the calorimeter as a mixture with $r=4n$ moles of carbon dioxide and b moles of water vapor; m_3 is the number of moles of oxygen entering the calorimeter during the flushing immediately following the actual combustion period and leaving the calorimeter as a mixture with c moles of water vapor; $(a\text{-}b\text{-}c)$ is the number of moles of water left in the calorimeter in the liquid state; and $a=3n$ is the total number of moles of water formed in the combustion. The quantity c also includes a very small amount of water left in the calorimeter in the gaseous state.

It is desirable to correct the results of each calorimetric experiment to a common basis for comparison. This can be done by adjusting all results to the basis of a "standard calorimetric process" defined by the equation

$$n\mathrm{C_4H_6(gas,\ 1\ atm},\ t_{25})+(m_1+m_2)\mathrm{O_2}$$
$$(\mathrm{gas,\ 1\ atm},\ t_{25})=[r\mathrm{CO_2}+m_2\mathrm{O_2}](\mathrm{gas,\ 1\ atm},\ t_{25})+$$
$$a\mathrm{H_2O(liq,\ 1\ atm},\ t_{25}) \quad (9)$$

The energy evolved in this reaction is q_c.

For the present experiments the various quantities have the values

$$m_1=\frac{11}{2}\,n,\ m_2=\frac{11}{4}\,n,\ r=4n,\ \text{and}\ a=3n.$$

The difference between the energy, q_c, evolved in the standard calorimetric process expressed by eq 9, and that evolved in the actual calorimetric process expressed by eq 8, but including the energy of ignition, is $q_c-q=-(q_g+q_v+q_i)$.

The energy associated with the adjustment of the composition of the carbon dioxide-oxygen mixture issuing from the calorimeter in the individual experiments to the average composition as expressed in the "standard calorimetric process" is negligible. The quantities q_g and q_v were evaluated by the relations:

$$q_g=\mathrm{C_1}[n(t_r-t_{25})]+$$
$$\mathrm{C_2}[m_1(t_r-t_{25})+m_2(t_r-t_m)+m_3(t_r-t_f)]+$$
$$\mathrm{C_3}[b(t_{25}-t_m)+c(t_{25}-t_f)]+$$
$$\mathrm{C_4}[(a-b-c)(t_{25}-t_f)]+\mathrm{C_5}[r(t_{25}-t_m)],$$

$$q_v=-(b+c)[\Delta Hv];$$

where $\mathrm{C_1}=80.1$, $\mathrm{C_2}=29.4$, $\mathrm{C_3}=33.6$, $\mathrm{C_4}=75.3$, and $\mathrm{C_5}=37.1$ are the approximate heat capacities of butadiene(gas), oxygen(gas), $\mathrm{H_2O}$(gas), $\mathrm{H_2O}$(liq), and $\mathrm{CO_2}$(gas), respectively, in j/deg mole, and $\Delta Hv=43{,}992$ abs j/mole is the heat of vaporization of water at 25° C and saturation pressure.

To obtain the values of the standard heat of reaction, $\Delta H°$, from the standard calorimetric process indicated by eq 9, it is only necessary to take account of the change in heat content with pressure at constant temperature for each gas from its given pressure to zero pressure, so that each substance will have the heat content of the thermodynamic standard state. Since this correction will not be significantly different for the two isomers, the ratio of the values of ΔH for the standard calorimetric process will also be the ratio of the values of $\Delta H°$ for the standard thermodynamic process.

VII. Results of the Present Investigation

The results of the calorimetric combustion experiments for 1,3-butadiene and 1,2-butadiene are given in tables 1 and 2, respectively. For these calculations, the value of E_s, the energy equivalent, was taken as approximately 154,446 j/ohm. The value of B were calculated from eq 3

TABLE 1. *Results of calorimetric combustion experiments on 1,3-butadiene*

Experiment	ΔR_c	Mass of carbon dioxide	q_g	q_s	q_i	B	Deviation from mean
	Ohms	*g*	*j*	*j*	*j*	*Ohms/g* CO_2	*Ohms/g* CO_2
1	0.388048	4.17091	+16.5	−342.3	31.3	0.0934941	−0.0000514
2	.381756	4.10179	−2.4	−331.2	31.3	.0935478	+.0000023
3	.381025	4.09487	+0.1	−360.3	31.3	.0935695	+.0000240
4	.397671	4.27289	−2.8	−355.4	31.3	.0935637	+.0000182
5	.384888	4.13689	−16.8	−352.2	31.3	.0935665	+.0000210
6	.390584	4.19985	−18.6	−362.7	31.3	.0935390	−.0000065
7	.391438	4.20192	−23.9	−236.5	31.3	.0935099	−.0000356
8	.378484	4.07076	−17.2	−389.7	31.3	.0935735	+.0000289
Mean						0.0935455	
Standard deviation of the mean						±.0000104	

TABLE 2. *Results of calorimetric combustion experiments on 1,2-butadiene*

Experiment	ΔR_c	Mass of carbon dioxide	q_g	q_s	q_i	B	Deviation from mean
	Ohms	*g*	*j*	*j*	*j*	*Ohms/g* CO_2	*Ohms/g* CO_2
1	0.384743	4.04783	−13.2	−304.9	31.3	0.0955079	−0.0000048
2	.380613	4.00684	−5.5	−345.8	31.3	.0955080	−.0000047
3	.388498	4.09171	−10.1	−368.8	31.3	.0954977	−.0000150
4	.395315	4.16322	−7.7	−383.4	31.3	.0955137	+.0000010
5	.397521	4.18337	−10.8	−352.4	31.3	.0955377	+.0000250
6	.388279	4.08829	−16.6	−364.3	31.3	.0955112	−.0000015
Mean						0.0955127	
Standard deviation of the mean						±.0000055	

From these data, the ratio of the heat of combustion of 1,2-butadiene to that of 1,3-butadiene is

$$(-\Delta Hc^\circ)_b/(-\Delta Hc^\circ)_a = B_b/B_a = 1.021029 \pm 0.000256. \quad (14)$$

The values previously reported [1] for the heats of combustion and formation of 1,3-butadiene (gas) are

$$C_4H_6(1,3\text{-butadiene, gas}) + \frac{11}{2}\,O_2(\text{gas}) = 4CO_2(\text{gas}) + 3H_2O(\text{liquid}), \quad (15)$$

$$-\Delta Hc^\circ_{298.16} = 607.91 \pm 0.23 \text{ kcal/mole.}$$

$$4C(c, \text{graphite}) + 3H_2(\text{gas}) = C_4H_6(1,3\text{-butadiene, gas}), \quad (16)$$

$$\Delta Hf^\circ_{298.16} = 26.75 \pm 0.23 \text{ kcal/mole.}$$

The heat of isomerization at 25° C thus becomes (from eq 7):

$$1,3\text{-butadiene (gas)} = 1,2\text{-butadiene (gas)} \quad (17)$$

$$\Delta H^\circ \text{ (isomerization)} = 12.78 \pm 0.16 \text{ kcal/mole.}$$

The heats of combustion and formation of 1,2-butadiene become:

$$C_4H_6(1,2\text{-butadiene, gas}) + \frac{11}{2}\,O_2(\text{gas}) = 4CO_2(\text{gas}) + 3H_2O(\text{liquid}), \quad (18)$$

$$-\Delta Hc^\circ_{298.16} = 620.69 = 0.28 \text{ kcal/mole.}$$

$$4C\ (c, \text{graphite}) + 3H_2(\text{gas}) = C_4H_6(1,2\text{-butadiene, gas}), \quad (19)$$

$$\Delta Hf^\circ_{298.16} = 39.53 \pm 0.28 \text{ kcal/mole.}$$

VIII. References

[1] E. J. Prosen and F. D. Rossini, J. Research NBS **34,** 59 (1945) RP1628.

[2] E. F. Mueller and F. D. Rossini, Am. J. Phys. **12,** 1 (1944).

[3] Selected Values of Chemical Thermodynamic Properties. National Bureau Standards. Values of Constants. (December 31, 1947.)

[4] G. P. Baxter, M. Guichard, and R. Whytlaw-Gray, J. Am. Chem. Soc. **69,** 734 (1947).

[5] F. D. Rossini and W. E. Deming, J. Wash. Acad. Sci. **29,** 416 (1939).

[6] E. J. Prosen and F. D. Rossini, J. Research NBS **27,** 289 (1941) RP1420.

[7] F. D. Rossini, BS J. Research **12,** 735 (1934) RP686.

[8] F. D. Rossini and J. W. Knowlton, J. Research NBS **19,** 249 (1937) RP1024.

[9] A. R. Glasgow, Jr., N. C. Krouskop, J. Beadle, G. D. Axilrod, and F. D. Rossini, Anal. Chem. **20,** 410 (1948).

[10] A. J. Streiff, E. T. Murphy, J. C. Zimmerman, L. F. Soule, V. A. Sedlak, C. B. Willingham, and F. D. Rossini, J. Research NBS **39,** 321 (1947) RP1833

[11] M. Shepherd, Anal. Chem. **19,** 77 (1947).

[12] E. J. Prosen and F. D. Rossini, J. Research NBS **33,** 255 (1944) RP1607.

[13] F. D. Rossini, BS J. Research **6,** 1 (1931) RP259.

[14] F. D. Rossini, BS J. Research **6,** 37 (1931) RP260.

[15] J. R. Eckman and F. D. Rossini, BS J. Research **3,** 597 (1929) RP111.

WASHINGTON, October 29, 1948.

Heats of Formation of Diborane and Pentaborane

Edward J. Prosen, Walter H. Johnson, and Florence Y. Pergiel

The heats of formation of diborane and pentaborane have been determined by measurements of the heats of decomposition into amorphous boron and hydrogen in a calorimeter. The heats of formation at 25° C, from amorphous boron and hydrogen, are 6.73 ±0.52 kcal/mole for diborane (gas) and 12.99 ±0.39 for pentaborane (gas).

1. Introduction

In order to ascertain the bond energy relations in the boron hydrides, precise values of the heats of formation of these substances from the elements are needed. Diborane, B_2H_6, and pentaborane, B_5H_9, were chosen for investigation as two of the simplest members of this class of compounds.

The measurements reported in this paper were made in 1948 but have not been previously published. No value for the heat of formation of pentaborane was available at that time. The value for the heat of formation of diborane given by Roth and Börger, −44 kcal/mole, [1, 2][1] was based on measurements of the heat of hydrolysis of diborane to boric acid, the heat of combustion of boron to boric oxide, and the heat of solution of boric oxide. This value was very uncertain because it depended directly upon the heat of combustion of elemental boron, a quantity which could not be determined with any precision. However, it was found that diborane and pentaborane could be decomposed quantitatively and rapidly at 600° C into amorphous boron and gaseous hydrogen. Hence this decomposition reaction could be employed calorimetrically to give values of the heats of formation of diborane and pentaborane independent of the value for the heat of combustion of boron.

2. Experimental Procedure

2.1. Materials

The diborane and pentaborane samples were obtained from the Naval Research Laboratory, Washington, D. C., through the courtesy of R. R. Miller. A similar sample of diborane supplied to the Ohio State University was found by the cryoscopic method to have a purity of 99.95 mole percent [3].

The pentaborane was produced by the fractional pyrolysis of diborane. A sample of the same lot supplied to the Ohio State University was found by the cryoscopic method to have a purity of 99.97 mole percent [4]. Analysis by the mass spectrometer showed no impurities other than boron hydrides with none heavier than B_5H_9 [5].

2.2. Apparatus

The calorimeter was of the isothermal-jacket type; the jacket temperature was maintained constant within ±0.001° C during each experiment. Details of the calorimeter assembly have been described in previous reports from this laboratory [6,7].

[1] Figures in brackets indicate the literature references at the end of this paper.

The calorimetric vessel used for the decomposition of diborane and pentaborane is shown in figure 1. It consisted essentially of a quartz tube (A) upon which was wound a nichrome wire heating coil (B) surrounded by a silver radiation shield (C) and a vacuum jacket (D). The heating coil had a total resistance of 190 ohms and was tapped (E) so that the upper portion had a resistance of 127 ohms. Quartz wool plugs (F) were inserted in the tube above and below the heating coil to retain the solid products within the heated zone. The exit vapors were carried out through the glass helix (G) to cool them to the calorimeter temperature.

Calorimeter temperatures were determined by means of a platinum resistance thermometer in conjunction with a Mueller bridge. The quantity of electrical energy was determined from the current, voltage, and time of current flow. The current and voltage were determined by means of a White double

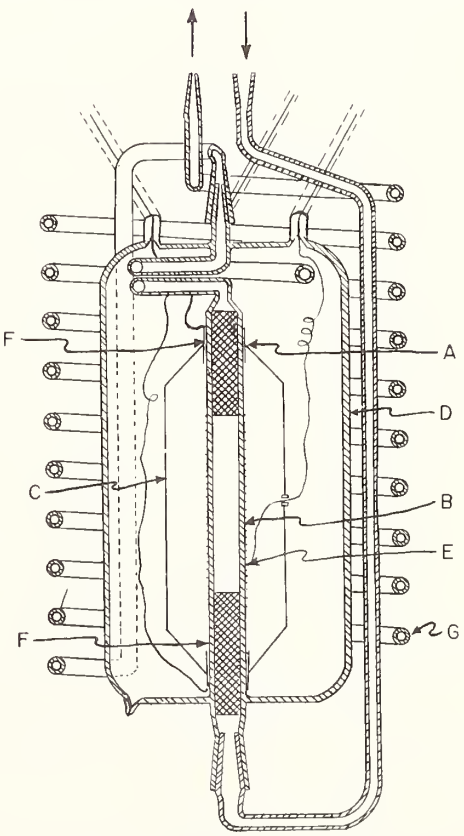

FIGURE 1. *Calorimetric reaction vessel.*

potentiometer from measurements of the potential drop across appropriate standard resistors included in the power circuit [8]. Timing of the experiments was done by reference to standard seconds-signals produced at the National Bureau of Standards. All equipment was calibrated in terms of standards maintained at the Bureau.

2.3. Procedure

a. Reaction Experiments

(1) *Diborane.* The gas train used for the diborane decomposition experiments is shown in figure 2. The diborane was contained in a steel cylinder fitted with a needle valve and connected to the system through a flowmeter and a mercury float valve. Before each experiment the cylinder was immersed in liquid nitrogen, and traces of hydrogen (produced by slow decomposition of diborane into higher boranes) were removed by evacuation. After removal of the hydrogen the valve was closed and dry ice was substituted for the liquid nitrogen; at the temperature of dry ice, the vapor pressure of diborane is approximately 2 atm and the vapor pressures of the higher boranes are negligible. Helium was passed through the system at a constant rate throughout the experiment. It was purified by passing successively over copper oxide at 600° C, ascarite, magnesium perchlorate, and phosphorus pentoxide before it entered the system.

Temperatures were observed at 2-min intervals during a 20-min "fore" rating period. At the end of this period the current was switched from an external "spill" resistor (having the same resistance as the heater) into the upper portion of the calorimetric vessel. After a warm-up period of 2 min the needle valve was opened, which permitted the diborane to pass into the vessel. The flow of diborane was cut off after 16 min and the float valve closed. Four minutes later the current was swtched to pass through both portions of the heater; this completed the decomposition of the polymerized material usually formed near the lower end of the upper portion of the heater. By means of appropriate resistors in the circuit, the current was nearly constant in both cases. During this time readings of current and voltage were made on alternate minutes, and temperature readings were made at 1-min intervals. When the desired calorimeter temperature was obtained the electric current was discontinued. Temperature measurements were continued at 1-min intervals until thermal equilibrium was reestablished, after which observations were made at 2-min intervals during a 20-min "after" rating period.

The gas mixture of helium and hydrogen passed out of the calorimeter through a trap cooled in liquid nitrogen, a copper oxide furnace maintained at 600° C, and a weighed absorption tube containing magnesium perchlorate and phosphorus pentoxide.

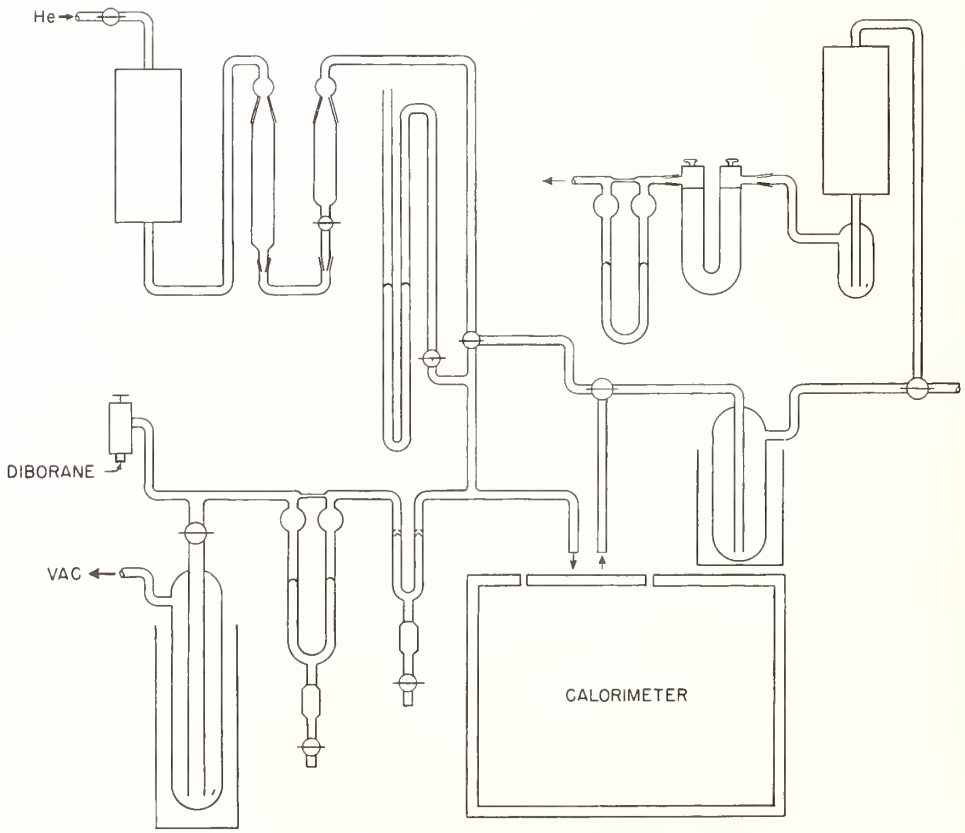

FIGURE 2. *Gas train used in thermal decomposition of diborane.*

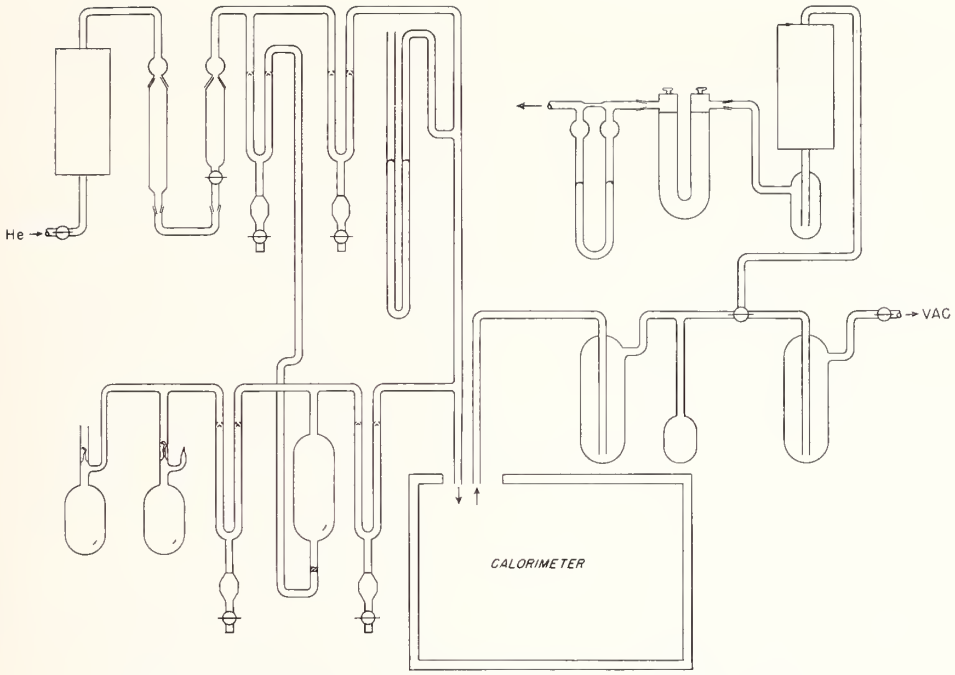

FIGURE 3. *Gas train for use in decomposition of pentaborane* (B_5H_9).

The trap was included as a safety measure, to prevent the diborane from reaching the furnace in the event of incomplete decomposition. No material was collected in the trap in any of these experiments.

The quantity of reaction was determined from the amount of hydrogen which was burned in the furnace and collected in the absorption tube as water.

(2) *Pentaborane.* The gas train used in the experiments with pentaborane is shown in figure 3. The pentaborane was inclosed in an internal breakoff ampoule. For each experiment the system was evacuated and a portion of the pentaborane transferred into the bubbling vessel. The experiments were carried out in the same manner as with diborane except that purified helium was bubbled through the pentaborane at 0° C in order to carry it into the calorimetric vessel. After each experiment, the remainder of the pentaborane in the bubbler, as well as that remaining in the original ampoule, was transferred to a second ampoule and sealed in vacuum.

b. Calibration Experiments

The calibration experiments were performed in exactly the same manner and using the same system as with the decomposition experiments except for omission of the boron hydride. Because the system used for pentaborane differed slightly from that used for diborane, a separate series of calibration experiments was performed.

3. Results

The results of the calibration experiments for the diborane system are given in table 1 in which E corresponds to the electrical energy added to the system, ΔRc the increase in resistance of the platinum thermometer, and $E_s = E/\Delta Rc$, the energy equivalent of the system.

The results of the diborane decomposition experiments are given in table 2, where q is the total energy absorbed by the system and is given by the following relationship:

$$(\Delta Rc)(E_s) = q.$$

This value of q when corrected for q_g, the correction calculated from the heat capacities of the gases involved, and subtracted from E, the electrical

TABLE 1.—*Results of the electrical calibration experiments on the diborane system*

Experiment	E	ΔR_c	E_s
	j	*Ohm*	*j/ohm*
1	49480.9	0.381239	129790
2	50329.8	.387803	129782
3	49804.4	.383708	129798
4	51630.9	.397799	129791
5	49551.6	.381761	129797
Mean			129792
Standard deviation of the mean			±3

TABLE 2. *Results of the diborane decomposition experiments*

Experiment	E	ΔR_c	q	q_g	q_c	B_2H_6	$-\Delta H$ (25° C)
	j	*Ohm*	*j*	*j*	*j*	*Mole*	*kj/mole*
1	51311.2	0.397528	51596.0	0.6	−284.2	0.010206	27.85
2	48536.9	.379034	49195.6	−2.2	−660.9	.021851	30.25
3	48557.9	.377216	48959.6	2.3	−399.4	.015966	25.02
4	49008.7	.379105	49204.8	1.1	−195.0	.007213	27.04
5	48704.1	.376538	48871.6	0.3	−167.2	.005444	30.71
Mean							28.17
Standard deviation of the mean							±1.05

energy added to the system, yields q_c, the energy absorbed by m moles of reaction, or:

$$E-(q-q_g)=q_c.$$

The heat of reaction at 25° C is then given by the ratio of q_c to m, or:

$$q_c/m=\Delta H \text{ joules/mole.}$$

To convert to the conventional thermochemical calorie, the following relationship was used:

$$1 \text{ calorie}=4.1840 \text{ joules.}$$

The results of the calibration experiments on the pentaborane system and the results of the pentaborane decomposition experiments are given in tables 3 and 4, respectively.

TABLE 3. *Results of the electrical calibration experiments on the pentaborane system*

Experiment	E	ΔP_c	E_s
	j	*Ohm*	*j/ohm*
1	48651.0	0.374654	129856
2	49904.1	.384457	129804
3	48058.8	.370289	129787
4	49314.9	.379834	129833
5	48547.3	.374191	129739
6	48495.9	.373680	129779
7	48657.3	.374996	129754
8	48529.6	.373886	129798
Mean			129794
Standard deviation of the mean			±14

TABLE 4. *Results of the pentaborane decomposition experiments*

Experiment	E	ΔP_c	q	q_g	q_c	B_5H_9	$-\Delta H$ (25° C)
	j	*Ohm*	*j*	*j*	*j*	*Mole*	*kj/mole*
1	49998.5	0.386650	50185.6	+0.4	−186.7	0.003409	54.77
2	49709.6	.384273	49876.3	−0.1	−166.8	.002889	57.74
3	49802.4	.385107	49984.6	+0.2	−182.0	.003560	51.12
4	49806.8	.385605	50049.2	+1.2	−241.2	.004353	55.41
5	49709.2	.385471	50031.4	+1.2	−321.0	.006037	53.17
6	51323.6	.397303	51567.5	+0.8	−243.1	.004508	53.93
Mean							54.36
Standard deviation of the mean							±0.91

The heats of decomposition obtained for the reactions of decomposition are given by the following equations:

$$B_2H_5(\text{gas})=2B(\text{solid, amorphous})+3H_2(\text{gas}),$$

$$\Delta H(25° \text{ C})=-6.73 \pm 0.52 \text{ kcal/mole,}$$

$$B_5H_9(\text{gas})=5B(\text{solid, amorphous})+9/2\ H_2(\text{gas}),$$

$$\Delta H(25° \text{ C})=-12.99 \pm 0.39 \text{ kcal/mole.}$$

The uncertainties assigned have been taken as twice the standard deviation of the mean of the experimental values, combined with reasonable estimates of all known sources of error.

By taking the amorphous form as the reference state of boron and 7.30 ±0.10 kcal/mole [9] for the heat of vaporization of pentaborane, the following heats of formation are obtained:

	ΔHf (25° C) kcal/mole
B_2H_6 (gas)	6.73 ±0.52
B_5H_9 (gas)	12.99 ±0.39
B_5H_9 (liquid)	5.69 ±0.40

4. Discussion

It was not possible to recover the finely divided boron quantitatively from the reaction vessel because of its tendency to adhere to the walls of the vessel as well as to the quartz wool plugs. It was therefore not feasible to obtain an accurate check on the completeness of the decomposition by determining the stoichiometric ratio between the masses of boron and hydrogen. In order to determine the presence of hydrogen, either chemically bound or adsorbed, samples of the boron produced were heated to 700° C in vacuum. Although traces of hydrogen were detected in some cases it is not likely that any significant error was introduced in the final result since the quantity of reaction in each case was based upon the mass of hydrogen evolved. Obviously, if all the boron-hydrogen bonds were of the same energy, the heat of decomposition as measured would be independent of the proportion of hydrogen removed in the process. The possibility that an extremely stable hydride was present was ruled out because portions of the residue treated with chlorine at 400° C were completely converted to boron trichloride [10]. The Constitution and Microstructure Section of the Bureau examined portions of the residue by X-ray diffraction methods. The absence of a pattern indicated that the boron was in an amorphous form.

In view of this information we conclude that the reaction of decomposition is quantitative and that the only products are amorphous boron and hydrogen. The thermal decomposition is probably the most convenient method for preparation of small quantities of high-purity boron.

5. References

[1] W. A. Roth and E. Börger, Ber. [B] **70,** 48 (1937).
[2] W. A. Roth, Z. Naturforsch. **1,** 574 (1946).
[3] E. M. Carr, J. T. Clarke, and H. L. Johnston, J. Am. Chem. Soc. **71,** 740 (1949).
[4] J. T. Clarke and H. L. Johnston (private communication).
[5] V. H. Dibeler, F. L. Mohler, L. Williamson, and R. M. Reese, J. Research NBS **44,** 489 (1950) RP2095.
[6] J. R. Eckman and F. D. Rossini, J. Research NBS **3,** 597 (1929) RP111.
[7] E. J. Prosen and F. D. Rossini, J. Research NBS **27,** 289 (1941) RP1420.
[8] E. J. Prosen and F. D. Rossini, J. Research NBS **33,** 255 (1944) RP1607.
[9] W. H. Evans and D. D. Wagman, (manuscript in preparation).
[10] E. H. Winslow and H. A. Liebhafsky, J. Am. Chem. Soc. **64,** 2725 (1942).

WASHINGTON, June 29, 1958.

JOURNAL OF RESEARCH of the National Bureau of Standards—A. Physics and Chemistry
Vol. 72A, No. 5, September–October 1968

Studies in Bomb Calorimetry. A New Determination of the Energy of Combustion of Benzoic Acid in Terms of Electrical Units

K. L. Churney and G. T. Armstrong

Institute for Basic Standards, National Bureau of Standards, Washington, D.C. 20234

(July 20, 1968)

The heat of combustion of NBS Standard Sample 39i of benzoic acid under standard bomb conditions has been determined in terms of electrical units. A value of $-26{,}434.0$ J g^{-1} was obtained. The total uncertainty in our determination is estimated to be ± 3.3 J g^{-1}. The uncertainty due to random errors was 1.7 J g^{-1} and is based on the appropriate factors for the Student t distribution at the 95 percent confidence limits for eleven determinations of the energy equivalent of the calorimeter and six determinations of the heat of combustion of benzoic acid. The principal systematic error, neglect of surface temperature correction for our calorimeter, has been assigned a value of ± 2.6 J g^{-1} until more reliable estimates of the correction can be made. Particular emphasis was placed on improving the precision of a calorimetric measurement over those previously obtained in this laboratory by the use of more sensitive auxiliary measuring equipment and more accurate procedures to evaluate the corrected temperature rise.

Key Words: Benzoic acid, heat of combustion; bomb calorimetry, procedures and errors; heat of combustion; bomb-calorimeter, electrical calibration; Dickinson calorimeter.

1. Introduction

Benzoic acid has served for many years as a reference material of known energy of combustion for calibrating bomb calorimeters. At the National Bureau of Standards (NBS), the Heat Division of the Institute for Basic Standards, or its predecessors, has certified the energy of combustion of various batches of benzoic acid in terms of electrical units for this purpose. Maintenance of a capability of a high degree of accuracy and precision in bomb calorimetry is a prerequisite for this certification activity.

The calorimetric measurements on which the certifications at NBS have been based have been made in most instances with a calorimeter of the same design, except for slight modifications, as that used by Dickinson [1].[1] In July of 1964, we started a study whose goal was to design a new bomb calorimeter capable of higher accuracy and precision than existing calorimeters. The first step in this project was a study of the performance of an existing Dickinson calorimeter (NBS 57662). The study was made in the hope that it would lead to a better understanding of the limitations inherent in the Dickinson calorimeter.

A second reason for making the study is that the last certification of benzoic acid in terms of electrical units at NBS was made in 1942 [2]. More recent certifications have been based upon intercomparison of benzoic acid samples. It appeared likely that a certification in terms of electrical units could now be made with greater accuracy than had been possible heretofore, because of the substantial improvement in the precision and accuracy of the auxiliary measuring instruments of the calorimetric station since 1942. Although there was no reason to suspect that the intercomparisons of samples had introduced undetected systematic errors in the certification of batches of benzoic acid, we wished to confirm the absence of such errors.

The general features of the calorimeter and its method of operation have been adequately described elsewhere [3, 4, 5]. A summary of pertinent details is given in sections 2 and 4.

The basis for the correction of the observed temperature rise of the calorimeter for the effects of heat transfer from its environment, Newton's cooling law, and of stirring energy is found in the discussion of Coops, Jessup, and Van Nes [4]. The particular method of calculation used in this work is described in section 5 in some detail because of the higher accuracy obtained by the use of fewer approximations.

[1] Figures in brackets indicate the literature references at the end of this paper.

Previous analysis of extensive calorimetric data from this laboratory had suggested that the uncertainty in our calorimetric measurements might be due mainly to the uncertainties in temperature measurements during the drift periods. Increasing the precision of the measurements of the resistance of the platinum thermometer led to a substantial improvement in the precision of measurement of the calorimeter temperatures but revealed the presence of small systematic deviations from Newton's cooling law. Modification of the calorimeter and our method of operating it suggested some possible explanations for these systematic deviations and reduced but did not entirely eliminate them as is discussed in sections 3, 5.1a, and 6.2.

A series of electrical calibrations to determine the energy equivalent of the calorimeter and a series of benzoic acid combustions to determine the energy equivalent, in terms of electrical standards, of the combustion of benzoic acid are described in sections 4 and 5. Presentation of the results is completed in section 6 by an analysis of random and systematic errors.

2. Experimental Apparatus

The calorimetric apparatus consists of a stirred-water calorimeter surrounded by an isothermal jacket. The calorimeter consists of a closed can which contains a stirrer, a platinum resistance thermometer placed near the can wall, a combustion bomb with fuse leads and handle, an electrical heater that fits snugly around the lower half of the bomb, and a weighed, fixed, quantity of water sufficient to be in contact with the calorimeter lid after the calorimeter has been assembled. The calorimeter temperature is always kept below that of the jacket.

2.1. Calorimeter and Jacket

The calorimeter and jacket are essentially the same as described previously by Jessup [6], except for the following modifications.

The calorimeter jacket has been enclosed by an air bath, kept near 27.5 °C with a regulation of ±0.2 °C by an on-off controller. The air bath was required to make sure the average jacket temperature did not change with time. Thermocouple measurements had shown the lid (i.e., top) of the jacket was about 0.006 °C colder than the rest of the jacket, presumably due to poor water circulation in the lid, when the room temperature was 3 °C below that of the jacket. The jacket temperature regulator was replaced by a commercially available proportional controller having reset action and a nickel resistance thermometer for a sensor.

To insure a constant stirring rate, the calorimeter stirrer was turned by a synchronous motor.

The oxygen combustion bomb and its internal fittings are those described previously [7], except for two changes. The fuses were made of 2 cm of 0.002-in-diam platinum wire rather than a combustible metal to eliminate any energy contribution due to fuse combustion as described by Prosen [5]. The stem of the bomb needle valve was modified so that the inside of the bomb could be directly connected to the pressure gage of the oxygen manifold during filling, for a more accurate pressure measurement.

The calorimeter heater is an improved version of a type described previously [8]. It consists of a 32-Ω heater element of glass-insulated, 0.010-in-diam Advance wire which was soft soldered at both ends to 18-gage, Formvar-covered, copper, current leads. The element was inserted in a $^3/_{16}$-in-diam 0.030-in-wall, soft copper tube. The tube was flattened against the element after the space between the tube and element was filled with epoxy-resin cement. The tube (sheath) length was selected so that, after the heater was coiled to fit the bomb, at least 20 cm of each current lead of the heater element was inside the calorimeter. The length of each current lead between the calorimeter and jacket was 5 cm. Of the two 26-gage copper potential leads, one was attached to a current lead at the calorimeter boundary, the other to the remaining current lead at the jacket boundary.

Four jacket terminals pass through the jacket to "temper" thermally the heater leads (or fuse leads in the case of a benzoic acid combustion). They are the same as those described previously [9], except the electrical insulation was changed to a 0.008-in-thick layer of Teflon tape and epoxy-resin cement. The insulation resistance both from the heater element to its tube sheath and from the jacket terminals to the jacket wall is greater than 100 MΩ at 100 V.

2.2. Calorimeter Temperature Measurement Equipment

The platinum resistance thermometer is of the Meyers type of construction [10], having a 20-cm-long, 7-mm-diam Pyrex sheath, and an ice-point resistance of about 25.5 Ω. The resistance element is wound in a single coil very close to the glass sheath to provide fast response and to minimize self-heating. For these experiments the thermometer head was protected from thermal drafts by a cylindrical aluminum shield covered with asbestos and aluminum. The thermometer leads are connected to the bridge via a selector box. The thermometer was reproduceably inserted to a depth of 21 cm in the calorimeter can (height, 23 cm).

The sensitivity of the measurement of the change in resistance of the platinum resistance thermometer was increased from 10^{-5} Ω (10^{-4} °C) to 10^{-6} Ω (10^{-5} °C). This was accomplished by replacing the G–2 Mueller bridge (smallest dial unit 10^{-4} Ω) by a G–3 Mueller bridge (smallest dial unit 10^{-5} Ω) and using a more sensitive detector of the bridge imbalance.

The main features of the G–3 Mueller bridge are discussed briefly elsewhere [10]. Special shielding of the bridge and alteration of the heater supply for the bridge thermostat have been described previously [11].

Two galvanometer systems were used with the bridge. The new and more sensitive system consists of a photoelectric amplifier, having a taunt suspension galvanometer, and secondary galvanometer. A ½-mm deflection of the secondary galvanometer corresponded to a change in thermometer resistance of 1 $\mu\Omega$ (1×10^{-5} °C), with bridge current reversal and a thermometer current of 2 mA. The less sensitive galvanometer system, essentially the same as that described previously [12], but with a somewhat more sensitive galvanometer, was used to measure the thermometer resistance only during the rapid temperature rise of the main period of an electrical calibration experiment.

2.3. Ignition Energy Circuit

The electrical energy required for ignition of the benzoic acid pellet was determined by measuring the voltage before (about 25 V) and after (about 24 V) the discharge of a capacitor having a measured capacitance of $(40.6 \pm 0.5) \times 10^3$ μF. The circuit is similar to that described by Boyd [13].

The fraction of the energy released by the capacitor that is dissipated in the part of the circuit external to the calorimeter was 0.25 ± 0.10. The first step in determining this number was to measure the corrected temperature rise caused by 50 complete discharges of the capacitor, when a short was connected across the fuse electrodes in the bomb interior. The fraction of energy dissipated external to the calorimeter for this particular experiment was calculated using the known capacitance, voltages, etc. The fraction dissipated in actual combustion experiment was calculated by combining this data with the measured lead resistances and the resistances between the bomb fuse terminals in the actual combustion experiments. The main source of the estimated uncertainty in the fraction is the assumption that the combustion fuse resistance does not change before it melts.

2.4. Electrical Calibration Circuits

The basic circuit for supplying electrical power to the heater has been described elsewhere [4].

Two separate, commercially available, Zener-diode-stabilized, d-c power supplies were used to supply electrical energy to the heater. One unit, with a range of 0–2 A and 0–60 V and operated in the constant-voltage mode, was used to supply power at levels of 60 and 110 W to the heater. The other unit, having a range of 0–5 A and 0–105 V and operated either in the constant-current or constant-voltage mode, was used to supply power at 270 W. The stabilities of these power supplies in the constant voltage mode was 2 to 10 ppm as inferred from measurements of heater voltage.

The time interval during which power is supplied to the heater was measured with a time counter accurate to within ± 0.0001 s.

The heater current is determined by measuring the voltage across a Reichsanstalt-type, 0.01-Ω standard resistor.

The potential drop across the heater is determined with a 1:1000 nominal voltage divider or volt-box connected to the heater potential leads.

The resistive elements of the volt-box are: (a) a commercially available unit consisting of ten[2] equal 10,000-Ω resistors and two 1,000-Ω resistors hermetically sealed in an oil-filled box, and (b) a 100-Ω standard resistor. Permanent copper links connect the 10,000-Ω resistors in series with the parallel combination of one[3] 1,000-Ω resistor and the standard resistor. Movable shorting bars are used to connect the 10,000-Ω resistors in parallel with this combination. The bars are made from copper, have a 1-cm-square cross section, and mercury-wetted surfaces to make electrical connections.

The volt-box is calibrated by measuring the resistance of the 100–1,000-Ω parallel combination and then the resistance of all the resistors connected in parallel. In calculating the volt-box ratio, use is made of the fact that, because of the close matching of the 10,000-Ω resistors, the ratio of series to parallel resistance of the 10,000-Ω resistor set is equal to 100:1 within 1 ppm [14].

The imprecision of the volt-box ratio in 9 determinations made during the course of the electrical calibrations was 0.6 ppm (standard deviation of a single determination). This is approximately the a priori estimated precision of a measurement. The inaccuracy was estimated to be between 2 and 10 ppm.

Potential measurements were made to 0.03 μV with a six-dial double potentiometer using the more sensitive of the two galvanometer systems described in section 2.2. The range of the potentiometer extends to 0.111111 V in steps of 0.1 μV. The potentiometer voltage reference consisted of three saturated, Weston standard cells mounted in an improved version of a constant temperature box similar to one described previously [15]. Since both short- and long- (3 months) term temperature regulation of the box, as indicated by a platinum resistance thermometer in the cell compartment, was within ± 0.001 °C, the standard cell voltage could be assumed to be constant to better than 1 ppm during the course of the electrical calibrations (see sec. 5.3). The potentiometer interdial corrections were determined in the laboratory before and after the set of electrical calibration experiments. The potentiometer ratio was checked more frequently using an auxiliary circuit similar to that described elsewhere [16]. Its constancy, based on eleven determinations during the course of the electrical calibrations, was 1 ppm (standard deviation of a determination).

The resistors of the auxiliary circuit and the volt-box as well as the standard current resistor were kept in a stirred-oil bath whose temperature was kept within 0.01° of 33.16 °C. At this temperature, the rate of

[2] The relative equality and stability (1 yr) of the resistors are ± 0.0015 percent and ± 0.0005 percent, respectively.

[3] The other 1,000-Ω resistor is used only when a volt-box ratio of 1:100 is required.

change of the resistances with temperature is extremely small. Because of the constancy of the bath temperature, the resistance of the resistors could be assumed to be constant to better than 1 ppm during the electrical calibration experiments.

The resistance ratios required in the calibration of the volt-box and potentiometer were measured with the Mueller bridge described in section 2.2.

2.5. Oxygen Handling Equipment

The oxygen manifold and associated purification equipment are essentially as described by Jessup [3]. A high-purity grade of commercially available oxygen [4] was further purified for use in the benzoic acid combustions. The final oxygen pressure is measured to 0.01 atm on a calibrated Bourdon pressure gage. The temperature of the oxygen in the bomb is measured to the nearest 0.1 °C with a calibrated mercury thermometer inserted in a brass cup that fits snugly around the bomb while the bomb is being filled.

3. Tests of the Apparatus

Numerous measurements of the variation of the thermometer resistance with time during drift periods not associated with the principal calorimetric measurements showed that the imprecision of the measurements, as indicated by the average deviation of the observations from the best smooth curve drawn through the data, could be reduced to a few microohms. This was done by making resistance measurements at 1 min intervals with the bridge commutator set in alternately the N and then (i.e., next minute) in the R positions. Bridge current reversal and interpolation to 10^{-6} Ω were made in the usual manner [17]. The effect of the time variation in the lead resistance was eliminated by calculating the resistance $R(t)$, at any time t, from the observed readings, adjusted for interdial corrections, $R'(t)$, $R'(t-1)$, $R'(t+1)$ according to eq (1).

$$R(t)=\frac{R'(t-1)}{4}+\frac{R'(t)}{2}+\frac{R'(t+1)}{4}. \qquad (1)$$

Proper operation of the bridge commutator was critical in making these more precise measurements. This required replacing the mercury in the switch every three to six experiments and periodic reamalgamation of switch contacts.

Small systematic deviations of the best smooth curves drawn through the values of $R(t)$ from the resistance-time curves predicted by Newton's cooling law were observed. The shape of these deviation curves differed. A study of possible causes of the deviations was inconclusive. The changes in the calorimeter jacket, calorimeter stirrer motor, and the thermal shielding of the thermometer head, mentioned in section 2, reduced but did not completely eliminate the deviations.

The stirring of the calorimeter was varied in order to test the possible effect of variation of the heat generated by stirring as a source of deviations. Although the study of this factor was incomplete, we found no clear evidence to indicate that random fluctuations of the energy of stirring of the water might cause deviations either when the stirrer was operated intermittently or when the stirrer was turning at a constant rate. The installation of a synchronous motor to turn the calorimeter stirrer was made to insure a constant rate. We did obtain some results suggesting that actual misalinement or flutter in the stirrer shaft might be a source of deviations.

To test the applicability of Newton's cooling law over a wider range of temperature than usually occurs in a drift period (0.01 °C or less), the average rate of change of the resistance of the thermometer was measured at six calorimeter temperatures below that of the jacket, 12 to 19 resistance measurements were made at each calorimeter temperature by the procedure given above. Resistances were averaged according to eq (1). The drift rate, $\Delta R(t)/\Delta t$, corresponding to a selected thermometer resistance, $R_S(t)$, was determined from the best straight line passing through the first order differences plotted as a function of time. The number of values of $R(t)$ at each calorimeter temperature, the value of $R_S(t)$, $\Delta R(t)/\Delta t$ for the selected values of $R(t)$, and the estimated average deviation of the first order differences from the straight line are given in columns 1, 2, 3, and 4 of table 1.

TABLE 1. *Calorimeter drift rate as a function of calorimeter temperature*

No. of values of $R(t)$	$R_S(t)$	$\Delta R(t)/\Delta t$, $\Omega \times 10^6$ min^{-1}		
		"Obs"	Av. dev.	"Obs"−"Calc." [a]
10	28.00717	568.7	0.5	−0.8
17	28.06315	460.7	0.7	+0.7
13	28.11692	355.0	0.6	+0.2
11	28.16559	260.0	0.7	+0.4
15	28.21188	169.0	0.4	0.0
13	28.25985	74.7	0.5	−0.5

[a] $\left(\frac{\Delta R(t)}{\Delta t}\right)_{calc} = 1956.35\,(28.29828 - R(t))$.

It may be shown that, if Newton's cooling law holds, $\Delta R(t)/\Delta t$ should be a linear function of $R(t)$ with an error of less than 3×10^{-8} Ω min^{-1} in $\Delta R(t)/\Delta t$ for our calorimeter and resistance thermometer. The differences between the "observed" values and those calculated from a least squares fit of the data, assuming that $R(t)$ has negligible error in comparison to $\Delta R(t)/\Delta t$, are given in column 5 of table 1. The root mean square deviation, 0.5×10^{-6} Ω min^{-1}, is substantially smaller than the value of 3.3×10^{-6} Ω min^{-1} obtained previously by Jessup [18]. Some of the differences is due to the lower sensitivity of Jessup's resistance measure-

[4] Supplier's impurity analyses were 10.0, 84.0, 0.18, and 15.9 molar ppm for argon, nitrogen, water, and methane, respectively.

ment (10^{-5} Ω) and some is due to the averaging effect of eq (1).[5] In any event, the random deviations from Newton's cooling law appear to be substantially less than those obtained previously. This is consistent with an improvement in the calorimetric measurements which is discussed further in section 6.1.

A summary of the magnitudes and types of deviations from Newton's cooling law during drift periods of the calorimetric measurements themselves is given in section 5.1.

4. Experimental Procedures

4.1. Benzoic Acid Combustions

The general experimental procedure involved in a benzoic acid experiment closely follows that given by Jessup [19]. Significant differences are given below.

The benzoic acid received no special treatment prior to the experiment but was used as it came from the bottle of NBS standard sample · 39i. Pellets of 1.51 ± 0.015 g were prepared and accurately weighed after ½-hr temperature equilibration in a platinum crucible in a balance having a readability of 1 μg.

After the bomb was filled to a pressure of 30 atm of oxygen, 15 to 20 min were allowed to elapse, to ensure temperature equilibration of the bomb and oxygen, before the final pressure and temperature were read.

The temperature of the calorimeter jacket was determined by measuring the resistance of the platinum resistance thermometer to ±10 μΩ as originally described in section 3 using bridge-current reversal.

Fifteen to 20 min after the calorimeter had been heated to a temperature about 3 °C below that of the jacket, measurements of calorimeter temperature were started. The preliminary calorimeter-temperature measurements with lower sensitivity were essential to establish the values of the drift rate and the differences between the readings with the commutator in the N and R positions as a preliminary step to the much more difficult measurements to follow. After 5 to 10 min of these readings, the galvanometer sensitivity was increased to permit measurements to ±1 μΩ, and these more precise measurements were carried out for an initial period of at least 12 min.

One minute after the final resistance measurement of the initial period, the fuse was ignited by discharging the capacitor and initial and final capacitor voltages were noted. Time-temperature measurements during the rapid temperature rise of the main period were made with the thermometer current reduced from 2 mA to 0.6 mA.

After the change in thermometer resistance was less than 0.002 Ω min^{-1}, resistance measurements at one minute intervals were resumed with alternate N and R commutator positions at a sensitivity of ±10 μΩ. Measurements to ±1 μΩ sensitivity were started after the drift decreased to 0.000200 Ω min^{-1} and continued through the remainder of the main period (defined to end 20 min after ignition) and a final period of at least 12 min. The jacket temperature was then remeasured as before.

Table 2 illustrates a typical set of resistance and time measurements made during a combustion experiment. The letters N and R refer to the bridge commutator settings. Columns labeled average resistance are values of $R(t)$ calculated by eq (1) using uncorrected rather than corrected dial readings. The course of the experiment with time can be readily followed by reference to table 2 while reading the foregoing text.

TABLE 2. *Observations of time and thermometer resistance during a combustion experiment*

Time	Resistance minus 28.0		Average resistance minus 28.0	Drift
	N	*R*		
Min	*Ohms*	*Ohms*	*Ohms*	*Ohms min⁻¹ × 10⁶*
0	0.18169			
1		0.18241		
2	.18296			
3		.18368		
4	.18422			
5		.18494		
6	.185487			
7		.186196		
8	.186747		0.186785	
9		.187451	.187412	627
10	.188000		.188037	625
11		.188698	.188661	624
12	.189246		.189283	622
13		.189943	.189906	623
14	.190492		.190527	621
15		.191183	.191148	621
16	.191733		.191769	621
17		.192427	.192389	620
18	.192967		.193005	616
19		.193660	.193622	617
20	.194199		.194235	613
21		.194882	.194849	614
22	.195434		.195465	616
23		.196110	.196076	611
24	.196659		.196686	609
25		.197330		
26	Ignition			
26.2892	.20			
26.4802	.21			
26.5710	.24			
26.6511	.26			
26.7207	.28			
26.7993	.30			
26.8762	.32			
26.9740	.34			
27.0828	.36			
27.2201	.38			
27.3731	.40			
27.4658	.41			
27.5742	.42			
27.7227	.43			
27.8993	.44			
28.1146	.45			
28.2697	.455			
28.4495	.460			
28.6790	.465			
29.0040	.470			
29.1801	.472			
29.3914	.474			
29.6697	.476			
29.8461	.477			
30.0682	.478			
30.2112	.4785			
30.3543	.4790			
30.4885	.4795			
30.7058	.4800			
30.9726	.4805			
31.1630	.4808			
31.4654	.4812			
32	.48175			
33		0.46229		
34	.48241			
35		.482614		

[5] See section 5.1a.

TABLE 2. *Observations of time and thermometer resistance during a combustion experiment*—Continued

Time	Resistance minus 28.0		Average resistance minus 28.0	Drift
	N	*R*		
Min	*Ohms*	*Ohms*	*Ohms*	*Ohms min*$^{-1}$ × 10^{6}
36	.48258+			
37		.....		
38	.482684			
39		.482830		
40	.482769			
41		.482915	0.482863	
42	.482854		.482906	43
43		.483000	.482948	42
44	.482938		.482989	41
45		.483080	.483031	42
46	.483024		.483074	43
47		.483166	.483116	42
48	.483107		.483158	42
49		.483250	.483200	42
50	.483192		.483241	41
51		.483331	.483282	41
52	.483274		.483323	41
53		.483413	.483364	41
54	.483355		.483405	41
55		.483496	.483446	41
56	.483437		.483488	42
57		.483580	.483530	42
58	.483522		.483572	42
59		.483664	.483613	41
60	.483603		.483654	41
61		.483746	.483695	41
62	.483684		.483736	41
63		.483830	.483778	42
64	.483769		.483819	41
65		.483908	.483859	40
66	.483852		.483900	41
67		.483989	.483941	41
68	.483934		.483983	42
69		.484076	.484025	42
70	.484013			

4.2. Electrical Energy Measurements

Much of the experimental procedure was similar to that outlined for the chemical heat measurements in the previous section. The procedure for making the electrical calibration measurements is essentially that outlined previously [4, 2].

The combustion bomb was prepared without a pellet or platinum fuse but contained the usual platinum crucible and the usual amounts of oxygen and water.

Just prior to a run, the temperature of the standard cell enclosure was measured. The emfs at the output leads of the volt-box and the 0.01-Ω standard current resistor were measured before and after a run when no power was supplied to the heater to obtain values of the residual (thermal) emf of the circuit.

Thermometer-resistance measurements during the rapid temperature rise (i.e., while the electrical power was on) of the main period were made in the same manner as in the benzoic acid experiments. Measurements of the potentials at the output of the volt-box and across the current resistor which were 0.054 and 0.018 V, respectively, for the 110 W calibration experiments were made between temperature measurements. (The time of each potential measurement was differentiated from those of the main period temperatures by actuating the timer-printer with the standard second signal to record two times, exactly 1 s apart, which bracketed the time of the corresponding measurement.) In this way it was possible to obtain up to eight measurements of both the heater current and voltage during a 5 min heating period.

At frequent intervals during the course of the calibration experiments, the volt-box was calibrated, the potentiometer ratio was determined, and the constancy of the resistance of the 0.01-Ω standard resistor was checked.

5. Calculation of Results of Calorimetric Experiments

A series of 6 benzoic acid combustion experiments and then a series of 16 electrical calibration experiments were carried out. The electrical calibration experiments are separated into three groups depending upon whether the amount of power supplied to the calorimeter heater was approximately 110, 60, or 270 W.

5.1. Calculations of the Corrected Temperature Rise

Values of corrected temperature rises are listed for the appropriate experiments in tables 3 and 4. Observed temperature rises were of the order of 2.82 °C, and the correction due to heat transfer between the calorimeter and jacket was about 1.5 percent of this value.

a. Treatment of Initial and Final Period Data

The observed readings of the bridge during the initial and final periods, illustrated in table 2, were converted to ohms by applying the various bridge corrections and then averaging according to eq (1). Temperatures corresponding to each $R(t)$ were calculated by the Callendar equation [10]. The parameters in this equation that are characteristic of our thermometer were determined by the Temperature Section of the Heat Division, NBS.

The calorimeter temperatures, $\theta(I, J)$, for the initial ($I=0$) and the final ($I=1$) drift periods were fitted to the integral form of Newton's cooling law, eqs (2).

$$\theta(I, J) = C(I) + D(I) \cdot P(J) \tag{2a}$$

$$P(J) = (1 - e^{-KJ})K. \tag{2b}$$

In eq (2), $C(I)$ and $D(I)$ are different constants for each drift period, J is the time of occurrence of the temperature relative to the start of the appropriate drift period, and K, the cooling constant of the calorimeter, is defined by eq (3).

$$K = [D(0) - D(1)]/[C(1) - C(0)]. \tag{3}$$

A consistent fit of the temperature-time data by eqs (2) and (3) was started by estimating values of $C(I)$, $D(I)$, and K from the first and last datum points of each drift period. Calculation of "improved" values

TABLE 3. *Benzoic acid combustion calculations*

Expt. No.	Mass	$F \times 10^6$	$\Delta\theta$	$m_s(1+F)/\Delta\theta$	E^i (cont)	ΔE_{IGN}	$-\Delta E$ (HNO_3)	A^*	$\frac{E \text{ (cal)}}{(-\Delta E_H)}$
	g		°C	g °C^{-1}	J °C^{-1}	J	J	(g °C^{-1}) $\times 10^6$	g °C^{-1}
1	1.523394	−189.8	2.849658	0.5344869	+1.43	+1.49	+0.49	−27.8	0.5344591
2	1.507283	−166.7	2.819376	0.5345267	+1.79	+1.60	+0.52	−39.3	0.5344874
3	1.492242	−166.9	2.791449	0.5344869	+1.80	+0.93	+0.70	−46.0	0.5344409
4	1.493978	−160.8	2.794708	0.5344880	+1.88	+1.23	+0.58	−46.6	0.5344414
5	1.525560	−157.2	2.853627	0.5345198	+1.93	+1.21	+0.58	−46.3	0.5344705
6	1.501083	−180.8	2.807857	0.5345043	+1.57	+1.38	+0.52	−33.8	0.5344705

Average 0.5344616
Std. dev. of experiment ..... 0.0000183(0.0034%)
Std. dev. of mean ..... 0.0000075(0.0014%)

* $A = \left[\frac{\Delta E_{IGN} - \Delta E \text{ (HNO}_3\text{)}}{(+\Delta\theta)} - E^i \text{ (cont)}\right] \frac{1}{(-\Delta E_H)}$.

TABLE 4. *Calculation of the energy equivalent of the calorimeter*

Expt. No.	$\int_0^T E_1 E_1 dt$ (p^2 s) $\times 10^{+3}$	$(F_2/F_1)\int_0^T E_r^2 dt$ (p^2 s) $\times 10^{+3}$	Q_T/F_1 (p^2 s) $\times 10^{+3}$	Q_c J	$\Delta\theta$ °C	$-E^i$ (cont) J °C^{-1}	E (cal) J °C^{-1}
Heater power 110 W							
7	3550.0634	1.1258	0.0377	38,955.397	2.757342	0.30	14,128.18
8	3559.4812	1.1288	.0377	39,058.739	2.764372	0.32	14,129.66
9	3615.7432	1.1467	.0378	39,676.104	2.808623	0.39	14,126.92
10	3605.5325	1.1434	.0378	39,564.063	2.800523	0.02	14,127.40
11	3585.7557	1.1372	.0378	39,347.050	2.785424	0.20	14,126.25
12	3591.6315	1.1390	.0378	39,411.526	2.789739	0.16	14,127.48
13	3578.4748	1.1348	.0378	39,267.158	2.779515	0.16	14,127.50
14	3591.6153	1.1390	.0378	39,411.348	2.789528	0.14	14,128.46
15	3588.6870	1.1381	.0378	39,379.216	2.787293	0.14	14,128.26
Heater power 60 W							
16	3575.0618	1.1342	0.0069	39,229.362	2.776922	0.07	14,126.99
17	3573.4132	1.1337	.0070	39,211.273	2.775357	0.07	14,128.44
Heater power 270 W							
18*	3582.3213	1.1348	7.3177	39,389.320	2.788869	0.13	14,123.89
19*	3548.3917	1.1240	7.3241	39,017.047	2.762050	0.13	14,126.25
20*	3506.1535	1.1107	7.2380	38,552.619	2.729664	0.16	14,123.74
21*	3588.2289	1.1368	7.2382	39,453.237	2.792813	0.16	14,126.86
22	3612.1828	1.1440	0.0208	39,636.866	2.805518	0.19	14,128.36

*Constant current mode of power supply; all others constant voltage mode.

of these constants proceeded by computing the deviations, $F(I, J)$, of the "observed" temperatures from those calculated by eq (2) using the initial estimates of $C(I)$, $D(I)$, and K. These deviations were fitted by least squares with deviation equations linear in $P(J)$ according to eq (4).

$$F(I, J) = B(0, I) + B(1, I)P(J). \quad (4)$$

The values of $B(0, I)$ and $B(1, I)$ were used to correct the initial estimates of $C(I)$, $D(I)$, and K. The cycle of calculations, performed by a high speed digital computer, was repeated until either the sum of the squares of the deviations of the initial and final drift periods increased or the values of K calculated on two successive cycles differed less[6] than 1×10^{-7} min^{-1}

The observed temperature rise was computed from the calculated values of initial and final temperatures using eqs (2) and the final values of $C(I)$, $D(I)$, and K.

This method of curve fitting assumes the values of $\theta(I, J)$ of each drift period are independent which cannot be so since the temperatures are calculated from observed resistances which were averaged according to eq (1).

It can be shown that, because of the use of eq (1), runs or deviations of the same sign should occur when the difference between "observed" and calculated temperatures are plotted as a function of time even though the errors are random. Usually, runs of three to five deviations of the same sign were observed. This indicates that in the case of random errors, those in the resistance measurements predominate. The systematic errors in the values of "observed" temperature and the calculated temperatures caused by using eq (1) are negligible.

Although the deviation plots sometimes showed systematic deviations from Newton's cooling law, they

[6] The latter "stop" was inserted because there is no assurance of a distinct minimum in the sum of the squares of the deviations. It was, in fact, the terminating step of all the calculations after two or three iterations. The value of 1×10^{-7} min^{-1} is based on the fact that the jacket temperature was constant to only about 1×10^{-4} °C, and K is approximately 2×10^{-3} min^{-1}.

were small. The average root mean square deviation of "observed" from calculated values of $\theta(I, J)$ was slightly less than 2×10^{-5} °C.

b. Treatment of Main Period Data

The correction to be added to the observed temperature rise due to heat transfer from the jacket and stirring energy is calculated according to a method discussed by Dickinson (see [20, 4]). In this method, the main period data is used to evaluate the parameter t_x, defined by eq (5), and the remaining parameters are determined from the values of $C(I)$, $D(I)$, and K determined from the drift period data in section 5.1a.

$$t_x = t_f - \frac{1}{(\theta_f - \theta_i)} \int_{t_i}^{t_f} (\theta - \theta_i) dt. \tag{5}$$

In eq (5), θ_i and θ_j are the temperatures at the beginning, t_i, and end, t_f, of the main period, respectively.

To keep the error in the calculation of the correction to the observed temperature rise to 1×10^{-5} °C in our experiments, t_x must be calculated to 0.1 s and the integral in eq (5) must be calculated with an accuracy of 1 part in 10,000. The following two procedures were adopted to minimize the calculation error.

First, the temperature-time data were graphed to eliminate gross errors and fill in gaps where data was sparse by superimposing corresponding portions of the main period of similar experiments.

Second, because eq (5) may be rewritten with an integral whose integrand is independent of temperature, temperatures of the main period were calculated in the same manner. Since virtually all the resistance measurements during the rapid temperature rise were made with fixed commutator position, the formula for the estimated correction for thermometer lead resistance applied to these readings was used throughout the main period. Thus, although the method of calculation of temperatures was in other respects the same as that for the initial and final periods, θ_i and θ_f in eq (5) are not quite the same as those used in calculating the observed temperature rise. We assumed the thermometer lead resistance correction varied linearly with the thermometer resistance in the main period from the average initial to the average final drift correction. Since the difference between these corrections was about 15 $\mu\Omega$ for all the experiments, the net effect of an error in the assumption is negligible in comparison to other errors in the treatment of the data of the main period.

The integral in eq (5) was evaluated using the spline numerical integration procedure whose characteristics are described in detail elsewhere [21]. Essentially, the method fits a piecewise cubic with continuous first and second derivatives to the data. Calculations were carried out with a high speed computer using a program written in the Dartmouth BASIC language [22]. This program was based on a subroutine originally written in FORTRAN [23].

5.2 Benzoic Acid Combustion Calculations

Since benzoic acid is certified as a secondary heat standard for use in determining the energy equivalent of bomb calorimeters, it is convenient to express its energy of combustion per unit mass of benzoic acid under so-called standard bomb-conditions [4]. Determination of the energy of combustion of benzoic acid under standard bomb conditions, ΔE_B, is carried out in two steps, the first of which is summarized in this section.

In order to compare the benzoic acid combustion data with the electrical calibration data, we defined the standard calorimeter to be the calorimeter can containing sufficient water so that their combined weight is 3750 g, the calorimeter lid, the electrical heater, and the combustion bomb with its standard contents, its external fuse leads and its handle. The standard bomb contents were defined to be 1 g of water, the platinum crucible, platinum fuse, and 0.441 moles of oxygen (30 atm at 25 °C).

By selecting the temperature to which the isothermal bomb process is referred to be the final temperature the calorimeter would have if the heat transfer from the calorimeter environment and stirring energy were zero, the ratio of the energy equivalent of the standard calorimeter, E(cal), in joules per degree, to ΔE_B, in joules per gram, can be calculated from the experimental results by eq (6) (see [20], [5]).

$$\frac{E\,(\text{cal})}{-\Delta E_B} = \frac{(1+F)m_s}{\Delta\theta} + \left[\frac{\Delta E_{\text{IGN}} - \Delta E_{\text{HNO}_3}}{(\Delta\theta)} - E^i\,(\text{cont})\right] \frac{1}{(-\Delta E_B)}. \tag{6}$$

In eq (6), $\Delta\theta$ is the corrected temperature rise, m_s is the mass (i.e., weight in vacuo) of benzoic acid in grams, ΔE_{IGN} is the electrical energy supplied to the calorimeter to ignite the benzoic acid, ΔE_{HNO_3} is the energy of formation of nitric acid produced in the actual combustion reaction, and E^i (cont) is the correction added to E(cal) to give the energy equivalent of the actual calorimeter prior to sample combustion. The quantity F is related to the energy of combustion, $\Delta E_B'$, per gram of benzoic acid under actual bomb conditions by eq (7).

$$\Delta E_B' = (1+F)\Delta E_B \tag{7}$$

Numerical values of F were calculated from the approximate formula given by Coops, Jessup, and Van Nes [4].

Since the second term on the right-hand side of eq (6) constitutes only a small contribution to the total, an approximate value of ΔE_B may be used in this term. For this we used $-26{,}434$ J g^{-1}. An error of 10 J g^{-1} in this value of ΔE_B would produce an error of only 1 ppm in $-E(\text{cal})/\Delta E_B$.

A summary of the calculations is given in table 3. In calculating F (col. 3), the pressure of oxygen at θ_h was calculated from observed pressures using the equation of state for oxygen given by Coops, Jessup, and Van Nes [4]. E^i(cont), listed in column 5, was evaluated using 1.21 J g^{-1} $°C^{-1}$ [4] for the heat capacity of benzoic acid and a value of 21.17 J mol^{-1}[20] for the constant volume heat capacity of oxygen at 30 atm. Measurement of ΔE_{IGN} is summarized in section 2.3 and the determination of $\Delta E(HNO_3)$ was made in the usual manner [4].

More accurate values of F were calculated by evaluation of the Washburn correction by the procedure described by Hubbard, Scott, and Waddington [20] using the computer program developed by Shomate [24]. A very slight difference was observed in the F values, for which a correction is made in the calculation of $(-\Delta E_B)$ at the bottom of table 5. (The dispersion of the values of $E(\text{cal})/(-\Delta E_B)$ was not altered significantly.)

5.3. Electrical Calibration Calculations

The energy equivalent of the calorimeter, $E(\text{cal})$, is related to the total electrical energy, Q_e, supplied to the calorimeter during a calibration experiment, by eq (8)

$$Q_e = [E(\text{cal}) + E^i(\text{cont})]\Delta\theta. \tag{8}$$

In eq (8), $\Delta\theta$ is the corresponding corrected temperature rise and E^i(cont) was defined in section 5. Q_e was evaluated by eq (9)

$$Q_e = F_1 \int_0^T E_V E_I dt - F_2 \int_0^T E_I^2 dt + Q_T. \tag{9}$$

In eq (9) the various terms on the right are, respectively, the energy calculated from the potentiometer measurements, the correction for current passing through the volt-box, and correction for transients (i.e., any voltages not measured with the potentiometer). E_V and E_I are the observed dial readings of the potentiometer at the output of the volt-box and across the current resistor, respectively after applying interdial and "zero" corrections. T is the length of time power is supplied to the heater. F_1 and F_2 are constants which depend upon the volt-box ratio, resistance of the current resistor, the standard cell voltage, and the calibration of the potentiometer.

The numerical values of the terms on the right of eq (9) divided by F_1 are given in the first three columns of table 4. The unit p in these tables stands for a "potentiometer unit" and is nominally 1 V. The values of Q_e, $\Delta\theta$, E^i(cont), and E(cal) are listed in the remaining columns of table 4.

Because of the constancy of the volt-box and potentiometer ratios and the inferred constancy of the standard current resistor and standard cell voltage to 1 ppm or better, F_1 and F_2 were assumed to be constants. This assumption causes negligible imprecision in E(cal) as compared to that from other sources. The numerical values of F_1 and F_2 are 1.09765196 $V^2\Omega^{-1}p^2$ and 1.099975×10^{-4}, respectively.

The standard cell voltage was determined by the NBS Electrochemistry Section of the Electricity Division by comparison with the NBS voltage standard. A correction of 1.4 microvolts [25] was added to this calibrated value since the average temperature of the cells during our measurements was 0.024 °C less than at the time the cells were calibrated.

The resistance of the standard current resistor was based on its certified resistance at 25 °C and the temperature coefficient of its resistance as determined by the supplier. The maximum error in this calculated value of resistance at the oil bath temperature (33.16 °C), as determined by ten potentiometric comparisons during the electrical calibration experiments of its resistance with that of a standard 0.1 Ω resistor calibrated by the NBS Resistance and Reactance Section, was found to be 0.002 percent or less. After our measurements were completed, a more accurate value for the resistance was determined by the NBS Resistance and Reactance Section. The corresponding correction to the data was made in the final calculation of $(-\Delta E_B)$ in table 5.

The first potentiometer measurements were made some 10 to 25 s after power was applied to the calorimeter heater. A total of 6, 13, and 2 measurements of E_V or E_I were made for the 110, 60, and 270 W experiments, respectively. Smoothed values of E_V and E_I were obtained from separate plots of the observed values as a function of time; the time dependence, more or less unknown, of the 270 W measurements had to be inferred from other considerations [26]. Values of the integrals in eq (9) were computed with the spline integration subroutine of the computer program used in the calculation of the integral in eq (5).

After the electrical calibrations were completed it was found that large voltage transients occur when the power source supplying 270 W to the calorimeter heater in the constant current mode is switched from the dummy heater to the calibration circuit. These transients had disappeared well before the first measurements of E_V and E_I were made with the potentiometer. Subsequent examination of the voltage-time characteristics of this power source in the constant voltage mode and of the power source used to supply 110 and 60 W to the calorimeter heater in the constant voltage mode also indicated the presence of transients, but these were much smaller.

Numerical values of the energy supplied to the calorimeter by these transients are based on separate determinations of the transient voltage-time curves, as observed on an oscilloscope, for the power supplies operated in the appropriate mode of operation. Corrections to account for the slightly different average values of power supplied to the heater in the actual electrical calibrations were made assuming the length of time required to switch the power supply from the dummy to the calorimeter heater was constant.

TABLE 5. *Summary of calculation of* $(-\Delta E_B)$

Expt. No.	Number of expts.	Heater power	Average E(cal), J °C^{-1}	Standard deviation of an experiment, J °C^{-1}	Standard deviation of average, J °C^{-1}	95% confidence limits J °C^{-1}
7–15	9	110 W (constant voltage	14,127.79	0.99 (0.007%)	0.33	0.76
16–17	2	60 W (constant voltage)	14,127.72	0.99	0.73	1.60
18–21	4	270 W (constant current)	14,125.19	1.6	0.80	2.55
22	1	300 W (constant voltage)	14,128.36	.....	.....	.....
Adopted value			14,127.79	0.99 (0.007%)	0.30	0.68

Summary of benzoic acid combustions

Expt. No.	Number of expts.	Average	E(cal)/$(-\Delta E_B)$, g °C^{-1}	Standard deviation of an experiment, g °C^{-1}	Standard deviation of average, g °C^{-1}	95% confidence limits g °C^{-1}
1–6	6	.....	0.534461.6	(0.0034%)	0.0000075	0.0000193

Calculation of $-\Delta E_B$

Nominal $(-\Delta E_B)$	26,433.69 J g^{-1}
Correction for $R_{a,01}$	+0.21 J g^{-1}
Correction for F	+.15 J g^{-1}
Corrected $(-\Delta E_B)$ =	26,434.05 J g^{-1}
with an uncertainty interval (random) of	1.7 J g^{-1}

5.4. Summary of results

The calculations of the energy equivalent of the calorimeter are summarized at the top of table 5. Ninety-five percent confidence limits are calculated by multiplying the standard deviation of the mean by the appropriate factor of the Student t-distribution. Assuming equal precision, standard deviations computed for experiments 7–15 and for 16–17 are pooled together. Comparison of the average values of E(cal) listed in table 5 for the three heater powers used in experiments 7 through 21 show they lie within their combined uncertainty (random) intervals. However, the results of experiments 18–22 were not used in computing a weighted average for E(cal) for the following two reasons.

First, it will be noted from columns 2 and 4 of table 4 that the contribution of Q_T to E(cal) is 0.2 percent in the case of experiments 18–21. For the other experiments, the power supplies were operated in the constant voltage mode and the contribution of Q_T to E(cal) is less than 0.0012 percent. Since we feel that a systematic error in the estimate of Q_T of 20 percent is not unreasonable, the difference between the average E(cal) of experiments 18–21 and the remainder is probably caused by a systematic error due at least in part to the error in Q_T.

Second, it will be noted that experiments 18–22 were carried out with the highest heater power and, thus, the shortest time necessary to warm the calorimeter 3 °C. This resulted in the unfortunate situation that we were able to make only a few measurements of heater current or voltage when the change in voltage, or current, was the most rapid. We feel the uncertainty introduced in E(cal) by the uncertainty in our estimates of the time dependence of the voltage, or current may be appreciable. Thus, the agreement of experiment 22 with 7–17 is regarded as being somewhat fortuitous. Experiment 22 was given zero weight on the basis that we suspect its uncertainty is considerable larger than experiments 7–17.

The results of the benzoic acid combustions and the value determined for ΔE_B for benzoic acid are summarized at the bottom of the table 5. The precision of ΔE_B was calculated as suggested by Rossini [27]; the contribution of the imprecision due to the various factors taken as constants in determining E (cal) was neglected since it was estimated to be 10 ppm.

6. Appraisal of Experimental Results

6.1. Random Errors

The standard deviation of a single combustion experiment with this particular calorimeter had never before been lower than 0.012 percent, for an extended series of measurements. It is clear from table 5 that the precision of the present measurements is substantially better than the previous work.

We were particularly interested to see whether or not we could account for the standard deviation of a measurement of either $-E$(cal)/ΔE_B or E(cal) in terms of the various factors we might expect to vary from experiment to experiment.

Common to both sets of measurements were the uncertainty in the corrected temperature rise and the absence of a buoyancy correction to the weight of the water placed in the calorimeter can.

The uncertainty in the corrected temperature rise was evaluated from the variances of the estimates of the various parameters appearing in eqs (2) and (3), using the usual propagation of error formulas [27] and assuming that the "average" root mean square deviation of $\theta(t)$ for the initial and final drift periods

may be treated as a random error. These "averages" were arbitrarily multiplied by $\sqrt{2}$ since they are probably too small due to the use of eq (1) (see sec. 5.1a). The error in the integral in eq (5) was based on the approximations that the main error is contributed by the errors in the times recorded during the rapid temperature rise of the main period and that the integral may be computed by the trapezoidal rule.

The uncertainty due to the absence of the buoyancy correction in the calorimeter weight was estimated from the known variation in air density during the benzoic and experiments (12 mg/l [7]) and the approximate volume of the calorimeter can plus water (2.59 l). The resulting percentage error was arbitrarily multiplied by two because it is quite evident from the method used to adjust the weight of water in the can (see [3]) that the aforementioned variation in air density is a minimum estimate. Other factors, such as convection currents, may also make a substantial contribution to the weighing error.

The random error in $E(\text{cal})/\Delta E_B$ due to the uncertainty of the mass of the benzoic acid sample is based on a conservative estimate of ± 10 μg for a sample weight of 1.5 g.

The estimates of the varous errors contributed by the parameters which make up F_1 are based on the deviations of their measurements. The standard current resistor, $R_{0.01}$, was assumed to have a stability of 2 ppm.

The estimate of the random error in E(cal) due to the random error in the integrals in eq (9) was based on the approximation that 13 smoothed pairs of values of E_V and E_I separated by 30 s time intervals were numerically integrated by the trapezoidal rule. The errors in the smoothed values of E_V and E_I were taken as $\pm 2 \times 10^{-7}$ potentiometer units.

The estimate of the random error due to the heater leads is based on the analysis given by Ginnings and West [28]. The dimensionless parameters L_s and L_c of that analysis were calculated to be 0.34 and 0.28, respectively. The variation in the heater lead resistance was estimated to be ± 0.002 Ω; the heater resistance is 32 Ω.

A summary of the errors and a comparison with the observed standard deviation of an experiment is given in table 6. The discrepancy between the observed and estimated values for the electrical calibrations is probably greater than the uncertainty of our estimates.

6.2. Systematic Errors

One of the main assumptions customarily made in using a stirred-water "isoperibol" calorimeter is that the correction to the temperature rise due to heat transfer from the calorimeter jacket and heat delivered by the stirrer can be computed from Newton's cooling law and temperatures measured inside the calorimeter.

It is generally understood that this assumption would be valid if the calorimeter temperature were strictly uniform throughout the calorimeter.[8] Real calorimeters have, of course, temperature gradients or, equivalently, temperature differences due to the effects of lags. Thus, the surface temperature of the calorimeter, which determines the rate of heat transfer between the calorimeter and jacket, is in general different from that measured by the thermometer, even though it is placed as close to the calorimeter wall as is practical.

The effect of a temperature gradient on calorimetric measurements has been analyzed to some extent for "isoperibol" calorimeters [29, 30, 31], and in detail for aneroid adiabatic calorimeters [32]. Harper [29] has shown that if the lag of the temperature measurement system (i.e., including both thermometer and electrical detecting system) is the same throughout a calorimeter experiment then the lag causes no error in the corrected temperature rise. White [30], in effect, considers the temperature gradient to be the superposition of those due to (1) heat transfer from the jacket and stirring, and (2) heat released in the calorimeter during the main period. By an argument identical to that used by Harper, he showed that the lag due to the first of these sources causes no error in the corrected temperature rise, while the lag due to the second source will cause an error. However, if the latter lag is a constant which is independent of the source of heat (i.e., electrical heater or combustion bomb), then it will cause no error in the heat of combustion of benzoic acid. White felt that the constancy of the lag due to different heat sources could be verified by appropriate experiments.

[7] Square root of the sum of squares of the deviations divided by the number of measurements minus one.

[8] Convective heat transfer between the calorimeter and jacket must also be negligible. For this discussion, we assume this is so.

TABLE 6. *Estimated random errors in* $-\text{E}(cal)/(-\Delta\text{E}_\text{B})$ *and* $\text{E}(cal)$

	Benzoic acid $(-E\ (\text{cal})/\Delta E_B)$	Electrical calibrations $(-E\ (\text{cal}))$
	%	%
Corrected temperature rise	0.0022	0.0019
Bouyancy correction	0.0018	0.0018
Mass of benzoic acid	0.0007	.....
$\int_0^7 E_V E_I dt$	.....	0.0003
k/E'_{sc}	.....	0.0001
E_{sc}	.....	0.0001
$R_{0.01}$	.....	0.0002
Volt box ratio	.....	0.0001
Heater leads	.....	0.0005
Estimated standard deviation of a measurement	0.0030	0.0027
Observed standard deviation of a measurement	0.0034	0.0070

TABLE 7. *Summary of values of* $(-\Delta E_B)$ *for benzoic acid*

Author	Sample	Value	Uncertainty
		$J\,g^{-1}$	$J\,g^{-1}$
Jessup and Green [2, 18, 33] (1934)	39d, 39e	26,432.0	±2.6
Prosen and Rossini [35] (1939–41)	39e	26,434.7	±2.2
Jessup [2, 33] (1942)	39e, 39f, B	26,433.8	±2.6
Coops et al. [31] (1946–8)	39b, 39f, VUS	26,438.0	±4
Coops et al. [31] (1954)	39b, VUS	26,435.0	±4
Challoner et al. [34] (1954)	C	26,436.0	±4
This work (1966)	39i	26,434.0	±3.3

Coops et al. [31], have suggested one method of making the lag due to different heat sources the same and have incorporated this in the design of their calorimeter.

An experimental test that has frequently been applied is that the lag is a constant if it can be shown that the energy equivalent of the calorimeter is invariant with the power supplied to the electrical heater. This criterion has been shown to be incorrect by West [32] for a calorimeter in which heat flow equations are linear. It is interesting to note that part of this argument depends upon showing that the contributions to the correction on the observed temperature rise of the temperature transients due to turning the electrical heater on and off exactly cancel. Indirect evidence that this cancellation is the case for our calorimeter is given in section 7. This conformity of our calorimeter with West's analysis of behavior of transients suggests that the remainder of West's argument may be applicable to the Dickinson calorimeter. The invariance of the energy equivalent found in the electrical experiments with varying electrical power (see table 5), thus, does not provide information about possible systematic errors.

A series of tests was carried out to see whether or not measurements based on the average surface temperature of the calorimeter in place of that registered by the platinum thermometer would give a different value of ΔE_B for benzoic acid. On the basis of these tests, which must be considered to be preliminary in nature, it was found that there is a difference between the temperatures of the calorimater surface and the water in the vicinity of the resistance thermometer and that this difference varies with time in the electrical calibrations in a different way than in the benzoic acid experiments. Because of certain experimental difficulties, we assigned an uncertainty to the difference in values of ΔE_B calculated from these observations that was about the same as the magnitude of the difference. Until a more reliable estimate based on more accurate tests is obtained, we have somewhat arbitrarily assigned an uncertainty of ± 0.01 percent of ΔE_B to take into account the possible correction for the effect of surface temperature.

The net contribution of other sources of systematic errors in the electrical calibrations is estimated to be at most ± 0.004 percent of ΔE_B.

6.3. Discussion of Results

In table 7, we have listed the more recent determinations of $(-\Delta E_B)$ for benzoic acid in joules per gram of sample.[9] Samples indicated by the number 39 followed by a letter refer to batches of the benzoic acid standard sample issued by NBS. B refers to a sample of 39e purified by fractional crystallization from benzene. VUS and C refer to benzoic acid samples from sources other than NBS and are described in the corresponding references.

Uncertainty intervals listed in table 7 are those cited by the authors except for the work of Jessup and Green [2, 18, 33] which we assumed to be equal to the later work of Jessup [2]. The bounds for the uncertainty interval for our own work was computed by the procedure recommended by Rossini [27] as $\sqrt{(1.7)^2+(1.1)^2+(2.6)^2}$.

Aside from our own work, only that of Challoner, Gundry, and Meetham [34] incorporates an uncertainty due to the effect of surface temperature. In the latter, a correction of -0.046 ± 0.0057 percent had to be applied to the energy equivalent of the calorimeter to correct for the difference in surface temperature effects during the main period of an electrical calibration and a benzoic acid combustion experiment. Our preliminary experiments suggest that the magnitude of the surface temperature correction is not insignificant for our results although it is smaller than that of Challoner et al. A substantial contribution to the uncertainty of our results has been allowed because of the unknown magnitude of our surface temperature correction. It would be preferable, in spite of the difficulty of measuring it, to evaluate the correction experimentally in absolute calorimetric measurements unless the calorimeter has been specifically designed to eliminate the error.

[9] We have been informed by private communication from Mosselman and Dekker [36], and from Head [37], of very recent electrical determinations of the energy of combustion of benzoic acid in their respective laboratories. These determinations are both based on measurements made in calorimeters containing water flow channels of the type devised by Coops et al. [31], and both are reported to be in excellent agreement with the value we list for this work in table 7. The work of Mosselman and Dekker includes some measurements on NBS Standard Sample 39i.

7. Appendix. Analysis of Main Period of the Electrical Calibration Experiments

If the temperature transients due to turning the electrical heater on and off make no net contribution to the corrected temperature rise, the two areas between the main period curves of the electrical calibrations and the straight lines given by eqs (10a), (10b), and (10c) should be equal since the heater power does not vary with time.

$$\theta(t)=\theta_i+(d\theta/dt)_i(t-t_i); \qquad t_i\leq t\leq t_1 \qquad (10a)$$

$$\theta(t)=\theta_3+(d\theta/dt)_3(t-t_3); \qquad t_1\leq t\leq t_2+t_b \qquad (10b)$$

$$\theta(t)=\theta_f+(d\theta/dt)_f(t_f-t); \qquad t_2+t_b\leq t\leq t_f. \qquad (10c)$$

Equations (10a) and (10c) are linear extrapolations of the initial and final drift period curves into the main period, and the constants θ_3, t_3 and $\left(\frac{d\theta}{dt}\right)_3$ of eq (10b) are determined from a linear least squares fit of the main period data during the rapid temperature rise. The times t_1 and t_2+t_b are the times of intersections of eq (10b) with eq (10a) and (10c).

To test whether or not the areas are equal, we noted that if they are, then the time t_1 should be approximately equal to time[10] t_b and both should be independent of the power supplied to the heater or $(d\theta/dt)_3$. Comparison of columns 3 through 5 of table 8 shows this is very nearly true. Further, the equality of the areas means that the integral in eq (5) for t_x is the area enclosed by the lines of eqs (10a) through (10c) and θ_i. Corrected temperature rises computed using values t_f-t_x determined in this manner differed by less than one part in 10^5 from those listed in section 5. The latter are based on values of t_f-t_x determined by the more accurate spline integration procedure.

TABLE 8. *Average main period characteristics, electrical calibration*

Heater power watts	No. of Expts.	t_1 min	t_b min	$(d\theta/dt)_3$ °C min^{-1}	t_2 min	t_{max} min
60	2	0.238	0.224	0.252	11.2	12.5–13
110	9	0.242	0.235	0.480	5.8	8.5
270	5	0.230	0.254	1.15	2.5	4–5.5

8. References

[1] Dickinson, H. C., Bull. BS **11**, 189 (1914).
[2] Jessup, R. S., J. Res. NBS **29**, 247 (1942) RP1490.
[3] Jessup, R. S., NBS Monograph 7, February 26, 1960.
[4] Coops, J., Jessup, R. S., and Van Nes, K., Calibrations of Calorimeters for Reactions in a Bomb at Constant Volume, ch. 3, Experimental Thermochemistry, Vol. **1**, F. D. Rossini, Editor (Interscience Publishers, Inc., New York, N.Y., 1956).
[5] Prosen, E. J. Compounds Containing Carbon, Hydrogen, Oxygen, and Nitrogen, ch. 6, Experimental Thermochemistry, Vol. **1**, F. D. Rossini, Editor (Interscience Publishers, Inc., New York, N.Y., 1956).
[6] Jessup, R. S., ibid, figures 1a, 1b, and Appendix 7.1e.
[7] Jessup, R. S., ibid., Appendix 7.1d.
[8] Domalski, E. S., and Armstrong, G. T., J. Res. NBS **69A** (Phys. and Chem.), No. 2, 137 (1965).
[9] Jessup, R. S., ibid., p. 20, figure 1c.
[10] Stimson, H. F., Precision Resistance Thermometry and Fixed Points, ch. 9, Temperature, Its Measurement and Control in Science and Industry, Vol. **II**, H. C. Wolfe, Editor, American Institute of Physics (Reinhold Publishing Corp., New York, 1955).
[11] Armstrong, G. T., Wong, P. K., and Kreiger, L. A., Rev. Sci. Instr. **30**, 339–343 (1959).
[12] Jessup, R. S., ibid., Appendix 7.1c.
[13] Boyd, R. H., Rev. Sci. Instr. **35**, 1086, 1964.
[14] Pailthrope, R. M., and Riley, J. C., An Improved Technique for Establishing Resistance Ratios, ESI Bulletin No. 35 (Electro Scientific Industries, Portland, Oreg., November 1962).
[15] Mueller, E. F. and Stimson, H. F., J. Res. NBS **13**, 699 (1934), RP739.
[16] Osborne, N. S., Stimson, H. F., Ginnings, D. C., J. Res. NBS **23**, 197, 261 (1939), RP1228.
[17] Jessup, R. S., ibid, p. 7.
[18] Jessup, R. S. and Green, C. B., J. Res. NBS **13**, 469 (1934), RP721.
[19] Jessup, R. S., NBS Monograph 7, Sec. 3.2 and 4.
[20] Hubbard, W. N., Scott, D. W., and Waddington, G., Standard States and Corrections for Combustions in a Bomb at Constant Volume, ch. 5, Experimental Thermochemistry, Vol. **I**, F. D. Rossini, Editor (Interscience Publishers, Inc., New York, N.Y., 1956).
[21] Walsh, J. H., Ahlberg, J. H., and Nilson, E. H., J. Math. and Mech. **11**, (No. 2), 225 (1962).
[22] Darmouth Basic Library, Code: Spline, Converted to Basic Language by Messina, C., NBS, September (1965).
[23] Katsanis, T., NASA Technical Note, D-2546, December (1964).
[24] Shomate, C. H., Fortran IV Computer Program for Reduction of Heat of Combustion Calorimetric Data, Code 5052 (U.S. Naval Ordnance Test Station, China Lake, California, January 1967).
[25] Hamer, W. J., NBS Monograph 84, January 15, 1965.
[26] Ginnings, D. C., West, E. D., Principles of Calorimetric Design, ch. 4, Experimental Thermodynamics, Vol. **I**, Calorimetry of Non Reacting Systems, J. P. McCullough, Editor (Butterworth and Co., Ltd., In press).
[27] Rossini, F. D., Assignment of Uncertainties to Thermochemical Data, ch. 14, Experimental Thermochemistry, Vol. **I**, F. D. Rossini, Editor (Interscience Publishers, Inc., New York, N.Y., 1956).
[28] Ginnings, D. C., West, E. D., Rev. Sci. Instr. **35**, 965 (1964).
[29] Harper, D. R., J. Res. NBS **8**, 659 (1912).
[30] White, W. P., The Modern Calorimeter (Reinhold Publishing Corp., New York, 1928), p. 89, p. 36. See also J. Am. Chem. Soc. **40**, 1861–1863, 1918 and Phys. Rev. **31**, 568–570, 1910.
[31] Coops, J., Adriaanse, N., Van Nes, K., Rec. Trav. Chim. **75**, 237 (1956).
[32] West, E. D., J. Res. NBS **67A** (Phys. and Chem.), No. 4, 331 (1963).
[33] Jessup, R. S., J. Res. NBS **36**, 421 (1946), RP1711.
[34] Challoner, A. R., Gundry, H. A., Meetham, A. R., Phil. Trans. Roy. Soc. (London), **A247**, 553 (1955).
[35] Prosen, E. J. and Rossini, F. D., J. Res. NBS **33**, 439 (1944), RP1619.
[36] Mosselman, C., and Dekker, H., The Free University, Amsterdam, Private Communication.
[37] Head, A. J., Natl. Physical Laboratory, Teddington, private communication.

[10] We assume the transient can be represented by a single exponential.

JOURNAL OF RESEARCH of the National Bureau of Standards—A. Physics and Chemistry
Vol. 72A, No. 2, March–April 1968

Constant Pressure Flame Calorimetry With Fluorine
II. The Heat of Formation of Oxygen Difluoride*

Reatha C. King and George T. Armstrong

Institute for Basic Standards, National Bureau of Standards, Washington, D.C. 20234

(December 27, 1967)

The heats of the following reactions were measured directly in an electrically calibrated flame calorimeter operated at one atm pressure and 303 °K.

$$OF_2(g) + 2H_2(g) + 99H_2O(l) \rightarrow 2[HF \cdot 50H_2O](l)$$

$$F_2(g) + H_2(g) + 100H_2O(l) \rightarrow 2[HF \cdot 50H_2O](l)$$

$$\tfrac{1}{2}\ O_2(g) + H_2(g) \rightarrow H_2O(l)$$

The reactants and products were analyzed for each of the reactions. From these heats we calculated the corresponding heats of formation, as follows:

$OF_2(g)$ $\Delta H^\circ_{f298.15} = +24.52 \pm 1.59$ kJ mol^{-1} ($+5.86 \pm 0.38$ kcal mol^{-1})
$HF \cdot 50H_2O(l)$ $\Delta H^\circ_{f298.15} = -320.83 \pm 0.38$ kJ mol^{-1} (-76.68 ± 0.09 kcal mol^{-1})
$H_2O(l)$ $\Delta H^\circ_{f298.15} = -285.85 \pm 0.33$ kJ mol^{-1} (-68.32 ± 0.08 kcal mol^{-1})

The uncertainties indicated are the estimates of the overall experimental errors. The value of the average O—F bond energy in OF_2 was calculated to be 191.29 kJ mol^{-1} (45.72 kcal mol^{-1}).

Key Words: Bond energy (O—F), flame calorimetry, flow calorimetry, fluorine, heat of formation, heat of reaction, hydrogen fluoride (aqueous), oxygen, oxygen difluoride, reaction calorimetry, water.

1. Introduction

Thermochemical data for the fluorine oxidizers are very important for their present-day applications. This group of oxidizers includes elemental fluorine, and its compounds such as OF_2, ClF_3, ClF_5, and BrF_3. These substances are typically very reactive and combine with most other elements and compounds, yielding large heats of reaction and in many cases the highest valence state of the oxidized element. Two important uses of these oxidizers are for the production of fluorides, and as possible ingredients in rocket propellants and explosive systems. Because of their reactivity, they make possible chemical reactions which have not been investigated, e.g., reactions at extremely low temperatures.

Until a few years ago, very few thermochemical studies involving these materials had been conducted. This lack of work was caused mainly by the nonexistence of corrosion-resistant construction materials and the unavailability of sufficiently pure samples the fluorides. In recent years several of the problems hindering earlier research have been solved, and precise calorimetry has been demonstrated to be possible.

For measuring heats of reactions of the fluorine oxidizers, a new flame calorimetric apparatus has been set up in this laboratory. An earlier version of this apparatus has already been described [1, 2].[1] An investigation of the heat of formation of oxygen difluoride is the first study carried out with the new apparatus and is described in this presentation.

For many years there has been interest in the heat of formation of oxygen difluoride. In 1930, von Wartenberg and Klinkott [3], and Ruff and Menzel [4], reported two different thermochemical studies on this compound. In various reviews of thermochemical properties [5–8], the data from these studies have been reevaluated repeatedly in attempts to derive a selected "best" value for the heat of formation of this compound. For some time, the selected value for

*This research was sponsored by the Air Force Office of Scientific Research under Order No. OA3 1SSA 65–8. For the first paper of this series see Reference [1].

[1] Figures in brackets indicate the literature references at the end of this paper.

$\Delta H^\circ_{f298.15}[OF_2]$ was +7.6 kcal mol^{-1} [5]. In 1965 Bisbee, et al. [9] reported on a more recent study from which they derived $\Delta H^\circ_{f298.15}[OF_2] = -4.06$ kcal mol^{-1}. In spite of the large amount of earlier work, there thus remained considerable uncertainty in the heat of formation of oxygen difluoride and, at the start of this work, it was not clear whether the compound was exothermic or endothermic. The results of the earlier experimental work are compared with those from the present study in another section of this paper. For comparison with the present experiments, it is important to mention here the reactions which were studied in the earlier investigations.

The measurements of von Wartenberg and Klinkott were carried out in a flow system in which they reacted OF_2 (g) with (1) KOH (excess KOH aq 40%), (2) [6KI + 2HF] (in excess aq), and (3) HBr (excess HBr, aq 45%). They measured the heats of reaction and derived a value for the heat of formation of oxygen difluoride based on each reaction. Ruff and Menzel used a flame calorimeter to measure the heat of the overall reaction of combustion of OF_2 with hydrogen and neutralization of the product HF in NaOH (aq). In the same apparatus they also measured the heats of the $F_2 - H_2 - NaOH$ and the $O_2 - H_2$ reactions. The latter measurements provide the auxiliary heat data needed for calculating $\Delta H^\circ_f[OF_2]$. Bisbee, et al. reacted oxygen difluoride with hydrogen in a combustion bomb, which contained water for solution of the product HF. For calculating $\Delta H^\circ_f[OF_2]$ they obtained their auxiliary data for the HF (aq) from the literature. It is interesting to note that in the earlier work, three different calorimetric methods were used. With well-developed procedures, suitably selected reactions for study, and pure reaction materials, it seems possible that each of the above calorimetric methods could lead to a reliable value for $\Delta H^\circ_f[OF_2]$. However, it appears that these methods were not used to their best advantage in the earlier work.

There are few known reactions of oxygen difluoride which are suitable for a thermochemical study for deriving $\Delta H^\circ_f[OF_2]$. Because the magnitude of this heat-of-formation value is small, it is desirable to derive it from a reaction with a small heat effect. Such reactions with oxygen difluoride unfortunately tend to lead to multiple products, which are not readily recovered and separated for quantitative analysis. Under ordinary conditions fluorine and oxygen do not combine directly to form oxygen difluoride.

With the above points in mind, the $OF_2 - H_2 - H_2O$ reaction was selected for this study despite the large heat effects to be expected. This reaction leads to only a few products, goes readily to completion, is amenable to analysis of reactants and products, and requires auxiliary data that can be measured in the same apparatus. Oxygen difluoride was reacted with hydrogen in a flame, and then the product hydrogen fluoride was dissolved in water present in the reaction vessel. Using the same apparatus and similar procedures, heat measurements were made also for the $F_2 - H_2 - H_2O$ and $O_2 - H_2$ reactions.

The reliability of the heat-of-formation value derived is increased by several factors inherent in this experimental plan. (1) The hydrogen fluoride is dissolved in water, yielding a well-defined thermodynamic state for the acid. (2) Dissolving the hydrogen fluoride inside the calorimeter lessens the possibility of loss of the acid by corrosion and retains it for later quantitative analyses. (3) Because the auxiliary data are measured in the same way as the principal reaction, several of the systematic errors cancel in the calculation of $\Delta H^\circ_f[OF_2]$. This plan is similar to that used by Ruff and Menzel. Our work differs from theirs mainly in the solution of the hydrogen fluoride in water instead of aqueous sodium hydroxide, and in the design of the reaction vessel.

2. Experimental Apparatus and Procedures

2.1. The Samples

a. Hydrogen

A commercially available high purity grade of hydrogen was used. A mass spectrometric analysis was performed directly on the contents of the cylinder and the composition (mole percent) of the gas was: H_2, 99.9; H_2O, 0.04 ± 0.02; and N_2, 0.05 ± 0.01. The hydrogen was used directly from the cylinder.

b. The Oxidizer Gases

Commercially available samples of oxygen, fluorine, and oxygen difluoride were used. Each of the samples was transferred from the large cylinder to a spherical weighable container for the analyses and calorimetric experiments. The design of the sample containers has already been described [1, 2]. They were constructed of Monel and equipped with either Monel or 316-stainless-steel valves with Teflon packing. The weight of a typical bulb was approximately 150 g. Extensive analyses were carried out for each of the gases and the procedures used are described in detail in the Appendix.

Oxygen. The oxygen was of high purity and is the grade used in this laboratory for bomb combustion experiments. The purity was reported by the supplier to be greater than 99.99 percent. It was analyzed for argon and nitrogen by mass spectrometry and gas chromatography, respectively. The composition of the sample is estimated to be oxygen, 99.987; nitrogen, 0.009; and argon, 0.004 weight percent.

Fluorine. The fluorine sample was of ordinary commercial quality and therefore not of the high purity desirable for a definitive thermochemical study of the hydrogen-fluorine reaction. While being sampled, the gas was passed over activated sodium fluoride for removal of hydrogen fluoride.

The total analysis of the fluorine sample was obtained using a combination of analytical methods. The total mole percent fluorine was determined by the mercury absorption technique and the relative amounts of the constituents of the residual gas were measured with mass spectrometry and gas chromatography. The chromatographic method was developed to provide a check on the results from the mass spectrometric method, which we have usually used

for analysis of the residual gas. The results from the two methods were in good agreement (see appendix). Table 1 gives the complete analysis of the fluorine sample.

TABLE 1. *Analysis of the fluorine sample*

Constituent	Mole percent total impurities [a]		Mole percent in fluorine sample	Weight percent
	I [b]	II	(based on II)	
F_2			98.75	98.92
N_2	61.8	62.0	0.77	0.54
O_2	28.6	31.3	.39	.33
Ar	0.2	0.2	.0025	.003
CO_2	3.4	1.2	.015	.017
CF_4	5.0	4.4	.055	.128
SiF_4		0.03	.0004	.001
SO_2F_2	0.3	.3	.0037	.010
C_2F_6		.28	.0035	.013
SF_6		.08	.0010	.004
C_3F_8		.08	.0010	.005
C_3F_6 (unsat.)		.07	.0009	.005
Remaining fluorocarbons	0.6	.06	.0007	

[a] Mass spectrometric analysis of volatile impurities after removal of F_2 by reaction with mercury.

[b] Sample pressure of I was factor of ten less than that of II. Analysis of I serves only for comparison of the analysis for major impurities.

Oxygen difluoride. The supplier's analysis of the oxygen difluoride sample showed it to contain: OF_2, 99.25; O_2, 0.69; and CO_2, 0.06 weight percent, and 0.01 volume percent CF_4. The gas was reported to contain no free fluorine. Kesting, et al. [10] compared the methods of gas chromatography, iodimetry and infrared spectroscopy for analysis of OF_2 and their tests show that gas chromatography yields the most reproducible and accurate results.

Because of the importance of the analysis to the accuracy of the calorimetric data, the oxygen difluoride sample was reanalyzed in this laboratory by gas chromatography, following procedures similar to those described by Kesting. The results from two of the analyses are shown below.

	Analysis I	Analysis II	Av
	Mole %		wt. %
OF_2	99.07	99.10	99.36
O_2	0.76	0.73	0.45
CF_4	.06	.07	.11
CO_2	.10	.10	.08

For qualitative identification, an infrared spectrum of the sample was obtained and is shown in figure 11 (appendix).

2.2. Reaction Vessel and Flow System Designs

a. The Reaction Vessel

The general method is to react the oxidizer in a flowing atmosphere of excess hydrogen and then to form the aqueous acid solution of the products. The overall design is illustrated in figure 1. In the upper chamber (A) the oxidizer and hydrogen (excess) are mixed, ignited, and reacted in a flame. The effluent

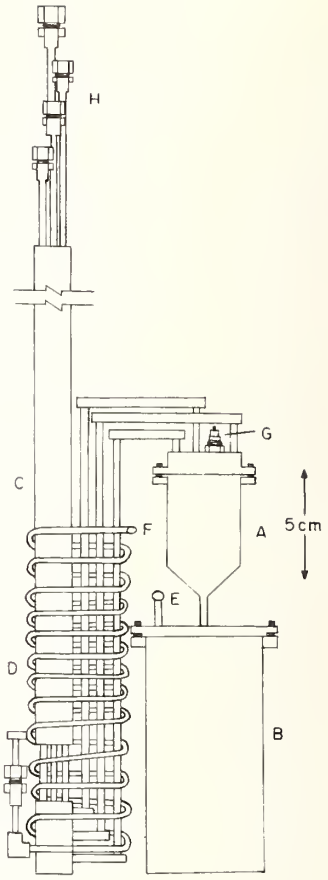

FIGURE 1. *Burner for fluorine flame calorimetry.*

A, Combustion chamber; B, Primary solution vessel; C, Heat exchanger; D, Cooling coil; E, To secondary solution vessel; F, From secondary solution vessel; G, Igniter; H, Inlet and Outlet connectors.

hydrogen removes the reaction products to the lower chamber (B), which is the primary solution vessel and contains 100 cm^3 of water. A gas dispersion system forces the gas mixture as fine bubbles through the aqueous solution, to cause complete removal of the hydrogen fluoride from the flowing hydrogen, and simultaneously to mix the solution making it homogeneous in concentration and temperature.

The gases are brought to the burner from the exterior of the calorimeter system by Monel tubes passing through the heat exchanger (C). The exit gas enters from the coiled tube (D) into the lower end of the outer tube of the heat exchanger, and while leaving the calorimeter, circulates among the small tubes which contain the entering gases. The outlet (E) on the primary solution vessel connects to a smaller vessel which is seen in the foreground in the complete burner assembly shown in figure 2. For an experiment this secondary vessel contains 20 cm^3 of water. As can be seen by reference to figures 1 and 2, the effluent gases leave the secondary solution vessel at F and pass through a helix of Monel tubing before entering the heat exchanger. Except for the primary solution vessel, the reaction vessel is composed almost entirely of

FIGURE 2. *Assembly of reaction vessel.*

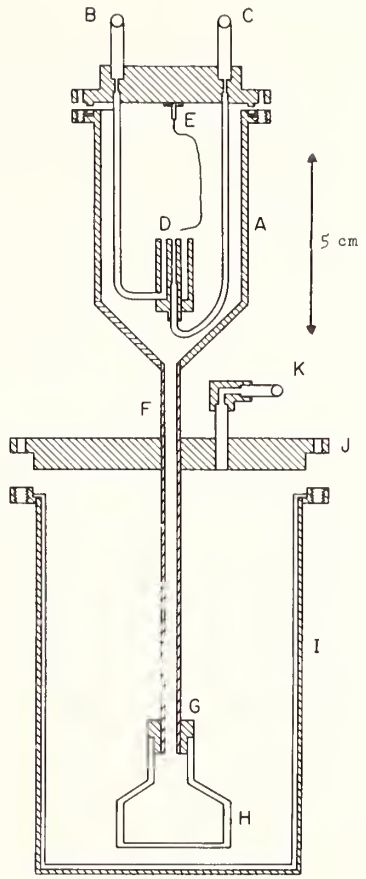

FIGURE 3. *Combustion chamber and primary solution vessel.*

A, Combustion chamber; B, Hydrogen inlet; C, Oxidizer inlet; D, Flame position; E, Spark electrode; F, Platinum tubing; G, Teflon adapter; H, Polyethylene gas disperser; I, Primary solution chamber; J, Lid for solution vessel; K, To secondary solution vessel.

Monel and silver-soldered at all of the permanent joints.

Details of the combustion chamber are shown in figure 3. The inlet tubes for the reacting gases, the igniter, and the flame tip are attached to the lid of the combustion chamber so that they are readily accessible when the lid is removed. The oxidizer is introduced through inlet C, and the major part of the hydrogen atmosphere enters through inlet B. Additional hydrogen is introduced through a third gas inlet (not shown). The joint between the cover and the combustion chamber is made by a Teflon gasket placed in a groove on the flange of the cup.

The reaction is initiated with an electric spark from a high voltage electrode which is a nickel rod, insulated by Teflon from a Monel sheath. A calcium fluoride disk is placed over the electrode (E) to further shield it from the reaction heat and product hydrogen fluoride.

The platinum tube (F) leading into the solution chamber is fitted with a polyethylene cap having a porous lower surface. The cap is held in place with a small Teflon adapter (G). The primary solution vessel is made of nickel-plated copper and has a Teflon liner. The flange on the liner makes the seal when the vessel is closed.

The water in the secondary solution vessel removes any hydrogen fluoride from the effluent gas that may be transferred from the primary solution. This provision assures also that upon leaving the burner the effluent gas flows through a solution for which the partial pressure of HF does not change during the experiment. In the primary solution vessel, the liquid contains no HF during the fore-period, but contains about two weight percent hydrogen fluoride in the final drift. The vapor pressure of hydrogen fluoride over the final solution is about 0.048 mm Hg at 25 °C [11]. Consequently, very little hydrogen fluoride is transferred to the secondary solution.

b. The Flow System

The layout of the gas flow system is similar to that used previously for flame calorimetric work in this laboratory [1, 2]. The components of the flow system are schematically shown in figure 4. Preceding the calorimeter are three flow lines which connect to inlet ports on the reaction vessel. These consist of the two flow lines for hydrogen, and one for the oxidizer.

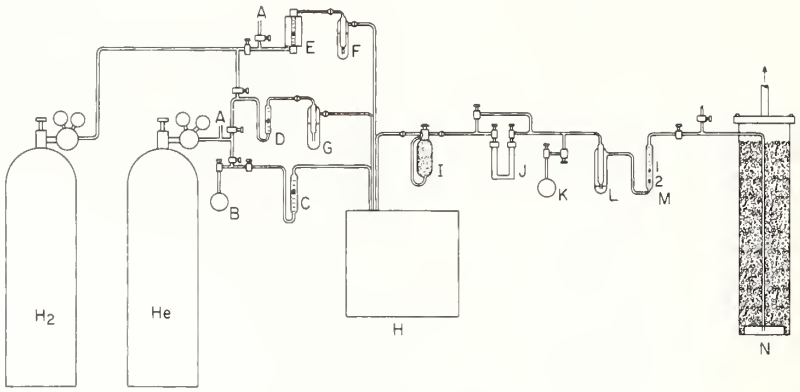

FIGURE 4. *Flow system.*

A, Flow inlet (helium); B, Oxidizer sample container; C, Flowmeter (oxidizer); D, Flowmeter (hydrogen, II); E, Flowmeter (hydrogen, I); F, Saturator (I); G, Saturator (II); H, Calorimeter; I, Absorber (magnesium perchlorate); J, Absorber (sodium fluoride); K, Sampling bulb; L, Bubbler (Kel-F oil); M, Flowmeter (effluent gas); N, Fluorine absorption tower.

The oxidizer line begins with the spherical sample bulb at B. Not shown in the diagram is an absorber of magnesium perchlorate placed immediately after the helium cylinder. Predrying of the helium is desired for the helium that enters the fuel line, but as is explained below, dried helium is not necessary for the hydrogen lines. The flow rate of the oxidizer was regulated by manual adjustment of the valves.

Each hydrogen line includes a flowmeter and weighable "saturator." The saturator is Pyrex and with the water, weighs about 69 grams. The hydrogen entering the reaction vessel is saturated with water to compensate for the water removed by the effluent hydrogen.

The items after the calorimeter used in these experiments are the absorption bulb (I), the sampling bulb (K), the bubbler (L), and the flowmeter (M). The absorption bulb contains magnesium perchlorate and is used to measure the amount of water removed from the reaction vessel by the effluent hydrogen. The final flowmeter is useful in monitoring the reaction. The remaining items serve the same purpose as described earlier [1].

2.3. The Calorimeter and Its Operation

The calorimeter is similar in design to the Dickinson Calorimeter [12], with modifications which were introduced by Prosen, et al. [13]. It is enclosed in a constant-temperature submarine-shield in the surrounding water bath. The calorimeter can is separated from the enclosure by a 1/2-in air space. It is supported by three metal pegs and has a volume of 5.5 liters. The calorimeter lid has three holes for bringing out the platinum resistance thermometer, the leads to the electrical calibration heater, and the flow lines to the reaction vessel. The reaction vessel and most of the heat exchanger are immersed in the stirred water of the calorimeter. The water is stirred at a rate of 300 rpm. The reaction vessel is placed on a small brass platform, supported by three small cones. This positions the bottom of the reaction vessel about 1/4 in above the bottom of the calorimeter can.

In the manner customary in this laboratory, temperature measurements were made with a calibrated platinum resistance thermometer, used in conjunction with a G–2 Mueller bridge and a high-sensitivity galvanometer. A displacement of 0.5 mm on the galvanometer scale represented 10 $\mu\Omega$ on the bridge or one-tenth millidegree. At 0 °C the thermometer has a resistance of 25.4668 Ω.

The temperature of the jacket water was kept constant at 32 °C by an automatic regulating system consisting of a thermistor sensing element, linear dc microvolt amplifier, strip-chart recorder (-5 to $+5$ μV), current-adjusting-type controller, and a 50-W magnetic power amplifier [14]. The jacket bath has two heaters, a 14-Ω heater for raising the jacket temperature to 32 °C, and a 131-Ω heater for temperature control. A 500-mA meter is connected between the magnetic amplifier and the control heater. The thermistors form two opposite arms of a Wheatstone bridge circuit of which the two remaining arms are formed by adjustable temperature-insensitive resistors. Each thermistor arm of the bridge consists of four bead thermistors of about 1000 Ω each. The thermistors are encased in flattened thin-wall copper tubing and are immersed in the jacket water near the heaters and stirrer. A 1.5-V mercury cell supplies a current of 0.040 mA to the bridge. The current is kept very small so that self heating of the thermistor elements remains below 0.001 °C. The temperature was usually controlled to better than ± 0.0015 °C.

a. Electrical Calibration System

The calibration heater was made from B&S gage No. 30 Advance wire covered with a double layer of glass insulation. The current leads were 22-gage copper wire and the heater sheath was thin copper tubing flattened onto the resistance wire. The resistance of the heater was 23 Ω. The heater was formed in a 1-in o.d. coil which was suspended from the calorimeter lid. The ends of the sheath passed through a small copper plug which was fastened securely to a ring on the lid.

The potential leads are attached so that there is a negligible disturbance in the current leads [15]. The first potential lead is soldered to the current lead just inside of the copper sheath at the physical boundary of the calorimeter. The three leads are then brought up to a copper plate and the second potential lead is attached at the point where the current lead contacts the copper plate. Then all four wires are coiled on the lower side of the plate and cemented firmly in place. By means of a bakelite rod, which passes through a tube in the submarine lid, the copper plate is secured firmly against the lower side of the submarine lid to achieve good thermal contact with the calorimeter shield.

The power for the electrical calibration was obtained from a precision regulated power supply. The unit has a power output of about 500 W maximum, with a current range from 0–5 A and a voltage range from 0–103 V. The supply was operated in the constant current mode.

With the parameters and switching arrangement in these experiments, operation in the current mode gave more constant current and voltage readings. The double-pole, double-throw switch which connects the calibration heater and a dummy heater of similar resistance alternately into the circuit posed a problem in the calibrations. While interchanging the heaters, a transient voltage appeared. In a separate investigation [16] the magnitude and decay time of this transient voltage were observed. Because the transients were over in about ten seconds, while the heating periods were usually about sixteen minutes long, we believe that this effect does not significantly affect the accuracy of the calibrations performed. Current and voltage readings were made on alternate minutes. The time interval for the electrical heating was measured with an electronic counter, with an internal quartz oscillator generating at 100 kHz, which gave the time readings to 10^{-5} second. The timer was actuated by the switching arrangement which initiated the heating to the calorimeter.

Other equipment used in measuring the electrical energy input consisted of a 0.01 Ω standard resistor, a volt box with a ratio of 20,000 to 20 Ω, a thermostated standard cell, and a Wolff Diesselhorst potentiometer. During the calibration experiments the calibration of the potentiometer was checked daily. Details on a similar calibration circuit are given by Churney and Armstrong [16]. The resistors, potentiometer, and standard cells were calibrated at the National Bureau of Standards.

b. The Ignition System

A high voltage coil was used for the igniter and the sparking was timed with an electric clock connected in the ignition circuit. The sparking power was measured in blank experiments to be 1.4 J sec^{-1}.

c. Conduct of an Experiment

Preliminary Actions. Before and after each experiment, the oxidizer-sample container, saturators, and magnesium perchlorate absorber (see figure 4) are weighed to 0.1 mg. In preparing the reaction vessel, the sparking lead is positioned over the flame position and demineralized water is added to the primary and secondary solution vessels and then the reaction vessel is assembled. The weight of the calorimeter can with water is adjusted to 5950 ± 0.0005 g on a 6-kg capacity balance. This weight also includes the support for the reaction vessel. Immediately the reaction vessel is positioned and the calorimeter is covered with its lid from which is suspended the calibration heater. Then the remaining assembly of the calorimeter and its accessories is completed.

Reactions. The three inlet flow lines are purged with helium to remove air and a flowing hydrogen atmosphere is established in the hydrogen inlets. The total flow rate of hydrogen varied, depending on the reaction being studied, from about 350 to 450 cm^3 min^{-1}. Though the oxidizer line is initially flushed with helium, no gas is flowing through this line during the initial drift period. After a fore drift period of about 20 min, during which time-temperature readings of the calorimeter are made, the reaction is initiated by simultaneously initiating the sparking and releasing gas from the sample bulb. The sparking is discontinued when there is certainty that the fuel has ignited. This is usually after 10 to 15 seconds of sparking. The increase in the rate of the temperature rise of the calorimeter and the decrease in the flow rate of effluent gas are the main signals that the reaction is taking place smoothly.

In most experiments, a 2.5–2.7 deg temperature rise was achieved in a 15- to 18-minute reaction period. Near the end of the reaction period the oxidizer sample container is closed and the material remaining in the flow line is flushed into the burner with helium. The helium flow is reduced and continued for the remainder of the experiment while hydrogen flows through the other lines. After the reaction experiments the solution in the primary solution vessel is transferred, with washings, to a weighed 250-cm^3 polyethylene bottle. The secondary solution (20 cm^3) is also recovered for titration.

Calibrations. The procedure for conducting the calibration experiments is similar to that used for the reactions. The solution vessels contain 100 and 20 cm^3 water, respectively. A hydrogen flow through the bubblers is maintained at a rate comparable to that used for the reactions. The regulation of the helium flow in the oxidizer flow line constitutes the main difference between the gas handling procedures for the calibration and reaction experiments. In the calibrations a small flow of helium is maintained in the oxidizer line throughout the experiment, whereas for the reactions the helium flow is begun at the end of the reaction period.

d. Calculations

All of the values for the corrected temperature rise were calculated on an electronic computer with a computer program developed by Shomate [17]. For the calculation, it was necessary to give the computer the following data: (1) dial corrections for the Mueller bridge; (2) time and resistance readings taken during

the reaction and drift periods of the experiment; and (3) constants for the platinum resistance thermometer. A comparison of some hand-calculated and computer-calculated values showed that the program satisfactorily calculates the corrected resistance change, ΔR(corr); the initial and final drifts; the conversion factor, $\frac{dR}{dt}$; the initial and final temperatures for the reaction; the correction to the temperature rise, Δt(corr); the corrected temperature rise, Δt_c; and the cooling constant.

The definition, 1 cal = 4.184 J, was used for expressing the results in calories. All atomic weights were taken from the 1961 Table of Atomic Weights based on Carbon 12, adopted by the International Union of Pure and Applied Chemistry [18]. The heat capacity data used for the gases and liquid water are tabulated below. The heat of vaporization of water was taken as 2,439 and 2,428 J/g at 298.15 and 303.15 °C, respectively [19]. Values for the heat capacity of aqueous hydrogen fluoride were obtained from the work of Thorvaldson and Bailey [20].

Substance	$C_{p^{298.15}}$ J mol^{-1} deg^{-1}	Reference
F_2(g)	31.30	[8]
O_2(g)	29.355	[8]
OF_2(g)	43.30	[8]
H_2(g)	28.823	[8]
H_2O(l)	75.2911	[8]

e. Water Removal from the Reaction Vessel

One general problem encountered in all the experiments was to account for and minimize loss of water from the reaction vessel. This was done by using a weighable drying tube on the outlet of the calorimeter and weighable saturators on the inlet tubes. The water entering and leaving the calorimeter could thus be monitored and the net change kept to a small value. The largest part of the residual heat effect due to condensation or evaporation could be presumed to form part of the causes of the initial and final drift rates, along with heat of stirring and heat transfer by conduction between the calorimeter and jacket. However, by keeping the net change in the amount of water small, it is believed that the uncertainty introduced by assuming the associated heat effects were constant would also be small. With this assumption, the results which are given in table 2, do not require further discussion. However, it is interesting to note the consistency in the signs of the differences for a given set of experiments.

A net removal of water is observed for all of the calibration experiments. This is consistent with the use of the helium in the oxidizer line throughout the experiment. Because the helium is not passed through a saturator, it causes a removal of water from the reaction vessel. The signs in the changes of water in the reaction vessel during the reaction experiments nearly correlate with the amounts of excess hydrogen used. The stoichiometric and actually used reactant ratios are summarized below.

TABLE 2. *Water changes in reaction vessel*

Expt. No.	Water removed g	Water carried in g	Increase g
	Electrical calibrations		
4	0.8033	0.5246	−0.2787
5	.8084	.4813	−0.3271
6	.7025	.4644	−0.2381
7	.7478	.4637	−0.2841
	Oxygen-hydrogen reaction		
1	0.6680	0.6483	−0.0197
2	.6483	.7264	+0.0781
3	.8313	1.0051	+0.1738
4	.8676	0.8887	+0.0211
5	.9486	.9740	+0.0245
6	.9345	.9461	+0.0116
	Oxygen difluoride-hydrogen reaction		
7	0.5466	0.5656	+0.0190
8	.7458	.7135	−0.0323
9	.7069	.7288	+0.0219
10	.6102	.6805	+0.0703
11	.5034	.6186	+0.1152
	Fluorine-hydrogen reaction		
1	1.4000	1.0715	−0.3285
2	1.2908	1.0127	−0.2781
3	1.1670	1.0396	−0.1274
5	0.9910	0.8310	−0.1591
6	1.0987	1.0397	−0.0590
7	0.8431	0.7853	−0.0578
8	1.0606	.9651	−0.0955
9	0.9137	.8323	−0.0814
10	.8322	.7700	−0.0622

reaction		stoichiometric	actual
O_2-H_2	n_{H_2}/n_{O_2}	2	2.8–3.4
F_2-H_2	n_{H_2}/n_{F_2}	1	4
OF_2-H_2	n_{H_2}/n_{OF_2}	2	4

A much larger excess of hydrogen was used in the fluorine reactions. This shows in the net removal of water from the reaction vessel, compared to the deposition of water observed for the other reactions.

3. Electrical Calibration Results

A series of seven electrical calibration experiments was conducted and the data are given in table 3. Included in this table are the experiment number; the average calorimeter temperature, t(av); the correction to the temperature rise, Δt(corr); the corrected temperature rise, Δt_c; the average current; average voltage; heating time; electrical energy; and the energy equivalent of the calorimeter. For the seven experiments the average value for the energy equivalent was 21887.9 J (°C)$^{-1}$ with a standard deviation of the mean of 0.006 percent.

TABLE 3. *Calibration of the calorimeter*

Expt. No.	1	2	3	4	5	6	7
t (av)....°C	30.37	30.36	30.38	30.39	30.37	30.38	30.48
Δt (corr)....°C	0.04724	0.04976	0.04658	0.04332	0.04878	0.04709	0.04368
Δt_c....°C	2.73616	2.75413	2.72360	2.71066	2.74159	2.77289	2.55693
Current....A	1.62580	1.62770	1.62706	1.62711	1.62770	1.62817	1.62737
Voltage....V	37.3949	37.4378	37.4236	37.4280	37.4385	37.4483	37.4282
Time....sec	984.857	989.160	979.206	974.077	984.874	995.612	918.805
q....J	59875.9	60276.9	59624.3	59320.7	60016.8	60704.6	55964.0
E....J(°C)$^{-1}$	21883.2	21886.0	21891.7	21884.2	21891.2	21892.2	21887.2

4. Examination of the Reaction Products

The corrosivity of fluorine and hydrogen fluoride is a general problem to be minimized and checked in these experiments. This was partly accomplished by using Monel as the construction material for the flow line and combustion chamber. Prior to the experiments these parts of the flow system were exposed to a flowing fluorine atmosphere to condition the surfaces. Consequently, all of the fluorine released from the weighed sample bulb should enter into the reaction with hydrogen.

Most of the corrosion problem in these experiments was caused by the product hydrogen fluoride. The appearance of the combustion chamber after the experiments suggested that more corrosion resulted from the hydrogen fluoride in the F_2-H_2 reaction than from the HF-H_2O mixture in the OF_2-H_2 reaction.

The solutions and washings from the primary solution vessel were transferred to a weighed polyethylene bottle from which weighed aliquots were taken for titration with standard sodium hydroxide solution. After the analyses for H^+, samples of these solutions were analyzed by atomic spectrophotometry for Cu^{++}, Ca^{++}, Ni^{++} and Ag^+. These results for the F_2-H_2-H_2O and OF_2-H_2-H_2O reactions are given in table 4.

TABLE 4. *Quantities of metal ions in hydrofluoric acid solutions*

Expt. No.	Ag	Ca	Cu	Ni	n_{HF} equiv
	μ moles				(total)
F_2-H_2-H_2O Reaction					
1	<0.05	<0.3	7.4	20.0	0.00005
2	<.05	<.3	9.0	16.1	.00005
3	<.05	<.3	2.2	9.1	.00003
4	<.05	<.3	1.5	3.9	.00001
5	<.05	<.3	1.5	4.5	.00001
6	<.05	<.3	3.2	8.4	.00002
7	<.05	<.3	0.6	3.9	.00001
8	<.05	<.3	<.1	4.7	.00001
9	<.05	<.3	1.2	7.7	.00002
10	<.05	<.3	3.5	10.0	.00003
OF_2-H_2-H_2O Reaction					
1	0.3	1.4	16.1	32.9	0.00010
4	<.05	0.9	15.1	23.4	.00008
7	<.05	.9	16.8	29.2	.00009
Blank	<.05	<.1	<0.1	<0.2	

For the fluorine reaction, the solution from each experiment was analyzed, and in the OF_2 reaction solutions from three selected experiments were tested. The blank is a sample of the demineralized water used for the solutions. Because the blank showed no ions (outside the uncertainty intervals), we concluded that the metal ions resulted from the corrosion of the reaction vessel.

The total amount of corrosion cannot be determined from these tests. The total quantity of aqueous fluoride salts amounts to less than 10 percent of the deficiency of HF. (Compare n_{HF}(equiv) in table 4 with Δn_{HF}(obs-calc) in tables 7 and 9.) However, the tests do reveal some interesting features about the reactions.

The solutions from the fluorine reaction contain a smaller concentration of the metal ions, in spite of the more corroded appearance of the reaction vessel. It is possible that only the metal fluorides that exist in the vapor phase near the flame position are flushed downward by the effluent gas in this reaction. On the other hand, the product HF(aq) in the oxygen difluoride reaction may dissolve some metal fluorides and serve as a transport medium to the solution. Approximately 1 g of water was formed in each experiment, more than enough to wet the surfaces of the combustion chamber. Much more erosion of the CaF_2 disk was observed for the OF_2 reaction. This is consistent with the larger amount of Ca^{++} present in the solution, and suggests that the CaF_2 is slightly dissolved by the HF(aq), and then transferred to the solution.

5. Reaction Heat Measurements

5.1. Oxygen-Hydrogen Reaction

For six of the nine experiments on this reaction (series I) the contents of the calorimeter were the same as for the electrical calibrations. In the other three experiments (series II), the water in the solution vessel was omitted, so that the product water could be weighed and compared with the amount calculated from the weighed quantity of oxygen reacted. In these three experiments the water was flushed from the reaction vessel with helium and absorbed in magnesium perchlorate outside the calorimeter [21]. The data for the experiments are given in table 5.

m_s is the mass of sample and m_{O_2} is the mass of oxygen, based on the analysis given in section 2.1.b. m_{H_2O} (obs) is the measured mass of water formed in the reaction and m_{H_2O}(obs)/m_{H_2O}(calc) is the ratio of the observed to calculated quantities of water. t(av) is the average temperature of the calorimeter during the reaction and is the reference temperature for the reaction. Δt(corr) and Δt_c are respectively, the correction to the temperature rise and the corrected temperature rise.

TABLE 5. O_2-H_2 *reaction*

a. Heat measurements

	Series I						Series II		
Expt. No.	1	2	3	4	5	6	7	8	9
m_{H_2}, g	3.3032	3.3850	3.4945	3.2208	3.2248	3.2376	3.2342	3.2325	3.1527
m_{O_2}, g	3.3028	3.3846	3.4941	3.2204	3.2244	3.2372	3.2338	3.2321	3.1523
m_{H_2O}(obs), g	[a]	[a]	[a]	[a]	[a]	[a]	3.6417	[b]	3.5517
m_{H_2O}(obs)/m_{H_2O}(calc)							1.0001		1.0006
t_{av}, °C	30.36	30.38	30.43	30.31	30.32	30.32	30.34	30.34	30.37
Δt(corr), °C	0.06586	0.06620	0.05722	0.04966	0.05286	0.05159	0.07163	0.06773	0.06378
Δt_c, °C	2.70570	2.77304	2.86490	2.64052	2.64704	2.64914	2.67368	2.67882	2.61481
m_{H_2O}(in soln vessels), g	119.64	119.64	119.64	119.64	119.64	119.64	0	0	0
Δe_1, J(°C)$^{-1}$	7.8	7.5	8.2	7.6	7.6	7.6	7.6	7.6	7.4
Δe_2, J(°C)$^{-1}$	0	0	0	0	0	0	−499.9	−499.9	−499.9
E(calorim), J(°C)$^{-1}$	21895.7	21895.4	21896.1	21895.5	21895.5	21895.5	21395.6	21395.6	21395.4
q(obs), J	59243.2	60716.8	62730.1	57815.5	57958.3	58004.2	57205.0	57315.0	55944.9
n_{H_2}/n_{O_2}	2.81	2.88	3.02	3.35	3.35	3.23	2.96	2.96	3.20

b. Corrections to the heat measurements

q(ign), J	23.2	16.0	11.5	19.6	22.4	18.2	16.4	10.5	17.1
q(temp), J	−37.5	−40.3	−25.1	−42.0	−28.0	−38.9	−18.4	−46.4	−38.5
q'(vap), J	271.5	278.1	371.1	256.6	279.5	265.3			
q''(vap), J	36.3	39.6	29.1	26.2	26.1	26.1			
q'''(vap), J							−366.9	−227.6	−181.6
q^{iv}(vap), J							−33.9	−33.8	−33.8
Total, J	293.5	293.4	386.6	260.4	300.0	270.7	−402.8	−297.3	−236.8
q_{H_2}, J	58949.7	60423.4	62343.5	57555.1	57658.3	57733.5	57607.8	57612.3	56181.7
n_{H_2O}, mol	0.20644	0.21154	0.21838	0.20128	0.20154	0.20234	0.20212	0.20202	0.19702
q_{O_2}/n_{H_2O}, kJ mol^{-1}	285.55	285.64	285.48	285.95	286.09	285.33	285.02	285.18	285.16

[a] Water formed was not measured.
[b] Attempt to measure water was unsuccessful.

m_{H_2O}(in soln vessels) is the total mass of water in the solution vessels. Δe_1 is the correction to the energy equivalent for the water formed in the reaction (the heat capacity of half the water formed). Δe_2 is the correction for the omission of water from the solution vessel. E(calorim) is the energy equivalent of the calorimeter corrected for the deviations from the standard calorimeter. q(obs) is the observed heat effect.

q(ign) and q(temp) correct for the ignition energy and the energy required to temper the reacting gases from room temperature to t(av), the average calorimetric temperature during the reaction. q(ign) was calculated from the sparking power, 1.4 J sec^{-1} and the measured sparking times. q(temp) was calculated from the heat capacities and the measured amounts of the gases reacted.

q'(vap) is a correction for the addition of water to the reaction vessel during the reaction period by the reacting hydrogen. The hydrogen that enters into reaction is saturated with water, which condenses and is not carried out of the calorimeter. The amount of water added to the calorimeter is calculated from the volume of hydrogen reacted (based on stoichiometry of reaction) and the vapor pressure of water at the room temperature. q'(vap) is then the heat of condensation of this water at t(av).

In contrast, the helium used for purging the oxidizer line causes a net removal of water from the solution vessel. We reason that if the gas flow were begun at the time when one-half of the temperature increase is achieved, no correction would be needed for the vaporization of the water because the heat effect would then be properly accounted for by the final drift rate measurements. q''(vap) is a correction for the energy of vaporization of the additional water that would have been removed from the solution vessel had the helium flow been started at t_m at the rate that was continued through the final drift period. q'(vap) and q''(vap) apply to all experiments with water in the solution vessel, whereas the corrections q'''(vap) and q^{iv}(vap) pertain only to the experiments in which the product water was measured. q'''(vap) is the amount of heat required to vaporize the water removed from the reaction vessel by the hydrogen and helium during the reaction. This quantity of water was measured by weighing the absorber immediately after the experiment, and using another weighed absorber for collecting the water remaining in the reaction vessel. q^{iv}(vap) is the heat of vaporization of the water in the vapor phase in the reaction vessel.

We have assumed that the nitrogen impurity present in the hydrogen and the oxygen sample does not react and therefore no correction was applied. Under the conditions the nitrogen impurity may react to give NH_3. No test was made for NH_3 in these experiments. In similar calorimetric work Rossini [21] reported the presence of nitrogen in his oxygen sample. For some of his experiments in which oxygen was burned in a hydrogen atmosphere, he tested the product gases for NH_3 and found the amount present to be negligibly small.

The heat of the oxygen-hydrogen reaction is given in table 6. The values given represent averages for the number of experiments shown in parentheses. The data are given for 303.4 °K and 298.15 °K. The factor, σ, is the standard deviation of the mean. As mentioned above, the series II measurements were conducted mainly for confirming the amount of reaction. Because water was not contained in the solution vessels for these measurements, we believe that the heat

TABLE 6. *Heat of the oxygen-hydrogen reaction*

$H_2(g) + \frac{1}{2}O_2(g) = H_2O(l)$

	$-\Delta H^\circ_{303.4}$	$-\Delta H^\circ_{298.15}$	σ
Series I (6) ..... kJ mol^{-1} ...	285.67	285.84	0.12
Series II (3) ..... kJ mol^{-1} ...	285.12	284.30	.....
Series I (6) ..... kcal mol^{-1} ...	68.28	68.32	0.03
Series II (3) ..... kcal mol^{-1} ...	68.14	68.18	.....

σ is the standard deviation of the mean.

data are less reliable than the series I data. The fact that they are less negative suggests that all of the heat from the reaction was not dissipated by the effluent gas. We do not propose the value found here, $\Delta H^\circ_{298.15} = -68.32$ kcal mol^{-1}, as a replacement for Rossini's determination [21], but use the agreement with the earlier work as an indication of the general validity of these and other experiments conducted in this study.

5.2. Fluorine-Hydrogen-Water Reaction

Ten experiments were conducted for the F_2-H_2-H_2O reaction. For the first five experiments only the oxidizer flow line was conditioned with fluorine, whereas in the remaining experiments the flow line and combustion chamber were conditioned. On this basis the data for the experiments are presented in two series.

The data for these experiments are given in table 7. The heat measurement data have been explained for the oxygen reaction. Δe is a correction to the energy equivalent for the hydrogen fluoride formed in the reaction (one half the heat capacity of the hydrogen fluoride). n_{H_2O}/n_{HF} is the ratio of the moles water in the solution vessel to the moles of hydrogen fluoride formed in the reaction, as determined by the analyses of the solutions.

For the reaction quantities, $n_{HF}(F_2)$ and $n_{HF}(CF_4)$ are the numbers of moles of HF produced from F_2 and CF_4, respectively. They were calculated from the analyses in table 1. The deficiency of HF in these experiments varied greatly. For the ten experiments, the values of $n_{HF}(obs)/n_{HF}(calc)$ ranged from 0.9772 to 0.9964, with a mean of 0.9844. We assume that the deficiency of HF is caused by corrosion. However, the erraticity of the recovery is difficult to explain.

The ignition, vaporization, and gas temperature corrections are the same as described above. q_{O_2}, q_{CF_4}, and q_{CO_2} are corrections for the reactions of the impurities. These corrections were calculated on the basis of eqs (1), (2), and (3).

$$\Delta H_{R,298.15\,^\circ K} \quad [8]$$

$$H_2(g) + \tfrac{1}{2}O_2(g) \rightarrow H_2O(l) \qquad -68.32 \text{ kcal(mol } H_2O)^{-1} \qquad (1)$$

$$2H_2(g) + CF_4(g) + 50H_2O(l) \rightarrow 4[HF{:}50H_2O](l) + C(c) \qquad -84.2 \text{ kcal(mol } CF_4)^{-1} \qquad (2)$$

$$2H_2(g) + CO_2(g) \rightarrow C(c) + 2H_2O(l) \qquad -42.59 \text{ kcal(mol } CO_2)^{-1} \qquad (3)$$

TABLE 7. F_2-H_2-H_2O *reaction*

a. Heat measurements

	Series 1					Series 2				
Expt. No.	1	2	3	4	5	6	7	8	9	10
m_s ..... g ...	3.5504	2.7483	2.7084	1.3165	2.7981	2.9859	2.4623	2.6524	3.1136	2.4048
Δt(corr) ..... °C ...	0.05552	0.03351	0.03381	0.07354	0.02279	0.07565	0.02937	0.03237	0.04481	0.05046
Δt_c ..... °C ...	2.71469	2.10439	2.07278	1.01125	2.14415	2.29429	1.89230	2.04004	2.39349	2.61824
t(av) ..... °C ...	30.35	30.73	30.73	30.02	30.74	30.16	30.78	30.69	30.51	30.30
Δe ..... J(°C)$^{-1}$ ...	1.8	1.4	1.4	1.0	1.4	1.6	1.6	1.4	1.6	1.8
E(calorim) ..... J(°C)$^{-1}$ ...	21889.7	21889.3	21889.3	21888.9	21889.3	21889.5	21889.5	21889.3	21889.5	21889.7
q(obs) ..... J ...	59423.7	46063.6	45371.7	22135.2	46933.9	50220.9	41421.5	44655.0	52392.3	57312.5
n_{H_2O}/n_{HF}	30.4	38.9	39.8	82.9	38.2	35.8	44.3	40.9	34.8	31.8

b. Reaction quantities

n_{F_2} ..... mol ...	0.09243	0.07155	0.07051	0.03427	0.07284	0.07773	0.06410	0.06905	0.08111	0.08864
$n_{HF}(CF_4)$ ..... mol ...	.00020	.00016	.00016	.00008	.00016	.00016	.00012	.00016	.00016	.00020
n_{HF}(calc) ..... mol ...	.18506	.14326	.14118	.06862	.14584	.15562	.12832	.13826	.16238	.17748
n_{HF}(obs) ..... mol ...	.18277	.14267	.13965	.06706	.14532	.15502	.12545	.13596	.15938	.17453
Δn_{HF}(obs-calc) ..... mol ...	−.00229	−.00059	−.00153	−.00156	−.00052	−.00060	−.00287	−.00230	−.00300	−.00295
n_{HF}(obs)/n_{HF}(calc)	.9876	.9959	.9891	.9772	.9964	.9961	.9776	.9833	.9815	.9833

c. Corrections to heat data

q(ign) ..... J ...	17.6	30.0	14.8	19.6	23.2	22.4	19.0	23.8	30.2	24.1
q'(vap) ..... J ...	122.6	100.3	100.3	56.9	90.8	120.9	89.9	95.8	109.2	104.0
q''(vap) ..... J ...	31.4	24.3	25.5	14.2	22.4	26.3	21.4	21.3	25.1	30.7
q(temp) ..... J ...	−15.5	−7.3	−13.8	−1.5	−25.1	−11.1	−15.5	−14.6	−19.2	−34.9
$q(O_2)$ ..... J ...	205.8	159.8	159.8	74.0	165.7	177.0	142.0	154.4	182.8	200.0
qCF_4 ..... J ...	17.6	14.1	14.1	6.7	14.1	14.1	10.5	14.4	14.1	17.6
$q(CO_2)$ ..... J ...	1.7	1.7	1.7	.8	1.7	1.7	1.7	1.7	1.7	1.7
q(diln) ..... J ...	−12.2	−6.5	−5.3	7.0	−6.1	−7.1	−1.0	−3.4	−8.0	−11.7
Total (1)	369.0	306.4	297.1	163.7	286.7	344.2	268.0	293.4	335.9	331.5
q(corros) ..... J ...	764.	197.	510.	520.	173.	200.	958.	767.	1001.	984.
Total (2)	1133.0	503.4	807.1	683.7	459.7	544.2	1226.0	1060.4	1336.9	1315.6
$q_{F_2}(1)$ ..... J ...	59054.7	45757.2	45074.6	21957.5	46647.2	49876.7	41153.5	44361.6	52056.4	56981.0
$q_{F_2}(2)$ ..... J ...	58290.7	45560.2	44564.6	21437.5	46474.2	49676.	40195.5	43594.6	51055.4	55997.0
$q_{F_2}(1)/n_{HF}(F_2)$ ..... kJ mol^{-1} ...	319.45	319.76	319.63	320.36	320.20	320.83	321.01	321.23	320.90	321.42
$q_{F_2}(1)/n'_{HF}$ [a] ..... kJ mol^{-1} ...	323.46	321.08	323.14	327.82	321.35	322.08	328.36	326.67	326.95	326.86
$q_{F_2}(2)/n'_{HF}$ ..... kJ mol^{-1} ...	319.28	319.70	319.48	320.06	320.16	320.78	320.72	321.02	320.66	321.21

[a] $n'_{HF} = n_{HF}(obs) - n_{HF}(CF_4)$.

q(diln) corrects for diluting the acid solution from a concentration, HF:nH$_2$O, to HF:50H$_2$O. Total (1) is the sum of the corrections to this point and total (2) includes q(corros), a correction for the corrosion of the combustion chamber. Equation (4) is the corrosion reaction assumed and shows the heat of reaction used for calculating q(corros) [22]. The number of moles of reaction (4) is taken to be n_{HF}(obs-calc)/2.

$$F_2(g) + Ni(c) \rightarrow NiF_2(c) \qquad -159.5 \text{ kcal(mol } F_2)^{-1} \qquad (4)$$

The corrections Total (1) and Total (2), table 7, were applied to the observed heat effect to give $q_{F_2}(1)$ and $q_{F^2}(2)$, respectively. We now have three ways of calculating the results. Referring to experiment (1) for example, in the first way the heat of reaction corrected by Total (1) to give $q^{(1)}_{F_2}$ is presumed to be caused by the measured amount of F_2 introduced, giving $q_{F_2}(1)/n_{HF}(F_2) = 319.45$ kJ mol^{-1}. In the second way the same heat of reaction is attributed to reaction of enough fluorine to form the observed amount of HF, giving $q_{F_2}(1)/n'_{HF} = 323.46$ kJ mol^{-1}. In the third way the deficiency of HF is attributed to corrosion forming NiF_2(c), introducing an additional energy correction, q(corros), and allowing a new total energy, $q_{F_2}(2)$ to be attributed to the amount of F_2 needed to form the observed HF. This gives $q_{F^2}(2)/n'_{HF} = 319.28$ kJ mol^{-1}, which we consider to be the best representation of the data. All experiments are treated each way at the bottom of table 7.

The results of two series of five measurements each are summarized in table 8 in which the results obtained by the three methods are listed in columns (1), (2), and (3), respectively. The calculation in column (3) is preferred for reasons described above and experiments of series 2 are considered to be preferable because of a better conditioning procedure for the reaction vessel. Hence, the value $\Delta H^\circ_{303} = -76.69$ kcal mol^{-1} is selected for use in later calculations. This value, corrected to 298.15° gives

$$\Delta H^\circ_{f298.15}[HF \cdot 50H_2O] = -76.68 \text{ kcal mol}^{-1}.$$

TABLE 8. *Heat of fluorine-hydrogen-water reaction*

$\frac{1}{2}F_2(g) + \frac{1}{2}H_2(g) + 50H_2O(l) = [HF \cdot 50H_2O](l)$

	(1) $-\Delta H^\circ_{303}$	σ	(2) $-\Delta H^\circ_{303}$	σ	(3) $-\Delta H^\circ_{303}$	σ
Series 1 (5)..... kJ mol^{-1}...	319.88	0.17	323.37	1.21	319.74	0.15
Series 2 (5)..... kJ mol^{-1}...	321.08	0.11	326.18	1.07	320.87	0.11
Series 1 (5)..... kcal mol^{-1}...	76.45	0.04	77.29	0.29	76.42	0.04
Series 2 (5)..... kcal mol^{-1}...	76.74	0.03	77.96	0.25	76.69	0.03

σ is the standard deviation of the mean.

5.3. The OF_2-Hydrogen-Water Reaction

The data obtained for this reaction are shown in table 9. No new features are involved. The experiments in series 1 were conducted before the electrical cali-

TABLE 9. OF_2-H_2-H_2O *reaction*

a. Heat measurements

	Series 1						Series 2						
Expt. No.	1	2	3	4	5	6	7	8	9	10	11	12	13
m_s..... g..	2.9080	3.4370	3.0869	3.5261	3.4556	3.4512	3.4558	3.4015	3.3549	3.3785	3.4021	3.4929	3.4651
Δt(corr)..... °C..	0.05253	0.04624	0.05224	0.04464	0.05456	0.05402	0.05216	0.05179	0.05348	0.05228	0.04842	0.04621	0.04681
Δt_c..... °C..	2.34591	2.77485	2.49106	2.84661	2.78877	2.78491	2.78889	2.74369	2.70657	2.72699	2.74267	2.81633	2.79548
t(av)..... °C..	30.16	30.37	30.25	30.41	30.38	30.38	30.39	30.37	30.37	30.36	30.50	30.45	30.42
Δe ..... J(°C)$^{-1}$..	3.8	4.0	3.9	4.0	3.9	3.9	3.9	3.9	3.9	3.9	3.9	4.0	4.0
E..... J(°C)$^{-1}$..	21891.7	21891.9	21891.8	21891.9	21891.8	21891.8	21891.8	21891.8	21891.8	21891.8	21891.8	21891.9	21891.9
q(obs)..... J..	51356.0	60746.7	54533.8	62317.7	61051.2	60966.7	61053.8	60064.3	59251.7	59698.7	60042.0	61654.8	61198.4
n_{H_2O}/n_{HF}.....	52.6	44.6	49.4	43.2	44.3	44.4	44.4	45.1	45.8	45.5	45.3	43.8	44.3

b. Reaction quantities

n_{OF_2}..... mol..	0.05351	0.06224	0.05680	0.06488	0.06359	0.06351	0.06359	0.06259	0.06173	0.06217	0.06260	0.06427	0.06376
$n_{HF}(CF_4)$..... mol..	.00016	.00016	.00016	.00016	.00016	.00016	.00016	.00016	.00016	.00016	.00016	.00016	.00016
n_{HF}(calc)..... mol..	.10718	.12664	.11376	.12992	.12734	.12718	.12734	.12534	.12362	.12450	.12536	.12870	.12768
n_{HF}(obs)..... mol..	.10669	.12602	.11380	.13009	.12682	.12634	.12658	.12462	.12266	.12355	.12399	.12811	.12686
Δn_{HF}(obs − calc)..... mol..	−.00049	−.00062	+.00004	+.00017	−.00052	−.00084	−.00076	−.00072	−.00096	−.00095	−.00137	−.00059	−.00082
n_{HF}(obs)/n_{HF}(calc).....	.9954	.9951	1.0003	1.0013	.9959	.9934	.9940	.9942	.9922	.9924	.9890	.9954	.9936

c. Corrections to heat measurements

q(ign)..... J..	17.1	18.9	19.3	14.0	21.6	21.6	16.8	19.6	18.5	14.8	14.8	19.0	19.9
q'(vap)..... J..	140.6	155.0	130.9	162.7	179.1	169.4	148.1	146.1	143.9	154.8	165.7	156.9	148.1
q''(vap)..... J..	31.8	55.6	43.6	45.2	53.1	53.1	53.1	45.2	50.6	50.6	49.8	50.6	50.6
q(temp)..... J..	−22.8	−36.8	−30.1	−35.6	−22.0	−28.4	−38.2	−42.0	−40.2	−34.2	−29.3	−37.0	−41.5
q(diln)..... J..	+1.8	−1.0	−.4	−2.2	−1.0	−1.0	−1.0	−.5	−.5	−.5	−.5	−1.0	−1.0
$q(O_2)$..... J..	234.3	274.0	245.6	285.8	274.0	274.0	274.0	274.0	268.6	268.6	268.6	279.9	279.9
$q(CF_4)$..... J..	14.1	14.1	14.1	14.1	14.1	14.1	14.1	14.1	14.1	14.1	14.1	14.1	14.1
$q(CO_2)$..... J..	8.8	10.5	10.5	10.5	10.5	10.5	10.5	10.5	10.5	10.5	10.5	10.5	10.5
Total (1)..... J..	425.7	490.3	433.5	494.5	529.4	513.3	477.4	467.0	465.5	478.7	493.7	493.0	480.6
q(corros)..... J..	240.	303.	0	0	254.	411.	372.	352.	469.	465.	670.	288.	401.
Total (2)..... J..	665.7	793.3	433.5	494.5	783.4	924.3	849.4	819.0	934.5	943.7	1163.7	781.0	881.6
$q_{OF_2}(1)$..... J..	50930.2	60256.4	54100.2	61823.2	60521.7	60453.4	60576.4	59597.3	58786.2	59220.0	59548.2	61161.8	60717.8
$q_{OF_2}(2)$..... J..	50690.2	59953.4	54100.2	61823.2	60267.7	60042.4	60204.4	59245.3	58317.2	58755.0	58878.2	60873.8	60316.8
$q_{OF_2}(1)/n_{OF_2}$..... kJ(mol)$^{-1}$..	951.79	952.82	952.47	952.88	951.75	951.87	952.61	952.18	952.31	952.55	951.25	951.64	952.29
$q_{OF_2}(1)/n'_{OF_2}$[a]..... kJ(mol)$^{-1}$..	956.17	957.51	952.13	951.71	955.66	958.21	958.33	957.69	959.77	959.96	961.85	956.10	958.45
$q_{OF_2}(2)/n'_{OF_2}$..... kJ(mol)$^{-1}$..	951.66	952.70	952.13	951.71	951.64	951.69	952.45	952.04	952.12	952.35	951.03	951.52	952.12

[a] $n'_{OF_2} = [n_{HF}(obs) - n_{HF}(CF_4)]/2$.

brations were performed, and those in series 2 were conducted later. Otherwise, the procedures used were identical. The average recovery of hydrogen fluoride was better than 99.5 percent. q(corros) for this system was calculated from eq (5) using the heat of reaction given there and a number of moles equal to Δn_{HF}(obs-calc)/2.

$$OF_2(g) + Ni(c) + H_2(g) = H_2O(l) + NiF_2(c)$$

$$-233.78 \text{ kcal (mol } OF_2)^{-1} \qquad (5)$$

The treatment is the same as for the fluorine reaction. The three alternative calculations of the reaction energy are shown at the bottom of table 9 and in table 10, of which the preferred one is based upon the amount of energy, adjusted for the energy of corrosion, and the amount of hydrogen fluoride actually observed. This is given as $\Delta H^\circ_{303}(3)$ of table 10.

TABLE 10. *Heat of* OF_2-H_2-H_2O *reaction*

$OF_2 + 2H_2 + 99H_2O = 2[HF \cdot 50H_2O]$ (*l*)

	$-\Delta H^\circ_{303}(1)$	σ	$-\Delta H^\circ_{303}(2)$	σ	$-\Delta H^\circ_{303}(3)$	σ
Series 1.....kJ mol^{-1}...	952.26		955.23		951.92	
Series 2.....kJ mol^{-1}...	952.12		958.88		951.95	
Total (13 expts).....	952.18	0.14	957.20	0.80	951.94	0.14
Series 1 kcal mol^{-1}.	227.60		228.31		227.51	
Series 2 kcal mol^{-1}.	227.56		229.18		227.52	
Total (13 expts).....	227.58	0.033	228.78	0.19	227.52	0.033

σ is the standard deviation of the mean.

6. Discussion of Errors

The uncertainties are summarized in table 11 for the three reactions and for the calculation of the heat of formation of OF_2(g). The observed standard deviation of the OF_2-H_2-H_2O measurements is 0.14 kJ mol^{-1} or 0.015 percent and that for the electrical calibrations is 0.015 percent. Hence the overall imprecision in the experiments expressed in 2-sigma limits is

$$\pm 2\sqrt{(0.015)^2 + (0.015)^2}$$

$$= \pm 0.042 \text{ percent } (0.40 \text{ kJ mol}^{-1}).$$

Systematic errors in calibration are 0.02 percent for "irrelevance" and 0.02 percent for the transient. Systematic errors in the reaction heat measurements are 0.02 percent for uncertainty in the oxygen content of the sample, and 0.02 percent for uncertainty in the correction for corrosion. Each of these sources of error is explained below. Assuming that these errors are independent we apply them as the square root of the sum of the squares and obtain 0.040 percent (0.38 kJ mol^{-1}) as the overall systematic error. The overall uncertainty in the heat of reaction is, therefore the sum of 0.042 and 0.040 or 0.082 percent (0.78 kJ mol^{-1} or 0.19 kcal mol^{-1}).

The error treatments for the two other reactions are summarized in much the same way. The systematic errors for the O_2-H_2 experiments do not include any uncertainties for analysis or corrosion, but do include systematic errors listed for the calibration. To place these on the same basis as the other calculations, we combine these two systematic errors as the square root of the sum of the squares.

In estimating the uncertainty in the heat of formation of OF_2 we combine the contributions in joules for the three reactions in the following way. The random errors and the chemical errors, which are presumed to be independent for the various reactions, are added without regard to sign; and the systematic calibration errors are added with due regard for the sign with which the reaction equations are added, in order to obtain their contributions to the uncertainty in the heat of formation of OF_2. These contributions, listed

TABLE 11. *Summary of errors*

$\Delta H_{R\ 303\ °K}$ kJ mol^{-1}	951.94		320.88		285.67		
	OF_2-H_2-H_2O		F_2-H_2-H_2O		1/2 O_2-H_2		OF_2
	%	kJ mol^{-1}	%	kJ mol^{-1}	%	kJ mol^{-1}	kJ^{-1}
Random errors:							
Calibration (σ_c).....	0.015	0.14	0.015	0.05	0.015	0.04	.....
Reaction measurement (σ_r).....	.015	.14	.034	.11	.042	.12	.....
Imprecision 2 $\sqrt{\sigma_c^2 + \sigma_r^2}$.....	0.042	0.40	0.074	0.24	0.089	0.25	1.13
Systematic errors:							
Irrelevance of calib.....	0.02	0.19	0.02	0.06	0.02	0.06	.....
Transient.....	.02	.19	.02	.06	.02	.06	.....
Total systematic calib.....	.028	.27	.028	.09	.028	.08	0.01
Analysis.....	.02	.19	.02	.06	.....	.....	.....
Corrosion.....	.02	.19	.02	.06	.....	.....	.....
Total chemical.....	.028	.27	.028	.09	.....	.....	.45
Overall systematic error.....	0.040	0.38	0.040	0.13	0.028	0.08	0.46
Uncertainty.....	0.082	0.78	0.114	0.37	0.117	0.33	1.59
Uncertainty (kcal mol^{-1}).....	.....	0.19	.....	0.09	.....	0.08	0.38

in the right-hand column of table 11, are added to obtain 1.59 kJ mol^{-1} (0.38 kcal mol^{-1}) for the uncertainty in the heat of formation of OF_2(g).

Recent experiments in this laboratory have indicated that to obtain accurate heat measurements in calorimetric studies such as these, using the Dickinson calorimeter, the chemical energy and the energy from the calibration heater should be liberated at nearly the same position in the calorimeter [16]. This would tend to cancel the effect of temperature gradients on the surface of the calorimeter. In the experiments described in this paper, the heater was near the side of the calorimeter (closer to the thermometer), whereas the reaction vessel was near the center. The earlier investigation shows that the energy equivalent determined from the electrical energy measurements may be inappropriate for the calorimeter as used in the chemical energy measurements. This possible uncertainty in the calibration is listed here as the "irrelevance" error and is estimated to have an upper limit of 0.02 percent for these experiments. It is noted that this error probably affects all of the heat measurements by the same fractional amount. It would thus cause an effect too small to be observed in the heat of formation of OF_2 which is calculated from differences between the measurements reported here; however, it could have an observable effect on the values for $\Delta H^\circ_{f298.15}[HF \cdot 50H_2O[(l)$ and $\Delta H^\circ_{f298.15}[H_2O(l)]$. The close agreement of the value found for the latter quantity with that reported by Rossini suggests that no important error is involved.

The "transient" effect has already been discussed in the description of the calibration procedures. Exact measurements of the effect were not made, but the maximum systematic error that could arise from this source was calculated to be 0.02 percent.

On the basis of earlier work [1, 2], we believe that the error in the analysis of the fluorine sample is 0.02 percent. Assuming that this amount of uncertainty is distributed among the F_2, N_2, and O_2 analyses, different values for n_{HF}(calc), q_{O_2}, and q(corros) are obtained (table 12). The variations amount to less than .02 percent.

We can demonstrate the validity of the overall corrosion correction applied in the following way. In figure 5 we have plotted the heats of reaction, corrected and uncorrected for corrosion, versus the percentage correction for corrosion for the F_2-H_2-H_2O and OF_2-H_2-H_2O reactions. The data plotted are obtained from tables 7 and 9, respectively. The data were fitted to the lines shown by the method of least squares and the equations are shown on the illustration. For both reactions there is a linear variation of the uncorrected heat of reaction with the q(corros) which was essentially eliminated, when q(corros) was applied. This illustration also shows why, in tables 8 and 10, the standard deviation of the mean of $\Delta H(3)$ is much less than for $\Delta H(2)$. The application of q(corros) smooths out an effect present in varying degrees in each of the experiments.

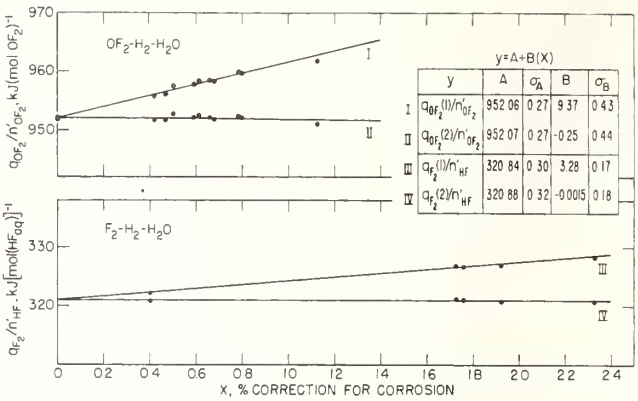

FIGURE 5. *Plot showing the variation of the heats of the* $F_2-H_2-H_2O$ *and* $OF_2-H_2-H_2O$ *reactions versus the percentage correction for corrosion.*

(X = q(corros) × 100/q(1), tables 7 and 9)

7. The Heat of Formation of Oxygen Difluoride. The (O-F) Bond Energy

We summarize the heat measurements and the heat of formation of OF_2 in table 13. The calculated heat of formation at 303.4 °K becomes the same value at 298.15 °K to yield $\Delta H^\circ_{f298.15}[OF_2(g)] = +5.86 \pm 0.38$ kcal mol^{-1}. The uncertainty shown represents the estimated accuracy based on the errors discussed. The value for the average O—F bond energy in OF_2 is calculated from this value for $\Delta H^\circ_f[OF_2(g)]$, using $\Delta H^\circ_f[O(g)] = 59.553$, and $\Delta H^\circ_f[2F(g)] = 37.75$ kcal mol^{-1} [8], to be 45.72 kcal mol^{-1}.

TABLE 12. F_2-H_2-H_2O *reaction*

Expt. #8 wt F_2 sample, 2.6524 g			
Column 1	2	3	4
F_2 (%)	98.92	98.90	98.90
N_2 (%)	0.54	0.56	0.54
O_2 (%)	.33	.33	.35
CF_4 (%)	.13	.13	.13
n_{HF}(calc)	0.13826	0.13824	0.13824
n_{HF}(obs)	.13596	.13596	.13596
Δn_{HF}(obs-calc)	.00230	.00228	.00228
q(corros) J	767.0	761.0	761.0
q_{O_2} J	154.3	154.3	165.7
sum of q(corros) and q_{O_2} J	921.3	915.3	926.7
q(obs) J	44655.0	44655.0	44655.0
% change in ΔH_R		−0.013	+0.012

TABLE 13. *The heat of formation of* OF_2

	$\Delta H_{R,303\ °K}$ kcal	
$OF_2(g) + 2H_2(g) + 99H_2O(l) \longrightarrow 2[HF \cdot 50H_2O](l)$	-227.52 ± 0.19	(6)
$F_2(g) + H_2(g) + 100H_2O(l) \longrightarrow 2[HF \cdot 50H_2O](l)$	-153.38 ± 0.18	(7)
$1/2\ O_2(g) + H_2(g) \longrightarrow H_2O(l)$	-68.28 ± 0.08	(8)
$F_2(g) + 1/2\ O_2(g) \longrightarrow OF_2(g)\ \Delta H^\circ_{f298.15}[OF_2(g)] = +5.86$ kcal ± 0.38		(9)

In table 14 we give the reactions investigated in the earlier work and compare the value reported for $\Delta H^\circ_{f298.15}[OF_2(g)]$ with the value [+5.86 ± 0.38 kcal

TABLE 14. *Earlier thermochemical studies involving* $OF_2(g)$

	Temp °K	$-\Delta H^\circ$ kcal mol^{-1}	$\Delta H_{f298}[OF_2]$	Ref
1. $OF_2(g)+2KOH$ (excess KOH aq 40%)$=[2KF+H_2O]$ (aq KOH)$+O_2(g)$	291	125.75	+6.9	[3, 6, 23]
2. $OF_2(g)+[6KI+2HF]$ (excess aq soln)$=[4KF+2KI_3+H_2O]$ (aq KI + HF soln)	291	176.55	+1.4	[3, 6, 23]
3. $OF_2(g)+4HBr$ (excess HBr aq 45%)$=[2HF+2Br_2]$ (aq HBr)$+H_2O$	291	134.36	+8.8 Av $+5.7\pm2$ [a]	[3, 6, 23]
4. $OF_2(g)+2H_2(g)+2NaOH$ (excess aq 20%)$=2NaF$ (in aq NaOH)$+3H_2O(l)$		254.9		[4, 23]
5. $\frac{1}{2}O_2(g)+H_2(g)=H_2O(l)$		68.5		[4, 23]
6. $F_2(g)+H_2(g)+2NaOH$ (excess aq 20%)$=2NaF$ (in aq NaOH)$+2H_2O(l)$		181.7	$+4.7\pm2$ [a]	[4, 23]
7. $OF_2(g)+H_2(g)$ (excess)$+nH_2O(l)=[2HF+(n+1)H_2O](l)\{n=\infty\}$		222.93	-4.06 ± 2.2 [a]	[9, 23]
8. The present work (see table 13)			$+5.86\pm0.38$	

[a] Estimated overall uncertainty given in original report.

mol^{-1}] derived from the present study. Our value agrees consistently with those reported by von Wartenberg and Klinkott [$+5.7\pm2$ kcal mol^{-1}], and Ruff and Menzel [$+4.7\pm2$ kcal mol^{-1}], but differs from Bisbee's results [-4.06 ± 2.2 kcal mol^{-1}].

In the various reviews which have been conducted on these studies so far, the biggest improvement in the re-evaluation of the original data has been to substitute current auxiliary data for the reactions studied by von Wartenberg and Klinkott. Ruff and Menzel measured the heats of principal reaction (4) and the auxiliary reactions ((5) and (6)) for calculating their value for $\Delta H^\circ_{f298.15}[OF_2]$. Bisbee's value for $\Delta H^\circ_{f298.15}[OF_2]$ will change as improvements are made in the $\Delta H^\circ_{f298.15}[HF, aq, \infty]$, the principal auxiliary data on which their results are based. However, it seems unlikely that the $\Delta H^\circ_{f298.15}[HF, aq, \infty]$ will ever be revised by an amount that will change the sign of their value for $\Delta H^\circ_{f298.15}[OF_2]$.

No attempt will be made here to review completely the earlier studies. However, in re-examining the work of Bisbee et al., we note several points about their experiments which may lead to a less negative observed heat of reaction, and therefore explain the more negative heat-of-formation value which they reported. They give little information on the (1) analysis of the sample, (2) the technique used to insure mixing of the solution, (3) the corrosion by the product HF, and (4) the quantitative basis for the heat of reaction. Each of these aspects of their experiments is very important in the accuracy of the work. For example, oxygen is a usual impurity in the OF_2 produced by the present-day method ($F_2 + NaOH$) and would react with H_2 under the conditions of these experiments. These authors mention no test for oxygen and therefore no correction for its heat of reaction.

The measurements were made in a stationary bomb, using a fairly massive internal container for $OF_2(g)$ which was ruptured to initiate reaction with H_2. The reaction products consisted of H_2O and HF in a condensed phase, formed in the presence of excess $H_2O(l)$. The formation of a homogeneous HF(aq) phase was presumed. However, experience in reactions in which condensation occurs in a stationary bomb indicates that much of the condensation would occur on the walls and would form droplets of a solution quite different from the bulk solution. Mixing these two solutions would evolve heat in addition to that which was measured. The massive OF_2 ampoule could also retain significant quantities of heat for an appreciable time, and the complete equilibration of the heat distribution was not described. Both of these processes would appear to act in the same direction, causing the measured amount of heat to be less than could have been evolved if equilibrium had been achieved. If any errors of these types exist in the experiments, a less negative heat of formation would be indicated for OF_2 than was reported.

The authors wish to acknowledge assistance received from several staff members of the National Bureau of Standards. Mr. James Baylor of the Shops Division made several valuable suggestions for the design of the reaction vessel. Mr. William Dorko and Mr. E. E. Hughes performed the mass spectrometric analyses, and Mr. T. C. Rains performed the analyses for metal ions in the hydrofluoric acid solutions.

8. Appendix

8.1. The Analyses of the Oxidizer Gases

a. Oxygen

The oxygen sample was transferred from the large cylinder to the weighing containers with a manifold of a type also used for filling oxygen combustion bombs [16]. Prior to being filled the container was evacuated and then purged three times with 2–3 atm of oxygen. Finally, the container was filled to about 14 atm. Although further purification probably was unnecessary, during the filling procedure the oxygen was passed through a column of CuO, heated to 500 °C, and through successive columns of Ascarite and magnesium perchlorate.

The oxygen in the weighing bulb was analyzed for argon by mass spectrometry. The concentration of argon was found to be 29 ± 10 parts per million. Nitrogen was determined by gas chromatography using the method reported by Kyryacos and Boord [24]. The equipment consisted of a commercially available chromatograph equipped with an electrically

heated column oven, a thermal conductivity cell, and a strip-chart recording potentiometer (−0.2 to +1.0 mV). Molecular Sieve Type 5A was used as column material with helium as carrier gas. The sample was introduced into the column with a commercial gas sampling valve, modified with a 10-cm³ sample loop. Nitrogen could not be detected in smaller samples. The reliability of the method was checked with one-cm³ samples of air.

The conditions are given on the chromatogram in figure 6. The small effect attributed to nitrogen was quite reproducible, and verified by the injection of air.

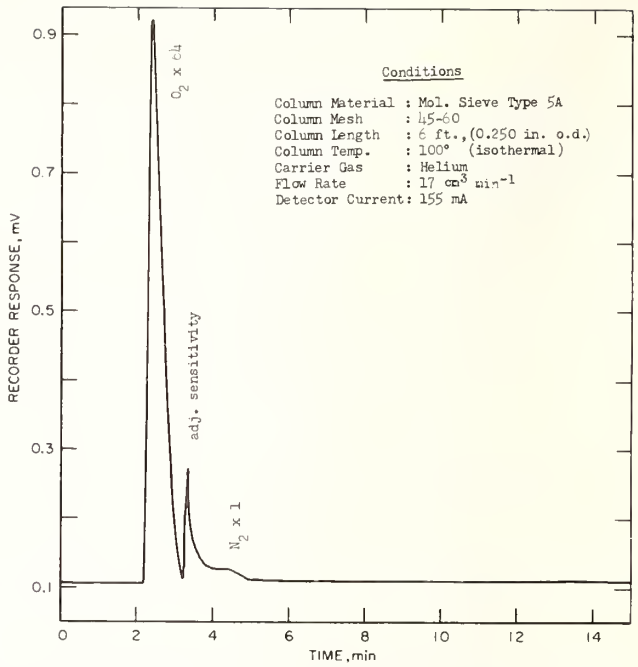

FIGURE 6. *Chromatogram of the oxygen sample on Molecular Sieve Type 5A.*

b. Fluorine

The fluorine was transferred to the spherical sample containers using the manifold and apparatus shown in figure 7. The general procedure for filling the containers consists of (1) evacuating the containers and connecting lines, (2) conditioning and purging the manifold and parts of the connected apparatus with fluorine, (3) filling the bulbs to the desired pressure, and (4) disposing of the fluorine in the connecting lines. To insure that the bulbs were conditioned thoroughly, they were filled repeatedly with a low pressure of fluorine (2 atm), and emptied. Finally they were filled to a working pressure of 13 atm.

Mercury absorption is a well-known technique and has been used extensively for the analysis of fluorine [1, 25, 26]. Although this method appears to be satisfactory, there is some question as to whether the mercury selectively absorbs fluorine from other reactive gases like NF_3 and OF_2 which possibly are present as impurities. These substances may react with mercury under the conditions of the test and produce some N_2 and O_2 which are the major impurities ordinarily contained in fluorine.

The chromatographic procedures developed for analysis of the residual gas are independent of the mass spectrometric method. However, the qualitative identification of the impurities obtained in the latter method is useful for selection of chromatographic column materials.

In addition to the usual chromatographic equipment, the method developed requires (1) a fluorine source, (2) a flask containing mercury for reaction of the fluorine, (3) a loop for containing chromatographic samples of the residual gas, (4) a soda-lime column for disposal of fluorine, and (5) a vacuum source. All of these items were arranged around a manifold as shown in figure 8.

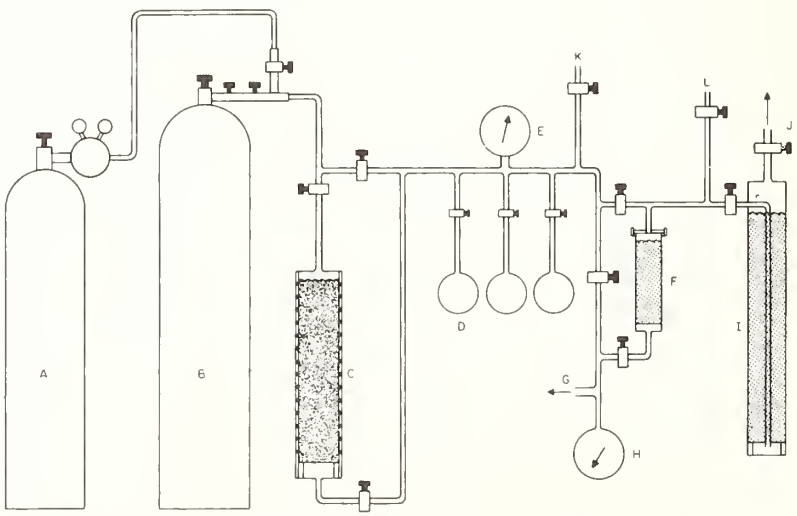

FIGURE 7. *Gas sampling manifold and connected apparatus* (F_2 *and* OF_2).

A, Nitrogen; B, Fluorine or oxygen difluoride; C, Sodium fluoride column; D, Sample bulbs; E, Pressure gauge; F, Fluorine absorption tower; G, Vacuum source; H, Vacuum gauge; I, Fluorine absorption tower; J, Outlet to hood; K, L, to calorimeter flow system.

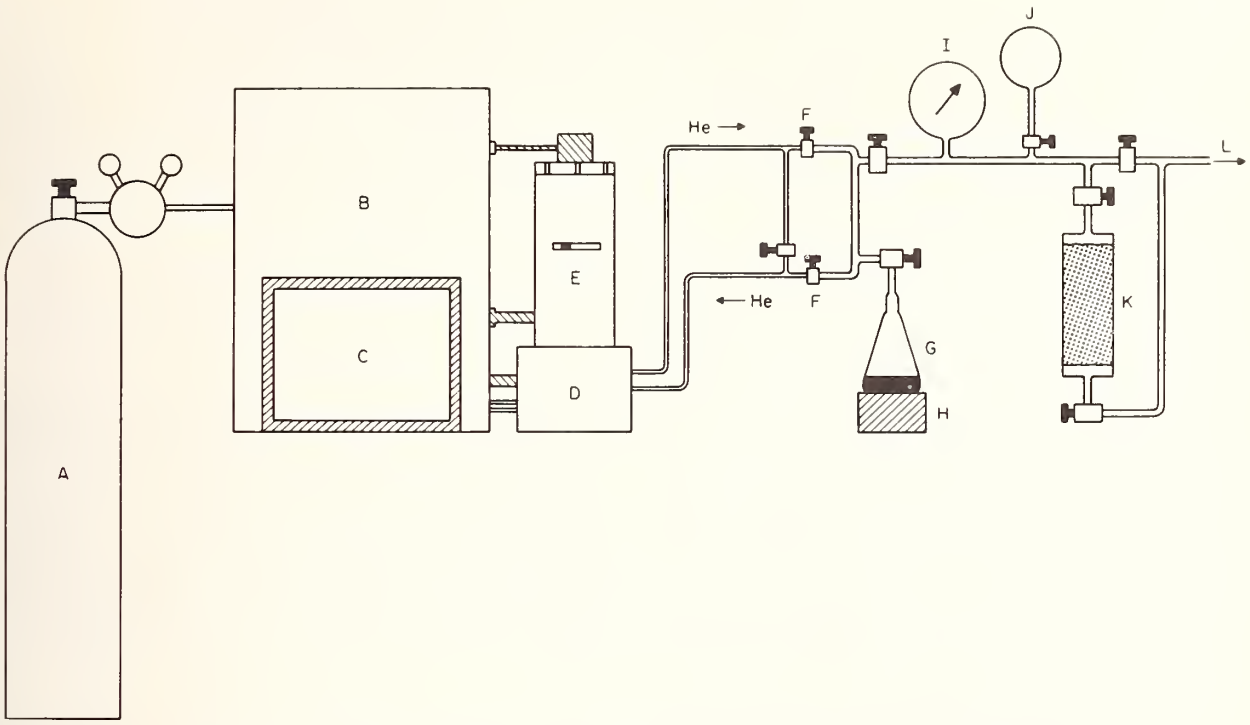

FIGURE 8. *Manifold and apparatus for chromatographic analysis of impurities in fluorine.*
A, Helium; B, Chromatograph; C, Recorder; D, Detector block; E, Column heater; F, Valves; G, Flask with mercury (300-cm³ flask); H, Magnetic stirring motor; I, Vacuum gauge; J, Fluorine sample; K, Fluorine absorption tower; L, Vacuum source.

The equipment preceding valves (F) is ordinarily used in chromatographic analyses and has been described for the oxygen analyses. The steps in the preparation of the system to receive the sample are: (1) close valves (F) and then evacuate remaining parts of system; (2) close flask and admit small amount of fluorine from container (J) for conditioning manifold; and (3) remove fluorine from lines by evacuation through soda-lime column (K). The conditioning procedure is repeated several times. The sample is then introduced by placing one atm of fluorine in the flask. A surface film forms on the mercury which prevents further reaction until the mercury is agitated. The flask contains a Teflon-covered magnet and is placed on a magnetic stirring motor so that the mercury can be agitated with the flask in place. However, to insure complete reaction of the fluorine, it is preferable to disconnect the flask from the manifold so that it can be shaken vigorously by hand. After the fluorine has completely reacted, the flask is reconnected to the manifold and the sample loop is evacuated. Appropriate valves are adjusted so that when the flask is opened the residual gas expands into the sample loop. To introduce the sample into the chromatograph, the valves are adjusted so that the helium from the chromatograph flushes the residual gas into the column. The reaction flask is left in place so that the analyses can be repeated.

Mass spectrometric analyses on other samples of residual gas from commercial fluorine had shown that the major impurities were nitrogen, oxygen, carbon tetrafluoride, and carbon dioxide, with smaller amounts of silicon tetrafluoride, sulfur hexafluoride and fluorocarbons. On this basis Molecular Sieve Type 5A and silica gel were selected for the chromatographic column materials. Molecular Sieve Type 5A, used in the procedure of Kyryacos and Boord [24], separates nitrogen from oxygen, but shows no separation efficiency toward the other impurities. Silica gel [10] separates oxygen plus nitrogen from the carbon tetrafluoride and carbon dioxide. Typical chromatograms are shown in figures 9 and 10, respectively. The conditions for the analyses are given on the chromatograms. The peak components were checked with injections of air, pure carbon tetrafluoride and carbon dioxide. Prior to the analyses both columns were conditioned at 300 °C under a flowing helium atmosphere.

After the chromatographic analyses, the sample loop was disconnected from the chromatograph at the two valves, F. On one valve a Pyrex breakoff-tip type ampoule was attached, and the ampoule and connecting lines were evacuated. The ampoule was filled with residual gas from the flask and sealed. A mass spectrometric analysis was performed on this sample. The results from the two methods are compared in table 15. Considering that these are two completely different techniques, the results are in good agreement. This agreement suggests that the chromatographic method may be developed further and used routinely as a second way of analysing for the impurities in ordinary commerical fluorine, which is usually reported to be of a purity of not better than 98 percent.

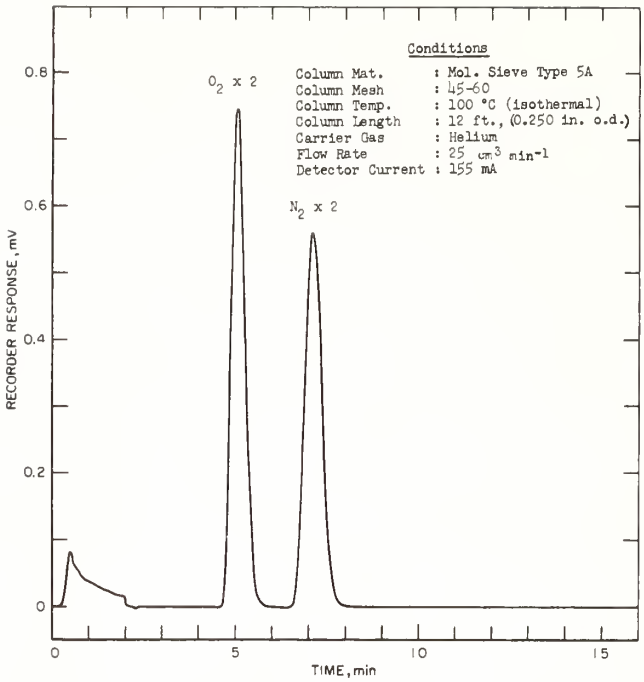

FIGURE 9. *Chromatogram of impurities in the fluorine sample on Molecular Sieve Type 5A.*

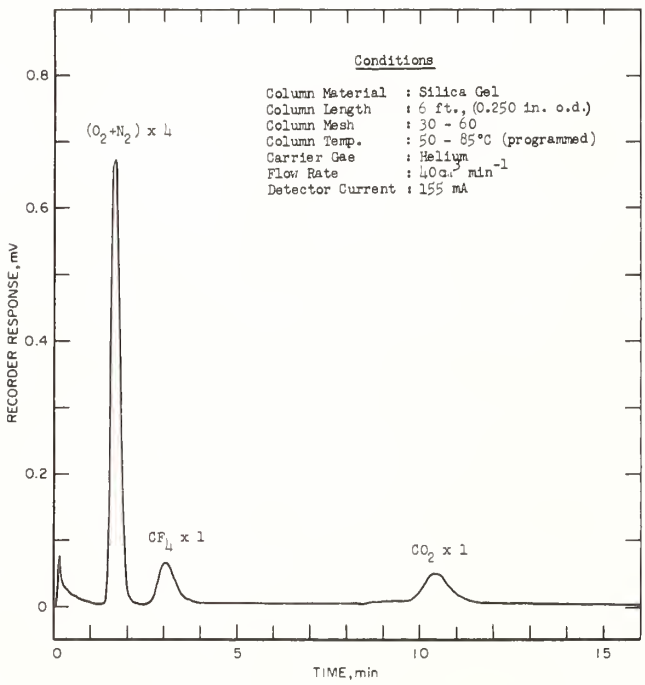

FIGURE 10. *Chromatogram of Impurities in the fluorine sample on silica gel.*

The data in tables 1 and 15 show a difference between the relative amounts of oxygen and nitrogen in the residual gas in the flask used for chromatography, compared to the residual gas used from the

TABLE 15. *Comparison of chromatographic and mass spectrometric analyses for impurities in fluorine*

Impurity	Mole percent of total impurities	
	Chromatography	Mass spectrometry
N_2	45.	42.6
O_2	47.	47.7
CF_4	3.6	2.8
CO_2	4.6	5.1
SO_2F_2		0.22
Ar		.2
SiF_4		1.1
C_2F_6		0.21
C_3F_8		.04

spherical bulbs. The larger amount of oxygen impurity in the Erlenmeyer flask suggests that some oxygen may have arisen from the mercury because there was 1000g mercury in the Erlenmeyer flask, as compared to 150g of mercury in the flask used for the analysis given in table 1. There is reason to believe that the analysis can be improved by conditioning the mercury and flask surfaces also with a small amount of fluorine, prior to filling the flask with the one atmosphere of gas needed for the analysis.

c. Oxygen Difluoride

The oxygen difluoride was transferred to the sample containers using the same manifold and equipment shown in figure 7. The procedures used were the same as those used in sampling the fluorine, except that the oxygen difluoride was not passed over the sodium fluoride. The sample containers were filled to approximately 8 atm with OF_2.

An infrared spectrum of the oxygen difluoride sample was made and compared with spectra in the literature [27, 28]. The cell was Pyrex with silver chloride windows. The windows were clamped in place and sealed to the cell with Kel-F O-rings. The spectrum is shown in figure 11. An absorption band presumed to be due to the impurity CF_4, is indicated.

The equipment used for the chromatographic analyses already has been described for the oxygen and fluorine analyses. The OF_2 sample container is connected to a loop which can be purged with helium from the chromatograph. Silica gel was used for the column material. Prior to the analyses, the column was conditioned at 350° for one hour under a flowing helium atmosphere. The other conditions for the analyses are given on figures 12 and 13 which show the chromatograms obtained.

In the complete chromatogram, four peaks were obtained. These were verified to be due to O_2 (or air), OF_2, CF_4, and CO_2. Analyses were made with the column temperature at 0° and 50 °C. At 0 °C nearly complete separation was achieved between the O_2 and OF_2 (figure 12), but the CO_2 peak was either very slurred or the fraction did not elute at this temperature. At 50 °C, the separation between the O_2 and OF_2 was poor but separation and elution of CO_2 could be obtained by temperature programming. After elution of the O_2 and OF_2, the column was temperature-programmed to a final temperature of 150 °C for

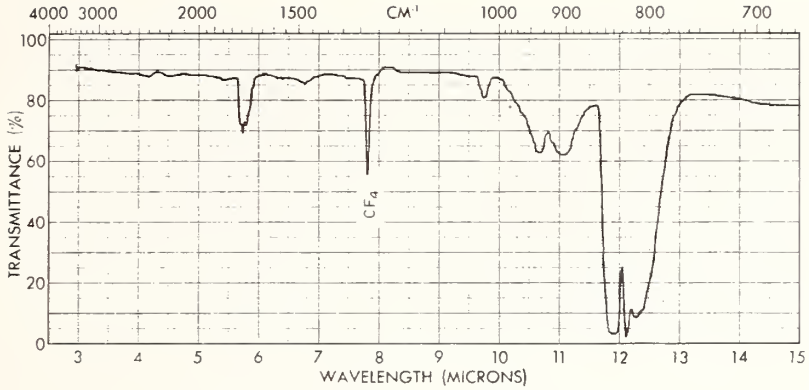

FIGURE 11. *IR spectrum of the* OF_2 *sample.*
Note CF_4 band at 780 microns.

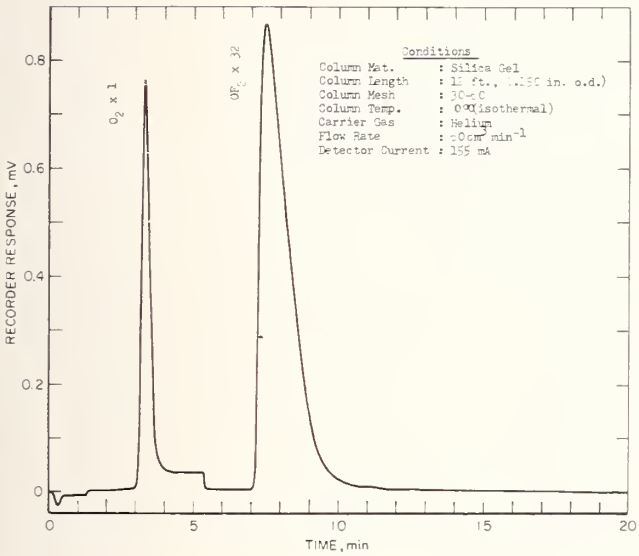

FIGURE 12. *Chromatogram of the* OF_2 *sample on silica gel (0 °C).*

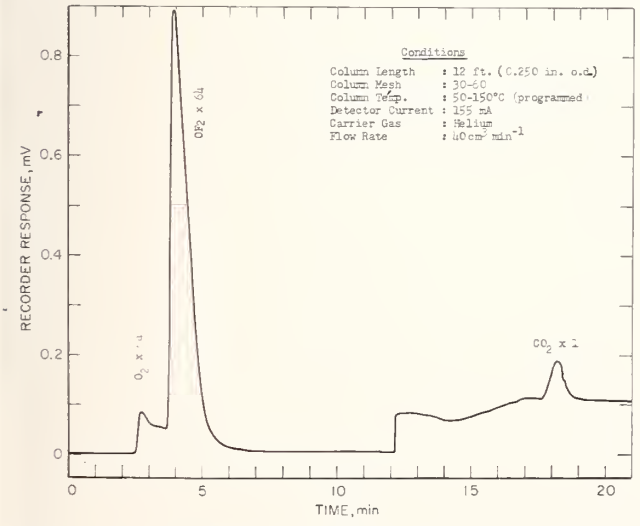

FIGURE 13. *Chromatogram of the* OF_2 *sample on silica gel (50 °C).*
(The column was programmed to 150 °C beginning at 12 mins.)

elution of the CO_2 (fig. 13). In agreement with Kesting's observations [10], the CF_4 eluted on the "tail" of the OF_2 fraction. The CF_4 peak was evaluated from other chromatograms obtained with the instrument set on the most sensitive scale.

Repeated analyses were made on several bulb fillings and the results were quite reproducible. We accepted the findings of Kesting, et al. [10], that the peak area percent for the observed components (OF_2, CO_2, O_2, CF_4) was very nearly equal to mole percent. The peak areas were evaluated both analytically and by counting squares.

Several preliminary analyses were carried out before a procedure was accepted for these experiments. Because of the reactivity of the OF_2, it is conceivable that OF_2 reacts with the silica gel. During preliminary analyses at various column temperatures, it was noted that extraneous peaks appeared at a temperature of 75 °C, and also that even at 50°, the mole percent of OF_2 decreased while the mole percent of O_2 increased. These preliminary analyses suggest that silica gel is not a generally useful column material for chromatographic analyses of the reactive inorganic fluorides. However, under the proper conditions silica gel has good separation efficiency toward OF_2 and inert component impurities such as O_2 and CF_4.

9. References

[1] G. T. Armstrong and R. S. Jessup, J. Res. NBS **64A** (Phys. and Chem.) No. 1, 49 (1960).
[2] G. T. Armstrong, Experimental Thermochemistry, Vol. II., Ch. 7, ed. H. A. Skinner (Interscience Publishers, Inc., New York, N.Y., 1962).
[3] H. v. Wartenberg and G. Z. Klinkott, Z. anorg. u. allgem. Chem. **193,** 409 (1930).
[4] O. Ruff and W. Menzel, Z. anorg. u. allgem. Chem. **190,** 257 (1930).
[5] W. H. Evans, T. R. Munson, and D. D. Wagman, J. Res. NBS **55,** 147 (1955) RP2614.
[6] R. C. King and G. T. Armstrong, Interagency Chemical Rocket Propellant Group, Thermochemistry Working Group, Bulletin of the Fifth Meeting March 15–17, 1967, Vol. 1., Chemical Propulsion Information Agency, Publication CPIA No. 146, pp. 69–96, May 1967.

[7] JANAF Thermochemical Tables, PB 168370, Dow Chemical Co., Midland, Michigan (Clearinghouse for Federal Scientific and Technical Information, Springfield, Va., August 1966).
[8] D. D. Wagman, W. H. Evans, I. Halow, V. B. Parker, S. M. Bailey, and R. H. Schumm, Selected Values of Chemical Thermodynamic Properties. Part 1. Tables for the First Twenty-Three Elements in the Standard Order of Arrangement, NBS Tech. Note 270-1 (U.S. Government Printing Office, Washington, D.C. 20402, 1965).
[9] W. R. Bisbee, J. V. Hamilton, R. Rushworth, T. J. Houser, and J. M. Gerhauser, Advan. Chem. Ser. **54,** 215 (1965).
[10] W. R. Kesting, General Chemical Division, Allied Chem. Corp., Baton Rouge, La., private communication; W. R. Kesting, J. E. Crosslin, and B. W. Bridwell, Analysis of Oxygen Difluoride, Report of the Analytical Chemistry Working Group, 22nd Meeting, ed., John W. Gunn, Jr. (Chemical Propulsion Information Agency, Nov. 3, 1965.)
[11] J. C. Brosheer, F. A. Lenfesty, and K. L. Ellmore, Ind. Eng. Chem. **39,** 423 (1947).
[12] H. C. Dickinson, Bull. BS **11,** 189 (1915).
[13] E. J. Prosen, W. H. Johnson, and F. Y. Pergiel, J. Res. NBS **62,** 43 (1959) RP2927.
[14] E. D. West and D. C. Ginnings, Rev. Sci. Instr. **28,** 1070 (1957).
[15] D. C. Ginnings and E. D. West, Rev. Sci. Instr. **35,** 965 (1964).
[16] K. L. Churney and G. T. Armstrong, submitted for publication J. Res. NBS.
[17] C. H. Shomate, Computer Calculations of Combustion Bomb Calorimetric Data, Technical Progress Report 327, NOTS TP 3288, U.S. Naval Ordnance Test Station, China Lake, Calif., August 1963.
[18] A. E. Cameron and E. Wichers, J. Am. Chem. Soc. **84,** 4175 (1962).
[19] N. S. Osborne, H. F. Stimson, and D. C. Ginnings, J. Res. NBS **23,** 197 (1939) RP1228.
[20] T. Thorvaldson and E. C. Bailey, Can. J. Res. **24,** 51 (1946).
[21] F. D. Rossini, J. Res. NBS **6,** 1 (1931) R.P.259; see also Chapter 4 Experimental Thermochemistry, ed. F. D. Rossini (Interscience Publishers, Inc., New York, N.Y., 1956).
[22] E. Rudzitis, E. H. Van Deventer, and W. N. Hubbard, J. Chem. Eng. Data **12,** 133 (1967).
[23] W. H. Evans, National Bureau of Standards, private communication.
[24] G. Kyryacos and C. E. Boord, Anal. Chem. **29,** 787 (1957).
[25] L. A. Bigelow, Chem. Revs. **40,** 110 (1947).
[26] H. Schmitz and H. J. Schumacher, Z. anorg. u. allgem. Chem. **245,** 221 (1940).
[27] H. J. Bernstein and J. Powling, J. Chem. Phys. **18,** 685 (1950).
[28] E. A. Jones, J. S. Kirby-Smith, P. J. H. Woltz, and A. H. Nielsen, J. Chem. Phys. **19,** 337 (1951).

(Paper 72A2-487)

6. Heat Transfer

Journal of Research of the National Bureau of Standards Vol. 57, No. 6, December 1956 Research Paper 2726

Heat Conduction Through Insulating Supports in Very Low Temperature Equipment[1]

R. P. Mikesell and R. B. Scott

An apparatus is described that is used to measure the heat conduction through insulating supports of storage vessels for cryogenic liquids and presents the data obtained from the conduction measurements. Two types of supports were tested: (1) multiple-contact supports in the form of stacks of thin metallic plates or spirally wound strips, and (2) nonmetallic spheres. The high thermal resistance of the multiple-contact supports arises from the numerous relatively poor contacts between the individual plates. Some special treatments of the plates were tried, and two of these, perforating and dusting, were found to be effective. Pyrex-glass spheres were also found to be excellent insulators, but, of course, are not as rugged as a stack of metal plates. Of the untreated plates tested, those of stainless steel (0.0008 inch thick) were found to be the best insulators per unit length of stack. The heat conduction through these plates, at a load pressure of 1,000 pounds per square inch, was found to be 2 percent of the conduction by a solid sample of the same metal having the same dimensions.

1. Introduction

The most efficient containers for storing and transporting low-temperature liquids, such as liquid oxygen, nitrogen, and hydrogen, are the vacuum-jacketed type known as Dewar vessels. In the past, several types of heat insulators have been used to bridge the vacuum space and furnish support for the inner container. For small laboratory-type Dewars, the design of insulators is not a major problem, but when designing a vacuum-insulated container of several hundred liters or more, which must have ruggedness to withstand the shocks and vibration of transportation by any type of carrier, the problem of insulating supports becomes a serious one.

The recent development of a large aluminum Dewar at the Bureau's Cyrogenic Engineering laboratory included the design of some new type insulating supports, which were of such a nature that their insulating properties could not be computed from the thermal conductivity of the materials from which they were constructed. For this reason, an apparatus was constructed to measure the heat conduction through these supports. Some of the supports were found to have such good insulating and structural properties that it is believed they will have an extended usefulness, and that information obtained from the tests will have general value in the design of Dewar equipment.

2. Experimental Details

2.1. Description of Apparatus

In order to simulate conditions actually encountered in practice, the calorimeter for measuring the heat conduction was itself a Dewar vessel. With this apparatus it was possible to measure the total heat conduction of the specimen when it was subjected to loads ranging from approximately 30 pounds to approximately 1,050 pounds and under the following temperature conditions: (1) room temperature to liquid-nitrogen temperature (296° to 76° K), (2) liquid-nitrogen to liquid-hydrogen temperature (76° to 20° K), and (3) room temperature to liquid-hydrogen temperature (296° to 20° K). These temperatures are the boundary conditions encountered in liquid-hydrogen Dewars, which are provided with a liquid-nitrogen-cooled radiation shield between the liquid hydrogen and the room-temperature shell.

The apparatus (fig. 1) was designed so that the calorimeter is a metal Dewar with the test specimen acting as a separating and insulating member. The specimen is placed between the bottom plate of the inner container, into which is poured liquid nitrogen or hydrogen, and the bottom plate of the outer container, which is at room temperature or liquid-nitrogen temperature. A 5-liter Dewar containing liquid nitrogen surrounds the calorimeter when it is required to have the exterior wall of the calorimeter at liquid-nitrogen temperature.

The outside container is secured in a vertical position by means of the ○-ring flange, which rests upon a wall bracket not shown in the diagram. The ○-ring seal is completed by a top flange, through the center of which passes a tube (8–18 stainless steel, 1¼-in. outside diameter, 1/16-in. wall), which is connected to the inner container. The vacuum system, consisting of a cold trap, diffusion pump, and forepump, is connected to the outer container.

The central tube serves both as the neck of the calorimeter-Dewar and as the compression member for transmitting the load from the fulcrum point of the lever arm to the specimen. This vertical load is the force resulting from a movable weight mounted on a lever arm. A metal bellows permits the central tube to move vertically through guides that also prevent horizontal motion. The brass plate is soldered to the bellows, is sealed to the outer container by means of an ○-ring and is secured in position by four screws. The unit consisting of the inner container or calorimeter, the central tube, the bellows, and the top flange may be easily withdrawn from the outer container to enable one to change the test specimen.

[1] This work was sponsored by the U. S. Atomic Energy Commission.

In order to reduce heat radiation from the side, the surfaces that face the insulating vacuum are covered with bright aluminum sheet. To intercept radiation from above, horizontal metal disks are placed along the central tube both inside and outside.

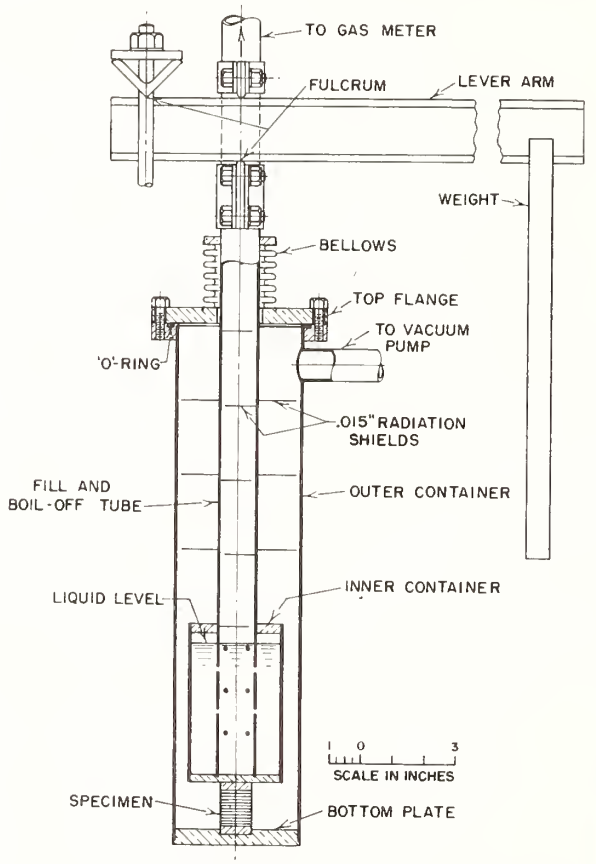

FIGURE 1. *Cross section of the calorimetric apparatus.*

2.2. Test Specimens

The specimens measured in the tests are described n tables 1 and 2.

The round plates (A, fig. 2) 1 in. in diameter, are mounted between brass end plates of the same diameter. Nylon threads tied through small holes in the plates keep them in place. The rectangular plates are mounted in the same manner, with the diagonal of each rectangle approximately the same length as the diameter of the circular end plates. The spheres (B, fig. 2) are held between two stainless-steel plates, each of which has three matching spherical depressions of somewhat larger diameter than that of the spheres (spheres $\frac{3}{16}$-in. radius, depression $\frac{1}{4}$-in. radius). This assembly is also tied together with threads to prevent dislodgment of the spheres during test.

TABLE 1. *Nonmetallic spheres*

Specimen	Dimensions	Comments
Three Pyrex-glass-spheres.	Each sphere, 0.375-in. diameter.	Made from semipolish No. 774 clear chemical glass, manufactured by the J. R. Kilburn Glass Co., Chartley, Mass.
Three soda lime spheres.	Average diameter of spheres, 0.42 in.	Manufactured by Hans L. Landay, Boulder, Colo.
Three ceramic spheres.	Each sphere, 0.39-diameter.	Made from Coors type AB–2 ceramic "high-strength alumina", manufactured by the Coors Porcelain Co., Golden, Colo.
Three Micarta linen-impregnated spheres.	Each sphere, 0.375-in. diameter.	Manufactured by Westinghouse Elect. Mfg. Corp.

TABLE 2. *Multiple-contact specimens (metallic)*

Specimen	Number of plates	Dimensions	Comments
Monel round plates:			
Clean plates	52	1-in. diameter, 0.017-in. thickness	Greased with Dow-Corning high-vacuum grease.
Greased plates	52		
Type 304 stainless-steel round plates:			
Clean plates	49	1-in. diameter, 0.0195-in. thickness	
Type 302 stainless-steel round plates:			
Clean plates	315	1-in. diameter, 0.0008-in. thickness	
Clean plates	313		
Clean plates	209		Dusted with a thin layer of manganese dioxide.
Clean plates	148		
Dusted plates	345		
Type 304 stainless-steel rectangular plates:			
Clean, plain plates	92	$\frac{9}{16}$ by $\frac{3}{4}$ in., 0.004-in. thickness	
Clean, perforated plates	107	$\frac{9}{16}$ by $\frac{3}{4}$ in., 0.004-in. thickness. 18 $\frac{7}{64}$-in.-diameter holes comprise approximately 40% of total area of a plate.	
Alternate layered stack of plain and perforated plates.	61 of each	$\frac{9}{16}$ by $\frac{3}{4}$ in., 0.004-in. thickness. 18 $\frac{7}{64}$-in.-diameter holes comprise approximately 40% of total area of a plate.	The holes of each plate were staggered with respect to the holes of the adjacent plate.
Dusted plain plates	110	$\frac{9}{16}$ by $\frac{3}{4}$ in., 0.004-in. thickness	Holes of adjacent perforated plates were staggered.
Teflon layered stack of plain plates	110	$\frac{9}{16}$ by $\frac{3}{4}$ in., 0.004-in. thickness	The metal plates were separated from each other by Teflon film 0.00025-in. thick.

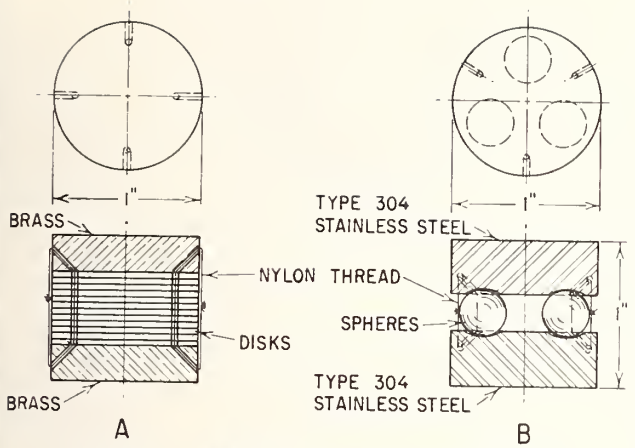

FIGURE 2. *Method for mounting the specimens.*

2.3. Experimental Procedure

With the specimen in place, the calorimeter supplied with liquid hydrogen or nitrogen, the required load applied, and an adequate vacuum (less than 10^{-5} mm Hg) in the insulating space, the volume of gas evaporated from the calorimetric liquid is determined with a wet test gas meter. Readings are continued until a constant rate of evaporation gives assurance that equilibrium has been reached. Volume determinations are adjusted to standard conditions and corrected for the partial pressure of water vapor in the meter. Several sets of readings are made with applied load on the specimen.

The rate of heat flow through the specimen cannot be calculated directly from the evaporation rate because (1) part of the evaporation of the liquid during the measurements is caused by heat transfer other than through the specimen, and (2) the relation between evaporation rate and heat conducted through the specimen is not quite linear because some of the heat flowing down the central tube is intercepted by the cold gas flowing up the tube; thus less heat is conducted down the tube when the rate of evaporation of the liquid is increased. Instead of trying to determine the magnitude of these incidental heat leaks, their effects were taken into account simply by calibrating the apparatus with a known heat input. This was done by lifting the inner container until it no longer made contact with the specimen and conducting another series of measurements of the gas evolved when known values of electric power were supplied to a heater immersed in the liquid in the inner container. The amount of heat conducted through the specimen during a test measurement is assumed to be the same as that supplied to the heater to produce a given rate of evaporation. This assumption is justified if the conditions during the measurements of heat conduction with applied loads are maintained during the calibration measurements.

3. Data and Discussion

3.1. Accuracy of the Data

The values of heat conduction obtained with this apparatus are accurate in most cases to approximately 10 percent. The main causes of error were the following: (1) The fluctuations in the magnitude of the incidental heat leaks, though small, did become important in the measurement of the conduction through the very good insulators, and (2) there were small changes in heat conduction resulting from variations in the exact manner of mounting or loading the specimen.

3.2. Untreated Stacked Plates

Six multiple contact specimens were tested between nitrogen (76° K) and room temperature; five of these were stacks of stainless-steel plates, and the sixth was a stack of Monel plates. Two specimens were tested between liquid-hydrogen temperature (20° K) and liquid-nitrogen temperature (76° K). Since the support of a Dewar is, in most cases, loaded warm, i. e., the load is applied when the support is at room temperature, the data for each specimen, with the exception of the Monel stack, is presented for warm loadings. The Monel stack was loaded cold, i. e. the load was applied when one end of the specimen was at nitrogen temperature. It was found that the conduction by a stack of plates (0.004 in.) subjected to a high pressure was approximately 30 percent greater when the stack was loaded warm than when it was loaded cold.

The results on clean multiple-contact, metal supports [2] are shown in figures 3a, 3b, and 3c, wherein the heat current per unit area is plotted as a function of the pressure on the specimen. The heat conduction through the plates increased with the pressure for two reasons: (1) the area of contact surface was increased, and (2) the heat paths became shorter through a given stack of plates. The conduction was found to be proportional to something less than the first power of the pressure, there being a tendency for the curves to level off as increased pressure had less effect. Thus, the stack of plates acted as a good insulator, even at the higher pressures.

The points below a pressure of 300 psi were not especially reliable because the exact values of the lower pressures, as well as the measured conduction rates, are somewhat in doubt.

Figure 4, on which these same curves are plotted on log-log paper, shows the conduction to be proportional to approximately the 0.67 power of the pressure for the nitrogen- to room-temperature range, and proportional to approximately the 0.86 power for the hydrogen- to nitrogen-temperature range. As the heat conduction by a stack of plates was found to be proportional to less than the first power of the load, it is concluded that such a support should be designed for high loading per unit area,

[2] Such an arrangement for use as an insulating support is the subject of a patent application for the AEC by B. W. Birmingham, E. H. Brown, R. B. Scott, and P. C. Vander Arend.

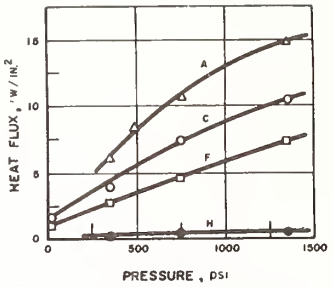

FIGURE 3a. *Heat conducted as a function of mechanical pressure of stacks of type 302 round stainless-steel plates, each plate 0.0008 in. thick.*

A (△), 148 plates; C (○), 209 plates; F (□), 313 plates; H (●), 315 plates. Boundary temperatures for A, C, and F are 76° and 296° K; for H, 20° and 76° K.

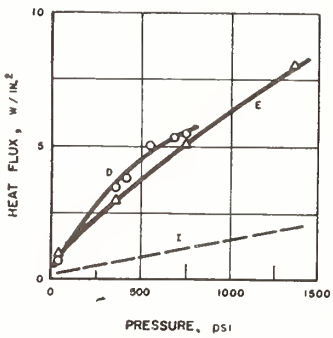

FIGURE 3b. *Heat conducted through stacks of thick plates where the boundary temperatures are 76° and 296° K.*

D (○), a stack of 52 round Monel plates, 0.017 in. thick; E (△), a stack of 49 type 304 round, stainless-steel plates, 0.0195 in. thick. Curve I shows the conduction that would occur through a stack of 0.0008in. plates the same height as the stack of 0.0195-in. plates. The conduction is extrapolated from the conduction by a stack of 313 plates, 0.0008 in. thick.

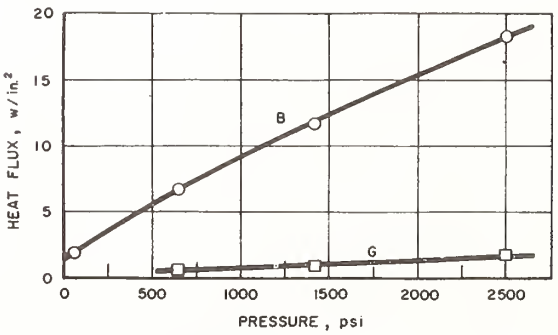

FIGURE 3c. *Heat conducted through a stack of 92 type 304 rectangular, stainless-steel plates, 0.004 in. thick.*

The boundary temperatures for B (○) are 76° and 296° K; for G (□), 20° and 76° K.

i. e., the cross-sectional area should be made as small as is consistent with strength and other design considerations.

The concept of thermal resistance is introduced here as an aid in comparing and correlating data on different specimens. Thermal resistance is defined as the temperature difference divided by the

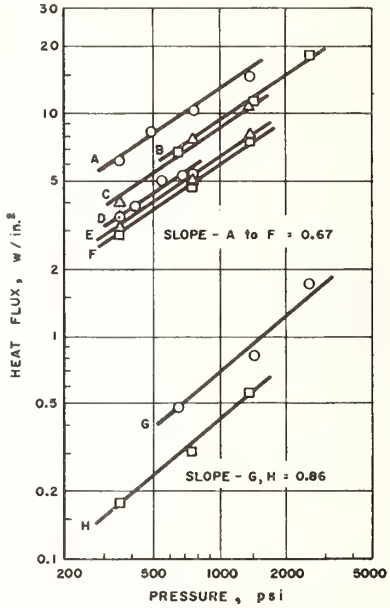

FIGURE 4. *A log-log presentation of the data given in figures 3a, 3b, and 3c, demonstrating that the heat current is approximately proportional to the 0.67 power of the pressure in the upper temperature range (76° to 296° K), and to the 0.86 power of the pressure in the lower temperature range (20° to 76° K).*

A (○), 148 plates, 0.0008 in. thick; B (□), 92 plates, 0.004 in. thick; C (△), 209 plates, 0.0008 in. thick; D (○), 52 plates, 0.017 in. thick; E (△), 49 plates, 0.0195 in. thick; F (□), 313 plates, 0.0008 in. thick; G (○), 92 plates, 0.004 in. thick; H (□), 315 plates, 0.0008 in. thick.

heat current (in analogy to its electrical equivalent). Thermal resistance is temperature dependent, but it is permissible to use an average value for comparing two stacks under the same temperature difference. As there were a large number of stacked plates in these tests, it was reasonable to expect that the resistance would be proportional to the number of plates, i. e., that the end effects would be negligible.

Three specimens of the 0.0008-in.-round stainless-steel plates were tested, each with a different number of plates. In figure 5 it is shown that the thermal resistance of a stack of plates varies linearly with the number of plates in the stack. Thermal resistance of unit area per plate as a function of the thickness of each plate is shown in figure 6. For many design applications a certain volume may be available for the insulating member. Hence, consistent with strength and cost considerations, it is desirable to know what thickness the plates should have to provide adequate heat insulation. Thermal resistance of unit area per unit length of stack as a function of plate thickness is plotted in figure 7. The length of the stack was determined by multiplying the number of plates by the thickness of each plate; this calculated length was in close agreement with the length measured when the stack was subjected to a pressure of 1,000 psi. Points for the curves of figures 6 and 7 are taken from the curves of figures 3a, 3b, and 3c for the

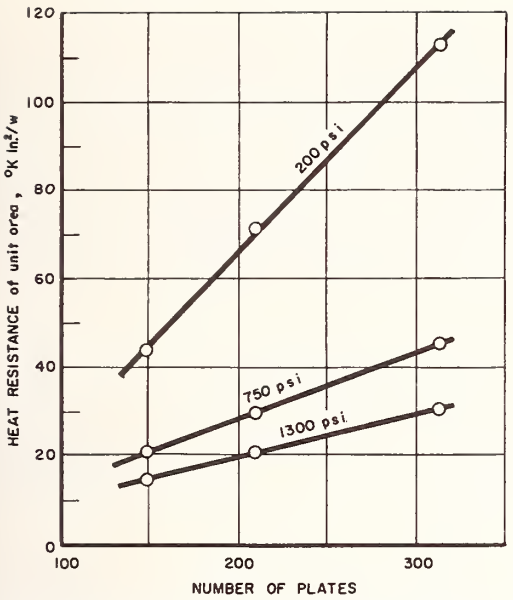

FIGURE 5. *Observed linear increase of the thermal resistance with the number of plates contained in a stack.*

The plate thickness is 0.0008 in.; the boundary temperatures are 76° and 296° K.

0.0008-in. stainless-steel round plates, the 0.0195-in. stainless-steel rectangular plates, and the 0.004-in. stainless-steel round plates. It is seen that the 0.0195-in. stainless-steel round plates had a higher thermal resistance per plate than the others, the explanation being that the thin plates were pressed into better contact with each other with a given applied pressure. However, for a given length of stack, the thin plates produced a greater total thermal resistance. This is shown by the dotted curve, I, figure 3b. No implication is intended that the slopes of approximately ½ and —½ of the lines of figures 6 and 7 have any significance other than that of representing the observations. It is probable that for different loads or plate thicknesses these would have other values.

The heat conduction through a stack of plates was considerably less than the conduction by a solid member of the same metal having the same dimensions, showing that the difference in conduction was due mainly to the total contact resistance of the specimen.

The conduction through a stack of 0.0008-in.-thick stainless-steel plates under a pressure of 1,000 psi was found to be approximately 2 percent of the conduction by a solid member; for the 0.0195-in. stainless steel round plates at 1,000 psi, 8.5 percent; for the 0.004-in.-thick stainless-steel rectangular plates at 1,000 psi, 4.5 percent; and for the 0.017-in.-thick Monel round plates at 600 psi, 6.5 percent.

The 0.0008-in. and the 0.004-in. plates were tested between liquid-nitrogen and liquid-hydrogen temperatures. Table 3 shows the comparison between these specimens. In the case of both the 0.0008-in. and the 0.004-in. plates, the specimen was loaded warm at the higher pressures; the load was reduced to the lower pressures after the specimen was cold. The

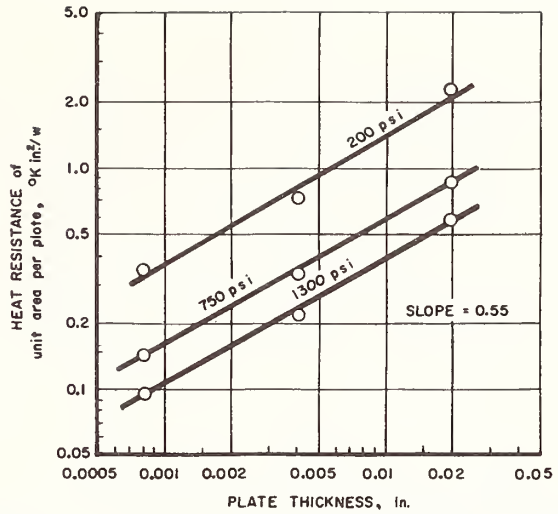

FIGURE 6. *A log-log presentation demonstrating that the heat resistance per plate increases approximately as the square root of the individual plate thickness.*

The boundary temperatures are 76° and 296° K.

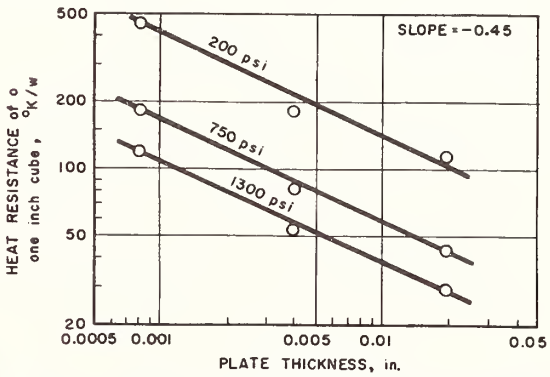

FIGURE 7. *A log-log presentation demonstrating that the heat resistance per unit length of a stack varies approximately as the inverse square root of the individual plate thickness.*

The boundary temperatures are 76° and 296° K.

ratio of the heat conducted between 296° and 76° K to that conducted between 76° and 20° K is of interest. The conduction ratio of a solid member of the same type of metal and the same dimension between the two temperature intervals would be 9 to 1. The greater ratio in the case of the stacked plates is an indication that the thermal resistance of the contacts increases as the temperature is decreased.

TABLE 3. *Comparison of 0.0008-in. and 0.004-in. plates*

Pressure	Specimen plates	Conduction ratio (Conduction at 76° to 296° K÷conduction at 20° to 76° K)
psi	*in.*	
754	0.0008	15.5 to 1
1,346	.0008	13.3 to 1
1,407	.004	14.2 to 1
2,509	.004	10.6 to 1

3.3. Specially Treated Stacked Plates

a. Dusted Plates

Because the objective of the work was to devise sturdy supports with the best possible insulating properties, methods of decreasing the heat conduction were studied. S. C. Collins of Massachusetts Institute of Technology predicted that a very slight coat of dust would greatly increase the thermal resistance. He had observed that a few dust particles detectable only under a microscope were sufficient to spoil the effectiveness of a thermal switch. Manganese dioxide was chosen to be the insulating dust for several reasons. It is only a fair conductor of heat and has moderate hardness. It can be ground into a fine powder that will cling to the surface of the plates, so that little of the dust is lost in the assembling of the supports. The dust coat on each plate was of such a small magnitude that the total length of the multiplate specimen was not significantly changed. The results for the dusted plates, as illustrated in figure 8, curves A and E, show that the heat resistance of unit area per plate of the stack of dusted plates is much higher than that of the stack of clean rectangular plates.

b. Perforated Plates

Another good insulating device was found to be a stack of perforated rectangular plates. The results on these plates are shown in figure 8, curve B. Figure 9 shows the plan of a perforated plate. The net area is 60 percent of the area of a plain rectangular plate. The thermal resistance of these plates was found to be higher than that of the plain rectangular plates because of the smaller area of the perforated plates and because the plates were stacked in such a manner that the holes of the adjacent plates did not aline, resulting in longer heat paths through the stack. Because the production of the perforated plates that might be used for an insulating support in a specific case was found to be expensive, it was also decided to try stacking the perforated and plain rectangular plates in alternate layers. In comparing the thermal resistance of the stacks of the three types of rectangular plates, each tested at a total load of 422 lb, it was found that the stack of plain plates had a resistance of 0.260° K-in.^{2}-watt^{-1} per plate; the stack of perforated plates, 0.420, and the alternate layered stack, 0.370.

c. Teflon-Separated Plates

A stack of rectangular plates with thin (approximately 0.00025 in.) films of Teflon placed between them was found to be a comparatively poor insulator at the low pressures. The high compressibility of the plastic resulted in a greater area of contact between it and the metal layers than would be realized between metal layers alone. However, at the higher pressures, the Teflon-layered stack was a good insulator, the area of the thermal contact having approached a constant value. At all pressures the plastic acted as a good insulator because of its low thermal conductivity. The conduction curve for the Teflon-layered plates is shown in figure 10, curve D.

d. Greased Plates

The application of grease to the Monel plates of a stack resulted in a decrease of heat resistance of nearly 16 percent at a pressure of 600 psi, as shown in figure 10, curve B (the stack of greased plates was loaded cold). A very thin layer of Dow-Corning high-vacuum grease was applied to each plate. The considerable increase in conduction by the greased plates may be explained in this manner: The coating of grease filled in the small spaces between the plates,

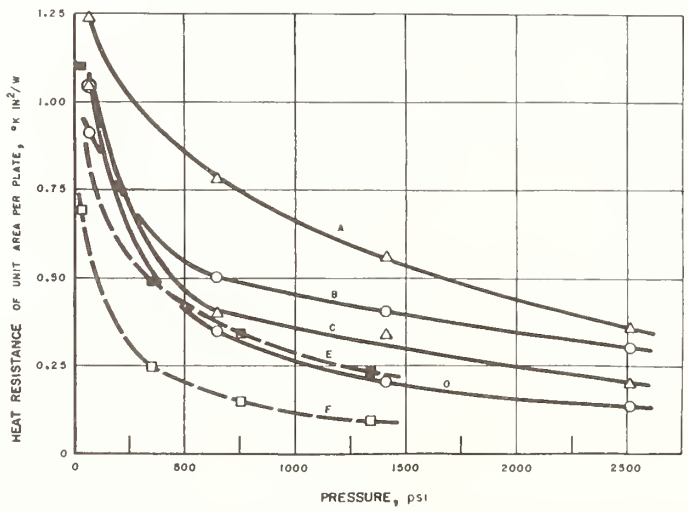

FIGURE 8. *Comparison of the heat resistance of clean plates with that of specially treated plates.*

The boundary temperatures are 76° and 296° K. A (△), a stack of 0.004-in. manganese-dioxide-dusted plates; B (○), 0.004-in. perforated plates; C (△), alternate layered stack of 0.004-in. plain and perforated plates; E (■), 0.0008-in. dusted plates; D (○), 0.004-in. clean plates; F (□), 0.0008-in. clean plates.

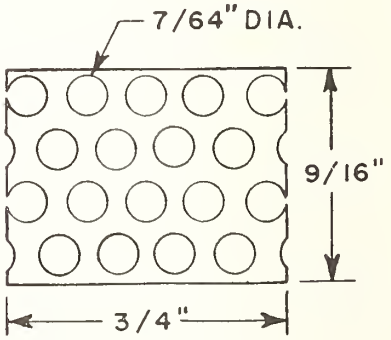

FIGURE 9. *A perforated plate.*

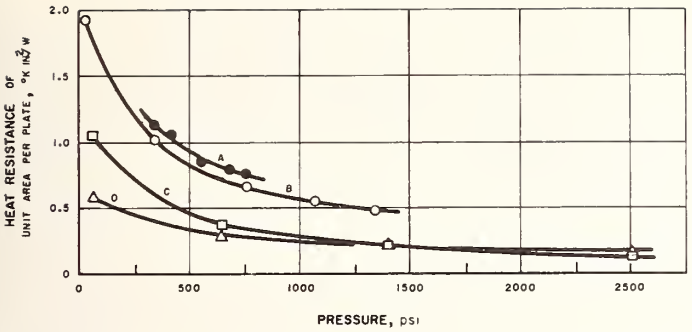

FIGURE 10. *Comparison of the heat resistance of clean plates with that of specially treated plates.*

The boundary temperatures are 76° and 296° K. A (●), a stack of 0.017-in. clean Monel plates; B (○), 0.017-in. greased Monel plates; C (□), 0.004-in. clean plates; D (△), 0.004-in. Teflon-separated plates.

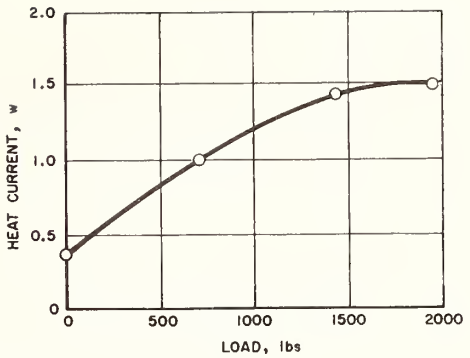

FIGURE 11. *Heat conducted as a function of total load on a type 304 stainless-steel strip, 0.0021 in. thick, 1 in. wide, which is dusted with manganese dioxide and rolled into a tight coil.*

The boundary temperatures are 76° and 296° K.

resulting in a more positive thermal contact. It is seen, therefore, that caution should be taken when one assembles a stack of plates, keeping each plate as clean as possible.

3.4. Application of Multiple-Contact Supports

A liquid-hydrogen Dewar, designed at the NBS–AEC Cryogenic Engineering Laboratory, was constructed with multiple-contact supporting members. Each of these separating members was made by tightly rolling a strip of type 304 stainless steel into a coil, the strip being 0.0021 in. thick, approximately 400 ft long and 1 in. wide. The inner diameter of the coil was approximately 2 in. and the outer diameter approximately 5 in. The coil was tested for conduction in an apparatus similar in operation to the original multiple-support testing equipment. The results of the conduction tests between nitrogen and room temperature, using a strip dusted with manganese dioxide, are shown in figure 11. It was not feasible to compute the heat conduction by a coil from the conduction by a stack of plates because it was not known how much heat flowed along the circumference of the coil nor how large was the effective cross-sectional area through which the heat flowed.

3.5. Nonmetallic Spheres

The results of tests on nonmetallic spheres are shown in figures 12a, 12b, 12c, and 12d, wherein the heat current per sphere is plotted as a function of the load per sphere. Each of the spheres in its socket made little more than point contact at no load. The conduction increased with increasing loads because the area of contact was increased, but it tended to level off at the higher loads as this area approached a constant value. The dependence of conduction on pressure also varied with the type of material of the sphere, e. g., if the material was soft, the sphere would flow slightly at the higher loads, resulting in a greater area of contact.

It is seen that of the four types of spheres tested, ceramic was found to be the best conductor and Pyrex glass was found to be the poorest conductor of heat. A load has more effect on the flow of heat through the ceramic spheres because the contact resistance has proportionally more effect in the case of the better conductor. Although the conductivity of Micarta is less than that of Pyrex, the conduction through the Micarta spheres was found to be greater than through the Pyrex spheres, possibly because of the slight flow of Micarta at the higher loads.

There was a small error due to a comparatively small temperature drop across the stainless-steel plates that were used for support of the spheres. The conduction through the spheres was actually greater than was measured.

In all cases, the conduction from 76° to 20° K is very much less than that from approximately 296° to 76° K. This is a consequence not only of the smaller temperature interval but also of the great decrease of the thermal conductivity of noncrystalline materials below 76° K.

Because the purpose of these measurements was to provide information about members that would be expected to have usefulness as insulating supports, some tests were conducted on the spheres to determine their crushing strength. The Pyrex-glass spheres failed at approximately 2,000 lb per sphere (two measurements). The ceramic spheres supported 10,000 lb each without failure.

The conduction data on the spheres should be considered in relation to their compressive strength. At first sight it appears that the higher strength of the ceramic spheres offsets their larger thermal conduction. This, of course, assumes that they will be used at high loads. If a support is designed for loads that would take the full advantage of the strength of the ceramic spheres, it would be necessary to provide hard bearings for the spheres to rest against, possibly of the same ceramic material. For average loads, the Pyrex spheres would be the most suitable.

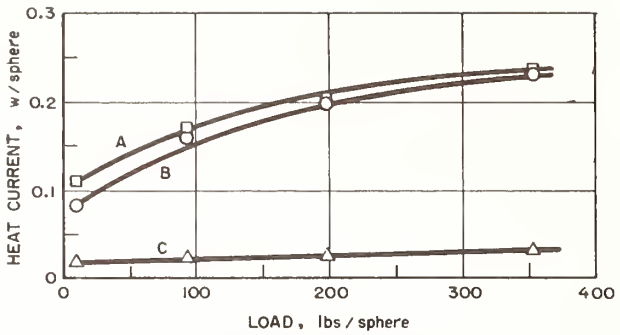

FIGURE 12a. *Heat conducted through Pyrex glass spheres, each sphere 0.375 in. in diameter.*

A (□), T_1=20° K, T_2=296° K; B (○), T_1=76° K, T_2=296° K; C (△), T_1=20° K, T_2=76° K.

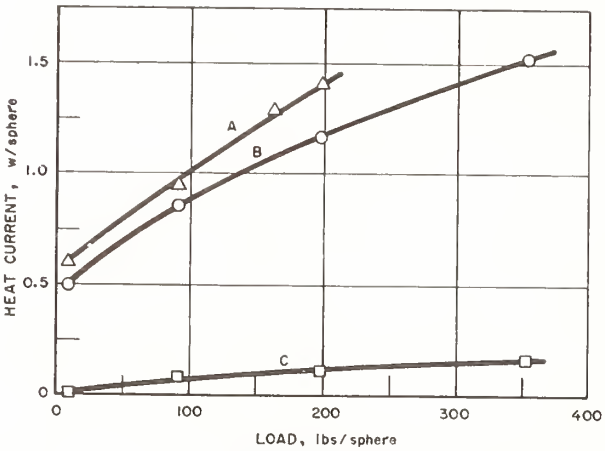

FIGURE 12b. *Heat conduction through ceramic spheres, each sphere 0.39 in. in diameter.*

A (△), T_1=20° K, T_2=296° K; B (○), T_1=76° K, T_2=296° K; C (□), T_1=20° K, T_2=76° K.

4. Previous Experiments

The use of multiple contact members as insulating supports was suggested by the experience of other workers who had to go to great pains to obtain good thermal contact in a vacuum.

R. B. Jacobs and C. Starr, in an effort to design a good thermal switch, carried out experiments at MIT in 1939 [3] wherein the heat conducted between two optically flat metallic surfaces in close contact with each other in a vacuum was measured as a function of contact pressure. Three different thermal switches were tested, one made of copper, another of silver, and the third of gold.

In 1949, S. C. Collins directed experiments [4] at MIT similar in nature to the Jacobs and Starr experiment. The thermal resistance between optically flat copper surfaces was measured.

In both these experiments it was found necessary to apply considerable pressure to obtain low thermal resistance.

[3] R. B. Jacobs and C. Starr, Thermal conductance of metallic contacts, Rev. Sci. Instr. **10**, 140 (April 1939).

[4] As described in a private communication from D. B. Chelton, who was working with Collins in 1949.

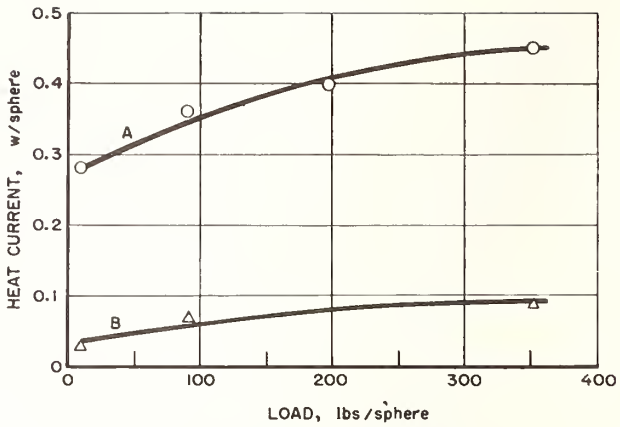

FIGURE 12c. *Heat conducted through Micarta spheres, each sphere 0.375 in. in diameter.*

A (○), T_1=76° K, T_2=296° K; B (△), T_1=20° K, T_2=76° K.

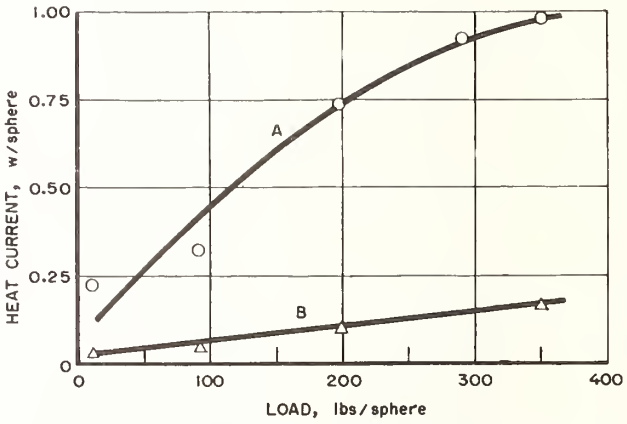

FIGURE 12d. *Heat conduction through soda lime spheres, each sphere 0.42 in. in diameter.*

A (○), T_1=76° K, T_2=296° K; B (△), T_1=20° K, T_2=76° K.

5. Conclusions

The most important conclusions to be drawn from these results are (1) the principle of multiple thermal contacts offers the designer of cryogenic equipment a simple rugged support that occupies small space, (2) the best assembly tested consisted of a stack of stainless-steel plates, 0.0008 in. thick. Its thermal conduction when supporting a load of 1,000 psi was only 2 percent of that of a solid conductor of the same dimensions, (3) the insulating value of such a support is enhanced by introducing a tiny amount of dust (MnO_2) between the plates, and (4) for best results the support should be designed for high loading per unit area.

The authors thank R. L. Powell for his assistance in designing the apparatus and developing the experimental procedure.

BOULDER, COLO., August 30, 1956.

JOURNAL OF RESEARCH of the National Bureau of Standards—A. Physics and Chemistry
Vol. 66A, No. 4, July–August 1962

Thermal Conductivity of Gases. I. The Coaxial Cylinder Cell[1]

Leslie A. Guildner

(April 13, 1962)

By combining appropriate geometric configuration and mathematical analysis with improved measuring techniques, the cell constant of a coaxial cylinder thermal conductivity cell was determined within 0.1 percent.

An analysis of the rate of heat transfer in such a cell showed a way to treat the data so that the error contribution of experimental deviations from idealized conditions is kept small. The principal considerations are:

1. That heat transport by convection is significantly large in a dense gas. This transport was analyzed mathematically from basic principles. The agreement of experimental results with the analysis indicated that the expressions are valid and that the convective heat transport could be accounted for with little more error than was involved in the precision of the heat transfer measurements.

2. That the heat transfer in a vacuum corresponds to the heat transfer by radiation and solid contacts in the presence of a gas. The uncertainty was that associated with the accuracy of determining the vacuum values.

3. That other effects were small enough to be computed and corrected for without increasing the uncertainty of the values of the thermal conductivity.

1. Introduction

The coaxial cylinder thermal conductivity cell, with large diameter of inner cylinder relative to the conductivity gap width, is one of the forms of apparatus often used to determine the thermal conductivity of gases. Over a period of several years, refinements were made in the design of a cell, in the analysis of heat transfer, in measurement techniques and in the treatment of the data. It is the purpose of this paper to set forth a summary of considerations which are applicable to measurements with a cell of this general type.

The heat guards at the ends of a coaxial cylinder cell can be designed so that the geometric form of the conductivity gap is simple. It is then possible to make a reliable mathematical analysis of the heat transfer by conduction. Consistent with a nearly exact mathematical analysis, special techniques were used for measuring the cell dimensions with improved accuracy.

At sufficiently high gas densities, convective heat transport becomes significant in a coaxial cylinder cell. When the axis of the cell is vertical, the heat transport by convection can be analyzed from basic principles. This analysis indicates the proper measurements to be made and the required treatment of the data.

Other effects which should be accounted for—asymmetry of the heat flow, radiation from the emitter and conduction through the mounting pins, and the temperature gradient in the body of the metal—are considered. The significance of these effects will be clearer after understanding some of the details of a cell, which will be described in the next section.

[1] This work was performed at the Massachusetts Institute of Technology and sponsored by Project SQUID, which is supported by the Office of Naval Research, Department of the Navy, under contract Nonr 1858(25) NR–098–038. Reproduction in full or in part is permitted for use of the United States Government.

2. Apparatus

The cell shown in figure 1 was made of silver. It consisted of an emitter EM, surrounded by a receiver RE. The emitter was located by seven Pyrex pins

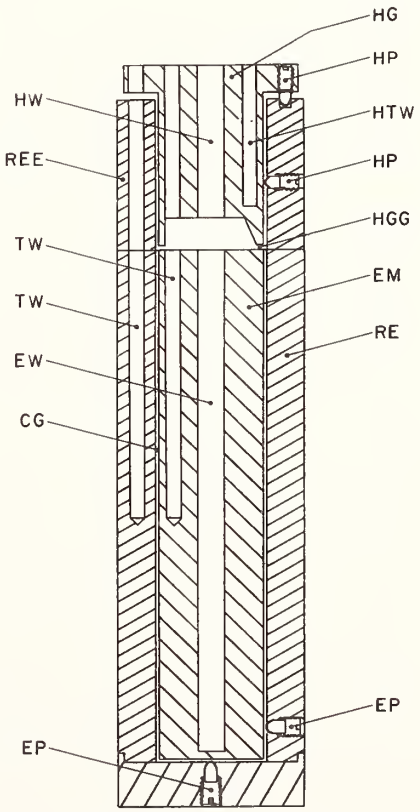

FIGURE 1. *Vertical cross section of coaxial cylinder cell.*

EP, one on the axis at the bottom, three spaced uniformly around the receiver near the bottom, and three (not shown) similarly spaced near the top. Electrical energy was supplied to the emitter by a heater in the heater well *EW*. The heater was made from Nichrome ribbon uniformly wound on a machined Grade "A" "Lava" form. The temperature or the temperature difference was measured by thermocouples inserted in the thermocouple wells *TW* of the emitter and receiver. The junctions were at two levels in the receiver and emitter, one level being midway along the emitter close to the bottom of the wells, and the other level just below the top of the emitter. The thermocouples were installed between the wall of the well and an inserted rod of silver. The thermocouple wires were insulated by thin sheets of mica, and they were packed tightly in the thermocouple wells.

A heat guard *HG* provided a continuation of the conductivity gap *CG*. It was positioned by six Pyrex pins *HP*, three spaced uniformly around the side and three around the top. The top pins were adjusted so that the width of the heat guard gap *HGG* was equal to the width of the conductivity gap. The heat guard temperature was maintained as close as possible to the temperature of the emitter, by introducing electrical energy from a heater in the heat guard heater well *HW*. The temperature was measured by a thermocouple whose junction was placed near the bottom of the heat guard thermocouple well *HTW*.

The leads from the emitter heater and the emitter and receiver thermocouples passed through the heat guard or the corresponding portion of the receiver, the receiver extension *REE*. (The receiver extension surrounding the heat guard was separate to facilitate assembly.) The thermocouple leads were insulated with mica and in order to improve heat transfer were held against the walls of the thermocouple wells, by means of a split rod of silver, which was wedge shaped.

The mounting pins were made in three parts: a Pyrex rod, 3 mm in diameter with a 60° included angle conical point, a pure aluminum holder, and a silver screw. The lengths of Pyrex and aluminum were chosen such that their composite expansion was close to that of silver over the temperature range 0 to 400 °C.

The dimensions of this cell, although not essential to the discussion in this paper, are used for illustration, and were approximately:

Conductivity gap	0.068 cm
Heat guard length	3.8 cm
Emitter diameter	2.2 cm
Emitter length	11.4 cm.

The dimensions should be chosen so that $\Delta r/\bar{r} \leq 0.1$. The length of the emitter should be sufficient for 90 or 95 percent of the heat transfer to take place radially, and the length of the heat guard should be enough to reduce unaccountable heat loss from the emitter satisfactorily. The choice of the size of the conductivity gap represents a compromise. On the one hand, a narrow gap makes the ratio of the heat transfer by conduction large relative to the heat transfer by radiation and also very effectively makes the relative heat transport by convection small. On the other hand, when the gap is made too narrow, the uncertainty in the value of the cell constant is increased. The choice of dimensions will depend upon the objectives of the investigation.

3. The Cell Constant

3.1. Mathematical Treatment

We can obtain the cell constant from the assumption that the rate of heat transfer, $\dot{q}$, is proportional to the temperature gradient and the surface area. In the steady state, we can integrate the temperature gradient over the region of heat flow, so that $\dot{q}=CK\Delta t$, where C is the cell constant, K is the thermal conductivity, and Δt is the temperature difference across the region in the steady state condition.

The principal terms of the cell constant can be evaluated by considering the radial heat flow across a section of length l of an infinite coaxial cylinder and the linear heat flow across a circular section of radius r_1 of two infinite parallel plates at the bottom. The determination of an accurate cell constant requires that recognition be made of the additional heat flow which takes place at the heat guard gap and at the bottom corner of the emitter. If both the conductivity gap, Δr, and the heat guard gap are small compared to the radius of the emitter, r_1, the conductivity gap and adjacent portion of the heat guard gap can be treated as if planar. In figure 2, the relaxation solution for the gas isotherms near the heat guard shows that the perturbing effect of the gap has practically vanished within two gap widths in any direction. Therefore, it is proper to employ the Schwarz-Christoffel transformation which is valid for an infinite cell. The transformations for both the heat guard gap and the bottom corner are given in Carslaw and Jaeger, [1][2] pp. 444 and 445. In an analogous manner to the solution for the bottom corner given on pp. 453–454, the correction terms for the heat guard gap may be found. On the assumption that the heat flow over the length of the cell takes place as if unperturbed, the deviations may be combined as a factor times half the heat guard gap, which is to be added to the length of the cell. If the heat guard gap is equal to the conductivity gap, Δr, the added length is [3]

$$c_2=0.923\ \Delta r/2.$$

The bottom corner of the emitter adds a term to the cell constant of $2\pi r_1 \times 0.559$ for equal conductivity gaps on the sides and bottom. Thus, the total rate of heat transfer by gas conduction is

$$\dot{q}=K\left[\frac{2\pi(l+c_2)}{\ln r_2/r_1}+\frac{\pi r_1^2}{\Delta r}+2\pi r_1\times 0.559\right]\Delta t \qquad (1)$$

where r_2 is the inner radius of the receiver. The

[2] Figures in brackets indicate the literature references at the end of this paper.
[3] See appendix 1.

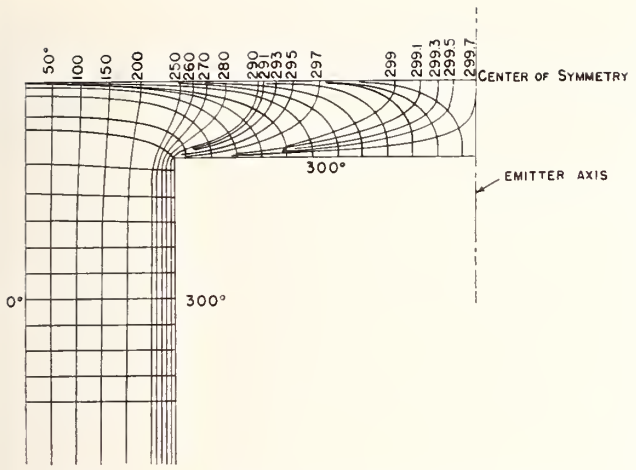

FIGURE 2. *Relaxation solution of the heat guard gap.*

cell constant is

$$C=\pi\left[\frac{2(l+c_2)}{\ln r_2/r_1}+\frac{r_1^2}{\Delta r}+1.118r_1\right]. \qquad (2)$$

From eq (2), we find 99.4 percent of the heat transfer from the cell illustrated in figure 1 is accounted for by the two principal parts: 94.9 percent by radial heat flow, 4.5 percent by linear heat flow. The transfer from the heat guard gap amounts to 0.25 percent, and the transfer from the bottom corner amounts to 0.33 percent.

3.2. Measurement of Receiver and Emitter Radii

Both to increase the flow of heat by conduction and to reduce the heat transferred by convection, the conductivity gap should be kept as small as will permit the accurate determination of the cell constant. For the case of $\frac{\Delta r}{r_1} \ll 1$, the rate of heat transfer by conduction from a section of length l of an infinite coaxial cylinder is $\dot{q}=\frac{2\pi\bar{r}Kl\Delta t}{\Delta r}$ within a relative error of $\frac{1}{3}\left(\frac{\Delta r}{2\bar{r}}\right)^2$, or 0.03 percent for $2\bar{r}=2.2$ cm and $\Delta r=0.068$ cm. The equation serves to emphasize that for the same error in the cell constant two orders of higher accuracy of length measurements are required to determine the conductivity gap, than the radii themselves.

The measurements of the two radii were made with a super-micrometer as measurements of two outer diameters, the one directly, the other by use of a "falling probe." If a "probe" is allowed to fall by its own weight, as shown in figure 3, the gap between the probe and the outer cylinder can be calculated from the air flow [2]. In an annulus formed by two coaxial cylinders of radius r_p and r_2, length L, and gap $m=r_2-r_p$, the volume of gas of viscosity η flowing in time θ with a difference of pressure

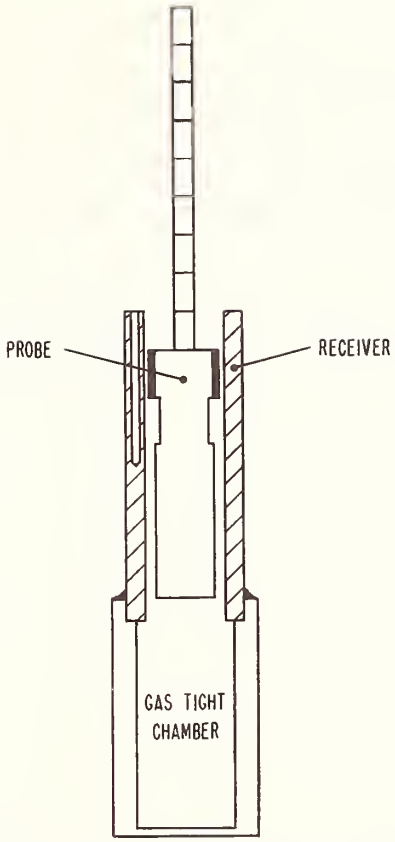

FIGURE 3. *Falling probe device for inner diameter measurement.*

$\Delta p=\Delta w\cdot g$ and average pressure $\bar{p}$ can be expressed within a relative error of $\frac{m^2}{60\,r_p^2}$ as

$$\Delta V=\frac{\pi\bar{p}\Delta w g\bar{r}m^3\theta}{6\eta p_2 L}$$

$\bar{r}=(r_p+r_2)/2$ and p_2 is the atmospheric pressure.

With the volume expressed as the probe displacement

$$m^3=\frac{6\eta p_2 r_2^2\Delta lL}{g\bar{p}\Delta w\bar{r}\theta} \qquad (3)$$

where g is the gravitational constant and Δl is the distance of fall in time θ and Δw is weight of probe.

The average inner radius of the receiver is determined by adding the gap, m, to the radius of the probe, r_p. The determination of the gap, m, was precise within 2.5×10^{-5} cm.

The measurement of $2r_p$ was precise within 2.5×10^{-5} cm, as well as $2r_1$, the outer diameter of the emitter. The sum of $m+r_p$ for varying m was consistent within 2.5×10^{-5} cm. Thus with differences of radius between receiver and emitter as small as 0.06 cm, the length of Δr was determined to an accuracy within 0.1 percent.

4. Convection

In general, the hydrodynamical equation for nonturbulent flow of a fluid of velocity $\bar{v}$, viscosity η, pressure p, and density ρ is (div η grad) $\bar{v}$=grad $p-\rho g$, where g is the acceleration of gravity [3]. For two infinite vertical plates at uniform temperatures $t_0-\Delta t/2$ and $t_0+\Delta t/2$, the equation reduces to

$$\eta \frac{d^2 v_z(x)}{dx^2}=(\rho-\bar{\rho})g.$$

The axes are taken with the origin at the midpoint between the planes. The x-axis is normal to the planes, the y-axis is horizontal, and the z-axis is vertical. The average density, $\bar{\rho}$ is the density at $x=0$.

If the separation of the planes is Δr, $t(x)=t_0+\frac{x\Delta t}{\Delta r}$ and

$$\rho=\bar{\rho}[1-\alpha(t-t_0)]=\bar{\rho}-\frac{\bar{\rho}\alpha x\Delta t}{\Delta r}, \text{ where } \alpha=-\frac{1}{\bar{\rho}}\left(\frac{\partial\rho}{\partial t}\right)$$

Since $v=0$ when $x=-\frac{\Delta r}{2}$ and $x=\frac{\Delta r}{2}$,

$$v(x)=\frac{\alpha\bar{\rho}g\Delta t\,x}{6\bar{\eta}\Delta r}\,[\Delta r^2/4-x^2] \tag{6}$$

In a closed system, the circulation takes place as a single stream, reversing direction at the top and bottom. Conservation of mass requires a term second order in Δt which does not affect the heat transport by more than 1 percent for actual measurement, hence it was neglected.

The heat transported per unit horizontal distance is

$$\dot{q}=c_p\int_{-\Delta r/2}^{\Delta r/2} v(x)\rho(x)\Delta t(x)dx=\frac{\Delta r^3 g}{720}\,\frac{\alpha\rho^2 c_p\Delta t^2}{\eta}$$

where c_p is the specific heat capacity and the average density is indicated without the bar. The horizontal distance in the cell is very nearly $2\pi\bar{r}$. Then the rate of heat transport per degree is

$$\dot{q}/\Delta t=\frac{2\pi\bar{r}\Delta r^3 g}{720}\,\frac{\alpha\rho^2 c_p\Delta t}{\eta}. \tag{7}$$

If the total heat transfer is studied as a "conductivity," $\dot{q}/C\Delta t$, a portion is due to convection, which may be written as

$$K_{\text{conv}}=\frac{\dot{q}_{\text{conv}}}{C\Delta t}=\frac{2.6\times10^{-6}\alpha\rho^2 c_p\Delta t}{\eta}. \tag{8}$$

The value 2.6×10^{-6} combines the constants of eq (7) and the value of the cell constant C for the cell of figure 1.

The neglect of terms of higher order in Δt for $\rho(x)$ affects K_{conv} detectibly near the critical point of CO_2. When $\Delta t<5$ deg C, these terms need not be considered for other measurements to be reported.

Engineering investigations of convection have been analyzed by use of several correlating functions. It may seem at times as if serious discrepancies exist when the correlation is extended to inappropriate conditions. Let us consider three dimensionless quantities:

(1) The Grashof-Prandtl product

$$\text{Gr}\cdot\text{Pr}=\frac{g(\Delta r)^3\alpha\rho^2 c_p\Delta t}{\eta K}; \tag{9}$$

(2) The Grashof number

$$\text{Gr}=\frac{g(\Delta r)^3\alpha\rho^2\Delta t}{\eta^2};$$

(3) The Reynolds number

$$\text{Re}=\frac{\rho\bar{v}x_0}{\eta},$$

where the average velocity $\bar{v}=\frac{(\Delta r)^2\alpha\rho g\Delta t}{192\eta}$ and $x_0=\Delta r/2$.

Then

$$\text{Re}=\frac{g(\Delta r)^3\alpha\rho^2\Delta t}{384\eta^2}. \tag{10}$$

Thus the Grashof number and the Reynolds number are functionally the same for a gas in a vertical gap. Within the range of pressure and temperature such that the Eucken factor, $K/\eta c_v$, is a constant and that $\gamma=c_p/c_v$ is a constant, the Grashof-Prandtl product and the Reynolds number will serve equally well for the correlation of laminar convective effects.

The ratio of K_{conv} to K_{gas} can be found by dividing eq (8) by K_{gas}, and is functionally $(\Delta r/l)$ (Gr·Pr). It can be seen from eq (8)/K_{gas} that the criterion of Kraussold, that convection is insignificant[4] for Gr·Pr$<$1000, leads to different error limits depending upon $\Delta r/l$. For the cell of figure 1, Gr·Pr=1000 involves a relative heat transfer by convection of 8×10^{-3}.

Representing a ratio of the heat transport of convection to conduction, Gr·Pr is a logical correlating function for heat transport by laminar convection. Over the range of variables that eq (9)/eq (10) is a constant, either will serve as a criterion for the initiation of turbulent convection. Near the critical point, however, $c_p\to\infty$ and $\gamma\to\infty$. Since the Eucken factor does not vary greatly, Gr·Pr can become enormous while the Reynolds number remains small. The Reynolds number depends upon the velocity resistance per se, and it is the fundamental quantity, not Gr·Pr, which should be used as the criterion for initiation of turbulent flow.

The purpose of this section is to demonstrate how the data can be treated to give the heat transfer by thermal conduction alone. Measurements must be made under conditions of laminar flow. For CO_2, Onsager and Watson [4] have shown that with

[4] Worse yet is the statement that convection does not exist for Gr·Pr<1,000. The author hopes this idea will take its place with the phlogiston theory!

apparatus of the planar, vertical type, turbulence commences at a value of the Reynolds number of about 25. Often it is clear that $Re << 25$. If there is uncertainty, the Δt for transition from laminar to turbulent flow should be determined experimentally. At constant pressure and constant average gas temperature, eq (8) indicates that $\dot{q}/\Delta t$ versus Δt is linear for laminar flow. By straight line extrapolation of $\dot{q}/\Delta t$ versus Δt to zero Δt, the heat transport by convection is eliminated.

The essential requirements of eq (8) are confirmed by the results. The heat transport correlates well versus $\frac{\alpha \rho^2 c_p \Delta t}{\eta}$. The $\dot{q}/\Delta t$ versus Δt extrapolations are linear within the precision of the data, except for very large values of eq (8) where second order effects may be detectible. The values of Δt calculated from eq (10) (indicated by an asterisk on some extrapolation isotherms in the next paper) are in satisfactory accord with the experimental measurements.

5. Asymmetry of the Heat Flow

5.1. Coaxial Centering

If the emitter is not centered perfectly the geometrical factor of $\ln r_2/r_1$ should be replaced by $\cosh^{-1}[(r_2^2+r_1^2-d^2)/2r_1r_2]$, where d represents the displacement of the two axes. For the cell of figure 1, an error of 7×10^{-4} cm in the centering would make a difference of only one part in 100,000 in the cell constant.

5.2. Heat Loss From the Bottom of the Emitter

The cell with a single heat guard loses heat on the bottom as well as on the sides. With a uniform heater winding this leads to an asymmetric temperature distribution, which becomes larger as the gas thermal conductivity becomes larger. A reasonable approximation permitting mathematical treatment assumes uniform heat flow from the center heater to the emitter, no heat flow on the heat guard end, and the heat flow across the conductivity gap proportional to the temperature difference. The solution for this problem is

$$-K_{Ag}\Delta t/2\dot{q}=h\sum\frac{\pm\sqrt{\alpha_n^2+h^2}\cos(\alpha_n z)\phi_0(r;n)}{\alpha_n^2([\alpha_n^2+h^2]l+h)\phi_1(a;n)}$$

where $h=AK$, A is the total exterior surface area, K is the thermal conductivity of the substance in the gap, and K_{Ag} the thermal conductivity of silver.[5]

$$a\leq r\leq b$$

$$0\leq z\leq l$$

$$\phi_0(r;n)=I_0(r\alpha_n)[\alpha_nK_1(b\alpha_n)-hK_0(b\alpha_n)]+K_0(r\alpha_n)[\alpha_nI_1(b\alpha_n)+hI_0(b\alpha_n)]$$

$$\alpha_n\phi_1(a;n)=\left(\frac{\partial\phi_0}{\partial r}\right)_{r=a}=I_1(a\alpha_n)[\alpha_nK_1(b\alpha_n)-hK_0(b\alpha_n)]-K_1(a\alpha_n)[\alpha_nI_1(b\alpha_n)+hI_0(b\alpha_n)]$$

and the α_n are the ordered positive roots of $h=\alpha_n\tan(\alpha_n l)$. The value of $\sqrt{\alpha_n^2+h^2}$ is taken positive or negative in accord with the sign of $\sin\alpha_n l$.

The functions I_0, I_1, K_0, and K_1 are Bessel functions of complex argument. The result shows that the average temperature of the emitter is not at the center but at

$$z=0.66l \text{ for } K=5.95\times10^{-5},$$

$$z=0.675l \text{ for } K=5.95\times10^{-4},$$

$$\text{and } z=0.697l \text{ for } K=11.90\times10^{-4}.$$

Conductivities calculated from the average of the top and center temperatures must be increased by the factor indicated in figure 4. This factor is accurate enough that usually no significant error is involved, and could be reduced by adding measurement of the temperature difference at the bottom of the cell.

6. The "Blank" and Conduction of Pins

When the cell is evacuated, the heat transferred by radiation and by conduction of the pins can be treated as a measurement of a "conductivity," called a "blank." The present cell had a blank at 0 °C of 0.138×10^{-5} cal cm^{-1} sec^{-1} deg C^{-1}, about 4 percent of the conductivity of CO_2 at the same temperature and 1 atm pressure. It was estimated that no more than half of the heat transfer of that blank was due to conduction of the pins.

It was assumed that the conductivity of a gas could be found by deducting the blank from the value of the apparent conductivity for zero temperature difference. However, the blank may not adequately represent the heat transfer in the presence of a gas for the following reasons:

(1) The conduction of heat across the pin-emitter interface may increase in the presence of a gas.

(2) The temperature distribution in the pins may perturb the heat transfer in the gas significantly.

In the first case, if the pressure of the pins against the emitter is high enough, the effect of the gas on the conduction across the contact interface is negligible. Ascoli and Germagnoli [5] showed that the temperature difference across a steel-aluminum interface with 8 μin. finish became nearly constant in a vacuum once the pressure of contact reached 100 kg/cm². For N_2 at 1 atm, the temperature difference across the interface with the same heat flux became nearly constant at 50 kg/cm² contact pressure, and at 100 kg/cm² was equal within experimental error to the corresponding vacuum value. Boeschoten and Van Der Held [6] found three times the heat conduction in the presence of 1 atm of helium as in a vacuum at 35 kg/cm² contact pressure. The inference from the preceding investigation is that at 100 kg/cm²,

[5] If the cell were made of another material, the corresponding thermal conductivity would be used in place of K_{Ag}.

the ratio would be 1.5/1. Rough surfaces approach the behavior of smooth surfaces as the contact pressure is increased. These measurements were performed upon a steel-aluminum interface rather than a Pyrex-silver interface used in the present apparatus. However, the ability of silver to conform to the harder surface of Pyrex is at least as great as for aluminum to conform to steel. The pins were forced into the silver sufficiently that indentations 0.003 to 0.005 in. deep were made in the emitter, which is to say with sufficient force to exceed 1500 kg/cm^2, the tensile strength of silver. The Pyrex pins were held in an aluminum sleeve such that the composite expansion of the two materials approximately matches the expansion of the cell material from 0 to 400 °C. Consequently the centering of the emitter and the contact pressure between the pin and the emitter should be maintained over the temperature range. Hence it can be expected that gases of low conductivity caused an insignificant change in the rate of transfer of heat through the pins. In helium, the uncertainty in pin conduction should not exceed 0.1 percent of the gas conduction.

The additional heat transfer through the gas, which arises because the temperature distribution in the pins does not follow the radial gradient, can be evaluated by relaxation methods, and leads to the result that an 18 percent increase of conduction for the area of the surface occupied by the base of the pin will be observed when the conductivity of the gas is 10 percent that of Pyrex. The area occupied by the bases of seven pins was 0.4 percent of the total surface area of the receiver so that at a gas conductivity of 3×10^{-4} cal cm^{-1} sec^{-1} deg C^{-1} an increase of conduction of 0.07 percent will be observed. If the conductivity of the fluid reached the value of Pyrex, the pins would have no effect on the temperature gradient, and at low values of gas conductivity, the effect is about the same as at a conductivity of 3×10^{-4} cal cm^{-1} sec^{-1} deg C^{-1}.

7. Radial Temperature Gradient in the Emitter and Receiver

A correction, in general small, must be made for the fact that the thermocouples are placed in the body of the emitter and receiver. This is a power series of $K_{corr}=K_{meas}\ [1+aK_{meas}+(aK_{meas})^2+\ .\ .\ .]$ of which only the first corrective term is large enough to be significant. For the dimensions of the silver conductivity cell in figure 1, $a=10.70$ cm sec deg C/cal.

8. Discussion of Other Cells

There are only a few forms of thermal conductivity cells suitable for accurate absolute determinations of the thermal conductivity of gases. The "hot wire" cell is an extreme case of a coaxial cylinder cell, with a small radius of the emitter, but the cell constant cannot be determined with the accuracy possible for a larger radius of emitter. The heat transfer analysis is complicated, and in a dense gas convection is difficult to control because of the large temperature gradient near the wire.

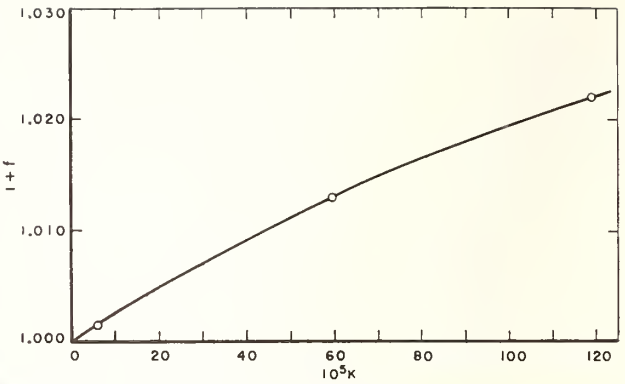

FIGURE 4. *Correction to the conductivity for asymmetric heat flow.*

A coaxial cylinder cell with heat guards at both ends would not have the end heat flow which requires the corrections given in figure 4. However, there is an uncertainty in the results due to a possible heat flow between the emitter and heat guards. When the emitter is suspended or held in place by sleeve or rod connections with the heat guards (as is customary for this design), the increased conduction possible by a slight difference in temperature between the emitter and guards will increase significantly the uncertainty of the thermal conductivity determination. The uncertainty is reduced if the thermal conductivity is relatively large, and if the emitter-receiver temperature difference is large. In order to avoid these restrictions, the suspension method could probably be modified.

In principle the flat plate cell, with an emitter and guard above the receiver, should not be affected by convection. In dense gas, there is good possibility that many such cells have had significant convection transfer from "chimneys," but that no special measurements were made to check. However, by proper design, it can be expected that convection difficulties would be eliminated. The cell constant can be determined with about the same accuracy as for the coaxial cylinder cell, but instability of the flat plate cell alinement affects the cell constant directly. By contrast, a change of the coaxial cylinder cell alinement affects the cell constant comparatively little.

9. Conclusions

By use of a heat guard and receiver extension which extends the conductivity gap of a coaxial cylinder, the conduction across the gap can be expressed accurately. In combination with special measuring techniques involving a "falling probe," the value of the cell constant can be obtained to an accuracy within ±0.1 percent.

The coaxial cylinder cell must be used with the axis vertical in order to permit analysis of convective heat transport. It was deduced mathematically and found experimentally that the apparent conductivity is affected by laminar convection linearly with the temperature difference. The temperature difference which causes the Reynolds number, eq (10), to be

25 defines the highest temperature difference for which laminar flow can be expected. The effects of convection can be eliminated by extrapolating the apparent conductivity versus the temperature difference to zero temperature difference, provided the measurements lie in the range of laminar flow.

For high accuracy, corrections must be made to the data for asymmetry of heat flow, perturbation of the temperature gradient by the mounting pins, and the temperature gradient in the emitter and receiver. Of course, the rate of heat transfer in a vacuum is deducted. There has now been sufficient quantitative measurement to show that the radiation and pin transfer should remain constant within 0.1 percent in the presence of a gas.

Of the various types of cells used for measuring the thermal conductivity of gases, the coaxial cylinder cell and the flat plate cell offer the most promise of accurate results.

10. References

[1] H. S. Carslaw and J. C. Jaeger, Conduction of heat in solids, 2d Ed., Oxford Univ. Press, London, 1959.
[2] W. H. MacAdams, Heat transmission, 2d Ed., McGraw-Hill Book Co., Inc., New York, 1942.
[3] R. C. Jones and W. H. Furry, Rev. Mod. Phys. **18,** 151 (1946).
[4] L. Onsager and W. W. Watson, Phys. Rev. **56,** 474 (1939).
[5] A. Ascoli and E. Germagnoli, Energia Nucleare **3,** 113 (1956).
[6] F. Boeschoten and E. F. M. Van Der Held, Physica **23,** 37 (1957).

11. Appendix

Given the conductivity gap h and heat guard gap $2k$.[6] We identify the points, $A\ B\ C\ D\ E\ F\ G\ H$ in the complex z-plane. These points are transformed in the t-plane by the Schwarz-Christoffel transformation, which is

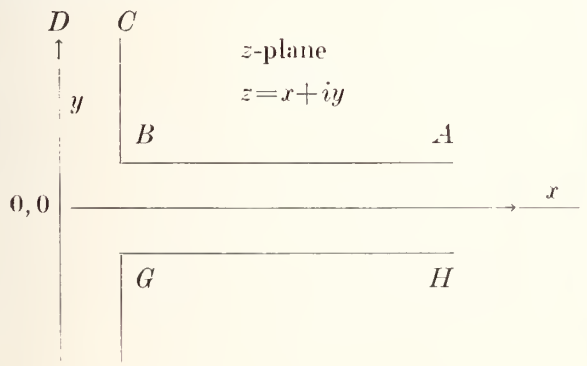

$$z=-iC\left\{\frac{\sqrt{1-a^2}}{2a}\ln\frac{[t+a][1-at+\sqrt{(1-a^2)(1-t^2)}]}{[t-a][1+at+\sqrt{(1-a^2)(1-t^2)}]}+\sin^{-1}t\right\}+\pi\frac{C\sqrt{1-a^2}}{2a};$$

$$C=2k/\pi; \qquad a^2=k^2/(h^2+k^2).$$

[6] Note that the symbolism is that of Carslaw and Jaeger, and in general should not be identified with the symbolism of the rest of the paper.

Points A, H, C, D, E, and F are assumed to lie at infinity in the z-plane. Corresponding values of the points are shown for the t-plane.

t-plane
$t=\zeta+i\xi$

A	B	C,D	$0,$	0	E,F	G	H
$-\infty$	-1	$-a$	0	0	a	1	∞

By use of the conformal mapping function

$$\pi w=\ln[(t+a)/(t-a)]$$

the points in the z-plane are transformed to the indicated points in the w-plane.

w-plane
$w=u+iv$

C	$A,$	H	F
$-\infty$	0	0	∞
D	0	0	E
$-\infty-i$	$0,$	$-i$	$\infty,-i$

Thus in the w-plane, heat flow between two infinite parallel plates can be studied.

If the heat flow to $w=u-i$ is studied, this corresponds to the heat flow to $DE=-iy$ in the z-plane. By substituting $\pi w=\ln\left(\frac{t+a}{t-a}\right)$ and $w=u-i$, $z=-iy$,

$$-iy=-ih(u-i)-\frac{ih}{\pi}\ln\frac{[1-at+\sqrt{(1-a^2)(1-t^2)}]}{[1+at+\sqrt{(1-a^2)(1-t^2)}]}$$

$$-\frac{2ik}{\pi}\sin^{-1}t+h.$$

For u (and y) large, $t\to+a^-$

$$y=hu+\frac{h}{\pi}\ln(1-a^2)+\frac{2k}{\pi}\sin^{-1}a.$$

The heat transport to DE per unit width per unit temperature difference is, in the w-plane, Ku (where K is the thermal conductivity of the medium).

$$Ku=K\left(\frac{y}{h}-\frac{1}{\pi}\ln[1-a^2]-\frac{2k}{\pi h}\sin^{-1}a\right).$$

Thus, there are two corrective terms to be added to the normal term y/h for the steady heat flow between two planes distant h apart. For the case that the heat guard gap ($2k$) is equal to the conductivity gap (h)

$$a^2=1/5.$$

Where the conduction is regarded as unperturbed along FG and BC, we can get a relative correction to the normal term for infinite plates over the distance of the heat guard gap by taking $y=2k=h$. Then

$$Ku=K\left(1-\frac{1}{\pi}\ln\left[1-a^2\right]-\frac{1}{\pi}\sin^{-1}a\right)$$

or we may add a length to the emitter equal to one half the heat guard gap times the factor in parenthesis, i.e.,

$$c_2=k\left(1-\frac{1}{\pi}\ln\left[1-a^2\right]-\frac{1}{\pi}\sin^{-1}a\right)$$

$$=k(1-0.0766)=0.9234k.$$

(Paper 66A4-168)

JOURNAL OF RESEARCH of the National Bureau of Standards—C. Engineering and Instrumentation
Vol. 67C, No. 2, April–June 1963

A Radial-Flow Apparatus for Determining the Thermal Conductivity of Loose-Fill Insulations to High Temperatures

D. R. Flynn

(November 28, 1962)

A description is given of an apparatus used for determining the thermal conductivities of loose-fill granular materials in the temperature range 100 to 1,100 °C. The method used in making these determinations was that of radial heat flow through a hollow cylinder of specimen material contained between a central ceramic core and an outer ceramic shell. The heat flow through the specimen was determined by measurement of the power input to a heater in the central ceramic core. The radial temperature drop through the specimen was inferred from temperatures measured in the core and in the shell, thus avoiding entirely the problems of measuring a temperature difference within the specimen material. Experimental results with an estimated uncertainty of 3 percent or less are presented for diatomaceous earth having a density of 0.15 g/cm³, and for aluminum oxide powders having densities of 0.40 and 0.44 g/cm³. A discussion of the test method is given, with attention to possible sources of error.

1. Introduction

Various loose-fill thermal insulations are used, in conjunction with appropriate guarding, to reduce extraneous heat flows in several thermal conductivity measuring devices under development in the Heat Transfer Section at the National Bureau of Standards. Since such heat flows cannot be entirely eliminated, it is necessary to know the approximate thermal conductivity of these insulations in order to effect appropriate corrections. In designing an apparatus for determining the thermal conductivity of these insulations, it was decided to aim for an accuracy of 5 percent or better, because of the general interest in thermal conductivity of loose-fill materials, both from an engineering and from a theoretical viewpoint.

The purpose of this paper is to describe an apparatus and method used for determining the thermal conductivity of loose-fill materials. Experimental results are presented for diatomaceous earth and aluminum oxide powder in the temperature range from 100 to 1,100 °C. Factors affecting both the precision and accuracy of the measurements are discussed.

2. Method

Radial heat flow in a hollow cylinder of loose-fill insulating material was selected as the method for the measurements. A cross section of the essential elements of the apparatus is shown in figure 1. The specimen was contained within the annular space between the outer radius, a, of the ceramic core and the inner radius, b, of the concentric shell. A known quantity of heat per unit time generated electrically in the ceramic core flowed radially through the specimen to the concentric ceramic shell. The ceramic core had a concentric ring of equally spaced holes at a radius, r', parallel to the axis, each containing a heater wire. Temperatures were measured by an axial thermocouple in the ceramic core and by tangential thermocouples in the ceramic shell at radius c, only one of which is shown in figure 1.

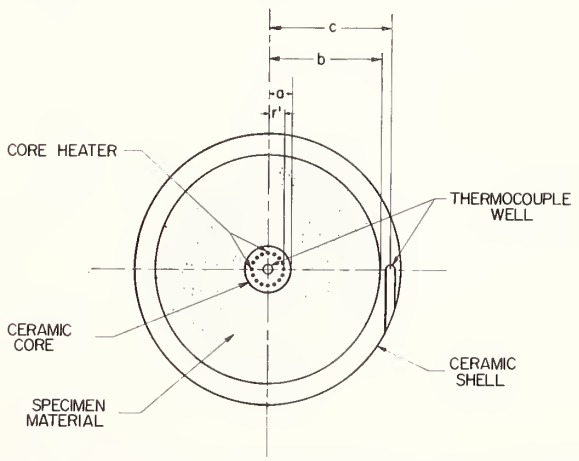

FIGURE 1. *Horizontal cross section of the essential elements of the apparatus.*

In figure 1, if the cylindrical surfaces $r=a$ and $r=b$ are each isothermal, the heat flow between these surfaces will be radial except near the ends. In general, the thermal conductivity of the specimen material will vary with temperature, and the heat flow rate, q, through a cylindrical element of unit axial length is

$$q=-2\pi kr\frac{dT}{dr}. \tag{1}$$

Temperature is denoted by the symbol T, the temperature-dependent thermal conductivity by k, and the radial coordinate by r. For reasonable temperature differences, the thermal conductivity of the specimen material can be assumed to vary linearly with temperature; then (1) becomes

$$q=-2\pi\bar{k}\{1+\alpha(T-\bar{T})\}r\frac{dT}{dr}. \quad (2)$$

$\bar{k}$ is the thermal conductivity at an arbitrary reference temperature, $\bar{T}$, and α is the corresponding temperature coefficient of thermal conductivity. Integration of (2) yields, after substitution of boundary conditions,

$$q=\frac{2\pi\bar{k}(T_a-T_b)}{\ln b/a}, \quad (3)$$

where T_a is the temperature at $r=a$, T_b is the temperature at $r=b$, and $\bar{k}$ corresponds to the temperature $\bar{T}$, which is given by

$$\bar{T}=\frac{T_a+T_b}{2}. \quad (4)$$

If the circle of heater wires at $r=r'$ were a continuous cylindrical heat source, the entire region $r<r'$ inside the heater circle would be isothermal. For the case of a finite number of line heat sources at $r=r'$, the temperature measured at the axis is equal to the average temperature at the radius of the heater circle [1][1] (see also sec. 5). The heat flow to the surface of the core per unit length is given by

$$q=\frac{2\pi k_c(T_0-T_a)}{\ln a/r'}, \quad (5)$$

where T_0 is the temperature measured in the axial well, and k_c is the thermal conductivity of the ceramic core material, corresponding to a temperature $(T_0+T_a)/2$.

Similarly, for the outer ceramic shell,

$$q=\frac{2\pi k_s(T_b-T_c)}{\ln c/b}, \quad (6)$$

where T_c is the temperature measured at $r=c$, and k_s is the thermal conductivity of the ceramic shell material at $(T_b+T_c)/2$.

If there are m heater wires at $r=r'$, each generating heat at the rate q' per unit length, the total heat generated per unit length of core is

$$q=mq'. \quad (7)$$

Combination of eqs (3), (5), (6), and (7) yields

$$\bar{k}=\frac{mq'\ln b/a}{2\pi\left\{T_0-T_c-\frac{mq'}{2\pi}\left(\frac{\ln a/r'}{k_c}+\frac{\ln c/b}{k_s}\right)\right\}}, \quad (8)$$

which is the equation used for purposes of calculation of all thermal conductivity data presented in this paper.

3. Experimental Procedure

3.1. Apparatus

A vertical cross section of the thermal conductivity apparatus is shown in figure 2. The specimen was contained in the annular space between the central ceramic core, which was supported at both ends, and the concentric ceramic shell, which was supported by Transite end pieces. The space between the ceramic shell and the outer stainless steel case contained a loose-fill thermal insulation.

The ceramic shell was a hollow mullite cylinder, 61 cm long, with an inner radius of 3.2 cm and an outer radius of 3.8 cm. A helical groove (about 1.6 turns/cm) on the outer surface was wound with three separate heaters of 0.10 cm Kanthal A–1 heater wire. The main shell heater was 41 cm in length; the upper and lower shell heaters were 5 cm in length. A length of 5 cm at each end was not wound. The upper and lower shell heaters provided extra heat needed to offset end losses, so that longitudinal temperature differences in the central region could be minimized.

The central core was an extruded mullite rod, 46 cm long and 1.27 cm in diameter. Sixteen equally spaced holes, 0.08 cm in diameter, extended the entire length of the rod. The centers of the holes formed a circle of 0.43 cm radius. The core heater, which provided the heat flowing radially through the specimen, consisted of a continuous length of platinum-20 percent rhodium (0.05 cm diam) wire threaded back and forth through the 16 holes. Current lead wires to this heater, and lead wires to its two voltage taps located at the upper end of the ceramic core, were brought in through the hollow ceramic upper support for the core. The core was supported below by a ceramic pin, as shown in figure 2. Both the upper and lower supports were provided with small platinum-20 percent rhodium heaters to minimize longitudinal heat flow at the ends of the ceramic core.

Temperatures in the apparatus were determined by means of six platinum: platinum-10 percent rhodium thermocouples. These thermocouples were fabricated from calibrated thermocouple wire, 0.04 cm in diameter.

Three thermocouples were positioned in the ceramic shell at the midplane of the apparatus. These were inserted into tangential holes (fig. 1) located 120° apart at a radius of 3.5 cm. The temperature, T_c, in (6) and (8) was obtained by taking the average of the temperatures indicated by these three thermocouples. Two additional tangential thermocouples were located in the ceramic shell, one 15 cm above and one 15 cm below the midplane of the apparatus.

Temperatures in the core were measured by means of a thermocouple which was located in a 0.25-cm diam axial well and which could be moved vertically

[1] Figures in brackets indicate the literature references at the end of this paper.

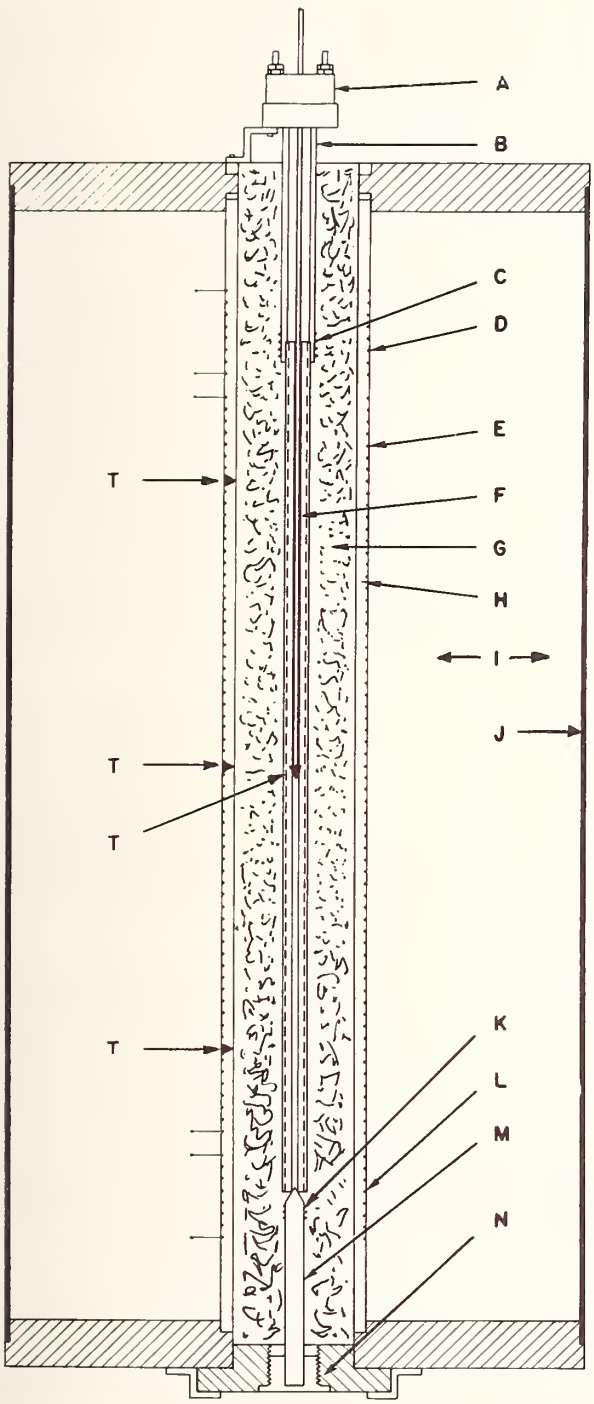

FIGURE 2. *Vertical cross section of the apparatus for determining the thermal conductivity of powders.*

A. Terminal head for current and voltage leads.
B. Ceramic support tube.
C. Upper support heater.
D. Upper shell heater.
E. Main shell heater.
F. Ceramic core.
G. Specimen.
H. Ceramic shell.
I. Shell insulation.
J. Stainless steel case.
K. Lower support heater.
L. Lower shell heater.
M. Ceramic support rod.
N. Removable plug.
T. Thermocouple.

by exterior manipulation. A scale fixed above the apparatus indicated the position of the thermocouple junction. The temperature measured at midlength was designated as T_0.

3.2. Instrumentation

The three heaters on the ceramic shell were fed by variable voltage transformers, which in turn were fed by a voltage regulating transformer. These heaters were individually regulated by on-off controllers actuated by thermocouples located in the ceramic shell adjacent to the heater windings. The heaters on the ceramic core supports were manually adjusted by means of variable voltage transformers.

The ceramic core heater, which provided the heat flowing radially through the specimen, was powered by a 28-v, 4-amp, regulated d-c power supply, with a small bank of power resistors in series for adjusting to the desired heater current. Power input to the ceramic core heater was determined by measuring the d-c current through the heater and the voltage drop across the entire length of heater wire in the core. These measurements were made using calibrated shunt and volt boxes and measuring their output voltages by means of a precision d-c potentiometer.

The noble metal leads of the six measuring thermocouples were brought to an isothermal zone box at room temperature. A thermocouple with one junction in the zone box and one in an ice bath was placed in series with a double-pole selector switch, so that each measuring thermocouple was automatically referenced against the ice bath [2]. Thermocouple voltages were read to 0.1 μv on the precision potentiometer.

3.3. Test Procedure

The specimen material was placed in the annular space between the ceramic core and the ceramic shell through the opening at the top of the apparatus. The bulk density of the specimen in place was computed from the weight of specimen material and the volume of the test chamber.

The shell temperature controllers were set at the desired temperature, which for the first test in any series was about 100 °C, and all heaters were turned on. The controllers and power for the heaters at the top and bottom of the ceramic shell were adjusted, if necessary, until the temperatures indicated by the upper and lower tangential thermocouples agreed to within 1 or 2 deg C with the average temperature of the three midplane tangential thermocouples. The power to the core heater was adjusted to attain the desired radial temperature drop across the specimen, and the power to the heaters on the ceramic core supports was adjusted until a traverse of the thermocouple in the axial hole indicated the desired longitudinal temperature distribution.

When a satisfactory steady-state condition was obtained, the test data were recorded. With the axial thermocouple in the midplane position, three sets of readings (at about 20 min intervals) were

taken of all thermocouples and of the output of the volt box and shunt box. At the end of these readings, the axial thermocouple was moved to a position near the top of the ceramic core. After this thermocouple again reached thermal equilibrium, its output was read on the potentiometer. Readings were taken at 5 cm intervals over a region 15 cm or more on either side of the midplane. When a complete set of data had been taken, the apparatus was adjusted to a new temperature level, as desired for the next test.

3.4. Calculation of Results

Calculations of thermal conductivity values by means of eq (8) were performed by means of a digital computer. The data input to the computer consisted of the average emf readings for each thermocouple and the average readings from the volt and shunt boxes. Equations for the estimated thermal conductivities of the ceramic core and shell as functions of temperature, and for temperatures as a function of thermocouple emfs, were contained in the computer program.

4. Results

4.1. Diatomaceous Earth

Test results for a specimen of commercial diatomaceous earth are presented in figure 3. The in-place bulk density of the specimen was 0.15 g/cm³. The temperature difference across the specimen during the various tests was from 30 to 60 deg C.

The open squares in figure 3 represent results obtained in five tests before heaters were placed at the ends of the ceramic core to minimize axial heat flows. For these five tests, the temperature difference between the ceramic core and shell was 10 to 25 percent less at positions 15 cm from the midplane than it was at the midplane. (These data, as well as those presented below, were calculated using eq (8); the effect of a nonuniform axial temperature distribution is discussed in sec. 5.2.)

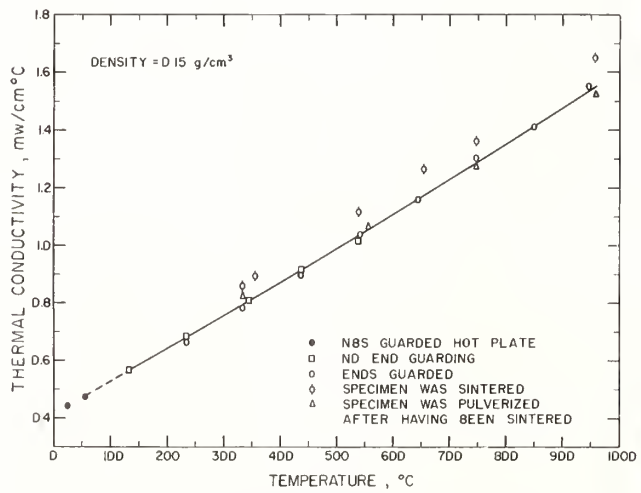

FIGURE 3. *Thermal conductivity of a diatomaceous earth as a function of temperature.*

After these five tests, the specimen was removed and heaters were installed on the ceramic core supports. The same sample was then reinstalled as the specimen, and the data represented by the open circles were taken in order of increasing mean temperature. After the test at a mean temperature of 946 °C, tests were conducted at several lower temperatures and finally at a maximum temperature. The results of these tests, indicated in figure 3 by circles with vertical lines through them, were significantly higher than those of previous tests. Removal of the specimen indicated that a slight sintering had occurred.[2] The powder appeared to be slightly fused together, but was easily broken apart. The same sample was pulverized by hand, replaced in the apparatus, and the test results indicated by the open triangles were obtained.

The curve drawn through the data points in figure 3 is the quadratic equation of least-mean-squares fit to the open squares, circles, and triangles. The equation for this line is

$$\bar{k}=0.414+1.114\left(\frac{\bar{T}}{1000}\right)+0.072\left(\frac{\bar{T}}{1000}\right)^2, \qquad (9)$$

where $\bar{k}$ is expressed in milliwatts/cm-deg C and $\bar{T}$ in °C. For all data points except the circles with vertical lines through them, the standard deviation of a point, estimated from the residuals about the fitted line, is 0.013 mw/cm-C, corresponding to 1.3 percent at 500 °C.

The solid circles shown in the lower left hand corner of figure 3 represent results of tests made on a sample of diatomaceous earth from the same container, at the same density, in the NBS guarded hot-plate apparatus (ASTM C177).

Figure 4 presents some literature data on diatomaceous earth of various densities [3, 4]; the curve from figure 3 is reproduced for comparison. There is substantial agreement between the results of this investigation and those from the literature, taking density into consideration.

4.2. Powdered Alumina

Test results for an aluminum oxide powder are presented in figure 5. This alumina was produced at the National Bureau of Standards by ignition of hydrated aluminum chloride in a muffle furnace at 1,150 °C. The method of production and some of the properties of this type of alumina powder have been described [5].

[2] An uncontaminated diatomaceous earth should melt at the temperature of fusion of silica, which is well above any temperatures obtained in these tests. A commercial diatomaceous earth, however, may contain sufficient clay to produce sintering at temperatures as low as 800 °C. No tests were conducted to determine the actual temperature at which sintering began for the diatomaceous earth discussed in this paper. In general, diatomaceous earth should be used with caution at temperatures above 800 °C if sintering would cause difficulties.

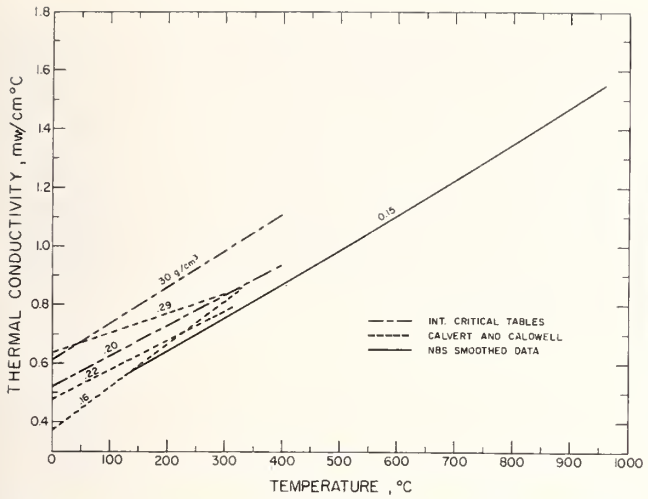

FIGURE 4. *Comparison of diatomaceous earth thermal conductivity results with literature data.*

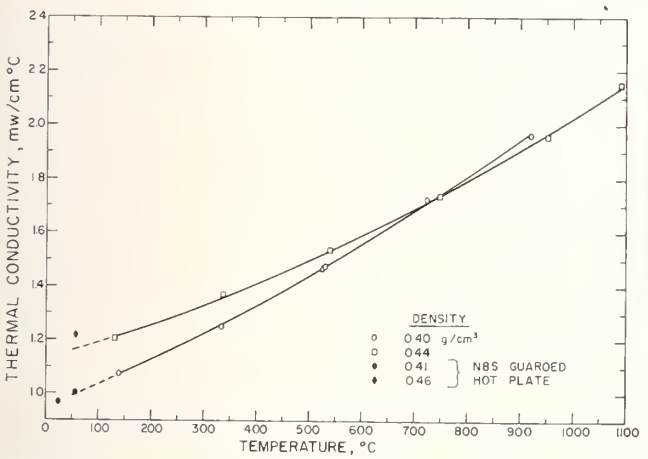

FIGURE 5. *Thermal conductivity of an aluminum oxide powder as a function of temperature.*

The data indicated by the open squares in figure 5 were taken in order of increasing mean temperature on a specimen having a bulk density [3] of 0.44 g/cm³. The curve drawn through the squares is the quadratic equation of least-mean-squares fit. The equation for this line is

$$\bar{k}=1.130+0.566\left(\frac{\bar{T}}{1000}\right)+0.333\left(\frac{\bar{T}}{1000}\right)^2, \quad (10)$$

where $\bar{k}$ is expressed in mw/cm-C and $\bar{T}$ in °C. The estimated standard deviation of a point is 0.010 mw/cm-C, corresponding to 0.7 percent at 500 °C.

The data indicated by the open circles were taken in order of increasing mean temperature on a specimen having a bulk density of 0.40 g/cm³. The specimen was the same sample as that previously tested, but was intentionally packed to a lower bulk density. After the tests up to 919 °C, a test, indicated by an open triangle, was made at 526 °C. The curve drawn through the open circles and the triangle is the quadratic equation of least-mean-squares fit to these points. This equation is

$$\bar{k}=0.947+0.841\left(\frac{\bar{T}}{1000}\right)+0.296\left(\frac{\bar{T}}{1000}\right)^2, \quad (11)$$

in the same units as above. The estimated standard deviation of a point is 0.011 mw/cm-C, corresponding to 0.8 percent at 500 °C.

The solid circles shown in the lower left-hand corner of figure 5 represent results of two tests made in the NBS guarded hot-plate apparatus on a sample of alumina powder, taken from the same batch as the sample installed in the ceramic core apparatus, having a bulk density of 0.41 g/cm³. The solid diamond shown represents a guarded hot-plate test on the sample of alumina which had been tested in the ceramic core apparatus at higher temperatures. The in-place bulk density for this test was 0.46 g/cm³.

The higher density specimen (0.44 g/cm³) had a room temperature thermal conductivity about 20 percent higher than that of the lower density specimen (0.40 g/cm³). However, the curves corresponding to these different densities converged with increasing temperature and crossed at about 730 °C. This crossing of the curves is believed to arise from increased radiation within the larger pores of the lower density material.

5. Discussion of Test Method

5.1. Determination of Temperature Difference Across the Specimen

Measurement of the temperature difference across the specimen, using the core and shell thermocouples shown in figure 1, represents a departure from the procedure used in radial flow methods for loose-fill materials described in the recent literature [6, 7]. The possibility of chemical contamination of thermocouples by the specimen material is greatly reduced, and the often-difficult problem of determining and maintaining the distance between thermocouples located within the specimen material is avoided. However, with the method of measurement used here, account must be taken of temperature drops in the core and shell, and at their interfaces with the specimen if necessary, to obtain the temperature drop across the specimen.

The thermocouple in the axial hole at midlength of the central ceramic core is located in a region where there are substantially no temperature gradients, and therefore the thermocouple accurately attains the temperature of its environment without disturbing the heat flow pattern. The theory of a harmonic logarithmic potential function shows that

[3] Later checks of the packing procedure used for this specimen indicate a possible uncertainty of 0.02 g/cm³ in the reported in-place bulk density. All other densities reported are believed to be accurate to within 0.005 g/cm³.

the value of the temperature at the center of a circle is equal to the average of its values over the circumference of the circle [8,9]. Hence, the temperature measured at the axis of the core is equal to the average temperature at the fictitious surface, $r=r'$. The difference between the average temperature of the fictitious surface at $r=r'$ and the average temperature of the surface of the core at $r=a$ may be computed from (5). It is to be noted that eq (5) is valid regardless of the distribution of heat sources on the circle $r=r'$, as has also been shown by Peavy [1] in analyzing the two-body system of the specimen and the core with line heat sources.

Similarly, the temperature difference, T_b-T_c, from the inner surface of the shell to the radius of the tangential thermocouples may be computed from (6).

The uncertainty in determining the temperature difference between the axial thermocouple in the core and the three thermocouples in the shell is estimated[4] to be less than 1 percent. The computed temperature drops in the core (T_0-T_a) and in the shell (T_b-T_c) were less than 2.4 percent and 0.6 percent, respectively, of the temperature drop through the specimen for all of the results presented in section 4, using the best available values for the thermal conductivities of the mullite core and shell, the uncertainties in which may have been as much as 30 percent.

The effective radius, r', of the virtual heating surface in the core is uncertain by not more than the radius of the heater holes, thus introducing an additional error of not more than 25 percent of T_0-T_a. Similarly, the effective radius, c, to the tangential thermocouple wells is uncertain by not more than the radius of the wells, thus introducing an additional error of not more than 35 percent of T_b-T_c. Combining the errors arising from the uncertainties in k_c and k_s and those from ln a/r' and ln c/b, the estimated uncertainties in T_0-T_a and T_b-T_c are 40 and 50 percent, respectively, thus introducing an additional uncertainty in T_a-T_b of 1.3 percent. For fine powders of low thermal conductivity, such as those tested, errors due to thermal contact resistance between the specimen and the surfaces of the core and shell are believed to be negligible. Thus, combining uncertainties, the temperature drop across the specimen (the expression in braces in the denominator of eq (8)) is considered to be known with an uncertainty of 1.5 percent.

5.2. Longitudinal Heat Flow

Equation (8) was derived on the assumption of no longitudinal heat flow. For an apparatus of finite length, having imperfect end guarding, the effects of axial heat flow should be considered. Jakob [11] considered the effect of axial heat flow for the symmetrical case in which both ends of the core are at the same temperature but are at a temperature different from that at the center. An analysis is presented here which allows different temperatures at the two ends of the core, and also takes into account the effect of core temperature distribution on the power measurement if the electrical resistivity of the heater wire varies linearly with temperature.

A simplified cross-sectional view of the apparatus is shown in figure 6. It is assumed that the surface $r=b$ is isothermal at temperature T_b and that temperatures are measured in the core at three positions equally spaced along the axis. It is assumed that, for the purpose of analyzing longitudinal heat flow, a transverse cross section of the core can be treated as being isothermal.

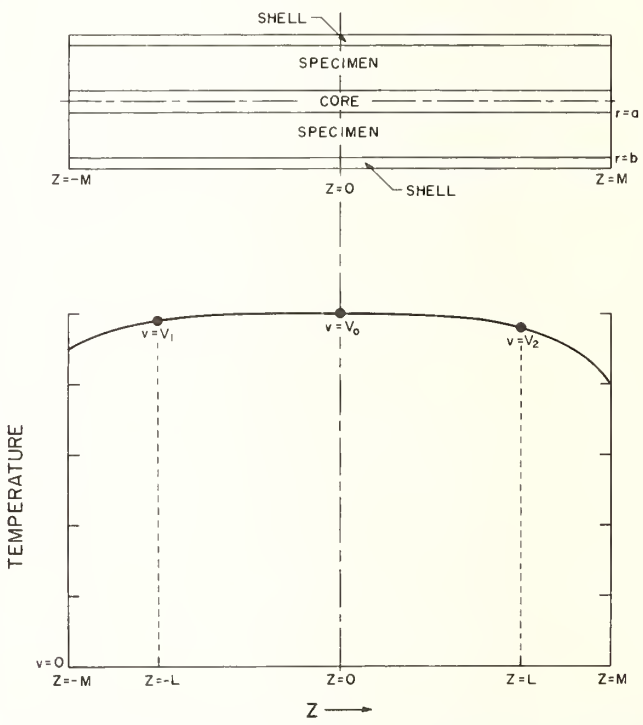

FIGURE 6. *General core temperature profile used in analyzing effects of longitudinal core temperature imbalance.*

Neglecting longitudinal heat flow in the specimen, the differential equation for heat flow along the core can be written as

$$\frac{d^2v}{dz^2}-\frac{2\pi\bar{k}v}{C\ln b/a}=-\frac{mq'}{C}, \tag{12}$$

where

$v=T-T_b$, T being the temperature at any point along the core;

$z=$longitudinal coordinate;

and

$C=$the longitudinal thermal conductance per unit length of the core, including heater wires and holes.

In general, the rate of heat generation, q', per unit length of heater wire will not be constant if the electrical resistivity of the heater wire varies appreciably

[4] All estimated uncertainties in this paper represent the author's estimate of the "two-sigma" limit. All uncertainties are combined using standard propagation of error formulas (see, for instance, Davies [10]).

with temperature. For reasonable temperature variations, the electrical resistance per unit length of heater wire can be assumed to be a linear function of temperature,

$$\rho=\rho_0(1+\gamma v), \tag{13}$$

where ρ and ρ_0 are the electrical resistances of a unit length of heater wire at temperatures T and T_0, respectively, and γ is the fractional change in electrical resistivity per unit change in temperature. The rate of heat generation per unit length of heater wire is

$$q'=I^2\rho=I^2\rho_0(1+\gamma v), \tag{14}$$

where I is the electrical current flowing through the heater. Equation (14) must be substituted into (12).

The conditions which are to be satisfied are

$$\begin{aligned} &v=V_1 \text{ at } z=-L.\\ &v=V_0 \text{ at } z=0\\ &v=V_2 \text{ at } z=L \end{aligned} \tag{15}$$

Substitution of these conditions into the solution of (12) yields

$$v=V_0+\left(\frac{V_1+V_2-2V_0}{2}\right)\frac{\cosh \mu z-1}{\cosh \mu L-1}+\left(\frac{V_2-V_1}{2}\right)\frac{\sinh \mu z}{\sinh \mu L}, \tag{16}$$

in which

$$\mu^2=\frac{1}{\bar{k}'}\left[\frac{2\pi\bar{k}}{\ln (b/a)}-\gamma m I^2\rho_0\right]. \tag{17}$$

The thermal conductivity of the specimen is given by

$$\bar{k}=\frac{mI^2\rho_0 \ln (b/a)}{2\pi V_0}\left[1+\gamma V_0+\frac{V_1+V_2-2V_0}{2V_0\cosh \mu L-(V_1+V_2)}\right]. \tag{18}$$

The total power delivered by the core heater is determined by the current, I, through the heater and the voltage drop, E, across the total length of heater wire in the core. The total resistance of the heater is given by

$$R=E/I=\rho_0(1+\gamma\bar{V})S \tag{19}$$

where S is the total length of heater wire and $\bar{V}$ is the average temperature of the core heater, obtained by integration of (16) over the entire length, $2M$, of the core,

$$\bar{V}=\frac{1}{2M}\int_{-M}^{M} v\,dz=V_0+\left(\frac{V_1+V_2-2V_0}{2}\right)\frac{\sinh \mu M}{\mu M(\cosh \mu L-1)}. \tag{20}$$

Equation (18) can be rewritten as

$$\bar{k}=\bar{k}'\left[1+\frac{V_1+V_2-2V_0}{1+\gamma\bar{V}}\left\{\frac{1}{2V_0\cosh \mu L-(V_1+V_2)}-\frac{\gamma(\sinh \mu M-\mu M)}{2\mu M(\cosh \mu L-1)}\right\}\right] \tag{21}$$

where

$$\bar{k}'=\frac{mEI \ln (b/a)}{2\pi V_0 S} \tag{22}$$

is the apparent value of thermal conductivity obtained if no corrections are made for the effects of axial heat flow. Since $\bar{k}$ is defined in terms of μ and μ in terms of $\bar{k}$, iterations are necessary in order to obtain $\bar{k}$. A first approximation to $\bar{k}$ is given by $\bar{k}'$; substitution of $\bar{k}'$ into (17) yields a value of μ which can be used in (21). The resultant $\bar{k}$ can be used to obtain a better value of μ, etc. The convergence is quite rapid in all practical cases; the first approximation did not introduce an inaccuracy greater than 0.003 percent in $\bar{k}$ for the case to be discussed below. Equation (22) corresponds to (8), the equation that was used for purposes of calculation; EI/S corresponds to q', and V_0 corresponds to the expression in braces in the denominator of (8). The first expression in the braces in (21) represents the correction for axial heat flow; the second expression represents the correction in power measurement to take account of the variation of electrical resistance with temperature. It is of interest to note that, for a positive value of γ, these corrections are of opposite sign.

Data were presented in section 4.1 for which the temperature difference between the ceramic core and the substantially isothermal ceramic shell was 10 to 25 percent less at positions 15 cm from the midplane than at the center. As seen in figure 3, the results for these tests were not appreciably different from the conductivities obtained later when the core was substantially uniform in temperature along its length.

In order to investigate more thoroughly the effects of axial heat flow in the apparatus, a series of five tests was conducted in which the ends of the ceramic core were held at temperatures different from that in the core at the midplane. These tests were all conducted at a mean temperature of 525 °C, with the alumina powder specimen discussed in section 4.2.

The ceramic shell was maintained approximately isothermal over a central region of at least 30 cm length. The core temperature at positions 15 cm above and below the midplane was varied by adjustment of the small heaters at each end of the ceramic core. The results of these tests are shown in figure 7, where the percent departure of the thermal conductivities from their mean value is plotted against the quantity $(V_1+V_2)/2V_0$. The solid circles represent experimental data; the solid curve is the straight line of least-mean-squares fit to the data. A straight line was used because, for the various values of parameters involved, the departure can be shown to be a nearly linear function of $(V_1+V_2)/2V_0$ for values

not too different from 1.0. The slope of the straight line in figure 7 was used to compute the value for μ of 0.29 cm^{-1} where γ was taken as 8.0×10^{-4} deg C^{-1}, V_0 as 44 deg C, L as 15 cm, and M as 23 cm. Substitution of this value of μ into (17) yields for the longitudinal conductance of the core, C', a value of 0.06 w-cm/C. This value agrees with the estimated longitudinal conductance of the ceramic core and heater wires.

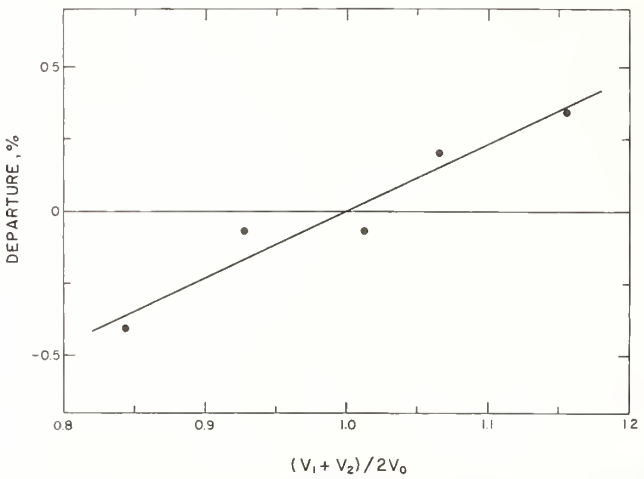

FIGURE 7. *Effect of longitudinal core temperature imbalance,* $(V_1+V_2)/2V_0$, *on thermal conductivity values obtained for alumina powder.*

With the exception of those tests in which core end heaters were not used, all data presented in section 4 gave values of $(V_1+V_2)/2V_0$ between 0.85 and 1.15. From figure 7, it is seen that this corresponds to an uncertainty of less than 0.4 percent in the thermal conductivity values obtained using (8). Values of $(V_1+V_2)/2V_0$ could be held between 0.95 and 1.05 without undue difficulty, if desired, thus further reducing this uncertainty.

5.3. Eccentricity

It has been assumed that the outer surface of the ceramic core and the inner surface of the ceramic shell were concentric cylinders. Since concentricity may not always be possible, the effect of eccentricities should be considered. The thermal resistance between two eccentric parallel circular cylinders is given by Carslaw and Jaeger [12] and is, in the notation of this paper,

$$\frac{T_a-T_b}{q}=\frac{1}{2\pi\bar{k}}\operatorname{arccosh}\frac{a^2+b^2-e^2}{2ab}, \qquad (23)$$

where e is the eccentricity, or the distance between the centers of the two cylinders.

From (23), the thermal conductivity is given by

$$\bar{k}=\frac{q}{2\pi(T_a-T_b)}\operatorname{arccosh}\frac{1+\lambda^2-\epsilon^2(\lambda-1)^2}{2\lambda}, \qquad (24)$$

where, following El-Saden [13], the dimensionless eccentricity $\epsilon=e/(b-a)$ varies between zero (concentricity) and one (cylinders in contact), and $\lambda=b/a$ is the ratio of the radii.[5,6]

For the case of eccentric cylinders, if (3) is used instead of (24) to compute the thermal conductivity of the specimen, an error will be introduced. Since it is of general interest, the percent error due to neglecting the effect of eccentricity is shown in figure 8 plotted against dimensionless eccentricity, ϵ, for several radius ratios, $\lambda=b/a$.

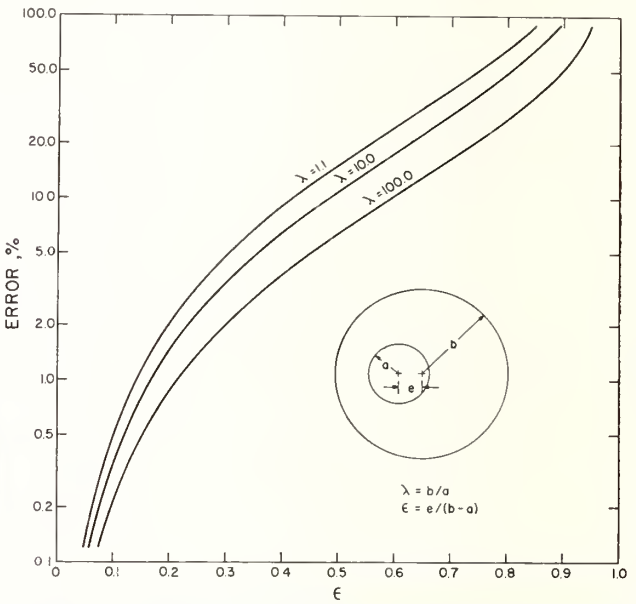

FIGURE 8. *Calculated error in thermal conductivity due to neglecting the effect of eccentricity for radial heat flow between isothermal cylinders.*

For the apparatus described in this paper, the ratio λ was approximately 5.0. The dimensionless eccentricity as defined above was less than 0.05, so that the uncertainty due to eccentricity was less than 0.1 percent.

5.5. Precision and Accuracy of Results

The precision of measurement is indicated by the standard deviations (estimated) of the data, which are of the order of 1 percent.

The accuracy of the reported measurements is more difficult to estimate. The total power generated in the core heater was known to within 0.1 percent. The length of wire between the potential taps at room temperature was known to within 0.2 percent. Thermal expansion could have increased this length by 1 percent at 1,000 °C if friction between the heater wire and the ceramic core at points of contact did not prevent free longitudinal expansion of the wire in the holes. Because the

[5] Equation (24) can also be derived from the last equation presented by El-Saden. To convert El-Saden's eq (38) to the form presented above, it is helpful to make use of the identity $\operatorname{arccosh} x-\operatorname{arccosh} y=\operatorname{arccosh}(xy-\sqrt{(x^2-1)(y^2-1)})$.

[6] Making use of the identity $\operatorname{arccosh} x=\ln(x+\sqrt{x^2-1})$, eq (24) reduces to the equivalent of (3) for the case of concentric cylinders ($\epsilon=0$).

effect of expansion was uncertain, no expansion corrections were made. The heat flowing radially through the specimen is further in question by not more than 0.4 percent in an extreme case, due to the uncorrected effects of longitudinal temperature variations along the core (see sec. 5.2).

In section 5.1, it was estimated that temperature drops across the specimen were determined with an uncertainty of 1.5 percent. Uncertainties in the ratio of the shell radius to that of the core did not introduce more than 0.2 percent uncertainty in the results. The error due to possible eccentricity of the ceramic core in the ceramic shell did not exceed 0.1 percent. Combining all of the uncertainties discussed, uncertainties in the thermal conductivity results presented in section 4 are estimated to be less than 2 percent at 100 °C, and, because of heater wire expansion, 3 percent at 1,000 °C.

5.5. Comments

It is felt that the type of central heater used in this apparatus has advantages which may recommend it to others interested in radial heat flow measurements. The particular advantages of this arrangement are, (1) the measuring thermocouple in the core attains the temperature to be measured and does not interfere with the pattern of heat flow, (2) the measuring thermocouple is well protected both mechanically and chemically but still can be easily removed for calibration or renewal, and (3) temperatures can be measured at any desired longitudinal position using the same thermocouple.

By means of suitable modifications, the equipment described could be extended to cryogenic temperatures, or to more elevated temperatures. If required, the accuracy of measurement could be improved over that attained in the apparatus described by taking careful account of all the factors discussed in sections 5.1 and 5.2. Applications for which a heated core of this type might be advantageous include determination of forced or natural convection from cylinders and determination of the thermal conductivity of pipe insulations or fluids. In the latter case, convective effects would need to be excluded by extrapolating results obtained with small temperature differences to zero temperature difference.

The experimental measurements were performed by C. T. Siu and J. E. Griffith. The author thanks T. W. Watson for conducting the various tests on the NBS guarded hot plate apparatus. The very helpful suggestions and comments by B. A. Peavy and H. E. Robinson are gratefully acknowledged.

6. References

[1] B. A. Peavy, Steady state heat conduction in cylinders with multiple continuous line heat sources, J. Research NBS **67C** (Eng. and Instr.) No. 2. 119–127 (Apr.-June 1963).

[2] W. F. Roeser, Thermoelectric thermometry, J. Appl. Phys. **11,** pp. 404–405 (1940); also in Temperature, Its Measurement and Control in Science and Industry, p. 202 (Reinhold Publishing Corp., New York, N. Y., 1941).

[3] International Critical Tables, Vol. II, p. 315 (McGraw-Hill, New York, N.Y., 1927).

[4] R. Calvert and L. Caldwell, Loss of heat from furnace walls, Ind. Eng. Chem. **16,** pp. 483–490 (1924).

[5] J. I. Hoffman, R. F. Leslie, H. J. Caul, L. J. Clark and J. D. Hoffman, Development of a hydrochloric acid process for the production of alumina from clay, J. Research NBS **37,** p. 409 (1946) RP1756.

[6] R. G. Deissler and D. S. Eian, Investigation of effective thermal conductivities of powders, National Advisory Committee for Aeronautics RM E52C05 (1952).

[7] M. J. Laubitz, Thermal conductivity of powders, Can. J. Phys. **37,** p. 798 (1959).

[8] O.D. Kellogg, Foundations of Potential Theory, p. 223 (Frederick Ungar Publishing Co., New York, N. Y., 1929; reprinted by Dover Publications, Inc., New York, N. Y., 1953).

[9] W. J. Sternberg and F. I. Smith, The Theory of Potential and Spherical Harmonics, pp. 74–76 (The Univ. of Toronto Press, Toronto, Canada, 1946).

[10] O. L. Davies, Statistical Method in Research and Production, 3d ed., pp. 40–41 (Hafner Publ. Co., New York, N.Y., 1957).

[11] M. Jakob, Heat Transfer, Vol. 1, pp. 246–250 (John Wiley and Sons, Inc., New York, N. Y., 1949).

[12] H. S. Carslaw and J. C. Jaeger, The Conduction of Heat in Solids, 2d ed., p. 451, equation 19 (Oxford Univ. Press, 1959).

[13] M. R. El-Saden, Heat conduction in an eccentrically hollow, infinitely long cylinder with internal heat generation, J. Heat Transfer, Trans. ASME, Series C, **83,** 510 (1961).

(Paper 67C2–126)

JOURNAL OF RESEARCH of the National Bureau of Standards—C. Engineering and Instrumentation
Vol. 71C, No. 4, October–December 1967

Measurements of the Thermal Conductivity and Electrical Resistivity of Platinum from 100 to 900 °C*

D. R. Flynn and M. E. O'Hagan**

Institute for Applied Technology, National Bureau of Standards, Washington, D.C. 20234

(August 17, 1967)

1. Introduction

Standards and standard reference materials are the basis of a consistent and accurate measuring system. The need for standard reference materials in thermal conductivity measurements is two-fold. In the first place, such materials are required for comparative measurements in which the thermal conductivity of the material under test is determined in terms of that of the standard reference material. Secondly, such materials are required in evaluating the accuracy of apparatus designed for thermal conductivity measurements. The degree to which the measured value of the thermal conductivity of the standard reference material agrees with the accepted value is a check on the accuracy of the apparatus in which the measurements were made.

The basic requirements for any standard reference material are that it be stable, reproducible and appropriate for the measurements at hand, and that the property in question be uniform throughout the material. In the case of standard reference materials for thermal conductivity other desirable requirements are that the standard be usable over a wide range of temperature, that it be chemically inert so as not to be affected by or affect other materials in the system and that the thermal conductivity of the reference material be close in value to that of the materials which are to be measured in terms of it.

The advantages of using platinum as a thermal conductivity reference material have been pointed out by Powell and Tye [1][1] and by Slack [2]. Platinum is available in high purity in pieces of substantial size. It has a fairly high melting point (1769 °C on the 1948 International Practical Temperature Scale), has no known transition points, and is relatively stable chemically in air and other atmospheres, with the exception of hydrogen, even at high temperatures [3, 4]. Its thermal conductivity, although relatively high for use as a reference material with nonmetals, is about the geometric mean for metals and alloys.

Since the thermal conductivity of a pure metal is strongly correlated with the electrical conductivity of the metal, it is highly desirable that the electrical conductivity of a metal which is intended for use as a thermal conductivity reference material be very stable under varying heat treatments. The stability of the electrical conductivity of platinum is evidenced by the fact that the International Practical Temperature Scale is defined by a platinum resistance thermometer in the temperature range −182.97 to +630.5 °C [5, 6]. Studies are currently underway at NBS [7] and other laboratories to investigate the possibility of extending to the gold-point (1063 °C) the range over which a platinum resistance thermometer is used to define the temperature scale.

*This research was the subject of a dissertation submitted by M. E. O'Hagan to the Faculty of The School of Engineering and Applied Science, The George Washington University, in partial satisfaction of the requirements for the degree of Doctor of Science. This work was supported in part by Engelhard Industries, Inc., Newark, New Jersey, who supplied the platinum and financial assistance in the form of a grant to the National Bureau of Standards. M. E. O'Hagan was supported in part by Grant AFOSR-1025-66 from the Air Force Office of Scientific Research and in part by the Institute for Industrial Research and Standards, Dublin, Ireland.

**Present address: Institute for Industrial Research and Standards, Dublin, Ireland.

[1] Figures in brackets indicate the literature references at the end of this paper.

Platinum appears to be, in every way save one, an ideal material to use as a thermal conductivity reference standard. The exception is that the spread among the literature values for the thermal conductivity of platinum is considerable, to say the least.

Powell, Ho, and Liley [8] show a plot of essentially all of the published thermal conductivity data for platinum through the year 1965. The spread in the data increases from about 10 percent at room temperature to over 30 percent at 1000 °C. Even if many of the older data are discounted, the picture is not particularly improved. O'Hagan [9] has summarized the methods used for previous measurements of the thermal conductivity of platinum and also has summarized the characterizations of the various samples.

Prior to the measurements of Powell and Tye [1], all thermal conductivity values reported for platinum at temperatures above 100 °C were obtained by methods in which the temperature gradient in the specimen was produced by Joule heating due to passage of an electric current directly through the specimen. While the results of all but one [10] of these higher temperature investigations employing electrical methods essentially agree with one another, they disagree with those of later investigations [1, 11, 12], which employed nonelectrical methods. This raised the question as to whether or not electrical methods yield results that are intrinsically different from those of nonelectrical methods. This could mean that the theory which has been used in analyzing electrical methods is in error, or it could mean that heat conduction is significantly dependent on electric current density, at least in the case of platinum.

The considerations discussed above pointed to the need for a comprehensive investigation of the thermal conductivity of platinum. It was felt that both an absolute steady-state method *without* an electric current flowing in the specimen, and also an absolute steady-state method *with* a current flowing in the specimen should be employed.

As regards the nonelectrical method, experience at NBS with guarded longitudinal heat flow methods indicated that such a method could be made to yield accurate results on a material having as high a thermal conductivity as platinum, provided a specimen of sufficient cross-sectional area was used. With a fairly conductive metal, there were no particular advantages in going to a radial heat flow method; furthermore, to do so would have required a much larger sample.

As regards the electrical method, an arrangement utilizing quite large current densities would be more likely to reveal deviations due to a dependence of thermal conductivity on current density. It was also desirable to use the same method as that used by most of the previous investigators. Fortunately, these two desiderata both pointed to the necked-down sample configuration utilized for measurements on platinum by Holm and Störmer [13], by Hopkins [14], and by Cutler, et al. [15].

To give a direct and accurate comparison between the two methods it was considered desirable to combine both sets of measurements in one apparatus and on the same specimen thereby eliminating a number of uncertainties which would arise in comparing data derived from measurements in different apparatus and on different specimens. The above considerations led to an apparatus, described in section 3, in which thermal conductivity measurements can be made by both the usual longitudinal heat flow method and by an electrical method.

It was also felt that thermal conductivity measurements should be made on platinum samples of at least two purities. Samples were obtained of a high purity platinum (resistance thermometer grade) and of a somewhat lower purity platinum (commercial grade). As of this writing, only the measurements on the lower purity platinum sample have been completed. The results obtained on that sample are presented in this paper and are compared with the results of other investigators.

2. Description of Sample

In order for a valid comparison to be made between the results of different investigators who measure on a particular kind of material, it is necessary that their specimens be characterized as extensively as possible so that differences in specimens may be accounted for. For this reason a number of pertinent measurements were made in an attempt to characterize the specimen used in the present investigation. These measurements and the results thereof are described below.

The platinum was provided by Englehard Industries, Inc., in the form of a solid bar 2.04 cm in diameter by 31 cm long, and was classified as being of commercial purity. The fabrication and cleaning procedures used in preparing the platinum have been described by O'Hagan [9].

The as-received bar was annealed in air for 5.5 hr at 770 °C in a horizontal tubular furnace and furnace cooled at a rate of approximately 120 deg/hr. Shortly thereafter the bar was accidentally dropped causing it to deform slightly at one end. After correcting the damage the bar was reannealed for 1.5 hr at 680 °C and furnace cooled at a rate of approximately 90 deg/hr. Its thermal conductivity was then measured in the NBS Metals Apparatus [34, 35] over the temperature range −160 to +810 °C [32].

Following these measurements the bar was machined and ground to 25.4 cm long by 2.000 cm diam. The density of this bar was measured (see below) and the electrical resistance was measured at ice and liquid helium temperatures (see below). The thermal conductivity specimen (18.4 cm long by 2.000 cm diam) was then fabricated from one end of this bar. A length of 6.4 cm was cut from the other end for separate low temperature thermal conductivity measurements [33]. The remaining disk, approximately 1 cm long, was reserved for metallographic and spectrographic analyses.

A thin neck, approximately 0.1 cm in diameter and 0.3 cm long, was machined in the thermal conductivity specimen at approximately 4 cm from one end. To cleanse this necked-down region of oil and any con-

tamination contracted from the cutting tools, the following cleaning procedure was followed. Degreasing was effected by immersion for half an hour in trichlorethylene vapor. The neck was then pickled for 10 min in hot 50 percent nitric acid. Following this the neck was washed in distilled water, pickled for 10 min in 50 percent hot hydrochloric acid, and again washed in distilled water. There was equal likelihood of the rest of the specimen having slight surface contamination as a result of machining but its effect on the bulk properties of the specimen would not be nearly as grave as the corresponding effect in the neck region. It was considered sufficient to clean the surface of the specimen with toluene and carbon tetrachloride.

A general qualitative spectrographic analysis, performed by the NBS Spectrochemical Analysis Section on the 2-cm-diam by 1-cm-long platinum disk mentioned above, detected Ag (10–100 ppm), Pd (10–100 ppm), Fe (< 10 ppm), and Mg (< 10 ppm). O'Hagan [9] reported the results of a quantitative spectrographic analysis made on a portion of a 0.05 cm wire drawn from the same platinum ingot as the thermal conductivity specimen.

Photomicrographs were also made of the platinum disk cut from the bar sample. They showed grain size to be of the order of 0.02 cm. No evidence appeared of inclusions of foreign matter or of any irregularities in microstructure. Hardness measurements were made on the original platinum bar, after the second anneal, using a Vickers Pyramidal Diamond Tester with a 10 kg load. Values ranged from 36.5 to 38.0 Vickers hardness number.

The density of the bar, when it was 25.4 cm long, was determined by mass and dimensional measurements to be 21.384 g/cm^3 at 21 °C, accurate to within ± 0.002 g/cm^3. This density is an average value for the whole bar and there is no guarantee that the density was uniform to that degree throughout the bar.

The ratio of the resistance at the ice-point temperature to that at the boiling point of helium at atmospheric pressure is a measure of the extent and condition of impurities in a material and of the crystallographic state of the material. This ratio was determined on the 2-cm-diam bar.

The ice-point resistances were measured both before and after the helium point measurements. The current was supplied from a regulated d-c power supply and was measured using a calibrated resistor and a precision potentiometer. The voltage drops in the specimens were measured on a high precision 6-dial potentiometer. In each case the resistance was measured at three or four different current levels and the value corresponding to zero current obtained by extrapolation. The ratio of the resistance of the sample at the ice-point to that at the helium-point was found to be 393. This value is believed to be accurate to within 1 percent. However, it corresponds to an average value over a considerable length of the sample and the sample may not have been uniform in purity throughout.

A set of knife edges of known separation was fastened to the 2-cm bar during the first set of ice-point resistance measurements. The knife edges acted as potential taps. Using the known separation of the knife edges and the cross-sectional area of the bar, the ice-point resistivity, corrected to 0 °C dimensions, was determined to be 9.847$\mu\Omega$ cm, accurate to within $\pm 0.010\mu\Omega$ cm.

A length of 0.05 cm platinum wire, drawn from the same ingot as the thermal conductivity sample, was electrically annealed in air for 1 hr at about 1450 °C. The electromotive force of this wire versus the platinum standard Pt 27 [16] was measured by the NBS Temperature Section with the reference junctions at 0 °C. The values obtained (at 100 deg intervals) increased in an essentially linear manner from 0 μV at 0 °C to +15 μV at 1100 °C. This indicates that the sample used in the present investigation was less pure than Pt 27.

The temperature coefficient of resistance, $\alpha = (R_{100} - R_0)/100R_0$, between the ice-point and the steam-point is often used as an indication of the purity of resistance thermometer grade platinum. The limiting value of α for extremely pure platinum is given by Berry [17] to be 0.003928_9. The size and low resistance of the thermal conductivity specimen precluded a highly accurate direct determination of α on the specimen using existing equipment. On the basis of the electrical resistivity measurements (described later) on the necked-down portion of the specimen, α had a value in the range $0.003876 \leq \alpha \leq 0.003916$. The relatively large uncertainty in α arises from the use of platinum versus platinum—10 percent rhodium thermocouples to measure the temperature near 100 °C. Berry [17] gives a plot which correlates α with the ratio of the resistance of a sample at absolute zero to that at the ice-point. He also correlates the resistance at absolute zero with that at the helium-point. On the basis of Berry's correlations, the ice-point to helium-point resistance ratio for the thermal conductivity specimen used in the present investigation corresponds to $0.003907 \leq \alpha \leq 0.003916$. This is not inconsistent with the range of values obtained from the electrical resistivity measurements.

Although α could have been measured directly with high accuracy on the 0.05 cm platinum wire, this was not done since the results would not necessarily be valid for the 2 cm bar, owing to possible differences in purity and annealing. Corruccini [18] gives an empirical expression, due to Wm. F. Roeser, correlating α with the electromotive force versus Pt 27 with the junction at 1200 °C and the reference junctions at 0 °C. Extrapolation of the emf measurements mentioned above, indicates an emf of +16 μV at 1200 °C, corresponding on the basis of Roeser's expression, to $\alpha \approx 0.003914$ for the 0.05 cm wire drawn from the same material as was used to fabricate the thermal conductivity specimen.

A cooperative project, involving NBS and several producers of thermometric grade platinum, is currently underway to study the properties of pure platinum. If as a result of this project, it appears that further characterization is indicated for the platinum used in the present investigation, such characterization will be performed on material which is being reserved for that purpose.

3. Method and Apparatus

3.1. Method

As discussed in the introduction, it was decided to build a single apparatus in which thermal conductivity could be measured by both an absolute guarded longitudinal heat flow method (nonelectrical method) and by a method in which a necked-down portion of the sample was heated directly by passage of an electric current (electrical method). The specimen configuration selected for these measurements is shown in figure 1. The specimen (A) was raised to the desired temperature level by means of the heaters Q_1 and Q_3. In the longitudinal heat flow method, the heater, Q_2, located slightly above the center of the bar produced a temperature gradient along the portion of the bar below Q_2. Heat from this heater was prevented from flowing up the bar by adjusting Q_3 so that there was negligible temperature difference across the necked-down region of the specimen. Lateral heat losses from the bar were minimized by matching the temperature distribution along the guard to that along the specimen. Thermal conductivity was calculated from the measured temperature distribution along the lower portion of the bar, the power input to the central heater, and the geometry.

In the electrical method, where the sample was directly heated by passage of an electric current, the voltage drop across the necked-down region of the specimen was measured as a function of current, while the maximum temperature rise in the neck was computed from the change in electrical resistance (due to a given change in current) and the temperature coefficient of resistance of the material. The thermal conductivity was determined from the voltage drop across the neck, the computed maximum temperature rise in it, and the electrical resistivity of the material.

The apparatus is described in detail in this section. The experimental test procedures and calculation procedures for the nonelectrical method are described in sections 4.1 and 4.2; those for the electrical method are described in sections 5.1 and 5.2.

3.2. Mechanical Configuration

The mechanical configuration of the apparatus is illustrated diagrammatically in figure 2 and described in detail below.

a. Specimen

The specimen (A) was a bar 2 cm in diameter by 18.4 cm long with a 0.11 cm diam by 0.33 cm long neck machined in it 4.1 cm from the upper end. A special technique, described by O'Hagan [9], had to be developed for machining the neck due to its structural

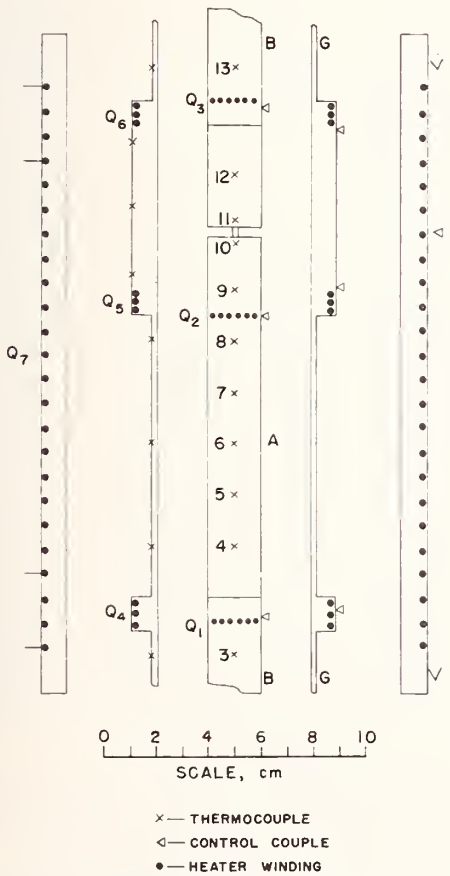

FIGURE 1. *Schematic diagram showing locations of heaters and thermocouples in the apparatus.*

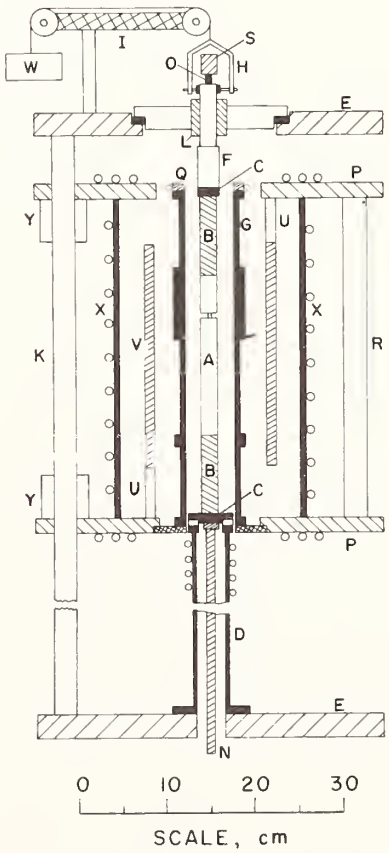

FIGURE 2. *The apparatus (components are identified in the text).*

weakness. Hollow molybdenum extensions (B) of the same diameter as the specimen were screwed to the specimen (A) at both ends. The open ends were brazed to copper blocks (C) that served as heat sinks. The molybdenum extensions were filled with high purity "coral" alumina. The lower end of the specimen assembly (B–A–B) was bolted to, but electrically insulated from, a brass flange which was welded to a water-cooled brass column (D). This column was firmly bolted to plate (E) which served as a base for the apparatus.

One of the major problems with the necked-down specimen was that of protecting the neck from mechanical strain due to tension, compression, torsion, or bending. Any clamp supporting the neck would have had to be electrically insulated from the specimen and differential thermal expansion between the clamp and specimen could have introduced strain in the neck. As an alternative to a clamp it was decided to counterbalance the load on the neck due to the weight above it so that there would be only a small net force on the neck. The weight of platinum above the center of the neck was computed from dimensional measurements and from the measured density of the specimen, and the components extending from the upper end of the specimen were weighed before assembly.

The counterweight (W) was suspended from a string which passed over two pulleys and attached to an aluminum hanger (H). The pulley wheels were mounted on low-friction bearings having a starting force of less than 1 g each. A molybdenum well (F), which was brazed to the upper copper block (C), passed through a linear bearing (L) which served to maintain the upper part of the specimen in precise alinement with the lower part, and presented negligible resistance to the free vertical motion of the specimen resulting from thermal expansion. This bearing was mounted on the upper plate (E) but electrically insulated from it. The two aluminum plates (E, E) were connected by three tie bars (K) to form a rigid framework for maintaining proper specimen alinement. An auxiliary device, described by O'Hagan [9], prevented the upper part of the specimen from rotating but still allowed free vertical motion. Current was introduced to the specimen via a copper rod (N) at the lower end and through a hollow molybdenum electrode (O) at the upper end. The upper electrode was brazed to a copper support (S) which was fastened to, but electrically insulated from, the upper plate (E). The molybdenum well (F) contained a liquid metal alloy into which the electrode dipped thereby affording a flexible current connection. The buoyant force of the liquid metal on the electrode contributed to the load on the neck and was compensated for in the counterweight. The electrode was fixed but the molybdenum well moved upwards with the specimen due to thermal expansion during test runs. This changed the buoyant force and consequently put a load on the neck. The maximum change in buoyant force was only 3 g, however, which would not strain the neck significantly. The liquid metal used was a gallium-indium eutectic alloy chosen primarily for its low vapor pressure and its comparatively low freezing temperature of 15.7 °C. The requirement for low vapor pressure was dictated by a need to evacuate the system. Preliminary tests were run to evaluate the uncertainty in buoyant force due to surface tension and sticking of the gallium-indium to the molybdenum surfaces. A very definite hysteresis effect was observed as the electrode was moved relative to the well and then returned to its initial position. The largest uncertainty in buoyant force was determined to be about 4 g. The choice of molybdenum as the electrode and well material stemmed from its compatability with gallium, which reacts with most other metals, and from the fact that molybdenum is wetted by gallium. The current feed-in system also served as a heat sink for the upper part of the specimen assembly. The hollow molybdenum electrode was internally cooled by circulating water at a temperature higher than the freezing point of the gallium-indium eutectic alloy.

b. Furnace and Guard

The inner core (G), or the guard as it is called, was a molybdenum tube of 5.7 cm inside diameter. Since the inner core acted as a thermal guard to prevent heat losses from the specimen, it was considered more desirable to make it from metal rather than from ceramic so that the temperature distribution along it could be more easily controlled and more accurately measured. The bottom of the guard was attached to a water-cooled brass plate (P). A water-cooled brass ring (Q) was attached to the upper end of the guard. The outer furnace core (V) was an aluminum oxide tube supported top and bottom by three 1-cm diam aluminum oxide rods (U).

The exterior portion of the furnace consisted of a water-cooled shell (X) supported between two water-cooled plates (P). Attached to the upper plate of the furnace was a split nut. This nut engaged a lead screw mounted between the plates (E, E) and by turning the screw the furnace could be moved up or down. Ready access to the specimen was thereby afforded. The three rods (K) acted as guide rods for the furnace. Six linear bearings (Y) attached to the furnace plates ensured alinement and permitted the furnace to move up and down freely. The correct vertical location of the guard relative to the specimen was determined when a probe attached to the upper end of the guard made electrical contact with a plate attached to the molybdenum well at the upper end of the specimen assembly. When the furnace had been positioned, the indicating probe attached to the guard was removed.

The space between the specimen and the molybdenum guard and that between the guard and the water-cooled shell were filled with fine high-purity aluminum oxide powder of low thermal conductivity and low bulk density (0.16 g/cm^3).

c. Environmental System

The entire apparatus was mounted inside a 24-in diam metal bell jar to enable operation in an inert atmosphere. A 4-in oil diffusion pump and a 5 cfm mechanical pump were used to evacuate the system prior to refilling with argon or helium. Initial evacua-

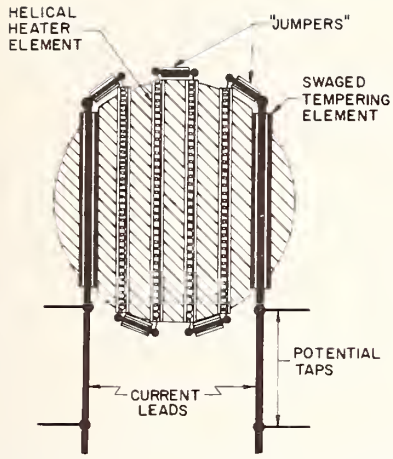

FIGURE 3. *Schematic diagram showing the construction of the specimen heater.*

tion was controlled to avoid disturbance of the fine powder insulation.

3.3. Thermal Configuration

The heater and thermocouple locations on the specimen and guard are shown in figure 1.

a. Specimen

The heaters, Q_1 and Q_3, used to raise the mean temperature of the sample were located in the molybdenum extensions. These heaters consisted of six series-connected helical coils of 0.02 cm diam platinum—thirty percent rhodium wire insulated from the surrounding metal by thin-wall aluminum oxide tubing. Platinel [2] thermocouples were attached adjacent to heaters Q_1 and Q_3 for use in controlling the temperatures at these locations.

The central heater, Q_2, was contained in six holes drilled through the platinum bar and was constructed as shown in figure 3. The inner four holes were 0.1 cm in diameter and accommodated helical elements contained in thin-wall aluminum oxide tubing. The elements were made from 0.013 cm diam platinum—10 percent rhodium wire, the outside diameter of the helix being 0.05 cm and the pitch 0.025 cm. The outer two holes were 0.16 cm in diameter and accommodated "swaged elements" having platinum—10 percent rhodium sheaths insulated from platinum—10 percent rhodium heater wires by compacted MgO powder insulation. The swaged elements were a snug fit in the holes so that there was good thermal contact between the sheath and the bar, and consequently good thermal coupling between the heater and the bar. The six elements were connected in series as in heaters Q_1 and Q_3. Platinum heater leads, 0.05 cm in diameter, were welded to the ends of the swaged elements. The good thermal contact in the swaged elements ensured that the temperature at the ends of the heater closely approximated that of the specimen. Moreover, the current leads extended radially from the heater in an isothermal plane. The combined result was to minimize heat losses via the leads. Two 0.02 cm platinum—10 percent rhodium potential leads were welded to each of the current leads, one at the junction of the heater and the current lead, and the other about 1 cm back along the current lead. The two platinum—10 percent rhodium potential leads together with the intervening section of platinum current lead served as a differential thermocouple to determine the temperature gradient in the current lead. By taking potential readings with the current flowing in the forward and reverse directions, the IR drop in the current leads could be accounted for and the temperature gradients therein determined. These data were used in computing heat flows along the leads. The potential drop across the inner taps was used in computing the power generated in the heater. The distances from the heaters to the nearest thermocouples and potential taps were such that perturbations in heat flow and electric current flow generated by the presence of the heaters decayed to an insignificant level at the position of the thermocouples or potential taps (see appendix B of O'Hagan [9]).

Five thermocouples, spaced 2 cm apart, were located in the gradient zone of the specimen, with the lowermost one (designated 4 in fig. 1) being 2 cm from the end of the specimen. The thermocouples were fabricated from 0.020 cm diam platinum and platinum—10 percent rhodium wires which were annealed in air at about 1450 °C for ½ hr and then butt-welded together. They were pressed into 0.018 cm wide by 0.023 cm deep horizontal slits in the surface of the specimen thereby replacing the metal removed in machining the slits. By virtue of the fact that the specimen was fairly pure platinum with essentially the same absolute thermoelectric power as the platinum leg of the thermocouple the junction of each thermocouple was effectively at the point where the platinum—10 percent rhodium leg first made contact with the specimen, and the temperature measured was the temperature at that point. The platinum—10 percent rhodium wire emerging from its groove extended a short way around the specimen in the same isothermal plane—insulated from the specimen in broken ceramic tubing—so as to minimize the amount of heat conducted away from the junction. Similar thermocouples were located in the molybdenum extensions, three in each, to measure the temperature distribution along them. This information was essential to the mathematical analysis of the system.

Additional thermocouples were located on either side of the neck (locations 9, 10, 11, and 12 in fig. 1). These were fabricated from annealed 0.038 cm diam platinum and platinum—10 percent rhodium wire and pressed into slits. In addition to measuring temperature, these thermocouples were wired at the selector switches so that the platinum legs could be used to measure voltage drops across the neck when an electric current was flowing through the neck. With no current flowing, the platinum—10 percent rhodium legs, in

[2] Platinel has a high thermal emf, approximately that of Chromel P versus Alumel. The negative leg of the thermocouple is 65 percent Au, 35 percent Pd alloy (Platinel 5355) and the positive leg is 55 percent Pd, 31 percent Pt, and 14 percent Au (Platinel 7674).

conjunction with the platinum neck, could be used as a differential thermocouple to control the differential temperature across the neck in the longitudinal heat flow method of measurement.

b. Guard

The guard had three heaters, Q_4, Q_5, and Q_6, at positions corresponding to those on the specimen assembly. All three were swaged heaters with platinum—10 percent rhodium sheaths and heating elements, and MgO insulation. They were pressed into grooves machined in the guard, thus giving good thermal contact. The end heaters (Q_4 and Q_6) were used to keep the guard at the desired temperature. The central heater (Q_5) was used to produce a temperature gradient in the guard matching that in the specimen.

The guard was electrically grounded but the heaters were isolated. Platinel control thermocouples were peened into the guard adjacent to each of the heaters.

Twelve thermocouples were located on the guard, three in the gradient zone, three in the isothermal zone, and three in each of the end zones. All the thermocouples were 0.038 cm platinum versus platinum − 10 percent rhodium with the junctions pressed into slits machined in the guard. The thermocouple wires were taken one turn around the guard in broken ceramic tubing in an isothermal plane and cemented to the guard with high purity alumina cement. This helped to temper the thermocouple leads and reduce the amount of heat conducted away from the junction by the leads. Within the furnace all the thermocouples were insulated in single-bore ceramic tubes. For the remainder of their lengths the wires were insulated in flexible fiber-glass sleeving. All the thermocouples, both from the guard and the specimen assembly, went to a junction box mounted on the inside of the feedthrough ring. There they were torch welded to identical wires which were taken through wax vacuum seals to an ice bath. All the Platinel control couples went to terminal strips on the upper plate of the furnace. There they were spot-welded to Chromel P and Alumel wires coming from the temperature controllers.

The aluminum oxide outer core (V) was provided with a heater winding (0.1 cm diam molybdenum) to bring the furnace as a whole to temperature and to reduce heat losses from the molybdenum guard and the power load on its heaters. A Platinel control thermocouple was mounted on the outer core (V).

3.4. Instrumentation

a. Temperature Control

In the longitudinal heat flow method of measuring thermal conductivity, the platinum—10 percent rhodium legs of the outer pair of thermocouples in the neck region were used in conjunction with the necked-down portion of the specimen as a differential thermocouple to control the power to heater Q_3, and thus maintain essentially a zero temperature differential across the neck. The signal from this thermocouple was amplified by a chopper-stabilized d-c amplifier and fed into a current-adjusting-type proportional controller incorporating automatic reset control and rate control. The output of the proportional controller regulated the power to the heater by means of a transistorized current amplifier fed by a regulated d-c power supply. In the electrical method of measuring thermal conductivity, an electric current flowed through the specimen and the above system of control could not be employed. In this case the Platinel control couple adjacent to heater Q_3 was put in series opposition with a signal from an adjustable constant voltage source and the resultant signal fed to the proportional controller which regulated the power to Q_3. The external signal was manually adjusted to give zero temperature differential across the neck.

The specimen heater (Q_2) was fed constant voltage ($\pm 0.01\%$) from a regulated d-c power supply. Power to heater Q_1 and to the three guard heaters (Q_4, Q_5, and Q_6) was supplied by variable-voltage transformers, which in turn were fed by voltage-regulated isolation transformers. Power to each heater was regulated by individual thermocouple-actuated controllers. Power to the heater winding (Q_7) on the alumina core was supplied by a variable-voltage transformer fed by a voltage-regulated isolation transformer. The current was manually ratioed among the three heater sections. The total power to this heater was regulated by a single thermocouple-actuated controller. All heaters were supplied by separate isolation transformers or power supplies to minimize current leakage effects.

b. Temperature Measurement

The noble metal leads of the thermocouples were brought to an ice bath, where they were individually joined to copper leads. The copper leads went in shielded cables to a bank of double-pole selector switches of the type used in precision potentiometers. The selector switches were housed in a thermally insulated aluminum box with 1 cm thick walls. The copper leads were thermally grounded to (but electrically insulated from) the switch box to minimize heat transfer directly to the switches. The emfs of the specimen thermocouples were read on a calibrated six-dial high-precision potentiometer to 0.01 μV, using a photocell galvanometer amplifier and a secondary galvanometer as a null detector. (Due to thermal emfs in the potentiometer and circuitry, these emfs were probably not meaningful to better than ± 0.05 μV.) The emfs of all other thermocouples were read on a second precision potentiometer to 0.1 μV using an electronic null detector.

c. Power Measurement

Power input to the specimen heater was measured using a potentiometer in conjunction with a high-resistance volt box to measure the drop across the inner set of potential taps, and a standard resistor in series with the heater to measure the current.

d. Resistance Measurement

All electrical resistance measurements were made by measuring the current (from a 0–100 A regulated d-c power supply) flowing through the specimen, utilizing a calibrated 0.001 Ω standard resistor, and by measuring the appropriate voltage drop in the specimen, using a potentiometer.

4. Longitudinal Heat Flow Method

4.1. Experimental Procedure

a. Preliminaries

The furnace was heated to 150 °C and the system evacuated to 3×10^{-4} torr. Initial pump-down was through a needle valve to give a sufficiently low rate so as not to disturb the very light powder insulation. When the pressure had fallen below 10^{-1} torr, the diffusion pump was turned on, pumping initially through the needle valve, and, when the pressure was below 10^{-2} torr, through the 4-in port. After pumping for 24 hr, the pumps were turned off and the system backfilled with high purity (99.99%) argon. The argon was bled in slowly through a needle valve to avoid disturbing the powder. The pressure was allowed to build up to almost 1 atm before the valves were shut off and the cycle of evacuating and backfilling repeated. The final argon pressure after the second backfilling was about three-quarters of an atmosphere.

The cooling-water flows to the system were adjusted to the desired levels as indicated on flow-meters. The water was pressure-regulated to maintain constant flow rate. A control thermocouple on the specimen was wired to shut all the heaters off if its temperature exceeded a predetermined level. This was a safety precaution in the event of an interruption in the cooling-water flow.

The test procedures are described in detail below. To facilitate the discussion let us refer to figure 1. The region of the specimen below the specimen heater, Q_2, will be referred to as the lower part of the specimen, and the region above Q_2 as the upper part of the specimen.

b. Description of Tests

In the longitudinal heat flow method of measuring the thermal conductivity each datum point was computed by simultaneous solution of three tests:

1. an "isothermal" test with no power input to the specimen heater (Q_2) and with the temperature distribution on the guard adjusted to closely match that on the specimen.

2. a "matched" gradient test with sufficient power input to the specimen heater to maintain the desired longitudinal temperature gradient in the specimen and with a matched temperature distribution on the guard.

3. an "unmatched" gradient test with the power input to the specimen heater and the temperature at the center of the measuring span the same as in the "matched" gradient test, and with the temperature distribution on the guard parallel to that on the specimen but 10 deg cooler.

Matched Gradient Test

The furnace temperature was raised by means of heater Q_7. The power to the specimen heater, Q_2, was adjusted to give a temperature gradient of 5 deg/cm in the lower part of the specimen. Power to Q_3 was automatically controlled, using a proportional controller, to maintain a minimum temperature drop across the neck. The Pt-10 percent Rh legs of thermocouples 9 and 12 were used in conjunction with the necked-down portion of the specimen as a differential thermocouple activating the proportional controller. The temperature drop across the neck never exceeded 0.1 deg. The specimen was maintained at the required mean temperature by thermostatting the power to the lower heater Q_1.

The temperature distribution along the guard was forced to match that along the specimen by adjusting the controllers for heaters Q_4, Q_5, and Q_6. Temperatures at corresponding locations on the specimen and the guard generally agreed to within 1 deg.

After allowing time for the system to come to equilibrium, readings were taken of the thermocouple emfs and the voltage and current to the specimen heater, Q_2. Normally these data were taken three times over a period of about 2 hr. The temperatures never drifted more than a few hundredths of a degree from one set of readings to the next and the three sets of data were averaged. When the drift between the first and second sets of readings was less than 0.01 deg, the third set of readings was not taken. On completion of the last set of readings, the voltage drops between the inner and outer taps of each current lead were measured with the heater current flowing normally and then reversed.

Unmatched Gradient Test

Upon completion of the "matched" gradient test the controllers for the guard heaters Q_4, Q_5, and Q_6 were adjusted to lower the temperatures on the guard by 10 deg while maintaining the temperature distribution parallel to that on the specimen. With the guard at the lower temperature heat losses from the specimen to the surrounding insulation were significantly increased and the heat flow in the specimen reduced. As a result, the temperature gradient in the specimen and its mean temperature were decreased. The power to heater Q_1 was adjusted to restore the specimen to the initial mean temperature. The system was then allowed to equilibrate and the same data were taken as for the "matched" gradient test.

Isothermal Test

For the "isothermal" test heater Q_2 was shut off and heater Q_1 adjusted until the specimen was approximately isothermal. No adjustments had to be made to Q_3 as the controller automatically adjusted to maintain $T_{11} - T_{10} = 0$. The guard heaters were likewise adjusted until the temperature distribution on the guard once again matched that on the specimen. When the system was in equilibrium, the data mentioned above were taken, with the exception of the power to the specimen heater which was shut off.

At 1100 °C an additional "matched" gradient test was run after the three regular tests were completed. The extra data obtained in this test served as a check on drifts in thermocouple calibrations during the testing period.

c. Testing Sequence

All of the measurements described above were made at a number of temperatures. Tests were first run in air at 100 °C, then in argon at 100, 300, 500, 700, 600, 400, and 200 °C in that order. One of the guard heaters would short out at about 750 °C and consequently the upper limit on the first run was 700 °C. After completing that run in argon the system was evacuated and backfilled with helium (99.99% pure) to a pressure of about three-quarters of an atmosphere. The helium, having a much higher thermal conductivity than argon, changed the effective thermal conductivity of the insulation surrounding the specimen. Tests were run in helium at 200 and 400 °C to experimentally evaluate heat losses from the specimen to the insulation. The system was then opened up and the trouble with the guard heater corrected. The furnace was filled with fresh powder insulation, the powder being packed lightly around the neck to ensure that the necked-down region was uniformly filled with insulation. The system was refilled with argon as described at the beginning of this section and tests were run at 300, 700, 900, and 1100 °C. Heater Q_3 burned out while tests were being conducted at 1100 °C by the electrical method and those tests were incomplete. The thermocouples started drifting at 1100 °C and losing their calibration due to contamination. Consequently, it was decided to terminate the tests at that point.

4.2. Calculation Procedures and Uncertainties

For one-dimensional steady-state heat flow, the total heat flow, Q, through the specimen is given by

$$Q=-\lambda A\frac{dT}{dz}, \tag{1}$$

where λ is the thermal conductivity, A is the cross-sectional area of the specimen, T is the temperature and z is the longitudinal coordinate. For moderate temperature ranges, the thermal conductivity of the specimen can be assumed to vary linearly with temperature; then (1) becomes

$$Q=-\lambda_0 A\{1+\beta_0(T-T_0)\}\frac{dT}{dz}, \tag{2}$$

where λ_0 is the thermal conductivity of the specimen at a reference temperature, T_0, and β_0 is its corresponding temperature coefficient. The difference between the heat flows in two tests is given by

$$Q-Q'=-\lambda_0 A\left[\left(\frac{dT}{dz}\right)-\left(\frac{dT}{dz}\right)'\right] -\lambda_0 A\beta_0\left[(T-T_0)\left(\frac{dT}{dz}\right)-(T'-T_0)\left(\frac{dT}{dz}\right)'\right], \tag{3}$$

where quantities of one test are distinquished from those of the other by use of primes. If we define the reference temperature as

$$T_0=\frac{T(dT/dz)-T'(dT/dz)'}{(dT/dz)-(dT/dz)'} \tag{4}$$

the second term on the right-hand side of (3) vanishes, and the thermal conductivity at the reference temperature, T_0, is given by

$$\lambda_0=\frac{-(Q-Q')}{A[(dT/dz)-(dT/dz)']}. \tag{5}$$

The purpose of computing the thermal conductivity from data corresponding to two different powers was to correct for errors that did not depend on the power transmitted through the specimen. The most obvious errors of this type are thermocouple errors. In a simultaneous solution each thermocouple in effect measures a temperature difference so that errors in calibration of the thermocouples cancel out to first order. Further possible sources of error will become evident below. Determination of λ_0 involved measurement of the cross-sectional area of the specimen, the total heat flow in the specimen and the longitudinal temperature gradient in the specimen for each of the two tests. These quantities were evaluated at the position of the middle thermocouple in the measuring span.

a. Cross-Sectional Area

The effective cross-sectional area of the specimen, after correction of the measured diameter for surface roughness, was determined to be 3.1331 cm² at 21 °C. The uncertainty [3] in this area was estimated to be less than 0.02 percent. The diameter at temperature t (°C) was computed from that at 25 °C using the equation

$$D_t=D_{25}(0.99978+8.876\times10^{-6}t+1.311\times10^{-9}t^2). \tag{6}$$

This equation was derived from smoothed thermal expansion data for platinum [19]. The cross-sectional area was then computed from the diameter.

b. Heat Flow

The total heat flow through the specimen at the position of the center thermocouple was calculated using the expression

$$Q=P-q_a-q_b-q_n-q_i-q_c, \tag{7}$$

where P is the measured electrical power input to the specimen heater;

q_a and q_b are the heat losses along the two leads carrying current to the specimen heater;

q_n is the heat loss across the necked-down portion of the specimen;

[3] Uncertainties stated in this paper represent either (a) statistical uncertainties based on results of calibrations or (b) limits to errors conservatively estimated by the authors.

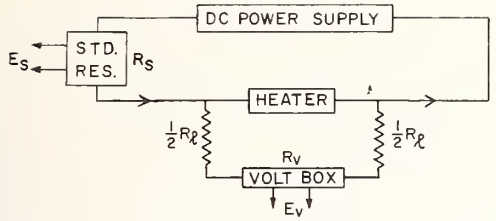

FIGURE 4. *Circuit diagram for the specimen heater.*

q_i is the heat loss into the insulation surrounding the specimen; and

q_c is the heat loss down the thermocouple wires and ceramic tubes next to the specimen.

Each of the quantities in (7) is considered separately below.

Power Input to Specimen Heater (P): The electrical circuit for the specimen heater is illustrated diagrammatically in figure 4. The power input to the heater was computed using

$$P = nE_v(1 + R_l/R_v)(E_s/R_s - nE_v/R_v), \tag{8}$$

where E_v is the voltage drop across the output of the volt box as measured with a potentiometer, n is the resistance ratio of the volt box, E_s is the voltage drop across the standard resistor, R_s, as measured with a potentiometer, R_l is the total resistance of the potential leads and R_v is the total resistance of the volt box.

The potentiometer, voltbox, and shunt box were each calibrated to 0.01 percent or better. The emf of the standard cell was known to 0.01 percent or better. The correction terms in (8) for the voltage drop in the potential leads and for the current through the voltbox were small (a few tenths of a percent) and uncertainties in these corrections could not have introduced more than 0.01 percent additional error in P. Thus the percentage uncertainty in the measured electrical power input was less than 0.05 percent.

Heat Flow in Current Leads (q_a, q_b): The circuit diagram in figure 4 shows only one set of potential leads coming from the heater. In fact there were two sets as shown in figure 5, but only the inner set, i.e., the potential taps closer to the heater, was used in measuring the power input to the heater. The two sets of potential leads were required in measuring heat conduction along the current leads. The current leads were platinum and the potential leads platinum-10 percent rhodium. Consequently, each current lead could be used along with its two potential leads as a differential thermocouple to measure the temperature drop, ΔT, between the potential taps. With current flowing to the heater the voltage drop measured between 1–2 or 3–4 was the algebraic sum of the IR drop between adjacent potential taps (where I is the current

FIGURE 5. *Arrangement of potential leads for the specimen heater.*

and R is the resistance of the current lead between the potential taps) and the Seebeck emf due to the temperature drop, ΔT, between the potential taps. Assuming no heat losses from the current leads, it can be shown [9, 20–26] that the heat conducted along the leads is given by

$$q_{a,b} = \frac{\lambda\rho}{R}\Delta T - \frac{I^2R}{2}, \tag{9}$$

where ρ is the electrical resistivity of the current lead and λ its thermal conductivity. By taking measurements with the current flowing forward and reversed, R and ΔT were determined for each lead, and consequently q_a and q_b.

The heat conducted along the leads, as determined using (9), was less than 0.05 percent of the heat flowing in the specimen. These corrections were sufficiently accurate that no errors larger than 0.02 percent are believed to have been introduced into the measured thermal conductivity values by uncertainties in q_a and q_b. We will discuss below the possible magnitude of heat losses from the current leads into the surrounding powder insulation.

Heat Flow across Neck (q_n): Referring to figure 1, it is seen that heat could be conducted across the necked-down region of the specimen by the neck itself and by the powder insulation surrounding it. The conductance of the powder was $\kappa\pi(b^2 - a^2)/2l$ where κ is the thermal conductivity of the powder, b the radius of the specimen, a the radius of the neck, and $2l$ the length of the neck. The conductance of the specimen between thermocouple positions 10 and 11 was λF where λ is the thermal conductivity of the specimen and F is a geometric factor which was determined from the corresponding equation for electrical conductance, $I = \sigma FV$, where I is the current, σ the electrical conductivity and V is the voltage drop between the thermocouples. These data were available from measurements by the electrical method. The heat flow across the necked-down region was given by

$$q_n = \left[\lambda F + \kappa\frac{\pi(b^2 - a^2)}{2l}\right]\Delta T, \tag{10}$$

where it is assumed that the temperature differential across the insulation was the same as that measured between the thermocouples.

The correction for heat flow across the necked-down region of the specimen was always less than 0.05 percent of P. Errors in the temperature drop across the neck due to possible inhomogeneities in the thermocouple leads or to stray thermal emfs would, for the most part, cancel since they were common to q_n and q_n' (i.e., corresponding to Q and Q'). At 300 °C a series of tests were run in which the temperature drop across the neck was held in turn at about −5, 0, and +5 deg, a range 20 times larger than that which occurred during normal measurements. The corresponding values for $(q_n - q_n')$ were about +1 percent, 0 percent, and −1 percent, respectively, of

P. The three thermal conductivity values obtained, using (10) to effect the correction for heat flow across the neck, fell within a range of less than ± 0.02 percent. For normal tests, in which the temperature across the necked-down region was maintained quite small, it is felt that any uncertainty in the measured thermal conductivity values due to this source was less than 0.02 percent.

Heat Loss into the Insulation (q_i): In order to determine q_i, the heat exchange between the specimen and the surrounding insulation, it was necessary to perform an extensive mathematical analysis. If the temperature distribution along the guard exactly matched that along the specimen there would have been no radial heat exchange between the specimen and the guard. However, there would still have been an exchange of heat between the specimen and the surrounding insulation in order to provide the longitudinal heat flow in the insulation adjacent to the specimen.

The heat flow from an elemental length of the surface of the specimen was

$$dq_i = 2\pi a \kappa \left(\frac{\partial \theta}{\partial r}\right)_{r=a} dz, \tag{11}$$

where a is the radius of the specimen, κ the thermal conductivity of the insulation, θ the temperature in the insulation relative to an arbitrary fixed temperature, r the radial coordinate, and z the longitudinal coordinate. The net heat flowing across the surface $r=a$ between z_1 and z_2 was

$$q_i(z_1, z_2) = 2\pi a \int_{z_1}^{z_2} \kappa \left(\frac{\partial \theta}{\partial r}\right)_{r=a} dz, \tag{12}$$

where κ is, in general, temperature dependent. Let us define a new potential, ξ, that satisfies the relation

$$\kappa_0 \nabla \xi = \kappa(\theta) \nabla \theta, \tag{13}$$

where $\kappa_0 \equiv \kappa(0)$. Integrating (13),

$$\xi = \frac{1}{\kappa_0} \int_0^{\theta} \kappa(\theta) d\theta, \tag{14}$$

where we have selected the integration constant so that $\xi = 0$ when $\theta = 0$. Writing (12) in terms of ξ we get

$$q_i(z_1, z_2) = \kappa_0 D(z_1, z_2), \tag{15}$$

where

$$D(z_1, z_2) = 2\pi a \int_{z_1}^{z_2} \left(\frac{\partial \xi}{\partial r}\right)_{r=a} dz. \tag{16}$$

The factor $D(z_1, z_2)$ was determined by analyzing the heat flow in the hollow cylinder of powder insulation between the specimen and the guard, using the measured temperature distributions along the specimen assembly and along the guard cylinder as boundary conditions. Polynomial expressions relating temperature to longitudinal position were used to describe these temperature distributions in the regions between the heaters. In the intervening regions near the heaters, smoothing cubics [27] were used which provided continuity of temperature and longitudinal temperature gradients. The evaluation of $D(z_1, z_2)$ is described more fully in appendix A.

Since the heat flow in the specimen was to be evaluated at the position of the center thermocouple in the gradient region, all the heat loss to the insulation from the location of the heater down to the position of the center thermocouple had to be considered. In addition, heat losses in the region between the specimen heater and the neck had to be considered since these had to be provided by the specimen heater. The neck, in effect, could be considered as the upper end of the specimen for purposes of this analysis, since any heat exchanges between the powder and the specimen above the neck did not affect that part of the specimen below the neck as long as zero temperature differential was maintained across the neck. Therefore, in evaluating q_i, the limits of integration for $D(z_1, z_2)$ were the position of the center thermocouple (z_1) and the position of the center of the neck (z_2).

The correction $(q_i - q_i')$ for heat exchange with the powder insulation was potentially a large source of error and considerable effort was expended to, first, keep this correction small and, second, evaluate it accurately. Evaluation of this correction, as seen from (15), required a knowledge of the integral, $D(z_1, z_2)$, and of the thermal conductivity, κ_0, of the insulation. Numerous factors could have adversely affected the determination of $D(z_1, z_2)$. The use of logarithmic functions to define the radial temperature distribution across the ends of the hollow cylinder of insulation was an approximation. However, it is easily shown that the potential distribution near the specimen was not significantly affected by the boundary conditions at the remote ends of the extensions.

In the mathematical analysis it was assumed that the temperatures on the inner surface of the guard were the same as the temperatures measured on the outer surface. The molybdenum guard had high thermal conductivity so that any radial temperature gradients in the guard would be small and the associated errors would tend to cancel on simultaneous solution of the gradient and isothermal tests. Angular variations in the temperature distribution on the guard could have arisen if the specimen and guard were not concentric or if the insulation between the specimen and the guard was not packed uniformly. Great care was taken to avoid both of these conditions. Any angular variations would have been approximately the same for two tests at the same mean temperature and so the associated errors would in large part cancel under simultaneous solution. Such would not be the case for errors arising from uncertainties in the longitudinal positions of the thermocouples since the temperature distribution along the guard cylinder in

the gradient test differed from that in the isothermal test. The necessary steps were taken to ensure that the longitudinal position of the guard was accurately known relative to that of the specimen, and the location of the thermocouple slits both on the guard and on the specimen assembly were measured accurately prior to installation of the thermocouples.

The details of the actual temperature distributions in the heater regions where smoothing cubics [27] were used could conceivably have influenced $D(z_1, z_2)$. Except for the regions of Q_2 and Q_5, such effects should have been about the same in the gradient and in the isothermal tests, and hence would have canceled on simultaneous solution of these tests. Since the guard heaters were on the outside of a considerable thickness of high-conductivity metal, we feel that the temperature on the inside surface of the guard cylinder varied smoothly with position in the regions of the guard heaters. Thus, no significant errors were believed to be introduced by the use of a smoothing function in the region of Q_5.

R. W. Powell [28] has pointed out that a possible additional source of error, not specifically discussed by O'Hagan [9], is heat loss into the powder insulation from the external platinum jumpers which connected the elements of heater Q_2 (see sec. 3.3a and fig. 3). There were five such jumpers, each about 0.3 cm long, contained in aluminum oxide tubing to electrically insulate them from the specimen. Although the heat generated in the jumpers was only a small fraction of the total heat generation in the heater, these jumpers were heated, by conduction from the helical heater coils inside the specimen, to a temperature above that of the specimen. This would have resulted in a heat flow into the powder insulation surrounding the jumpers. A portion of this heat would have flowed back into the specimen but, at least in principle, a net portion of the power input to the specimen heater could have been lost from the heater jumpers with a corresponding error in the measured thermal conductivity values.

Since the temperature rise of the jumpers was dependent upon the power input to the specimen heater, the heat loss discussed in the previous paragraph was not eliminated, or even reduced, by the simultaneous solution of a matched gradient test and an isothermal test. The use of an unmatched gradient test also did not help in evaluating this source of heat loss. The smoothing functions used were quite adequate for the isothermal tests but did not truly represent the temperature distributions in the region of Q_2 for the gradient tests. In view of the importance of this potential source of error, heat loss from the jumpers is considered further in appendix B, where a mathematical analysis is used to approximately evaluate this source of error. This analysis indicates that errors in the measured thermal conductivity values due to heat loss from the jumpers on heater Q_2 were less than 0.2 percent at 100 °C and less than 0.5 percent at 900 °C.

A calculation (see appendix I of O'Hagan [9]), based on the degree of tempering provided by the swaged elements to which the heater current leads were attached, indicated that the current leads were only 1 to 2 deg C hotter than the adjacent specimen material. By comparison to the discussion of heat loss from the jumpers (see appendix B), which may have been over 100 deg C hotter than the specimen, we see that any errors due to heat loss from the heater leads into the powder insulation were negligible.

In analyzing the data the "isothermal" test was combined with the "matched gradient" test and with the "unmatched gradient" test to give two equations of the form (5). Inspection of eqs (5), (7), and (15) shows that the value obtained for λ_0 depends in a linear manner on the value assumed for κ_0. The effective thermal conductivity of the insulation surrounding the specimen depends on the density of the powder and the pressure and type of gas present, and is best determined under experimental conditions. This was done by simultaneous solution of two equations of the form (5) which yielded values both for the thermal conductivity of the specimen, λ_0, and the thermal conductivity of the insulation, κ_0. The thermal conductivity values obtained for the aluminum oxide insulation, in argon and in helium, were given by O'Hagan [9].

If there was a significant heat exchange between the specimen and the insulation that was not being adequately corrected for, one would expect a systematic difference between the values obtained for the thermal conductivity of the specimen in helium and those obtained in argon, due to the large difference between the thermal conductivity of the powder in the different atmospheres. In fact, however, the values measured in helium fell within the scatter band of those measured in argon indicating that any uncorrected heat exchanges were certainly less than 0.2 percent, the width of the scatter band (see sec. 4.3).

For all of the tests taken the correction $|q_i - q_i'|$ was less than 0.1 percent of P. It is felt that $D(z_1, z_2)$ and κ_0 were each known to better than 10 percent and hence the uncertainty in $(q_i - q_i')$ less than 0.02 percent of $(P - P')$. However, in view of all the factors which conceivably could have influenced this correction, an uncertainty of 0.1 percent is assigned to the measured thermal conductivity values due to possible errors in $(q_i - q_i')$. To this must be added the uncertainty due to heat loss from the jumpers on heater Q_2.

Heat Loss along Thermocouple Wires and Insulators (q_c): The heat loss, q_c, along the thermocouples and ceramic insulators next to the specimen was computed from the expression

$$q_c = \sum_{i=1}^{n} C_i \left(\frac{dT}{dz}\right), \tag{17}$$

where C_i is the longitudinal thermal conductance of the ith wire and its insulator, n is the total number of wires crossing the plane where the thermal conductivity was evaluated, and dT/dz is the temperature gradient at that plane. Each C_i was computed from the thermal conductivities and dimensions of the wire

and insulator. This correction was rather large, falling from about 0.8 percent at 100 °C to 0.3 percent at 1100 °C, the falloff being due to the rapidly decreasing thermal conductivity of the ceramic tubing. Although the thermal conductivity of the thermocouple wires was known fairly accurately (5%) the thermal conductivity of the ceramic tubing was known only approximately (15%). Furthermore, the cross-sectional areas of the wires and tubing were not accurately known (5%). Thus the total conductance of the wires and the ceramic tubing was only known to about 25 percent. The corresponding uncertainty in the measured thermal conductivity values was 0.2 percent at 100 °C and 0.1 percent at 900 °C.

Departure from Steady-State: The ratio of heat absorbed (or released) to that conducted in the specimen is given approximately by

$$\frac{wcAL(dT/dt)}{\lambda A(dT/dz)}=\frac{L}{D}\frac{(dT/dt)}{(dT/dz)}, \tag{18}$$

where w is density, c is specific heat, A is area, L is total length of specimen below the necked-down region, dT/dt is time rate of temperature change, λ is thermal conductivity, dT/dz is temperature gradient, and $D=\lambda/wc$ is thermal diffusivity. Temperatures in the system did not drift at a rate greater than 0.03 deg/hr (i.e., 10^{-5} deg/sec); the length, L, was about 14 cm; the temperature gradient was 5 deg/cm; and the thermal diffusivity of platinum in the temperature range 0–1100 °C is always greater than 0.2 cm^2/sec [12]. Hence the ratio of heat absorbed (or released) to that conducted was less than ± 0.02 percent. No correction was made for departure from steady-state conditions.

Total Uncertainty in Heat Flow: Using standard propagation of error formulas, the estimated uncertainty in $(Q-Q')$ was 0.4 percent at 100 °C and 0.7 percent at 1100 °C.

c. Temperature Gradient

The temperature gradient in the specimen was computed from the measured temperatures at the five thermocouple positions in the gradient region. The separations between thermocouple grooves at room temperature were accurately measured before the thermocouples were installed; the separation at elevated temperature was computed using (6). Since temperature gradients in the specimen were rather small (less than 5 deg/cm) it was essential that the conversion of thermocouple emfs to temperature not introduce any additional uncertainties. The equation

$$E=15.83952\left(\frac{t}{1000}\right)-9.18328\left(\frac{t}{1000}\right)^2$$

$$+7.30572\left(\frac{t}{1000}\right)^3-1.92753\left(\frac{t}{1000}\right)^4$$

$$-2.50480\,(1.0-\exp[-4.18312(t/1000)]), \tag{19}$$

where t is temperature (°C) and E is emf (mV), was found to fit to within 1 μV the calibration data for the platinum versus platinum−10 percent rhodium thermocouple wire from which the specimen thermocouples were fabricated. This equation was used for converting the thermocouple voltages to temperatures.

The temperature gradient was computed by evaluating the slope, at the center thermocouple location, of the quadratic equation of least-squares fit to the five temperatures and thermocouple positions. The uncertainty in the temperature gradient due to uncertainties in effective thermocouple positions is estimated to have been less than 0.2 percent. Errors in reading thermocouple emfs did not introduce an uncertainty of more than 0.05 percent for the temperature gradients used. Errors due to heat conduction along thermocouple leads should have been negligible and were certainly less than 0.05 percent (see Appendix G of O'Hagan [9]). Due to the use of a simultaneous solution of a gradient and an isothermal test, errors in the measured temperature gradient due to variations between individual thermocouples are estimated to have been less than 0.05 percent. It is estimated that the conversion of thermocouple emfs to temperatures introduced errors of less than 0.2 percent in the temperature gradients.

The estimated overall uncertainty in the temperature gradient is estimated to have been 0.3 percent.

d. Mean Temperature

In addition to the uncertainties discussed above in the area, heat flow, and temperature gradient, there is an uncertainty in the temperatures to which the thermal conductivity values correspond. For a 0.5 deg uncertainty in temperature, the associated uncertainty in thermal conductivity is less than 0.001 percent at 100 °C and less than 0.02 percent at 900 °C.

4.3. Results

The experimental values obtained for the thermal conductivity of our platinum specimen by the longitudinal heat flow method are given in table 1. The

TABLE 1. *Experimental values for the thermal conductivity of platinum as measured using the longitudinal heat flow method*

The values given are corrected for thermal expansion.

Test	Run	Atmosphere	Mean temperature °C	Thermal conductivity W/cm deg
1	1	Air	99.6	0.715
2	1	Argon	99.8	.715
3	1	Argon	301.0	.728
4	1	Argon	501.5	.753
5	1	Argon	701.2	.784
6	1	Argon	601.3	.769
7	1	Argon	400.2	.740
8	1	Argon	201.7	.721
9	1	Helium	199.6	.721
10	1	Helium	400.6	.740
11	2	Argon	300.0	.729
12	2	Argon	701.3	.786
13	2	Argon	900.0	.822
14	2	Argon	1100.5	(.866)[a]

[a] See text.

TABLE 2. *Typical set of data from measurements of the thermal conductivity of platinum by the longitudinal heat flow method*

The data correspond to Test No. 6 in table 1.

		Matched gradient	Unmatched gradient	Isothermal
Temperature distribution along the specimen, °C	T_4	580.4	579.0	600.7
	T_5	590.9	588.9	600.6
	T_6	601.3	598.8	600.3
	T_7	611.7	608.9	600.1
	T_8	622.1	619.0	600.0
Temperature gradient at the location of thermocouple T_6, deg/cm	$\frac{dT}{dz}$	5.18	4.96	−0.09
Power generated in specimen heater, W	P	12.818	12.853	.0
Heat flow across the necked-down region, W	q_n	0.003	−0.008	−.002
Heat flow along the current leads, W	q_a	.004	.017	.002
		.003	.006	.002
Heat flow to the insulation, W	q_a	.006	.542	.027
Heat flow along the thermocouple wires and insulators, W	q_c	.051	.049	−.001

TABLE 3. *Summary of individual uncertainties contributing to the overall uncertainty in the thermal conductivity results obtained using the longitudinal heat flow method*

Source of uncertainty	Uncertainty, %	
	100 °C	900 °C
Cross-sectional area	0.02	0.02
Heat flow		
Power input to specimen heater	.05	.05
Heat flow in current leads	.02	.02
Heat flow across neck	.02	.02
Heat loss into the insulation	.3	.6
Heat loss along thermocouple wires and insulators	.2	.1
Departure from steady-state	.02	.02
Temperature gradient	.3	.3
Mean temperature	.001	.02
Combined[a]	0.5	0.7

[a] Each combined uncertainty was obtained by taking the square root of the sum of the squares of the individual uncertainties.

thermal conductivity values given there have been corrected for thermal expansion of the specimen. A typical set of data, including the various correction terms, is given in table 2.

A cubic equation of least-squares fit was found to fit the data (corrected for expansion) from the longitudinal heat flow method with the residuals having a standard deviation of 0.08 percent. This was significantly less than the standard deviation of the residuals from a parabola. The equation, valid over the range 100 to 900 °C, is

$$\lambda = 0.713 + 0.683 \times 10^{-5} t + 0.173 \times 10^{-6} t^2 - 0.513 \times 10^{-10} t^3, \qquad (20)$$

where t is temperature in °C and λ is in W/cm deg. Departures of the data points from (20) are plotted in figure 6. With the exception of the point at 1100 °C all the data points, including the two obtained in helium, fall within ±0.1 percent of the curve. There were no significant differences between the values obtained on heating and cooling in the first run and those from the second run. At 1100 °C the thermocouples started drifting giving rise to significant uncertainties in temperature measurement. After completing the "matched" gradient, "unmatched" gradient, and "isothermal" tests at 1100 °C a second "matched" gradient test was run. Two values for the thermal conductivity were obtained by simultaneous solution of each of the two "matched" gradient tests with the "isothermal" test. The first value (0.820) was below the value predicted by (20) and the second value (0.905) was above it. Assuming that the temperature drifts were linear with time, interpolation to the time of the "isothermal" test gave a value of 0.866 for the thermal conductivity of the specimen at 1100 °C. This value is 0.6 percent above the value given by extrapolation of (20) to 1100 °C. The 1100 °C point, due to the larger uncertainty associated with its value, was not used in deriving (20).

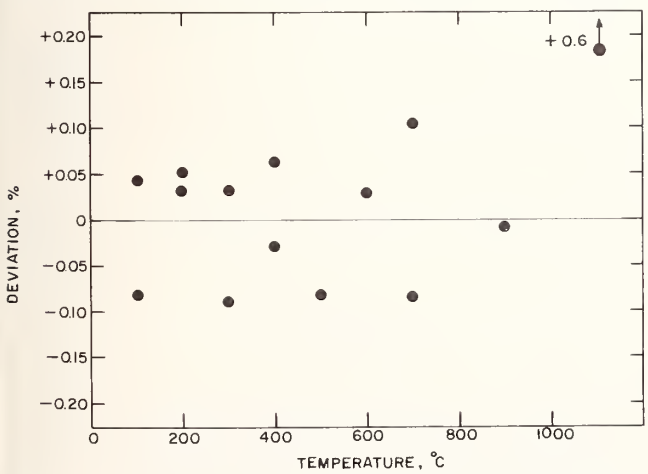

FIGURE 6. *Percentage departures from eq (20) of the thermal conductivity data points obtained by the longitudinal heat flow method.*

The thermal conductivity values corresponding to (20) are believed to be uncertain by not more than 1 percent over the temperature range 100 to 900 °C. The estimated uncertainties arising from the various known sources of error are summarized in table 3; these uncertainies were discussed in section 4.2.

5. Electrical Method

5.1. Experimental Procedure

Measurements of thermal conductivity by the method in which the sample was heated directly by passage of an electric current were made following each measurement by the longitudinal heat flow method. Thus the preliminary procedures and testing sequence described in section 4.1 also apply to these measurements. Power to heaters Q_1 and Q_3 was controlled to maintain T_{10} and T_{11} constant with $|T_{11} - T_{10}|$ less than 0.2 deg. Temperatures along the guard in the region opposite the neck were maintained at the same value as T_{10}. Data were taken with currents (both normally and reversed) of approximately 10, 58, 82, and 100 A dc flowing through the specimen. These

current levels correspond approximately to even increments of power generation. Readings were taken of thermocouples 9, 10, 11, and 12 (see fig. 1) on the specimen and of the guard thermocouples between heaters Q_5 and Q_6. The voltage drops between the platinum legs of thermocouples 10 and 11 and also between 9 and 12 were measured with the current being measured simultaneously on another potentiometer.

The temperatures never drifted more than a few hundredths of a degree during a test (approximately three-quarters of an hour), and although the current showed drifts of 0.05 percent the measured resistances remained constant to 0.01 percent with current and voltage being read simultaneously.

5.2. Calculation Procedures and Uncertainties

Consider a conductor of arbitrary geometry which is perfectly insulated, both thermally and electrically, except for the ends where electric current enters and leaves the conductor. Joule heat will be generated in the conductor by the electric current. Let T_m be the maximum temperature in the conductor. Let V be the voltage drop between two surfaces, one on either side of the surface of maximum temperature, which are both at some lower temperature, T_0. It is shown in appendix C, where earlier work is referenced, that the following relation holds:

$$\frac{V^2}{8}=\int_{T_0}^{T_m}\lambda\rho dT=\int_0^{\theta_m}\lambda\rho d\theta, \tag{21}$$

where $\theta=T-T_0$, $\theta_m=T_m-T_0$, λ is the thermal conductivity of the conductor, and ρ is the electrical resistivity of the conductor.

Equation (21) shows that the maximum temperature rise, θ_m, in an electrically heated conductor with negligible lateral heat losses and with both its ends held at the same temperature is a function only of the voltage drop V across it, and of the thermal and electrical conductivities of the material, and is independent of the geometry of the conductor provided the geometry is such as to make lateral heat losses negligible. If the maximum temperature rise can be measured as a function of the applied potential, $\lambda\rho$ is readily determined.

The maximum temperature rise, θ_m, can be measured indirectly using the specimen as its own resistance thermometer. This method was employed by Holm and Störmer [13] and Cutler et al. [15], and requires that the temperature coefficient of resistance of the material be known over the temperature range of interest and that it be large enough to yield sufficient sensitivity. Platinum satisfies both requirements very well and the resistance method of measuring the maximum temperature rise was adopted in the present experiments.

It is shown in appendix C that the following relation holds for a perfectly insulated conductor:

$$\frac{R_0}{R}=\frac{1}{F}\int_0^{\theta_m}\frac{\lambda\rho_0(1+\gamma_0\theta)d\theta}{F}, \tag{22}$$

where

$$F\equiv+\left\{2\int_0^{\theta}\lambda\rho d\theta\right\}^{1/2} \tag{23}$$

and R is the electrical resistance between the two surfaces, one on either side of the surface of maximum temperature, which are both at the same temperature, T. The quantities R_0 and ρ_0 are the values R and ρ would have if the conductor were isothermal at some reference temperature, T_0. The quantity γ_0 is the coefficient of linear thermal expansion at T_0.

Assuming that λ and ρ can both be represented by linear functions of temperature—a valid assumption over small temperature intervals—we can write:

$$\rho=\rho_0(1+\alpha_0\theta), \tag{24}$$

$$\lambda=\lambda_0(1+\beta_0\theta), \tag{25}$$

$$\lambda\rho=\lambda_0\rho_0(1+\eta_0\theta), \tag{26}$$

where α_0 is the temperature coefficient of resistance evaluated at $\theta=0$, β_0 is the temperature coefficient of thermal conductivity evaluated at $\theta=0$ and $\eta_0=\alpha_0+\beta_0$. The term in $\alpha_0\beta_0\theta^2$ in (26) has been neglected. Substituting the above expression for $\lambda\rho$ into (23) and integrating we get

$$F(\theta,\theta_m)=+\left[2\lambda_0\rho_0\left\{\theta_m\left(1+\frac{\eta_0}{2}\theta_m\right)-\theta\left(1+\frac{\eta_0}{2}\theta\right)\right\}\right]^{1/2} \tag{27}$$

If the integration is evaluated for $T=T_0$, or $\theta=0$, we have, from (27) and (21),

$$F=\left[2\lambda_0\rho_0\theta_m\left(1+\frac{\eta_0}{2}\theta_m\right)\right]^{1/2} \tag{28}$$

and

$$V^2=8\lambda_0\rho_0\theta_m\left(1+\frac{\eta_0}{2}\theta_m\right). \tag{29}$$

Substituting F from (27) into (22) and performing the indicated integration we have for $\theta=0$,

$$\frac{R_0}{R}=\frac{\beta_0+\gamma_0}{\eta_0}+\frac{\alpha_0-\gamma_0}{\eta_0}\frac{1}{G}\arctan G, \tag{30}$$

where

$$G^2\equiv 2\eta_0\theta_m\left(1+\frac{\eta_0}{2}\theta_m\right). \tag{31}$$

The coefficients α_0 and β_0 are the "true" coefficients in that they correspond to electrical resistivity and thermal conductivity values which have been corrected for thermal expansion. If one considers "apparent" coefficients α_0' and β_0' which correspond to "apparent" thermal conductivity values which have not been

corrected for thermal expansion, then it is apparent that $\alpha_0=\alpha_0'+\gamma_0$, $\beta_0=\beta_0'-\gamma_0$, $\eta_0=\eta_0'$, and (30) can be written as

$$\frac{R_0}{R}=\frac{\beta_0'}{\eta_0'}+\frac{\alpha_0'}{\eta_0'}\frac{1}{G}\arctan G, \tag{32}$$

where, reiterating, α_0', β_0', and $\eta_0'=\alpha_0'+\beta_0'$ are apparent coefficients corresponding to electrical resistivity and thermal conductivity values which have not been corrected for thermal expansion. Thus the maximum temperature rise in the conductor can be computed without knowing the coefficient of expansion.

Equation (30) gives θ_m implicitly in terms of known measured parameters, and its value can be determined by iteration. In practice it would generally be necessary to measure R at at least two different levels of heating current and then extrapolate to zero current to obtain R_0. Once θ_m is obtained using (30), its value can be used in conjunction with (29) to obtain the thermal conductivity. In the present investigation, R and V were measured at four or five different current levels. The data obtained were analyzed as described below.

An adjusted voltage, V^*, was defined as:

$$V^{*2}=\frac{V^2}{1+\frac{\eta_0}{2}\theta_m}. \tag{33}$$

In the limit of small $\alpha_0\theta_m$, (30) reduces to

$$\frac{R-R_0}{\alpha_0 R_0}=\frac{2}{3}\theta_m. \tag{34}$$

An adjusted resistance, R^*, was defined for the case where $\alpha_0\theta_m$ is not sufficiently small for (34) to be valid:

$$R^*=R_0\left(1+\frac{2}{3}\alpha_0\theta_m\right). \tag{35}$$

In the limiting case of small $\alpha_0\theta_m$, (35) reduces to (34) and R^* to R.

Substituting (33) and (35) into (29), we obtain

$$V^{*2}=12\lambda_0\rho_0\frac{R^*-R_0}{\alpha_0 R_0}. \tag{36}$$

Differentiating (36) and rearranging, we obtain

$$\lambda_0=\frac{\alpha_0 R_0}{12\rho_0}\frac{dV^{*2}}{dR^*}. \tag{37}$$

The thermal conductivity values in the electrical method were obtained from the slope of the V^{*2} versus R^* curve, using (37). From (33) and (35) we see that

$$\frac{dV^{*2}}{dR^*}=\lim_{\alpha_0\theta_m\to 0}\frac{dV^2}{dR}. \tag{38}$$

In the analysis given in appendix C and also that given just above, we explicitly assumed that there was no loss or gain of either electric current or heat across the surface of the conductor. In the present investigation a necked-down sample was employed, the neck and the specimen as a whole being surrounded by an insulating powder. Since this insulating powder had an electrical conductivity many orders of magnitude lower than that of the specimen material, the assumption of no flow of electric current across the boundaries was completely valid. The powder surrounding the neck prevented heat loss by convection, and radiation through the powder was negligible. However, the powder conducted heat away from the neck and it was necessary to analyze this heat loss and develop an appropriate correction for it. Since most of the temperature rise between thermocouple positions 10 and 11 was in the neck itself, only heat losses from the neck were considered and other heat exchanges were neglected. O'Hagan [9] has shown that in the presence of small heat losses from the neck, (37) is replaced by

$$\lambda_0=\frac{1}{1+C}\frac{\alpha_0 R_0}{12\rho_0}\frac{dV^{*2}}{dR^*}, \tag{39}$$

where

$$C=\frac{\kappa_0}{\lambda_0}\Omega \tag{40}$$

κ_0 being the thermal conductivity of the powder insulation at the reference temperature, T_0, and λ_0 the thermal conductivity of the specimen at T_0. The geometrical factor, Ω, is given by

$$\Omega=\frac{64}{\pi^3 a^2}\left(\frac{2l}{\pi a}\right)^3\frac{K_1(\pi a/2l)}{K_0(\pi a/2l)}\frac{\rho_0^2}{R_0^2}, \tag{41}$$

where $2a$ is the diameter of the neck and $2l$ is the length of the neck, and K_0 and K_1 are the modified Bessel functions of second kind and order zero and one, respectively.

The calculation procedure used was as follows: At any given nominal temperature, measurements were made at n current levels. An approximate value for R_0 was computed from the resistance corresponding to the lowest current level, for which Joule heating was minimal and the neck was nearly isothermal. For each experimentally determined resistance a corresponding approximate value of θ_m was computed using (34). Values of α_0' were computed from the data obtained in the resistivity measurements (see sec. 5.3a). Using this value of θ_m as the first trial value, Newton-Raphson iteration was used to compute the value of θ_m which satisfied (30).[4] Values for R^* and V^{*2} were then computed from (35) and (33) respectively. Since it was impractical to hold T_0 (i.e., the average temperature of thermo-

[4] Values for β_0' computed from the thermal conductivity values obtained by Watson and Flynn [32] on the same specimen were used.

couple locations 10 and 11) at exactly the same value for different current settings, it was necessary to adjust slightly the V^{*2} and R^* values to correspond to a common reference temperature. A straight line of least-squares fit through these values of R^* and V^{*2} gave R_0 as the ordinate intercept and dV^{*2}/dR^* as the slope. This value for R_0 was a more accurate value than the initial value used, as it was based on an extrapolation to $I=0$. The calculation was then repeated using this value of R_0. This in turn led to improved values for R_0 and dV^{*2}/dR^*. The iteration converged in a few passes and the final values for R_0 and dV^{*2}/dR^* were used in (37) to compute the apparent thermal conductivity. Using this apparent value for λ_0, and eqs (40) and (41), the correction factor for heat losses from the neck was computed and used in (39) to give the final value for the thermal conductivity.

a. Electrical Resistivity

The electrical resistivity values were computed from

$$\rho_0=\rho_{\text{ice}}R_0/(R_0)_{\text{ice}}, \tag{42}$$

where ρ_{ice} is the independently measured ice-point resistivity, R_0 is the resistance of the necked-down region at zero current, and $(R_0)_{\text{ice}}$ is the value of R_0 extrapolated to the ice point. These values were then corrected for thermal expansion. The uncertainty in ρ_{ice} was not more than 0.1 percent. The uncertainties in the measured values of R_0 did not exceed 0.05 percent. However, an additional uncertainty must be assigned to the values of R_0 due to the uncertainty in the temperature to which these values correspond. Quite conservatively, temperatures were known to within 0.5 deg, corresponding to 0.14 percent of R_0 at 100 °C and 0.04 percent at 900 °C. The uncertainty in $(R_0)_{\text{ice}}$, which was based on an extrapolation, was estimated to be less than 0.25 percent. At lower temperatures the uncertainties in R_0 were correlated with the uncertainty in $(R_0)_{\text{ice}}$ so that the uncertainties in $R_0/(R_0)_{\text{ice}}$ were lower than the uncertainties in either R_0 or $(R_0)_{\text{ice}}$ at lower temperatures but not necessarily at higher temperatures. The overall uncertainty in electrical resistivity was estimated to be less than 0.1 percent at 0 °C and less than 0.4 percent at 900 °C.

The thermal conductivity was computed, using (39), from the ratio R_0/ρ_0. Since ρ_0 was taken from a smoothed curve, this quantity was further uncertain by the scatter in the individual R_0 data points around a smooth curve, or about an additional 0.05 percent (see sec. 5.3a). The overall uncertainty in R_0/ρ_0 was probably less than 0.4 percent.

b. Temperature Coefficient of Resistance

The uncertainty in the sensitivity, α_0, of the specimen as a resistance thermometer was essentially the uncertainty in the sensitivity of the thermocouples used plus a small uncertainty in the resistance measurements and the thermocouple emf measurements. That this is so is seen by considering that R_0 was measured as a function, say $R_0=f(E)$, of the thermocouple emf, E. Then

$$\alpha_0=\frac{1}{R_0}\frac{dR_0}{dT}=\frac{1}{f(E)}\frac{df(E)}{dE}\frac{dE}{dT}\equiv g(E)\frac{dE}{dT}. \tag{43}$$

The uncertainty in the sensitivity, dE/dT, of the thermocouples is estimated to have been less than 0.2 percent while the uncertainty in the resistance and voltage measurements was less than 0.05 percent. Thus α_0 is believed to have been known with an uncertainty of less than 0.25 percent.

c. Slope of V^{*2} Versus R^* Curve

The voltage drop across the neck and the resistance of the neck were each measured with an uncertainty of about 0.02 percent. The change in the resistance of the neck for the different current levels was small compared to the resistance itself, so that any error in measuring resistance would be greatly magnified in computing the rate of change of resistance as a function of the voltage drop. For all of the data taken, the departures of the R^* values from the least-squares straight line fitted to the R^* and V^{*2} values were less than 0.01 percent and for a majority of the tests they were less than 0.005 percent. However, since $(R-R_0)\ll R$, the small scatter in R was highly magnified in calculating dV^{*2}/dR^*. What departures did exist tended to be systematic rather than random and tended to indicate that the plot of R^* versus V^{*2} was very slightly concave downward rather than linear, as assumed. Such an effect could possibly have been due to neglecting higher order terms in the temperature dependence of the thermal conductivity and the electrical resistivity. The uncertainty in dV^{*2}/dR^* is estimated to have been less than 1.5 percent.

d. Heat Loss Correction

The uncertainty in the heat loss correction, C, may have been as large as 50 percent of C. For the tests in argon this corresponds to an uncertainty in the measured values for the thermal conductivity of the specimen of 0.1 percent at 100 °C and 0.6 percent at 900 °C. For the tests in helium the corresponding uncertainties were 0.5 percent at 200 °C and 0.7 percent at 400 °C.

e. Departures From Theory

In the derivation of the mathematical expressions used to compute thermal conductivity in the electrical method, there were a number of explicit or implicit assumptions made which could lead to erroneous results if these assumptions were not valid.

It is shown in appendix C that the Thomson effect cancels out to first order provided the temperatures at the two potential taps (used to measure V) are approximately the same. The requirement that the potential taps be at the same temperature is also necessary for the Seebeck emf and Fermi energy terms in (C–50) to drop out. In all of the measure-

ments, the temperatures at the inner potential taps (thermocouple positions 10 and 11) agreed within 0.2 deg or better, as compared with values of θ_m (for 100 A current) ranging from 35 deg at 100 °C to 100 deg at the highest temperatures. Neglecting the Seebeck term in (C–50) for $|T_2 - T_1| < 0.2$ deg corresponds to an uncertainty in the measured thermal conductivity values of less than 0.05 percent. Neglecting the Fermi energy term in (C–50) also involves an uncertainty of less than 0.05 percent (see O'Hagan [9, p. 127]).

It is explicitly assumed in appendix C that the conductor is homogeneous and isotropic; this should be a valid assumption for platinum of the purity used in the present investigation.

As stated in appendix C, the electron current is considered to be the only mass current. In principle it would be possible for platinum, or any impurities which might be present, to migrate under the influence of the electric potential gradient (electromigration) or under the influence of the temperature gradient (Soret effect). If such mass motion existed there would be an associated entropy flow and equation (C–4) and all following equations in appendix C would have to be modified to include a term involving the mass current density and its associated entropy transport. A rigorous analysis including mass migration would be quite complex and was felt to be beyond the scope of the present investigation. However, a qualitative discussion of the probable effect of such mass motion, if it were to occur is given below.

In electromigration, the energy flow is proportional to the electric field. Similarly, the energy flow due to the Thomson effect is essentially proportional to the electric field. Thus if one were to introduce an electromigration term into (C–4) and rigorously go through the analysis, the equivalent expression to (C–31) would include an electromigration term of a form analogous to (i.e., proportional to the electric field) the term in (C–31) involving the Thomson coefficient. Provided this term were small compared with the first two terms in (C–35) it would, to first order, cancel in a similar manner to the way the Thomson term canceled, provided the temperature at the two potential taps were the same and the medium was homogeneous and isotropic. Physically what happens is that the energy transport due to electromigration adds to the energy transport by conduction on one side of the surface of maximum temperature and subtracts on the other side, with no net effect on the maximum temperature rise in the conductor or on the voltage drop between the potential taps, at least to first order. To reemphasize, the temperatures at the taps must be the same for this cancellation to occur and also the medium must be homogeneous and isotropic.

In the Soret effect, the energy transport is proportional to the temperature gradient. Thus the ratio of energy transport due to the Soret effect to that due to heat conduction by other mechanisms is independent of the temperature gradient. The Soret effect is a diffusion process, similar to heat conduction. For a homogeneous medium, therefore, the Soret effect simply behaves as an additional mechanism for "heat conduction" and thus is a legitimate augmentation (or depletion, depending on the sign of the heat of transport) of the thermal conductivity and should be included in the total thermal conductivity value.

For the conditions of the present experiments, there would be no errors involved due to electromigration or Soret effect provided the medium remained homogeneous and isotropic. Both of these effects can change the distribution of impurities and vacancies in a solid. During the experiments the current was in one direction through the specimen about one-half of the time and in the other direction about one-half of the time. Thus, it is doubtful if there was significant inhomogenity introduced due to electromigration effects, even if they were occurring. The Soret effect, if large enough, could cause a redistribution of impurities in the specimen.

For platinum of the purity used, the thermal conductivity at high temperatures would not be expected to be significantly affected by changes in the impurity and vacancy distribution. All of the data at low temperatures, where impurity concentration could affect the thermal conductivity, were taken before the specimen was heated to temperatures where significant mass migration was likely to occur. In view of the above discussion it is felt that neither electromigration nor Soret effect had any adverse effect on the results.

5.3. Results

a. Electrical Resistivity

The ice-point resistivity was determined on the platinum bar before the neck was machined in it (see section 2). The value obtained was

$$(\rho_0)_{\text{ice}} = 9.847 \pm 0.010 \mu\Omega \text{ cm}, \tag{44}$$

corrected to 0 °C dimensions.

In conjunction with the electrical method of measuring thermal conductivity, the resistance of the necked-down region of the specimen at each temperature was determined at a number of current levels. The resistance, R_0, at temperature T_0, was evaluated by extrapolation to zero current as described in section 5.2. In the first series of tests, or the first run as it will be referred to, measurements were made in the following order: 100, 300, 500, 700, 600, 400, and 200 °C in argon; and 200 and 400 °C in helium. The apparatus was then opened up for repair of the guard heater as described in section 4.1c. In the second series of tests, or the second run as it will be referred to, measurements were made at 300, 700, 900, and 1100 °C in argon, in that order.

The values for the resistance of the neck obtained during the second run were about 1.5 percent higher than the values obtained at corresponding temperatures in the first run. This increase in resistance was observed both for measurements at the inner potential taps (10, 11) and for measurements at the outer potential taps (9, 12), indicating that the increase in values

were due either to contamination or to a change in the geometrical factor of the necked-down region rather than to, for example, a short circuit which changed the effective position of one of the potential taps. Since data taken in the first run at lower temperatures after the sample had been heated to 700 °C agreed quite closely with results obtained before the sample was heated to 700 °C, it is felt that there was no evidence indicating that any chemical contamination of the necked-down region occurred during the first run. Furthermore, 700 °C is rather too low a temperature to expect any significant contamination of platinum in a relatively clean environment. Exactly what happened is not known but it is believed that the necked-down region suffered some slight geometrical change between the first and second runs, perhaps while the guard heater was being repaired. In determining the electrical resistivity, data from the first run had to be treated separately in view of this change in the geometric factor.

A quadratic equation was fitted, by the method of least squares, to the measured values of R_0 from the tests in air, argon, and helium from the first run. The equation, extrapolated to 0 °C and normalized to the ice-point resistivity, (44), gave

$$\rho = 9.847(1 + 0.3963 \times 10^{-2} t - 0.5389 \times 10^{-6} t^2) \qquad (45)$$

as the electrical resistivity (corrected for thermal expansion) of the neck from 0 to 700 °C, t being in °C and ρ in $\mu\Omega$ cm. The standard deviation of the residuals from this equation was 0.03 percent. Departures of the data points from this equation are plotted in figure 7 where the overall scatter is seen to be ± 0.05 percent. All but three of the points fall within 0.025 percent of the curve and there is no significant difference between the values obtained on heating and cooling.

A second quadratic equation was fitted to the data points (corrected for thermal expansion) at 300, 700, and 900 °C obtained in the second run. The equation, normalized to the value given by (45) at 700 °C, gave

$$\rho = 9.767(1 + 0.4033 \times 10^{-2} t - 0.5802 \times 10^{-6} t^2), \qquad (46)$$

t being in °C and ρ in $\mu\Omega$ cm. While the geometric factor of the neck changed between the first and second runs there is no reason to believe the resistivity would have changed. Any strains introduced when the geometric factor changed would have annealed out at 700 °C. Thus normalizing the data from the second run to that from the first run at 700 °C is felt to be justified. The departures of the normalized data points at 300, 700, 900, and 1100 °C from the values given by eq (45) are indicated by triangles in figure 7. The 1100 °C data point was not used in deriving (46). The thermocouples started to drift at 1100 °C due to contamination so that greater uncertainty had to be assigned to data obtained at that temperature. The 1100 °C data point agrees with the extrapolated value given by equation (46) to within 0.02 percent. The deviations from the quadratic equation (45) at the higher temperatures as shown in figure 7 are in line with what one would expect. Recent measurements at NBS [29] in conjunction with work toward extending platinum resistance thermometry to the gold point showed that the measured resistance of a certain high purity platinum resistance thermometer at the gold point (1063 °C) was about 0.07 percent below the value obtained by extrapolating the Callendar equation [5] for that thermometer from 630.5 °C to the gold point (1063 °C). Laubitz and van der Meer [30], in measuring the electrical resistivity of high purity (99.999% pure) platinum, found that between 800 and 1200 °C their experimental results fell consistently below the values extrapolated from an equation similar to (45) by an average amount of 0.10 percent.

As stated in section 5.2a, the uncertainty in the electrical resistivity values is estimated to be less than 0.1 percent at 0 °C and less than 0.4 percent at 900 °C.

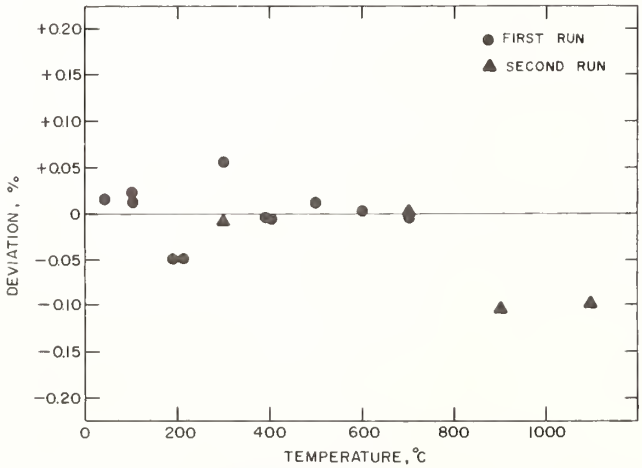

FIGURE 7. *Percentage departures from eq (45) of the electrical resistivity data points.*

The values obtained during the second run have been normalized at 700 °C, as discussed in the text.

b. Thermal Conductivity

The experimental values obtained for the thermal conductivity of the platinum sample by the electrical method are given in table 4. The values for ρ_0 and α_0 used in computing these thermal conductivity values were computed using (45) in the first run and (46) in the second run. The thermal conductivity values given in table 4 have been corrected for thermal expansion. A typical set of data is given in table 5.

The following equation, obtained by the method of least squares, was found to fit the thermal conductivity data (corrected for thermal expansion) obtained in air and in argon, using the electrical method, with a standard deviation of 0.30 percent:

$$\lambda = 0.716 - 0.247 \times 10^{-5} t + 0.182 \times 10^{-6} t^2 - 0.783 \times 10^{-10} t^3, \qquad (47)$$

where t is temperature in °C and λ is in W/cm deg.

TABLE 4. *Experimental values for the thermal conductivity of platinum as measured using the electrical method*

The values given are corrected for thermal expansion.

Test	Run	Atmosphere	Mean temperature °C	Thermal conductivity W/cm deg
1	1	Air	99.8	0.719
2	1	Argon	99.7	.716
3	1	Argon	299.9	.732
4	1	Argon	500.0	.749
5	1	Argon	700.1	.779
6	1	Argon	599.6	.763
7	1	Argon	400.3	.738
8	1	Argon	202.0	.720
9	1	Helium	199.9	.722
10	1	Helium	400.2	.745
11	2	Argon	300.1	.731
12	2	Argon	699.9	.774
13	2	Argon	900.0	.804

TABLE 5. *Typical set of data from measurements of the thermal conductivity of platinum by the electrical method*

The data correspond to Test No. 6 in table 4.

Heating current through necked-down region....A...	I	10.0	57.6	81.7	100.1
Average temperature at thermocouple locations 10 and 11....°C...	T_0	599.5	599.6	599.6	599.6
Voltage drop between platinum legs of thermocouples 10 and 11....mV...	V	12.03	70.80	102.14	127.52
Electrical resistance between platinum legs of thermocouples 10 and 11....mΩ...	R	1.2086	1.2290	1.2509	1.2734
Calculated temperature rise in necked-down region....deg...	θ_m	0.8	25.5	52.2	80.2
Square of adjusted voltage drop....$(mV)^2$...	V^{*2}	145.	4930.	10090.	15456.
Adjusted resistance....mΩ...	R^*	1.2086	1.2292	1.2513	1.2746

Reference temperature....°C...	T_0	599.6
Electrical resistivity at reference temperature.... $\mu\Omega$ cm...	ρ_0	31.16
Electrical resistance corresponding to reference temperature...mΩ...	R_0	1.2079
Temperature coefficient of resistivity at reference temperature....deg^{-1}...	α_0	0.001032
Temperature coefficient of thermal conductivity at reference temperature....deg^{-1}...	β_0	0.000267
Correction for heat loss....	C	0.0077
Correction for thermal expansion....percent....		0.56
Computed value for thermal conductivity of specimen....W/cm deg...	λ_0	0.763

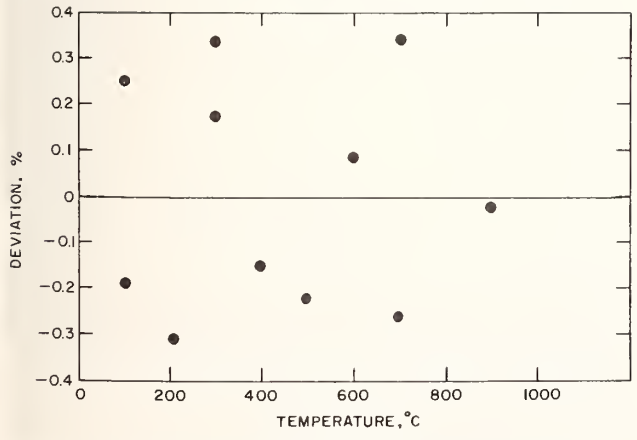

FIGURE 8. *Percentage departures from eq (47) of the thermal conductivity data points obtained by the electrical method.*

This equation is valid from 100 to 900 °C. Deviations of the data points from eq (47) are plotted in figure 8. The scatter is random and there are no significant differences between values obtained on heating and cooling or between the first run and the second run. The value obtained in helium at 200 °C agrees within 0.05 percent of the value given by (47) but the measurement in helium at 400 °C shows a deviation of +0.9 percent. The measurements in helium were made during the first run and there is a possibility that the powder insulation did not uniformly and completely fill the necked-down region. If the powder did not completely fill the space, the boundary conditions assumed in deriving the heat loss corrections would not have been met. Any errors in the heat loss correction would be amplified in helium, particularly at the higher temperature, due to the high thermal conductivity of this gas. In the second run the powder was carefully packed around the neck so that the necked-down region was completely and uniformly filled with insulation. The two data points obtained in helium were not used in deriving (47).

The thermal conductivity values corresponding to (47) are believed to be uncertain by not more than 2 percent over the temperature range 100 to 900 °C. The estimated uncertainties arising from the various known sources of error are summarized in table 6; these uncertainties were discussed in section 5.2.

TABLE 6. *Summary of individual uncertainties contributing to the overoll uncertainty in the thermal conductivity results obtoined using the electrical method*

Source of uncertainty	Uncertainty, %	
	100 °C	900 °C
Geometrical factor (R_0/ρ_0)	0.4	0.4
Temperature coefficient of resistance	.25	.25
Slope of I^{*2} versus R^* curve	1.5	1.5
Heat loss correction (tests in argon)	.1	.6
Seebeck effect	.05	.05
Temperature coefficient of Fermi energy	.05	.05
Combined[a]	1.6	1.7

[a] Each combined uncertainty was obtained by taking the square root of the sum of the squares of the individual uncertainties.

6. Comparison of Results With Other Investigations

The smoothed experimental results given in sections 4.3 and 5.3 are tabulated in table 7. The electrical resistivity values correspond to equation (45) from 0 to 700 °C and to (46) at 800 and 900 °C. The thermal conductivity values for the longitudinal heat flow method and the electrical method correspond to eqs (20) and (47), respectively. The values for the Lorenz function, $\lambda\rho/T$, were computed from the smoothed values for the electrical resistivity, ρ, the two sets of values for thermal conductivity, λ, and the absolute temperature, T.

In this section the results of other investigations on platinum are compared with the results of the present

investigation. Since many investigators do not correct their thermal conductivity and electrical resistivity results for thermal expansion, it was necessary to convert all data to a common basis in order to make valid comparisons.

TABLE 7. *Smoothed experimental values for thermal conductivity, electrical resistivity, and Lorenz function of platinum*

All values are corrected for thermal expansion.

Temperature °C	Electrical resistivity $\mu\Omega$ cm	Thermal conductivity W/cm deg		Lorenz function l^2/deg^2	
		Longitudinal method	Electrical method	Longitudinal method	Electrical method
0	9.847	.....	.....	.....	.....
100	13.70	0.715	0.717	2.62×10^{-8}	2.63×10^{-8}
200	17.44	.721	.722	2.66	2.66
300	21.08	.729	.729	2.68	2.68
400	24.61	.740	.739	2.70	2.70
500	28.03	.753	.750	2.73	2.72
600	31.35	.768	.763	2.76	2.74
700	34.56	.785	.776	2.79	2.76
800	37.65	.803	.790	2.82	2.77
900	40.63	.822	.804	2.85	2.78

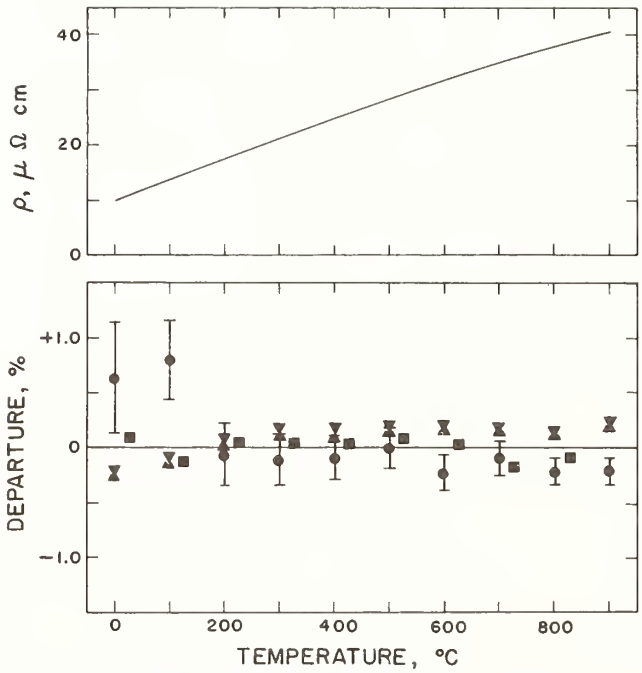

FIGURE 9. *Electrical resistivity of platinum: comparison of previous data with the results of the present investigation.*

- Powell and Tye [1]. Reported purity was 99.999 percent for both samples tested. The ratio of the ice point to helium point resistivity of their No. 1 specimen, which was purer than their No. 2 specimen, was previously reported by Powell, Tye, and Woodman [11] to be about 760. The uncertainties shown represent possible round-off error due to results only being reported to nearest 0.1 $\mu\Omega$ cm.
- ▲ Laubitz and van der Meer [30]. The reported purity was 99.999 percent. The ratio of ice point to helium point resistivity was about 1890.
- ▼ Roeser [31]. His sample was probably thermometric grade platinum having a purity of about 99.999 percent.
- ■ Martin, Sidles, and Danielson [37]. The values shown correspond to their sample which had a reported purity of 99.999 percent and a ratio of ice point to helium point resistivity of 5000.

6.1. Electrical Resistivity

The electrical resistivity values reported for platinum by Powell and Tye [1], Laubitz and van der Meer [30], Roeser [31], and Martin, Sidles, and Danielson [37] are compared with the results of the present investigation in figure 9. The reported purities and resistivity ratios for the different samples are given in the figure caption.

6.2. Thermal Conductivity

The thermal conductivity values reported for platinum by Powell and Tye [1], Laubitz and van der Meer [30], and Martin, Sidles, and Danielson [37, 60] are compared with the results of the present investigation in figure 10. The base line in this figure is a weighted average of the two sets of data obtained in the present investigation, the data from the longitudinal heat flow method being given twice the weight that was given to the data from the electrical method, which had a larger uncertainty. The derived curve of Slack [2] is also shown in figure 10; this represents essentially all of the thermal conductivity values reported for platinum prior to 1962 with the exception of the data of Krishnan and Jain [10].

The previously unreported data of Watson and Flynn [32] shown in figure 10 were made at NBS on the bar from which the specimen for the present in-

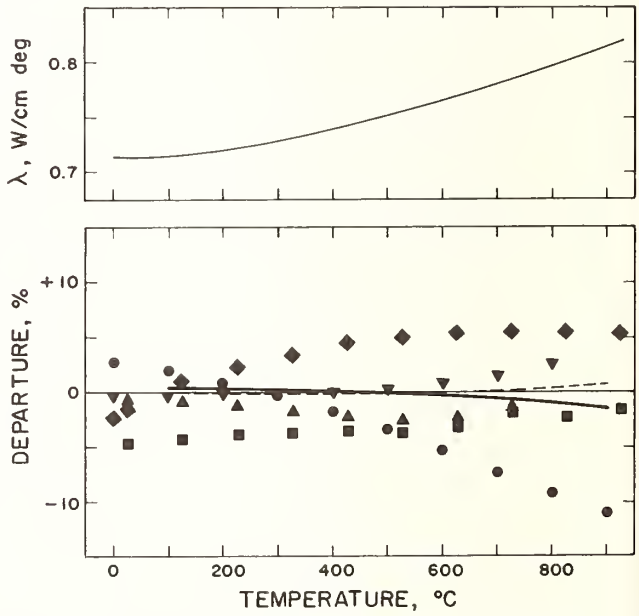

FIGURE 10. *Thermal conductivity of platinum: comparison of previous data with the results of the present investigation.*

The curve in the upper drawing and the baseline in the lower drawing correspond to a weighted average of the two sets of data from the present investigation with the data from the longitudinal heat flow method being given twice the weight of the data from the electrical method.

- --- Present investigation—longitudinal heat flow method.
- — Present investigation—electrical method.
- ▼ Watson and Flynn [32]—same sample as that used in the present investigation.
- ◆ The curve of Slack [2].
- ● Powell and Tye [1].
- ▲ Laubitz and van der Meer [30].
- ■ Martin, Sidles, and Danielson [37], the values shown correspond to their sample D.

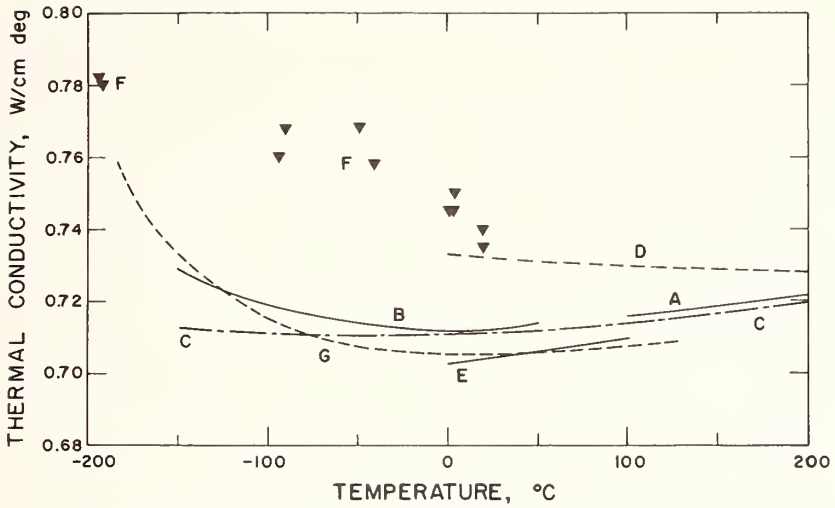

FIGURE 11. *Thermal conductivity of platinum: comparison between existing low temperature data and those of the present investigation.*

A. Present investigation: the curve shown is that obtained by the longitudinal heat flow method.
B. Halpern and Flynn [33]; measurements made on a portion of the sample used for the present investigation.
C. Watson and Flynn [32]; measurements made on a portion of the sample used for the present investigation.
D. Powell and Tye [1].
E. Bode [38].
F. Powell, Tye, and Woodman [39]; measurements made on one of the samples of Powell and Tye [1].
G. Moore and McElroy [40]; measurements made on one of the samples of Powell and Tye [1].

vestigation was later machined. Watson and Flynn made their measurements in air in a longitudinal heat flow apparatus which has been described by Watson and Robinson [34] and by Ginnings [35].

Several recent sets of thermal conductivity values for platinum at lower temperatures are displayed in figure 11. The data of Powell and Tye [1], curve D, were also shown in figure 10. The data of Bode [38], curve E, were obtained using a longitudinal heat flow method; Bode stated that he considered his values to be accurate to within 0.5 percent. Since the present investigation was begun, Powell, Tye, and Woodman [39], curve F, have used a longitudinal heat flow method to make low temperature thermal conductivity measurements on one of the samples of Powell and Tye. Also during this time, Moore and McElroy [40], curve G, have made thermal conductivity measurements on the same sample which Powell, Tye, and Woodman [39] used for their investigation. In the temperature range shown in figure 11, the thermal conduc-

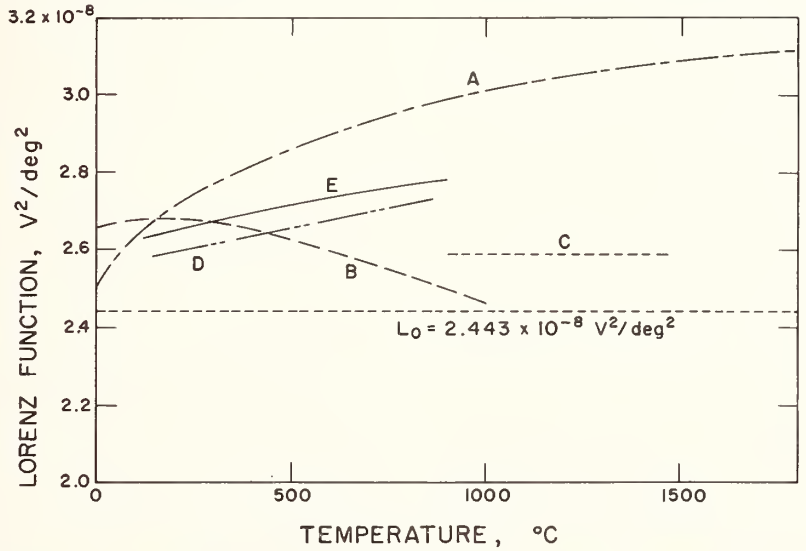

FIGURE 12. *Lorenz function for platinum: comparison between existing data and those of the present investigation.*

A. Slack [2].
B. Powell and Tye [1].
C. Wheeler [36].
D. Martin, Sidles, and Danielson [37]: the values shown correspond to their sample D.
E. Present investigation; the curve shown was computed from the thermal conductivity values obtained by the longitudinal heat flow method.

tivity of platinum could be affected by small differences in purity and this may account for some of the differences shown. However, the measurements of Powell, Tye, and Woodman [39] and those of Moore and McElroy [40] were carried out on the same sample; hence the differences between the results of these investigators must be presumed to be due to experimental errors.

Additional references to previous measurements of the thermal conductivity of platinum are given by Powell, Ho, and Liley [8]. Ciszek [61] has recently reported some high temperature thermal diffusivity measurements for platinum.

Values obtained for the Lorenz function of platinum are compared with those of other investigators in figure 12. The present measurements indicate a Lorenz function increasing above the theoretical value as the temperature increases. Laubitz and van der Meer [30] point out that such behavior of the Lorenz function can be understood qualitatively if one assumes a low Fermi energy for platinum.

7. Conclusions

The good agreement among the thermal conductivity values obtained for platinum by two different methods in the present investigation and by an independent measurement by Watson and Flynn [32] lend considerable weight to these results. The values indicate that the thermal conductivity of platinum increases with temperature as found by Laubitz and van der Meer [30] rather than being essentially independent of temperature as found by Powell and Tye [1]. However, there remains the possibility that there is a real difference between the samples of Powell and Tye [1] and those of other investigators. In order to explore this possibility, measurements should be made at high temperatures in another laboratory on one of the actual samples of Powell and Tye. Steps are being taken to see if this can be done.

The results of the present investigation indicate that electrical methods of measuring thermal conductivity can yield equivalent results to those obtained by the more conventional nonelectrical methods, at least for the conditions of this investigation. This can be interpreted as indicating that the thermal conductivity of platinum does not depend significantly on electric current densities in the range less than $10^4 A/cm^2$.

Before platinum can be established as a thermal conductivity reference standard, additional measurements by the same method on samples of differing purity are indicated. It is intended to repeat the measurements described in this paper on a sample of platinum of higher purity than that used in the present investigation.

We appreciate the advice and assistance provided by Henry G. Albert and A. V. Lincoln, both of Engelhard Industries, Inc. We thank Henry E. Robinson, Chief, Environmental Engineering Section, NBS, and Adjunct Professor of Engineering, The George Washington University, for his advice and support. The intricate and difficult machining required for this project was done by Raymond Chidester. Much good advice in matters of fabrication came from John Hettenhouser.

NOTE: Appendixes 8, 9, and 10, have been omitted from this copy.

11. References

[1] Powell, R. W. and Tye, R. P., The promise of platinum as a high temperature thermal conductivity reference material, Brit. J. Appl. Phys. **14,** 662 (1963).

[2] Slack, G. A., Platinum as a thermal conductivity standard, J. Appl. Phys. **35,** 339 (1964).

[3] Hill, J. S. and Albert, H. J., Loss of weight of platinum, rhodium, and palladium at high temperatures, Engelhard Industries, Inc. Technical Bulletin, **IV,** 59 (1963).

[4] Galagali, R. J., Change of platinum resistance by hydrogen, Brit. J. Appl. Phys. **15,** 208 (1964).

[5] Stimson, H. F., The international temperature scale of 1948, J. Res. NBS **42,** 209 (1949) RP 1962.

[6] Stimson, H. F., International practical temperature scale of 1948, text revision of 1960, J. Res. NBS **65A** (Phys. and Chem.), No. 3, 139 (1961).

[7] Evans, J. P. and Burns, G. W., A study of stability of high temperature platinum resistance thermometers, in Temperature, Its Measurement and Control in Science and Industry, **3,** Part 1, p. 313 (Reinhold, 1962).

[8] Powell, R. W., Ho, C. Y., and Liley, P. E., Thermal conductivity of selected materials, NSRDS–NBS 8 (Nov. 25, 1966).

[9] O'Hagan, M. E., Measurements of the Thermal Conductivity and Electrical Resistivity of Platinum from 373 to 1373 °K, Doctoral Dissertation, The George Washington University (Aug. 1966).

[10] Krishnan, K. S. and Jain, S. C., Determination of thermal conductivities at high temperatures, Brit. J. Appl. Phys. **5,** 426 (1954).

[11] Powell, R. W., Tye, R. P., and Woodman, M. J., Thermal conductivities and electrical resistivities of the platinum metals, Platinum Metals Rev. **6,** 138 (1962).

[12] Martin, J. J. and Sidles, P. H., Thermal diffusivity of platinum from 300 to 1300 °K, Report No. IS–1018, contribution No. 1614 of the Ames Laboratory of the U.S. Atomic Energy Commission (1964).

[13] Holm, R. and Störmer, R., Messung der Wärmeleitfähigkeit einer Platinprobe ein Temperaturgebeit 19 bis 1020 °C, Wiss. Veroff. Siemens-Werk **9,** 312 (1930). (An unpublished English translation for NBS was made by Joint Publications Research Service.)

[14] Hopkins, M. R., The thermal and electrical conductivities of metals at high temperatures, Z. Phys. **147,** 148 (1957).

[15] Cutler, M., Snodgrass, H. R., Cheney, G. T., Appel, J., Mallon, C. E., and Meyer, C. H., Jr., Thermal conductivity of reactor materials, Final Report GS–1939, General Atomic Division, General Dynamics Corporation, San Diego (30 January 1961).

[16] Wichers, E., The History of Pt 27, in Temperature, Its Measurement and Control in Science and Industry, **3,** Part 1, p. 259 (Reinhold, 1962).

[17] Berry, R. J., Relationship between the real and ideal resistivity of platinum, Canad. J. Phys. **41,** 946 (1963).

[18] Corruccini, R. J., Annealing of platinum for thermometry, J. Res. NBS **47,** 94 (1951) RP2232.

[19] Kirby, R. K., NBS, private communication (Dec. 1965).
[20] Meissner, W., Thermische und elektrische Leitfähigkeit einiger Metalle zwischen 20° und 373° abs., Ann. Phys. **47,** 1001 (1915).
[21] McFee, R., Optimum input leads for cryogenic apparatus, Rev. Sci. Instr. **30,** 98 (1959).
[22] Neighbor, J. E., Leads power in calorimetry, Rev. Sci. Instr. **37,** 497 (1966).
[23] Mallon, R. G., Optimum electrical leads of aluminum and sodium for cryogenic apparatus, Rev. Sci. Instr. **33,** 564 (1962).
[24] Sobol, H. and McNicol, J. F., Evaporation of Helium I due to current-carrying leads, Rev. Sci. Instr. **33,** 473 (1962).
[25] Stein, R. P., A solution of the steady linear heat-flow equation with heat generation and conductivity an arbitrary function of temperature, J. Appl. Mech. **26,** 685 (1959).
[26] Ginnings, D. C. and West, E. D., Heater lead problem in calorimetry, Rev. Sci. Instr. **35,** 965 (1964).
[27] Peavy, B. A., Determination and smoothing of Fourier coefficients representing sectionally discontinuous functions on a finite surface, J. Res. NBS **71C** (Engr. and Instr.) No. 2, 93 (1967).
[28] Powell, R. W., Thermophysical Properties Research Center, private communication to D. R. Flynn (Oct. 1966).
[29] Evans, J. P., NBS, private communication (Aug. 1966).
[30] Laubitz, M. J. and van der Meer, M. P., The thermal conductivity of platinum between 300 and 1000 °K, Canad. J. Phys. **44,** 3173 (1966).
[31] Roeser, Wm. F., in American Institute of Physics Handbook, Second Edition, p. 4–13 (McGraw–Hill Book Co., 1963). The values given in this reference have been adjusted to correspond to temperatures expressed on the International Practical Temperature Scale of 1948. The original reference is to the work of W. F. Roeser as given in Temperature, Its Measurement and Control in Science and Industry, p. 1312 (Reinhold, 1941).
[32] Watson, T. W. and Flynn, D. R., NBS, private communication (Jan. 1966).
[33] Halpern, Carl and Flynn, D. R., NBS, private communication (Aug. 1966).
[34] Watson, T. W. and Robinson, H. E., Thermal conductivity of some commercial iron-nickel alloys, Trans. ASME J. Heat Transfer **83C,** 403 (1961).
[35] Ginnings, D. C., Standards of heat capacity and thermal conductivity, in Thermoelectricity, edited by Paul H. Egli, p. 320 (Wiley, 1960).
[36] Wheeler, M. J., Thermal diffusivity at incandescent temperatures by a modulated electron beam technique, Brit. J. Appl. Phys. **16,** 365 (1965).
[37] Martin, J. J., Sidles, P. H., and Danielson, G. C., Thermal diffusivity of platinum, Report No. IS–1261, contribution No. 1810 of the Ames Laboratory of the U.S. Atomic Energy Commission.
[38] Bode, K-H, Messung der Wärmeleitfähigkeit von reinem Platin zwischen 0 °C und 100 °C, PTB Mitteilungen Nr. **5,** 416 (1964).
[39] Powell, R. W., Tye, R. P., and Woodman, Margaret J., The thermal conductivity and electrical resistivity of polycrystalline metals of the platinum group and of single crystals of ruthenium, J. Less-Common Metals **12,** 1 (1967).
[40] Moore, J. P., and McElroy, D. L., Oak Ridge National Laboratory, private communication (Mar. 1967).
[41] Huntington, H. B., and Ho, S. C., Electromigration in metals, J. Phys. Soc. Japan **18,** Supplement II, 202 (1963).
[42] Ho, S. C., Hekenkamp, T. and Huntington, H. B., AEC Document Code No. RPI–1044–1, Contract HT(30–1)–1044 (Apr. 1, 1964).
[43] O'Boyle, D., Observations of electromigration and the Soret effect in tungsten, J. Appl. Phys. **36,** 2849 (1965).
[44] Callen, H. B., The application of Onsager's reciprocal relations to thermoelectric, thermomagnetic, and galvanomagnetic effects, Phys. Rev. **73,** 1349 (1948).
[45] De Groot, S. R., Thermodynamics of Irreversible Processes (Interscience, 1951).
[46] Domenicali, C. A., Irreversible thermodynamics of thermoelectric effects of inhomogeneous, anisotropic media, Phys. Rev. **92,** 877 (1953).
[47] Domenicali, C. A., Irreversible thermodynamics of thermoelectricity, Rev. Mod. Phys. **26,** 237 (1954).
[48] Domenicali, C. A. Stationary temperature distribution in an electrically heated conductor, J. Appl. Phys. **25,** 1310 (1954).
[49] Leech, J. W., Irreversible thermodynamics and kinetic theory in the derivation of thermoelectric relations, Canad. J. Phys. **37,** 1044 (1959).
[50] Ziman, J. M., Electrons and Phonons (Clarendon Press, Oxford, 1960).
[51] Beaumont, C. F. A., Connection between macroscopic and microscopic transport phenomena in solid conductors, Am. J. Phys. **33,** 547 (1965).
[52] El-Saden, M. R., Theory of nonequilibrium thermodynamics with application to the transport processes in a solid, Trans. ASME, J. Heat Transfer, Paper No. 65–HT–1 (1965).
[53] Onsager, L., Reciprocal relations in irreversible processes, Part I, Phys. Rev. **37,** 405 (1931).
[54] Onsager, L., Reciprocal relations in irreversible processes, Part II, Phys. Rev. **38,** 2265 (1931).
[55] Callen, H. B., Thermoelectric and thermomagnetic effects in electrochemical constants, NBS Circular 524, 141 (1953).
[56] MacDonald, D. K. C., Thermoelectricity–An Introduction to the Principles (Wiley, 1962).
[57] Davidson, P. M., The theory of the Thomson effect in electrical contacts, Proc. Inst. Elec. Engrs. **96,** Part 1, 293 (1949).
[58] Holm, R., Electric Contacts: Theory and Application, 4th ed. (Springer-Verlag, 1967).
[59] Llewellyn Jones, F., The Physics of Electrical Contacts (University Press, Oxford, 1957).
[60] Martin, J. J., Sidles, P. H., and Danielson, G. C., Thermal diffusivity of platinum from 300 to 1200 °K, J. Appl. Phys. **38,** 3075 (1967).
[61] Ciszek, T. F., The Thermal Diffusivity and Electrical Resistivity of Platinum at Temperatures Above 1000 °K, Master's Thesis, Iowa State University (1966).

(Paper 71C4–258)

Emissivities of Metallic Surfaces at 76°K

M. M. Fulk and M. M. Reynolds*
National Bureau of Standards, Boulder, Colorado
(Received October 15, 1956; revised manuscript received July 29, 1957)

Heat transport by radiation between surfaces at 300°K and 76°K was measured to evaluate the effective emissivities of a number of technical grade or commercially available metals with unknown metallurgical history. The surface with the lowest total hemispherical emissivity was an unbuffed silver-plated surface. It was found that the emissivity of surfaces was lowest when used without any mechanical working and that the ability to absorb radiant energy varied with the length of time the surface was kept cold, even at a pressure less than 10^{-6} mm Hg, indicating surface contamination by residual gases.

I. INTRODUCTION

THERE have been a number of researches on vacuum jacketed vessels since the work of Dewar, but the subject does not seem to have been studied as carefully as the practical importance would seem to justify. Owing to the importance of low-temperature research and to the constantly expanding technological uses of low-temperature equipment and liquefied gases, more information is needed for the optimum design of cryogenic and cryostatic equipment.

Many experimental data on reflectivity, emissivity, and absorptivity of various materials over a wide range of temperatures and wavelengths of radiation are available. There is, however, considerable difficulty in translating this information into numbers that can be used in the design of low-temperature equipment, except in a few special cases. This hindrance has left obscure many points that are of considerable interest in evaluating surfaces and their performances in low-temperature equipment.

The present work was undertaken to obtain more information about heat transport by radiation and how it depends on materials and their surfaces. The measurements of emissivities were made under conditions that exist in practical vacuum vessels rather than being a study of the most pure metallic surfaces to check theoretical arguments.

The metals used in this study were either technical grade or commercially "pure" with unknown metallurgical history. Their surfaces were cleaned of grease, dirt, etc., but retained their normal oxide coat that is acquired at room temperature.

In most low-temperature equipment there is seldom a surface at a temperature greater than 300° or 400°K facing the low-temperature parts. This means that the wavelengths (λ) of thermal radiation encountered are practically all greater than 2 microns (μ) and 98% of the total radiation has wavelengths greater than 4 microns. The present interest is therefore confined to $\lambda > 4\,\mu$ where the frequency is comparable to or smaller than the collision frequency of electrons in most common metals.[1]

Biondi[2] and others have shown that the absorptivity of copper becomes nearly independent of λ for $\lambda > 2\,\mu$. After reaching the region where $\lambda > 4$ or $5\,\mu$ most metals are practically "flat" in their reflectivity (r) with increasing λ. Thus it is seen that the assumption of "grayness" for the surface of metals for $\lambda > 4\,\mu$ is fairly safe. Emissivity (e) may be used in substitution for absorptivity (a) or $(1-r)$ even though the temperature of the radiator and absorber are not the same but both less than about 400°K. Therefore in the following it is assumed that $e = a = (1-r)$ for the conditions under consideration. The terms "emissivity" and "absorptivity" have been used interchangeably, although strictly speaking these measurements were determinations of the "absorptivity."

There are a number of works treating various aspects of the interaction of light with metals and concerning the anomalous skin effect in metals.[1,3]

The bibliography by J. R. Partington[4] on metallic reflection is fairly complete.

There are also a number of works[2,5] giving measured values of r, a, and e at low temperatures.

The effects of surface films on metallic reflection have

* Now at Titan Chemical Industries, Inc., Colorado Springs, Colorado.

[1] N. F. Mott and H. Jones, *Properties of Metals and Alloys* (Oxford University Press, New York, 1936). R. E. Peierls, *Quantum Theory of Solids* (Oxford University Press, New York, 1955).

[2] M. A. Biondi, Phys. Rev. **96**, 534 (1954).

[3] R. B. Dingle, Physica **19**, 311, 348, 729 (1953). J. R. Beattie and G. K. T. Conn, Phil. Mag. **46**, 989 (1955). T. Holstein, Phys. Rev. **88**, 1427 (1952); **96**, 535 (1954). R. G. Chambers, Proc. Roy. Soc. (London) **A215**, 481 (1952). R. G. Chambers, Physica **19**, 365 (1953). G. E. H. Reuter and E. H. Sondheimer, Proc. Roy. Soc. (London) **A195**, 336 (1948). R. W. Ditchburn, *Light* (Interscience Publishers, Inc., New York, 1955). König, *Handbuch der Physik* (Springer-Verlag, Berlin, 1928), Vol. XX, pp. 197–253. H. Rubens and E. Hagen, Ann. Physik **11**, 873 (1903). J. A. Stratton, *Electro-Magnetic Theory* (McGraw-Hill Book Company, Inc., New York, 1941).

[4] J. R. Partington, "Physico-Chemical Optics," Vol. IV of *An Advanced Treatise on Physical Chemistry* (Longmans Green and Company, London, 1955).

[5] K. G. Ramanathan, Proc. Phys. Soc. (London) **A65**, 532 (1952). M. Blackman *et al.*, Proc. Roy. Soc. (London) **A194**, 147 (1948). F. J. Zimmerman, J. Appl. Phys. **26**, 1483 (1955). K. Weiss, Ann. Physik **6**, 1 (1948). H. Cheung, unpublished thesis, Georgia Institute of Technology (1955).

been considered by a number of workers and will not be taken up here.[6]

The bibliographies in the references given will serve as guides to most work on metallic reflection, and for those engaged in radiation exchange problems the *Table of Radiant-Interchange Configuration Factors*[7] may be very helpful.

II. APPARATUS

A. Description

The method of measurement consisted of metering the gas "boil-off" from liquid nitrogen contained in a Dewar-like calorimeter. The inside surface was the sample material that absorbed the heat transport by radiation from the warm outside wall facing the sample across the vacuum space. The heat absorbed by the inside surface evaporated the liquid nitrogen and the gaseous nitrogen was measured with a gas flowmeter. The arrangement is shown in Fig. 1(B).

Various forms of Dewar-like calorimeters were used to measure the heat transport by radiation between surfaces in vacuum. One calorimeter was made of Lucite, another glass, and others of metals. Figure 1 shows schematically the various geometries and designs used so that various surfaces could be easily substituted and yet provide as closely comparable results as possible.

Figure 1(A) shows the form of the internal neck shields used to stop radiation down the neck into the liquid nitrogen can or ball. The forms of external shields can be seen in Figs. 1(B) and 1(C). The radiation shields in the tops of the calorimeters in Fig. 1 were "black" on top and "polished" underneath.

Aluminum rods were added to the inside cans to prevent superheating and bumping caused by the hydrostatic head of liquid nitrogen. The gas pressure in the vacuum space was always reduced to less than 10^{-6} mm Hg except in the case of the Lucite unit. In the Lucite unit two to four measurements at different pressures were made and extrapolated back to 10^{-6} mm Hg.

The calorimeters were usually calibrated electrically with the outside and inside of the calorimeter at 76°K. This calibration gave the solid support and neck radiation correction as a function of boil-off rate. Those calorimeters not calibrated electrically were "calibrated" by running a well-known surface.

After calibration it was found that the radiant heat transfer to the surfaces at low temperature was large compared to the "corrections." The "corrections" could have been ignored and the determinations would still have been well within the estimated accuracy of 5%.

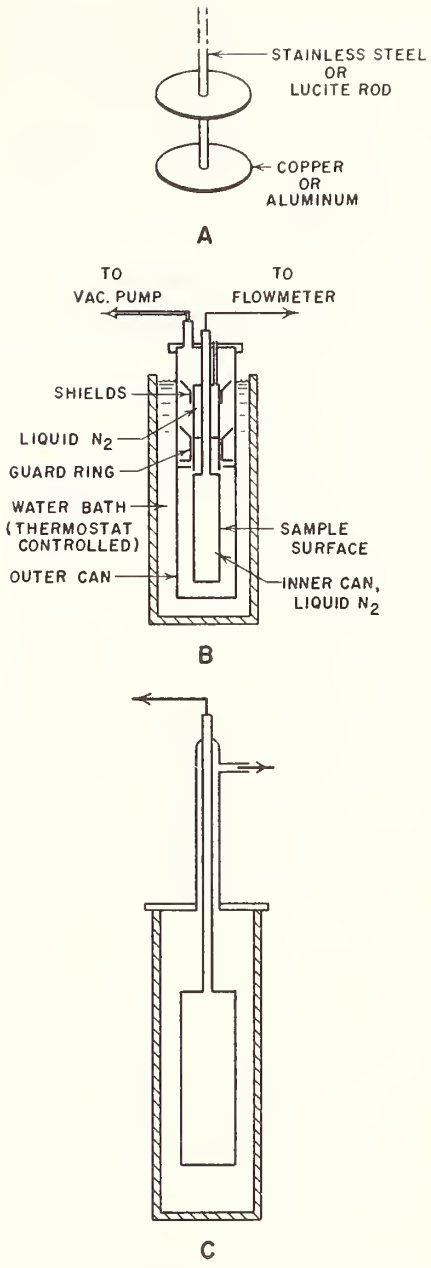

FIG. 1. Schematic diagrams of the various forms of Dewar-like calorimeters and their respective radiation shields, used to study the total hemispherical absorptivity of surfaces at 76°K for 300°K thermal radiation. (A) Internal neck shield to stop radiation down boil-off tube—used in all units. (B, C) Metal units. Note: All "shields" were "black" on top and "shiny" underneath.

The temperature drop through the wall of the calorimeter can for the Lucite unit was estimated at a maximum of 0.1°K, and the temperature drop through the walls of the metal calorimeters was of the order of 0.01°K.

For a given metal sample the values were easily reproducible within 2% and in the better calorimeters 1% or less.

[6] C. S. Taylor and J. D. Edwards, Heating, Piping and Air Conditioning (January, 1939). P. Drude, Ann. Physik **36**, 532, 865 (1889). C. Hilsum, J. Opt. Soc. Am. **44**, 188 (1954). F. A. Lucy, J. Chem. Phys. **16**, 167 (1948). O. S. Heavens, *Optical Properties of the Solid Films* (Academic Press, Inc., New York, 1955).

[7] D. C. Hamilton and W. R. Morgan, Technical Note 2836, *Radiant-Interchange Configuration Factors* (National Advisory Committee for Aeronautics, Washington, D. C., 1952).

TABLE I. Total hemispherical absorptivity of metals at 76°K for 300°K thermal radiation.[a]

Metal	Surface treatment	a_h
Aluminum	0.001 in Kaiser foil unannealed	0.018
	0.0015 in Cockron home foil	0.018
	0.0015 in. Hurwich home foil—mat side	0.021
	0.0015 in. Hurwich home foil—bright side	0.022
	0.020 in. cold acid cleaned	0.028
	0.020 in. hot acid cleaned, Alcoa process	0.029
	0.020 in. Alcoa No. 2 reflector plate	0.026
	0.020 in. Alcoa No. 2 reflector plate sanded with fine emery	0.032
	0.020 in. Alcoa No. 2 reflector plate cleaned with alkali	0.035
	0.020 in. wire brush, emery paper, steel wool, cold acid	0.045
	0.020 in. wire brush	0.06
	0.020 in. Liquid honed[b]	0.014
	Aluminum vaporized onto both sides of 0.0005 in. plastic Mylar	0.04
	Aluminum sprayed onto stainless steel	0.07
	Aluminum sprayed onto stainless steel and wire brushed	0.06
Brass, yellow	0.001 in. Shim stock (65% Cu, 35% Zn)	0.029
Cadmium	A very mossy and smeared-looking plated surface	0.03
Copper	0.005 in. Millrun sheet (annealed)	0.015
	0.005 in. dilute chromic acid dip	0.017
	0.005 in. wet polished with pumice	0.018
	0.005 in. dry polished with plastic polishing wax abrasive	0.019
	0.005 in. electrolytically cleaned	0.017
	0.020 in. liquid honed[b]	0.088
	0.005 in. fine emery	0.023
	Commercial copper sphere—polished	0.03
	Commercial copper sphere—Oakite No. 33 cleaned	0.03
Copper	Commercial copper sphere—Alleghany silver spray coated	0.01
	Commercial copper sphere—tinned	0.02
Chromium	Chromium plate on copper	0.08
Gold	0.0015 in. Foil	0.010
	0.0005 in. Foil	0.016
	0.000040 in. Foil	0.023
	0.00001 in. Leaf	0.062
Gold plate	0.0002 in. on stainless steel 1% silver in gold	0.025
	0.0001 in. on stainless steel 1% silver in gold	0.027
	0.00005 in. on stainless steel 1% silver in gold	0.028
	0.0002 in. on copper, 1% silver in gold	0.025
	24K gold plate on stainless steel	0.017
	Gold vaporized onto both sides of 0.0005 in. Mylar plastic	0.02
Lead	0.004 in. foil (commercial sheet)	0.036
Nickel	0.004 in. foil	0.022
Rhodium	Rhodium plated on stainless steel	0.078
Silver	Sheet	0.008
	Silver plate (careful preparation) nickel strike on stainless steel	0.009
	Silver plate (careful preparation) nickel and copper strike on stainless steel	0.007
	Allegheny Silver Spray Process on stainless steel	0.009
Stainless steel	0.005 in. type 302 sheet	0.048
	Commercial ball type 302	0.07
Tin	0.001 in. foil	0.013
	Tinned copper ball	0.02
Zinc	0.0065 in. foil	0.02
50–50 Solder	0.002 in. solder surface on 0.005 in. copper sheet	0.03

[a] All values were calculated on the basis of the equation

$$q=\frac{e_i e_0 A_i \sigma}{e_0+e_i(1-e_0)A_i/A_0}(T_0^4-T_i^4).$$

Since $e_0>0.8$ and $A_i/A_0\sim 0.5$ this equation reduces in our case to $q=e_i A_i \times\sigma(T_0^4-T_i^4)$ within experimental error. e = emissivity, A = area, σ = Stefan-Boltzmann constant, T = temperature, q = heat transport by thermal radiation, and the subscript 0 = outside and i = inside.

[b] Abrasive carried in a liquid jet.

B. Cryogen Level Effect

Test runs were performed with different quantities of liquid nitrogen in the calorimeters to determine if boil-off varied with level. In the glass and plastic units, which would have shown the most effect, there was no level effect down to 60–70% full with surfaces of less than 0.10 emissivity. All readings were taken with the calorimeter essentially full, in the metal units as well as in the glass and Lucite units, since all calorimeters were level-sensitive for large heat leak.

C. End Effects

The end effect was estimated[5,7] to be less than 5% and was ignored in the following determinations of emissivity. The neck radiation error was determined in the electrical calibration of the original unit.

End effects, spurious radiation leak problems, and calibration, etc., can be eliminated in the cylinder-in-cylinder case by building two identical units, except for length. Thus the differences in readings are simply related to the area differences. This refinement was not justified by the accuracy needed at the time of these measurements.

D. Materials

The metals used are readily available and likely to be used in experimental low-temperature work and cryogenic engineering.

Some samples in the form of thin sheet or foil were wrapped on the inner can and held in place with fine copper wire. Thermal contact was established with a thin layer of Apiezon-L vacuum grease. Other surfaces were the can itself or metals electroplated, sprayed, or melted onto the surface of the can. The outside wall facing the sample surface was made "black" ($e>0.8$) with metal black and paints.

III. RESULTS

Table I contains a representative selection of materials checked at 76°K for their total hemispherical

absorptivities for 300°K thermal radiation. The over-all accuracy was estimated to be 5%.

Table II shows the effect of lowering the temperature on the absorptivity of a surface for 300°K thermal radiation.

IV. DISCUSSION

The equation

$$q=\frac{e_i e_0 A_i \sigma}{e_0+e_i(1-e_0)A_i/A_0}(T_0^4-T_i^4)$$

was used to calculate all values in the tables, where e=emissivity, A=area, σ=Stefan-Boltzmann constant, T=temperature °K, q= heat transport by thermal radiation, and the subscripts 0=outside and i=inside. The warm wall of calorimeter had an emissivity of 0.8 or greater and the ratio of A_i to A_0 was about 0.5. The problem was assumed to be more nearly a diffuse rather than a specular reflecting problem so the above equation reduced in this case to $q=e_i A_i \sigma(T_0^4-T_i^4)$, within experimental error.

The factors affecting the absorptivity of a surface include material, purity, temperature, thickness, roughness, surface coat, wavelength of radiation with its angle of approach, and the number of scattering impurities in the surface to the depth of penetration of the radiation wavelength under consideration.

TABLE II. Total hemispherical absorptivity of metals at 76°K and 20°K for 300°K thermal radiation (showing effect of lowering temperature).

Metal	Surface treatment	Temperature of surface	a_h
Silver	plated on copper	76	0.017
		20	0.013
Nickel	plated on copper	76	0.033
		20	0.027

Metal surfaces at low temperatures change with time in their total heat transfer ability. Figure 2 shows the change in ability of surfaces at 76°K to absorb heat from a 300°K surface as a function of time. This increase was attributed to the adsorption or condensation of residual gases on the surfaces of the metals—since the surfaces recovered their original e after being warmed to 300°K and pumped.

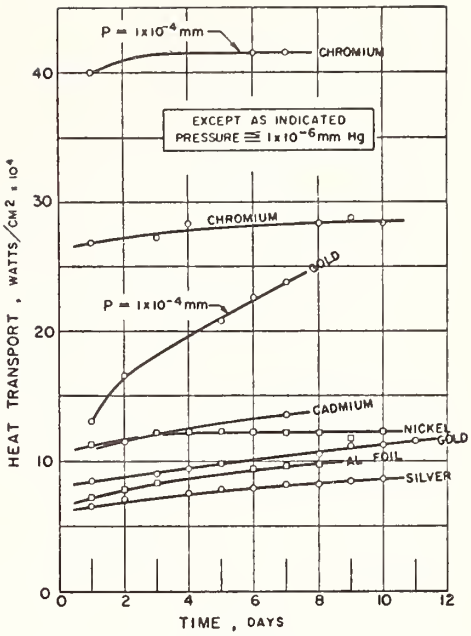

FIG. 2. The change in ability of a 76°K surface to absorb heat from 300°K surface as a function of time. This change was attributed to the absorption of gases. The surfaces were various metals electroplated on to a copper calorimeter can and the calorimeter was pumped to a pressure less than 10^{-6} mm Hg, except where noted.

Electroplating would appear an easy solution to many thermal radiation problems but there are attending difficulties. There is a wide spread in the properties of electroplated surfaces. They have to be as pure as possible, dense and fairly thick if plated on to an insulator or metal of low electrical conductivity. Purity and density of plate are more important than the highly polished look the electroplater likes to give to a surface. The visual appearance of a surface is not a very good criterion for the performance of this surface beyond 4 μ. It was found that the absorptivity of some surfaces increased if mechanically polished. This observation was noted at least as early as 1947 by M. Blackman *et al.*

V. ACKNOWLEDGMENTS

This work was sponsored by the U. S. Atomic Energy Commission. The authors wish to thank J. Brown, O. Park, J. Schrodt, and D. Weitzel for their assistance in the work.

Reprinted from JOURNAL OF APPLIED PHYSICS, Vol. 28, No. 12, 1464–1467, December, 1957

Journal of Research of the National Bureau of Standards Vol. 59, No. 5, November 1957 Research Paper 2805

An Apparatus for Measurement of Thermal Conductivity of Solids at Low Temperatures

Robert L. Powell, William M. Rogers, and Don O. Coffin

A description is given of an apparatus used for determining the thermal conductivities of solids in the temperature range 4° K to 300° K. The apparatus is especially suited to the determination of thermal conductivity over a large temperature interval, enabling coverage of the temperatures between the normal boiling points of liquefied gases. Illustrative results are given for an insulator, polytetrafluoroethylene, and for a high-conductivity commercial coalesced copper. The thermal conductivity of the insulator increases monotonically from 0.56 milliwatt per centimeter per degree K at 5° K, to 2.32 at 80° K. The thermal conductivity of the copper has a maximum of 24.9 watts per centimeter per degree K at 21° K, and a value of 8.15 at 5° K. The methods of data analysis and estimation of errors are given.

1. Introduction

Data on thermal conductivity are necessary for the selection of suitable construction materials, and the prediction of operating characteristics of low-temperature apparatus used in research and industry. In addition, accurate thermal conductivity values for pure metals and controlled alloys are important in the development and verification of theories of electronic transport phenomena in metals. The apparatus described in this paper is well suited to the measurement of thermal conductivity of metals and commercial alloys; it is also usable for poor conductors such as plastics and other dielectric solids.

2. Experimental Apparatus

2.1. General Description

The method of determining thermal conductivity by axial heat flow through a long cylindrical sample is used. A pictorial diagram of the apparatus is shown in figure 1. The apparatus is similar, in many respects, to some of those described in the review by Olsen and Rosenberg [5].

The cryostat consists of concentrically mounted sample, thermal shield, vacuum container, glass Dewar, Dewar support, and outside metal Dewar.

The sample rod is clamped to the heat sink at the top; the sample heater is attached to the bottom of this rod. The temperature distribution along the sample is measured by means of eight thermocouples attached to thermocouple holders positioned along the rod. Heat losses by gas convection and conduction are made negligible by evacuating the region surrounding the sample. Losses by radiation and conduction along the lead wires are reduced by enclosing the sample rod within a symmetric cylindrical thermal shield maintained at approximately the same temperature and axial gradient as the sample. Measurements of the temperature, thermal gradient,

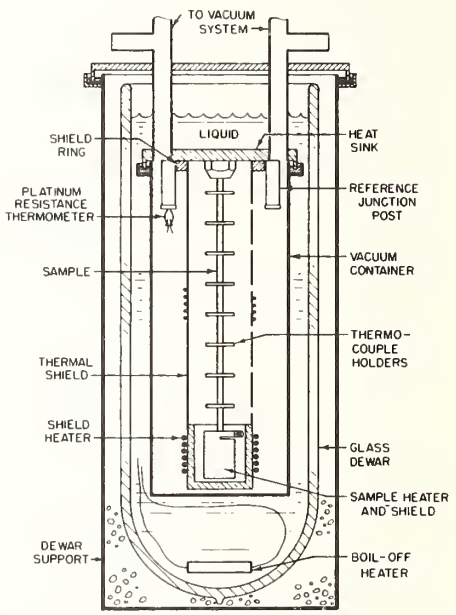

FIGURE 1. *Thermal conductivity apparatus.*

and power input to the sample, combined with data on the cross-sectional area, permit a calculation of the thermal conductivity of the sample based upon Fourier's equation for steady state, linear heat flow.

The heat sink is maintained at a constant low temperature by a refrigerant, usually a liquefied gas. This refrigerant, poured into the glass Dewar from a central fill tube, surrounds the heat sink and vacuum can. The glass Dewar is supported by a metal container that is, in turn, sealed to a top plate. For temperatures below 80° K in the internal apparatus, the Dewar support container is further surrounded by a metal Dewar containing liquid nitrogen, reducing heat conduction down into the colder refrigerant. The associated vacuum, electrical control, and measuring equipment are located on nearby racks and benches.

[1] Now at the Los Alamos Scientific Laboratory, Los Alamos, New Mexico.

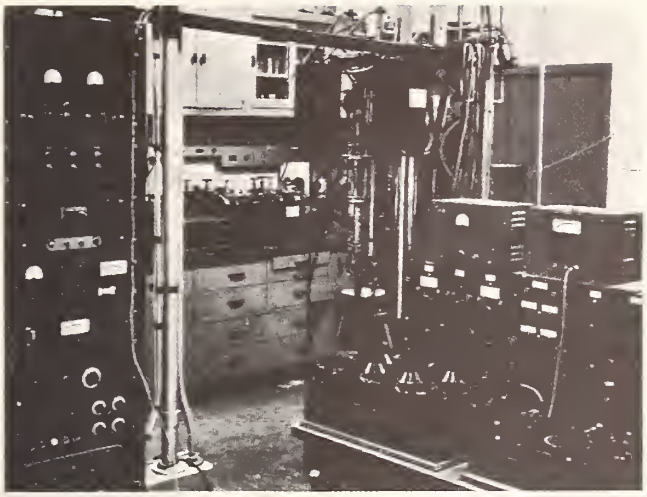

FIGURE 2. *Cryostat and associated equipment.*

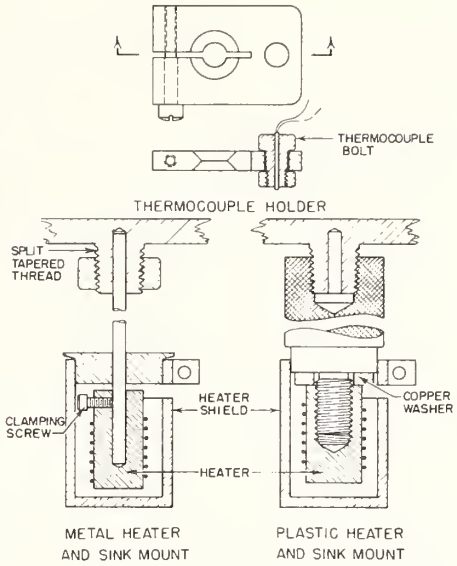

FIGURE 3. *Heaters and thermocouple holders.*

Figure 2 is a photograph of this assembly. Two similar cryostats are used concurrently to increase the data output.

2.2. Sample Assembly

Metal and alloy sample rods are 0.367 cm in diameter and 23.2 cm long; plastic samples are 2.54 cm in diameter and 20.5 cm long. The metal and alloy rods are turned, then ground to the final diameter with a tolerance of 0.0005 cm. Because of their larger size, the plastics are turned with a tolerance of only 0.001 cm. When required, the sample is annealed after the last grinding operation. Then the thermocouple holders shown in figure 3 are attached, and the holders are placed on the sample with their centers 2.54 cm apart by means of gage blocks. The thermocouple holders have a thin interior edge that gives, essentially, line contact between the holder and the sample. The actual distances between flat surfaces on the holders are measured by a vernier height gage with an attached precision dial test-indicator. The accuracy is about 0.0005 cm. The average diameters of the sample are measured between the thermocouple holders to about the same accuracy.

The samples are attached to the heat sink by a clamping action for metals, or an internal tapered screw thread for plastics as is shown in figures 1 and 3. The details of the sample heaters are also included in figure 3. The heater for a metal sample is slipped onto the rod and clamped with a small screw. In order to improve the thermal contact, mercury is placed in the hole that surrounds the lower end of the metal sample. The heater for plastic samples is screwed on so that it presses against a large copper washer used to increase the heater-to-sample contact area. Both heater blocks made of copper are wrapped with No. 36 or 40 AWG constantan heater wire in a single layer held in place with G. E. 7031 air-drying varnish. The sample heaters have a resistance ranging from 175 to 500 ohms for metals, and from 500 to 1,000 ohms for plastics. The power measuring circuits limit the current to a maximum of about 100 ma, and the voltage to a maximum of about 16 v. A small sample heater shield is attached to the sample by a split collet-and-screw clamp, so reducing radiation losses. These shields are covered on all exposed surfaces with aluminum foil to further reduce radiation.

2.3. Thermal Shielding, Tempering, and Controls

Several factors, such as gas conduction, radiation, and wire conduction, can lead to consistent errors in the experimental determinations of thermal conductivity. Heat losses by gas conduction or convection are reduced to an insignificant amount by baking out and evacuating the system to at least 10^{-5} mm of Hg while the system is at room temperature. Cooling of the system during experimental runs further reduces the residual gas pressure.

Heat losses by radiation and lead wire conduction are greatly reduced by surrounding the sample with a cylindrical thermal shield as shown in figure 1. The bottom, middle, and top of the shield are held at approximately the same temperature as the sample at the corresponding elevation. To provide a good thermal contact to the heat sink when the shield is bolted in place, the upper shield fastening ring is made of copper. The bottom of the shield is also made of copper to provide a nearly isothermal region surrounding the sample heater. The longer intermediate section of the shield is made of thin stainless steel to reduce the power input necessary to maintain any given temperature gradient. The shield is split in two, vertically, to allow rotation of the front half during the mounting and assembling of the sample.

The two halves are bolted together near the bottom, and a copper bar is soldered across the bottom to improve thermal contact. A mounted sample and the split shield are shown in figure 4.

Three heaters are wrapped on the shield to supply power necessary to maintain the proper thermal gradient. The main shield heater, wrapped back and forth across the bottom copper section, is made of 32 AWG constantan wire and has about 100 ohms resistance. The other two heaters at the midpoint and near the top, made of 45 AWG constantan, have about 300 ohms resistance. All three are kept in place with air-drying varnish. All wires connected to the sample pass through the shield and are cemented to it at areas close to the same temperature as that of their point of contact on the sample. These wires are 10 to 20 cm in length between the sample and shield.

The temperature difference between the sample heater and a horizontally opposed point on the lower copper section of the shield is measured with a gold-cobalt versus copper thermocouple. Potential differences of about 0.1 μv can be detected, corresponding to from 0.02° K at liquid helium temperatures, to 0.002° K at room temperature. Similar differential thermocouples are at midpoint and near the top.

The thermal electromotive forces developed across the middle and top differential thermocouples are measured with a d-c amplifier-galvanometer. To bring about thermal balance between the shield and sample, as indicated by null readings on the two upper differential thermocouples, the a-c voltages supplied to the heaters at the middle and top of the shield are adjusted manually. If the shield is hotter than the sample at either one of the two upper points, there is no way to obtain thermal balance. The lower, or main, differential thermocouple is the sensing device for a heater servomechanism. The approximately correct voltage for the bottom shield heater is adjusted manually by varying two autotransformers in series.

Heater and thermocouple wires are wrapped back and forth upwards on the shield for thermal tempering and then are wound on the posts attached to the heat sink. Two of the six cylindrical copper posts are shown in figure 1. The winding on the posts allows most of the heat conducted down the wires from above to be shorted to the liquid bath. One of the posts serves as a reference junction block for the eight measuring thermocouples; another is used to hold a platinum resistance thermometer that indicates the reference temperature. The others are used for thermal tempering only.

The heat sink and posts are machined from free-cutting leaded copper, assuring both good conductivity and machinability [6]. The vacuum chamber cylinder is soldered onto a lip of the heat sink with Rose's Alloy. Two thin stainless steel tubes serve as mechanical support for the internal apparatus, as exit tubes for the wires, and as pumping lines for evacuation of the inside chamber.

For measurements at liquid nitrogen, hydrogen, or helium temperatures, the entire apparatus is surrounded by liquid nitrogen in a large metal Dewar. To further reduce heat transfer to the internal apparatus, all the wires are again tied down thermally to a copper post inserted into the pumping line just above the top plate. The wires are brought out from the vacuum space through a hard wax seal. Near the top of the apparatus is a thermally insulated junction box where the various small wires from the cryostat are soldered to larger copper wires, usually 22 AWG, which lead to the control panel and measuring instruments.

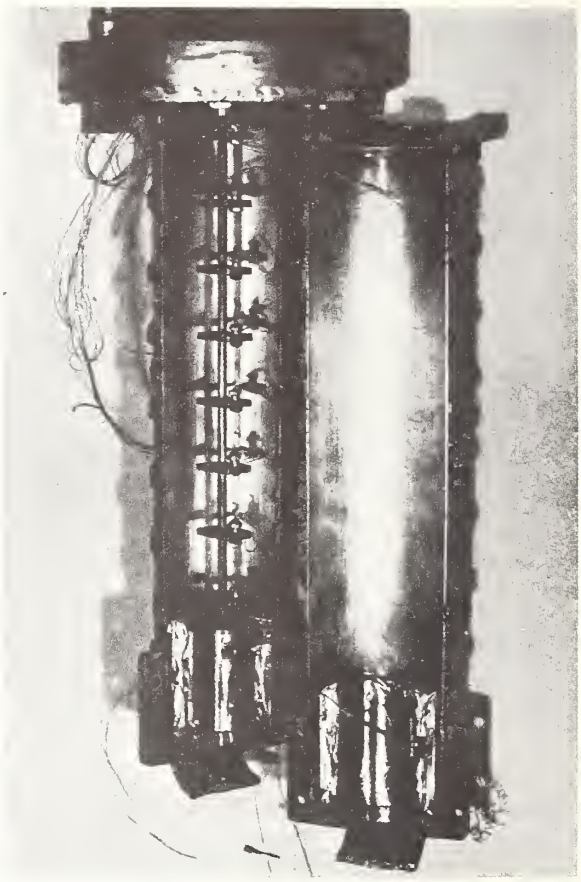

FIGURE 4. *Mounted sample.*

2.4. Measuring Apparatus

The reference junction temperature for the thermocouples is assumed to be the same as that of the thermometer post. The measuring thermometer is a strain-free capsule platinum resistor with an ice point resistance of about 25 ohms, which is embedded in one of the posts attached to the heat sink. The resistance of this thermometer, calibrated down to 12° K by the Temperature Measurements Section of the Bureau, is measured on a five-dial Mueller bridge. When actual readings are not being taken, this thermometer is switched to a resistance recorder. This switching allows a drift of the heat sink tem-

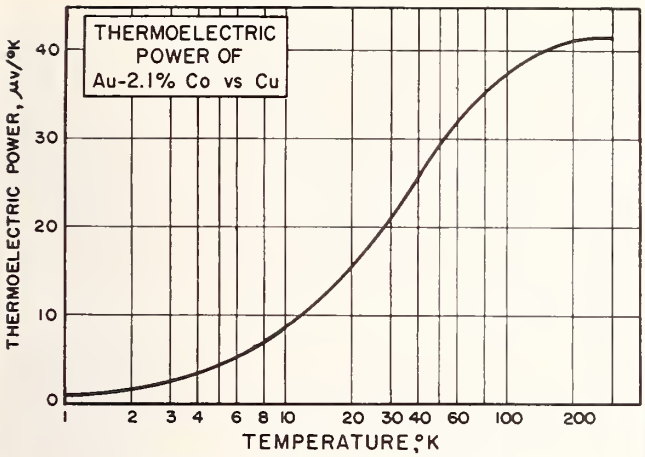

FIGURE 5. *Thermocouple calibration.*

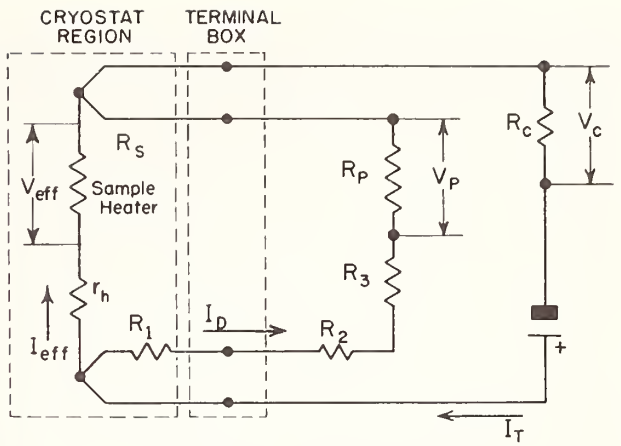

FIGURE 6. *Heater circuit.*

perature to be observed without continual manual measurements. With liquid helium, the temperature of the heat sink is obtained from a reading of the barometric pressure by using the 1955 d compromise temperature scale [2].

Wire of 5-mil diameter, composed of gold with 2.1 atomic percent of cobalt, is used for the common element of the eight thermocouples [1]. The common reference junction is on one post of the heat sink. The external common lead and the separate wires going to each thermocouple junction on the sample are standard thermocouple copper. The thermocouple combination was calibrated in a separate apparatus. Different spools of gold-cobalt wire with the same nominal composition have been found to vary in sensitivity by about 5 to 10 percent. A graph of the sensitivity of the spool that was used is shown in figure 5. Each thermocouple junction has one separate external lead and is measured with reference to the common junction at the heat sink. The junctions are electrically insulated by epoxy resin from the thermocouple bolt and, therefore, from the holder, sample, and ground. The thermocouple leads are soldered to larger wires at the junction box. The voltages are read on a 5-dial Wenner potentiometer, usually to 0.01 μv.

A determination of the power to the sample heater is obtained by measuring the d-c voltage and current. Figure 6 shows the circuit diagram. The total current passes through a calibrated 1-ohm NBS—type resistor, R_c; the voltage developed across it is measured on a Rubicon type-B potentiometer. The effective current passes through the sample heater R_s and the lead resistances r_h. The currents range from several milliamperes to about 100. The voltage across the heater is divided across three calibrated resistors, arranged to give either 2 to 1 or 11 to 1 voltage division. Resistor R_3 is 10 K ohms; R_p is either 10 K ohms for 2 to 1 voltage divider ratio, or 1 K ohm for 11 to 1 ratio. The voltage, measured on the same potentiometer as the current, ranges from 1 to about 16 v. The four calibrated resistors are in an oil bath maintained at 25° C by a commercial mercury thermostat and infrared heating unit.

Galvanometer unbalance voltages from the bridge and two potentiometers are directed to a commercial d-c breaker amplifier rather than the more commonly used moving-coil galvanometers. The input selector switch to the amplifier can be set to any of the galvanometer terminals of the bridge or potentiometers, or to some of the differential thermocouples between the sample and shield. The high sensitivity and several-million-fold amplification of the breaker amplifier allow interpolation one figure beyond the last dial setting on either the Mueller bridge or the Wenner potentiometer. The signal from the amplifier is switched to a l-v, center zero, d-c voltmeter for precise readings, or to a slow-speed recorder for following temperature drifts or approach to equilibrium.

Standard low-level electric techniques have been used: that is, all wires are shielded; a special common ground wire is used; the bridges are on insulated ground plates; and all terminals, switches, batteries, and standard cells are thermally insulated.

2.5. Auxiliary Equipment

A photograph of the equipment is shown in figure 2. The vacuum control unit is behind the cryostat; the power panels and control are on the left. The sample space is evacuated through nominal 1-in. tubes by an oil diffusion pump. Between the system and the diffusion pump is a metal cold trap that can hold liquid nitrogen over a weekend without refilling. Between the diffusion pump and the rotary mechanical pump is a 2-liter reservoir that, with its valve to the mechanical pump closed, can normally hold the diffusion-pump output for 4 hr before the pressure builds up to 100 μ. In parallel with the cold trap, diffusion pump, and reservoir, is a bypass line for pumping the system down initially without breaking the vacuum in the cold trap or diffusion pump. The pressure in the sample system is measured with a commercial ion gage when it is below 1 μ, and with a thermocouple gage when above that. The pressure in the reservoir, that is, the back pressure of the diffusion pump, is measured on another thermo-

couple gage system that has shutoff relays controlling the diffusion pumps and ion gage. Whenever the back pressure goes above 100 μ, an alarm light turns on, and the power to the diffusion pump and ion gage turns off.

The liquid refrigerant can be either maintained at a reduced pressure by a high-capacity mechanical pump, or vented directly to an explosion-proof exhaust system. These vent lines are necessary to reduce the explosion danger during liquid hydrogen tests. The vapor space over the liquid is connected to a mercury manometer, permitting measurement of the vapor pressure of the bath.

The power panel supplies both a-c and d-c voltage to the heaters and electronic equipment. The d-c voltage is obtained from a large bank of nickel-cadmium batteries in a nearby room. The current through the main sample heater, which is adjusted by four variable decade resistors, is read preliminarily on a precision multirange milliammeter. The a-c power is obtained from a 110-v regulated power supply. Power to each of the shield heaters is controlled by two autotransformers in series. The a-c power supply also furnishes voltage to a millivolt recorder, breaker amplifier, and the main shield heater servomechanism.

2.6. Measurement Techniques

For each metal sample, the thermocouple holders are mounted in a temperature-controlled shop room, where the dimensions are also measured. After these preliminary measurements, the sample is mounted in the heat sink and the heaters and thermocouples are attached. The sample is not heated or soldered after assembly of the thermocouple holders, and it is subjected to as little mechanical strain as possible during insertion into the cryostat. After this assembly, the shield is closed and bolted; then the vacuum can is soldered into place with Rose's Alloy. The sample space and tubes are evacuated and baked out for several days, usually over a weekend. The liquid refrigerants are not placed into the glass Dewar until the pressure in the cryostat is down to at least 10^{-5} mm of Hg.

Experimental runs are usually begun at liquid helium temperatures, after precooling first with nitrogen, then with hydrogen; and then the runs are continued at the hydrogen triple point, hydrogen boiling point, nitrogen triple point, nitrogen boiling point, carbon dioxide sublimation point, and then ice point. Normally, about six series of measurements at various temperature gradients are made in each temperature range. Two sets of measurements are made for each gradient to insure against reading errors or lack of steady state. The over-all temperature differences across the sample vary from 1° K to a sufficiently large temperature necessary to overlap readings in the next higher temperature range. The approach to steady-state conditions is observed by amplifying the unbalance emf from the Wenner potentiometer with the input switch set for the lowest thermocouple. The amplified signal is switched to the millivolt recorder, and, when this thermocouple emf no longer drifts with time, precise measurements of the voltage, current, and temperatures are begun. Measurements are also made at each sink temperature with no power input and with the normal vacuum space filled with helium exchange gas at a pressure of several hundred microns. Because the apparatus should be isothermal under these conditions, these readings give the "zero" corrections for the thermocouples. These corrections are attributed primarily to inhomogeneous emf's and are assumed to be constant for a particular sink temperature.

Subsidiary measurements are made afterwards on a short section of the sample. They include mounting and polishing of the metal for photomicrographs of grain structure, measurement of hardness, measurement of density, and spectrographic or chemical analyses.

3. Analyses of Data

3.1. Basic Calculations

The fundamental equation of heat flow is utilized in its differential form:

$$\dot{Q}=-\lambda A\frac{dT}{dx}$$

where $\dot{Q}$ is the heat flux, λ is the thermal conductivity, and A the cross-sectional area. Because $\dot{Q}$ and A are essentially constants of the sample for each run,

$$\lambda=\frac{d(-\dot{Q}x/A)}{dT}.$$

Because we do not measure the temperature directly, but rather the thermocouple voltage E, we rearrange the equation to

$$\lambda=\frac{d(-\dot{Q}x/A)}{dE}\frac{dE}{dT}$$

where dE/dT is the thermoelectric power of the thermocouple at the given voltage E and for the given reference temperature.

Several corrections to a straightforward calculation of the heat power of the sample heater are necessary. The various components of the power circuit are shown in figure 6. Basically, the power is the product of the voltage and current through the sample heater. The effective current through the heater is given by

$$I_{eff}=I_T-I_D,$$

where I_T is the total current and I_D is the current through the divider circuit. The total current is given by the measured voltage V_C across the standard resistor divided by its resistance R_C. Similarly, the divider current is given by the measured divider voltage V_P divided by the resistance of the particular resistor R_P. The effective current is then

$$I_{eff}=\frac{V_C}{R_C}-\frac{V_P}{R_P}.$$

The effective voltage is

$$V_{eff}=\rho V_P-r_h I_{eff},$$

where $r_h I_{eff}$ is the temperature-dependent voltage developed across the heater leads between the shield and the sample, and ρ is the voltage divider ratio. The ratio is given by

$$\rho=\frac{R_1+R_2+R_3+R_P}{R_P},$$

where R_1 and R_2 are lead resistances (R_1 is temperature dependent), R_3 is a standard 10 K ohm resistor, and R_P is either 1 K ohm or 10 K ohm.

The cross section and distances along the sample are measured at room temperature. These dimensions are corrected for thermal contraction at each sink temperature range whenever thermal expansion data are available. A preliminary plot is made of $\dot{Q}x/A$ against E to check for points that are considered to have too large a deviation.

For the acceptable runs, the $\dot{Q}x/A$ and E are tabulated, and the values are processed by an IBM 650 digital computer. The program fits the $\dot{Q}x/A$ data by a least squares method to polynomials to the first, second, third, and fourth degree in E. Generally speaking, the first-degree polynomials give the best results for small temperature gradients, and the fourth-degree polynomials give the best for the large gradients. The computer is then programed to take the derivative of each of the polynomials, and then to multiply by the thermoelectric power of the thermocouples at each temperature. The final result is the thermal conductivity at 1-deg intervals based upon each of the above polynomials.

Thermal conductivities as a function of temperature for each run are then plotted on a large scale graph. Average or best curves are drawn through the many points for each range, and the various ranges are connected smoothly to give the complete graph.

3.2. Estimation of Errors

Three main sources of error appear in the apparatus described here: (1) Calibration of the thermocouples, (2) placement of the thermocouple holders, and (3) thermal contact resistance between the thermocouple and the sample. The first can be improved by a more complete and accurate thermocouple calibration. A new series of thermocouple calibrations to improve the range and accuracy of the data has been started in thermometry calibration apparatus. The second source of error has been practically eliminated because of better control of the dimensions and placement of the holders. The third source of error can be reduced by increasing the length of the thermocouple lead wire between the shield and the sample, and by obtaining better contact between the thermocouple bolt and its holder.

Even after improvement, the first and third will probably remain the main sources of error. The thermocouple measurements can be improved, but appreciable errors will still come from chemical inhomogeneities, mechanical strains, uncertainty in calibration, reduced sensitivity at the lowest temperatures, and thermal emf in the external circuitry. The thermocouple error is estimated to be less than 1 percent over most of the temperature range. This error will be systematic and cannot be estimated or eliminated by statistical methods. The error caused by thermal contact resistance can be estimated by deliberately holding the thermal shield hotter or colder than the sample.

Except for gas conduction and radiation at high temperatures, the other sources of error have been reduced to an insignificant amount, considering the larger errors mentioned above. Errors in the cross-sectional measurements are probably about 0.2 percent; inaccuracy in locating the actual contact point between the thermocouple holder and sample is about the same. Errors due to radiation below 100° K and conduction along lead wires were calculated to be below 0.1 percent. To check these radiation losses at higher temperatures, several trial runs with different gradients were made at the ice point. Apparently, for metals, an error of about 1 to 2 percent exists in the readings at that temperature as disclosed by a systematic dependence of the apparent conductivity on the gradient. Several runs were made with a residual helium gas pressure of approximately 1×10^{-5} mm Hg within the system. These runs differed by about 3 percent for most temperature ranges.

Experimental runs in each temperature range have been analyzed for internal consistency. The deviations from an average curve are usually less than 1 percent in the liquid helium and hydrogen ranges, and less than ½ percent at liquid nitrogen temperatures and above. These inconsistencies are apparently due to the combined result of the various errors mentioned above, the one exception being thermocouple calibration error, which is systematic. The inaccuracies increase if the sample has either a very high or a very low conductivity. The range of usable sample diameters is not as great as the variation in conductivity; therefore, at both extremes of conductivity, optimum measuring conditions cannot be obtained. Recent measurements on a very pure copper sample that had a conductivity maximum over 100 w/cm °K gave inconsistencies of about 5 percent between 4° K and 60° K. Measurements on very low conductivity alloys or plastics have about this same inaccuracy, and, in addition, are usually not reliable above 100° K because of the increasing significance of radiation exchange between the sample and shield.

Many control experiments have been carried out to test the self-consistency of the apparatus. Many of the runs overlap in temperature range. For example, some of the runs were carried out with the heat sink at 4° K and the bottom of the sample

around 25° K, thus overlapping runs made with the sink at 19.7° K. The conductivity curves from the lower ranges fit smoothly with the curves at the higher temperatures. Apparent conductivities from runs with different thermal gradients on the sample usually agree within the scatter normally characteristic of a single run. Various runs with different size samples and holders gave consistent results.

4. Results

4.1. Polytetrafluoroethylene

The graph of thermal conductivity of this plastic is given in figure 7. The estimated inaccuracy of the results is about 10 percent. The sample was extruded and had a density of 2.218 g/cm^3. Thermal contraction was calculated by using the data of Quinn, et al. [7] for the higher temperatures, and the data of Head and Laquer [3] for the low temperatures [4].

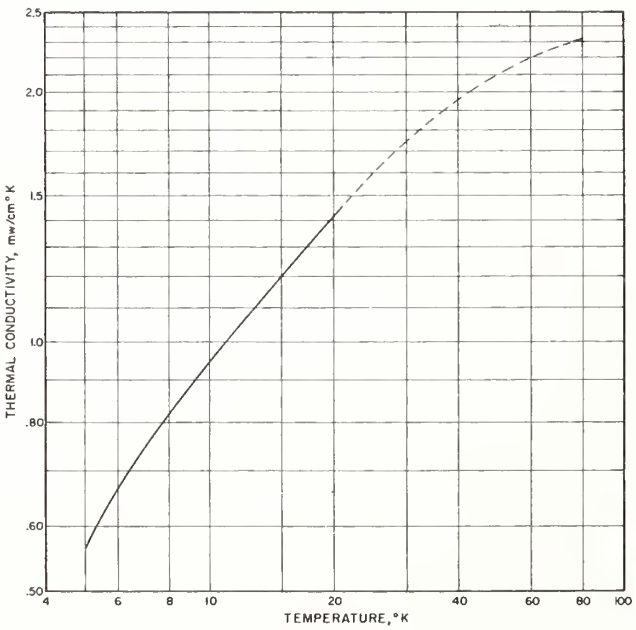

FIGURE 7. *Thermal conductivity of polytetrafluoroethylene.*
(The dashed lines indicate interpolated regions.)

4.2. Coalesced Copper

The graph of the thermal conductivity of this high-purity commercial copper is given in figure 8. The estimated inaccuracy of these results ranges from 2 to 5 percent. The sample had a mill specification giving the impurities by weight as 13 ppm O_2; 8 ppm Pb; 7 ppm Ni; less than 5 ppm each of Fe, As, and Sb; 2 ppm Sn; less than 1 ppm Te and Ag; and less than 0.5 ppm Bi. The sample was annealed 4 hr at 400° C, cooled slowly to 200° C, and then kept at 200° C for 8 hr. During the entire heating cycle, the sample was kept in a flowing helium atmosphere. The density of the sample was 8.90 g/cm^3, and its hardness on the Vickers diamond point system with a 10 kg weight was 54.1 in the longitudinal section, and 48.8 in the transverse.

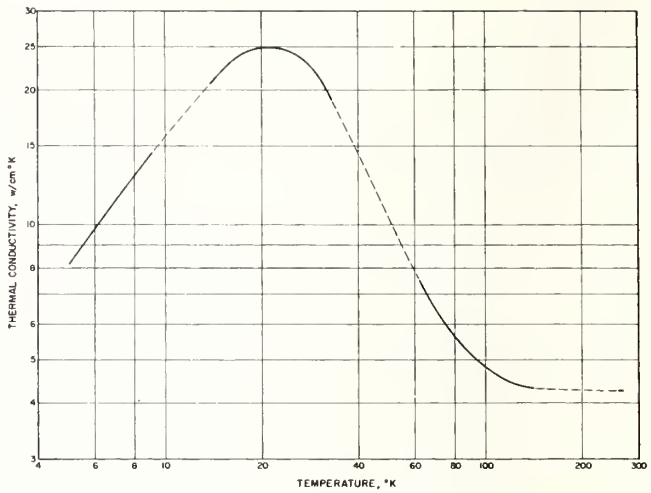

FIGURE 8. *Thermal conductivity of coalesced copper.*
(The dashed lines indicate interpolated regions)

The authors thank R. J. Corruccini, W. B. Hanson, and R. B. Scott for advice and assistance during the progress of this project, and G. A. Yates of the Phelps Dodge Copper Products Corp. for the generous supply of samples and fabrication information.

5. References

[1] G. Borelius, W. H. Keesom, C. H. Johansson, and J. O. Linde, Commun. Phys. Lab. Univ. Leiden, No. 206b.
[2] J. R. Clement, liquid helium vapor pressure—temperature scale. Distributed by the Naval Research Laboratory as an informal report (1955).
[3] E. L. Head and H. L. Laquer, Low temperature thermal expansion of various materials, Available from Office of Technical Services, AEC D–3706.
[4] Richard K. Kirby, J. Research NBS **57,** 91 (1956). Received after completion of the data analysis.
[5] J. L. Olsen and H. M. Rosenberg, Adv. Physics **2,** 28 (1953).
[6] R. L. Powell and D. O. Coffin, Rev. Sci. Inst. **26,** 516 (1955).
[7] F. A. Quinn, D. E. Roberts, and R. N. Work, J. Appl. Phys. **22,** 1085 (1951).

BOULDER, COLO., December 8, 1956.

Author Index

[Reference is to volume number, boldface, followed by page number of this volume.]

Author Index—Continued

Author Index—Continued

Subject Index

Subject Index—Continued

☆ U. S. GOVERNMENT PRINTING OFFICE : 1970 O - 379-831

Announcement of New Volumes in the NBS Special Publication 300 Series Precision Measurement and Calibration

Superintendent of Documents,
Government Printing Office,
Washington, D.C. 20402
Dear Sir:

Please add my name to the announcement list of new volumes to be issued in the series: National Bureau of Standards Special Publication 300, Precision Measurement and Calibration.

Name _____

Company _____

Address _____

City _____ State _____ Zip Code _____

(Notification key N–353)

(cut here)

Official SI Unit Names and Symbols

[For a complete statement of NBS practice, see NBS Tech. News Bull. Vol. 52, No. 6, June 1968.]

Name	Symbol	Name	Symbol
meter	m	newton	N
kilogram	kg	joule	J
seeond	s	watt	W
ampere	A	coulomb	C
kelvin [1]	K	volt	V
candela	cd	ohm	Ω
radian	rad	farad	F
steradian	sr	weber	Wb
hertz	Hz	henry	H
lumen	lm	tesla	T
lux	lx		

Additional Names and Symbols approved for NBS use

eurie [2]	Ci	mho	mho
degree Celsius [3]	°C	mole	mol
gram	g	siemens [4]	S

[1] The same name and symboi are used for thermodynamic temperature and temperature interval. (Adopted by the 13th General Conference on Weights & Measures, 1967.)
[2] Accepted by the General Conference on Weights & Measures for use with the SI.
[3] For expressing "Celsius temperature"; may also be used for a temperature interval.
[4] Adopted by IEC and ISO.

Table for Converting U.S. Customary Units to Those of the International System (SI)[5]

To relate various units customarily used in the United States to those of the International System, the National Bureau of Standards uses the conversion factors listed in the "ASTM Metric Practiee Guide", NBS Handbook 102. These are based on international agreements effeetive July 1, 1959, between the national standards laboratories of Australia, Canada, New Zealand, South Afriea, the United Kingdom, and the United States.

To convert from:

(1) inehes to meters, multiply by 0.0254 exaetly.
(2) feet to meters, multiply by 0.3048 exactly.
(3) feet (U.S. survey) to meters, multiply by 1200/3937 exactly.
(4) yards to meters, multiply by 0.9144 exactly.
(5) miles (U.S. statute) to meters, multiply by 1609.344 exactly.
(6) miles (international nautical) to meters, multiply by 1852 exaetly.
(7) grains (1/7000 lbm avoirdupois) to grams, multiply by 0.064 798 91 exactly.
(8) troy or apothecary ounces mass to grams, multiply by 31.103 48 . . .
(9) pounds-force (lbf avoirdupois) to newtons, multiply by 4.448 222 . . .
(10) pounds-mass (lbm avoirdupois) to kilograms, multiply by 0.453 592 . . .
(11) fluid ounees (U.S.) to cubic centimeters, multiply by 29.57 . . .
(12) gallons (U.S. liquid) to cubic meters, multiply by 0.003 785 . . .
(13) torr (mm Hg at O °C) to newtons per square meter, multiply by 133.322 exactly.
(14) millibars to newtons per square meter, multiply by 100 exactly.
(15) psi to newtons per square meter, multiply by 6894.757 . . .
(16) poise to newton-seconds per square meter, multiply by 0.1 exaetly.
(17) stokes to square meters per second, multiply by 0.0001 exactly.
(18) degrees Fahrenheit to kelvins, use the relation $T_{68}=(t_F+459.67)/1.8$.
(19) degrees Fahrenheit to degrees Celsius, use the relation $t_{68}=(t_F-32)/1.8$.
(20) curies to disintegrations per second, multiply by 3.7×10^{10} exactly.
(21) roentgens to coulombs per kilogram, multiply by $2.579\ 760\times10^{-4}$ exactly.

[5] Système International d'Unités (designated SI in all languages).